

Improved flood risk assessment:

New data sources and methods for flood risk modelling

kumulative Habilitationsschrift
zur Erlangung des akademischen Grades
doctor rerum naturalium habilitatus (Dr. rer. nat. habil.)
venia legendi: Hydrologie

vorgelegt der
Mathematisch-Naturwissenschaftlichen Fakultät
der Universität Potsdam

von

Kai Schröter

geboren am 19. Februar 1976 in Kronberg i. Ts.

Potsdam, June 2019

Published online on the
Publication Server of the University of Potsdam:
<https://doi.org/10.25932/publishup-48024>
<https://nbn-resolving.org/urn:nbn:de:kobv:517-opus4-480240>

Contents

Preface	9
Summary	11
1 Introduction	13
1.1 Background	13
1.2 Flood risk management	15
1.3 Challenges in flood risk management	17
1.3.1 Understanding flood risk systems	17
1.3.2 Analysing flood events and exploring new data sources	18
1.3.3 Modelling flood risk	19
1.3.4 Assessing flood impacts and modelling vulnerability	19
1.4 Objectives and outline	21
Part 1: Flood risk systems	25
2 A review of multiple natural hazards and risks in Germany	25
2.1 Introduction	26
2.2 Historic damage from natural hazards	28
2.3 Distribution and characteristics of natural hazards in Germany	31
2.3.1 Storms: Winter storms and convective storms	31
2.3.2 Inland and coastal floods	35
2.3.3 Extreme temperature	38
2.3.4 Earthquakes	39
2.4 Risk analyses and management	39
2.5 Conclusions	47
3 What made the June Flood 2013 in Germany an exceptional event? A hydro-meteorological evaluation	49
3.1 Introduction	50
3.2 Data and Methods	52
3.2.1 Data	52
3.2.2 Methods	54
3.3 Results	58
3.3.1 Meteorological conditions	58
3.3.2 Precipitation	59

3.3.3	Initial catchment state	63
3.3.4	Peak flood discharges	66
3.3.5	Index based classification	68
3.3.6	Sensitivity Analysis	70
3.4	Conclusions	71
4	The flood of June 2013 in Germany: How much do we know about its impacts?	77
4.1	Introduction	78
4.2	Data sources	82
4.2.1	Governmental reports	82
4.2.2	Communications on disruptions of road and railway traffic	83
4.2.3	Computer-aided telephone interviews	84
4.3	Impacts of the flood in June 2013	87
4.3.1	Flood impacts on human health	87
4.3.2	Overview of impacts on economic activities (and assets) on the regional and national scale	91
4.3.3	Impacts on economic activities – traffic disruptions	97
4.3.4	Impacts on economic activities at the asset scale: with a focus on business interruption of individual companies	102
4.3.5	Impacts on cultural heritage	103
4.3.6	Environmental impacts	104
4.4	Discussion and recommendations	105
4.5	Conclusions	110
5	Social media as an information source for rapid flood inundation mapping	113
5.1	Introduction	114
5.2	Challenge 1: Filtering social media information	115
5.2.1	State of the art and related work	115
5.2.2	Requirements	117
5.2.3	PostDistiller	117
5.3	Challenge 2: Utilization of the information from social media for rapid inundation mapping	122
5.3.1	State of the art and related work	122
5.3.2	Case study Dresden June flood 2013	124
5.4	Discussion	131
5.5	Conclusions	132
6	What are the hydro-meteorological controls on flood characteristics?	135
6.1	Introduction	136
6.2	Study area	137
6.3	Data and methods	139
6.3.1	Hydro-meteorological patterns	140
6.3.2	Regional flood model (RFM)	144
6.3.3	Flood event identification and characteristics	146
6.3.4	Linking patterns to flood events and their characteristics	148
6.4	Results	150

6.4.1	Evaluation of the regional flood model and of the reshuffling approach	150
6.4.2	Separate control of hydrological pre-conditions and meteorological event conditions on flood characteristics	151
6.4.3	Combined control of soil moisture patterns and weather patterns on flood characteristics	155
6.5	Discussion	157
6.5.1	Suitability of the developed approach	157
6.5.2	Hydro-meteorological controls on the flood characteristics	159
6.6	Conclusions	162
7	Spatially coherent flood risk assessment based on long-term continuous simulation with a coupled model chain	165
7.1	Introduction	166
7.2	Methods	168
7.2.1	Weather generator	168
7.2.2	Regional Flood Model (RFM)	168
7.3	Application to the Mulde catchment	171
7.3.1	Study area	171
7.3.2	Model set-up	172
7.4	Results and discussion	175
7.4.1	RFM model performance evaluation	175
7.5	Long-term simulation results: flood risk in the Mulde catchment	178
7.6	Conclusions	187
8	Large-scale, seasonal flood risk analysis for agricultural crops in Germany	189
8.1	Introduction	190
8.2	Methodology	191
8.2.1	Seasonal crop susceptibility	191
8.2.2	Seasonal flood probability	193
8.2.3	Superposition of flood seasonality and seasonal crop susceptibility .	193
8.2.4	Calculation of expected annual damage	197
8.3	Results and Discussion	198
8.4	Conclusions	205
Part 2: Vulnerability modelling for flood loss estimation		207
9	A review of flood loss models as basis for harmonization and benchmarking	207
9.1	Introduction	208
9.2	Methods used to build the inventory	209
9.2.1	Literature review strategy	210
9.2.2	Structure of the inventory	211
9.3	Observations on the flood loss model inventory	211
9.4	An illustration of model diversity	218
9.4.1	Challenges in model harmonization	222
9.5	Conclusions	225

10	How useful are complex flood damage models?	227
10.1	Introduction	228
10.2	Set up of validation exercise	230
10.2.1	Flood events	231
10.2.2	Empirical damage data collection	233
10.2.3	Consideration of observation uncertainty	234
10.2.4	Evaluation criteria	237
10.3	Damage models	237
10.3.1	Depth-damage function	238
10.3.2	FLEMOps+r	239
10.3.3	Regression Trees	239
10.3.4	Data based Bayesian networks	241
10.3.5	Expert Bayesian networks	243
10.4	Results and discussion	245
10.5	Conclusions	250
11	Tracing the value of data for flood loss modelling	253
11.1	Introduction	254
11.2	Data and Models	254
11.2.1	Empirical flood loss data	254
11.2.2	Loss models	255
11.3	Analysis framework	256
11.3.1	Split-sample validation experiments	256
11.3.2	Performance criteria and scores	256
11.4	Results and Discussion	258
11.5	Conclusions	262
12	Flood loss estimation using 3D city models and remote sensing data	263
12.1	Introduction	264
12.2	Data	266
12.2.1	Study area	266
12.2.2	Data sources	267
12.3	Methods	271
12.3.1	Model development	271
12.3.2	Software and data availability	274
12.4	Results	274
12.4.1	Variable selection	274
12.4.2	Model derivation and evaluation	276
12.5	Prototype	279
12.5.1	Implementation	279
12.5.2	Application example Dresden	281
12.6	Discussion	284
12.7	Conclusions	286

13 Multi-model ensembles for assessment of flood losses and associated uncertainty	287
13.1 Introduction	288
13.2 Setup of validation exercise	290
13.2.1 Flood loss models	290
13.2.2 Evaluation methods	291
13.2.3 Application cases	293
13.3 Ensemble construction and evaluation	296
13.3.1 Model rating	297
13.3.2 Ensemble-mean performance	298
13.3.3 Probabilistic application	309
13.4 Conclusions	312
14 Probabilistic, multi-variable flood loss modelling on the meso-scale with BT-FLEMO	315
14.1 Introduction	316
14.2 Data and methods	318
14.2.1 Case study area	318
14.2.2 Bagging Decision Tree (BT) based loss model for the micro-scale . .	318
14.2.3 Spatial scale transfer	320
14.2.4 Model validation	324
14.3 Results and discussions	325
14.3.1 Meso-scale BT-FLEMO	325
14.4 Loss estimates and model validation	327
14.5 Conclusions	331
15 Discussion, conclusions and outlook	333
15.1 Summary of achievements	333
15.2 Discussion	337
15.3 Concluding remarks and outlook	341
Annex 1	343
List of Figures	343
List of Tables	353
Bibliography	355

Preface

This thesis compiles 13 independent peer reviewed scientific articles in the research field of flood risk. The articles have been published in ISI journals except for one article in conference proceedings. These articles present results from research work at the German Research Centre for Geosciences GFZ, Section Hydrology, carried out in various research projects in which I have been actively involved:

- Federal Ministry of Education and Research (BMBF): Untersuchungen zur Bewältigung des Hochwassers 2013 (October 2013- February 2015)
- Centre for Disaster Management and Risk Reduction Technology (CEDIM): Forensic Disaster Analysis (May 2012- October 2015)
- European Institute of Technology (EIT), Climate-KIC: 3d city flood damage module (3DCFD) pathfinder project (July 2015 - December 2016)
- European Union Horizon 2020, Marie Skłodowska-Curie Action European Training Network System-Risk, A large-scales systems approach to flood risk assessment and management (ETN System-Risk) (since January 2016)
- European Union Horizon 2020, Oasis Innovation Hub for Catastrophe and Climate Extremes Risk Assessment (H2020 | Insurance) (since May 2017)

The financial support of all mentioned institutions as well as data provision by many other institutions is gratefully acknowledged.

Scientific work thrives on cooperation and discussion with colleagues and peers. Therefore, my sincere thanks are dedicated to all my coauthors and project partners. It has been a pleasure to work with you. In particular, I would like to acknowledge Bruno Merz and Heidi Kreibich for their scientific enthusiasm and for providing an inspiring and motivating work environment. Just as much I thank Annegret Thieken for her support and advice at the University of Potsdam, as well as Jeroen Aerts and Rob Lamb for being part of the advisory committee. I also thank all colleagues (current and former) and friends at GFZ Section Hydrology for the time shared during the last years and the fruitful discussions. Special thanks go to Stefan Lüdtke, for technical advice and solid espresso supply, and to Philip Bubeck for his valuable comments on this thesis.

Finally, I would like to thank my family and friends for having supported me over the past years. Especially my wife, daughter and son deserve a big thank you for being a great encouragement.

Potsdam, June 2019,
Kai Schröter

Summary

Floods are recurring natural phenomena. For human uses of the rivers and floodplains floods are a significant hazard causing major property, infrastructure and economic damage as well as loss of human life. Over the last decades large efforts have been undertaken to mitigate flood disaster risk. Despite of this, in this period a dramatic increase of damaging floods has been seen globally. In view of anthropogenic climate change and increasing exposure, losses are expected to further rise in the future. The reduction of flood disaster mortality, number of people affected, as well as economic loss are of high priority.

Flood risk management aims to reduce the likelihood and/or the impact of floods by taking actions to control the hazard in terms of frequency and intensity of flooding, lower the exposure by minimising the assets exposed, and reduce the vulnerability via preparedness. Flood risk is a dynamic challenge and changes to the components of flood risk are accelerating with increasing frequency of severe weather events, land use change and socio-economic transformations. The sustainable mitigation of flood impacts requires a rigorous implementation of integrated risk management on the foundation of profound knowledge about flood risk systems. This requires an improved understanding of interactions and feedbacks in cause-effect relationships, as well as triggers and controls of flood characteristics and impacts.

In this context, current research challenges are to deepen insights into flood risk systems and to increase the understanding of interactions and dynamics of underlying hazard, exposure and vulnerability processes. Rapidly increasing amounts and diversity of data require further efforts to enhance the capability to process large data sets, as well as to develop and test methods and models for less uncertain and more reliable flood risk assessments.

This thesis contains new insights and findings about flood risk systems and vulnerability modelling for loss estimation, covering three overarching topics:

- Flood event analysis,
- usage of new data sources, and
- innovating flood risk modelling.

This work includes a review of flood risk management in Germany and perspectives in the context of multi-hazard risk management. The flood event in June 2013 is analysed with regard to hydro-meteorological flood drivers and flood impacts. Controls on flood characteristics and impacts are further investigated using a simulation based approach. New data sources are explored in terms of social media data for rapid flood

inundation mapping and using data from 3D city models in combination with empirical post event survey data for flood vulnerability modelling. Further, the value of data and the usefulness of complex flood vulnerability models are examined. Approaches to flood risk modelling comprise the development of probabilistic flood vulnerability models using machine learning and multi model ensembles. New methods for deriving flood risk from long term continuous simulations of the flood risk chain and accounting for seasonal changes in flood risk are presented.

Flood characteristics and flood impacts are controlled by numerous processes and diverse factors which interact in a complex way. Unusual combinations of hydro-meteorological factors have been found to trigger even more severe floods than exceptional occurrences of individual factors. This knowledge can feed into the development of worst-case flood scenarios and for additional investigations of flood controls including the spatial and temporal variability of these factors, and their superposition. As non-linear and threshold behaviour within flood risk systems complicate the identification and analysis of relationships between controls on flood characteristics and impacts these connections are not yet fully understood.

An approach has been proposed to derive flood risk from continuous long-term simulations of the flood risk chain, covering processes from meteorological inputs to flood impacts and representing process interactions. According to modelling results, flood risk depends not only on the maximum flood intensity but also on flood volume and flood-plain hydraulics. Probabilistic multi-variable flood vulnerability models have been newly introduced and have been shown to be a major advancement in reliably estimating flood loss. Improvements in model predictive performance depends not only on the number of predictors but also on the model approach, and thus on the representation of damage processes.

Closely monitoring and documenting flood events provide the basis to inform worst case flood scenarios, to evaluate flood risk reduction strategies, and to develop improved models. Information about consequences of flooding are fragmented and require large efforts to compile useful datasets particularly for flood impacts. Tapping new data sources including volunteered geographic information and high resolution building information open up opportunities to complement established sensors and monitoring systems and amend insights to flood risk processes.

Flood risk assessment accounting for system behaviour does not only need methodological advancements but also require suitable technical frameworks to hold data as well as data analytics to collate and integrate data from diverse sources. Machine learning approaches have been successfully used to explore heterogeneous and high-dimensional datasets and to detect complex dependencies among variables.

The development and findings of this thesis present progress in several aspects of flood risk assessment and management. It contributes knowledge about flood risk systems and improved capabilities to analyse and make use of data in risk modelling. Consolidating the observation and analysis of extreme events, expanding the use of new technologies and open data, and increasing interoperability and transparency of data and models are needed to keep up with changing risk. These aspects mark directions of future research in the field of flood risk modelling.

1 | Introduction

1.1 Background

Floods have been responsible for 25 % of the total economic damage from natural disasters over the last 30 years (CRED, 2019). From 1994 to 2005 more than 2.5 billion people were affected and 66 million buildings were damaged by floods (CRED, 2015). According to IPCC (2012) and P. Ward et al. (2017) the global expected annual flood loss ranges in the order of USD 100 b.

Floods are hydrological extremes of the water cycle and characterize a situation of rising and overflowing of a body of water onto normally dry land (EC, 2007b). While floods are recurring natural phenomena, conflicts arise with human uses of the rivers and floodplains (White, 1945). For these interests and claims floods are a significant hazard causing major property, infrastructure and economic damage as well as loss of human life. Despite large efforts to mitigate flood disaster risk over the last decades, this period has seen a dramatic increase in economic flood losses globally (Bouwer, 2010; Luger et al., 2010). For the future, a further rise of losses is expected as a consequence of anthropogenic climate change and increasing exposure (Hirabayashi et al., 2013; Hallegatte et al., 2013; IPCC, 2012; Hoeppe, 2016; Winsemius et al., 2016; Willner et al., 2018). Hence, the further reduction of flood disaster mortality, and number of people affected, as well as the trend reversal to reduce economic loss remain high priority targets of the international community (UNISDR, 2015).

Catastrophic flooding as a recurring motif in written heritage, ancient myths, and chronicles of human history (Herget et al., 2015) underpins that flood control is a crucial component in the development of settlements and securing livelihoods of individuals and communities. With the background of historic and recurring flood experiences (Glaser and Stangl, 2004; Herget et al., 2015) as well as with a deepened understanding of historic flood hydrology (Benito et al., 2015; Swierczynski et al., 2013) it has been realized that the complete prevention of flood impacts is technically not feasible and economically not sustainable (White, 1936; Schanze, 2006).

Still, under the paradigm of flood protection, societies have largely relied on structural measures to control floods (White, 1936; Tobin, 1995; Werritty, 2006). However, closely tied to the resulting fallacious perception of safety, flood hazard and risk awareness decay and seriously undermine foresighted human adjustments to floods (Tobin, 1995; Pinter, 2005; Di Baldassarre et al., 2015; Di Baldassarre et al., 2018). Acknowledging the inadequacies of the flood hazard centred *promise of protection*, the International Decade of Natural Disaster Reduction from 1990 to 1999 (IDNDR) has encouraged a shift to more comprehensive catchment and risk-oriented approaches (UNDRO, 1991). Subse-

quently, *flood risk management* has received increasing attention and important progress has been made in research and practice (B. Merz et al., 2010a). In Europe, particularly the floods directive (EC, 2007b) has catalysed risk-oriented approaches to be increasingly pursued and operationalized in assessing and managing flood risk. In a nutshell, this development has entrenched flood risk as a basis for decision making, has expanded the range and variability of flood characteristics considered in flood scenarios, and has broadened the spectrum of mitigation measures by complementing or replacing technical flood defence schemes with spatial planning, precaution, early warning, risk transfer and other non structural measures (Kreibich et al., 2015).

In this development the concept of quantitative risk takes a central role (Haimes, 1998; E. Plate, 2002; B. Merz, 2006; Renn, 2008). In essence, quantitative risk is about probability and consequences (Kaplan and Garrick, 1981). In the case of floods, it combines floods as a source of danger with the likelihood of adverse consequences. Kaplan and Garrick (1981) formalise risk R as a set of triplets consisting of scenarios (s_i) describing possible incidents, the likelihood or probability of these scenarios (p_i), and the consequences (x_i), i.e. the metric of damage: $R = \langle s_i, p_i, x_i \rangle, i = 1, 2, \dots, N$. Hence, flood risk represents the damage that is exceeded with a given probability. Closely following this concept, natural sciences and engineering commonly define flood risk as the product of flood hazard, exposure and vulnerability (W. Kron, 2005; EC, 2007b; IPCC, 2012). In this definition flood **hazard** is an expression of the probability of the flood in a given area within a specified period of time, **exposure** represents the inventory of objects in the area in which a hazard may occur including their values at risk, and **vulnerability** reflects the propensity of the exposed objects to suffer adverse effects when impacted by a hazard event, thus describing the susceptibility of these objects to flood impacts (W. Kron, 2005; IPCC, 2012).

The practical implementation of the quantitative risk concept faces difficulties regarding the choice of scenarios, the quantification of probabilities, and estimation of consequences. Therefore, many simplifying assumptions are introduced as for instance using homogeneous return periods for flood scenarios within the entire catchment, and using return periods of discharges as a proxy for return periods of consequences. While this often feeds criticism, risk analysis and assessments offer systematic procedures to capture the system under study and provide the best available knowledge for flood risk management decisions (B. Merz, 2006). Ideally, the assumptions are made transparent and thus enable an informed discussion about priorities and social acceptance of risk. Importantly, the procedure of risk assessment builds an understanding of the interplay between natural and socio-economic processes in the flood risk system and has strongly influenced how societies deal with floods and manage flood risks (Bubeck et al., 2017). Hereinafter, the concept of flood risk management and the associated challenges for risk analyses and assessment to support sound decision making are discussed and the objectives and the outline of this thesis are presented.

1.2 Flood risk management

Changes in flood risk are induced by alterations to hazard, exposure or vulnerability. Therefore, flood risk management aims to reduce the likelihood and or the impact of floods by taking actions to control the hazard in terms of frequency and intensity of flooding, lower the exposure by minimising the number and values of objects exposed, and reduce the vulnerability via preparedness. In light of human interventions, land development, and non-stationary climate, flood risk is a dynamic entity. Hence, the management of flood risk must be seen as a continuous process in an iterative and interlinked adaptive cycle (Stern and Fineberg, 1996; DKKV, 2003b; PLANAT, 2004; Klijn et al., 2015; Bubeck et al., 2017; Cremades et al., 2018). In this line, flood risk management has been framed as a cyclic activity with the *analysis*, *assessment* and *mitigation* of flood risk as key components (E. Plate, 2002; Sayers et al., 2002; B. Merz, 2006; Schanze, 2006).

Flood risk analysis provides estimates for the likelihood of occurrence of flood loss. Risk curves or exceedance probability curves are a pivotal tool to describe the probability that various levels of flood loss will be exceeded. Usually flood risk analyses resort to the probability of flood peak discharges as a proxy for the probability of damage by applying methods of extreme value statistics to a sample of observed or modelled extremes (Gumbel, 2013; Embrechts et al., 1997).

In practice, loss estimates are usually available only for a few flood scenarios with certain exceedance probabilities, and thus provide discrete approximations of the flood risk curve (Apel et al., 2004; P. Ward et al., 2011). The integral of the risk curve corresponds to the expectation of the damage (ED) and is widely used as a metric for flood risk (B. Merz, 2006; B. Merz et al., 2009). However, aggregating risk to ED as a single number is controversial (Kaplan and Garrick, 1981; Haines, 1998) because this number is sensitive to the number, space and range sampled from the risk curve (B. Merz et al., 2009; P. Ward et al., 2011). Instead, the characteristics of the complete risk curve along the whole range from high to low probability events and associated uncertainty are important to understand the performance and complexity of the flood risk system under study (B. Merz and Thieken, 2009; B. Merz et al., 2015). For frequent (high probability) events it is important to know the threshold for the occurrence of loss. For low probability events as for instance overload events which go beyond the design level of flood defence schemes or failure scenarios and the resulting consequences need to be included in the analysis of flood risk. Therefore, an understanding of flood controls and system behaviour is needed providing insights into flood triggers, formation and dynamics of flood hazard and impacts.

Flood risk assessment incorporates risk estimates into decision making. It strives to optimally balance benefits in terms of avoided loss, gains from utilizing flood prone areas, and costs for the implementation and maintenance of mitigation measures. Cost-benefit analysis, multi-criteria analysis, and robust decision making have been put forward to provide clear and transparent decision frameworks required for efficient flood risk management (Cardona et al., 2012; Kreibich et al., 2014a). One important step in applying these methods is to comprehensively consider and weigh the social, economic and environmental dimensions of floods including direct and indirect forms of damage as well as their tangible and intangible effects (Messner et al., 2006). While ED is conveniently used to quantify economic efficiency of risk mitigation options in cost-benefit analysis,

intangible consequences cannot be taken into consideration in a straightforward manner (Nachtnebel, 2007; Kind et al., 2017; Hudson et al., 2019). Further, as ED multiplies the consequences of each scenario with its probability, in this calculation low probability high-impact events commensurate with high probability low-impact events (Haimes, 1998). This property represents a risk-neutral perspective, but neglects the actual risk perception of people and institutions affected which often implies a stronger aversion to low probability high-impact events (B. Merz et al., 2009; Kind et al., 2017). Multi-criteria analysis explicitly evaluates multiple conflicting criteria in decision making, and thus expands the number of factors taken into account. It enables risk managers to account for the various demands of multiple stakeholders and interests but there is a trade-off between comprehensive lists of criteria, clarity and direction in the assessment procedure (Renn, 2008).

Facing dynamics in risk, socio-economic developments, system modifications or changes in boundary conditions will continuously modify the basis for rational decisions. As such changes in future flood risk can hardly be predicted, robustness, expected regret and real options analysis have been proposed for designing risk management strategies under uncertainty (Hallegatte, 2009; Rosner et al., 2014; Mens and Klijn, 2015; Kind et al., 2017). Moreover, the assessment of risk confronts uncertainties regarding incomplete and inaccurate data, small sample sizes, imperfect models and unknown social preferences (Apel et al., 2004; B. Merz and Thieken, 2005; Bubeck et al., 2012; W. J. W. Botzen et al., 2013). Hence, flood risk assessment needs insights into flood risk processes, flood impacts and vulnerability to improve flood risk modelling. To gain more knowledge comprehensive investigations of flood events and the exploration of additional data sources are possible avenues (IRDR, 2011; Schröter et al., 2018b).

Building upon the knowledge and outcomes of risk analysis and assessment, *risk mitigation* involves the selection, planning and implementation of risk reduction strategies as well as the maintenance of existing measures before, their operation during, and their revision after flood events (Schanze, 2006). Risk mitigation embarks on a holistic and catchment oriented perspective with a diversified inventory of interventions regarding hazard, vulnerability and exposure. These interventions address all phases of the risk management cycle (DKKV, 2003b; PLANAT, 2004) including preparedness, prevention, response and recovery. The effects of diverse structural and non-structural measures as for instance spatial planning, private precaution, early warning, risk transfer, and emergency management need to be assessed from a catchment perspective taking interactions and feedbacks into account (Bruijn et al., 2017; Vorogushyn et al., 2018).

The performance assessment of combined risk reduction strategies in complex flood risk systems requires sophisticated methods and tools, but practical procedures are, in view of uncertainty and incomplete knowledge, inevitably based on numerous simplifying assumptions (Klemes, 2000; Apel et al., 2009). In this light, as a minimal requirement, robust risk reduction strategies need to ensure that the probability of extreme events and the consequences of flooding are reduced (Klemes, 2000; Nachtnebel, 2007). Confronting these limitations and uncertainties, the overarching goal of flood risk management is shifting from reinforcing the resistance to strengthening the resilience of flood risk systems. While resistance aims to avoid and withstand flood consequences, flood resilience intends to attenuate consequences by absorbing stress and maintaining functioning which is particularly important for overload events exceeding the resistance thresh-

old (Mens et al., 2011; Bruijn et al., 2017). Therefore, an understanding of effects and interactions of interventions within flood risk systems is important. Such knowledge is needed as a basis to represent these effects in flood risk models and tools.

1.3 Challenges in flood risk management

Flood risk management is a dynamic challenge and changes to the components of flood risk are accelerating with increasing frequency of severe weather events, land use change and socio-economic transformations. Facing an increasing trend in flood risk, the sustainable mitigation of flood impacts requires a rigorous implementation of integrated risk management on the foundation of profound knowledge about flood risk systems. This requires an improved understanding of interactions and feedbacks in cause-effect relationships, as well as triggers and controls of flood characteristics and impacts. In this context, in-depth analyses of flood events may give insights into flood risk in all its interlinked dimensions of hazard characteristics, vulnerability and exposure. Along this line, the availability and informative value of data has to be evaluated and novel sources of data need to be explored. For both, event analyses and data sources, there is a need to design coherent frameworks which enables the compilation of consistent datasets and testing their potential usefulness. Data analyses offer insights into flood risk systems and provide the foundation to improve methods for flood risk analysis and assessment. The integration of heterogeneous data sources offers opportunities to advance flood risk modelling including the estimation of impacts and modelling of vulnerability.

1.3.1 Understanding flood risk systems

The idea of a systems approach to flood risk is to widen the scope to a bigger picture in flood risk management (Tobin, 1995) and to account for the complexity of the flood risk system including nonlinearity, interdependencies, and non-stationarity (B. Merz et al., 2015). A generalized fluvial flood risk system comprises a chain of meteorological, hydrological, open channel flow, inundation and damage processes (B. Merz et al., 2006). Flood risk arises from these processes usually triggered by rainfall which forms runoff in the affected catchments depending on climatic, topographic, land cover and soil (moisture) conditions. The catchment runoff then concentrates in creeks and propagates within the river network. Discharges above the bankfull capacity induce inundations and affect exposed elements. While the image of a chain may suggest a sequence of processes, it is important to recognize that these components are interlinked having complex feedback effects which means that one driver may influence different risk components directly or indirectly and may be subject to dynamics which means that certain properties are changing over time (Klijn et al., 2015; Bruijn et al., 2017; Vorogushyn et al., 2018). An intuitive example is the building of dikes along a river reach which reduces the probability of flooding locally but as a downside this intervention may accelerate flood propagation with higher flood peaks and increasing flood hazard downstream (Pinter, 2005). An example for system-inherent dynamics is the changing vulnerability of agricultural crops with seasons: inundations may cause severe losses during the growing season until harvest, but cause no damage or be even beneficial, if following the harvest (Penning-Rowsell et al., 2005; Kuhlmann, 2007). Understanding and capturing the key

elements of such interdependencies and dynamics is crucial and requires a sound system framing. The definition of the system has to carefully determine the important processes and aspects which need to be considered in a certain detail or can be neglected (B. Merz et al., 2014a). Challenges remain regarding the understanding of interactions and feedbacks in cause-effect relationships, as well as dynamic changes, triggers and controls of flood characteristics and impacts.

1.3.2 Analysing flood events and exploring new data sources

The analysis of extreme floods is a powerful vehicle for gaining insights and better understanding of flood risk systems, dynamics, and interactions between hazard, exposure and vulnerability as key metrics of risk (Kreibich et al., 2017b). For flood risk management, event-centered multi-disciplinary investigations offer unique opportunities to learn and revise current strategies (Kreibich and Thieken, 2009; M. Kunz et al., 2013; DKKV, 2015). As extreme flood events are important triggers or accelerators for adaptation or precaution (Bubeck et al., 2012; Kreibich et al., 2017b), monitoring the societal responses to floods is valuable to understand how vulnerability to floods changes over time and how human behaviour dynamics can be integrated in flood risk assessment (Aerts et al., 2018). Importantly, the structured documentation of flood events including the impacts is an important element and a valuable basis for validating and improving risk analyses and risk models (Corbane et al., 2015; De Groeve et al., 2014; Schröter et al., 2018b). In this context, UNISDR (2015) defines monitoring and reporting requirements of disaster events with the aim to build a data basis of damages and people affected. Important tasks include the design and implementation of procedures and standards for data collection. This needs an understanding of which data are available how they can be accessed and what is their completeness and quality.

As data availability is a crucial aspect in flood risk assessment, the increasing volume, variety and velocity of data from a growing diversity of sensors and sources carries great potential, but so are the challenges (Ford et al., 2016). Volunteered Geographic Information (VGI) and citizen science are fast developing fields with promising contributions to keep data up-to-date and enhance monitoring of ongoing floods by complementing traditional data sources and to support flood risk management by providing real-time awareness and feedback during emergency response (Schnebele and Cervone, 2013; Assumpção et al., 2018; Tzavella et al., 2018; Irwin, 2018). These data offer additional levels of detail enabling better insights into the incidents, and interlinks of flood risk processes during extreme events. The challenge here is to explore novel ways of making use of data streams and leveraging the potential of open data sources. The domain of machine learning and data-mining provides efficient algorithms to analyse, integrate and make inferences from heterogeneous data. Applications comprise detection and extraction of relevant data, data integration and fusion from diverse sources (D'Addabbo et al., 2016; Giordan et al., 2018), data analytics regarding dependency relations (K. Vogel et al., 2018) as well as predictive modelling (L. Li et al., 2010; B. Merz et al., 2013). These approaches need to be tested and the usefulness of data has to be thoroughly evaluated.

1.3.3 Modelling flood risk

To provide quantitative estimates of flood risk and assess the benefits and costs of potential mitigation measures, simulation models are indispensable tools (Haimes, 1998). Flood risk models are representations of real systems based on mathematical equations which describe the various processes and aspects of flood hazard, exposure and vulnerability (B. Merz et al., 2006; Falter et al., 2016). In view of limited data available from observations flood risk models are useful tools to extend the range and variation within quantitative risk assessments. These models are increasingly applied for numerous tasks in flood risk management. This includes the evaluation of technical flood defence and alleviation schemes, the comparison of different disaster types, financial appraisal and catastrophe modelling in the insurance industry to quantify probable maximum losses, solvency requirements and premiums (W. Kron, 2005; Surminski and Thielen, 2017), scenario analyses (Hattermann et al., 2014; Felder et al., 2018) as well as risk mapping to increase risk awareness (Schmidt-Thomé et al., 2006; De Moel et al., 2009). Model application scales range from local (Apel et al., 2009) to large-scale/continental (Winsemius et al., 2013; Alfieri et al., 2014), as well as from retrospective (Zischg et al., 2018), to current and anticipatory flood risk estimation (Elmer et al., 2012; Winsemius et al., 2016; Hattermann et al., 2018).

Further, flood risk models are useful for explorative investigations as they create possibilities to gain insights as for instance by investigating the spatial distribution of risk (Falter et al., 2015), or studying the sensitivity of flood risk to changes in different drivers (Elmer et al., 2012; Metin et al., 2018).

However, with an increasing uptake and utilization of these models as well as with nearly realistic visualization of outcomes, discrepancies between expectations and model capabilities are emerging (P. Ward et al., 2015). For the outcomes to be useful, the purpose and limitations of the models must be respected (Klemes, 2000). Hence, uncertainty, reliability and validation of flood risk models are important issues on the agenda of flood risk research (B. Merz et al., 2010b). The advancement and integration of models to represent the different components of flood risk systems is needed to support comprehensive analyses regarding feedbacks, indirect or cascading impacts (Barendrecht et al., 2017; Koks, 2018).

Important challenges to move forward in flood risk modelling are to obtain an improved understanding of the underlying system and processes as well as the provision of high quality and more complete data appropriate to the scale of the analysis. This requires the development and implementation of novel modelling approaches which represent these processes, use these data and quantify the uncertainty associated with model outcomes.

1.3.4 Assessing flood impacts and modelling vulnerability

Societal change and economic development are dominant drivers of the observed increase in flood losses (Barredo, 2009; Paprotny et al., 2018b). With vulnerability having a key role in this development (Bouwer, 2010; Mechler and Bouwer, 2015; Kreibich et al., 2017b), the reduction of vulnerability is an important issue for effective flood risk management (Jongman et al., 2015). Moreover, exposure and vulnerability are sources of large uncertainty in flood risk assessments (Moel and Aerts, 2011; Apel et al., 2009) and

may affect decisions about investments in flood mitigation measures (Wagenaar et al., 2016). In order to reduce the uncertainties surrounding flood risk assessment, vulnerability modelling (as one component of flood risk models) deserves priority in flood risk research. As flood damaging processes are controlled by complex physical and socio-economic processes a deeper understanding of the dimensions of impacts, specific damaging processes, and the role of different factors as well as their interactions is needed to advance flood vulnerability models for loss estimation (Thieken et al., 2005; B. Merz et al., 2010b; B. Merz et al., 2013; K. Vogel et al., 2018). Investigations about vulnerability has expanded over the last decade, still many open questions remain regarding flood damage processes and linkages to flood hazard as well as appropriate implementations in vulnerability models. The majority of model developments focus on direct economic damage mostly to the residential and commercial sector. Approaches to estimate for instance damage to critical infrastructures or indirect impacts barely exist (B. Merz et al., 2010b; Bubeck et al., 2019). Flood vulnerability models require information about hazard (intensity), exposure and vulnerability characteristics (resistance) to provide an estimate of the relative damage or economic loss to the object affected by flooding (Thieken et al., 2005; B. Merz et al., 2010b). Established flood vulnerability models commonly describe complex damage processes using simple deterministic approaches (Meyer et al., 2013), but empirical damage data usually expose large scatter (B. Merz et al., 2004; Thieken et al., 2005). Using inundation depth as sole predictor is usually insufficient to explain this variability (B. Merz et al., 2010b; B. Merz et al., 2013). Additional loss determining variables have been identified including further hazard intensity characteristics like duration, contamination or return period of the event, as well as resistance factors such as precaution, flood warning, awareness (D. Smith, 1994; Penning-Roswell and Green, 2000; Thieken et al., 2005; Kreibich et al., 2010; Elmer et al., 2010). Accordingly, multi-variable models which incorporate additional variables as predictors have been developed (Zhai et al., 2005; Thieken et al., 2008b; Kreibich et al., 2010; Elmer et al., 2010) and have been shown to improve the reliability of flood loss estimates (Apel et al., 2009; B. Merz et al., 2013; Dottori et al., 2016; Sieg et al., 2017). In view of large uncertainties associated with loss estimates, probabilistic modelling approaches are emerging (K. Vogel et al., 2013; Kreibich et al., 2017a; Wagenaar et al., 2017) Challenges in vulnerability modelling are to integrate data into models to better represent flood damaging processes, assess and exploit their predictive value, and to quantify the uncertainty associated with model predictions.

1.4 Objectives and outline

Just as flood risk management is a continuous activity to adjust management strategies, flood risk research is consistently striving for gaining more knowledge (Haimes, 1998). Deepening insights and increasing the understanding of interactions and dynamics of underlying flood risk systems will advance methods and models for improved flood risk management decisions.

This habilitation thesis contributes to these efforts by expanding knowledge about flood hazard, vulnerability and risk derived from the *analyses of flood events*, exploration of *new data sources* and research on *flood risk modelling*. Based on these themes and taking up the research gaps outlined in the previous sections, the thesis investigates the following overarching questions:

- What do we learn by analysing flood events about controls and impacts and how do flood events need to be monitored and documented?
- How can we utilize information available from new data sources in flood risk assessment and modelling?
- How can we incorporate interactions and dynamics in flood risk systems in flood risk modelling and assessment?

The thesis consists of thirteen independent peer reviewed scientific articles (see Table 1.1) which have been published in ISI Journals except for one article which was published in conference proceedings. The author's contributions to these publications are documented in Annex 1.

The research contribution of these papers is grouped in two main parts. The first part deals with flood risk systems. Embedded to this thematic framework, the second part of the thesis focuses on flood vulnerability modelling for loss estimation. The structure of the thesis as a composition of research papers on these two levels is illustrated in Figure 1.1 with a grouping of the papers' contributions to the three overarching themes: *flood event analyses*, *new data sources*, and *flood risk modelling*.

The first part of the thesis, starts with a review of the current approach to flood risk management in Germany and perspectives on the broader context of multi-hazard risk management (Paper 1). Next, a series of three papers deals with event analysis and learning from the large-scale flood in June 2013 in Central Europe. The focus is on the role of hydro-meteorological flood triggers (Paper 2), flood impacts (Paper 3), and the use of social media (VGI) data as a source for rapid flood inundation mapping (Paper 4). The latter two papers also explore the availability and suitability of new data sources. Further three papers cover contributions to the topic of risk modelling by investigating controls on hydrological and loss characteristics of floods (Paper 5), the continuous long-term simulation of flood risk using a coupled model chain to account for system interactions and to derive flood risk directly from loss estimates (Paper 6), and the analysis of temporal dynamics of flood risk systems with regard to seasonal changes in flood risk of agricultural crops in Germany (Paper 7).

The second part provides a review of flood vulnerability models and their characteristics (Paper 8), compares and evaluates the performance of models with different

Table 1.1: List of Papers included in habilitation thesis

Paper	Citation
1	Kreibich, H., Bubeck, P., Kunz, M., Mahlke, H., Parolai, S., Khazai, B., Daniell, J., Lakes, T., Schröter, K. , 2014. A review of multiple natural hazards and risks in Germany. <i>Nat Hazards</i> 126. https://doi.org/10.1007/s11069-014-1265-6
2	Schröter, K. , Kunz, M., Elmer, F., Mühr, B., Merz, B., 2015. What made the June 2013 flood in Germany an exceptional event? A hydro-meteorological evaluation. <i>Hydrol. Earth Syst. Sci.</i> 19, 309327. https://doi.org/10.5194/hess-19-309-2015
3	Thieken, A.H., Bessel, T., Kienzler, S., Kreibich, H., Müller, M., Pisi, S., Schröter, K. , 2016. The flood of June 2013 in Germany: how much do we know about its impacts? <i>Nat. Hazards Earth Syst. Sci.</i> 16, 15191540. https://doi.org/10.5194/nhess-16-1519-2016
4	Fohringer, J., Dransch, D., Kreibich, H., Schröter, K. , 2015. Social media as an information source for rapid flood inundation mapping. <i>Nat. Hazards Earth Syst. Sci.</i> 15, 27252738. https://doi.org/10.5194/nhess-15-2725-2015
5	Nied, M., Schröter, K. , Lüdtke, S., Nguyen, V.D., Merz, B., 2017. What are the hydro-meteorological controls on flood characteristics? <i>Journal of Hydrology</i> 545, 310326. https://doi.org/10.1016/j.jhydrol.2016.12.003
6	Falter, D., Schröter, K. , Dung, N.V., Vorogushyn, S., Kreibich, H., Hundecha, Y., Apel, H., Merz, B., 2015. Spatially coherent flood risk assessment based on long-term continuous simulation with a coupled model chain. <i>Journal of Hydrology</i> 524, 182193. https://doi.org/10.1016/j.jhydrol.2015.02.021
7	Klaus, S., Kreibich, H., Merz, B., Kuhlmann, B., Schröter, K. , 2016. Large-scale, seasonal flood risk analysis for agricultural crops in Germany. <i>Environmental Earth Sciences</i> 75. https://doi.org/10.1007/s12665-016-6096-1
8	Gerl, T., Kreibich, H., Franco, G., Marechal, D., Schröter, K. , 2016. A Review of Flood Loss Models as Basis for Harmonization and Benchmarking. <i>PLOS ONE</i> 11, e0159791. https://doi.org/10.1371/journal.pone.0159791
9	Schröter, K. , Kreibich, H., Vogel, K., Riggelsen, C., Scherbaum, F., Merz, B., 2014. How useful are complex flood damage models? <i>Water Resour. Res.</i> 50, 33783395. https://doi.org/10.1002/2013WR014396
10	Schröter, K. , Lüdtke, S., Vogel, K., Kreibich, H., Merz, B., 2016. Tracing the value of data for flood loss modelling. <i>E3S Web of Conferences</i> 7, 05005. https://doi.org/10.1051/e3sconf/20160705005
11	Schröter, K. , Lüdtke, S., Redweik, R., Meier, J., Bochow, M., Ross, L., Nagel, C., Kreibich, H., 2018. Flood loss estimation using 3D city models and remote sensing data. <i>Environmental Modelling & Software</i> 105, 118131. https://doi.org/10.1016/j.envsoft.2018.03.032
12	Figueiredo, R., Schröter, K. , Weiss-Motz, A., Martina, M.L.V., Kreibich, H., 2018. Multi-model ensembles for assessment of flood losses and associated uncertainty. <i>Nat. Hazards Earth Syst. Sci.</i> 18, 12971314. https://doi.org/10.5194/nhess-18-1297-2018
13	Kreibich, H., Botto, A., Merz, B., Schröter, K. , 2017. Probabilistic, Multivariable Flood Loss Modeling on the Mesoscale with BT-FLEMO. <i>Risk Analysis</i> 37, 774787. https://doi.org/10.1111/risa.12650

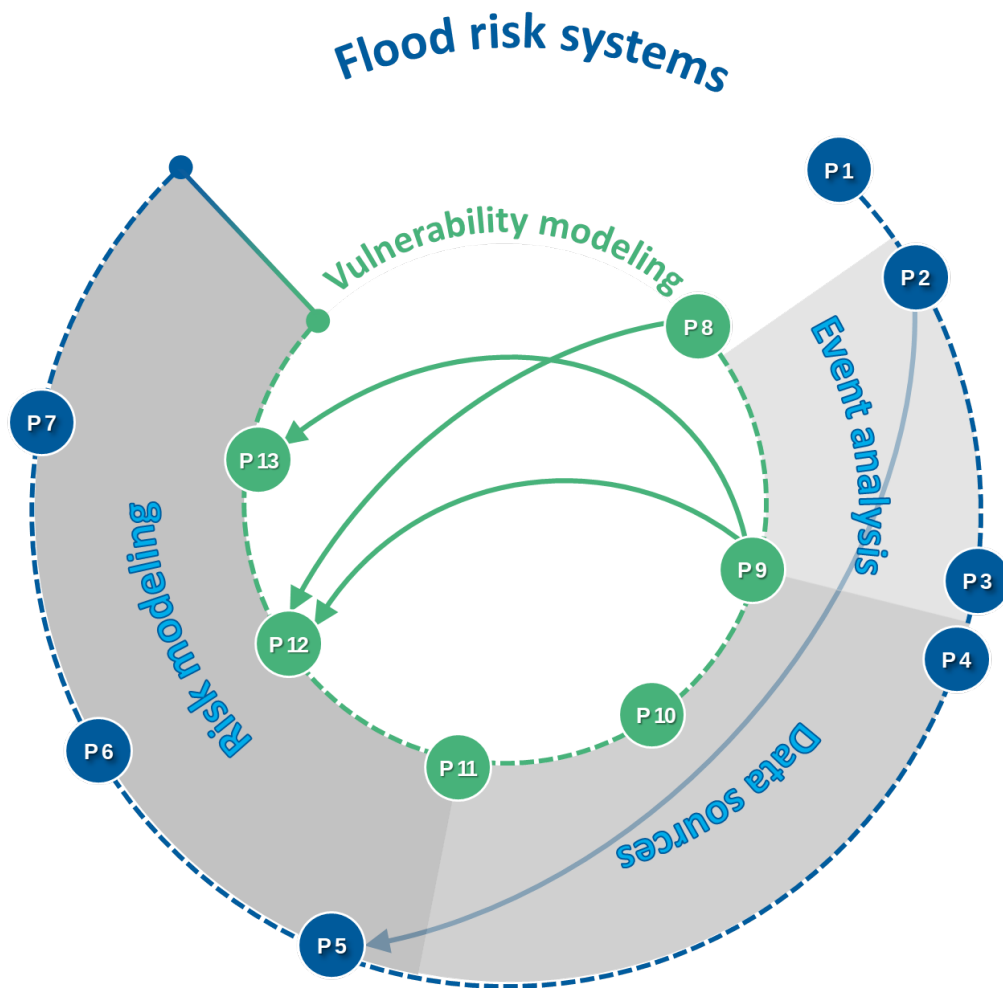


Figure 1.1: Thematic framework, overarching themes and composition of the thesis. Arrows indicate links between papers regarding methods, methodological approaches and interrelated research design

complexity and assesses their predictive performance in spatial transfer contexts by using data from different events and regions for model derivation (Paper 9). It further examines the value of data volume to improve loss model accuracy and reliability (Paper 10), as well as the expediency of open data sources for flood loss modelling (Paper 11). Finally, approaches to frame predictive uncertainty of flood vulnerability models are explored by using multi-model ensembles (Paper 12), ensemble based machine learning algorithms (Paper 13), and probabilistic modelling approaches (Paper 9).

Besides the thematic classification to event analysis, new data sources and risk modelling the contributing papers are interlinked regarding methods and interrelated research design. In this regard, Paper 2 explores the role of flood triggering factors and interactions of flood controls for large scale floods based on observed data, which is then extended and detailed by using a model based approach driven by synthesized data in Paper 5. The information gathered in the flood vulnerability model review in Paper 8 forms the basis for the pre-selection and composition of multi-model ensembles investigated in Paper 12. Papers 9, 12 and 13 are connected regarding the use of machine learning approaches for predictive analytics of flood losses.

Part 1: Flood risk systems

2 | A review of multiple natural hazards and risks in Germany

Manuscript Info

Authors information:

Heidi Kreibich
Philip Bubeck
Michael Kunz
Holger Mahlke
Stefano Parolai
Bijan Khazai
James Daniell
Tobia Lakes
Kai Schröter

Published as:

Kreibich H., Bubeck P.,
Kunz M., Mahlke H.,
Parolai S., Khazai B.,
Daniell J., Lakes T.,
Schröter K.

A review of multiple
natural hazards and
risks in Germany.

Nat. Hazards.

2014;74:2279.

doi:10.1007/s11069-014-1265-

6.

Abstract

Although Germany is not among the most hazard-prone regions of the world; it does experience various natural hazards that have caused considerable economic and human losses in the past. Moreover, risk due to natural hazards is expected to increase in several regions of Germany if efficient risk management is not able to accommodate global changes. The most important natural hazards, in terms of past human and economic damage they caused, are storms, floods, extreme temperatures and earthquakes. They all show a pronounced spatial and temporal variability. In the present article, a review of these natural hazards, associated risks and their management in Germany is provided. This review reveals that event and risk analyses, as well as risk management, predominantly focus on one single hazard, generally not considering the cascading and conjoint effects in a full multi-hazard and risks approach. However, risk management would need integrated multi-risk analyses to identify, understand, quantify and compare different natural hazards and their impacts, as well as their interactions.

2.1 Introduction

While Germany is not among the most hazard-prone regions of the world, similarly to many other countries world-wide, it experiences various natural hazards that cause considerable economic and human losses. (B. Merz and Emmermann, 2006) and list seventeen natural hazards with relevance for Germany, including for example, lightning, hail, torrential rain, and even hazards with extra-terrestrial causes like magnetic storms and meteorite impacts. Although there are no active volcanoes in Germany, there is still the possibility of future eruptions in the Eifel Volcanic Field, where several large eruptions had taken place during Middle and Late Pleistocene (Sirocko et al., 2013). Additionally, also hazards generated outside of the German territory, might have impacts on the society and economy in Germany. Examples are the Eyjafjallajökull eruption in 2010 which led to a shutdown of the European air traffic for several days directly damaging many airlines including e.g. the German Lufthansa; or the Thailand flood in 2011 which shut down scores of factories, damaging global car manufacturing and electronics industries. However, the most important natural hazards in terms of their historic impacts in Germany are summer and winter storms, floods, extreme temperatures and earthquakes (DAT, 2006). They all are characterized by pronounced spatial and temporal variability from small, local-scale events to country-wide events and durations from seconds up to months. Germany was particularly affected by hydro-meteorological hazards, while geo-hazards made up less than 10% of the damaging natural hazard events in Germany during recent decades (Munich Re, 2009). This is especially relevant given the predicted increase in hydro-meteorological hazards due to climate change in many parts of Europe (Watkiss et al., 2005). Furthermore, projections from global and regional climate models suggest an increase in the frequency, duration and intensity of extreme weather situations inducing heat waves in Germany over the next decades, e.g. (Fischer and Schär, 2009; Gosling et al., 2009; Meehl and Tebaldi, 2004). The potential for natural hazards to cause damage not only depends on the magnitude and frequency of the hazard, but also on how vulnerable an exposed community or critical infrastructure is to such hazards. Thus, due to the high population density and economic values exposed in Germany, e.g. (Kleist et al., 2006), many natural hazards are also damaging events (Munich Re, 2009). Facing challenges such as demographic change with increasing numbers of elderly and a less mobile population, as well as ongoing land use change with urbanization and soil sealing, damage due to natural hazards is expected to increase in Germany in the future (Barredo, 2007; Barredo, 2010).

To significantly mitigate risks due to natural hazards, an efficient, science-based integrated risk management scheme is necessary. Widely-used is the concept of the risk management cycle, which integrates all aspects of risk reduction and response, e.g. (DKKV, 2003b; PLANAT, 2004). This means, for instance, that reconstruction after a disaster already has to contain the foundations for improved preparedness for a possible natural hazard event in the future. The risk management cycle describes the consecutive phases that a society undergoes after it has been struck by a disaster: 1 emergency response during or immediately after a hazardous event; 2 recovery and reconstruction; 3 event and risk analysis; and 4 preparedness to reduce the risk (Figure 2.1). In case a society had already been affected by extreme events and/or is aware of the risks it might undertake preparedness measures, which consist of preventive, precautionary and preparative mea-

asures. Prevention aims to avoid damage primarily by appropriate land-use or structural measures, preparation tries to manage and cope with the catastrophe and precaution wants to mitigate damage mainly due to private risk reduction (Kreibich et al., 2005). Private precautionary measures include building precautionary actions such as improving the building structure to withstand a hazard; or preparative measures like collecting information and developing emergency plans; or risk precaution like signing an elementary insurance (DKKV, 2003b). Before, during and shortly after an event emergency measures are undertaken to further mitigate losses. The type and effectiveness of the response depends on the quality of preparedness. The resulting damage is influenced by the hazard characteristics, but also by the resistance or vulnerability of the exposed area, which might have been influenced by precautionary and emergency measures. For instance, (Thieken et al., 2005) suggests that the amount of flood damage is determined by impact parameters (hazard characteristics at the affected site, e.g. water depth) and resistance parameters (characteristics of the affected object, e.g. building type). During recovery one tries to repair the damage and to regain the same (or even a better) standard as before the event happened as quickly as possible. If societies are willing to learn from disasters, they invest in event and risk analyses as basis for risk reduction. Precautionary measures can often be implemented without large additional effort when extensive reconstruction needs to be undertaken anyhow. To assure efficiency, risk management strategies need to be developed on basis of comprehensive risk analyses integrated in decision-support frameworks, such as cost-benefit analysis, multi-criteria analysis or robust decision making (Kreibich et al., 2014a). In Germany, several risk analyses have been undertaken over various spatial scales for different regions, e.g. (Apel et al., 2009; Vorogushyn et al., 2012; Tyagunov et al., 2006; Heneka et al., 2006). These studies have predominantly focused on the risk analysis of only one hazard. In fact, only a few multi-risk assessments are available for Germany, e.g. (Grünthal et al., 2006)).

The new strategy for civil protection in Germany (BBK, 2010) follows an integrated risk management approach and demands amongst others comprehensive, comparable and standardised hazard and vulnerability assessments. Furthermore, the Environmental Impact Assessment and Strategic Environmental Assessment directives (EC, 2001; EC, 2011a; EC, 2014) can be seen as procedural platforms for integrated multi-hazard risk assessments. For instance, the shift towards integrated flood risk management policies can be observed in the European Flood Directive on the assessment and management of flood risks (EC, 2007b). The Flood Directive demands the development of management plans for areas with significant flood risk, which will be integrated in the long term with the river basin management plans of the Water Framework Directive (EC, 2000) contributing to integrated water management on the scale of river catchments.

The objective of this paper is to provide a review of the most important natural hazards, their consequences and risk management strategies in Germany. Knowledge gaps, i.e. research needs, particularly for multi hazard approaches are identified and some conclusions for an improved risk management are drawn.



Figure 2.1: The risk management cycle (adapted from (DKKV, 2003b; PLANAT, 2004))

2.2 Historic damage from natural hazards

In recent decades, Germany has been hit by various extreme natural hazard events. The international disaster database (DAT, 2006) lists 85 events, namely storms, floods, extreme temperatures, earthquakes, wet mass movements, and wildfires between 1950 and 2013. All together, these events have caused more than 10.000 fatalities and nearly 30 b EUR damage in Germany (Figure 2.2). Flood events hold the highest share of economic damage with about 50% of losses. The frequently occurring storm events hold the second highest share of economic damage with about 45%, and with about 7% the second highest share of fatalities (Figure 2.2). However, it needs to be noted, that storm surges, which are multi-hazard events composed of storms and coastal flooding are classified as 'storm' in the EM-DAT database (DAT, 2006). These include the extreme storm surge in the North Sea in 1962, which caused more than 300 fatalities in the city of Hamburg (Storch and Woth, 2008) and the storm surge caused by storm "Capella" in 1976 with 82 fatalities. Earthquakes are typically low probability, high impact events in Germany, and have caused relatively minor damage in recent decades (Figure 2.2). However, even for only a moderate magnitude earthquake, the total losses can be considerable due to the large number of people and the high value of the exposed assets in the densely populated and seismically active Rhine rift valley. Studies have shown that paleoseismologically constrained earthquakes with a magnitude (M_w) up to 6.7 (Camelbeek et al., 2000a) could produce losses of the order of tens of bs of euro (Grünthal et al., 2006).

The single event with the highest human loss was the heat wave in 2003 with more than 9.000 fatalities and EUR 1204 M damage (Table 2.1). The storm surge of 16–17th of February 1962 at the North Sea caused 347 fatalities and damage of EUR 438 M due

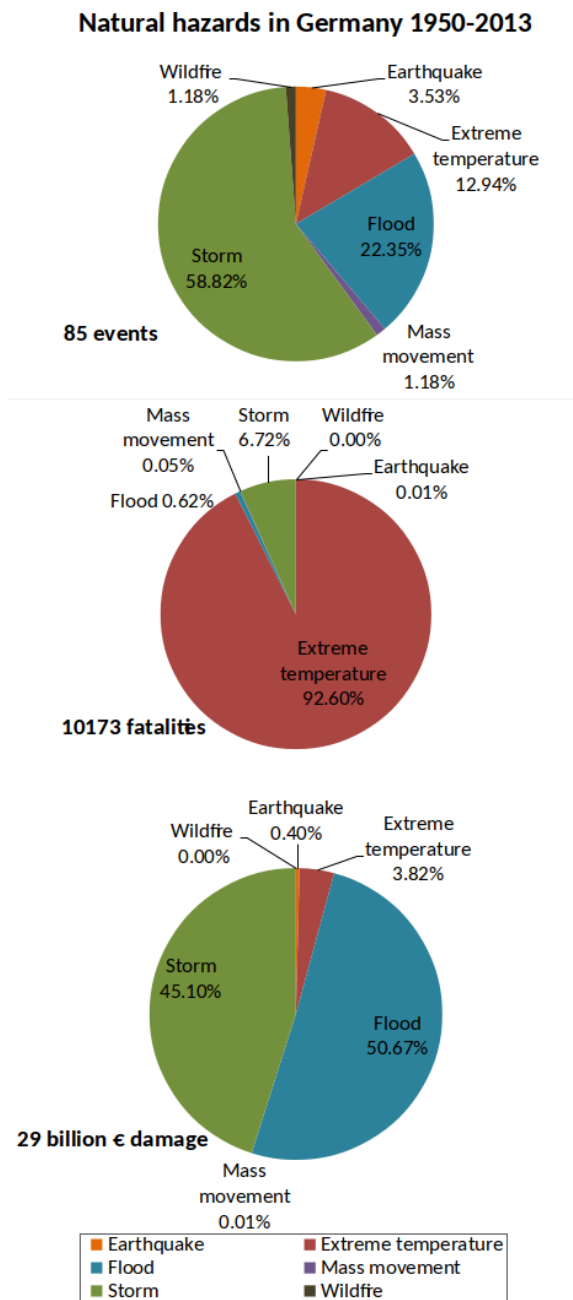


Figure 2.2: Distribution of the different natural hazards that caused fatalities and economic damage between 1950 and 2013 in Germany. Damage given in USD in EM-DAT are converted into EUR using the exchange rate of 1.37 as at December 2013 (DAT, 2006)

Table 2.1: Most severe events with respect to fatalities and economic loss in Germany between 1950 and 2013 according to (DAT, 2006)

Disaster	Date	Location	Fatalities	Est. damage [million *]
Events most severe in respect to fatalities				
Heat wave	Aug-03	Germany (western Europe)	9355	1204
Storm (surge)#	Feb-62	North Sea, Lower-Saxony, Schleswig-Holstein, particularly Hamburg	347	438
(Storm surge and) storm Capella#	Jan-76	Federal Republic of Germany, North Sea, particularly Hamburg	82	949
Events most severe in respect to economic damage				
Flood	May/June 2013	Elbe, Danube, Rhine and Weser catchments, particularly Saxony-Anhalt, Saxony and Bavaria	4	9416
Flood	Aug-02	Elbe and Danube catchments, particularly Saxony	27	8467
Storm Kyrill	Jan-07	Germany	11	4014

Events are classified as storm in EM-DAT. * All damage estimates refer to the year of the event, i.e. the original damage values, not inflation-adjusted. Damage given in USD are converted into EUR using the exchange rate of EUR 1 = USD 1.37 as of December 2013.

to a combination of storm and flood impact (Table 2.1). The events that caused the highest economic damage were the floods in May/June 2013 and August 2002 causing EUR 9.4 b and EUR 8.5 b damage, respectively, according to (DAT, 2006); Table 2.1). However, damage information is uncertain, e.g. estimates of total economic damage for the 2013 flood for Germany range between EUR 8.7 and EUR 12 b (Bundesregierung, 2013; Ratings, 2013; GDV, 2014; B. Merz et al., 2014b). And the 2002 flood damage was estimated at EUR 11.8 b by (W. Kron, 2004). Various flood types concurred during these events, partly one type triggering another. This was particularly obvious in 2002 in the city of Dresden, which was hit by four different flood types: (a) due to torrential rain, streams caused inundation on 12 August 2002; (b) the Elbe tributaries Weißeritz and Lockwitzbach brought flash floods from the Ore Mountains on 13 August 2002; (c) the Elbe River flooded more than 9.3 km² in the city on 17 August 2002; (d) finally, these extreme fluvial floods have triggered groundwater flooding which stayed for many months (Kreibich et al., 2005; Kreibich and Thielen, 2008). The most severe winter storm was Kyrill on 18 January 2007 with total losses of over EUR4 b ((Munich Re, 2012; DAT, 2006) Table 2.1). The most expensive hailstorm occurred on 28 July 2013 and caused EUR 3.5 b of damage (EM-DAT 2014). The cold wave of 1996/1997 resulted in 45 fatalities and EUR 240 M damage (Munich Re, 2012). The most significant earthquake in recent history was the Albstadt 1978 (MI 5.7, Mw 5.1) earthquake which damaged around 9000 structures and caused about EUR 63 M total insured losses.

As far as the accuracy and reliability of damage data are concerned, it must be noted that

the estimated damage arising from natural hazards are generally associated with high uncertainties due to the following reasons: there is a lack of standardized, consistent event documentation concerning damage. For example, depending on the severity of the event and on the loss compensation, flood damage is recorded by different organizations differently according to their own needs (R. Merz and Blöschl, 2008; B. Merz et al., 2012). Furthermore, event definition and categorisation are not trivial. Some of the damage data differ from source to source due to different allocation to a particular hazard, event or region (Handmer et al., 2005; W. Kron et al., 2012).

Many natural events are multi-hazard events which manifest in various perils. For instance, storms are not only associated with high wind speeds, but may also cause storm surges, torrential rain, hail, pluvial or flash floods (W. Kron et al., 2012; Gall et al., 2009) provide a good summary of the problems associated with damage databases of natural hazards. Thus, greater efforts to collect damage data from natural hazards according to standardized methods need to be taken, e.g. (Ramirez et al., 1988; Yeo, 2002; Changnon, 2003; Handmer et al., 2005)).

2.3 Distribution and characteristics of natural hazards in Germany

Natural hazards occur over different spatial and temporal scales. The duration of events differs significantly ranging from seconds to several months. Short events lasting only seconds to minutes are lightning, hail, tornados, mass movements like landslides, earthquakes and meteorite impacts (Bittner et al., 2009; Dotzek, 2000). Other events like torrential rain, flash floods, winter storms, wild fires, and floods last longer, i.e., from a few hours to several days. Particularly long events with durations from several days to a few months are cold and heat waves (Table 2.2). Small, local-scale events which affect an area up to 10 km² are, for example, torrential rain, flash floods, tornadoes, lightning and hail, as well as mass movements like landslides (Bittner et al., 2009). Fluvial floods and storm surges are regional events affecting coast lines or river valleys up to several 100 kilometres. In the same spatial category are earthquakes, volcanic eruptions and magnetic storms (B. Merz and Emmermann, 2006). Germany-wide events, i.e., events affecting an area of more than 500 km² are hazards like winter storms with wind fields up to 1000 km and track lengths up to 5000 km, as well as cold and heat waves (Table 2.2).

2.3.1 Storms: Winter storms and convective storms

Storms are transient disturbances of the mean atmospheric state, comprising different weather systems. For instance, storm cyclones have typical length scales of 1000 km, with convective storms or hailstorms having spatial extents of several kilometres to more than 100 km. Whereas storm cyclones, often referred to as winter storms, usually develop in a region of high baroclinity (high horizontal temperature gradient) over the North Atlantic Ocean in the winter half-year (October to March), short-lived severe convective storms are the result of thermal instability and large-scale lifting processes and, thus, are usually confined to the summer half-year (May to September). Despite their different characteristics, both weather systems can be associated with extreme winds, heavy

Table 2.2: Spatial-temporal characteristics of important natural hazards in Germany (adapted from (B. Merz and Emmermann, 2006; Bittner et al., 2009))

Natural hazards	Hazard prone region in Germany	Spatial scale	Temporal scale	Forecasting
Winter storms	Germany wide, particularly in the west	Width of the wind field up to > 1000 km; track length up to 5000 km	Few hours to few days; Clusters: several days	Possible
Hail	Germany wide, particularly in the south	Width of the hail streaks: several 100 m to some 10 km; length: some km to > 300 km	Minutes to few hours (depend on the track length)	Hardly possible (only forecast on the hail potential)
Tornados	Germany wide, particularly in lowlands in northwest Germany	Diameter: several meters to 500 m; track length: 10 km to > 100 km	Few seconds to over an hour, on average less than 10 minutes	Hardly possible (only forecast on the tornado potential)
Fluvial floods	Germany wide in river valleys	Several 10 km to several 100 km	Few hours to several days	Possible
Storm surges	North Sea coast, weaker also Baltic Sea coast	Several 100 km	Few hours to few days	Possible
Cold / heat waves	Germany wide, heat waves particularly in urban settings	Up to several 1000 km	Few days to few months	Possible
Earthquakes	Rhine rift valley and Vogtland area	Up to 100 km	Few minutes; after shocks: several days	Not possible

precipitation, and, in case of organized convective systems, significant hail. Therefore, it is common practice in the insurance industry to combine both perils into one category "storm".

Winter storms

Severe winter storms occur infrequently over Europe and Germany. According to the comprehensive study of Barredo (2010), 54 damaging winter storms (i.e., just over 1 per year) were registered in Central Europe between 1970 and 2008. The occurrence probability shows high annual and decadal variability, including considerable temporal clustering (Vitolo et al., 2009), which give rise to storm series such as those in 1990 (storms Daria, Herta, Vivian, Wiebke) or 1999 (Anatol, Lothar, Martin). Since European winter storms that affect Germany develop almost exclusively over the Atlantic Ocean, their frequency and intensity on the large scale decrease from north-to-south and west-to-east (see Figure 2.3a). On the local scale, the wind field is modified by the terrain's roughness and by orographic features, which lead to flow deflections and enhanced vertical exchange of horizontal momentum. The storm hazard map in Figure 2.3a (Heneka et al., 2006; Hofherr and Kunz, 2010) reveals considerable small-scale variations in the gust speeds, that are more or less directly connected to terrain variations.

The overall damage caused by winter storms is determined by impact parameters determined by the storm field (i.e., maximum wind speed and spatial extent), influenced by topography as well as by resistance parameters including structural and societal factors. Even if winter storms persist over several hours or even days, the duration of the storm is of minor importance (Pinto, 2012). Furthermore, the responsible factor for the damage is not the mean wind speed, but rather the gusts, which are short-term increases in the speed with durations of the order of seconds. The ratio between gusts and mean wind depends primarily on atmospheric stability and terrain's roughness (Brasseur, 2001) and usually lies between 1.8 and 2 during storms (Wieringa, 1986). Wind loads and damage are proportional to the third power of maximum wind speed, that is, the advection of kinetic energy (Klawns and Ulbrich, 2003). However, for specific events, in particular the 1990 storm series, higher order exponents between 4 and 5 were found empirically to better describe economic loss (Munich Re, 1993). Typical damage related to storms' wind speeds are defects on roofs, shingles, vinyl sidings, gutters, and - indirectly - to cars due to falling roof material, trees, branches, and other objects flown through the air. Extensive damage to power lines due to fallen trees may result in power outages for up to several days, potentially over large areas. Fatalities and personal injuries due to winter storm events occur rarely, and when they do occur, they are mostly due to indirect impacts, for example accidental deaths in automobiles due to traffic accidents or during clean-up efforts by forestry workers.

To estimate the damage potential of most severe storms, both the maximum gusts and the spatial extent of the storm field must be considered. For example, while the record gust speeds of storm Lothar (e.g. 259 km h⁻¹ at Wendelstein) were restricted to a comparatively small area, the storm field of Kyrill stretched over most parts of Germany. Thus, a storm with extreme gusts comparable to those from Lothar with the spatial extent of Kyrill would cause total economic damage far beyond the losses experienced up to now. However, the relation between spatial extent and storm intensity, including a definition of upper bounds, is still an open question.

Severe convective storms

In contrast to large-scale winter storms, severe thunderstorms possibly associated with extreme wind speeds, heavy precipitation and hail, are high-frequency perils. The

number of thunderstorm days in Germany range between 10 to 40 days per year. These storms usually have a limited extent and duration, causing a high spatial and temporal variability in the probability of occurrence and intensity. In cases of strong upper tropospheric forcing, however, organized convective storm events may also persist over several hours, affecting meso-scale regions larger than 500 km². Because thunderstorms are related to convective energy (Kunz 2007), their overall probability in Germany increases from north to south as shown by the lightning density presented in Figure 2.3b. Superimposed on this overall trend are local-scale variations with several hot spots, for example, in the regions south of Stuttgart and Munich. As shown by (Brombach, 2012; M. Kunz and M. Puskeiler, 2010) for damage causing hailstorms, it is probably the flow around the low mountain ranges that creates areas of flow convergence downstream, which in turn trigger or intensify convective storms in those regions.

Most of the damage caused by severe thunderstorms results from large hail. The most expensive hailstorm in history was the Reutlinger event on 28 July 2013 with an estimated insured loss of EUR 1.9 b (preliminary estimate of WGV; not considered in Table 2.1). In the federal state of Baden-Württemberg, for example, damage-causing hail occurs on up to 40 days per year. Due to a strong increase in the number of hail days in this area, almost 40% of all damage to buildings caused by natural hazards can be attributed to large hail (1986-2008; (M. Kunz and M. Puskeiler, 2010). The local-scale characteristics of hail and a lack of operational observation systems make statistical analyses on their probability and spatial variability very difficult. The main variables responsible for the impact of hail on vulnerable structures are the sizes of the hailstones, their number density, the footprint of damaging hail and the horizontal wind (Schuster et al., 2006). Most important is the number of large hailstones ($D > 5$ cm) rather than that of smaller ones. In addition to the vertical fall velocity, convective gusts further increase the hail kinetic energy up to a factor of five (Changnon, 1970) and shift the fall direction with the consequence that vertically-oriented surfaces, such as building shells, may also be affected. Damage to buildings, in particular roofing tiles, claddings, shutters and blinds, occurs for hail sizes in excess of 2 cm; for crops and other agricultural products, the limit is around 0.8 cm.

The largest hailstone that has been found so far in Germany had a maximum diameter of 14.1 cm (6 Aug. 2013, Undingen) according to the European Severe Weather Database (ESWD). This size may be considered as an upper limit for European hailstorms since no substantially larger hailstones have been recorded till now. The damage potential of severe hailstorms can be estimated from the few severe hail tracks with lengths of more than 300 km, yielding losses of up to EUR 3.1 b (Munich Re, 1999).

2.3.2 Inland and coastal floods

Floods are recurring natural phenomena which involve a temporary rise in the water level of a surface water body. Hence, floods can be broadly defined “as the temporary covering by water of land that is usually not covered with water” (EC, 2007b). In Germany, inland, pluvial and fluvial floods are caused by extraordinary rainfall events, sometimes in combination with snow melt. At the North Sea and Baltic coasts, storm surges pose the greatest potential flood hazard.

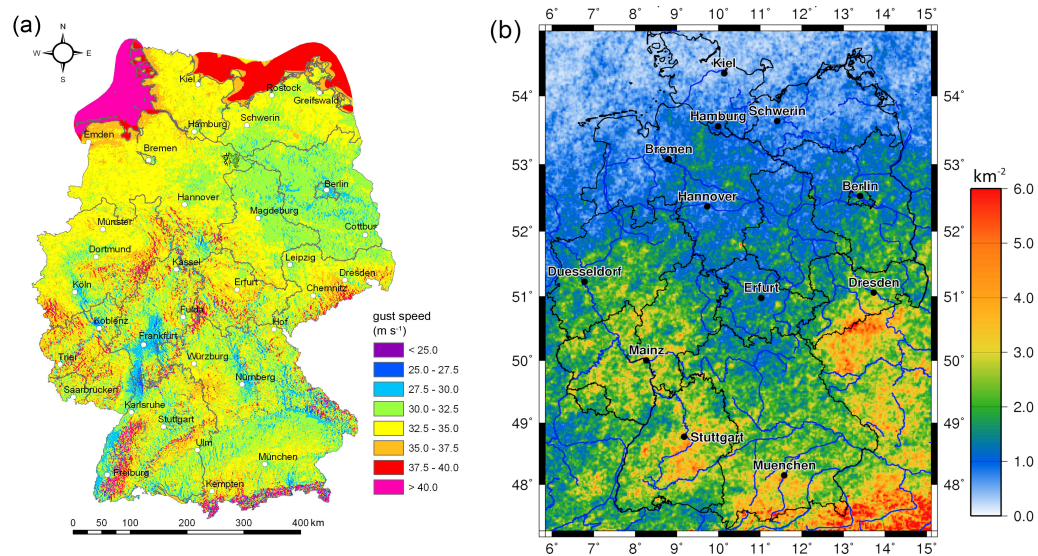


Figure 2.3: a: Maximum gust wind speeds in Germany on a $1 \times 1 \text{ km}^2$ grid for a 10-year return period according to model simulations and observations (1971-2000) obtained during the CEDIM www.cedim.de project “Risk Map Germany” (Hofherr and Kunz, 2010); b: lightning density in Germany obtained from the Siemens Network BLIDS 2000-2009 (Damian, 2011).

Inland floods

Pluvial floods are caused usually by high-intensity or prolonged rainfall periods. The flooding emerges from overland flow or ponding of water before it enters a drainage system or a water course. Pluvial floods are most often rather localised phenomena that may occur anywhere in Germany. However, flat regions and regions with a tendency for severe convective storms are more prone. Fluvial floods occur when discharges exceed the conveyance capacity and consequently overtop the river banks. These types of floods can be generally classified as those caused by either long persisting rain, short intense rain on saturated soils, local extreme rainfall in the course of thunderstorms, snowmelt or a combination of rainfall and snowmelt (R. Merz and Blöschl, 2003). The formation and development of fluvial floods is related to hydro-meteorological conditions as well as catchment conditions and characteristics. Basically, the flood regimes are subject to the geographical situation, the topographic relief and the hydro-morphologic structures. (Beurton and Thieken, 2009; Petrow and B. Merz, 2009; Petrow et al., 2009; Uhlemann et al., 2010) have carried out a comprehensive analysis of discharge observations in Germany. According to their findings, there are essentially three regions showing pronounced differences concerning the seasonal occurrence of floods. The western region (mainly the Rhine and Weser catchment areas) is dominated by winter flood events, which are triggered by westerly cyclonic systems that are sometimes combined with sudden warming, causing intense snowmelt or ice flow. These winter floods are characterised by a large spatial extend and rather long durations of 10 to 15 days on average

and up to two months in extreme cases (Uhlemann et al., 2010; Prudhomme et al., 2012). The eastern region (Elbe and Oder catchments) shows a considerable amount of comparable winter floods, but in addition, a notable fraction of summer and spring floods. The southern region (Danube catchment) shows a multimodal distribution of floods throughout the year. There are marked frequencies of floods both during the period of snow melt and in the summer months. In summer, southwest cyclonic patterns can possibly entail the occurrence of heavy convective rainfall causing local and flash flood events (Gaume et al., 2009). These summer flood events sometimes give rise to particularly high discharges. However, their spatial extent is usually limited to a few gauges or sub-catchments, respectively.

The amount of flood damage is determined by flood impact and resistance parameters (Thielen et al., 2005). Impact parameters reflect the flood characteristics at the affected site, such as water depth, flow velocity, duration of inundation, sediment concentration or contamination of flood water, e.g. (Penning-Rowsell and Green, 2000; Förster et al., 2008; Kreibich and Thielen, 2009; Kreibich et al., 2010)).

Resistance parameters depend on the affected object, such as the building type, applied precautionary measures, early warning and emergency measures, e.g. (D. Smith, 1994; Wind et al., 1999; Kreibich et al., 2005; Kreibich et al., 2007; Kreibich and Thielen, 2009). The importance of these parameters depends on the type of the flood, e.g., flow velocity is particularly important during flash floods and for damage to traffic infrastructure, whereas flood duration is particularly important for damage to agricultural crops (Förster et al., 2008; Tapia-Silva et al., 2011; Kreibich and Thielen, 2008; Kreibich et al., 2009). An overview about damage influencing factors considered in different flood damage assessments is provided by (B. Merz et al., 2010b).

Storm Surges

Storm surges are defined as abnormal and sudden rises of sea levels resulting from the combined effect of low atmospheric pressure and strong onshore winds (Danard et al., 2003). The severity of the emerging storm surge depends on the fetch, the wind velocity, the duration of the storm and the water depth (Woth et al., 2006; Malcharek, 2010). Ultimately, critical water levels develop from the superposition of storm surges with high tides, spring tides or external surges. In the North Sea and Baltic Sea regions, storms occur mainly during winter. This is related to the more pronounced temperature differences between the polar and sub-tropical masses of air, which induce the pressure gradient that causes the wind.

The atmospheric situations and local settings involved in the formation of storm surges and the occurrence of high water levels are quite different at the North Sea and Baltic coasts. In the North Sea region, storms develop from cyclones moving along the northern North Sea. These cyclones cause winds from westerly directions and induce storm surges at the German North Sea coast. Petersen and Rohde (1991) distinguish three different types of meteorological situations. This includes the Jutland, the Scandinavian and the Skagerrag types. The storms of the Jutland type are of rather short duration and mainly affect the coast of Schleswig-Holstein. The cyclones of the Scandinavian type sometimes remain quite stationary, causing persistent storms for several days from a north-westerly direction, affecting the German North Sea Coast. Storms

induced by cyclones of the Skagerrag type affect the entire coastline of the North Sea region (Malcharek, 2010).

Storm surges at the German Baltic Sea coast mainly occur from a meteorological situation with a strong high pressure area situated above Scandinavia, and with a cyclone simultaneously situated above central Europe extending as far as the coast of the Baltic countries. This setting brings about a strong pressure gradient inducing winds from the east. In addition to the meteorological conditions, the filling of the Baltic Sea basin, seiches, tides, as well as the local situation are crucial for the development of a storm surge (Graewe and Burchard, 2012; Mudersbach and J. Jensen, 2010) The filling of the Baltic Sea Basin, which is reflected in the current mean water level, as well as a swashing effect towards the southern and western parts of the coast which is induced by changes in the direction of the wind from west to east, contributes strongly to extreme water levels. Seiches as a sort of natural oscillation as well as tides are of a minor order of magnitude, but will also contribute to extreme water levels. Small water depths and the lateral extent of bights within the coastline give rise to locally diverse occurrences of extreme water levels (Graewe and Burchard, 2012).

Storm surges show several distinct characteristics that distinguish the relevant damaging processes from the ones occurring during fluvial flooding. Higher waves and flow velocities can cause considerably higher damages (Kelman, 2002) and salt water may lead to different damage compared to sweet water. According to (Nadal et al., 2010) only highly engineered, massive structural elements are capable of withstanding breaking wave forces. However, even though coastal floods show these different characteristics, basically the same approaches, e.g. depth-damage functions, are commonly used for damage assessment as for fluvial flooding, e.g. (Kok et al., 2005; Penning-Rowsell et al., 2005; Vanneuville et al., 2006).

2.3.3 Extreme temperature

Extreme temperature events are of high importance in Germany, encompassing heat waves as well as cold waves, e.g. (Kuttler, 2011). Both types of events are normally measured relative to the usual weather in the area and relative to normal temperatures for the season. There is no universal definition of a heat wave, i.e., an extreme event associated with particularly hot sustained temperatures leading to notable impacts on human health, economies, and ecosystems (Meehl and Tebaldi, 2004). For Germany, a heat wave is frequently defined by at least 5-7 days in a row with a daily temperature maximum of at least 30 degrees. A cold wave on the other hand is characterised by a rapid decrease in temperature within 24 hours to temperatures requiring substantially increased protection to agriculture, industry, commerce, and social activities (AMS, 2013). While there is no distinct definition on the duration of a cold wave it is generally understood to vary from a few days to several weeks. Moreover, studies have found that also the point in time when temperature extremes occur affects the risk: Extreme heat and cold were both found to be particularly hazardous at the beginning of the summer and winter season, respectively (Barnett et al., 2012). Extreme temperatures and especially heat stress events are particularly prevalent in urbanized areas because of the specifics of the urban climate and the associated urban heat island effect that exacerbate high temperatures (Gabriel and Endlicher, 2011). Within Germany, a regional concentration of high temperatures

can be allocated in the south-west (BMU, 2009).

Adverse impacts of extreme temperature events on human health have been identified in several studies and particularly urban heat stress has been linked to mortality, morbidity, as well as a reduced quality of life (Lagadec, 2004; Gabriel and Endlicher, 2011; Gosling et al., 2009) Heat waves may also cause crop failures and power outages due to increased electricity consumption by air conditioning. They may lead to cascading events like wildfires and droughts. Also, cold waves are associated with mortality, particularly when taking into account after effects like flu or pneumonia (Barnett et al., 2012). Additionally, cold waves can cause death and injury to livestock and wildlife as well as damage to buildings and infrastructure (e.g. bursting of water pipelines, material damage).

2.3.4 Earthquakes

While seismic activity in Germany is low, it is not negligible. In fact, a large part of the country lies within shallow-earthquake prone zones, as also indicated in the recently published European-Mediterranean Earthquake Catalogue (EMEC) (Grünthal and Wahlström, 2012).

In particular, it is noticeable that while the eastern Mediterranean is the most seismically active region in Europe, Germany is affected by some of the highest seismic activity north of the Alps. Most of the seismicity occurs in the Rhine rift valley, extending from Basel into the Benelux countries and, in particular, in the area around Cologne. Earthquakes occurring mainly as swarms also affect the Vogtland area. The strongest documented event occurred near Basel in 1356 ($M_w=6.2-6.6$, $I=IX$), with the epicentre just south of the current German border. Recent paleoseismic studies, e.g. (Camelbeeck and Meghraoui, 1998; Camelbeeck et al., 2000b; Vanneste et al., 2001) have found evidence of pre-historic earthquakes with $M_w=6.7$ in the Lower Rhine Embayment.

The seismic hazard map given in the DIN4149 shows expected macro seismic intensities with return period of 475 years (this threshold is based on the standard seismic hazard calculation of 10% probability of exceedance of a certain intensity level in 50 years). Although this map is likely to depict also where most of the largest seismic events are possibly occurring in Germany (along the Rhein Graben and the Vogtland area), seismic events might also occur outside of these area, where damages can therefore be significant due to the existence of old, non-renovated masonry structures that are not seismically resistant. Currently, the highest risk to earthquakes can be found in Baden-Württemberg, North Rhine-Westphalia and Thuringia. Very long return period earthquakes (>1000 years) with high magnitudes such as M_6+ earthquakes near the highly populated areas of Cologne/Ruhr region and Frankfurt meanwhile have a loss potential exceeding tens of bs of Euros (Allmann et al., 1998; Daniell, 2010).

2.4 Risk analyses and management

For an efficient and successful mitigation of risk, the creation of a culture of risk prevention has been called for within the last few decades. Such a culture should be based on a comprehensive analysis of the risk and an appraisal of potential risk-reducing measures. A key element is an open dialogue about risk and risk-reducing options, integrating all

stakeholders (DKKV, 2003a; B. Merz and Emmermann, 2006). Thus, one needs to involve different levels of decision-making in a federal country such as Germany, where risk management strategies are developed on country-, state- and municipal levels as well as the different sectors of governance, businesses and civil society in general. Integrated risk management should be a quasi-continuous, iterative process which should be closely linked to risk analyses and costing of natural hazards (Kreibich et al., 2014a). Thus, the two main elements of risk management - risk reduction via precautionary measures and well-coordinated disaster response - must be included in the risk management cycle (Figure 2.1; e.g. (Silver, 2001; DKKV, 2003a). Additionally, Kreibich et al. (2014a) propose an integrated cost assessment in risk management which is represented by the new cost assessment cycle. This involves the continuous monitoring of all costs associated with natural hazards risk management, comprising damage and risk mitigation costs. For systematically estimating damage, comprehensive risk analyses need to be undertaken considering all relevant hazards and their interaction, all affected sectors and damage categories (i.e. direct, business interruption, indirect, intangible damage). Such an integrated, comprehensive costing enables the early detection of inefficient risk management strategies and supports improved decision making for more efficient risk management (Kreibich et al., 2014a).

Risk Analyses

In Germany, several risk analyses which consist of assessments of hazard, exposure and vulnerability, have been undertaken on different spatial scales for different regions and hazards. In the natural sciences context, hazard is commonly characterised by the exceedance probability of potentially damaging events and their intensities. Exposure is characterised by the number or the value of elements at risk and their characteristics. Vulnerability analysis investigates how and to which extent the affected elements will be damaged. Kaplan and Garrick (1981) propose that for any risk analysis, the following three questions need to be answered: a) What can happen?; b) How likely is it that it will happen?; and c) If it does happen, what are the consequences?

To answer question a) in the context of a natural hazard risk analyses, it is necessary to identify and take into account all relevant natural hazards in the study area (Greiving and Fleischhauer, 2006; Kappes et al., 2012). Which hazards are relevant depends on the specific setting of the respective area and the objective of the study. The European Commission (EC, 2011b) proposes a set of criteria for the determination of significant hazards at national level in their guidelines for risk assessment and mapping. To answer question b) comparable hazard assessments focusing on the probability of occurrence of potentially damaging natural events for all identified hazards and their interactions need to be undertaken. To answer question c) the same coherent exposure data base of elements at risk needs to be used for all risk analyses in the multi-risk framework to enable a consistent comparison of risks from different hazards (Grünthal et al., 2006). On this basis, vulnerability assessments and damage estimations need to be undertaken for all hazard scenarios.

However, in practise, only a few studies take into account multiple hazards or even share the aim of taking into account all relevant hazards in the study area. This is especially true for scientific studies and is among multiple reasons probably due to the separation of disciplines with all the consequences for differing terminology, definitions,

approaches, etc. (WMO, 1999; Kappes et al., 2012). To be able to compare different natural hazard risk analyses, the following characteristics need to be the same for all analyses:

- Analyses need to be undertaken in the same study area, at the same spatial scales and with the same level of detail, i.e. basis and level of aggregation need to be the same, for instance, damage may be aggregated per municipality per year
- The same types of consequences need to be estimated, e.g. direct monetary damage to residential building, business disruption losses, casualties, affected population, etc.
- Representation of damage needs to be the same, e.g. absolute damage in monetary values, relative damage in percentage, damage per inhabitants, etc.
- Risk analyses need to be undertaken on basis of the same exposure data base.
- To compare the outcomes of the risk analyses, the estimated risk indicators need to be the same, e.g. risk curves, expected annual damage, etc.

An additional, advantage are comparable methods for probability assessment, e.g. the use of upper bounds.

Some examples of risk analyses undertaken in Germany are provided in the following. The hazard of severe winter storms is usually assessed by applying extreme value statistics to observations, model data, or a combination of both, e.g. (Kasperski, 2002; Pinto et al., 2007; Della-Marta et al., 2009; Hofherr and Kunz, 2010; Heneka and T. Hofherr, 2011). Because of the limited spatial extent of hailstorms and the lack of direct monitoring systems for hail, comprehensive and long-term statistics on hail are not available for Germany. The few available studies that estimate hail hazard or hail risk are based on proxies (i.e. indirect climate data) from remote sensing instruments such as radar (Zimmerli, 2005; Puskeiler, 2013) or satellite (Bedka, 2011; Punge et al., 2014)

Examples for flood risk analyses on various spatial scales are available. For instance, (Kreibich et al., 2011b) undertook a groundwater flood risk analysis focused on residential buildings for the city of Dresden (Figure 2.4). Groundwater flooding is often a cascading event triggered by fluvial floods which was the case in the city of Dresden during and after the extreme flood event in the Elbe catchment in August 2002 (Kreibich and Thielen, 2008). Other local flood risk analyses for single cities have been undertaken for instance by (B. Merz and Thielen, 2009; Apel et al., 2009). The ICPR Rhine-Atlas provides a catchment-wide estimated maximum damage potential (ICPR, 2001), while (Linde et al., 2011) estimate possible changes in future flood risk along the river Rhine. (Apel et al., 2006; Vorogushyn et al., 2012) undertook probabilistic flood risk assessments along the Rhine and Elbe rivers, respectively. Falter et al. (2014) presented a proof-of-concept exercise for large-scale flood risk assessments with the RFM-Regional Flood Model, which was applied to one of the largest catchments in Germany, the Elbe. However, so far no consistent flood risk analysis for the whole of Germany is available.

Two distinct approaches for heat wave risk analyses are common. First, spatially explicit analyses of vulnerability and risk are undertaken which target area-wide vulnerability indicators for different sectors using medium- to small-scale datasets, such as surface temperature, amount of green space in combination with aggregated socioeconomic

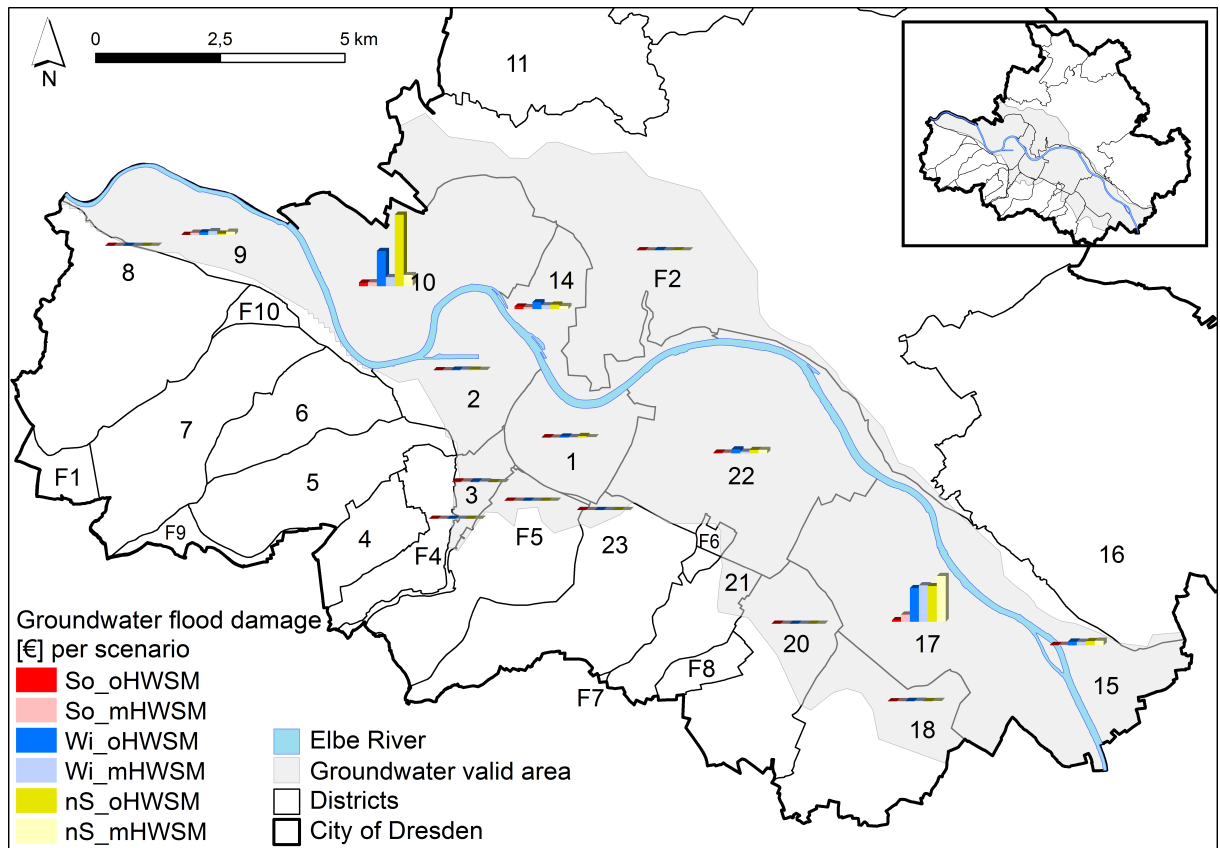


Figure 2.4: Groundwater flood damage to residential buildings in Dresden estimated on basis of different groundwater flood scenarios (adapted from (Kreibich et al., 2011b))

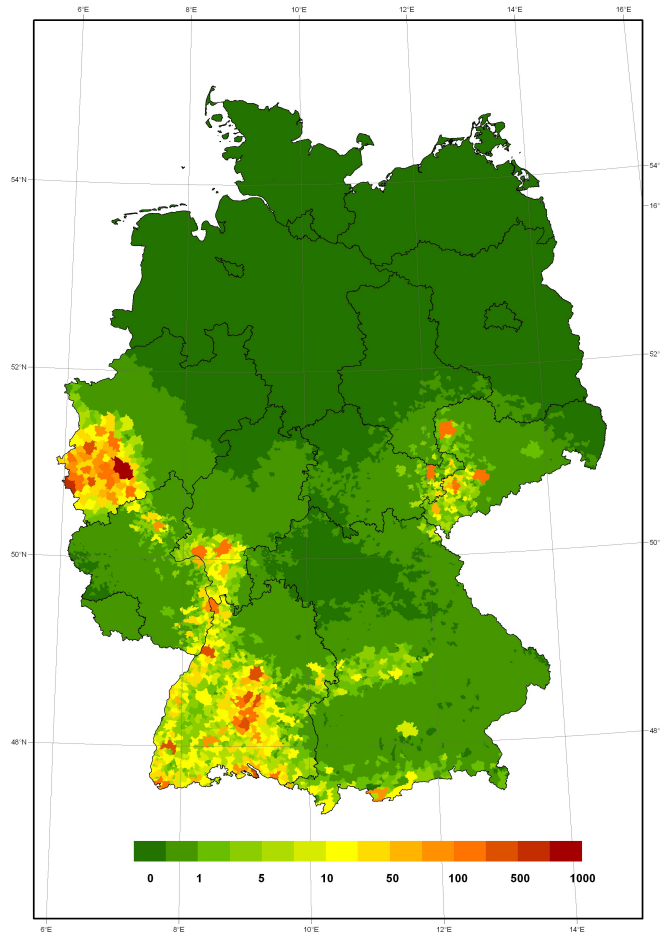


Figure 2.5: Estimated seismic risk [millions of Euro] in communities of Germany for an exceedance probability of 10% in 50 years (adapted from (Tyagunov et al., 2006))

datasets such as age or population density (Kropp et al., 2006). Second, individual-level vulnerability and risk analyses are undertaken that aim for a better understanding of underlying socio-economic influences on behaviour-driven exposure and adaptation capacities, e.g. (Leichenko, 2011; Harlan and Ruddell, 2011),

The spatial distribution of seismic hazard in terms of macroseismic intensities for an exceedance probability of 10% in 50 years outlines the main earthquake hazard zones (Grünthal et al., 1998). One quarter of the total area of Germany, containing about one third of the population, belongs to zones where the level of expected macroseismic intensity with a probability of exceedance of 10% in 50 years is equal or greater than VI, which might result in slight damage to normal buildings (Tyagunov et al., 2006); Figure 2.5. In some areas, e.g., south of Stuttgart and between Aachen and Cologne, the estimated macroseismic intensities are up to VIII-IX. For this reason, as well as for its economical importance, studies on seismic hazard in Germany have focused on the Cologne area, including efforts to account for site specific response, e.g. (Parolai et al., 2007).

These analyses have all focused on only one hazard and do not take into account that different hazard types independently, or triggering each other and causing cascading

effects, also affect many regions and societal groups. Only a few multi-risk assessments are available for Germany or Europe (Kappes et al., 2012). For example, (Grünthal et al., 2006) present a quantitative single-type multi-risk assessment for the city of Cologne, Germany. The natural hazards windstorm, flooding and earthquake were compared by risk curves showing the exceedance probability of the estimated economic losses in Euro. A common economic assessment of exposed assets was developed to compare the three hazard types on a consistent basis, but interrelations between the hazards were not considered. A novel multi-risk assessment, considering conjoint events of earthquakes damaging flood defences, for the city of Cologne is undertaken in the framework of the MATRIX project, with a specific focus on uncertainties ¹. (Schmidt-Thomé et al., 2006) show European flood and earthquake hazard maps as well as the resulting risk profiles resulting from a combination of hazard potential and vulnerability. A few multi-risk tools are available, and might be transferable to the German context. For example, the GIS based tool Hazus-MH can assess four types of hazards, namely floods, hurricanes, coastal surges, and earthquakes (Banks et al., 2014; Remo and Pinter, 2012). It includes hazard, exposure and susceptibility analyses and calculates direct economic damage, structural damage etc. Although Hazus was developed for the USA, its tools have been applied in other countries as well, e.g. in Bucharest, Romania (Lang et al., 2012) or in Ottawa, Canada (Ploeger et al., 2010). Another example is CAPRA, which is an open source platform for probabilistic risk analysis and decision making. Hazard assessments are combined with exposure and vulnerability assessments, allowing risk analyses of conjoint or cascade events on an inter-related multi-hazard basis, including earthquakes, tsunamis, cyclones, floods, landslides and volcanic hazards (<http://www.ecapra.org>; (Dyke et al., 2011). However, to the authors knowledge no attempt of their application to the German context was done yet. Thus, despite several published frameworks and approaches for multi-risk analyses, e.g. (Bovolo et al., 2009; Marzocchi et al., 2012; Schmidt et al., 2011), multi-risk assessments, including hazard interaction, are missing in Germany.

Risk Management

Integrated risk management should aim to mitigate risks from all relevant natural hazards. It considers preventive, precautionary and preparative measures. Prevention aims to avoid hazard, e.g. floods by appropriate land-use planning or structural measures like dykes or retention basins. Precaution sets out to mitigate damage mainly by private measures, sometimes enforced by laws or regulations. Preparation tries to manage and cope with the catastrophe. For an effective response forecast and early warning play an important role. Apart from technical aspects, risk reduction also requires effective communication with the aim of improving risk awareness since undertaking appropriate and effective measures demands often self-dependent actions by the potentially affected population. The composition of different management measures which shall form an efficient risk management strategy depends on the relevant hazards and other physical and socio-economic characteristics Table 2.3

Spatial planning can play an important role in the management of risks, and due to the spatial perspective requires a multi-hazard approach that considers all relevant

¹<http://matrix.gpi.kit.edu/>

Table 2.3: Indication of relevant risk management measures for storms, floods, extreme temperatures and earthquakes in Germany (++ = very relevant; + = relevant; (+) = partly relevant; - = not relevant/not applicable)

Actors	Measures	Storms	Floods	Extreme temp.	Earthquakes
Spatial planning	keeping hazard prone areas free of further development	-	++	-	(+)
	allocation of structural measures, e.g. dykes	-	-	++	-
	precautionary land use, e.g. supporting natural water retention, designing fresh air corridors in cities	-	+	++	+
Sectoral planning	Structural measures, e.g. dykes	+	++	-	-
	Increase risk awareness	+	+	++	++
Building regulation	Hazard adapted building construction, building precaution	++	+	++	++
Private households / companies	Private precaution including building precaution	+	+	++	++
	Preparative measures, e.g. emergency plans and exercises	(+)	+	+	++
	Risk precaution, e.g. signing an elementary insurance contract	++	+	-	+
Emergency response	Early warning systems	++	++	++	++

hazards threatening a certain area as well as the vulnerability of this area (Greiving and Fleischhauer, 2006). Spatial planning decides how certain spaces will be used; therefore, it influences vulnerability where natural hazards are apparent. Thus, the formulation of guidelines for harmonizing a successful planning process and a set of methodologies seems to be more promising than the formulation of general measures that should fit all hazards (Greiving and Fleischhauer, 2006). For instance, spatial planning aims to reduce exposure to floods but it is also an important means of mitigating heat waves in cities, e.g. via (re-)design of city quarters with respect to optimising micro- and local-scale climates (Kuttler, 2011) Besides, spatial planning may increase natural flood retention, and as such decreases flood hazard.

Structural and non-structural flood protection measures are the prevalent approach to prevent flood damage. The standard of structural fluvial flood protection e.g. via dykes varies considerably and ranges from 1/10 years at some parts of the Elbe River (IKSE, 2003) and 1/30 years e.g. at the city of Neu-Ulm at the Danube, to 1/1000 years along the upper Rhine (ICPR, 2001; Linde et al., 2011). Standards along the coast are based on a 100 year event and on historical extreme events and thus are in practice often higher than the 100 year design criteria (Safecoast, 2008).

Precautionary measures aiming to mitigate damage due to extreme wind speeds include, for example, changes in tree species, or deforestations in the vicinity of traffic networks. The German building code regulates the adaption of buildings and constructions to the current expected extreme wind characteristics (DIN, 2005), e.g. via the reinforcement of roof structures. However, convective gusts related to severe thunderstorms and hail risk have not been considered in the building code until now. The seismic resistant building codes only refer to multi-story buildings and have to be considered in relation to the location and year of construction of the building stock. They were first put in place in 1957 (DIN, 1981) with 2 unenforced zones), with revisions in 1972 (Baden-Württemberg) before enforcement in 1981 through the DIN4149 code. An East German code in 1988 (StBA) was then incorporated into DIN4149 in 1992 following reunification. A revision to DIN4149 in 2005 for all of Germany was also in line with Eurocode standards. Flood precautionary measures, for instance building retrofitting or flood-proofing of oil tanks, to be undertaken by flood-endangered residents and companies, are enforced by law (German Water Act to Improve Preventive Flood, 2005 (Deutscher Bundestag, 2010) , water laws of the federal states, e.g. Bayerisches Wassergesetz - BayWG (Staatskanzlei, 2010).

An important part of preparative measures are early warning systems. Early warning of extreme hydro-meteorological events is provided by authorities via public broadcasting, telecommunication and the internet, e.g. weather warnings² as well as heat wave warnings³ by the German weather service DWD. Flood early warning is provided by the flood centres of the federal states⁴. It is obvious that if authorities, as well as the warned population and companies, know what to do and act efficiently, they can significantly mitigate negative health effects as well as economic damage via emergency preparedness measures. In case of heat waves, efficient reaction is supported, for example, by the improvement of public health responses, access to air conditioning, safety nets in the form of social networks (Wilhelmi and Hayden, 2010). Other emergency measures

²<http://www.wettergefahren.de>

³<http://www.dwd.de/hitzewarnung>

⁴<http://www.hochwasserzentralen.info>

include, for instance, closing doors and windows or raising blinds before a storm event or safeguarding objects by moving them to flood safe areas or by using water barriers to prevent the water from entering buildings before floods, e.g. (Kreibich et al., 2007)).

Building insurance commonly covers fire and domestic water damage as well as damage due to storm and hail events. Thus, storm and hail risks to residential buildings and companies are commonly insured in Germany. Most insurance companies offer an optional supplement insurance covering other elementary risks like earthquake, flood, snow loading, and landslides. Not being covered by insurance up to now are heat-induced damages. Flood insurance coverage for companies and households is offered in areas with medium to low flood risk (Thieken et al., 2006b). These areas are identified via the zoning system 'ZÜRS' developed by the German Insurance Association GDV, which is based on flood maps in order to distinguish areas with a different flood probability (GDV, 2008; De Moel et al., 2009). The average market penetration of flood insurance is between 3% and 4% for building insurance, and 10% for household contents insurance (GDV, 2003; Landtag Rheinland-Pfalz, 2005; Bogenrieder, 2004). However, elementary insurance penetration is highly variable in different regions in Germany. The federal state of Baden-Württemberg, for example, has a very high density of insurance (up to 95%) for damage to buildings from natural disasters, as a result of the mandatory disaster insurance, which was extended to earthquakes in 1971, but was mandatory only until 1994. However, most house owners have not altered their contracts. The eastern German states also used to have a high density of multi-peril cover (including earthquakes and floods), but upon reunification the former State insurer was placed in the hands of the free market, which agreed to carry over only flood coverage (Schwarze and Wagner, 2007).

2.5 Conclusions

In this work a review of the most important natural hazards, their consequences and risk management strategies in Germany is presented. Germany experiences various natural hazards that have caused considerable economic and human losses in the past. In this respect, the most important natural hazards are storms (winter and summer), floods, extreme temperatures and earthquakes. The various natural hazards occur over different spatial and temporal scales and have different characteristics, which need to be taken into account for risk analyses and management strategies. Different hazards occur in the same regions and are partly interacting and triggering each other. An example is the storm surge in 1962, which was composed of storm and coastal flooding causing more than 300 fatalities in the city of Hamburg. However, risk analyses are usually carried out separately for the various pertinent hazards in a region, making it very difficult (or impossible) to compare different natural hazard risks and thus to prioritise, for instance, risk reduction investments. To assess the full spectrum of possible risks, comprehensive, harmonised and site-specific multi-risk assessments are needed. So far, risk management approaches for the different hazards in Germany are rather inconsistent and separate from each other. More comprehensive approaches for risk analyses and management are therefore necessary to enable the identification and utilisation of synergies. Particularly, spatial planning could play an important role due to its comprehensive, multi-sectoral

nature. For instance, the reduction of heat-stress and flood risk using water sensitive urban design provides an opportunity to integratively address both hazards.

3 | What made the June Flood 2013 in Germany an exceptional event? A hydro-meteorological evaluation

Manuscript Info

Authors information:

Kai Schröter
Michael Kunz
Florian Elmer
Bernhard Mühr
Bruno Merz

Published as:

Schröter K. , Kunz M.,
Elmer F., Mühr B.,
Merz B.
What made the June 2013
flood in Germany an
exceptional event?
A hydro-meteorological
evaluation.
Hydrol. Earth Syst. Sci.
2015;19,1:309-327.
doi:10.5194/hess-19-309-2015.

Abstract

The summer flood 2013 sets a new record for large-scale floods in Germany for at least the last sixty years. In this paper we analyze the key hydro-meteorological factors using extreme value statistics as well as aggregated severity indices. For the long-term classification of the recent flood we draw comparisons to a set of past large-scale flood events in Germany, notably the high impact summer floods from August 2002 and July 1954. Our analysis shows that the combination of extreme initial wetness at the national scale - caused by a pronounced precipitation anomaly in the month of May 2013 - and strong, but not extraordinary event precipitation were the key drivers for this exceptional flood event. This provides additional insights into the importance of catchment wetness for high return period floods on a large-scale. The data base compiled and the methodological developments provide a consistent framework for the rapid evaluation of future floods.

3.1 Introduction

In June 2013, wide parts of Central Europe were hit by largescale flooding. Particularly southern and eastern Germany were affected, but also other countries such as Austria, Switzerland, the Czech Republic, Poland, Hungary, Slovakia, Croatia and Serbia. Almost all main river systems in Germany showed high water levels: the Elbe between Coswig and Lenzen, the Saale downstream of Halle, and the Danube at Passau experienced new record water levels. Severe flooding occurred especially along the Danube and Elbe Rivers, as well as along the Elbe tributaries Mulde and Saale. In the Weser and Rhine catchments exceptional flood magnitudes were, however, observed only locally in some smaller tributaries. The area affected most in the Rhine catchment was the Neckar with its tributaries Eyach and Starzel. In the Weser catchment the Werra sub-catchment was affected most, in particular the discharges in the Hasel and Schmalkalde tributaries were on an exceptional flood level (BfG, 2013). As a consequence of major dike breaches at the Danube in Fischerdorf near Deggendorf, at the confluence of the Saale and Elbe Rivers at Rosenberg, and at the Elbe near Fischbeck, large areas were inundated with strong impacts on society in terms of direct damage and interruption of transportation systems (see Figure 3.14 at the end of the chapter for geographic locations).

Estimates on overall losses caused by the flooding in Central Europe are in the range of EUR 11.4 b (Munich Re, 2013) to EUR 13.5 b (Swiss Re, 2013), whereof EUR 10 b occurred in Germany alone. Official estimates of economic loss for Germany amount to EUR 6.6 b (Bundesregierung, 2013) These numbers are about 60% of the total loss of EUR 14.1 b (normalized to 2013 values) in Germany caused by the extreme summer flood in August 2002 (W. Kron, 2004; Thielen et al., 2005) which remains the most expensive natural hazard experienced in Germany so far.

The June 2013 flood was an extreme event with regard to magnitude and spatial extent as well as its impact on society and economy (Blöschl et al., 2013; B. Merz et al., 2014b). The Forensic Disaster Analysis (FDA) Task Force of the Center for Disaster Management and Risk Reduction Technology (CEDIM) closely monitored the evolution of the flood in June 2013 including the impacts on people, transportation and economy in near real time. In this way CEDIM made science-based facts available for the identification of major event drivers and for disaster mitigation. The first phase of this activity was done by compiling scattered information available from diverse sources including in-situ sensors and remote sensing data, the internet, media and social sensors as well as by applying CEDIM's own rapid assessment tools. Two reports were issued: the first report focused on the meteorological and hydrological conditions including comparisons to major floods from the past (CEDIM, 2013a), while the second one focused on impact and management issues (CEDIM, 2013b).

The subsequent phase of this FDA activity focused on the research question: What made the flood in June 2013 an exceptional event from a hydro-meteorological point of view? This question is analyzed in this paper. We expect this analysis to improve the understanding of key drivers of large-scale floods and thus contribute to the derivation of well-founded and plausible extreme scenarios.

In this context, the statement of BfG (2013) and Blöschl et al. (2013) that high initial soil moisture played an important role for the generation of this extreme flood are an interesting starting point. Klemes (1993) reasoned that high hydrological extremes are

more due to unusual combinations of different hydro-meteorological factors than to unusual magnitudes of the factors themselves. On the one hand, catchment wetness state is an important factor for the generation of floods (R. Merz and Blöschl, 2003). As such it is a useful indicator in flood early warning schemes, e.g. (Van Steenbergen and Willems, 2013; Alfieri et al., 2014; Reager et al., 2014) and is also incorporated in procedures for extreme flood estimation, e.g. (Paquet et al., 2013). On the other hand the contribution of catchment wetness to extreme floods has been shown to be of decreasing importance with increasing return periods of rainfall, e.g. (Ettrick et al., 1987; B. Merz and E. J. Plate, 1997). However, the interaction of various hydro-meteorological factors, primarily rainfall and soil moisture, has been studied mainly for small scale catchments, e.g. (Troch et al., 1994; Perry and Niemann, 2007). Only few studies examined the interplay of various hydro-meteorological factors for large-scale floods. One example is the work of Nied et al. (2013) who investigated the role of antecedent soil moisture for floods in the Elbe catchment (ca. 150,000 km²) and emphasized the increased occurrence probability of large-scale floods related to large-scale high soil moisture.

In this study, we examine key meteorological and hydrological characteristics of the June 2013 flood and compare them to two other large-scale high impact events, the August 2002 and July 1954 floods in Germany. The factors considered are antecedent and event precipitation, initial streamflow conditions in the river network and flood peak discharges. We evaluate these factors in a long-term context in terms of recurrence intervals using extreme value statistics based on a 50 years reference period. For this period the set of large-scale floods in Germany identified by Uhlemann et al. (2010) are updated and now comprises 74 flood events. Hence, the analysis is deliberately limited to the national borders of Germany in order to be able to compare the 2013 flood with the event set of Uhlemann et al. (2010). For a coherent comparison of the events we use available long-term datasets of precipitation and discharge observations. Besides the statistical analysis we derive different indices to rank the spatial extent and magnitude of the hydro-meteorological factors.

The spatial extent and hydrological severity of large-scale floods in Germany has been analyzed by Uhlemann et al. (2010) in terms of flood peak discharges using a specifically developed flood severity index. In our study we enhance this framework to include antecedent and event precipitation as well as initial streamflow as additional hydro-meteorological factors. We introduce severity indices for these factors to evaluate their relative importance among the event set. Precipitation and flood peak discharges are key figures which are commonly used to characterize cause and effect of floods. The antecedent precipitation index is a well-established parameter to approximate catchment wetness (Teng et al., 1993; Ahmed, 1995). Even though there are reasonable objections against API as it disregards soil and land use characteristics which influence soil hydrological processes, it provides sufficient information to compare the potential wetness between different large-scale floods. Initial streamflow is usually not considered in hydrological analyses of flood events but is a very relevant factor for dynamic flood routing processes (Chow, 1959) as it controls the load of a river section. The inclusion of this factor within a statistical analysis of large-scale flood events is, to the knowledge of the authors, done for the first time.

The paper is organized as follows. Section 3.2 describes the data and methods used to conduct the hydro-meteorological analysis of the June 2013 flood and the set of large-

scale flood events. Section 3.3 describes the meteorological situation associated with the flood in June 2013 and presents the results from the analysis of antecedent and event precipitation, initial river flow conditions and flood peak discharges. Detailed comparisons with the extreme summer floods of August 2002 and July 1954 are drawn. This section concludes with a sensitivity analysis of the procedure. In Section 3.4 we discuss the key findings and provide recommendations for future work. A map of geographical locations mentioned in the article can be found at the end of this chapter as well as some additional information regarding sensitivities.

3.2 Data and Methods

3.2.1 Data

Data base of large-scale floods

For the analysis of the meteorological and hydrological conditions prior to and during large-scale flood events in Germany and their relation to the climatological context, a consistent data base of precipitation and discharge data was compiled. For this, we considered a set of large-scale floods which had been first determined in a consistent way by (Uhlemann et al., 2010) for the period from 1952 to 2002. In this study, we used an updated event set from 1960 to 2009. These flood events are identified from daily mean discharge records at 162 gauges in Germany by screening these time series for the occurrence of peak discharges above a 10-year flood and significant flood peaks at other gauges within a defined time window that accounts for the time shift between hydraulically coherent peak flows. According to (Uhlemann et al., 2010), large-scale floods are characterized by a spatial extent of mean annual flooding which affects at least 10% of the river network considered in Germany. Applying this criterion, 74 large-scale floods are identified in the reference period 1960-2009. For each flood we derive consistent samples for hydro-meteorological factors including antecedent and event precipitation, initial streamflow conditions and peak discharges. A compilation of hydro-meteorological factors and related data sources, their spatial and temporal resolution, and the methods applied is presented in Table 3.1.

Meteorological datasets

For the triggering of large-scale floods the amount and spatial variability of precipitation are more important than the small-scale temporal variability. For this reason, we used 24-hour precipitation sums of REGNIE (regionalized precipitation totals) both for the reference period 1960-2009 and for the single events 2013 (April-June) and 1954 (June-July). The data set, compiled and provided by the German Weather Service (Deutscher Wetterdienst, DWD), is interpolated from climatological stations to an equidistant grid of $1 \times 1 \text{ km}^2$. The interpolation routine considers several geographical factors such as altitude, exposition, or slope by distinguishing between background monthly climatological elds and daily anomalies (see Rauthe et al. (2013) for further details). In cases

Table 3.1: Data sources, resolution and analysis methods for hydro-meteorological parameters

Hydro-meteorological factors	Data source	Spatial resolution	Temporal resolution	Analysis/classification
Precipitation	REGNIE DWD ¹⁾	1 sqkm	Daily Event-based	Maximum 3-day totals R3d. extreme value statistics based on annual series Precipitation index for all large-scale floods API quantification 30 days ahead of R3d; extreme value statistics based on partial series conditional on past flood events Wetness index for all past flood events Extreme value statistics based on partial series conditional on past events Initial hydraulic load index for all past flood events Extreme value statistics based on annual maximum series Flood severity index for all past flood events
Initial catchment state	Antecedent precipitation index API Ratio of initial river flow to mean annual flood	REGNIE DWD ¹⁾ Discharge gauges BfG ²⁾ /WSV ³⁾ and hydrometric services of federal states	1 sqkm Point information; 162 gauges and related sub-basins Daily mean Event-based	Daily Event-based Daily mean Event-based
Peak flood discharge	Discharge gauges BfG ²⁾ /WSV ³⁾ and hydrometric services of federal states	Point information; 162 gauges and related sub-basins	Daily mean Event-based	Daily mean Event-based

¹⁾German Weather Service, ²⁾German Federal Institute of Hydrology, ³⁾Water and Shipment Administration

of convective or orographic precipitation, where a very high density of stations is required, it can be expected that REGNIE underestimates the actual spatial variability of precipitation. However, since large-scale flood events are mainly driven by advective precipitation, this effect is of minor importance in the present study. Additionally, weather charts and sounding data are used to describe the characteristics of the atmosphere on the days with maximum rainfall.

Hydrological data sets

We use time series of daily mean discharges from 162 gauging stations operated by the water and shipment administration (WSV), the German Federal Institute of Hydrology (BfG) or by hydrometric services of the federal states. The same selection of gauges has been used by (Uhlemann et al., 2010) to compile the set of large-scale flood events in Germany. These gauges provide continuous records since 1952 and have a drainage area larger than 500 km². Basin areas vary from 521 km² to 159,300 km² with a median of 3,650 km² including a high percentage of nested catchments. For the flood in June 2013 raw data of daily mean discharges were available for 121 gauges mainly covering the central, southern and eastern parts of Germany which have been affected most by flooding.

Based on the procedure proposed by Uhlemann et al. (2010), the point observations of discharge peaks at the 162 gauges are regionalized to represent the flood situation in a particular river stretch and its associated catchment area. The regionalization scheme uses the location of the gauges and the hierarchical Strahler order (Strahler, 1957) which accounts for the branching complexity of the river network. A gauge is assumed as representative for an upstream river reach until the next gauge and/or the Strahler order of the river stretch decreases by two orders. In downstream direction, a gauge is representative until the Strahler order of the river changes by one order or a confluence enters the river which has the same Strahler order or one order smaller. The total length of the river network considered amounts to 13,400 km.

3.2.2 Methods

For the statistical analysis of the hydro-meteorological factors and their consistent comparison within the set of large-scale flood events, a clear event definition including its onset and duration is required. The start of an event determines the point in time for which we evaluate the different hydro-meteorological factors instantaneously (e.g. initial streamflow) forward (event precipitation, peak discharges) and backward in time (antecedent precipitation). Due to temporal dynamics of the precipitation fields across Germany, flood triggering precipitation affects different catchment areas at different days. Therefore, we do not consider a fixed event start date for the whole of Germany, but one that may vary in space and time, that is, from one grid point to another or from one sub-catchment to another, respectively.

Definition of event start dates

We considered two different definitions of the event start date. The first one is related to the onset of the large-scale floods compiled in the event set by Uhlemann et al. (2010).

It considers the flood response in the spatial series of mean daily discharges recorded at 162 gauges in Germany taking significant hydraulically coherent peak flows into account. The second is based on the maximum precipitation that triggers the floods. For this we quantify the highest 3-day precipitation totals (R3d) at each REGNIE grid point within a centered 21-day time window that spans from 10 days ahead to 10 days after the event start of a large-scale flood. The duration of the chosen time window considers the time lag which links flood triggering precipitation with discharge response, e.g. (Duckstein et al., 1993) and the travel times of flood waves along the river-course, e.g. (Uhlemann et al., 2010). Considering the R3d totals excludes local scale convective precipitation, which is relevant for local or flash floods but not for large-scale floods (R. Merz and Blöschl, 2003)

Event precipitation

The first day of the R3d period defines the meteorological event start for a given grid point. Depending on the space-time characteristics of the precipitation fields, these days will be more or less correlated for adjoined grid points. We have performed this analysis for maximum precipitation totals of 3 to 7 days duration and found that this variation does not imply considerable changes in the meteorological event start date. As shown in Figure 3.15 at the end of the chapter the spatial pattern of the 7 day totals do not differ largely from the R3d patterns for the flood events investigated. Therefore we use R3d as a reasonable figure for the meteorological start date of event precipitation.

For the statistical evaluation of event precipitation, annual maximum 3-day precipitation totals are determined for the reference period from 1960 to 2009 and for the two events of 1954 and 2013. Using extreme value statistics return periods are determined for the event-triggering R3d totals independently for each grid point.

Antecedent precipitation

The meteorological event starts (first day of maximum R3d) are used to calculate antecedent precipitation backward in time. We use the antecedent precipitation index (API) according to (Kohler and Linsley, 1951) as a proxy for the wetness conditions in a catchment in the period before the event precipitation. The relation between surface soil-moisture content and different versions of the API was shown, for instance by (Blanchard et al., 1981; Teng et al., 1993). We quantify API over a 30-day period prior to the meteorological event start dates at each grid point for each event of the large-scale flood set. API is given by the sum of daily precipitation weighted with respect to the time span (here: $m = 30$ days) of rainfall occurrence before the reference day:

$$API(x, y) = \sum_{i=1}^{30} k^i R_i(x, y), (m - i) \quad (3.1)$$

where $R_i(x, y)$ is the 24-hr total at a specific grid point (x, y) and i represents the day prior to the 3-day maximum, which ensures that event precipitation and antecedent precipitation are clearly separated. Usually a value between 0.8 and 0.98 is used for the depletion constant k (Viessman and Lewis, 2002). The potentiation of k with the number of days i assigns continuously decreasing weights to rainfall that occurred earlier. This relation approximates the decrease of soil moisture due to evapotranspiration and

percolation to deeper soil layers. In our study we selected a mean value of $k = 0.9$. For the statistical analysis of API and thus the calculation of return periods we use partial series which are derived using the meteorological event start dates identified for the 74 large-scale flood events in the period 1960-2009.

Precipitation and wetness indices

To further evaluate the importance of the hydro-meteorological factors R3d and API and to rank their spatial extent and magnitude for the floods in June 2013, August 2002 and July 1954 among the set of large-scale floods we introduce precipitation and wetness severity indices as aggregated measures:

$$S_X^k = \frac{1}{\Gamma} \sum_{i,j} \left\{ \frac{X_{i,j}^k}{X_{i,j}^{5-yr RP}} \right\} \mid X_{i,j}^k \geq X_{i,j}^{5-yr RP}, \quad (3.2)$$

where X is either R3d or API and $5-yr RP$ denotes the values for a 5-year return period. In this formulation, values of R3d and API, respectively, are considered at REGNIE grid points i, j that exceed the 5-year return values. For each event k the sum of the ratios of R3d and API to the 5-years return period are normalized with the mean area size Γ represented by the total number of REGNIE grid points in Germany.

Initial hydraulic load

To transfer the meteorological event start dates, possibly varying from grid cell to grid cell, to the discharge time series given at gauge locations, we need to spatially integrate and hence to average the event start dates for individual grid points within hydrological sub-basins. We use the sub-catchments of the 162 river gauges as spatial units. The resulting 'areal mean' dates per sub-catchment are used as the event start date for the hydrological analyses.

The streamflow situation at the beginning of the flood event provides information on the initial hydraulic load of the river cross section. An already increased discharge level may considerably strain the discharge capacity of a river section, and thus the superposition of the subsequent flood wave may increase the load on flood protection schemes and may aggravate inundations. For the statistical analysis of the initial streamflow conditions, we normalize the discharge values by calculating the ratio of the daily mean discharge on the event start date (Q_i) and the mean annual flood (MHQ:= mean of annual maximum discharges) for each of the $n = 162$ gauges. For each gauge a partial series is created by evaluating the ratio of Q_i and MHQ for the areal mean event start dates in the corresponding sub-catchment which are derived using the meteorological event start dates identified for the 74 large-scale flood events in the period 1960-2009.

Further, we introduce an initial load severity index representing the spatially weighted sum of the initial hydraulic load level in the river network for each event k :

$$S_{Q_i}^k = \sum_n \left\{ \lambda_n \times \left(\frac{Q_i}{MHQ} \right)_n \right\} \mid \left(\frac{Q_i}{MHQ} \right)_n \geq \left(\frac{Q_i}{MHQ} \right)_n^{5-yr RP} \quad (3.3)$$

where $5-yr RP$ denotes the flow ratio with a 5-year return period and the weights λ_n

correspond to the ratio of the river stretch length (l_n) associated with a certain gauge and the total length of the river network: $\lambda_n = \frac{l_n}{\sum_n l_n}$.

Peak discharge

Peak discharge (Q_p) is a key figure to characterize the magnitude of a flood at a specific location. Q_p is the integrated outcome of hydrological and hydraulic processes upstream of that location and provides important information for numerous water resources management issues in particular flood estimation and flood design. For the statistical evaluation of the observed flood peaks at each of the 162 gauges we use the annual maximum series (AMS) of daily mean discharges. We evaluate the spatial flood extent and magnitude using an aggregated measure of event severity. For this purpose we calculate the length of the river network L for which during event k the peak discharge Q_p exceeds the 5-year return period:

$$L^k = \sum_n \{ \lambda_n \times 100 \} \mid Q_p^k \geq Q_p^{5-yr RP} \quad (3.4)$$

where 5-yr RP denotes the discharge with a 5-year return period and the weights λ_n are defined as explained above. The flood severity index represents a weighted sum of peak discharges Q_p normalized by a 5-year flood using n as weights:

$$S_{Q_p}^k = \sum_n \left\{ \lambda_n \times \frac{Q_p^k}{Q_p^{5-yr RP}} \right\} \mid Q_p^k \geq Q_p^{5-yr RP} \quad (3.5)$$

Extreme value statistics

To calculate exceedance probabilities and return periods (T_n) for the various hydro-meteorological factors, i.e. R3d, API, Qi/MHQ and Q_p , observed for the June 2013, August 2002 and July 1954 floods, we applied the classical generalized extreme value distribution (Embrechts et al., 1997). Most appropriate and widely used in the case of precipitation is the Fisher-Tippett type I extreme value distribution, also known as Gumbel distribution, with a cumulative distribution function (CDF) of:

$$F(x) = \exp \left[-\exp \left(-\frac{x - \beta}{\alpha} \right) \right] \quad (3.6)$$

where α is the scale parameter affecting the extension in x-direction and β is the mode that determines the location of the maximum. This distribution is also suitable to the Qi/MHQ samples. For the statistical analysis of Q_p we fit a generalized extreme value distribution to the AMS of daily mean discharges. The CDF of the generalized extreme value distribution has a function of

$$F(x) = \exp \left\{ - \left[1 + \frac{\gamma(x - \zeta)}{\delta} \right]^{\frac{-1}{\gamma}} \right\} \quad (3.7)$$

where δ is the scale parameter affecting the extension in x-direction, ζ is a location parameter and γ is a shape parameter.

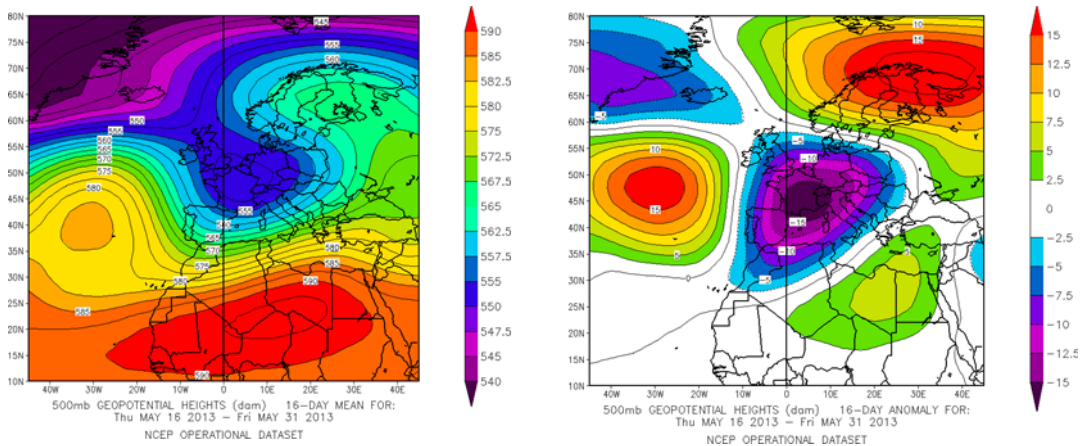


Figure 3.1: 500 hPa geopotential height, 16-day mean for 16 – 31 May 2013 (left) and anomaly in respect to the climatology based on 1979-1995 (right). Credit: Data/image provided by the NOAA/OAR/ESRL PSD, Boulder, Colorado, USA, from their Web site at <http://www.esrl.noaa.gov/psd/> (accessed 4 April 2014)

3.3 Results

3.3.1 Meteorological conditions

Large-scale Central European floods are mainly caused by the interaction of upper-level pressure systems, associated surface lows and the continuous advection of moist and warm air over long distances. In 2013, the second half of the month of May was exceptionally wet across most of Central Europe due to the unusual persistence of an extended upper air low pressure system (trough; Figure 3.1, left) that triggered several surface lows. The persistence of the quasi-stationary trough is reflected by a strong negative geopotential anomaly compared to the long-term mean (1979-1995) over France, Switzerland and north-western Italy (Figure 3.1, right). This trough was flanked by two upper air high pressure systems over north-eastern Europe and the North Atlantic Ocean, which caused a blocking situation. Therefore, Atlantic air masses from the west were prevented from entering Central Europe. On the other side, warm and humid air masses were repeatedly advected from south-eastern Europe northwards and eventually curved into Germany and Austria.

The intense and widespread rain that finally triggered the 2013 flood occurred end of May/ beginning of June. Responsible for the heavy rainfall was a cut-off low that moved slowly with its center from France (29 May) over northern Italy (30 May; Figure 3.2a) to Eastern Europe (1 June; Figure 3.2b). In the latter region, three consecutive surface lows were triggered by short-wave troughs that travelled around the cut-off low (CEDIM, 2013a). On the north-eastern flank of the upper low and near the secondary surface lows, warm and moist air masses were advected into Central Europe. Grams et al. (2014) identified evapotranspiration from continental landmasses of central and Eastern Europe as main moisture source. Due to the significant horizontal pressure gradient in the lower troposphere that prevailed from end of May to the first days of June, there was a constant and strong northerly flow of moist and warm air which caused substantial rain

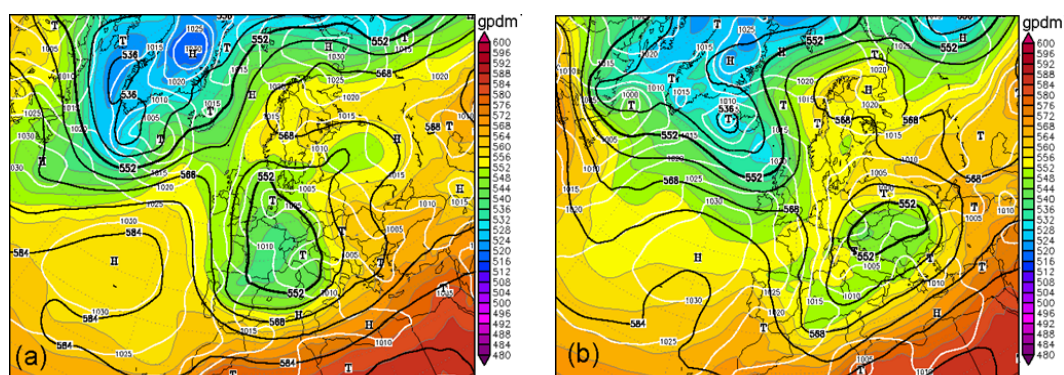


Figure 3.2: Weather charts for 30 May (a) and 01 June 2013(b) 00 UTC with analysis of 500 hPa geopotential height (black lines), surface pressure (white lines) and 1000/500 hPa relative topography (colors) from the Global Forecast System (GFS). Image credit: wetter3.de (Accessed 7 May 2014).

enhancement on the northern side of the west-to-east oriented mountain ranges, e.g. the Alps, Ore Mountains, and Swabian Jura.

In summary, the combination of large-scale lifting at the downstream side of the troughs, orographically-induced lifting over the mountains, and embedded convection in the mainly stratiform clouds due to unstable air masses resulted in prolonged and widespread heavy rainfall.

3.3.2 Precipitation

Highest precipitation totals within the 30-day period prior to the flood event start dates can be observed between three and four days ahead of the flood event start date (indicated by the zero in Figure 3.3), as shown by the time series of cumulated areal precipitation averaged over the upper Elbe (Figure 3.3a) and Danube (Figure 3.3b) catchments. Note that these characteristics are almost the same for the other two floods considered, 2002 and 1954, respectively. Especially for the Elbe catchment in May 2013, rain totals were high up to 17 days prior the event start, and higher compared to the other events (if the large totals 28 days ahead of the 2002 flooding are neglected). For the whole month of May 2013, the precipitation averaged over Germany was 178% of the long-term average for the period 1881-2012 (DWD-DeutscherWetterdienst, 2013). To better explain differences and similarities of the three flood events considered, we analyzed both maximum 3-day precipitation totals (R3d) as event precipitation and precipitation in the month before the flooding in terms of API. In both cases, the quantities are calculated independently at each grid point of the REGNIE gridded precipitation data (see Section 3.2.2).

Event precipitation

Maximum 3-day totals (R3d) in 2013 show high values in excess of 60 mm over southern and eastern Germany (Figure 3.4, left). The highest rain maximum with R3d = 346

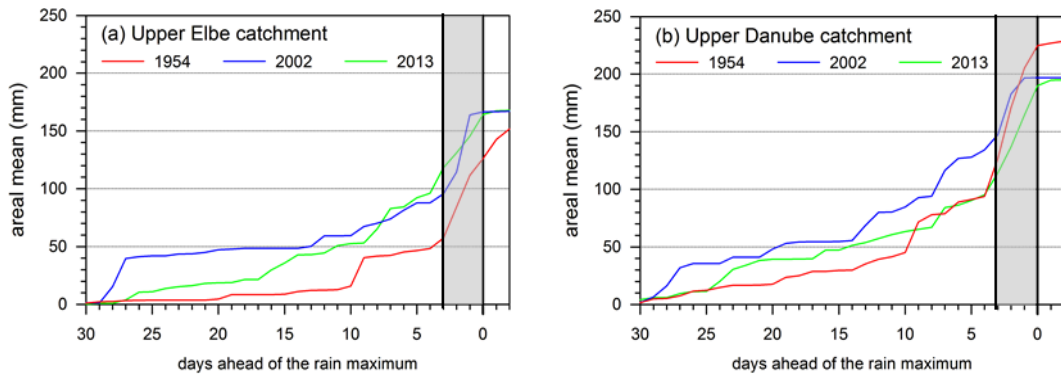


Figure 3.3: Time series of cumulated areal mean precipitation for the upper Elbe catchment in Germany up to the inflow of the Saale River (area: 63,171 km²; a) and for the upper Danube catchment in Germany (area: 51,379 km²; b). The x-axis marks the days prior to the 3-day maximum precipitation totals. Event precipitation is highlighted in grey.

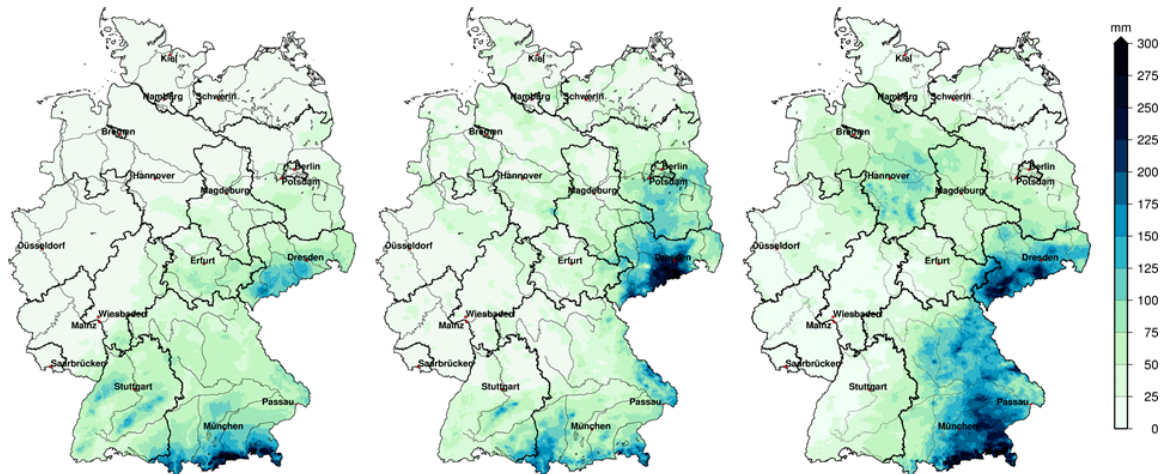


Figure 3.4: The 3-day maximum precipitation according to REGNIE data sets for June 2013 (left), August 2002 (middle) and July 1954 (right).

mm was observed at the DWD weather station of Aschau-Stein (31 May to 3 June 2013, 6 UTC), which is situated in the Bavarian Alps at an elevation of 680 m asl. This station also recorded the maximum 24-hr rain sum of 170.5 mm on 1 June 2013 (from 1 June 6 UTC until 2 June 2013 6 UTC). On that day, peak rainfall was recorded at many other stations in the federal states of Bavaria, Saxony, and Baden-Württemberg. Overall, the R3d maxima were registered almost homogeneously between 30 May and 1 June 2013 (Julian day 152, Figure 3.5 left). At the upper reaches of Danube and Elbe (German part) the maxima occurred one day later. Over the very eastern parts, especially near Dresden and Passau, the temporal difference was even two days. This consecutive shift of the main precipitation fields in west-to-east direction, i.e. following the flow direction of the Danube, caused an additional amplification of the high-water peaks.

Even if the flood-related rainfall in 2013 was mainly driven by meso-scale processes such as uplift related to the troughs and advection of moist air masses, the R3d map suggests that additional orographically-induced lifting over the mountains increased the

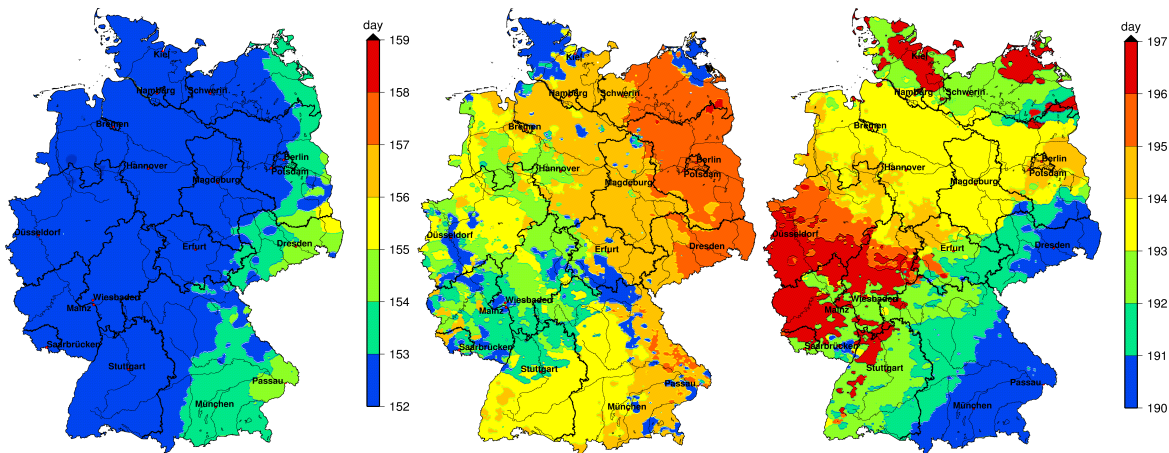


Figure 3.5: Day of the year at each REGNIE grid point where the event related maximum R3d total according to Figure 3.4 occurred (end of the 3-day total) for June 2013 (left), August 2002 (middle), and July 1954 (right). The day 152 corresponds to 1 June, 220 to 8 August, and 190 to 9 July. The indicated days refer to the end of R3d.

rain totals substantially. Highest rain sums occurred along the crests of the Ore Mountains (near Dresden), the Black Forest and Swabian Jura (west and east of Stuttgart, respectively), the Alpine Foothills (south of Munich) and the Bavarian Alps. Overall, the rain enhancement over the low-mountain ranges estimated from the ratio between areal rainfall over the mountains and adjacent low-lands was between 200 and 310%. This substantial local-scale increase in precipitation can be plausibly explained by the characteristics of the air mass on the large-scale. First of all, the lifting condensation level (LCL), which represents the level of the cloud base in case of synoptic-scale or orographic lifting, was very low on the first three days of June as observed at the sounding stations at Munich, Stuttgart, Meiningen, and K ummersbruck. The pressure levels were only around 920 hPa, i.e. near the surface (e. g. at K ummersbruck the LCL was on average 924.7 hPa / 765 m asl). A low LCL ensures that a large amount of atmospheric moisture, which decreases almost exponentially with elevation, basically can be converted into rain. Furthermore, precipitable water (pw) as the vertical integral of the specific water vapor content was large with values of up to 26 mm. The sounding at Stuttgart, for example, measured a pw value of 25.9 mm (1 June 2013, 12 UTC), which is even above the 90% percentile ($pw_{90} = 23.7\text{mm}$) obtained from all heavy precipitation events between 1971 and 2000 at the same station according to the study of (M. Kunz, 2011). Together with high horizontal wind speeds between 20 and 75 km h⁻¹ (850 hPa; around 1.5 m asl) this led to a substantial increase of the incoming water vapor flux (Fwv). This quantity can be considered as an upper limit of the conversion of moisture into precipitation (R. Smith and Barstad, 2004; M. Kunz, 2011) Thus, the high Fwv values observed during the first days of June 2013 plausibly explain the substantial orographic rainfall enhancement over the mountains.

To relate the June 2013 precipitation event to the climatological context, we quantify statistical return periods based on REGNIE data for the period from 1960 to 2009. In Figure 3.6 (left), the return periods are displayed only in the range between 5 and 200 years.

The estimated values of the return periods have been truncated to 200 years as statistical uncertainty substantially increases for larger return periods due to the short observation period of 50 years. Over the south-western parts of the Ore Mountains, the Swabian Jura and the very southern border of Bavaria, the return periods are in the range between 5 and 20 years. Only a limited number of grid points show peak values in excess of 100 or even 200 years, for example the aforementioned station of Aschau-Stein. Thus, one can conclude that the rainfall was unusually but not extraordinarily high, and hence cannot fully explain the dimension of the 2013 flood.

The most important rainfall characteristics that were decisive for the 2013 flood can be summarized as: (i) high - but not extraordinary - 3-day totals over parts of the Danube and Elbe catchments; (ii) substantial rainfall increase over the mountains that was decisive for the onset of the flooding; and (iii) areal precipitation occurring almost simultaneously with a slight temporal shift of two days between the western and eastern parts of Germany.

These meteorological conditions differ largely from those prevailing during the floods in 2002 and 1954. Areal 3-day rain totals averaged over the upper Elbe catchment (Germany only, upstream of the confluence of Elbe and Saale) were 49.3 mm compared to 75.9 mm in 2002 and 68.8 mm in 1954. Over the upper Danube catchment (Germany only), the mean areal rain was 75.7 mm compared to 62.5 and 111.2 mm in 2002 and 1954, respectively.

The most striking feature in 2002 was the extreme precipitation over the Ore Mountains reaching values of 312 mm in the 24 hours before 13 August 2002, 06 UTC, at the station of Zinnwald-Georgenfeld (Ulbrich et al., 2003b). The R3d totals (Figure 3.4, middle) show a larger area at the eastern parts of the Ore Mountains with values in excess of 300 mm. However, additional high rain totals were only observed at the southern border of Bavaria as well as over the Swabian Jura. This distribution is mainly caused by northerly flow in conjunction with a so-called Vb weather situation (Ulbrich et al., 2003b). Comparable to the 2013 event, flood triggering precipitation occurred with a shift of 2 days between the southern and eastern parts of Germany that correspond to the Danube and Elbe catchments, respectively (Figure 3.5, middle). Note that the regions with larger temporal differences in the occurrence of R3d maxima are not associated with high amounts of precipitation (see Figure 3.4). Application of extreme value statistics to R3d totals yields return periods of more than 200 years for the maxima. Return periods around 100 years are estimated for the lowlands north of the Ore Mountains (Figure 3.6, middle). Precipitation in that region also contributed to the large increase in runoff of the Elbe.

In 1954, most parts of Bavaria experienced 3-day accumulated rainfalls in excess of 150 mm (Figure 3.4, right). This was even the case for the lowlands in the north of Bavaria. Near the Alps as well as over the western parts of the Ore mountains, R3d reached values of 300 mm or even more. These extreme totals recorded within a time shift of only one day (Figure 3.5, right) correspond to statistical return periods of more than 200 years covering more than half of Bavaria (Figure 3.6, right). Thus, considering only the observed precipitation directly prior to the onset of the flooding, 1954 was certainly the most extreme event that occurred within the last 60 years.

The same conclusions can be drawn when considering 7-day instead of 3-day maxima

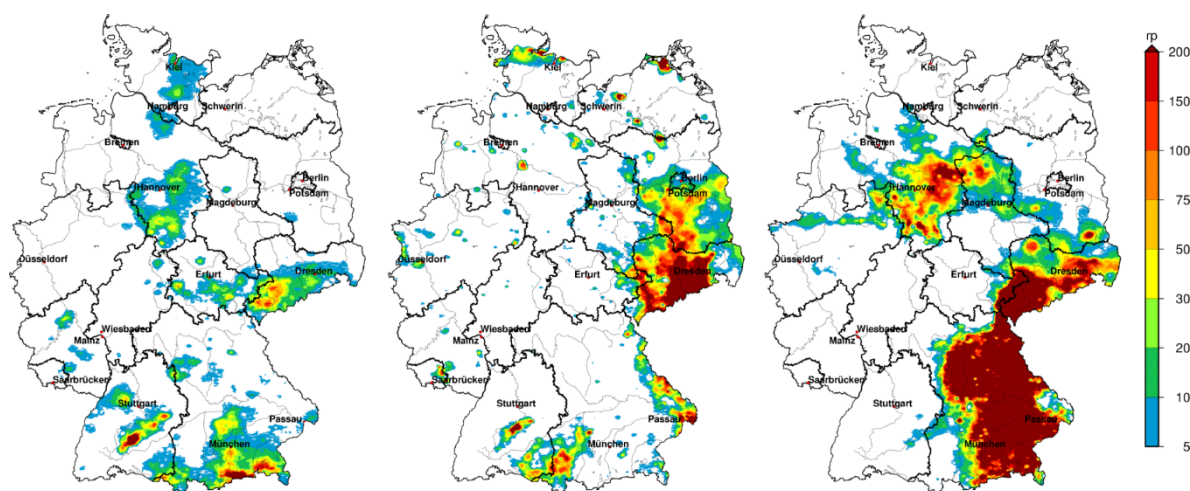


Figure 3.6: Return periods of 3-day maximum precipitation for each REGNIE grid point derived from data of the period from 1960 to 2009 for the corresponding rain totals displayed in Figure 3.4: June 2013 (left), August 2002 (middle), and July 1954 (right).

(see Figure 3.15). Of course, the rain totals increase for the longer accumulation period, for example over the Ore Mountains in 2013 or in Bavaria for 2002. The estimated return periods, especially in the Elbe and Danube catchments, are less affected by these changes - with the exception of an area in the North of Munich, where return periods in excess of 100 years can be identified for June 2013. Note that the high return periods for 7-day precipitation totals in June 2013 which are visible in North-West Bavaria are related to the Rhine catchment (see Figure 3.14).

3.3.3 Initial catchment state

Antecedent precipitation

In the next step, we assess initial catchment wetness by means of the antecedent precipitation index (API). This proxy is based on the starting date of R3d (day of the year shown in Figure 3.5 minus 3 days) and computed independently at each grid point of REGNIE. API reached high values between 100 mm and in excess of 150 mm over large parts of Germany, especially – and most importantly – over the catchments of Elbe and Danube (Figure 3.7, left). At a large number of grid points, especially in the upper Elbe catchment, the return periods are between 100 and 200 years, at some points even in excess of the latter (Figure 3.8, left). Note that the maximum that occurred between Hannover and Magdeburg was related to considerable flooding at the Aller, Oker and Leine Rivers in the Weser catchment for which no discharge data were available. The high rain totals in the month of May, especially those at the end of May (recall the increasing weighting of rain totals in API with decreasing temporal distance to R3d), resulted in very wet catchments and filling of storage capacities and thus very favorable conditions for high runoff coefficients.

Regarding the initial moisture conditions, it is found that API was significantly lower

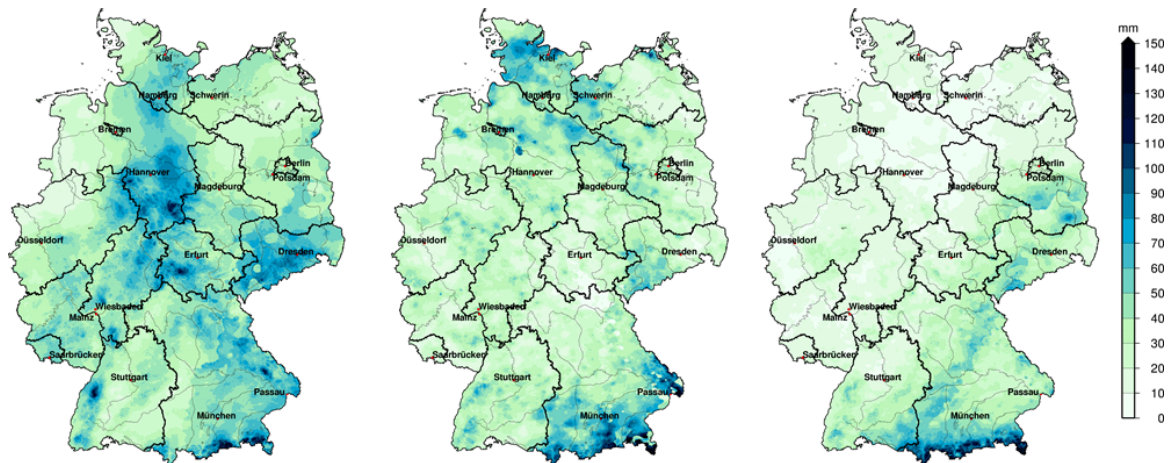


Figure 3.7: Antecedent Precipitation Index API over 30 days for the floods in June 2013 (left), August 2002 (middle), and July 1954 (right). See text for further details.

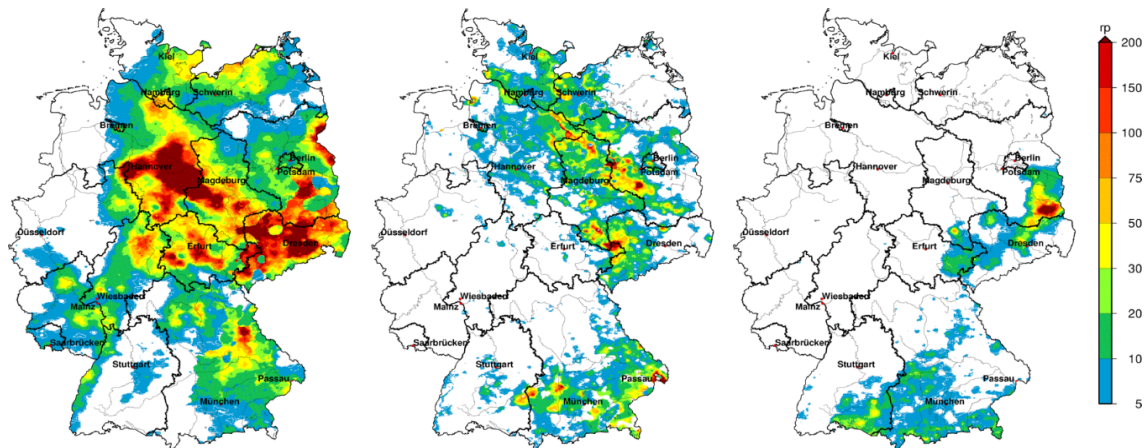


Figure 3.8: Return periods of the API displayed in Figure 3.7 derived from 30-day API of large-scale floods in the period from 1960 to 2009: June 2013 (left), August 2002 (middle), and July 1954 (right).

prior to the floods in 1954 and 2002, respectively (Figure 3.7). In both cases, high values of API up to 150 mm can be observed only over parts of the Bavarian Alps related to orographic precipitation induced by northerly flow directions. Whereas in 2013 the maxima of API correspond well with those of R3d, this is not the case for the two other events. Especially over the Ore Mountains and north of it, where highest rainfall was observed, API was below 50 mm in both cases, yielding return periods below 20 years at most of the grid points (Figure 3.8). The same applies to the API in the Danube catchment in 1954. Both in 2002 and 1954 high API values indicate that the initial wetness was comparatively high, but in general not in those regions where the event precipitation was highest (compare Figure 3.4 and Figure 3.7). Apart from areal precipitation as described above, this is the major difference to the 2013 event

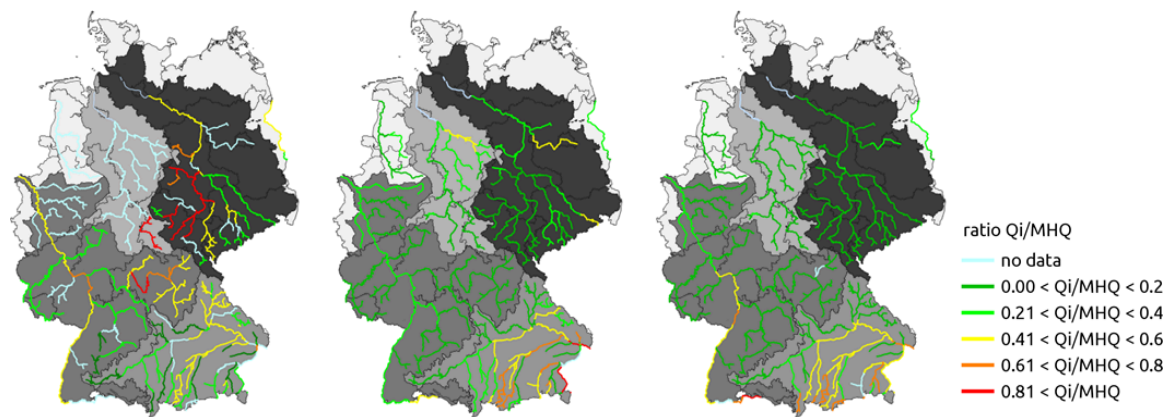


Figure 3.9: Initial flow ratio at meteorological event start Q_i normalized for MHQ (calculated from AMS 1950-2009) for June 2013 (left), August 2002 (middle), and July 1954 (right).

Initial hydraulic load

As a consequence of the large amounts of rainfall accumulated during the month of May, reflected by the extended areas of high API, also the initial hydraulic load in the river network was already clearly increased at the beginning of the event precipitation in 2013. In general, the pattern of increased initial hydraulic load in the rivers shown in Figure 3.9 (left) resembles the spatial distribution of high API values (Figure 3.7 left). This mostly applies to the central and south-eastern parts of Germany. Most prominent in this regard were the Saale River and its tributaries Wipper and Bode in the western part of the Elbe catchment with an initial flow ratio above 0.8 of MHQ. The Rhine, upper Main, Danube, with tributaries Naab and Isar and the Werra River were also affected. Note that for many gauges in the Weser and lower Rhine catchments no discharge data have been available for the June 2013 flood (see Figure 3.14 for geographic locations).

In comparison, for the August 2002 and July 1954 floods the initial hydraulic load of the river network was clearly lower with few exceptions (Figure 3.9). In August 2002, basically the Danube and its tributaries Inn, Isar, Lech and Regen showed a noticeable increase of initial river discharge (ca. 0.5 of MHQ). These catchments showed also high API values. Similarly, at the beginning of the July 1954 flood increased river discharges of about 0.4 to 0.8 of MHQ for the Danube and its southern tributaries are visible. Also the middle and upper parts of the Rhine show increased initial hydraulic loads in this range. The lower coincidence of regions of increased initial hydraulic load with regions of increased API for the July 1954 flood (compare Figure 3.7 and Figure 3.9) suggests that the increased initial hydraulic load particularly along the Rhine was induced by different mechanisms than high amounts of antecedent precipitation, presumably due to snow-melt in the alpine headwaters of the Rhine.

From the statistical extreme value analysis applied to the Q_i /MHQ samples at each gauge we obtain an estimate for the return period of the specific initial river flow situation for the June 2013, August 2002 and July 1954 floods. The results presented in Figure 3.10 show that for the June 2013 flood the initial flow ratios observed in central Germany, in particular at the upper Main (Rhine catchment), Werra (Weser catchment),

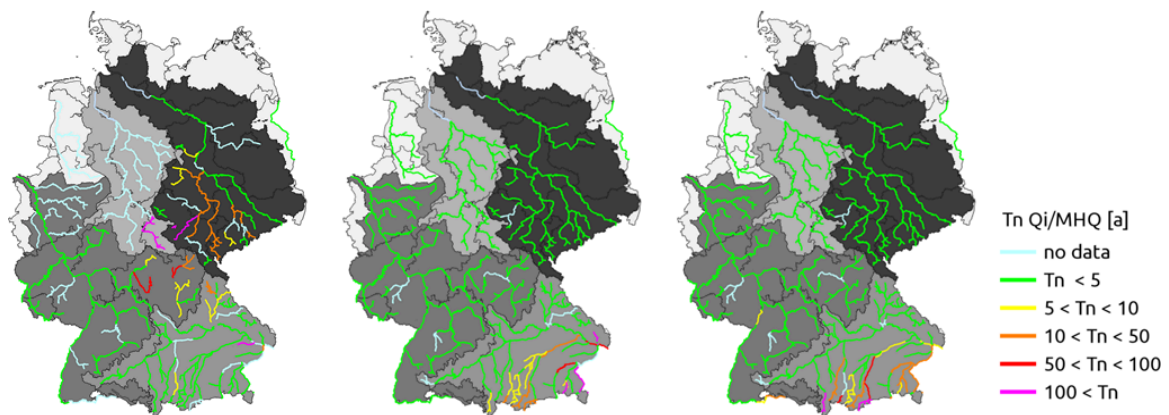


Figure 3.10: Return periods of initial flow ratio at meteorological event start (Q_i normalized for MHQ) derived from Q_i /MHQ ratios of large-scale floods in the period from 1969 to 2009: June 2013 (left), August 2002 (middle), and July 1954 (right)

Wipper, Saale, Weisse Elster, Mulde (Elbe catchment) and Naab and Vils (Danube catchment) exhibit return periods in the range of 10 to 50 years, in some river stretches even above 100 years. For the events in August 2002 and July 1954 comparable extremes are only observed for few river stretches in the Danube catchment including the Regen, upper Isar, Ilz, Inn and Salzach Rivers in 2002 and the upper Iller, Lech and Isar Rivers in 1954.

The initial hydraulic load of the river network (13,400 km) was clearly increased in June 2013 given the comparison to other large-scale flood events from the last 50 years. Hence, the aggravating effect of increased initial hydraulic load was stronger in June 2013 than in August 2002 and July 1954. However, extraordinarily high initial flow ratios occurred only in some river stretches, namely the Saale River and its tributaries.

3.3.4 Peak flood discharges

In June 2013, 45% of the total river network considered in Germany showed peak discharges above a 5-year flood. As can be seen in Figure 3.11 (left), all major catchments showed flooding, namely the Weser, Rhine, Elbe and Danube catchments. Particularly the Elbe and Danube Rivers and many of their tributaries were affected by extraordinarily high flood levels. In the Elbe catchment, flood peak discharges exceeded a return period of 100 years along the whole Elbe stretch between Dresden and Wittenberge, the Mulde, and the tributaries of the Saale River, Weisse Elster and Ilm. In the Danube catchment, the section of the Danube downstream of Regensburg as well as the Inn and Salzach Rivers experienced peak discharges with return periods above 100 years. In addition, the Isar, Naab and Iller Rivers showed flood peaks above 50-year return periods. Further, in the Rhine catchment, the Neckar and parts of the Main as well as the Werra River in the Weser catchment experienced peak discharges above the 50-year return period. New record water levels were registered at the Elbe between Coswig and Lenzen (along a total length of 250 km), at the Saale downstream of Halle, and at the Danube in Passau. Severe flooding occurred especially along the Danube and Elbe Rivers, as well as along the Elbe tributaries Mulde and Saale, in most cases as a consequence of

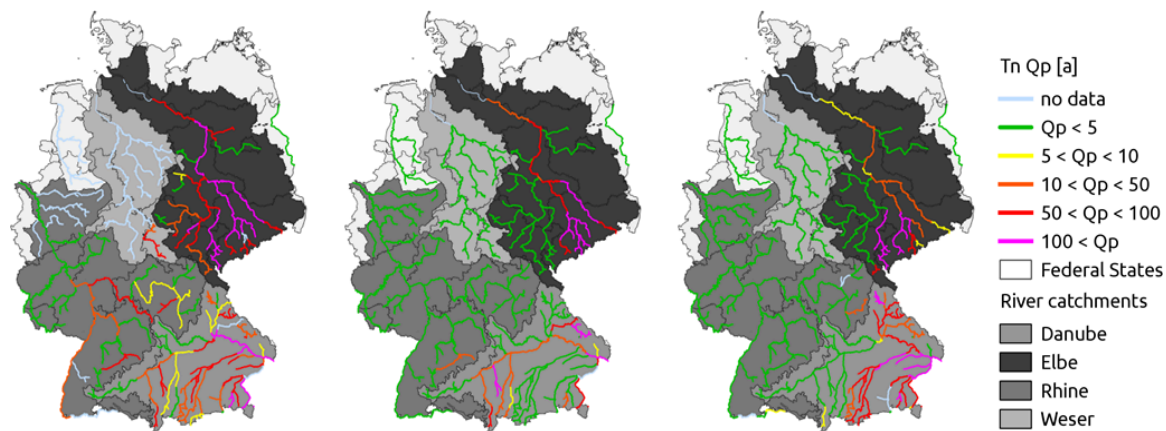


Figure 3.11: Regionalized return periods (T_n) of flood peak discharges for June 2013 (left), August 2002 (middle), and July 1954 (right). Gauge data were made available by the Water and Shipping Management of the Fed. Rep. (WSV) prepared by the Federal Institute for Hydrology (BfG) and environmental state offices of the federal states.

dike breaches. It is remarkable that large parts of catchments affected by flooding did not receive exceptional amounts of rain (see Figure 3.4). In particular, this applies to the upstream parts of the Saale, Werra and Main catchments. However, these regions show high amounts of antecedent precipitation and substantial initial hydraulic load.

The August 2002 and July 1954 floods show peak discharges in the order of 100 year return periods at the Elbe between Dresden and Wittenberg, in parts of the Mulde, Regen and Mindel and of 50 years at the Freiburger and Zwickauer Mulde and the Elbe downstream of Wittenberg to Wittenberge, (see Figure 3.11, middle and right panels). In July 1954 return periods of 100 years occurred at the Weisse Elster and Mulde in the Elbe catchment and the Isar, Rott and Inn in the Danube catchment. Flood peaks with a return period of 50 years were observed at the Danube downstream Regensburg, the Naab, Inn and Salzach as well as the upper Isar Rivers. However, as can be seen in Figure 3.11 (middle and right), the river stretches with high magnitude flood peaks are clearly less extended in August 2002 and July 1954: the index L describing the spatial flood extent amounts to 19% in August 2002, 27% in July 1954 and 45% in June 2013 (see Figure 3.14 for geographic locations).

The major differences of the flood in June 2013 in comparison to August 2002 and July 1954 are that the Elbe, the Mulde and the Saale Rivers were affected simultaneously by extraordinary flooding which by superposition of flood waves resulted in unprecedented flood levels particularly in the middle part of the Elbe. Further, nearly all tributaries of the Danube showed flood responses and jointly contributed to the record flood along the Danube downstream of Regensburg. Also the Rhine and Weser catchments were considerably affected even though the magnitude of the peak discharges was not as extreme as in the Elbe and Danube catchments.

Table 3.2: Severity indices for June 2013, August 2002 and July 1954 floods

Index	Jun-13	Aug-02	Jul-54
Precipitation index (S_{R3d})	16.9	30.1	55.2
Wetness index (S_{API})	114.1	47.3	21.1
Initial hydraulic load index (S_{Qi})	12.7	6	6.1
Flood severity index (S_{Qp})	74.6	35.4	49.8

3.3.5 Index based classification

We evaluate the importance of the individual hydro-meteorological factors within the different flood events using the severity indices introduced in section 2.3. The precipitation-, wetness-, initial hydraulic load- and flood severity indices enable us to compare the 74 past large-scale flood events with regard to the spatial extent and magnitude of each hydro-meteorological factor. This allows for the identification of singularities in terms of extreme situations associated with individual events. The index values for the June 2013, August 2002 and July 1954 events are listed in Table 3.2.

Among these events, the June 2013 flood is characterized by the highest wetness, initial hydraulic load and flood severity indices which are more than twice the values of the August 2002 flood and with regard to wetness more than five times the value of the July 1954 flood. In contrast, the precipitation index of July 1954 exceeds the value of June 2013 by a factor of three and is nearly twice as high as for the August 2002 event. These proportions emphasize the prominent role of extreme antecedent precipitation and increased initial hydraulic load in the river network as key factors for the formation of the extreme flood in June 2013.

Figure 3.12 shows a scatterplot of the precipitation and wetness indices of the 74 past large-scale floods in Germany. The June 2013 flood is the most extreme in terms of the wetness index, whereas the July 1954 flood is by far the most extreme in terms of the precipitation index. To explore the relationship between precipitation and wetness indices as flood drivers and the flood severity index as dependent variable, we apply a locally-weighted scatter plot smooth (LOWESS) model (Cleveland, 1979). For this locally weighted linear least-squares regression, the tri-cube weight function and a span of 50% are used. The span specifies the percentage of data points that are considered for estimating the response value at a certain location. The performance of the LOWESS model to explain the variation of flood severity is expressed in terms of Root Mean Square Error (RMSE) which can be interpreted as the standard deviation of unexplained variance.

The inclined orientation of the response surface indicates that both precipitation and wetness are equally relevant factors to explain resulting flood severity. According to this model, flood severity index values above around 0.5 (normalised values) increase approximately proportionate with precipitation and wetness severity. However, both the concave shape of the response surface, visible for precipitation and wetness index values below 0.5 (normalized values), and the moderate performance of the LOWESS model to explain variability of flood severity (RMSE = 13.2) suggest that additional factors and

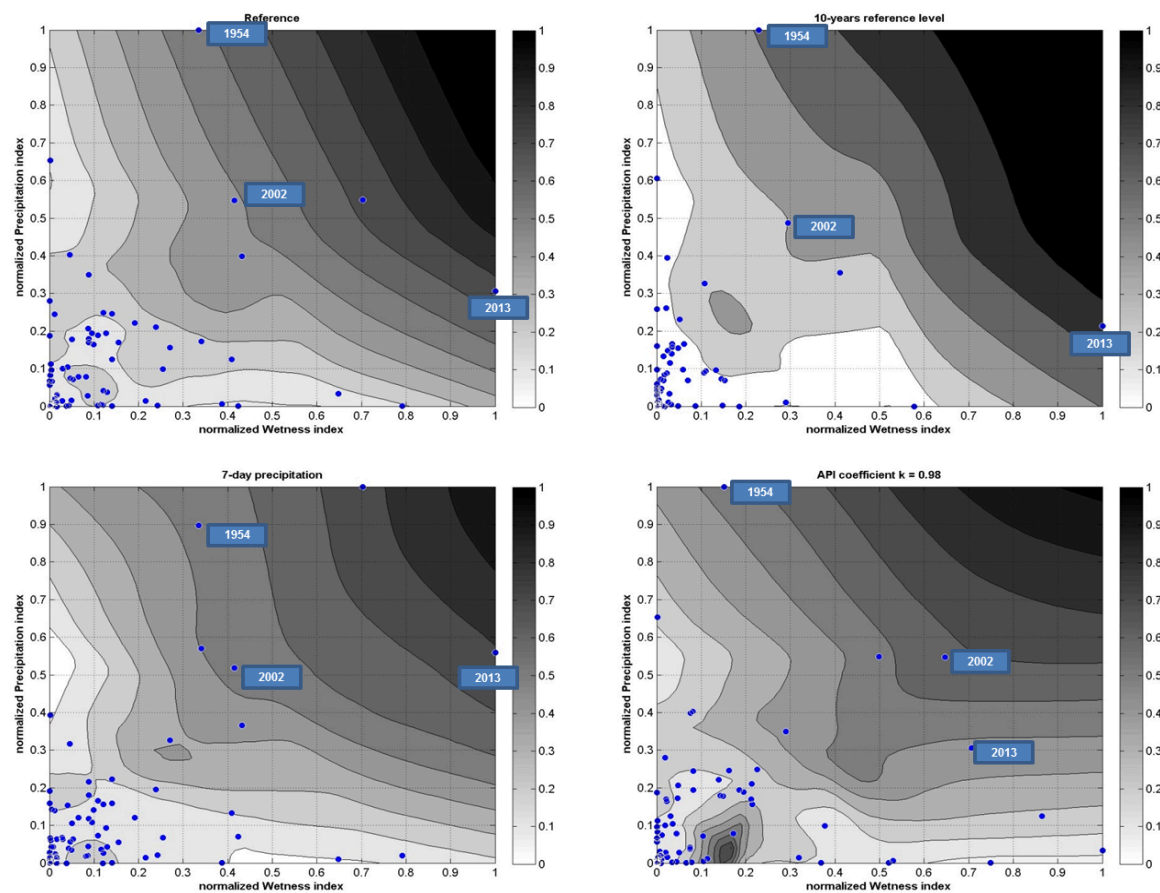


Figure 3.12: Locally-weighted scatter plot smooth (LOWESS) for the relationship between precipitation and wetness indices as predictors for the flood severity index (grey color code) of past large scale flood events in Germany. Top left: Reference (5-years return period as reference level for severity indices, R3d, API 30 days, $k = 0.9$), top right: 10-years return period as reference level for severity indices, bottom left: R7d, bottom right: API $k=0.98$. Note that all severity indices have been normalized to the respective maximum values and that the upper right corners do not contain observed data.

Table 3.3: Variation scenarios examined within sensitivity analysis

Scenario	Code	Reference	Variation
Duration event precipitation	R7d	3 days	7 days
Duration antecedent precipitation	API15	30 days	15 days
Depletion constant API	API k0.8	k = 0.9	k = 0.8
	API k0.98	k = 0.9	k = 0.98
Return period reference level flood severity	S10a	5 years	10 years
	S25a	5 years	25 years
Return period reference level precipitation severity	P10a	5 years	10 years
	P25a	5 years	25 years
Return period reference level wetness severity	W10a	5 years	10 years
	W25a	5 years	25 years
Return period reference level initial hydraulic load severity	I10a	5 years	10 years
	I25a	5 years	25 years

characteristics influence this relationship. The spatial variability and the corresponding degree of areal overlaps of the factors as well as other hydrological processes, for instance snow melt or seasonal variations in base flow, play a role in this regard.

3.3.6 Sensitivity Analysis

To check the robustness of our evaluation of the flood in June 2013, it is important to revisit the specifications of parameters of the methodology. Besides, depending on the focus of the analysis the use of different return periods as reference levels for the assessment of severity may be of interest. We examine the implication of varying duration of event precipitation and antecedent precipitation index period as well as different values for the depletion constant for the calculation of API, as well as different return periods as reference levels for the calculation of severity indices following a one-at-time sensitivity analysis design (Saltelli et al., 2000). The scenarios examined are listed in Table 3.3. To assess the implications of these variations on the evaluation of the flood events, we are interested in the changes in the ranking of the flood events with regard to different severity indices. For this purpose, we compare the reference set-up which has been used to introduce the methodology to the outcomes from the different variations in terms of Spearman’s rank correlation coefficient (ρ). Lower rank correlations mean larger differences in the outcomes and indicate a larger sensitivity to these variations.

The implications of these variations are moderate. The correlation coefficients between the reference scenario and these variations are above 0.83 (see Figure 3.13). The most sensitive variations are related to changing the return periods used as reference level for the calculation of flood severity and wetness severity indices to 25 years (S25a and W25a). This is followed by duration of event precipitation (R7d) and increasing the depletion constant, i.e. the weight of earlier precipitation within the calculation of API (API k0.98). We track the implications on the outcomes of the LOWESS model for these variations (see Figure 3.12 bottom left and right panels for R7d and API k0.98). Further, we examine the changes in LOWESS model outcome for the variation of return periods used as reference level for the calculation of severity indices, i.e. 10-years and 25-years. Increasing the return period used as reference level for the calculation

of severity indices, implies a reduced range of precipitation or discharge observations, and hence, an increased focus on local extremes. For the 25-years level this leads to a pronounced clustering of precipitation and wetness index values below 5 (not shown). Exceptions are the floods in July 1954, August 2002 and June 2013. Using a 10-years return period as reference level the scattering of data points is also low resulting in a less well-defined model for precipitation indices below 0.3 (normalized values) and wetness indices below 0.2 (normalized values, Figure 3.12 top right panel). The interpolated surface indicates a stronger inclination towards the wetness index which suggests that flood severity increases disproportionately with catchment wetness. Varying the duration of event precipitation to seven days (R7d) shifts the attention to events which are more related to west cyclonic circulation patterns, and thus is rather associated with winter floods (Beurton and Thielen, 2009) but also with the autumn flood in October 1998 (Uhlmann et al., 2010). Accordingly, the October 1998 flood yields the highest precipitation severity index in Figure 3.12 (bottom left panel). The increase of the depletion coefficient k within API corresponds to an almost equally weighting of the precipitation over the antecedent precipitation period. As a result three floods achieve higher wetness indices than the flood in June 2013 even though the flood severity of these events is clearly lower. According to the resulting LOWESS model interpolation (see Figure 3.12 bottom left panel) the importance of catchment wetness for flood severity is reduced.

Overall, across the variation scenarios examined the relationship between precipitation and wetness indices as flood drivers and the flood severity index as dependent variable is largely comparable. The floods of July 1954, August 2002 and June 2013 remain among the most severe events and mainly determine the shape of the LOWESS model response surface in the region of high severity indices. Hence, the main finding of the index-based classification which points out that both precipitation and wetness are equally relevant factors to explain flood severity remains valid.

3.4 Conclusions

This study provides new insights into the characteristics of hydro-meteorological factors that caused the flood in June 2013 and presents a statistical evaluation of the associated return periods. The data-based approach further comprises aggregated index values which consider both the spatial extent and magnitudes of the different hydro-meteorological factors and allows for the comparison to past and future large-scale flood events. The results of this analysis proved robust against variations in parameters within the calculation procedure. The large-scale flood data base and the methodological framework developed enable the rapid assessment of future floods based on precipitation and discharge observations.

The results illustrate that the sequence of prevalent circulation patterns in May 2013 put an important boundary condition for the extraordinary precipitation anomaly observed. For this flood, diverse hydro-meteorological factors showed exceptional characteristics. First, the development of event precipitation and in particular the substantial orographic rainfall enhancement was driven by a very low lifting condensation level in combination with high amounts of precipitable water in the atmosphere. This was continuously sustained by the strong influx of high water vapor resulting from a strong

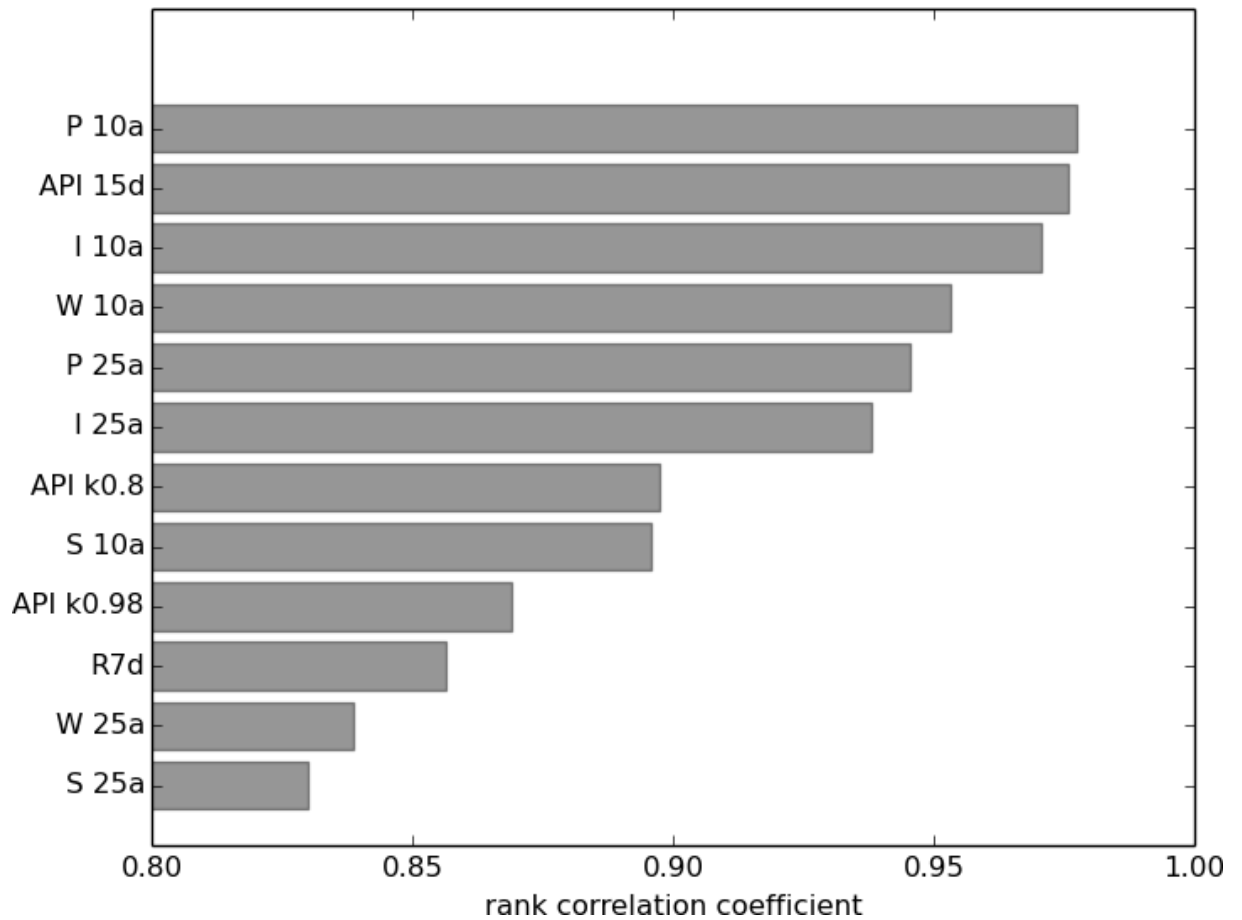


Figure 3.13: Spearman's rank correlation coefficients between the reference scenario and the variations examined within the sensitivity analysis; for the scenario definition see Table 3.3

and persistent flow of air from the north to north-east. Second, during the weeks before the onset of the flood, enormous amounts of antecedent precipitation occurred over large parts of Germany. As the areas of high antecedent and event precipitation were amply overlapping, the wet initial conditions strongly intensified the runoff response to event precipitation. Hence, particularly the large areal superposition and interplay of event precipitation and wet initial catchment conditions turns out as key drivers for the exceptional hydrological severity of the flood in June 2013. In the Saale catchment the increased initial hydraulic load in the river network has been an additional aggravating factor. In the Danube, the movement of the event precipitation field from west to east, i.e. following the streamflow direction, amplified the superposition of the flood waves from the tributaries. Third, the spatial extent of high magnitude flood peaks marks a new record for large-scale floods in Germany for at least the last sixty years and set new record water levels along extensive river sections in Germany.

In comparison, the flood in August 2002 was triggered in Germany by extremely intense precipitation which was relatively localized in the Ore Mountains. Initial wetness showed considerably high values in some parts of Germany but these areas did not coincide largely with event precipitation. The flooding in July 1954 was for the main part caused by exceptional amounts of event precipitation affecting large parts of Bavaria. In comparison to August 2002 and June 2013, initial wetness was a less important factor in Germany. However, at the Northern ridge of the Alps initial wetness contributed to flood generation in the Salzach and Inn Rivers (Blöschl et al., 2013).

Our results show that the influence of catchment wetness is a considerable factor for high-return period, large-scale floods in Germany. In this regard we support the hypothesis that hydrological extremes are rather a consequence of unusual combinations of different hydro-meteorological factors than of unusual magnitudes of the factors themselves as stated by (Klemes, 1993). Using the knowledge gained about the characteristics, the range of magnitudes and interactions of the various hydro-meteorological factors associated with large-scale floods from the past 60 years, we can advance the derivation of plausible extreme scenarios. In this regard, the data base compiled for large-scale floods in Germany may be analysed concerning the possibilities of coinciding extremes of individual hydro-meteorological factors as for instance the combination of initial wetness observed in June 2013 and event precipitation as in July 1954. Of course, the development of such scenarios requires an in-depth analysis of synoptic meteorological situations and the corresponding transition of related weather conditions. The hydrological evaluation of such extreme scenarios could provide new insights for large-scale flood hazard assessment, planning scenarios for national disaster response, spatial risk as well as cumulated flood losses. These insights may find further use in advanced approaches for flood frequency analysis and design flood estimation, e.g. (R. Merz and Blöschl, 2008; Paquet et al., 2013).

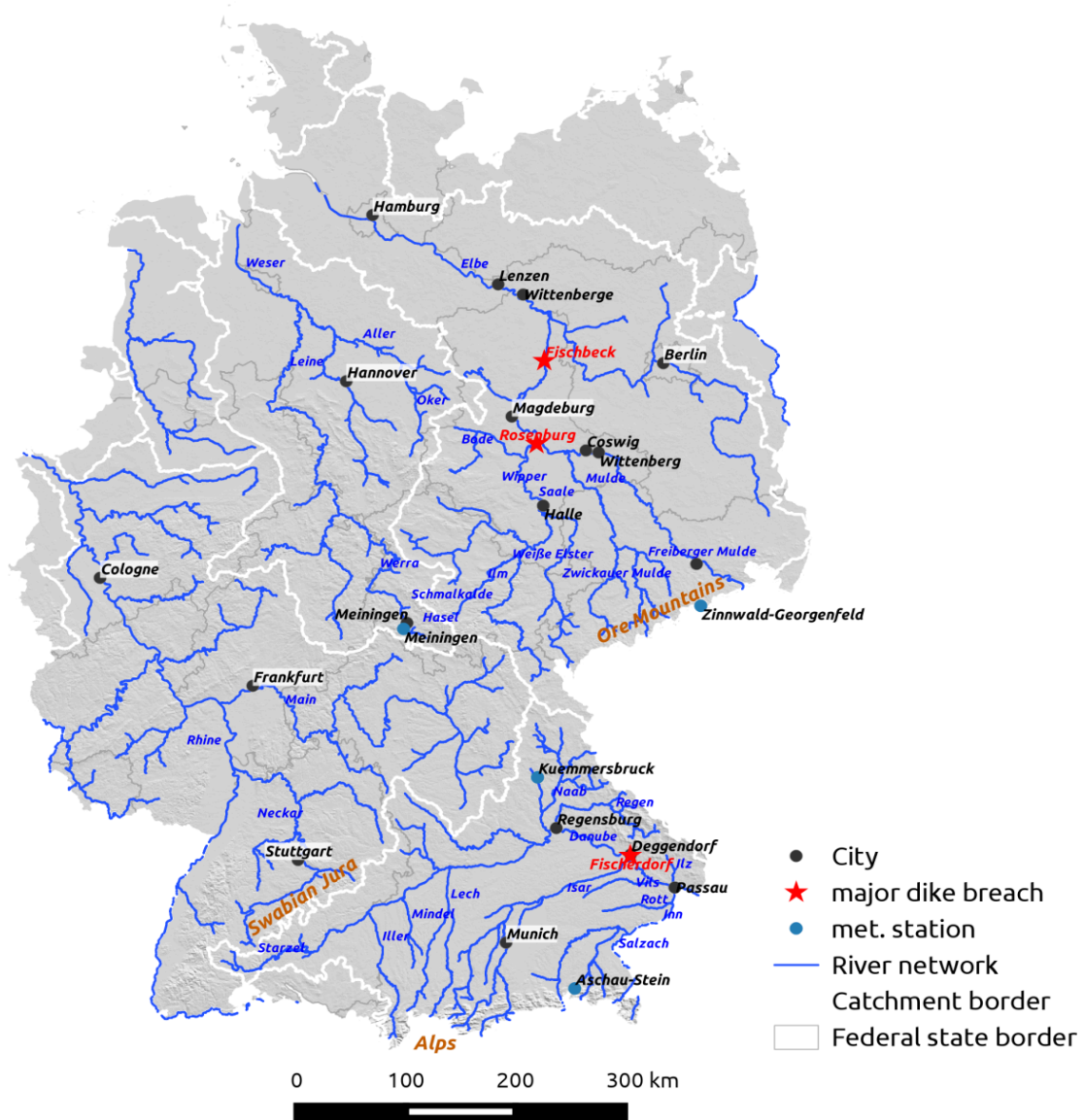


Figure 3.14: Outline map of referred geographic locations.

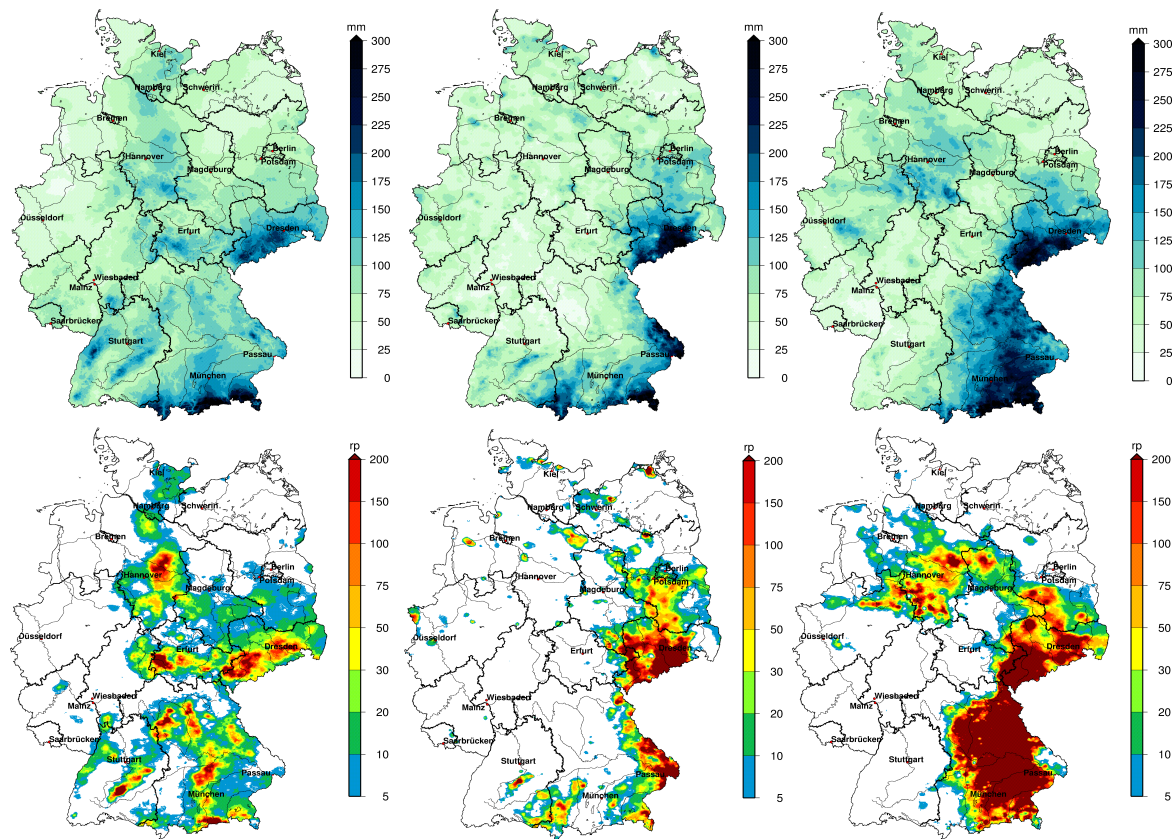


Figure 3.15: Same as Figures 3.4 and 3.6, but for 7-day maximum precipitation (top line: 7-day maximum precipitation; bottom line: Return periods June 2013, left; August 2002, middle; July 1954, right).

4 | The flood of June 2013 in Germany: How much do we know about its impacts?

Manuscript Info

Authors information:

Annegret Thieken
Tina Bessel
Sarah Kienzler
Heidi Kreibich
Meike Müller
Sebastian Pisi
Kai Schröter

Published as:

Thieken A., Bessel T.,
Kienzler S., Kreibich H.,
Müller M., Pisi S.,
Schröter K.
The flood of June 2013
in Germany:
How much do we know
about its impacts?
Nat. Hazards Earth Syst. Sci.
2016;16,6:1519-1540.
doi:10.5194/nhess-16-1519-
2016.

Abstract

In June 2013, widespread flooding and consequent damage and losses occurred in Central Europe, especially in Germany. The paper explores what data is available to investigate the adverse impacts of the event, what kind of information can be retrieved from these data and how good data and information fulfil requirements that were recently proposed for disaster reporting on the European and international level. In accordance with the European Floods Directive (2007/60/EC), impacts on human health, economic activities (and assets), cultural heritage and the environment are described on the national and sub-national scale. Information from governmental reports is complemented by communications on traffic disruptions and surveys of flood-affected residents and companies. Overall, the impacts of the flood event in 2013 were manifold. The study reveals that flood-affected residents suffered from a large range of impacts, among which mental health and supply problems were perceived more seriously than financial losses. The most frequent damage type among affected companies was business interruption. This demonstrates that the current scientific focus on direct (financial) damage is insufficient to describe the overall impacts and severity of flood events. The case further demonstrates that procedures and standards for impact data collection in Germany are widely missing. Present impact data in Germany are fragmentary, heterogeneous, incomplete and difficult to access. In order to fulfil, for example, the monitoring and reporting requirements of the Sendai Framework for Disaster Risk Reduction 2015-2030 that was adopted in March 2015 in Sendai, Japan, more efforts on impact data collection are needed.

4.1 Introduction

In June 2013, large-scale flooding occurred in many Central European countries, i.e. in Switzerland, Austria, the Czech Republic, Slovakia, Poland, Hungary, Croatia, Serbia, and particularly in Germany. In 45% of the German river network peak flows exceeded the five-year flood discharge (Schröter et al., 2015). Using an adapted method of (Uhlemann et al., 2010) that determines and assesses large-scale flooding based on discharge data from 162 gauges from all over the country, the flood of June 2013 can be regarded – in hydrological terms – as the most severe flood in Germany over at least the past 60 years (Merz et al., 2014). However, the extreme flood of August 2002 remains the most damaging event with an overall loss of EUR 11.6 b (as of July 2005; (Thielen et al., 2006b)). The event of 2013 was especially characterised by extraordinary high antecedent moisture. During the second half of May 2013 exceptional rainfall amounts had been witnessed due to a quasi-stationary upper-level trough over Central Europe. This circulation pattern triggered a sequence of surface lows on its eastern side, a process that was also referred to as repeated Rossby Wave Breaking (RWB) (Grams et al., 2014) and that repeatedly transported warm and humid air from South-East Europe to Central Europe (Schröter et al., 2015). Notably continental evapotranspiration was the main moisture source as revealed by Grams et al. (2014). By the end of May, rainfall totalled to 178% of the average monthly amount and record-breaking soil moisture was observed in 40 % of the German territory (DWD-Deutscher Wetterdienst, 2013) . Accordingly, Schröter et al. (2015) also reported high initial streamflow levels in the river network.

First local flooding was caused by a thunderstorm on 18th May 2013 in the southern part of Lower Saxony, where anew heavy rainfall and flooding occurred a week later (NLWKN, 2014) . However, the large-scale flooding was mainly triggered by rainfall between 31st May and 2nd June 2013. These rainfall amounts were considerable – especially over mountains – but not exceptional (Schröter et al., 2015). However, in combination with the wet soils and above-average initial streamflow levels, high flood peaks resulted in the upper catchments of the rivers Rhine and Weser in the western part of Germany as well as in many parts of the catchments of the rivers Danube in southern Germany and Elbe in East Germany.

Flood discharges above a five-year-return period were observed in many rivers reaches in Germany between 21st May 2013 and 20th June 2013. Over a length of approximately 1,400 km in the river network even 100-year flood discharges were exceeded. Therefore, widespread inundation occurred as depicted in Figure 4.1. At several locations, embankments were unable to withstand the floodwater resulting in dike breaches and inundation of the hinterland. As a result, 12 out of the 16 federal states were affected by the flood, from which eight declared a state of emergency (see Figure 4.2a for a geographic overview).

Particularly affected areas are detailed in Figure 4.1a to d, i.e. the areas inundated by a dike breach at Fischbeck at the river Elbe (Figure 4.1a), at the confluence of the rivers Saale and Elbe at Klein Rosenberg-Breitenhagen (Figure 4.1b) and in Deggendorf-Fischerdorf at the confluence of the rivers Isar and Danube (Figure 4.1c). The city of Passau (Figure 4.1d) is commonly known as “Three-River-City” since it is located at the confluences of the rivers Danube, Inn and Ilz. Due to its special geographic-topographic situation no flood defence schemes are in place. In 2013, the water level of 12.89 m above

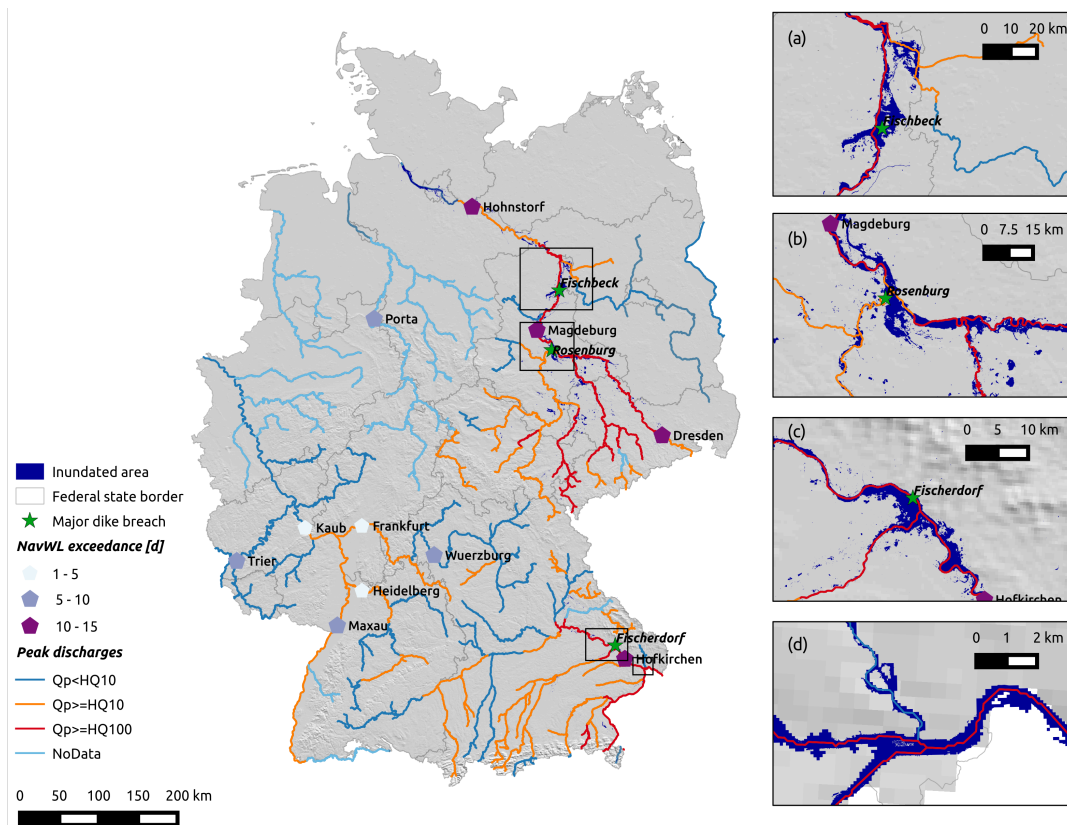


Figure 4.1: River reaches with flood discharges (Q_p) exceeding a 10-year-discharge ($HQ10$) or a 100-year discharge ($HQ100$), exceedance of highest navigable water level ($NavWL$) in days at selected gauges (data source: (BfG, 2014a), p. 152), as well as hot spots of inundation in June 2013 including major dike breach locations; details for a) Fischbeck, b) confluence of the rivers Saale and Elbe, c) Fischerdorf at the confluence of the rivers Isar and Danube as well as d) the city of Passau (Source: (Schröter et al., 2015), based on satellite images of TerraSAR-X and MODIS).

gauge zero nearly reached that of a flood event in 1501, which is with 13.20 m above gauge zero the highest water level ever recorded in Passau (BfG, 2013).

While the meteorological and hydrological aspects of the flood event were published in scientific journals already a few months after the flood, e.g. (Blöschl et al., 2013; Grams et al., 2014; B. Merz et al., 2014a; Schröter et al., 2015), only little information is available on the flood impacts. However, the societal significance of natural hazards such as floods only becomes visible through their effects on human society, its assets and activities. Accordingly, the crucial dimension when it comes to the assessment of events is not the flood hazard, but the flood risk. In this context, flood hazard is defined as the exceedance probability of potentially damaging flood situations and is often assessed by a frequency analysis of the discharges or the water levels at a given point within a specified period, usually a year (B. Merz and Thielen, 2004). Flood risk statements, in contrast, do include information about the consequences of flood situations, for example direct losses or fatalities. Hence, flood risks are not solely dependent on the flood hazard, but also on the vulnerability of the affected society. This is determined by the use of the flood-prone areas, i.e. the exposure of human beings, infrastructures and buildings to flooding (also referred to as elements at risk or damage potential), as well as the susceptibility of these elements to inundation. The extent of vulnerability and risk is strongly influenced by the resilience of the affected society or its ability to resist: the better the preventive and protective measures, early warning systems and emergency response have been developed, the less severe the resulting damage will be.

In general, adverse effects of floods are divided into direct and indirect damage (K. Smith and R. C. Ward, 1998). While direct damage, such as fatalities and injured people as well as damaged or destroyed buildings, are directly caused by a physical contact of the element at risk with the flood water, indirect damage occur in space and time outside the actual event. Among these effects are traffic and business disruptions, but also migration or long-term psychological illnesses.

Accounting for all impacts and costs of a particular event is complicated for many reasons (M. Downton and Pielke, 2005). To begin with, damage to buildings seems to be monetised easily since the goods concerned are traded on the market (B. Merz et al., 2010b). The damage costs can thus be estimated on the basis of the necessary repair works and materials in a first instance. For some applications such as cost-benefit analyses, however, the financial damage that is based on repair and replacement costs has to be depreciated by the betterment that the damaged structures underwent during reconstruction; taxes also have to be excluded (see B. Merz et al. (2010b). A monetary estimate can also be put on disruptions of operations, turnover losses or costs incurred by delivery detours. However, further indirect costs of disasters along production chains are difficult to measure and can often only be assessed by models (Greenberg et al., 2007; Meyer et al., 2013). Moreover, many losses (and benefits) associated with a flood event are intangible and difficult to monetarise or even to count. Many health effects due to flooding, but also damage to cultural heritage or the environment can only be monetised – if at all – through indirect assessments, based on, for example, the willingness of the population to pay for the restoration of a cultural heritage site or a recreational area, as well as to avert evacuation (see Meyer et al. (2013) for an overview). Furthermore, even big flood events have direct and indirect benefits, for example donations, relief funds or other (financial) support provided to affected regions, which should be crosschecked

with the costs. Finally, flood losses might differ and depend on the spatial and temporal scale of the assessment, for example the property (asset), local, regional, national or international scale as defined by De Groeve et al. (2013), as well as on the overall context of the analysis and its underlying monetary assessment.

The true costs of flood events may hence include hidden costs, such as health effects and long term societal impacts, and hidden benefits caused by, e.g. extra compensation payments, which are difficult to identify and quantify (M. Downton and Pielke, 2005). Due to this complexity, there is currently a clear focus on accounting direct damage costs or primary effects of actual events (Pielke Jr. and Landsea, 1998) by using economic and/or human indicators (IRDR, 2015a). While human indicators such as the number of people killed, injured or evacuated can be determined fairly reliable shortly after the event, a reliable estimate of the direct economic or financial costs of an event can often only be made after several years when all repair works and compensation payments have been completed. Using flood damage data provided by the National Weather Service (NWS) in the USA, (M. Downton and Pielke, 2005) demonstrated that reliable loss figures require regular data updates and consistent definitions of the damage components included. Data consistency is, however, difficult to assess if sub-amounts such as damage in different sectors or damage to movable and fixed items, are not explicitly recorded (Blong, 2004; M. W. Downton et al., 2005). Further potential biases of loss data are outlined by Gall et al. (2009).

In contrast to meteorology and hydrology, very little standardisation and institution-alisation prevails regarding (flood) loss documentation (Kreibich et al., 2014a), although the lack of reliable, consistent and comparable data is seen as a major obstacle for effective and long-term loss prevention (Changnon, 2003). Enhanced efforts to collect loss data and the development of transparent methodologies and standardized datasets have been constantly demanded since an accurate, comparable and consistent impact database is required for many applications, among others:

- to assess the influences of climate, population growth, land use and policies on trends in losses and damage (M. W. Downton et al., 2005),
- to improve risk assessment methods by calibrating and validating loss models with real data (De Groeve et al., 2013),
- to identify drivers and root causes of disasters and to deepen our understanding of damaging processes (disaster forensic; (DKKV, 2012),
- to set priorities between competing demands for national and international budget allocations (Guha-Sapir and Below, 2002),
- to evaluate policy successes and failures on the basis of trends and spatial patterns of damage,
- to think about new policies (insurance, climate policies),
- to set priorities of research funding, and
- to evaluate contributions of science to real-world outcomes (M. Downton and Pielke, 2005).

Since damage information is assumed to be collected more systematically and comprehensively for a major flood than for a small event and information is more likely to be shared among different agencies and institutions (M. Downton and Pielke, 2005), this paper explores what data is currently available to describe the impacts of the flood event of June 2013 and what can be learnt from them about the types and severities of flood impacts in different sectors. Finally, it will be discussed how good current data and information are and what could be done to create better impact data.

In consistency with the European Floods Directive (2007/60/EC) that aims to establish a framework for the assessment and management of flood risks in Europe and to reduce adverse consequences of flooding for human health, economic activities (and assets), cultural heritage, and the environment, predominantly data and impacts on these domains are explored in this paper. Further, we mainly concentrate on direct flood impacts on different scales, i.e. from the national down to the property (asset) scale, due to the above-mentioned complexities and problems that are associated with indirect and long-term effects. In the next section, the used data sources are introduced, before the actual flood impacts are presented per damage type and scale (if applicable) in Section 4.3. This part of the paper is accompanied by an overall evaluation of the data content and quality in comparison to recently published guidelines on recording disaster losses (Corbane et al., 2015; IRDR, 2015a), which will be introduced in each section dealing with a damage category. The paper ends with an overview of the data requested by the guidelines and those gathered for the flood of 2013, from which recommendations on future event documentation and loss data collection are derived.

4.2 Data sources

Three main data sources were used for this study: i) governmental reports on the flood in June 2013, ii) communications on disruptions of road and railway traffic, and iii) computer-aided telephone interviews among flood-affected residents and companies.

4.2.1 Governmental reports

General information on the flood impacts was collected from official governmental reports on the flood on the federal/national level, e.g. (BMF, 2013; BMI, 2013; BfG, 2014a; GMLZ, 2014), as well as on the subnational level of the affected states (*Länder*; e.g. (Saxon State Chancellery, 2013; Saxony-Anhalt Ministry of the Interior, 2013)). In addition, enquiries on the overall losses detailed per economic sector and affected municipality were directed at the Federal Ministries of the Interior and of Finance as well as at the respective ministries of flood-affected states in spring 2014. All ministries responded; most of them referred to the numbers reported in the application of the German Federal Government to the European Union Solidarity Fund from July 2013 (BMF, 2013). Some states updated their loss estimates; almost none provided numbers on a finer spatial level. For Saxony, some numbers are documented per administrative district (*Landkreis*) by the Saxon State Chancellery (Saxon State Chancellery, 2013); Bavaria reported costs for emergency services on the level of the seven Bavarian administrative regions (*Regierungsbezirke*; StMI, pers. communication in June 2014). The most recent numbers were published in an answer to a minor parliamentary enquiry (Parliament, 2015).

In this paper, these governmental reports were used to retrieve information on the general human and economic indicators proposed by (De Groeve et al., 2014; Corbane et al., 2015; IRDR, 2015a) on the national and the subnational level. In addition, the reports provided insight into expenses for emergency services as well as into impacts on cultural heritage and the environment.

4.2.2 Communications on disruptions of road and railway traffic

Since the European Floods Directive (2007/60/EC) addresses impacts on economic activities, disruption of transportation plays an important role. Therefore, communications on the disruption of road and railway traffic were analysed.

Road traffic

In order to capture the impact of the June 2013 flood on road traffic systematically, all communications contained in police traffic reports for the period between 15th May and 31st December 2013 with respect to flooding were filtered out and the retrieved information was saved in a database. An example of a police traffic report with respect to the flood event reads as follows: '4th June 2013, 11.30 am: B96 Hoyerswerda in the direction of Bautzen, between junctions Zeissig and Neu Buchwalde traffic obstructions in both directions due to flooding, traffic obstruction due to flood, both directions of traffic closed, a detour has been instated' (Source: (Police, 2013), own translation).

All situations that posed an obstruction to road traffic, such as a closed road on one side or on both sides, narrowing of lanes, obstructions by traffic (e.g. by emergency vehicles) as well as dangers (e.g. an increase in game crossing the road due to the flood) were further considered as traffic obstruction. Repeated identical reports were merged so that they counted as one traffic obstruction. However, should a piece of information in the report change, for example the stated section of the affected road, then the report was captured as a new traffic obstruction. A traffic obstruction was deemed to have ended, as soon as

- information in the report changed so that this could be captured as a new traffic obstruction,
- it had been reported that the street was traversable once again or that the danger on the road had passed,
- the traffic obstruction did not appear in the police traffic reports any longer.

Railway transportation

The German Railways Corporation (*Deutsche Bahn AG*; DB) provided several internal communication maps, in which the railway segments that were interfered due to extreme weather conditions or flooding are indicated. The maps cover the time period between 3rd June 2013 and 1st July 2013 with, however, some days without any information. On other days, especially at the beginning of the flood event, the maps were updated several times a day. Besides the geographic information, the type of interference, i.e. low-speed routes, platform or route closures, is reported in the maps. Further, the press releases of

the DB were used to retrieve additional information.

4.2.3 Computer-aided telephone interviews

To capture more detailed flood effects on the level of individual properties (assets, households), information from flood-affected residents and companies was systematically gathered.

Flood-affected residents

Computer-aided telephone interviews (CATI) were conducted among households in the flood-affected regions of Germany nine months after the event. On the basis of information from affected municipalities, flood reports or areas experiencing flooding, street lists were compiled and the telephone numbers of residents potentially affected by the flood were searched. For the survey on the 2013 event, a comprehensive survey was conducted, i.e. all the searched telephone numbers were contacted. In total, 1652 interviews were completed between 18th February and 24th March 2014 with affected residents. In the survey, the term 'affected' was defined as a household that had suffered (financial) flood damage in May or June 2013. The spatial distribution of the surveyed households is illustrated in Figure 4.2b.

Similarly to former surveys (see (Thieken et al., 2005; Kienzler et al., 2015), the main objective was to investigate how financial flood losses are influenced by other factors, for example flood characteristics or private mitigation. However, after the June 2013 flood, some questions were posed regarding flood effects on health and wellbeing as well as on the assessment of the (governmental) aid for reconstruction. Overall, the questionnaire addressed the following topics (in the order of appearance):

- Hydraulic characteristics of the flood at or in the building;
- Early warning and emergency measures;
- Contamination of the floodwater;
- Evacuation;
- Clean-up work and recovery;
- Adverse flood effects, including effects on health and wellbeing, and perceived severity;
- Physical and financial flood damage to the building and the household contents;
- Building ownership and further information on the residential building (or the rented apartment);
- Previously experienced flood and flood awareness;
- Long-term preventive and protective measures undertaken by the affected household and motivation (not) to do so;

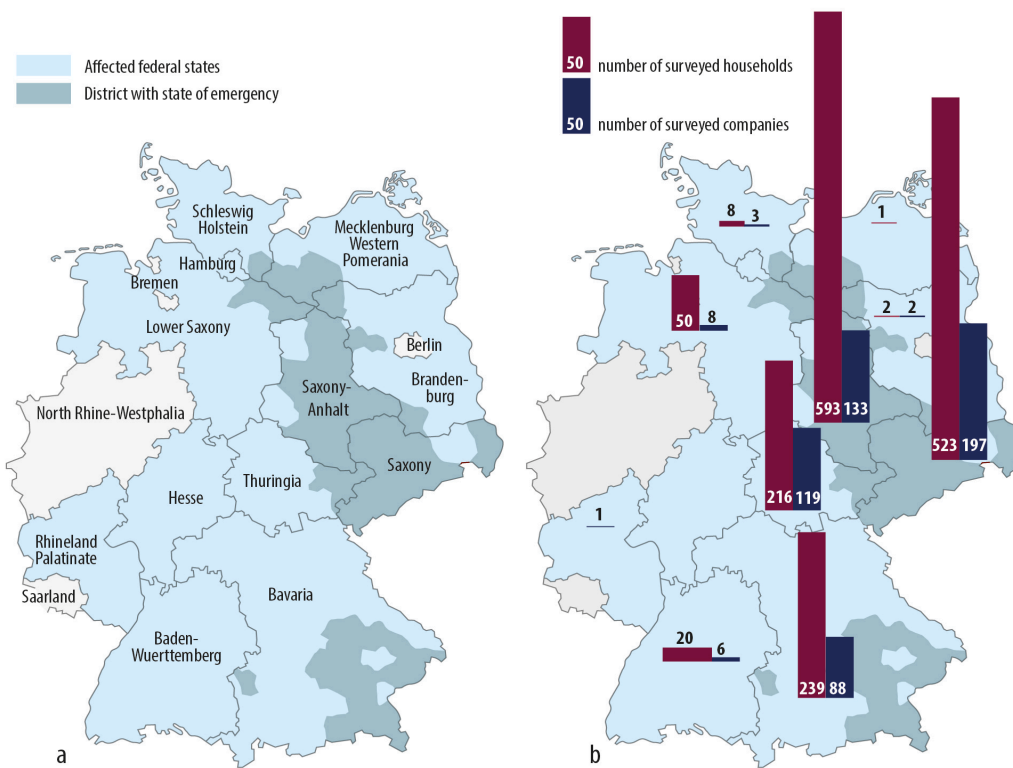


Figure 4.2: Geographic overview of affected federal states and districts that declared a state of emergency (a) as well as the number of surveyed households and companies (b).

- Aid and financial compensation;
- Socio-demographic information.

Information on health effects and the perceived severity of different damage types presented in section 4.3.1.2 of this paper are based on this survey.

The above-mentioned former surveys that were conducted a few months after the floods in 2002, 2005 and 2006 (see (Kienzler et al., 2015) were complemented by a follow-up household survey in autumn 2012 (n = 910 households), i.e. ten years after the flood in 2002. The survey focused on long-term (health) effects of the flood as well as property-level mitigation measures. These data are used in section 4.3.1.2 to illustrate short and long-term flood effects on affected residents.

Flood-affected companies

Companies that had been affected by the flood in June 2013 were surveyed with regard to the losses incurred and the circumstances influencing the type and amount of damage before, during and after the event. For the sampling procedure, street lists were compiled on the basis of information obtained from municipalities, flood reports or mapped inundation areas and were further used to determine the telephone numbers of companies potentially affected by the flood. To include some large-sized companies in the random sampling as well, these were searched additionally from flood reports.

Affected companies were surveyed from mid of May to mid of July 2014. Again, the term 'affected' was defined as an enterprise that had suffered (financial) flood damage. The information was gathered through CATI with the individual in the company who was best placed with providing information on the flood. In total, 557 interviews were completed. The spatial distribution of the surveyed companies is illustrated in Figure 4.2b. The interviews lasted 15 to 35 minutes on average; the questionnaire covered approx. 90 questions on the following topics (in the order of appearance):

- Company description (sector, size, number of buildings, assets, perceived vulnerability with regard to flooding, etc.);
- Hydraulic characteristics of the flood on the company grounds;
- Early warning and emergency measures;
- Contamination and clean-up work;
- (Financial) flood damage (to buildings, operational facilities, merchandise, products and warehouse inventory, motor vehicle inventory; due to interruptions of operations);
- Reconstruction, compensation, plans to relocate;
- Previously experienced floods;
- Long-term preventive and protective measures at the property-level.

Results presented in section 4.3.4 of this paper are based on this survey.

4.3 Impacts of the flood in June 2013

4.3.1 Flood impacts on human health

The effects of flooding on health can be significant and may concern both, physical and mental health. Physical health effects are deaths due to drowning, electrocution, heart attacks, vehicle-related accidents etc. as well as injuries, illnesses and infections that require medical assistance and result directly from the flood, for example due to a lack of sanitation, contaminated water, chemical hazards or mildew (within wet or insufficiently reconstructed buildings; (IRDR, 2015a). Mental health effects might be acute or long-term due to a loss of family members or friends, displacement, destruction of homes, delayed recovery and water shortages (Menne and Murray, 2013). Recurrent flash backs, nightmares, sleeplessness (insomnia), angst, panic and depression are some examples for mental health effects and might even lead to a posttraumatic stress disorder (PTSD). Limited access to health facilities during and after a flood event, in particular medical treatment and nursing of flood-affected or evacuated people suffering from chronic diseases, is a further issue related to this domain (Menne and Murray, 2013), but this is usually reported as part of the physical and economic damage (see section 4.3.2).

Human indicators in disaster loss databases are commonly related to physical health or the displacement and movements of people caused by the flooding; mental health effects are usually not explicitly reported. For example, (IRDR, 2015a) proposes the numbers of dead, missing, injured and exposed people as primary human impact indicators, while the numbers of homeless, evacuated, relocated and affected people are regarded as secondary. Some indicators, e.g. dead and missed people, are mutual exclusive, others, e.g. homeless, evacuated and relocated people, are not since they correspond to consecutive management phases of a damaging event (IRDR, 2015a).

In the European guidance for recording disaster losses (Corbane et al., 2015), the number of deaths, missing people as well as directly affected people are recommended as minimum information that should be recorded with regard to human losses. All information should be provided on the NUTS 2 or NUTS 3 level (NUTS stands for Nomenclature of Territorial Units for Statistics). In Germany, NUTS 2 units mainly correspond to the 38 (former) administrative regions (*Regierungsbezirke*), while NUTS 3 units comprise the 402 urban and rural administrative districts (*kreisfreie Städte und Landkreise*). Since almost no information was provided for administrative levels below the federal states, an overview of human loss indicators (see 4.1 can currently be provided for this level (NUTS 1) only.

Overview of human loss indicators for the flood in June 2013

Table 4.1 illustrates that 14 people lost their lives in the June 2013 flood. Five fatalities can be allocated to Saxony-Anhalt (Saxony-Anhalt Ministry of the Interior, 2013), three to Baden-Württemberg (DieWelt, 2013), two to Bavaria (BMF, 2013) and one to Saxony (BMF, 2013). In fact, in the application of the German Government to the European Union Solidarity Fund, only eight (immediate) fatalities were reported. This number was later corrected to 14 (GMLZ, 2014). In addition, 128 people were injured and approximately 80,630 were evacuated in eight different federal states (GMLZ, 2014). In

general, 600,000 people in 1,800 municipalities were affected by the flood (BMF, 2013) ; Table 4.1). However, the term 'affected' is not clearly defined, nor is its relation to the categories 'injured' and 'evacuated' in terms of ex-/ inclusiveness. Due to this ambiguity, (IRDR, 2015a) recommends using exposed people, defined as the number of people who permanently or temporarily reside in the hazard area before or during the event, in a first instance, as this number can be more reliably determined from census data and geographic information on the flooded area. In principle, the disaggregated population density is mapped for all of Germany (Thieken et al., 2006a)) and could be used to determine the number of exposed people. However, the inundated areas depicted in Figure 4.1 were derived from satellite images that mainly contain inundated areas along the big rivers. Smaller inundated areas, especially at the beginning of the event, are not captured by these images. Therefore, the number of people exposed to the June 2013 flood has not been determined.

As a further human-related indicator, the number of helpers in emergency services and relief or aid organisations totalling to more than 1 M person days Germany was often reported in governmental reports dealing with the June 2013 flood and hence added to Table 4.1 although this indicator is not considered in any guideline for disaster documentation. This number does not include volunteers who helped to cope with the flood (damage) without being organised in an emergency service or an aid or relief organisation. With regard to the 2013 flood, the numbers illustrate that the magnitude of responders and helpers is similar to the amount of people directly affected by this widespread flood event.

Table 4.1 clearly demonstrates that the reporting of the federal states was not focussed on human losses. Only in the Bavarian report (Annex 6 in (BMF, 2013), numbers for all categories of Table 4.1 were mentioned. In most of the states, no numbers were explicitly reported although estimates are provided for the national level. Therefore, more transparent and systematic reporting procedures are needed to evaluate the quality of the aggregated data and to reach a comprehensive report on human losses that fulfils the minimum requirements proposed by Corbane et al. (2015) or IRDR (2015a).

Flood impacts on affected residents and perceived severity

To obtain more insights of the variety and severity of flood impacts on affected residents, the surveyed households (see section 4.2.3.1) were asked to indicate from a list of ten possible flood damages, which of these had affected them in June 2013 and how seriously they perceived each of the witnessed damage type. The answers could be graded on a scale of 1 (= damage was not serious at all) to 6 (= damage was very serious). The perceptions of all respondents to a particular damage type resulted in average assessments between 3.0 and 4.6 (Figure 4.3). The damage types that were assessed on average with 4.0 or worse – and were thus evaluated as serious – cited as a priority and included psychological stress or other stresses, reinstatement works (e.g. cleaning or repairs), supply problems (e.g. no electricity, water etc.) as well as damage to buildings and household contents (Figure 4.3). This highlights that mental health issues and disruption of daily life are of great importance for affected people.

Table 4.1: Overview of human loss indicators as recommended by (Corbane et al., 2015) or (IRDR, 2015a) accessible for the flood in June 2013 per federal state (data sources: BMF, 2013 including annexes; GMLZ, 2014 without annexes; ND: no data reported)

Federal State	Number of people					Number of helpers
	Died	Missed	Injured	Affected	Evacuated	
Baden-Wuerttemberg	3	human damage is mentioned, but not specified by numbers		ND	at least 200	18,394
Bavaria	2	0	9	80,000	13,600	40,000
Brandenburg	ND	ND	ND	25,000	3,500	ND
Hamburg	ND	ND	ND	ND	ND	ND
Hesse	ND	ND	ND	ND	ND	ND
Mecklenburg-Western Pomerania	ND	ND	ND	ND	ND	ND
Lower-Saxony	ND	ND	ND	ND	ND	ND
Rhineland-Palatinate	ND	ND	ND	ND	ND	ND
Saxony	1	ND	21	ND	33,700 (8,270 to 16,000 per day)	76,161
Saxony-Anhalt	5	ND	ND	ND	88,000	>120,000
Schleswig-Holstein	ND	ND	ND	ND	ND	660
Thuringia	ND	ND	ND	ND	ND	ND
Overall	14	ND	128	600,000	80,630	871,000 regional and 217,000 federal helpers (in person days)

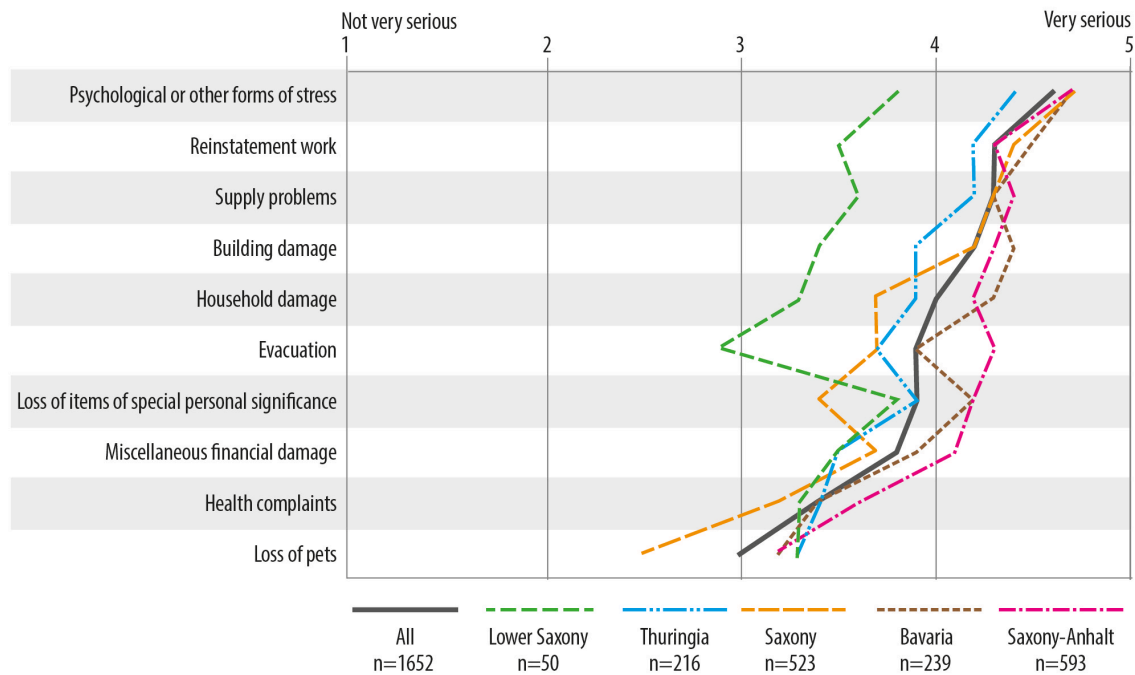


Figure 4.3: Average perception of the severity flood impacts witnessed by flood-affected residents and assessed on a scale of 1 (= impact was not very serious) to 6 (= impact was very serious).

Figure 4.3 further highlights that the perception of residents from Bavaria and Saxony-Anhalt is above average: six or seven types of flood impacts were on average assessed by 4.0 or worse. In contrast, residents from Thuringia and Lower-Saxony perceived most impacts as less severe. In Thuringia, only averages for three types of impact (psychological stress or other stresses, reinstatement works and supply problems) exceeded 4.0. In Lower-Saxony, there is even no impact that was perceived that seriously (Figure 4.3). This pattern reflects the hydrological severity of the flood as depicted in Figure 4.1.

Figure 4.3 further elucidates that the flood situation did not only have a great impact on the mental health of the affected persons, but also – to a lesser degree – on their physical health. To shed some light on the underlying medical conditions, all respondents who had reported mental or physical health effects (84.4%) were surveyed in more detail. In an open question regarding the type of stress undergone and grievances in detail, uncertainty about the future, worries with regard to family, existence and subsistence, and the future, fears of loss, panic, trauma, shock, crying fits or nervous breakdowns were cited most frequently. In addition to these, sleep disorders or nightmares were mentioned, as well as feeling restless, tense and nervous or agitated.

Physical symptoms manifested themselves most frequently in the form of states of exhaustion or lack of sleep; joint, bone, muscle or nervous complaints; infections, inflammation, (skin) irritations or the exacerbation of pre-existing illnesses or conditions. It is noteworthy that the management of the flood situation aggravated in the case of persons with chronic illnesses or conditions.

Psychological stress is, however, not limited to the period of the actual flood event,

but can still remain in existence a long time afterwards. The above-mentioned surveyed group of affected persons with health impairments was therefore additionally asked about the extent to which they were still stressed by the flood event at the time of the interview (answer scale from 1 = 'I am not stressed by it any longer /I feel like I did before the event' to 6 = 'I am still very stressed by it'). Slightly more than a third of the respondents (35%) were still very or extremely stressed as a result of the flood as much as nine months after the event (answers 5 and 6); by contrast, a further third hardly felt stressed any longer or not at all (answers 1 and 2).

However, the 2013 flood was still very prevalent in the minds of all the residents affected. This is clearly evident from the results to the question: 'How often have you thought about the June 2013 flood over the past six months?' At the time of the survey, i.e. approximately nine months after the event, 35% of all the affected persons still thought about the 2013 flood once or several times a day, 50% still at least once a month to several times a week (Figure 4.4). This distribution of answers clearly differs from the answers of affected persons who were asked the same question in autumn 2012, i.e. ten years after having witnessed the severe flood of August 2002 (Figure 4.4). On the one hand the comparison illustrates the extent to which a flood can change daily life and thinking, on the other hand the long-term and ongoing impression that an extreme flood can leave behind is evidenced: ten years after the event of August 2002, only 20% of respondents stated that they never thought of the event in the six months preceding the interview. Nevertheless, 8% still thought of it approximately daily. However, it is worth noting that the thoughts about the flood were not negative throughout: the experience of solidarity and a sense of community were often positively highlighted.

According to Kuhlicke et al. (2014), affected households in Saxony that had been flooded up to three times in recent years (i.e. in 2002, 2006 or 2010, and 2013), perceived the flood impacts more severe than households that had been affected by flooding in 2013 for the first time. In addition, households that already suffered flood damage several times thought considerably more often about resettlement which might have severe consequences for flood-prone communities that do not get flood protection (Kuhlicke et al., 2014).

In conclusion, the survey among flood-affected residents highlights the importance of physical and particularly mental health issues caused by flooding. This is contrasted by the little attention this domain received in official governmental flood documentations and reports in Germany.

4.3.2 Overview of impacts on economic activities (and assets) on the regional and national scale

In industrialised countries, economic or financial losses caused by natural hazards are a major concern and achieve a lot of attention during and after disastrous events. Quick and reliable loss estimates are requested by the (re-)insurance industry as well as by governmental institutions. However, data on economic or financial losses are fairly uncertain (B. Merz et al., 2004; M. Downton and Pielke, 2005; M. W. Downton et al., 2005). To assess impacts of natural hazards on the economic activities according to the European guidance for recording disaster losses (Corbane et al., 2015), indicators describing the physical number of damaged items should be distinguished from indicators that

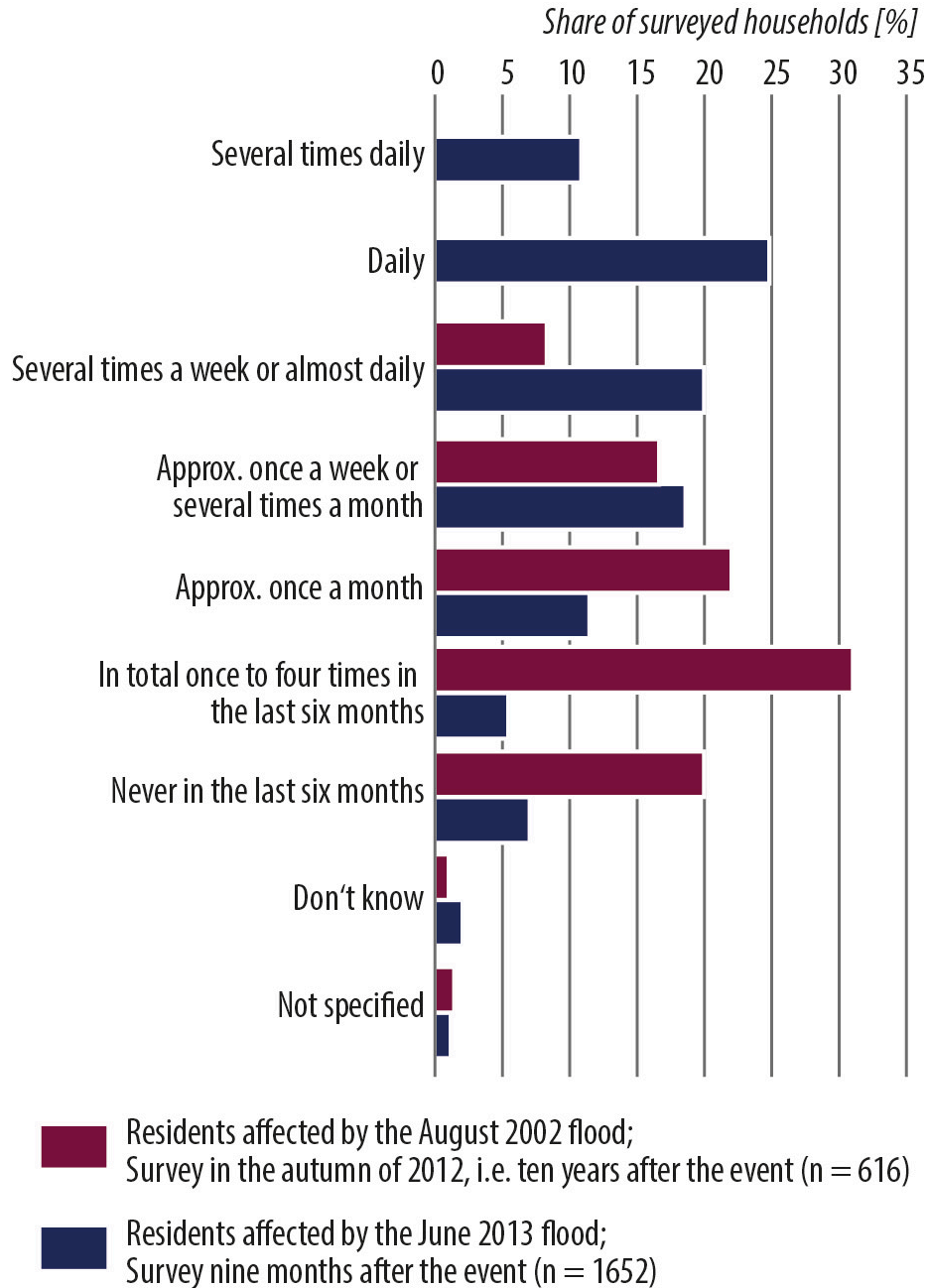


Figure 4.4: Frequency of the flood memories of affected private households in the six months preceding the survey (information is given in percentages of respondents; the first two categories of answers – (several times) daily – were not provided to the respondents in autumn 2012).

quantify financial losses (costs). As a minimum requirement, it is proposed that physical damage indicators should deliver information on the number of damaged or destroyed houses, educational centres (e.g. schools, kindergartens) and health facilities (e.g. hospitals). Optionally, further aggregated damage indicators can be provided, i.e. on the total area of destroyed or affected crops and woods (in hectares), the number of lost four-legged livestock, the number of damaged or destroyed governmental and administrative buildings, the number of damaged or destroyed industrial and commercial facilities as well as the length of damaged or destroyed roads and railways (in kilometres) and the number of damaged or destroyed transportation infrastructure such as bridges, airports and marine ports (Corbane et al., 2015). These physical damage indicators are further translated into economic monetary indicators, in particular into the overall direct tangible loss, i.e. the monetary value of the physical damage to capital assets. This loss should ideally be disaggregated over all sectors or loss owners and accompanied by information on the loss bearer. Expenditures for emergency services and clean-up are further costs to be recorded optionally (Corbane et al., 2015).

As a minimum requirement the overall direct damage should be reported on NUTS 2- or NUTS 3-levels (see section 3.1). As outlined above, almost no information was provided for administrative levels below the state-level (NUTS 1). Therefore, the overview of damage and losses can currently be provided for the NUTS 1-level only. Table 4.2 summarises the information that was collected for the flood of June 2013 on the minimum indicators on direct damage and economic loss as proposed by (Corbane et al., 2015).

Table 4.2: Damage and loss indicators as recommended by (Corbane et al., 2015; IRDR, 2015a) available for the flood of June 2013 in Germany per federal state (Data sources: (BMF, 2013; Saxon State Chancellery, 2013; Parliament, 2015), Brandenburg pers. communication in May 2014; Federal Parliament, 2015; ND: no data reported).

Overview of financial losses

Table 4.2 illustrates that data on the physical damage indicators are so fragmentary that they do not allow a sound interpretation. Only from the Saxon report (Annex 14 in BMF (2013) and Saxon State Chancellery (2013) , information for all minimum indicators recommended by Corbane et al. (2015) could be retrieved. Therefore, the overall (direct) financial loss given in Table 4.2 is further used as main indicator for the economic impact.

According to the Federal Ministry of Finance (BMF, 2013), the overall losses that incurred by the June 2013 flood amounted to EUR 8,154 M. This figure was communicated by the Federal Government in its application to the European Union Solidarity Fund mid of July 2013. The answers to our queries in spring 2014 (see section 4.2.1) indicate that this estimate will probably turn out to be too high. The most significant corrections were communicated by Saxony-Anhalt, the Federal Government and Saxony. The loss in Saxony-Anhalt, originally estimated at EUR 2.699 b, was reduced to between EUR 1.5 and 2 b (written communication from the Saxony-Anhalt Ministry of Finance dated 15th April 2014). In addition, the damage to the infrastructure of the Federal Government – this involves damage to the federal assets regarding railways, motorways and navigable waterways, as well as to the administrative buildings of the Federal Government – clearly lies below the EUR 1.484 b estimated initially (Table 4.2). In its response to a

Table 4.2: Damage and loss indicators as recommended by Corbane et al. (2015) and IRDR (2015) available for the flood of June 2013 in Germany per federal state (Data sources: BMF, 2013; Saxon State Chancellery, 2013; Brandenburg pers. communication in May 2014; Federal Parliament, 2015; ND: no data reported)

Federal State	Number of damaged or destroyed			Overall financial loss	
	Houses	educational centres (e.g. schools, kindergartens)	health facilities (e.g. hospitals)	reported in BMF (2013) [million EUR]	funds claimed by 30 June 2015 (Federal parliament, 2015) [million EUR]
Baden- Wuerttemberg	3,697	129	ND	74	59
Bavaria	13,000	ND	ND	1,308	760
Brandenburg	1,100	ND	ND	92	81
Hamburg	0	0	0	1	0
Hesse	ND	ND	ND	21	6
Mecklenburg- Western Pomerania	0	ND	ND	8	6
Lower-Saxony	ND	ND	ND	64	41
Rhineland- Palatinate	0	ND	ND	4	6
Saxony	13,000	widespread disruption, no numbers reported	no disruptions in hospitals	1,923	1,171
Saxony-Anhalt	ND	ND	ND	2,699	1,496
Schleswig- Holstein	ND	ND	ND	25	14
Thuringia	ND	ND	1 hospital (power failure)	452	187
Federal Government		— not applicable —		1484	114
Emergency response					71
Insured loss					1650
Total	>32,000	disruption mentioned, no numbers reported	ND	8,154	5,664

minor parliamentary enquiry concerning the flood relief funds, the Federal Government recently assumed that only a sum of approximately EUR 114 M was in question (Parliament, 2015). On the contrary, the Freestate of Saxony requires an additional amount of EUR 480 M for all repair works (Parliament, 2015). The same enquiry also provides recent amounts of losses that have been claimed to governmental relief funds by end of June 2015 (see Table 4.2). In contrast to the application to the European Union Solidarity Fund, these numbers, however, seem to include neither expenses for emergency response, nor insured losses. Losses that property owners bear themselves are probably also neglected in these figures. With these corrections and considerations, the total direct loss will probably range between EUR 6 and 8 b.

Even the most recent numbers indicate that the compilation of the overall financial losses is still preliminary. Many of the damage claims have not been resolved conclusively and to some extent unforeseeable losses that had been incurred but have not been reported may still appear. According to the administrative arrangement for the Act to Establish Reconstruction Funds passed in 2013, applications for reconstruction aid could be submitted until 30th June 2015. The period for final approval was recently extended to 30th June 2016 (Parliament, 2015). Only thereafter will it be possible to compile a conclusive loss statement.

Nevertheless, it is already possible to look at the spatial and sector-wise distribution of losses. Table 4.2 reveals that Saxony-Anhalt, Saxony and Bavaria are the three most affected federal states in terms of financial losses, each covering about 20% to more than 30% of the overall loss. For the flood of 2013, approximately 22% of all losses incurred in private households, 19% in the industrial and commercial sector, 7% in agricultural and forestry and almost 50% in governmental domains (infrastructure and emergency services; (BMF, 2013). This distribution can, however, considerably vary between federal states as is illustrated in Figure 4.5 taking Bavaria and Saxony as examples. While in Bavaria two thirds of the losses are allocated to private households as well as the commercial and industrial sectors, losses to the state and municipal infrastructure amount to around 60% in Saxony (Figure 4.5). This can be divided into 20% state infrastructure and 40% municipal infrastructure. With respect to state infrastructure, the biggest damage can be attributed to surface water bodies and flood defence systems belonging to Water Body Category I. In regard to municipal infrastructure, the largest share of the damage is allocated to streets and bridges, as well as to flood defence systems belonging to Water Body Category II (Saxon State Chancellery, 2013). More details about the type of the damage infrastructure were unfortunately not available for Bavaria. So the reason for the differences is still unclear. In addition the sector-wise loss distributions are based on the first loss estimates of the federal states and have not been updated. Further investigations could be carried out when the final losses and their allocation are recorded.

It is noteworthy that flood losses in Germany are generally divided into the sectors private households, industry and commerce, agriculture and forestry, state and municipal infrastructure as well as costs for emergency services in loss statements of the Federal Government and the federal states. To some extent, losses to cultural facilities, sport and recreational centres, churches and research institutions are also provided. Unfortunately not all the sectors are systematically dealt with in every flood event and state, and the definitions, which damage should be reported in which category, are not managed uniformly over space and time. This can be another reason for the differences in the loss

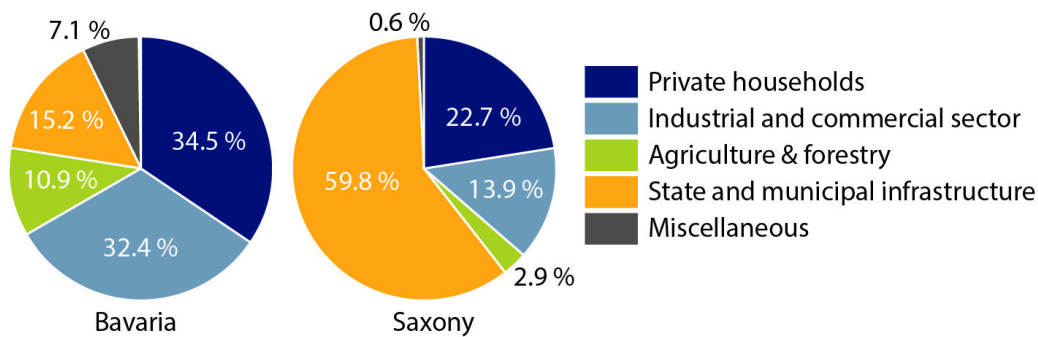


Figure 4.5: Distribution of the overall direct losses of the flood event in June 2013 according to loss-incurring sectors in the federal states of Bavaria (EUR 1.3 b) and Saxony (EUR 1.9 b) according to the Federal Ministry of Finance (BMF, 2013).

allocations reported by Saxony and Bavaria (see Figure 4.5). Moreover, in the case of changes to the overall loss estimates, the distribution among the sectors is often not updated. This considerably hinders a comparison of the overall financial or economic losses of different flood events and in different federal states (Thieken et al., 2010).

Of all losses, the insurance industry in Germany has covered around EUR 1.65 b (GDV, 2015). With EUR 900 M, the most insured damages occurred in the Freestate of Saxony, followed by Saxony-Anhalt (EUR 310 M), Bavaria (EUR 270 M) and Thuringia (EUR 140 M; GDV, 2014). 142 major claims – this equals to individual claims exceeding EUR 500,000 – were reported to the Association of the German Insurance Industry (GDV) with an overall damage total of EUR 257 M (GDV, 2015).

In addition, the Federal Government and all federal states launched flood relief funds containing a total amount of EUR 8 b. The parties agreed that losses of private households can be compensated up to 80%, whereas repair costs for damaged state and municipal infrastructure can be covered up to 100%. Further, private donations of EUR 108 M have been available (BMF, 2013). Altogether, the funds available for reconstruction exceed the total damage. Therefore, more reliable methods for first and immediate damage estimates are required. In order to evaluate the reasonability of first loss estimates reported by the federal states to the Federal Government, not only the estimation methods applied should be documented, but the numbers of physically damaged (or destroyed) items should be reported by default as proposed by (Corbane et al., 2015). For a first economic loss estimate, the number of damaged or destroyed items could be combined with standard repair costs per item. Further, damage indicators should be clearly defined and agreed upon so that the loss documentation of different states and events can be better compared.

Expenses for disaster response and emergency services

With the 2013 flood situation, distinctive needs arose for disaster response and appropriate support by personnel and technical resources in the affected federal states. While Baden-Wuerttemberg and Bavaria managed the flood situation predominantly with their

own teams and resources, as well as via bilateral cooperation, states like Saxony, Thuringia and Saxony-Anhalt used the coordination service offered by the German Federal Joint Information and Situation Centre (GMLZ). Further support was provided by federal states that were not affected by the flood, and in addition, the worst affected states mutually supported each other (BMI, 2013).

The assistance requests of individual federal states had already been brought to the attention of the GMLZ on 2nd June 2013. In total, the GMLZ processed 43 assistance requests from five affected states. Subsequently, around 5.15 M sandbags, 5,700 emergency rescue personnel and transport services for 1,000 tonnes of material were arranged in the course of the flood situation by 15th June 2013 (GMLZ, 2014). Material shortages occurred in the number of available sandbags. To meet the demand of the affected areas, the GMLZ arranged for five M sandbags from other federal states and Germany's European neighbours (BMI, 2013).

In total, 1.7 M voluntary workers are organized in (volunteer) fire brigades, relief and aid organisations as well as the German Agency for Technical Relief (THW). They form the cornerstone of Germany's disaster response. By 5th July 2013, the deployment of local fire brigades and aid organisations added up to around 871,000 person days (GMLZ, 2014); Table 4.1. Additionally, the Federal Government supported affected municipalities and states with its own resources. In the process, the Ministry of the Interior (BMI) coordinated the support staff of the Federal Police and the THW, while the Ministry of Defence coordinated the Federal Armed Forces staff. From the outset of deployment, the Federal Government provided help in the form of around 216,000 person days ((GMLZ, 2014); Table 4.1). Through this, the Federal Government incurred additional costs to the tune of EUR 59.9 M (BMF, 2013).

In general, the costs for emergency services and response are included in the overall loss estimates shown in Table 4.2. Three federal states explicitly reported their response costs, which amount to EUR 8.89 M in Bavaria (by 25th June 2014), EUR 1.70 M in Schleswig-Holstein and EUR 0.99 M in Thuringia. Related to the total amount of the other direct damages as of July 2015, the response costs of these federal states amount to 1.2%, 12.1% and 0.5% of the direct damage, respectively, which considerably differs from the 2% of the direct damage that is often used to estimate response costs ex-ante (see (Penning-Rowsell and T. Wilson, 2006; Pfurtscheller and Thieken, 2013). Since publicly accessible data in this domain is scarce despite well-established costing and reporting procedures, it is recommended explicitly reporting costs for emergency services and disaster response in loss documentations.

4.3.3 Impacts on economic activities – traffic disruptions

Apart from the direct damage to assets presented in Section 3.2, floods can have further adverse impacts on economic activities – also far beyond the flooded area –, for example if the transportation systems are affected. In general, roads, railways, waterways as well as airports play an important role for the transportation of goods and people. Therefore, traffic disruptions during the flood in June 2013 are analysed in this section although in the guidelines on loss documentation (Corbane et al., 2015) damage to the transportation system is only considered in terms of physical damage (see section 3.2). Traffic disruption include complete interruption of operations due to route closures as well as restrictions

to normal operations on damaged routes, for example: on dual track/carriage routes only one track/lane is usable, low-speed routes or diverted routes are implemented, or the transportation system is replaced by another mode of transport (e.g. railways are replaced by buses).

In the longer term, disruption of a particular mode of transport might lead to a loss of customers or a decline in customer satisfaction, for example with railway services. Such effects of flood events are, however, difficult to separate from other influencing factors. Therefore, the analysis focusses on traffic disruptions and interferences.

Disruption of navigation

If rivers are used as waterways, river reaches will be closed for navigation when a specified water level, i.e. the highest navigable water level (NavWL), is exceeded at the respective reference gauge. As depicted in Figure 4.1, such water levels were observed in June 2013 at several gauges on different Federal waterways and lasted for 15 consecutive days at maximum. The internationally important waterway at the Lower Rhine was, however, not affected by this flood (BfG, 2014a).

Disruption of the shipping traffic might last longer than the durations given in Figure 4.1, since the Federal Waterways and Shipping Administration first has to screen for new obstacles in the navigation channel before they can be regularly navigated again.

So far, no monetary assessments of the disruption of waterways have been undertaken (BfG, 2014a). Related costs are therefore not included in the figures of Table 4.2.

Disruption of road traffic

The flood event of 2013 led to flooding, dangerous situations and closures of streets in city centres, closures of regional roads and even of a Federal motorway (*Autobahn*). In total, 700 km of roads and 150 bridges were damaged in Germany (BMF, 2013). These impacts resulted in interferences of road traffic across almost all of Germany.

The chronological sequence of traffic obstructions on German roads is illustrated in Figure 4.6 and reflects the general development of the flood as described by Schröter et al. (2015) (see also section 4.1). Isolated reports of flood-related traffic obstructions emerged as early as 19th May 2013. As of 26th May, the flooding of the rivers Weser and Leine, particularly in the administrative districts of Braunschweig and in the Hanover region in Lower Saxony, was the presumed reason behind road closures. As of 31st May, numerous traffic obstructions occurred in almost all of the federal states, especially in the most affected, i.e. Bavaria, Saxony and Saxony-Anhalt. On 2nd June 2013, traffic obstructions had reached a maximum nationwide (Figure 4.6). Due to the flood developing over several days, it was only as of 6th June 2013 that traffic obstructions from the flood occurred at the lower reaches of the River Elbe.

More than 75% of reported traffic obstructions can be traced back to the actual flooding of streets or to flood danger (Figure 4.6). In addition to these, landslides especially in Baden-Wuerttemberg (Keller and Atzl, 2014) together with numerous uprooted trees contributed to approximately 20% of obstructions in road traffic. In more than 60% of the events, the roads had to be closed completely in both directions. Of the traffic obstructions, 10% occurred in city centres and on other urban roads. The federal trans-regional road network was affected by more than 50% of the traffic obstructions.

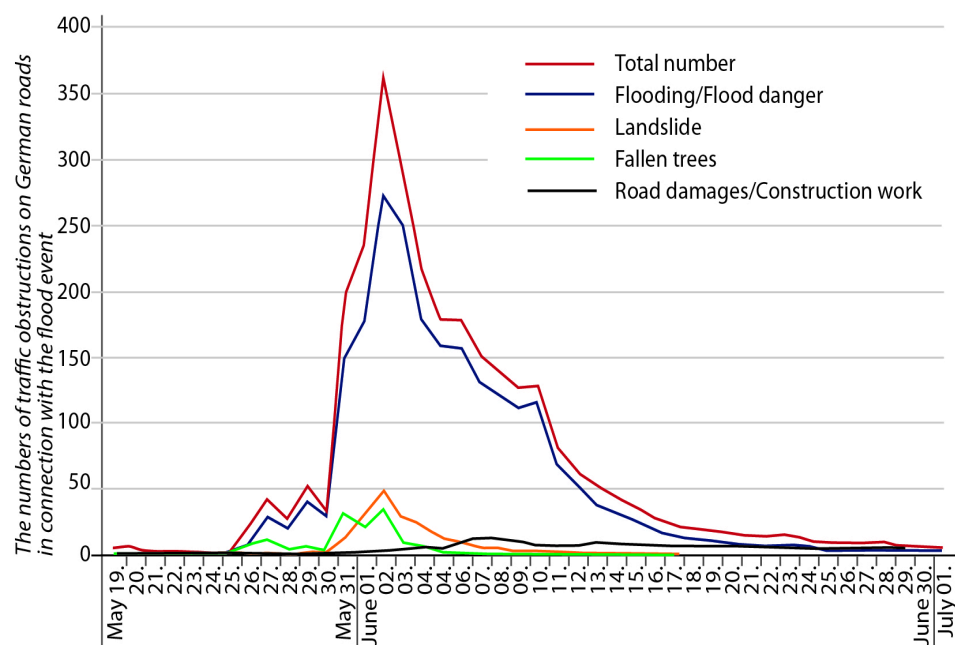


Figure 4.6: Chronological sequence of the number of traffic obstructions on German roads related to the flood event in the period from 19th May to 1st July 2013, subdivided into causes and as a total number.

Figure 4.7 illustrates the spatial distribution and duration of the traffic obstructions on an administrative district level. With traffic obstructions lasting more than 14,500 hours in total, traffic in Saxony was the most curtailed. The Saxon administrative districts of Meissen, Leipzig district, city of Dresden, Saxony's Swiss-East Ore Mountains and Central Saxony were equally affected by a very high incidence of traffic obstructions, as was the Hanover administrative region in Lower Saxony. However, it took only days to remove most of these after the flood had been cleared. In the administrative districts of Traunstein (Bavaria) and Tuebingen (Baden-Wuerttemberg) extensive construction work to damaged roads had to be conducted, which to some extent still affected regional traffic months afterwards.

The administrative districts denoted in red in Figure 4.7 therefore all display a high overall duration of traffic obstruction. This information does not, however, indicate any decisive conclusions arrived at as to the actual indirect cost due to detours etc. incurred.

Disruption of railway operations

One company that has been considerably affected by the flood event of 2013 is the German Railways Corporation (*Deutsche Bahn AG*). In June 2013, mudslides as well as the submergence or under-washing of tracks led to a variety of interferences of the normal rail traffic (Figure 4.8). Thus the morning of 3rd June 2013 saw 60 route closures and interferences, of which approximately 25 were in Bavaria as well as approximately 30 in Thuringia and Saxony. In the afternoon, further restrictions were reported on up to 15 routes. These could be lifted to some extent in the subsequent days. From 8th June 2013, when the flood attained the middle reaches of the River Elbe, this number increased to

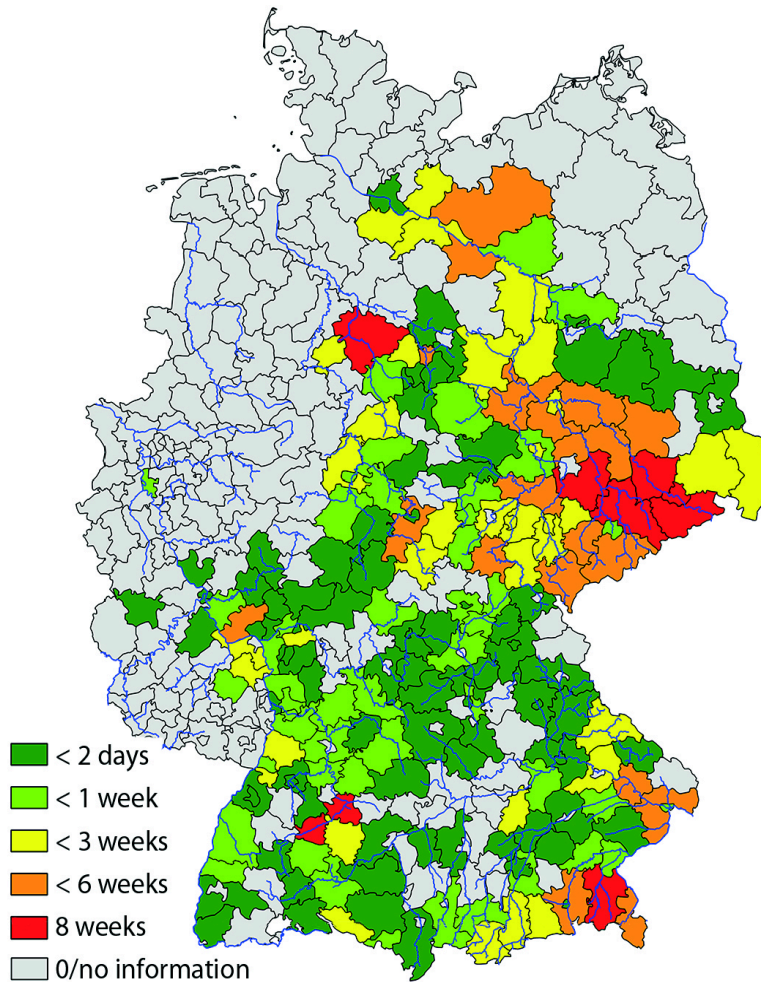


Figure 4.7: Overall duration of the obstructions in road traffic induced by the flood event shown in terms of administrative districts.

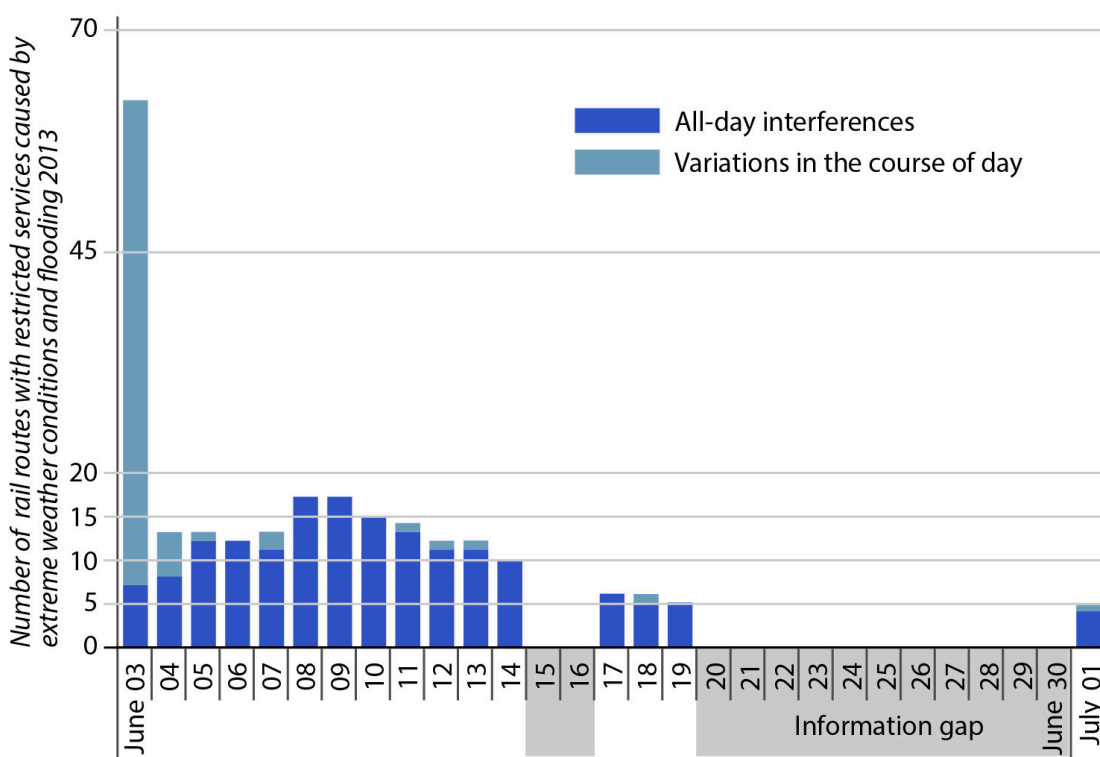


Figure 4.8: Number of train routes with disruptions or interferences caused by extreme weather conditions (low-speed routes, platform or route closures; Information source: German Railways Corporation's internal survey maps detailing interferences caused by extreme weather, in part updated several times a day).

17 routes.

In the medium term, primarily long-distance traffic had to bear the brunt of the flood after the dyke breach at Fischbeck on 10th June 2013 (Figure 4.1a) resulted in the flooding of an approximately 5 km long stretch at the town of Stendal. This meant that the high-speed rail line between Berlin and Hanover had to be interrupted until 4th November 2013, i.e. for almost five months (Bahn, 2013). For this reason, important connections between Berlin and the Ruhr district, Cologne and Bonn, as well as between Berlin and Frankfurt (am Main) were affected. A replacement timetable with diversions was deployed but led to travel time extensions of 30 to 60 minutes (Bahn, 2013). As a result, approximately 10,000 passenger trains and more than 3,000 goods trains had to be diverted (Deutsche Bahn, 2014). Due to the travel time extension, a third of passengers took a flight to or from Berlin, or continued their journey by car or intercity coach (Deutsche Bahn, 2014). The financial impacts of this disruption on the railway company itself and on further economic activities are difficult to evaluate and are hence not included in the numbers presented in Table 4.2.

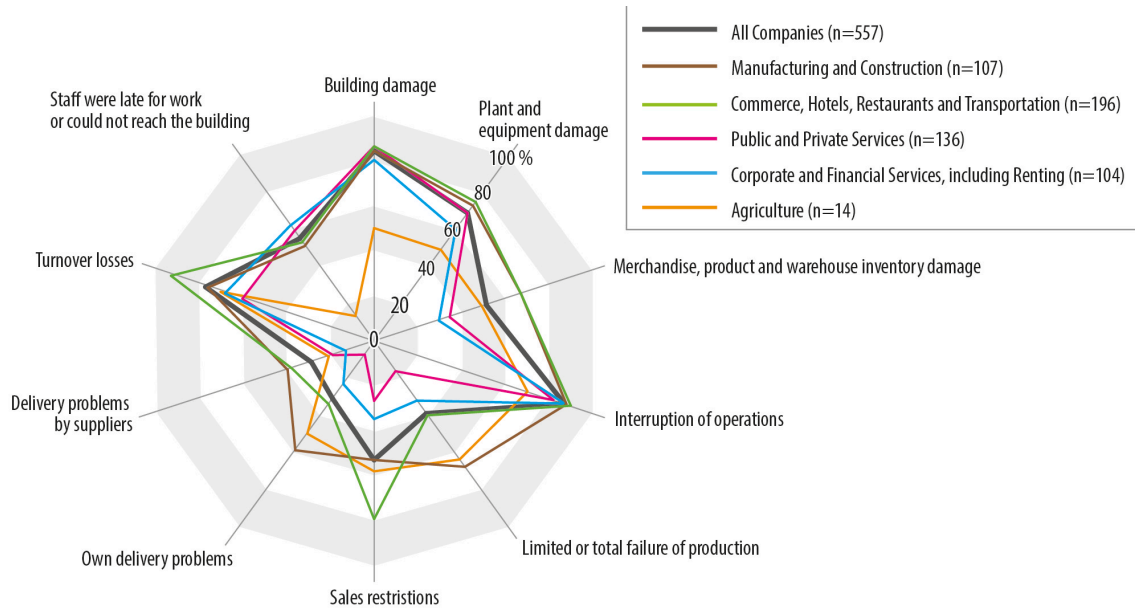


Figure 4.9: Share of surveyed companies that reported on the different flood impacts.

4.3.4 Impacts on economic activities at the asset scale: with a focus on business interruption of individual companies

Although the European Floods Directive (2007/60/EC) explicitly addresses the effects flooding has on economic ACTIVITIES, current loss guidelines and reporting emphasise adverse effects on ASSETS. In order to further complement the nationwide data that was presented in section 4.3.2 and focused on losses to assets, this section looks at the diverse impacts floods can have on individual companies. The data from the survey described in section 4.2.3.2 were used as basis for the analysis.

Flood impacts on companies comprise direct damage to buildings or merchandise, losses due to operational interruptions as well as indirect damage caused by delivery difficulties of suppliers (Figure 4.9). Most of the companies surveyed, i.e. 88%, indicated that they had been affected by business interruptions (Figure 4.9). This led to a similarly large percentage of turnover losses. When differentiating the analysis by sector, i.e. 1) agriculture, 2) manufacturing and construction, 3) commerce, hotel, restaurants and transportation, 4) financial and corporate services as well as 5) public and private services, some differences between the sectors are revealed. For example, own delivery problems and delivery problems by suppliers are most frequently reported by the manufacturing sector, while sales restrictions are most frequently reported by the commercial sector (Figure 4.9). Nevertheless, all sectors except for agriculture heavily suffered from damage to buildings as well as from business interruption. Thus losses caused by business interruption might be equally important than direct asset losses. Except for the amount on insured losses, they are, however, not included in the overall losses given in Table 4.2 since they are more difficult to assess than repair costs.

In general, different methods are available for the estimation of business interruption costs. The most prevalent approaches are 1) to apply a sector-specific reference value per

Table 4.3: Financial losses of companies affected by the flood in June 2013

Loss type	Number of surveyed companies (n)	Mean financial loss [EUR]	Median of the financial losses [EUR]
Business interruption	358	137,287	15,000
Damaged equipment	327	287,126	20,000
Damaged buildings	310	524,292	80,000
Damage to goods, products, and stocks	238	46,897	8,000
Damaged vehicles	26	26,765	16,500

unit affected or per day of interruption to estimate the loss of added value, 2) to compare production output between hazard and non-hazard years, and 3) to calculate production losses as a fixed share of the direct damage (Meyer et al., 2013). Since the first approach is the most reliable, the companies surveyed about the 2013 flood were further asked about the period of interruption of operations in their company, as well as how long it took for normal operations without any restrictions to resume afterwards (period of restricted operations). The median value of downtime, through complete interruption of operations or restriction of operations, amounted to two to eight weeks, respectively. In the case of the 2013 flood, there were, however, a number of companies that experienced far longer downtimes through interruption or restrictions of operations: the 75%-percentile of downtime through the interruption of operations due to the 2013-flood amounts to 60 days, the duration with restrictions of operations to 150 days. The average loss caused by business interruption (including restrictions) amounted to EUR 137,287 (n = 358; median: EUR 15,000). They were only exceeded by the losses of damaged equipment or buildings (see Table 4.3). Significant differences might, however, occur between different economic sectors, both in terms of downtimes through interruption of operations and in terms of loss share as was shown for the 2002 flood by Kreibich et al. (2007).

4.3.5 Impacts on cultural heritage

Although research and data on flood impacts predominantly deal with the impacts on economic assets, the European Floods Directive also addresses effects on cultural heritage. In fact, the flood in August 2002 severely damaged, for example the historic Semper opera house in Dresden (Saxony) and the Garden Kingdom in Dessau-Woerlitz (Saxony-Anhalt) approved as UNESCO world heritage and almost destroyed the flower gardens of the castle Weesenstein at the river Müglitz (Saxony; see DKKV (2003b)). Since the repair and reconstruction work of such assets is often very specific and sometimes undoable and since the value that people attribute to such places is beyond financial accounting, this category is treated differently in the European guidance for recording disaster losses: not necessarily financial losses, but lists of damaged cultural, historical and UNESCO world heritage assets are proposed as indicators for loss databases (Corbane et al., 2015); no minimum requirements apply.

Despite the difficulties of the monetarization of damages to cultural heritage, financial losses related to cultural assets are given in the report of the German government to the European Union Solidarity Fund. The overall amount of initially EUR 56 M (BMF, 2013)

accounts for only 1% of the overall financial losses listed in Table 4.2. Saxony-Anhalt, Thuringia and Saxony reported losses to cultural assets of more than EUR 10 M each, Bavaria more than EUR 6 M, Baden-Wuerttemberg around EUR 1 M and Schleswig-Holstein EUR 350,000. A detailed list of affected cultural, historic or heritage assets is, however, missing. Thuringia explicitly mentioned several damages to parks and gardens, for example the historic Greizer Landscape Park, a cultural place of national importance (Annex 16 in BMF (2013)). Schleswig-Holstein mentioned inundation of the historic and listed centre of the city of Lauenburg on the Elbe. Furthermore, it is known that the (historic) city centres of Passau (Bavaria) as well as Grimma and Meissen (Saxony) were flooded. In contrast to 2002, the Garden Kingdom in Dessau-Woerlitz (Saxony-Anhalt) was rarely inundated despite higher water levels due to the meantime betterment of the flood protection. Nevertheless, rising groundwater damaged one castle of this UNESCO world heritage site so that the restoration of the Garden Kingdom is with more than EUR 22 M one of the most expensive projects funded by the governmental disaster relief (Parliament, 2015). This demonstrates the high importance cultural heritage might have in individual cases.

4.3.6 Environmental impacts

Similar to the impacts on cultural heritage, it is difficult to quantify flood impacts on the environment (see Meyer et al. (2013)). In fact, some impacts that are adverse at first sight might be ambiguous due to the fact that floods are natural phenomena and ecosystems in floodplains are adapted to flooding. Nevertheless, the environment can be damaged, especially by inorganic and organic harmful substances that have dissolved or are transported with sediments and floodwater and enter freshwater systems. With regard to contaminants that are deposited in meadows, pastures and agriculturally used lands there is the risk of organisms absorbing them so that the contamination may sustain in food chains. Therefore, pollution must be regarded as the main indicator of adverse environmental flood impacts. Flooded protected ecosystem habitats and formation of new water bodies are further items that are considered by the European guidance for recording disaster losses (Corbane et al., 2015). However, no minimum requirements for loss documentation were suggested.

Adverse environmental effects might also occur, if floodplains or flood retention areas have not been used in a flood-adapted manner. For example, in August 2002, the intended flooding of the Havelpolders at the confluence of the rivers Elbe and Havel caused widespread fish deaths. The flooding submerged the agriculturally used areas and caused the sensitive plants, i.e. maize, to die off. The ensuing decay processes lowered the oxygen content in the water to such an extent that fish could no longer survive (DKKV, 2003b). In June 2013, 430,000 ha of agricultural land was flooded (BMF, 2013), but according to the State Office of Nature Conservation and Landscape Management in the Free State of Saxony no fish deaths were noticed (LFULG, 2013).

In the framework of river monitoring programmes, sediment load and water quality are frequently measured. Measurements are augmented during and after (extreme) flooding, particularly along the middle reach of the river Elbe due to past mining and industrial activities in the catchment of the river Mulde (Böhme et al., 2005; BfG, 2014a). The measurement programme along the middle reach of the river Elbe provides a wealth

of data on the quality of sediments, suspended matter and floodwater (BfG, 2014a).

In June 2013, an increased sediment load was observed in all main rivers, i.e. Rhine, Danube, Elbe and Weser (BfG, 2014a). In the rivers Rhine and Weser, the total load during the flood each amounted to about 20% of the average annual load. At many gauges on the rivers Elbe and Danube, even higher load were measured with a maximum of two thirds of the average annual load at the river Danube and even 80% of the average annual load at a spot on the river Elbe (BfG, 2014a).

In a few samples of water and suspended matter, increased concentrations of heavy metals and arsenic were detected, most probably originating from the Ore Mountains (*Erzgebirge*). The loads of heavy metals amounted occasionally to more than 100% of the annual load in 2012, reaching a maximum at the Magdeburg gauge. The loads were, however, comparable to those during former flood events, i.e. in 2002 and 2006 (BfG, 2014a).

In the suspended matter, greatly enhanced amounts of organic pollutants such as hexachlorocyclohexane (HCH) and derivatives of DDT (1,1,1-trichloro-2,2-bis-(p-chlorophenyl)ethane), i.e. DDD and DDE, were measured here and there (BfG, 2014a). These pesticides had been produced in chemical plants in Bitterfeld-Wolfen until 1973 (DDT) and 1982 (HCH) and process wastes had been dumped nearby in abandoned open pit mines causing severe pollution of soil and groundwater, e.g. (Thieken, 2001; Böhme et al., 2005).

In water bodies in Saxony, aggravating pollution was not experienced in June 2013; all the samples inspected were not toxic (LFULG, 2013). In contrast to this, the Bavarian State Office for the Environment (LfU, 2013) reported a high incidence of contamination by heating oil, especially in the area affected by the breach of the embankment at Deggendorf-Fischerdorf (see Figure 4.1c). Leaking heating oil from damaged tanks has repeatedly been observed during flood events in Germany and had already been identified as a major source for environmental damage during the Whitsun Flood of 1999 in Bavaria. As a consequence, one-off mandatory testing was introduced at that time for heating oil storage facilities with storage volumes of 1000 to 10,000 litres located in flood-prone areas; a measure which came into effect on 1st January 2001 (LfU, 2013).

It is noteworthy that oil leakage and contamination not only harms the environment, it also aggravates damage of flooded buildings considerably (see (Kreibich et al., 2005; Thieken et al., 2005). In the administrative district of Deggendorf, up to 150 buildings have to be destroyed and newly erected because of oil contamination (Bavarian Parliament, 2014). Since cost-effective and efficient technical fail-safety systems exist that counteract the floating of oil tanks, e.g. (Kreibich et al., 2011b), homeowners should be better informed about them. Since 2005, the Federal Water Act states that homeowners are obliged to mitigate damage according to their means. Additionally, the implementation of fail-safe measures ought to be monitored more consistently by public authorities (LfU, 2013).

4.4 Discussion and recommendations

In this paper, impacts of the flood of June 2013 in Germany were described with regard to the domains that are addressed by the European Floods Directive (2007/60/EC), i.e.

human health, economic activities (and assets), cultural heritage, and the environment. The investigation was further guided by the loss indicators proposed by (Corbane et al., 2015; IRDR, 2015a) for a consistent loss documentation and was complemented by analyses of traffic disruptions and further impacts perceived as important by affected residents and companies.

It is noteworthy that guidelines on disaster losses such as (Corbane et al., 2015; IRDR, 2015a) are expected to become more important in the future when it comes to the implementation and monitoring of the Sendai Framework for Disaster Risk Reduction 2015-2030 (SFDRR) that was agreed upon in Sendai, Japan, in March 2015 by the United Nations (UN). In the SFDRR, seven targets to be achieved by 2030 are listed, among others a substantial reduction of 1) (global) disaster mortality, 2) the number of affected people, 3) direct economic losses as well as 4) damage to critical infrastructure and disruption of basic services such as health and educational facilities (UNISDR, 2015). Apart from these targets, four priority areas for action are defined, in which systematically recorded, evaluated, shared and publicly accessible loss data play a vital role to understand and consequently mitigate the impacts of such events (UNISDR, 2015).

In case of the flood event in June 2013, data and information on the flood impacts could be presented for all four domains considered as relevant by the European Floods Directive (2007/60/EC) and the Sendai Framework SFDRR (Table 4.4). Table 4.4 further reveals that the data and information recorded for the 2013 flood do, however, often not meet the requirements of loss documentation as proposed by (Corbane et al., 2015; IRDR, 2015a). Therefore, the official reports were augmented by further data. The range of impacts portrayed in this paper (from direct to indirect damage caused by operational and traffic interruptions through to health and environmental effects) does convey an impression of the diversity of the impacts that flood event can have at different scales. The used data sets have, however, some strengths and weaknesses. It should be noted that the availability of survey data and traffic disruptions is rather an exception than a rule and does require high efforts and resources for data collection and data processing that may not be available for many events. Such data do, however, provide detailed insights into impacts on the property scale, their perception etc. The analysis shows that affected residents perceive psychological stress, reinstatement works and supply problems more seriously than damage to buildings or household contents. With regard to economic activities, traffic and business disruption are more widespread than damage to economic assets or infrastructure elements. The costs attached to these impacts are, however, currently not assessed and hence not included in the overall damage figures. Therefore, more efforts are needed to include such impacts in loss documentation – by indicators or in monetary terms.

On the contrary, rough data and information from governmental reports, media articles etc. are generally available for many events. For the flood of 2013, there is a clear emphasis of the national and regional reports on the cost assessment of damaged assets for an application to the European Union Solidarity Fund and for the creation of a national reconstruction fund. With regard to human losses common loss indicators such as the number of dead, missing, injured, and directly affected (or exposed) people are only entirely reported on the federal level (Table 4.1). In the reports of the affected states to the Federal Ministry of Finance (BMF, 2013), many specifications are lacking. It is obvious that human losses are not in the focus of an application to the European Union

Table 4.4: Overview of minimum information requested by recently published loss documentation guidelines (Corbane et al. 2015; IRDR 2015) and information reported for the 2013-flood

Domain	Minimum loss indicators proposed by Corbane et al. (2015) for a specific event	Primary loss indicators proposed by IRDR (2015)	Reported for the flood in 2013 by federal and state authorities
General items	<ul style="list-style-type: none"> -Reporting on NUTS 2-/NUTS 3-level - Hazard classification - Time of the event - Uncertainty assessment 	<ul style="list-style-type: none"> - No further specifications 	<ul style="list-style-type: none"> -Reporting only on NUTS 0-/NUTS 1-level; - NO data on NUTS 2-/NUTS 3-levels - No uncertainty assessment
Human health	<ul style="list-style-type: none"> - Deaths - Missing - Directly affected 	<ul style="list-style-type: none"> - Deaths - Missing - Injured - Exposed 	<ul style="list-style-type: none"> - Deaths - Injured - Affected - Evacuated - Number of helpers - Complete reporting only on the federal level
Economic activities and assets	<p>Total number of:</p> <ul style="list-style-type: none"> - houses destroyed - houses damaged - education centres (damaged or destroyed) - health facilities (damaged or destroyed) <p>Total economic (direct) loss of all sectors, owners and loss bearers</p>	<p>Economic loss as cumulative estimate of the amount of damage to property, crops, and livestock and to the flow of goods and services expressed in monetary terms (no distinction between direct and indirect impacts)</p>	<p>Direct damage (repair costs) in different sectors; in-/exclusion of insured losses, expenses for emergency response and indirect costs (e.g. caused by business interruption) is often unclear.</p>
Cultural heritage	No minimum requirements	Not considered	Lump sum of repair costs
Environment	No minimum requirements	Not considered	Extended monitoring of water quality, but no integrated assessment

Solidarity Fund. This lack of information is, however, contrasted by the importance that this damage type is given in European and international agreements and that affected residents attribute to physical and particularly mental health problems caused by the flooding. A more comprehensive documentation of human losses together with information on their contexts would be helpful to prevent such losses in future. This was partly undertaken by GMLZ (2014). Most of this information is, however, not publicly accessible as requested by the Sendai Framework (SFDRR).

Damage to economic activities and particularly to economic assets is the domain for which the most information is available, also on a subnational level since this was the focus of the report by BMF (2013). However, the annexes to (BMF, 2013) as well as Table 4.1 and Table 4.2 illustrate that the reports of the affected states to the Federal government differ in length, content and comprehensiveness. Some of the differences can be explained by the different relevance the flood had for the respective state, some by previously experienced flooding or a lack of experience with event documentation. In the future, economic indicators should by default be accompanied by information on the number of damaged or destroyed items (physical damage indicators), such as damaged buildings, enterprises, schools and health facilities as proposed by Corbane et al. (2015) (see Table 4.4). On the one hand, such information will reveal further impacts on the affected population (e.g. supply problems, access to health facilities). On the other hand, it will allow a better comparison and evaluation of the quality of the financial loss estimates reported by the states. The reasonability of first estimates could roughly be appraised by multiplying the numbers of damaged or destroyed item by an average loss per item or a rough damage estimation that is currently discussed for the monitoring of the SFDRR. Reasonable average losses could be derived from the survey data used in this paper. In addition, such an approach could help to balance different experiences with event documentation between states. It is of course not applicable to cases with complex structural damage.

Furthermore, economic sectors should be clearly defined and agreed upon so that the loss documentation of different states and for different events can be better compared. Finally, costs for emergency services and disaster response should be explicitly reported since costing and reporting procedures have been well established in civil protection. The loss reports on the 2013 floods suggest that this potential has not been fully exploited. Only some federal states explicitly provided costs of emergency services of the flood of 2013, others included them to infrastructure losses. This practise should be avoided since in the scientific literature these costs are sometimes regarded as indirect costs (e.g. (Van Der Veen et al., 2003)).

Further indirect costs due to traffic or business interruption are currently not included in the overall losses, but might be substantial. Our analysis reveals that traffic disruptions were widespread in 2013 and lasted partly for several weeks and even months. The descriptive assessment of the information gathered on traffic disruptions and interferences illustrate the consequences of the flood without going into the further effects this had on travel times, cancellations of trips or the monetisation of these impacts. The obstruction of shipping, road and railway traffic that is portrayed here was not taken into account in the loss specifications of the states that was presented in section 4.3.2 and therefore complements the description of flood impacts on (economic) activities. Still, more efforts are needed to derive financial losses of such impacts.

The survey among flood-affected companies further reveals that business interruption is the most frequently reported flood impact. Since methods to estimate the costs attached to this are in their infancies, this domain requires more attention in research. Data collected on the scale of individual companies can help to derive more reliable estimation models.

In June 2013, damage to cultural assets and heritage accounted only for a small share of the overall financial losses. In consistency with the guideline of Corbane et al. (2015), damaged historic, cultural and heritage places should be explicitly listed together with the scale of their importance, i.e. for the regional, national or international heritage.

With regard to environmental impacts, many measurements of sediment loads as well as of water and sediment quality are available. In 2013, a particular monitoring programme was launched at the middle reaches of the river Elbe due to past mining and industrial activities in the catchment of the river Mulde. In order to better evaluate these measurements, indicators should be developed which also assess the consequences of such contaminations. It is striking that environmental impacts were only addressed in the reports of the water authorities, although contamination by leaking oil tanks is a frequently observed and important driver for building damage (DKKV, 2015). In Germany, the number of floating and leaking oil tanks could thus serve as an important indicator for environmental damage. Since cost-effective and efficient technical fail-safety systems exist that counteract the floating of oil tanks, e.g. (Kreibich et al., 2011b), homeowners should be better informed about them. Their obligation to mitigate loss should be emphasized. Additionally, the implementation of fail-safe measures ought to be monitored more consistently by public authorities (LfU, 2013).

Altogether, it has to be concluded that the information provided in governmental reports from Germany hardly meet the requirements of European (Corbane et al., 2015) or international (IRDR, 2015a) guidelines for disaster loss documentation and databases, especially with regard to the spatial resolution and the documentation of human and physical loss (Table 4.4). Table 4.1 and Table 4.2 illustrate that more efforts are needed to reach comprehensive loss documentations that are also required for reporting on the progress of the implementation of the SFDRR. Present data and information on flood impacts in Germany appear to be fragmentary, incomplete, partly still preliminary and more often than not publicly inaccessible even for an extreme event such as the flood in June 2013. Since floods are among the most damaging natural hazards in Germany (Kreibich et al., 2014b) and insurance penetration is still low (GDV, 2014; GDV, 2015), transparent and systematic reporting procedures of flood impacts and a related database should be developed.

As a minimum effort, a template should be developed by a joint effort of the federal and state civil protection authorities that is not only usable for applications to the European Union Solidarity Fund but also fulfils minimum requirements of Corbane et al. (2015) and the SFDRR. This template should be developed before the next flood happens and should be accompanied by more robust methods and procedures for first loss estimations.

Ideally, such efforts should be embedded in a broader risk management context in order to not only monitor, but to reduce losses in the longer term. Investment decisions on risk reduction should be combined with an integrated risk management and their effects should be monitored and evaluated. Therefore, an information system on flood

impacts and costs should ideally include all relevant cost categories including costs for response and prevention (see (Meyer et al., 2013; Kreibich et al., 2014a). Hazard information should be clearly linked to data on damage and losses, preferably on an event basis with sub-national spatial resolution. Data collection and provision should be established as a continuous task and enforced by national legislation as (potential) data providers are often non-governmental entities, e.g. with regard to infrastructure. To ensure quality, data collection should be based on transparent rules and methodologies. The set-up of such a system can be done stepwise, but data gaps should be closed gradually. Needed research efforts should be systematically identified and funded and good/best practise examples should be studied and maintained. Only then, event impacts and the effectiveness of the risk reduction measures in place can be reliably evaluated.

4.5 Conclusions

At present, a lack of adequate cost assessment approaches and data on flood impacts limits our knowledge and understanding of appropriate prevention and risk management measures. In comparison to other scientific fields related to the hydrologic system, impact data are still scarce and methods on assessing losses and damage are in their infancies. Therefore, this paper explored what data is available to describe and quantify the impacts of the flood in June 2013, which was the most widespread flooding Germany witnessed over at least the past 60 years (B. Merz et al., 2014b).

The analysis shows that information about impacts in all four domains that are addressed by the European Floods Directive (2007/60/EC), i.e. human health, economic activities (and assets), cultural heritage, and the environment, is available, but considerably differs in detailedness, completeness and accuracy. The analysis further reveals that drawing up a balance sheet for the impacts of the event in June 2013 has not yet been completed in its entirety. It is further evident that the information currently available does not meet the standards for loss documentation that were proposed by Corbane et al. (2015) for member states of the European Union. Therefore, the establishment of national (and regional) disaster-related accounting systems should be further encouraged. In such an information system, all relevant cost categories including expenditures for risk reduction and response should be included. Furthermore, the system should enable a linkage of flood event indicators with (various) impact indicators in order to evaluate the success of (flood) risk management strategies and measures on the long run. Such an evaluation is required, for example, in progress reports on the Sendai Framework for Disaster Risk Reduction 2015-2030 (SFDRR) that was agreed in Sendai, Japan in March 2015. Only accurate, consistent and comparable databases will allow Germany to seriously monitor these internationally agreed targets.

The range of damages portrayed (from direct to indirect damages from operational and traffic interruptions through to health and environmental effects) conveys an impression of the diversity of the impact that flood events can have. Data collected on the scale of individual properties reveal that business interruption is the most frequently reported damage by affected companies and mental health issues as well as supply problems are perceived more seriously by affected residents than building damage or other forms of financial damage. These damage types receive, however, only little attention in govern-

mental reports on the flood of 2013 as well as in research. However, in the case of evaluating and accepting preventive and protective strategies, these can play an important or even decisive role. Therefore, efforts in these domains, starting from data collection to properly describe and understand the phenomena up to effective management strategies in order to reduce these impacts are needed.

5 | Social media as an information source for rapid flood inundation mapping

Manuscript Info

Authors information:

Joachim Fohringer
Doris Dransch
Heidi Kreibich
Kai Schröter

Published as:

Forhinger J., Dransch D.,
Kreibich H., Schröter K.
Social media as
an information source
for rapid flood
inundation mapping
Nat. Hazards Earth Syst. Sci.
2015;15,12:2725-2738.
doi:10.5194/nhess-15-2725-
2015

Abstract

During and shortly after a disaster data about the hazard and its consequences are scarce and not readily available. Information provided by eye-witnesses via social media are a valuable information source, which should be explored in a more effective way. This research proposes a methodology that leverages social media content to support rapid inundation mapping, including inundation extent and water depth in case of floods. The novelty of this approach is the utilization of quantitative data that are derived from photos from eye-witnesses extracted from social media posts and its integration with established data. Due to the rapid availability of these posts compared to traditional data sources such as remote sensing data, for example areas affected by a flood can be determined quickly. The challenge is to filter the large number of posts to a manageable amount of potentially useful inundation-related information as well as their timely interpretation and integration in mapping procedures. To support rapid inundation mapping we propose a methodology and develop the 'PostDistiller', a tool to filter geo-located posts from social media services which include links to photos. This spatial distributed contextualized in-situ information is further explored manually. In an application case study during the June 2013 flood in central Europe we evaluate the utilization of this approach to infer spatial flood patterns and inundation depths in the city of Dresden.

5.1 Introduction

Information provided by citizens via Internet can improve the information basis for disaster response after natural disaster (Poser and Dransch, 2010; Dransch et al., 2013). During the wildfire event in 2007 in California affected people posted information about the wildfires in their own neighborhood to an internet page to inform about the expansion and behavior of the fires (Sutton et al., 2008; Goodchild and Glennon, 2010). Another popular example is “Ushahidi”¹, a content sharing platform that collects and provides eyewitness reports of natural disasters like earthquakes (Haiti and Chile 2010, Christchurch 2011), winter storms (Washington, D.C. 2010), wildfires (Russia 2010) and floods (Missouri 2011 and Thailand 2011). Hirata et al. (2018) used the Ushahidi platform to test a procedure for collaborative flood mapping in Sao Paulo based on information provided by people equipped with mobile devices providing location data. Information provided by citizens offers several benefits for disaster assessment and management. It is highly up-to-date since eye-witnesses document their observations directly and as such improve situation awareness and assessment. Additionally, people may contribute information which cannot be captured by sensors since the phenomenon is not measurable or sensors are not available. Information from citizens can be conducive to rapidly describe the extent and intensity of the hazardous event as well as resulting impacts.

Rapid evaluations of hazardous events are needed for efficient response both in emergency management and in financial compensation and reconstruction planning. Estimates of monetary loss to be expected by a certain hazard scenario can be provided by damage models. In the presented research we follow the hypothesis that social media contain additional and/or even exclusive information which can be used to reasonably infer spatial flood patterns and inundation depths and thus provides an important basis for the estimation of flood damage. We investigate how information from social media, such as Twitter or Flickr, can contribute data for this task. The following challenges will be addressed:

- Challenge 1: Filtering information relevant for inundation mapping from the high amount of information posted in social media.

One major challenge related to utilization of information posted in social media is the huge volume of information created continuously to all kind of topics. Concepts and tools are required to facilitate extracting the information suitable for inundation mapping.

- Challenge 2: the utilization of the relevant information from social media for inundation mapping.

Information about the inundation situation and particularly about the flooding intensity in terms of inundation depth is essential for rapid loss estimation in case of floods. Inundation depth data are typically provided after the flood by terrestrial surveys of flood marks, evaluation of aerial or satellite images, or ex-post hydrodynamic-numeric simulations of the flood. Near-Real-Time information on inundation depths is, if at all, available from in situ (e.g. water level gauges) or derived from remote sensing products (e.g. satellite images) in combination with

¹<http://www.ushahidi.com/>

terrain elevation data. It has to be investigated if social media can provide relevant and rapid information for flood inundation area and depth.

Both challenges were addressed in a close and fruitful cooperation of flood experts and computer scientists. The computer scientists developed a tool 'PostDistiller' that combines various filtering methods with regard to selective contextual information reduction. The functionalities, components and implementation of PostDistiller are detailed in Section 5.2.3. This tool also provides a visual interface to assess the filtered information and to derive suitable data for flood inundation mapping. The flood experts investigated and evaluated the utilization of information provided by this tool. They examined how the information derived from social media complement the traditionally collected data. Additionally, they evaluated how it supports rapid inundation mapping.

5.2 Challenge 1: Filtering social media information

Information from social media comes along with several challenges (Abel et al., 2012): the filtering of relevant information, their provision to people who need them, and quality assessment of the data. The presented research focuses predominately on filtering and provision of data, data quality is treated implicitly.

5.2.1 State of the art and related work

To find meaningful information in the large amount of data, several approaches have been pursued so far: (1) filtering by keywords or by geographic queries, (2) filtering by crowdsourcing, (3) automatic filtering utilizing machine learning and natural language processing, and (4) interactive visual spatiotemporal analysis/geovisual analytics.

For harvesting social media posts for analysing user's response during or after a disastrous event, mostly the keyword search of the appropriate social media service is used. Vieweg et al. (2010), for instance, used terms like "grass fire" or "red river" to collect Tweets that contain terms related to the Oklahoma Grassfires and Red River Floods in spring 2009. The selection of the keywords affects the amount and quality of the returned Tweets, this has been shown by, e.g. Rogstadius et al. (2013) or Joseph et al. (2014). The geolocation of posts from social networks can be used as an alternative for disaster related and language-specific keywords for filtering. Herfort et al. (2014) examined the spatial relation between location based social media and flood events. Their results show that Tweets, which are geographically closer to flood-affected areas, contains more useful information capable to improve situational awareness than others.

Another approach to determine relevant social media posts is to classify them manually by crowdsourcing and to filter irrelevant declared data. Crowdsourcing as introduced by Howe (2006) means to distribute a specific task to an unknown set of volunteers to solve a problem by harnessing collective contribution rather than by an individual. Another form is to perform data processing tasks like translating, filtering, tagging or classifying this content by voluntary crowd workers (Rogstadius et al., 2011). These operations can be facilitated already during creation of social media posts by explicit user-driven assignment of predefined thematic keywords or hashtags, for instance #flood or #need, to allow easy extraction, filtering and computational evaluation of contained information

(Starbird and Stamberger, 2010). In this approach, in particular, the scalability is a problem, because due to the volume and velocity of the posts during the disaster response a high-speed processing is difficult even for a large group of volunteers (Imran et al., 2013).

For classification of text content in posts into relevant and non-relevant, also automatic approaches such as supervised classification and natural language processing (NLP) techniques based on machine learning are used. For instance, Sakaki et al. (2010) used a support vector machine (SVM) based on linguistic and statistical features such as keywords, number of words and context of target-event words for detection of earthquake events in Japan. Yin et al. (2012) developed a classifier that automatically identifies Tweets including information about the condition of certain infrastructure components like buildings, roads or energy supplies, during the Christchurch earthquake in February 2011 by utilizing additional Twitter-specific statistical features like number of hashtags and user mentions. Other important features as observed by Verma et al. (2011) are subjectivity and sentiment that can help also to find information contributing to situational awareness. However, Imran et al. (2013) have shown that pre-trained classifiers are suitable for the classification for a specific disaster event, but achieve significantly inferior results for another event of the same type. As a consequence classifiers have to be adjusted for each disaster event and for each task, e.g. event detection or damage assessment, in order to achieve the best possible accuracy in classifying relevant posts.

To connect the benefits of crowdsourcing (ad-hoc classification without need for training classifiers) and machine learning (scalability and automatic processing), Imran et al. (2014) present a system to use volunteers to manually classify part of the incoming data as training data for an automatic classification system.

Geovisual analytics approaches also allow filtering social media posts, putting focus on interactive visualisation and exploration rather than on completely automated machine learning methods. MacEachren et al. (2011) presented a geovisual analytics approach for collecting and filtering of geocoded Tweet content within a visual interface to support crisis management to organise and understand spatial, temporal and thematic aspects of the evolving crisis situations. Also Morstatter et al. (2013) used visualisation techniques for organising Tweets by these aspects, for instance time graphs, which show the number of Tweets matching a query per day, network graphs showing which matching Tweets were propagating most and heat maps, showing the spatial distribution of these Tweets.

The approach presented in this paper combines filtering and visualization methods. Keywords are used, as in most works presented here, for the retrieval of generally disaster-related data. From the collected subset of posts those can be filtered that are both temporally and spatially related to the concrete disaster event under study. A visual interface facilitates exploration of filtered posts with the purpose of deriving specific quantitative or qualitative data. Compared to the methods and procedures discussed in this paragraph, neither training classifiers (machine learning/natural language processing) nor a sufficiently large amount of volunteers (crowdsourcing) are necessary in our approach.

5.2.2 Requirements

Rapid impact assessment requires quick information about a specific hazardous event. This includes the type of impact, such as inundation, the affected area, and the time when the effect was observed. All posts containing such information have to be selected from the high amount of information posted to social media. Additionally, the selected posts have to be analysed to extract qualitative and quantitative information about the impact either from text, photos or videos which are enclosed in the post.

The selection of all relevant posts for a specific disaster event should be possible at any time when it is needed. Since not all social media services provide full retrieval of all posts at any time, two types of retrieval have to be available: The event-related on demand retrieval for social media that allow for permanent access to all posts, and the continuous retrieval for social media that provides posts only for limited time. The event-related on demand retrieval enables retrieval of posts by an accurately fitting query. In contrast, in the continuous retrieval, the event is not known in advance, therefore posts must be retrieved that generally refer to several types of natural hazards and their impacts, such as “flooding” or “inundation”. Continuous retrieval results in a collection of posts covering a variety of disasters, therefore, additional filters are necessary to select those posts that are relevant for the specific event under study.

The extraction of information related to the impact is dependent on the type of event. In our use case we focus on inundation mapping after floods, thus, information about inundation area and water depth have to be extracted. We focused on photos to extract this information, since photos have the following advantages. They show the relation of water level and parts of the environment, such as windows, roofs, or traffic signs; this facilitates estimating the inundation depth. Photos show also context information, for instance existing means for mobile flood prevention or near-by buildings. This context information supports the interpretation and verification of derived information. For example the photos context allows for verifying the posts geolocation. Apparent mismatches between the photo contents and its location can in most cases be recognized by locating posts in a map. Means are required to visually explore the selected photos and derive meaningful information.

5.2.3 PostDistiller

Components

Our approach to select relevant posts and to extract required information consists of three components: 1) the *PostCrawler* for retrieval of the posts, 2) the *PostStorage* for persistent storage, and 3) the *PostExplorer* for exploration and extraction of information from single posts (Figure 5.1). *PostCrawler* and *PostStorage* are generic components, the *PostExplorer* is adapted to the use case flood inundation mapping.

The *PostCrawler* retrieves and pre-processes disaster-related posts from social media services. Depending on the temporal availability of posts provided by the social media service, the posts are collected by either retrieving a data stream continuously, e.g. in Twitter, or an event-related set of data on demand, e.g. in Flickr. In case of continuous retrieval of posts general disaster-relevant search terms are applied for retrieval; they cover the type of hazard, e.g. flood, the perceptible triggers, e.g. heavy rain, and its

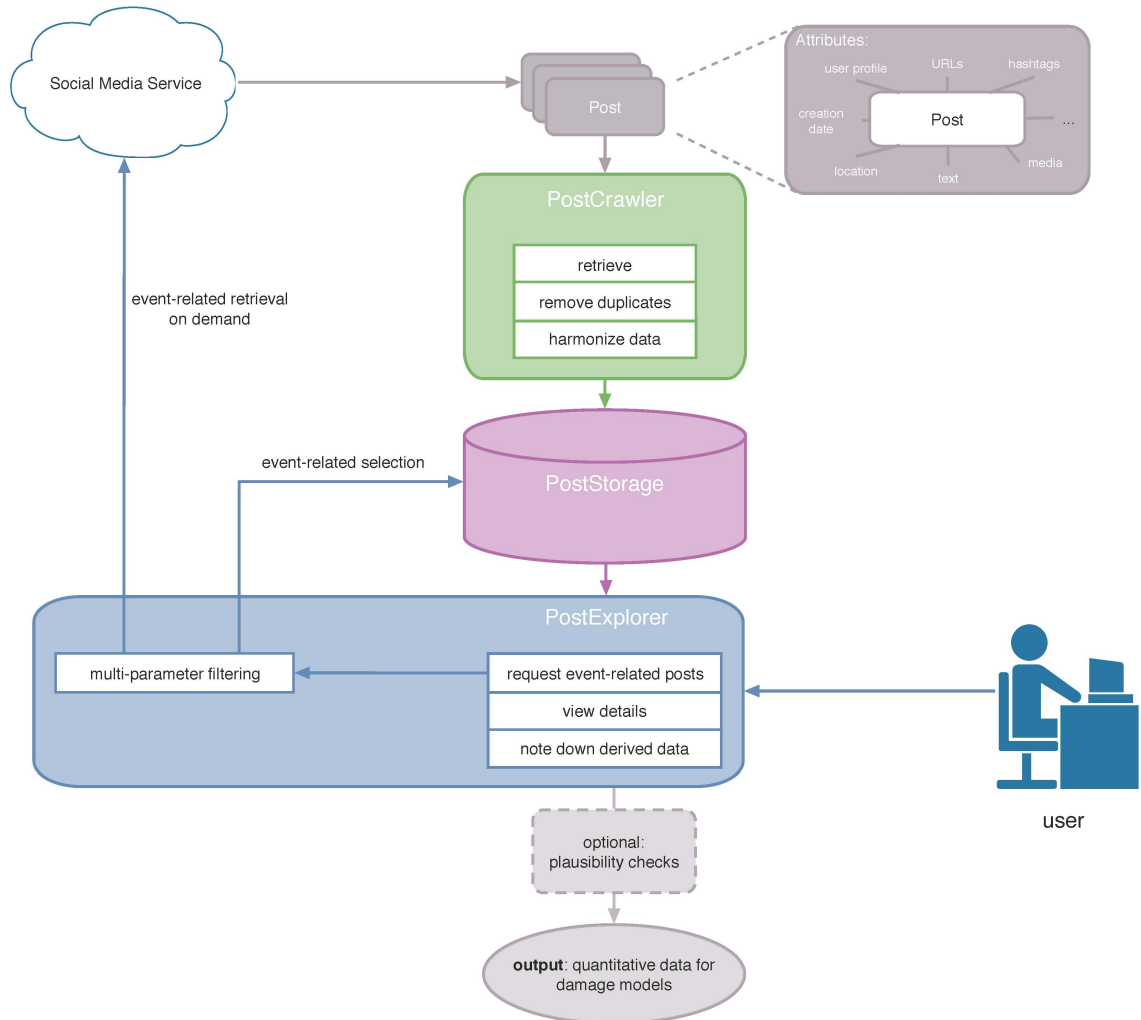


Figure 5.1: PostDistiller system architecture.

impacts, e.g. destructions and damage. For event-related on demand retrieval these search terms are stated more precisely regarding observable effects and consequences of the specific event, like overflowing rivers or flooded roads, as well as the affected area and corresponding time period. In both cases, the search terms can be customized by the user. After retrieval the posts are automatically pre-processed regarding duplicate handling, georeferencing, and harmonization of data format. Duplicates of posts, caused by forwarding of already published posts, are removed. Posts without explicit location information in form of geo-coordinates are automatically georeferenced if possible. The features date and location are harmonized with respect to their formal description. This becomes necessary since date and location can be contained at different attributes within the same post, for example the location in a Tweet can be given either in designated attribute coordinates or in the user profile. Using various social media services simultaneously, these features can also appear in different formats or encodings, e.g. as geographical coordinates as longitude and latitude or vice versa as latitude and longitude. The results of georeferencing and harmonization are added as extra attributes to the original post and saved in the *PostStorage*.

The collected posts from various social media services are permanently saved by the *PostStorage* in a database. The database stores all attributes of a post which are text, links to external media (images and videos), location, creation date, user profile, URLs and others. Data selection is possible by means of the harmonized attributes date and location and other attributes of the posts.

The *PostExplorer* facilitates the expert in various ways. It enables selecting relevant posts from the data base according to different post attributes. It supports exploring the information inherent in the post, and it enables to catch and store extracted information in the database. Data selection is realized by multi-parameter filtering. As natural disasters affect a limited region within a limited period of time, the posts will be filtered based on their publication date and location. Further filtering is achieved by considering the presence of links to extra media, like photos or videos. In addition, event-related text filters can be used to filter posts referring to concrete effects of a disaster, such as dike breaches. The selected posts are presented in an interactive visual interface for further exploration. In our use case the interface is configured to explore posts combined with fotos. It consists of four components which are shown in Figure 5.2: The first component allows for browsing through the filtered posts/photos and gives a quick overview about the whole number of selected posts and photos. The second component depicts single posts/photos and attached information (author, publication time, location, content) with respect to extract information about inundation. The third component shows a map with the location of filtered posts. It facilitates verifying if the coordinates from the posts metadata match with the place and context depicted in the photo. The fourth component provides fields to catch and store the extracted information to the data base. The expert can add the following information: the relevance of the post/photo for inundation mapping, if the presented situation is wet or dry, the inundation depth estimate, and an indication of the estimated reliability of the derived information. Information extraction from the photos is made by the analysts expertise, there is no automatic information extraction support up to now. In this regard the analyst assesses the relevance of the photo and derives an estimate of inundation depth by visually inspecting the photo contents. Objects and items visible in the photo may provide an indication for inundation depth,

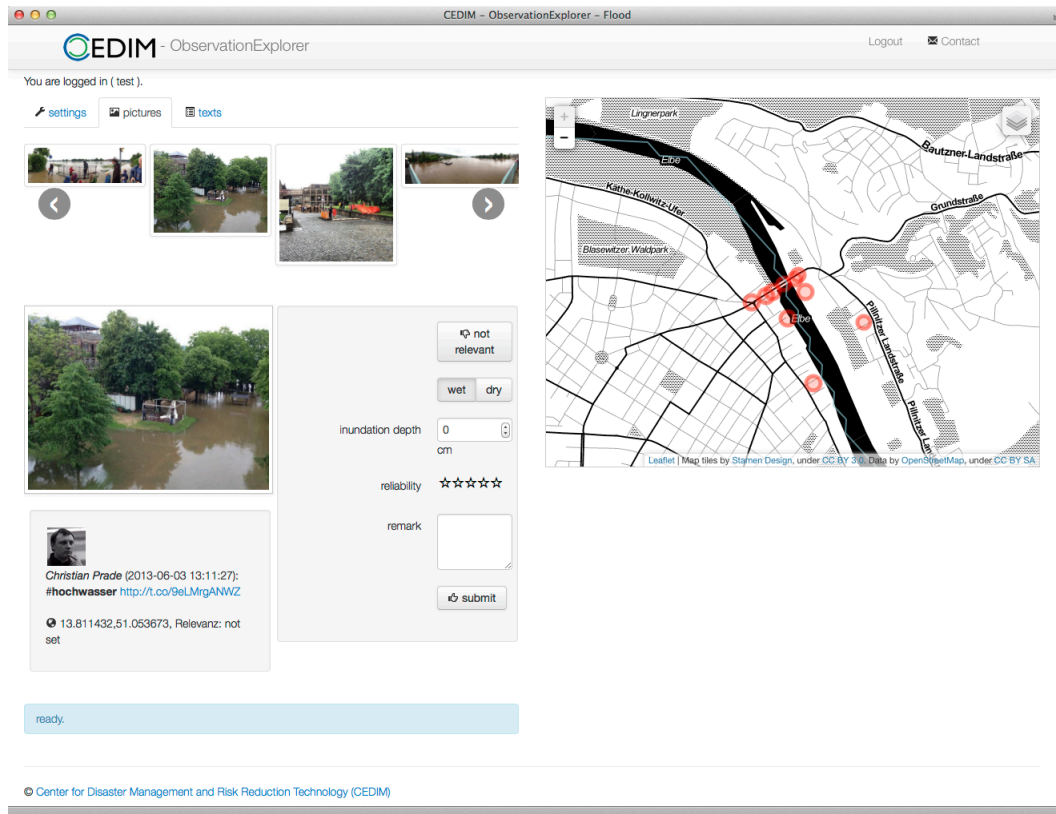


Figure 5.2: PostExplorer: media view and map view (map tiles by Stamen Design), under a Creative Commons Attribution (CC BY 3.0) license. Data by OpenStreetMap, under Open Data Commons Open Database license (ODbL).

e.g. flood water level in relation to buildings' windows, traffic signs or other street furniture. Experts may also subjectively rate the reliability of each estimate to provide an indicator for the consideration of uncertainties in a later stage.

Implementation

The implementations for *PostCrawler* and *PostStorage* are independent of specific disaster types, the *PostExplorer* is adapted for application during flood events as an example. In our use case we have chosen the social media platforms Twitter and Flickr as information source. Both services are characterized by open interfaces, moderate access restrictions and widespread use.

PostCrawler: We use the micro-blogging service Twitter for continuous retrieving of data and the content-sharing service Flickr for on demand retrieval. For continuous data retrieval the *PostCrawler* connects to Twitters freely available Streaming API and receives consecutively Tweets matching given filter predicates. For this purpose the *PostCrawler* performs the authentication procedures required by Twitter and requests the stream of Tweets, by giving appropriate disaster specific search terms, such as flood, inundation or damage. These search terms can be customized by the user to limit the amount of data while collecting. The *PostCrawler* for Twitter has been implemented in Java. To

access Twitter's Streaming API the Hosebird Client (hbc) ² is used. Tweets are received as documents in JavaScript Object Notation (JSON) consisting of attribute value pairs, like text: The flood cannot impress us or url: <http://t.co/YFdItwOr7t>. The Flickr-specific implementation of the *PostCrawler* connects to the representation state transfer (REST) interface of Flickr, authenticates itself and requests posts that contains corresponding event-related search terms in appropriate metadata (title, description or tags), for example elbe, water level or gauge. Time and area of the event are also included in the request. Selected documents are returned also in JSON format from Flickr. The *PostCrawler* for Flickr was programmed in Python. Access to the Flickr API is provided by the software library flickrapi ³. The pre-processing of collected posts is implemented as follows. Duplicate removal: Forwarded Tweets, so-called retweets, are identified by appropriate markings existing either in the text or the metadata, e.g. a preceding RT or in the attributes retweeted or retweeted_status. Those retweets are stored separately in order to avoid duplication. Data harmonization: Data Harmonization between both services is accomplished by parsing attributes, which include the location (in twitter: coordinates, and in Flickr: location) and creation date of the post (created_at and datetaken), and mapping each to a new shared attribute (coordinates and creation_date). Georeferencing: To add geo-coordinates to posts without explicit location information, the open source software package CLAVIN ⁴ (Cartographic Location And Vicinity INdexer) is used. It facilitates to extract the local entities from text related attributes and to find associated geo-coordinates using the OpenStreetMap dataset⁵ and GeoNames database ⁶.

PostStorage: To save pre-processed posts the open-source database system MongoDB ⁷ is used as backend for the *PostStorage*. MongoDB is a document-oriented data base that allows storage of JSON-like documents in the form they are delivered by Twitter and Flickr. This is different to common relational data bases which need predefined data schemes. By this means, it is possible to store posts from several Social media services without doing additional data conversion. Each attribute of the posts is indexable and queryable. The database supports indexes for numeric, text and date attributes, it also supports 2-D geospatial indexing. These indexes facilitate post selection from the data base in various ways. Spatial queries allow for easily retrieving posts from defined areas. The full-text search of MongoDB allows for filtering text according to search terms like flooded road or keywords/hashtags like #waterlevel.

PostExplorer: The *PostExplorers* functionality regarding data selection, data exploration, and data catchment is implemented following: Data selection is realized by multi-parameter filtering. Temporal filtering selects posts that are published in the chosen time period. Spatial filtering selects all posts based on whether associated position is located within the chosen target area, e.g. a river basin that is described internally by a 2-dimensional multipolygon. The media filtering is done by selecting all posts that contain one or more URLs in either the text itself or in the corresponding metadata. As we are interested in photos attached to collected posts, it is determined whether embedded

²<https://github.com/twitter/hbc>

³<http://stuvel.eu/flickrapi>

⁴<http://clavin.bericotechnologies.com/>

⁵<http://wiki.openstreetmap.org/wiki/Planet.osm>

⁶<http://www.geonames.org/>

⁷<http://www.mongodb.org/>

URLs point to images of popular photo-sharing services Instagram ⁸, TwitPic ⁹, Path ¹⁰ or Twitters own service. Appropriate filter parameters can be set by drop-down boxes that allow choosing a predefined event-type, e.g. flood. Depending on this selection, the user chooses the river basin to be examined from a predefined list (e.g. Elbe) as well as the time period of considered posts (e.g. from 05 May 2013 until 21 June 2013). For data exploration and data catchment an interactive visual interface has been set up to allow for directly interacting with the data base and the selected posts. The four components of the visual interface are realized as follows: The dataset of photos and text messages resulting from the filtering is presented in the visual interface. For overview the photos are listed in a sliding list. The sliding list shows four scaled-down versions of the filtered images at a time (component 1). By selecting a certain photo in this list, the corresponding post is displayed; it presents an enlarged version of the photo as well as the attributes associated to the post (component 2). The photos location derived from its coordinates is highlighted in the map view (component 4). Information that has been extracted from the photo by an expert is caught via input boxes and stored in the data base (component 4). The visual interface is implemented as a web-based user interface. As a web application the *PostExplorer* is a client-server application that is displayed in the users web browser and is executed on a web server. On the server side, the Python-based web application framework Flask ¹¹ is used. Flask is kept simple and minimal, but allows easy integration of existing libraries, e.g. such to interact with MongoDB, or to process and deliver documents in JSON through the Hypertext Transfer Protocol. In addition to the languages Hypertext Markup Language, we applied several means: Cascading Style Sheets and JavaScript to implement the web interface, and the JavaScript library Leaflet ¹² to implement the interactive map.

5.3 Challenge 2: Utilization of the information from social media for rapid inundation mapping

One challenge for rapid flood impact assessment is to obtain an overview of the flooding situation in which the main interests are spatial flood patterns and inundation depths. Social media content is promising to improve disaster response capabilities by adding supplementary information to improve situation awareness and assessment. However, the utility of this information source depends on the possibility to reasonably infer quantitative data on inundation depths. This will be tested within the use case of the June 2013 flood in the city of Dresden (Germany).

5.3.1 State of the art and related work

Given the aim to rapidly provide flood inundation depth maps, a pragmatic attitude towards data sources and quality is needed, meaning that any suitable information should be exploited as soon as it becomes available and might be discarded or updated when

⁸<http://instagram.com>

⁹<http://twitpic.com>

¹⁰<https://path.com>

¹¹<http://flask.pocoo.org>

¹²<http://leafletjs.com>

further data become available with time. In this light, the availability of data in space and time as well as the reliability of data sources are of particular importance.

Data sources which are usually used for inundation mapping are water level observations at river gauges, operational hydrodynamic-numeric model results or remote sensing data. In combination with topographic terrain data, which are available from topographic maps or digital elevation models (DEM), the inundation depth within the flooded areas can be estimated. The requirements for topographic data are considerable. This particularly concerns the accuracy of ground levels as well as the realistic representation of hinterland flow paths and flood protection schemes since these details locally control flooding. The advent of airborne laser altimetry as for instance LiDAR has significantly improved the resolution and vertical accuracy of DEMs within the lower range of decimetres (Mandlbürger et al., 2009; Bates, 2012).

Water level sensors are usually installed with tens of kilometres distance along a river course and only a fraction is equipped with online data transmission features. Depending on the sampling interval of the measurement network, water level values are available online within minutes to hours or days. Hence, during floods only limited point information of water levels is available for inundation mapping. Linear interpolation of water levels between gauging stations is straightforward to obtain an estimate of the flood level (Apel et al., 2009). The intersection of this level with a DEM then yields a map of inundated areas. The difference between ground levels and flood level is the inundation depth. However, this approach neglects non-stationary hydrodynamic processes, limitation of flow volume and effects of hydraulic structures. A higher spatial data density would be needed to approximate the actual characteristics of the water level gradient along a river more realistically.

Hydrodynamic-numeric models compute floodplain inundations by solving the hydrodynamic equations of motion for given geometric and hydraulic boundary and initial conditions. The spatial detail of the simulated inundation depths depends on the discretization level of the model set-up which is usually below 100 m horizontal resolution (Horritt and Bates, 2002; Falter et al., 2016). The Near-Real-Time application of hydrodynamic-numeric models is hampered by the need to provide appropriate estimates of initial and boundary conditions, to assimilate model simulations and observations (Matgen et al., 2007) and by considerable computational costs (Di Baldassarre et al., 2009). Computation time depends particularly on the size of the computational domain and its spatial resolution (Falter et al., 2013) and the complexity level of model equations ((Horritt and Bates, 2002). Alternatively, the inundated areas and inundation depths can be calculated in advance for a set of flood scenarios. However, the underlying assumptions of such scenarios might differ from the actual situation of a real event, e.g. dike breaches. The consideration of such unforeseen incidents is not feasible.

Remote sensing data allow for the detection of inundated areas by comparing before and during flood images (Y. Wang, 2002). In combination with a DEM the approximation of flood water levels and thus the estimation of inundation depth is feasible by detecting the flood boundary and extracting height information from the DEM (Zwenzner and Voigt, 2009; Mason et al., 2012). However, image acquisition is largely dependent on the revisiting time of orbital platforms which in turn is inversely related to spatial resolution (Di Baldassarre et al., 2009). During a flood it is not guaranteed that suitable remote sensing images are available within short time for the flood situation and the region of

interest. Further, the acquisition of images synchronously with the occurrence of flood peak, in order to capture maximum flood extent, is hard to achieve. This particularly applies for large areas due to dynamic flood processes. Usually, image delivery and processing is feasible within 24 - 48 h (Schumann et al., 2009).

In this light, social media show promise to fill the time gap until inundation depth information from other data sources might become available. The derivation of inundation depths from photos could complement observations from water level gauges with additional distributed in-situ information and support the inundation mapping process. (Schnebele and Cervone, 2013) show the complementary value of information extracted from photos and videos which have been compiled from a search on the internet for flood extent mapping. In urban areas the additional micro-level evidence on the flooding situation is valuable since remotely sensed information and flood inundation models experience difficulties in these areas (Zwenzner and Voigt, 2009; Apel et al., 2009). Despite these obvious opportunities of social media for rapid flood damage estimation, there are a number of challenges to overcome. This concerns the filtering of relevant information, the availability and the quality of information. As social media posts are not controlled or actively inquired there is no guarantee for their availability during the flood. The content and spatial coverage of the posts is very much depending on the caprice of tweeters. Data quality, credibility of information and uncertainty concerning location and inferred inundation depth are important issues (Poser and Dransch, 2010).

5.3.2 Case study Dresden June flood 2013

We investigate the usefulness of photos posted via Twitter and Flickr as an information source for rapid inundation depth mapping within the city of Dresden during the flood in June 2013 using PostDistiller. Urban areas are of specific interest because on the one hand potential flood damage is high and on the other hand the number of social media activists is large. The city of Dresden (Saxony, Germany) with almost 800 000 inhabitants is located on the banks of the river Elbe which has brought severe impacts from major floods, most notably the recent events in August 2002, April 2006 and June 2013. Therefore, flood awareness in Dresden is on a high level and comprehensive flood management concepts have been put into practice (Dresden, 2011).

During the June 2013 flood the peak water level at the gauge Dresden (Figure 5.3) was registered on 06 June 2013 with 876 cm above gauge datum (i.e. 111.3 mNN). Due to an elongated flood wave the water level remained above 850 cm (ca. HQ20) from 05 to 07 June 2013 which is a critical level for flooding in several quarters of Dresden e.g. Laubegast, Kleinschachwitz upstream and Pieschen Süd downstream of the city centre (see Figure 5.3, Landeshauptstadt Dresden, 2011).

Data and inundation mapping scenarios

Within the Dresden case study we use data from the water level gauge in Dresden (operated by the water and shipment administration (WSV)) and photos retrieved from Twitter and Flickr as information sources for rapid inundation mapping. Information on ground level is available from the DGM10 (Federal Agency for Cartography and Geodesy) which has a vertical accuracy of ± 0.5 to $\pm 2m$.

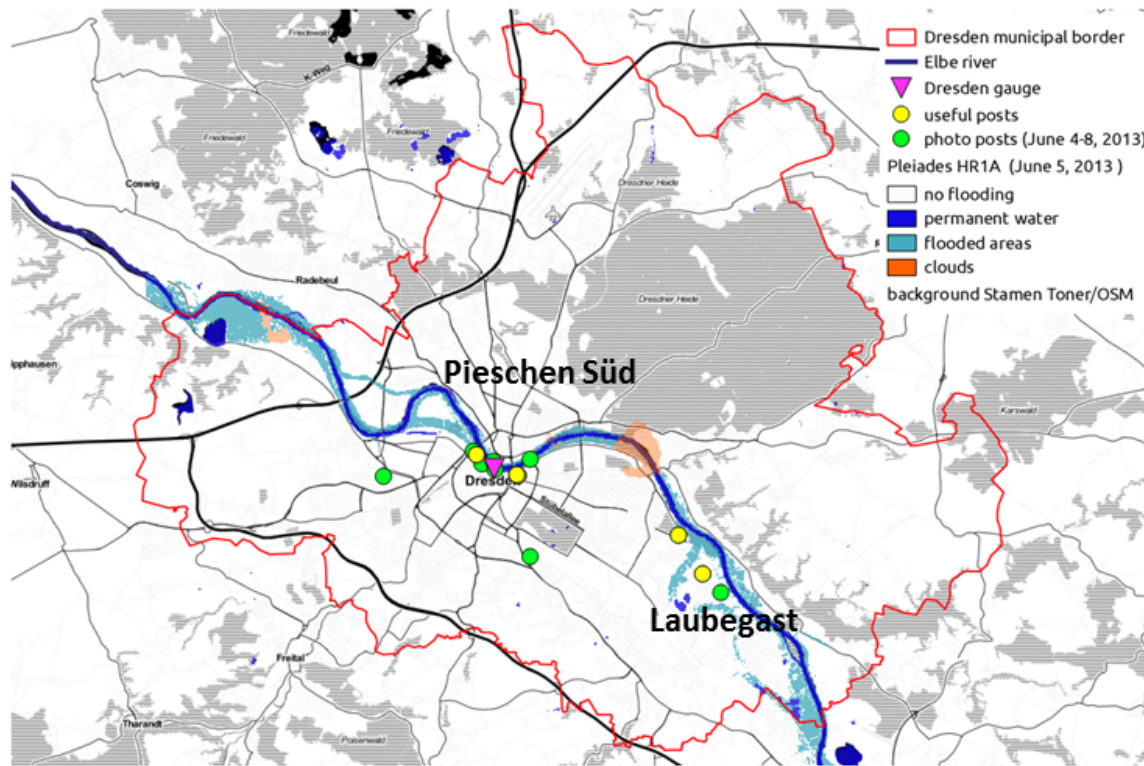


Figure 5.3: Study region and data sources for flood inundation depth mapping.

Further, for this study a footprint of flooded areas in Dresden is available from Perils AG¹³ which is based on Pleiades HR1A multispectral image taken on 05 June 2013 with a horizontal resolution of 50 cm. In this product a SPOT 5 multispectral image from 21 August 2011 has been used as a reference to classify flooded areas and permanent water surfaces. Even though this footprint has been released as a rapid inundation mapping product and might not meet the requirements of a careful documentation of flooded areas, in the context of this study it is a useful reference to evaluate the outcomes of the rapid inundation mapping procedures based on either water level observations or social media photo posts and DEM terrain data.

Inundation depth maps are derived for two scenarios: (a) online water level observations at the gauge Dresden and (b) information inferred from photos filtered from Twitter and Flickr services using the *PostCrawler*, *PostStorage* and *PostExplorer* implementation presented in this paper. The satellite based flood footprint is used to evaluate the mapping results in terms of inundation extent.

Results

Within scenario (a), the water level observation for the flood peak at the gauge Dresden retrieved online is intersected with the DEM10. Considering hydrodynamic flow processes the water level is not horizontal but inclined along the flow direction. In view of the elongated flood wave which led to almost constant high flood levels during the 06

¹³www.perils.org

and 07 June 2013 it is reasonable to assume quasi stationary flow conditions in the time period around the flood peak. Therefore, we assume that the gradient of the water level along the river is approximately parallel to the bottom slope (on average 0.27 ‰ between the upstream gauge Pirna and downstream Gauge Meissen). The inclined water level surface is intersected with the DEM in such a way that all areas below the water level are assumed to be inundated. The difference between the water surface and ground level is the inundation depth. The resulting inundation depth map is shown in Figure 5.6a.

In scenario (b) we utilize PostDistiller to extract information from the posts collected by *PostCrawler* and stored in the PostStorage which runs as a permanent service. The keywords used for the *PostCrawler* are terms related to flood and associated impacts both in English and in German language: flood: "Hochwasser", "Flut", "flood", "floods", "flooding", "inundation", "Sturzflut", "Überflutung", "Unterspülung", "Regen", "undermining".

Triggered by the decision to analyse the June flood 2013 in the Dresden region this data base is automatically filtered based on event related features which include the definition of the flood period of interest (05 May 2013 until 21 June 2013), the availability of geo-location information attached to the posts, and the location within the target study region. Within seconds the relevant posts are provided to the *PostExplorer* which enables subsequent manual filtering and visual inspection of photo contents for the estimation of inundation depth. Within a GIS environment the plausibility of photo locations and derived inundation depths are checked. In this step, the time window for acquisition time of photos is narrowed to the period from 05 to 07 June 2013 to exclusively capture the inundation situation around the occurrence of the flood peak at the water level gauge in Dresden. The process chain, the timeframe and the resulting numbers of tweets in each step are compiled in Figure 5.4 for this specific application example.

For the Dresden example a number of 84 geo-located posts with photos attached are available within the target time and area. As a result of plausibility checks and expert image evaluation a total number of 5 inundation depth estimates are derived for subsequent flood inundation mapping. To give an impression on the challenge to estimate inundation depth based on photo content the 5 useful photo posts, their location and the inundation depths estimates in the Dresden study region are shown in Figure 4.5. For instance photos 1 and 2 in Figure 5.5 show inundated roads but a dry sidewalk. This context enables the analyst to estimate inundation depth in the order of approximately 5 cm. Photo 4 in Figure 5.5 shows flood water on an open space between residential buildings. The orange waste bin which can be seen on this photo is not yet touched by the flood water which provides an indication to estimate inundation depth in the order of 20 cm.

Next, these point estimates of inundation depth are converted into water levels with reference to the base height level [mNN]. This is achieved by adding the inundation depth to the ground level height available from the DGM10 at the location of the photo. The resulting heights are sample points of the spatial continuous water level surface. Given the origin of these points they obviously do not show a regular spatial structure as for instance an equidistant grid. Further, the sample size of data points is rather small. Given these properties we follow the recommendations of J. Li and Heap (2014) for the selection of spatial data interpolation methods and apply a bilinear spline interpolation to obtain an estimate of the water level surface within the target area. Finally, the water

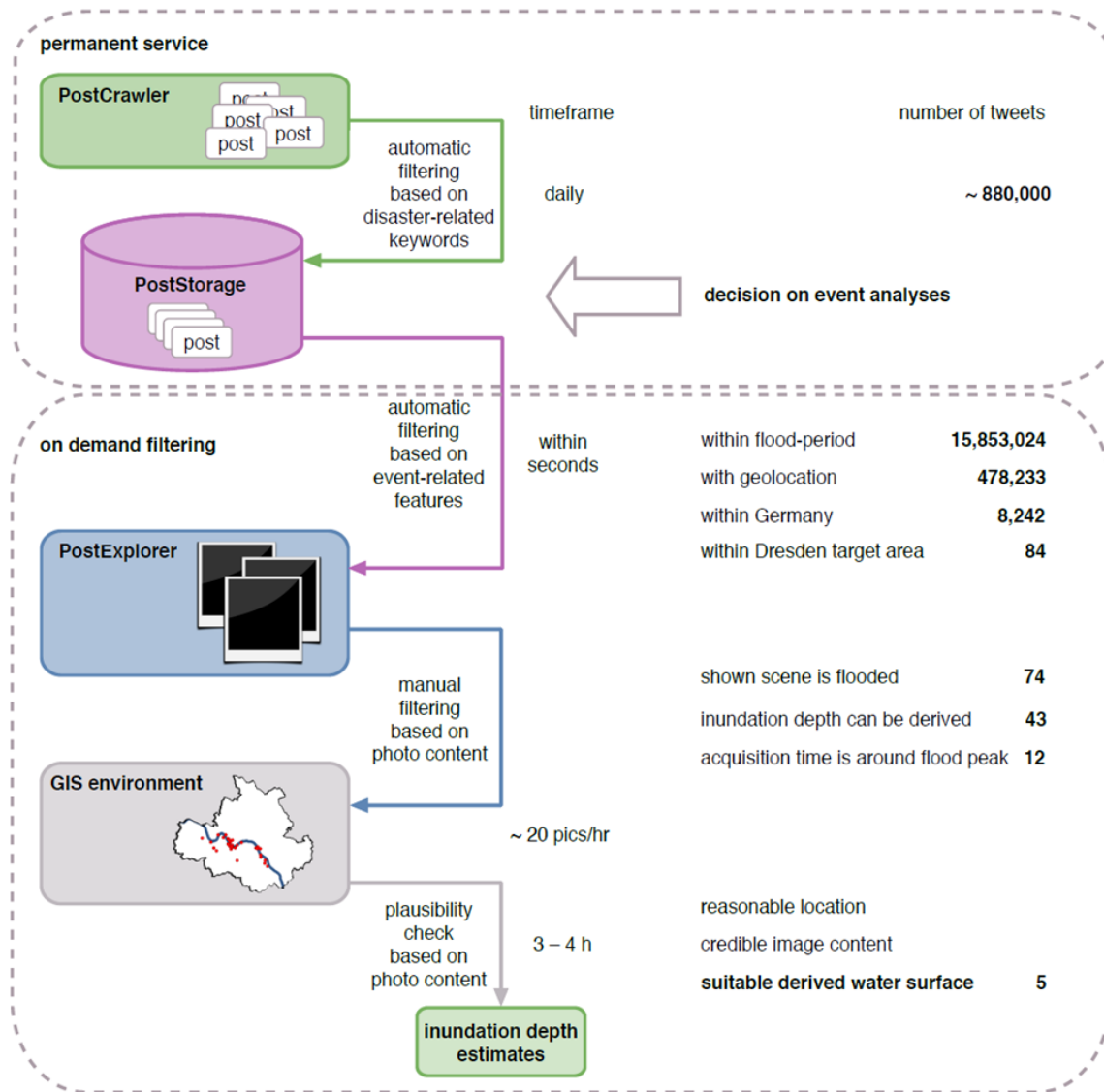


Figure 5.4: Process chain, timeframe and number of tweets for the Dresden flood in June 2013 handled within PostCrawler, PostStorage, PostExplorer and GIS environment for automatic and manual filtering of tweets.

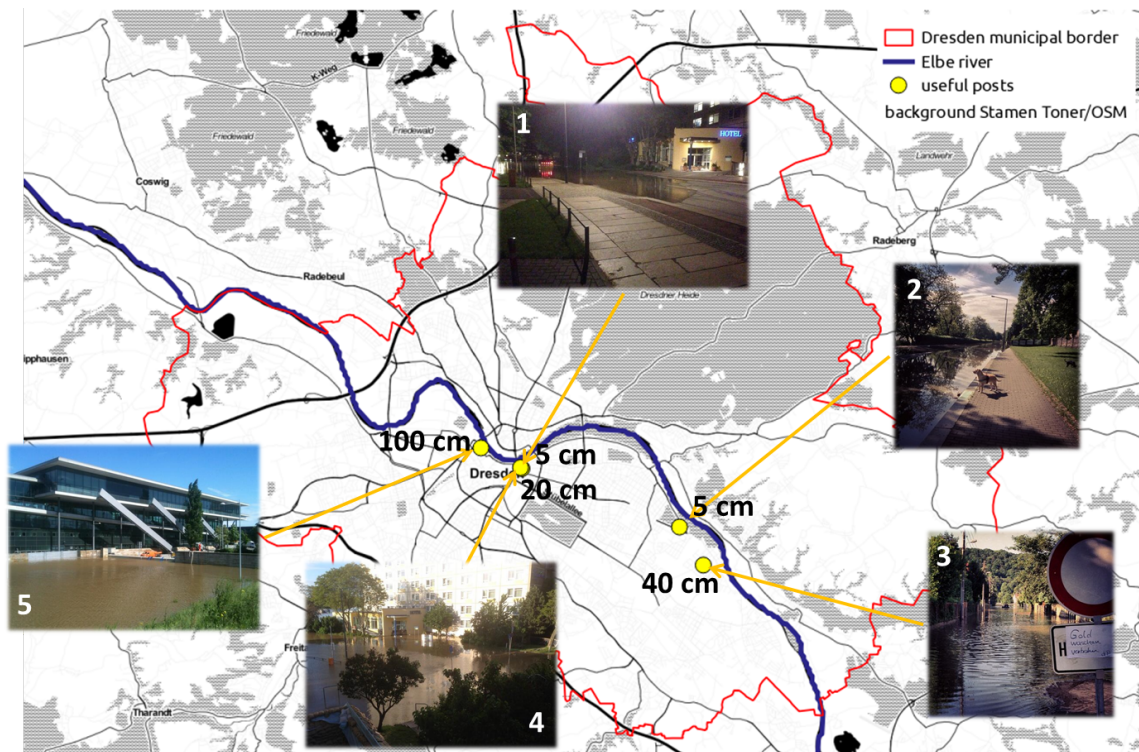


Figure 5.5: Location of useful photos retrieved with PostDistiller and inundation depths estimates (Photos by Denny Tumlrirsch (@Flitzpatrick), @ubahnverleih, Sven Wernicke (@SvenWernicke), Leo Käßner (@leokaesner)).

level surface is intersected with the DEM10 and the difference between the water surface and ground level provides the inundation depth within the inundated area. The resulting inundation depth map is shown in Figure 5.6b. All GIS processing tasks are conducted using the GRASS software (GRASS, 2014).

Evaluation

The inundation maps derived for both mapping scenarios using either (a) online water level observations at the gauge Dresden (Figure 5.6a) or (b) information inferred from photos filtered from social media (Figure 5.6b) are compared in terms of spatial inundation extent and inundation depths.

The water level surface of the inundation map derived from social media photos is on average 1.5 m above the water level surface of the online water level observation. Accordingly, the inundated area based on social media photos resulting from the intersection with the DEM is larger than using the online water level observation as can be seen from Figure 5.6a and b. The spatial distribution of the differences between both inundation depth estimates are given in Figure 5.6d. The differences have been calculated by subtracting scenario (a) from scenario (b) within the overlapping areas. This map of differences illustrates that the agreement of inundation depth estimates is best in the city centre of Dresden with differences smaller than 1 m. In contrast, in the upper part of the Elbe river in the region where additional point estimates of inundation depth are derived from social media photos the differences amount up to 4 m. This comparison reveals that, first, in the case that no water level observations are available, social media may provide useful alternative inundation depths estimates and, second, that through the spatial distribution of information source social media may also provide additional information to the inundation mapping process.

Both mapping approaches are contrasted with a flood footprint which is based on remote sensing data recorded on 05 June 2013 given in Figure 5.6c. This reference inundation map indicates inundations in Dresden in the district of Laubegast upstream and in Pieschen Süd downstream of the city centre (cf. Figure 5.3) the pattern of which reflects the former course of ancient river branches. From this comparison it is apparent that both mapping scenarios clearly overestimate inundated areas. This applies for the inundation mapping based on water level observations (scenario a) for the part downstream of the gauge in Dresden which is located in the city centre. In this scenario, for the upstream part no inundations are detected. In contrast, for the inundation mapping based on social media data (scenario b) also areas upstream of the gauge in Dresden are classified as inundated and provided with inundation depth information which is the outcome of the inundation depth estimates available from the social media photos in the district of Laubegast (cf. photos 2 and 3 in Figure 5.5). However, in this scenario (b) the extent of inundated areas in the target area is overestimated stronger than using solely water level observations in scenario (a). Both inundation depths mapping scenarios intersect the estimated water level with a 10 m DEM. This level of detail for the topographic terrain does not map dike crests, mobile flood protection walls and other flood protection schemes in place. Moreover, the spatial interpolation procedures neither account for hydraulic flow paths nor correct for puddles, i.e. low lying areas that are behind dams or walls and hence are not flooded actually. To overcome the weaknesses of the spatial

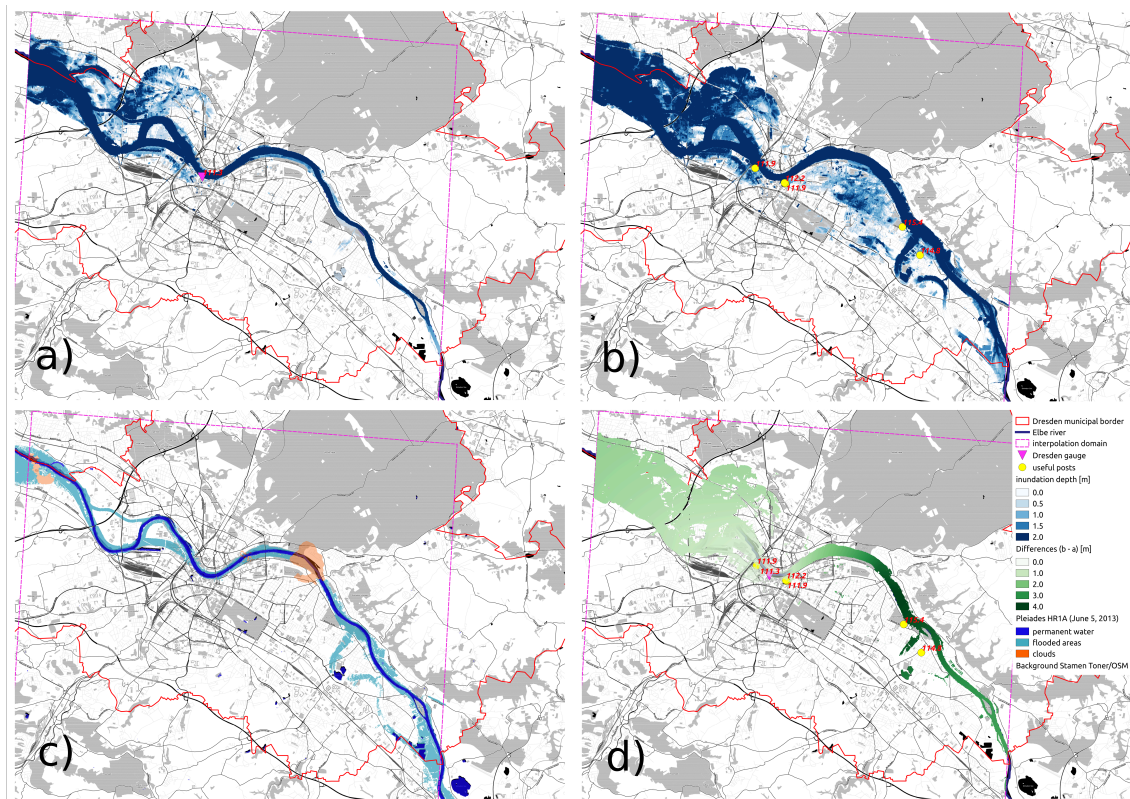


Figure 5.6: Inundation maps and inundation depths derived from online water level observations (panel a), social media content (panel b), inundated area from reference remote sensing flood footprint (panel c) and differences between inundation depths for overlapping areas in maps (a) and (b) (panel d).

interpolation schemes, the remote sensing based flood footprint could be used as a mask in order to spatially constrain the inundation depth maps. In our use case such an information update would have been available several hours later (at best 24 h after image acquisition).

5.4 Discussion

The methodology and tool for filtering the massive amounts of social media data described in this paper proved to be robust and effective within the application example for inundation mapping during the June 2013 flood in the city of Dresden. The filtering and data processing chain effectively supports the target oriented evaluation of photo content. For this example, the temporal demand of the processing chain to provide inundation depth maps is in the range of 2 to 8 h. This expenditure of time essentially stems from the effort to manually filter and evaluate the photos as well as GIS processing and thus depends on the amount of pictures to be analysed. Still, in comparison to alternative data sources for inundation depth mapping, e.g. remote sensing or hydraulic numeric modelling, the inundation depth map derived from social media is more rapidly available and proved a useful complement to water level gauge observations or are even an exclusive in-situ data source for the case that no water level gauge exists in the target area. Technical possibilities to further limit the pre selection of photos for instance by making use of automatic image analyses should be investigated to further improve the efficiency of the manual filtering and evaluation.

It is recognized from the comparison to the water level observations from the gauge in Dresden that the inundation depth estimates derived from photos for specific locations in Dresden in combination with the base height levels from the DGM10 provide decent water level elevations. The differences are in the order of decimetres which is acceptable for the purpose of rapid inundation mapping, particularly when no other information source is available. In this context, both the vertical accuracy level of the DGM10 which is around ± 0.5 to $\pm 2m$ and the vagueness of referencing inundation depth from the photo content, as illustrated in Figure 5.5, have to be borne in mind. Further, the potential difference of the location of the photo and the geolocation of the tweet as well as the offset from the photo shoot and the photo contents involves uncertainties concerning the horizontal location. Improvements concerning the vertical and horizontal accuracy of inundation depth estimates can be expected from using higher resolution LiDAR digital elevation models which may achieve vertical accuracies for terrain data in the range of $\pm 15cm$ (Mandlbürger et al., 2009) and thus also include details about dike crests, or from the integration of more detailed information about the reference environment as for instance available from 3-D-city models (Gröger and Plümer, 2012).

To reduce the inaccuracies concerning the spatial extent of flooding more exact topographic terrain data should be used and appropriately considered within spatial interpolation. Making use of ancillary data such as remote sensing flood footprints, or hydraulic numeric modelling results based on detailed topographic terrain data within spatial interpolation, e.g. External drift Kriging (Goovaerts, 1997) should be investigated.

The availability and the spatial coverage of information support from social media within the target area cannot be controlled but depends on the random activity of social

media users. Crowdsourcing, i.e. distributing the task of inundation depth estimation solves this problem by harnessing collective contributions (Howe, 2006) by actively pushing the acquisition of information via social media, and thus could enhance the reliability of this data source and to improve the coverage.

In summary, the results obtained from the application case in Dresden support the initial hypothesis that social media contain additional and potentially even exclusive information that is useful for inundation depth mapping as a basis for rapid damage estimation but also more general for improving the situation awareness and assessment during the flood event.

5.5 Conclusions

A methodology and tool to automatically filter and efficiently support the manual extraction of information from social media posts for rapid inundation mapping has been presented. In a first step the processing chain allows for filtering a manageable amount of potentially interesting social media posts within seconds. In the Dresden application case 84 potentially interesting posts were selected out of almost 16 Mio posts. In a second step PostDistiller supports to manually assess and filter the automatically derived posts according to relevance and plausibility of their content. Finally, information about inundation depth is extracted. All in all, estimates on inundation depth could be derived within three to four hours in the Dresden example. In comparison to traditional data sources such as satellite data, social media can provide data more rapidly.

The outcomes of the application case are encouraging. Strengths of the procedure proposed are that information for the estimation of inundation depth is rapidly available, particularly in urban areas where it is of high interest and of great value because alternative information sources like remote sensing data analysis do not perform very well. The photos provided represent a snapshot of the current situation and thus also help to improve situation awareness and assessment. In contrast, the detail of location information that can be extracted from social media posts is limited and inundation depths estimates are associated with uncertainty concerning the timing, location and magnitude. Another weakness is that appropriate social media information is not reliably available as it depends on the random behaviour of human sensors. Hence, the uncertainty of inundation depth data derived and the uncontrollable availability of the information source are major threats to the utility of the approach. Another disadvantage is related to the fact that the more photos are available the longer it takes to manually evaluate the photo contents and finally derive an inundation depth map. Automation and integrated quality assessment are crucial for any operational application of the tool.

Nevertheless, social media as an information source for rapid inundation mapping provide the opportunity to close the information gap when traditional data sources are lacking or are sparse. In particular the joint usage of different data streams seems to provide an added value. In this light, further research is required to (i) investigate technical possibilities to improve the pre selection of photos by making use of automatic image analyses, (ii) to integrate more detailed information on the reference environment as for instance provided by high resolution LiDAR DEM or 3d-city models, (iii) to use ancillary data such as flood footprints or hydrodynamic numeric modelling results in order

to constrain inundated areas and to continuously update inundation depth maps, and (iv), for the purpose of quality control, to develop a probabilistic mapping framework that accounts for the uncertainties involved in the different data sources and the final result.

6 | What are the hydro-meteorological controls on flood characteristics?

Manuscript Info

Authors information:

Manuela Nied
Kai Schröter
Stefan Lüdtke
Viet Dung Nguyen
Bruno Merz

Published as:

Nied M., Schröter K.,
Lüdtke S., Nguyen V.D.
Merz B.

What are the
hydro-meteorological
controls on flood
characteristics?

Journal of Hydrology
2017;545:310-326.

doi:10.1016/j.jhydrol.2016.12.003

Abstract

Flood events can be expressed by a variety of characteristics such as flood magnitude and extent, event duration or incurred loss. Flood estimation and management may benefit from understanding how the different flood characteristics relate to the hydrological catchment conditions preceding the event and to the meteorological conditions throughout the event. In this study, we therefore propose a methodology to investigate the hydro-meteorological controls on different flood characteristics, based on the simulation of the complete flood risk chain from the flood triggering precipitation event, through runoff generation in the catchment, flood routing and possible inundation in the river system and floodplains to flood loss. Conditional cumulative distribution functions and regression tree analysis delineate the seasonal varying flood processes and indicate that the effect of the hydrological pre-conditions, i.e. soil moisture patterns, and of the meteorological conditions, i.e. weather patterns, depends on the considered flood characteristic. The methodology is exemplified for the Elbe catchment. In this catchment, the length of the build-up period, the event duration and the number of gauges undergoing at least a 10-year flood are governed by weather patterns. The affected length and the number of gauges undergoing at least a 2-year flood are however governed by soil moisture patterns. In case of flood severity and loss, the controlling factor is less pronounced. Severity is slightly governed by soil moisture patterns whereas loss is slightly governed by weather patterns. The study highlights that flood magnitude and extent arise from different flood generation processes and concludes that soil moisture patterns as well as weather patterns are not only beneficial to inform on possible flood occurrence but also on the involved flood processes and resulting flood characteristics.

6.1 Introduction

Floods can be characterized by a variety of variables, such as flood magnitude and extent, event duration and flood loss. Depending on the perspective, the flood characteristics under consideration vary. The target variable for the (re-)insurance industry is flood loss and expected annual damage, e.g. (W. Kron et al., 2012; Pollner, 2012). Flood risk management requires details on flood magnitude and extent, e.g. (BfG, 2014a) to view the German flood risk map, whereas inundation duration and month of occurrence during the year are decisive for losses to agricultural crops and to flora, e.g. (Van Eck et al., 2006). The flood event characteristics are the outcome of atmospheric processes that deliver the water input to the catchment, runoff generation processes, as well as flood routing and inundation processes in the river system (B. Merz et al., 2014a; R. Merz and Blöschl, 2003). The interacting hydro-meteorological controls and the resultant spread of the event characteristics were illustrated by the disastrous Central European floods of August 2002 (Ulbrich et al., 2003a; Ulbrich et al., 2003b) and June 2013 (Conradt et al., 2013; B. Merz et al., 2014b), affecting amongst others the Elbe Basin. Although the event precipitation in 2013 was not as extreme as in 2002, the hydrological severity, a combination of spatial extent and frequency of the flood peaks, was much higher than in 2002 (Schröter et al., 2015). This can be explained by the particularly wet pre-event soil moisture conditions in 2013. For flood design, flood risk analysis and flood forecasting, it is therefore crucial to understand how the various flood characteristics are controlled by the hydrological catchment conditions and by the meteorological event conditions.

The control of the meteorological conditions and the pre-event catchment conditions on flood generation and magnitude has been acknowledged in many studies (Huza et al., 2014; Nied et al., 2014; Pathiraja et al., 2012; Schröter et al., 2015). However, systematic analyses are limited to small-scale catchments, e.g. (Ettrick et al., 1987; Huza et al., 2014; Paquet et al., 2013; Sivapalan et al., 2005) and flood forecasting, e.g. (Fundel and Zappa, 2011; Silvestro and Rebora, 2014). At the river basin scale, first attempts to study the interplay between catchment state and event conditions indicate the large influence of antecedent catchment conditions on flood magnitude and severity (Nied et al., 2013; Schröter et al., 2015). The control on further flood characteristics such as flood duration and losses has, to our knowledge, not been investigated.

With respect to the meteorological event conditions, numerous studies identified a link between flood occurrence and weather patterns which characterize the main modes of atmospheric state variability, e.g. (Duckstein et al., 1993; Jacobeit et al., 2006; Prudhomme and Geneviev, 2011). Few studies examined the relation between weather patterns and flood magnitude. For instance, Bárdossy and Filiz (2005) identified flood producing circulation patterns by relating them to positive increments of discharge time series. For the Elbe River basin, Nied et al. (2014) showed that different atmospheric circulation patterns favor different flood types such as long-rain floods or snowmelt floods. For the Elbe tributary Mulde in Germany, Petrow et al. (2007) found that Vb-weather systems have the highest flood potential for floods above the 5-year return period whereas floods of lower return period are caused by a variety of circulation patterns. For different regions in Britain, Wilby and Quinn (2013) detected that normalized flood magnitudes are on average greater under specific weather patterns and established a link between circulation patterns and spatial flood extent. Time-varying flood magnitudes were also

related to large scale oscillations such as the El Niño/Southern Oscillation (P. Ward et al., 2010; P. Ward et al., 2014; Waylen and Caviedes, 1986), the North Atlantic Oscillation (Bouwer et al., 2006) or to the decadal variability of the Asian monsoon (Delgado et al., 2012). However, investigations of how the meteorological event conditions in combination with the hydrological pre-event conditions control different flood characteristics besides flood magnitude are lacking.

We intend to fill this gap by studying the interacting control of soil moisture patterns, as a proxy for the hydrological pre-event conditions, and of weather patterns, as a proxy for the meteorological event conditions, over a variety of flood characteristics. These characteristics include not only indicators for flood magnitude and severity but also indicators which quantify the length of the flood-affected river system or the flood impact on society.

It is not feasible to base this analysis on historic flood events alone, since the sample would not be large enough to derive statistically robust conclusions. This would be particularly problematic for the indicators which describe the societal flood impacts. Flood impact data is not well documented and is plagued by inconsistencies (B. Merz et al., 2010b). Hence, we propose to generate a very large number of synthetic flood events. This includes their controls, i.e. spatially coherent patterns of event precipitation and catchment pre-conditions, as well as their consequences, i.e. spatio-temporal patterns of discharge, water stage, inundation, and losses. To this end, a model chain for assessing flood risk at the river basin scale, e.g. (Falter et al., 2016; Falter et al., 2015) is applied. This model chain consists of a hydrological catchment model, a 1D/2D hydraulic model for the processes in the river system, and a damage model. It is driven by synthetically generated patterns of event precipitation and antecedent catchment conditions derived by a resampling approach. In this way, the space-time consistency of controls, processes and their interactions is taken into account. The methodology is developed for the example of the Elbe River basin introduced in section 6.2. The Elbe catchment was chosen due its susceptibility to basin-wide flooding in the past years as well as due to the wealth of data and availability of models. Furthermore, both summer and winter floods are observed in the Elbe basin (Beurton and Thieken, 2009; Nied et al., 2014) which allows studying the controls on a broad range of flood types. Section 6.3 outlines the methodology, from the flood triggering precipitation and its associated weather patterns, through runoff generation compromising the soil moisture conditions, to flood identification and characterization. The results are presented and discussed in section 6.4 and 6.5. The paper finalizes by concluding remarks in section 6.6.

6.2 Study area

The Elbe/Labe Basin (Figure 6.1) is located in Central Europe encompassing 148,268 km². The river originates in the Giant Mountains (Czech Republic), 1386 m a.s.l., and flows after 1094 km into the North Sea (IKSE, 2005). Major tributaries are the Moldau/Vltava, the Eger/Ohe, the Mulde, the Saale, the Schwarze Elster and the Havel. The main riparian states are the Czech Republic and Germany.

The basin can be subdivided into three geomorphologic units: (1) The tide influenced Lower Elbe with an elevation mainly below 75 m a.s.l. encompassing 9% of the catchment

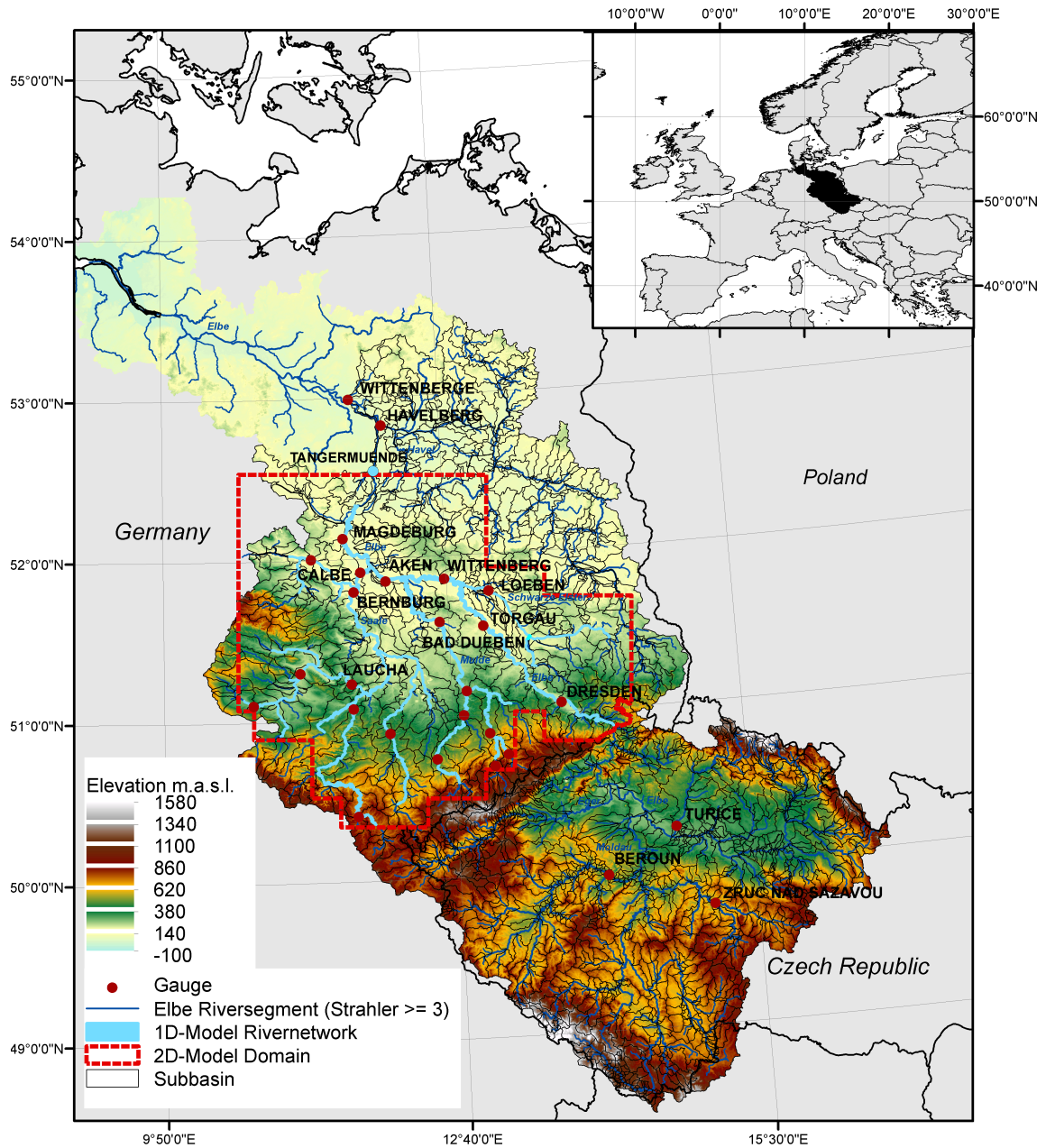


Figure 6.1: Topographic map of the Elbe River catchment, hydrologic model domain, 1D model river network and 2D model domain. Red dots show the gauges which are used to calibrate and validate the rainfall-runoff model, and to identify large-scale flood events. Map of the regional setting of the Elbe catchment (upper right). The map delineates the spatial extent the weather pattern classification is based on.

area, (2) the lowlands of the Middle Elbe (55% of catchment area) situated in an elevation zone below 200 m a.s.l., and (3) the Upper Elbe (36% of catchment area) characterized by hilly country, and low to high mountain ranges (IKSE, 2005). In the lowlands, sandy soils and glacial sediments dominate. In the valleys, loamy soils and in the western Elbe loess is found. In the highlands, cambisols are the main soil type (Hattermann et al., 2005).

Climate ranges from maritime in the Lower Elbe to continental in the Middle and Upper Elbe. Mean annual evapotranspiration is 455 mm (IKSE, 2005). Basin average mean annual precipitation is 715 mm (1961-1990). However, the variation within the basin is high (IKSE, 2005). In the Middle Elbe, mean annual precipitation is around 450 mm. In the mountainous regions, mean annual precipitation is above 1000 mm and strongly modified by the relief. In winter, precipitation is falling as snow. Snow melts predominantly in March, although it can persist until May resulting in a snowmelt influenced discharge regime.

The anthropogenic influence on the catchment is strong. 50.8% of the catchment is cropland, 30.2% forest and 10.2% grassland. Settlements account for 6.5% of the total catchment area (CORINE European Environment Agency, 2000). In the headwaters, dams have been built and along the river, dikes have been installed for flood protection purpose. Past mining activities strongly modified the Havel region.

Besides basin-wide floods, such as the disastrous summer floods of 2002 and 2013, small-scale flooding due to convective events is observed. In winter and spring, floods are predominantly generated by a combination of snowmelt and rainfall (IKSE, 2005; Nied et al., 2014; Petrow et al., 2007).

6.3 Data and methods

A process-based flood hazard and risk assessment is conducted in which soil moisture patterns are selected as a proxy for the hydrological pre-event catchment conditions and weather patterns are selected as a proxy for the meteorological event conditions. Based on 84 observed flood events in the Elbe catchment, the patterns' influence on flood generation has previously been illustrated (Nied et al., 2014). Their control on the flood characteristics is determined from an augmented sample generated by reshuffling daily fields of meteorological conditions. The reshuffling extends the available climate time series by taking into account the synoptic-scale dependence between large-scale circulation and local meteorology, as well as the seasonal variability. The reshuffled meteorological time series is used to drive the regional flood model (RFM). RFM has been developed to simulate flooding and its impact at the river basin scale (Falter et al., 2015). First, a continuous semi-distributed rainfall-runoff model simulates soil moisture as well as river discharge. Flood inundation and loss are determined by subsequently applying a hydrodynamic and a flood loss model. From these time series, flood events, their characteristics, as well as the involved soil moisture and weather patterns are identified. The relationship between patterns of hydro-meteorological conditions and flood occurrence as well as a variety of flood characteristics is deciphered by (i) conditional cumulative distributions functions to estimate the separate impact of soil moisture patterns and weather patterns on the flood characteristics, and (ii) by regression trees to analyze the combined

impact of soil moisture patterns and weather patterns on the flood characteristics. The analysis period is September 1957 to August 2002. In the following, the analysis steps (Figure 6.2) are presented in detail.

6.3.1 Hydro-meteorological patterns

Weather patterns and reshuffling

In the analysis period, the meteorological conditions are scrutinized on two scales: on the synoptic scale to characterize the large scale meteorological conditions and attribute them to floods and on the local scale to drive the RFM in high spatial resolution and derive the flood characteristics.

The synoptic scale is accounted for by daily weather patterns. To derive weather patterns, ERA-40 reanalysis data (Uppala et al., 2005) covering Europe (see Figure 6.1, upper right) are used. Daily fields ($1.125^\circ \times 1.125^\circ$) of geopotential height in 500 hPa representing atmospheric circulation, temperature in 500 hPa indicating e.g. melting conditions, and total column water vapor content indicating potential rainfall, were clustered by (Nied et al., 2014) into 40 weather patterns using the SANDRA algorithm (Philipp et al., 2007). The flood generating weather patterns vary seasonally and can be linked to different flood types (Nied et al., 2014). Figure 6.3 displays a selection of four weather patterns, which play a central role in this work. During weather pattern 19 subtropical air masses are transported to Central Europe. The pattern shows positive anomalies with respect to air temperature and negative anomalies with respect to precipitation in the Elbe catchment whereas weather pattern 26 is associated with positive anomalies in air temperature as well as precipitation. Wind directions are mostly westerly or north-westerly. Weather pattern 29 is a low pressure system over South Europe which transports warm and moist air masses towards Central/Eastern Europe. Flood-favoring 'Vb' cyclones are mostly assigned to this weather pattern. In case of weather pattern 34, moist air from the Mediterranean is transported towards the Elbe catchment.

For the characterization of the local meteorological conditions in the Elbe catchment and to drive the RFM (sect. 3.2), daily station data of precipitation amount, mean, maximum, and minimum air temperature, solar radiation and relative humidity are used. The station data were provided by the German Weather Service (DWD) and the Czech Hydrometeorological Institute, corrected for inconsistencies, data gaps and inhomogeneities (Oesterle, 2001; Oesterle et al., 2006).

These available climate time series are extended by a reshuffling approach which is similar to the concept of the Multi-Exponential Weather Pattern distribution, e.g. (Garavaglia et al., 2011; Paquet et al., 2013). In the reshuffling approach, the local meteorological data (i.e. precipitation amount, mean, maximum, and minimum air temperature, solar radiation and relative humidity) of all stations are grouped for each day. Afterwards, subsamples of the grouped data are derived for each month and prevailing weather pattern. The subsamples and the weather pattern time series are used to generate synthetic meteorological time series. Therefore, the grouped data are resampled by retaining the prevailing weather pattern and its month of occurrence. For instance, within the analysis period, a particular weather pattern occurs 62 times in August. The meteorological data of these 62 days are randomly exchanged. The replacement is executed for all combinations of weather patterns and months simultaneously. In doing

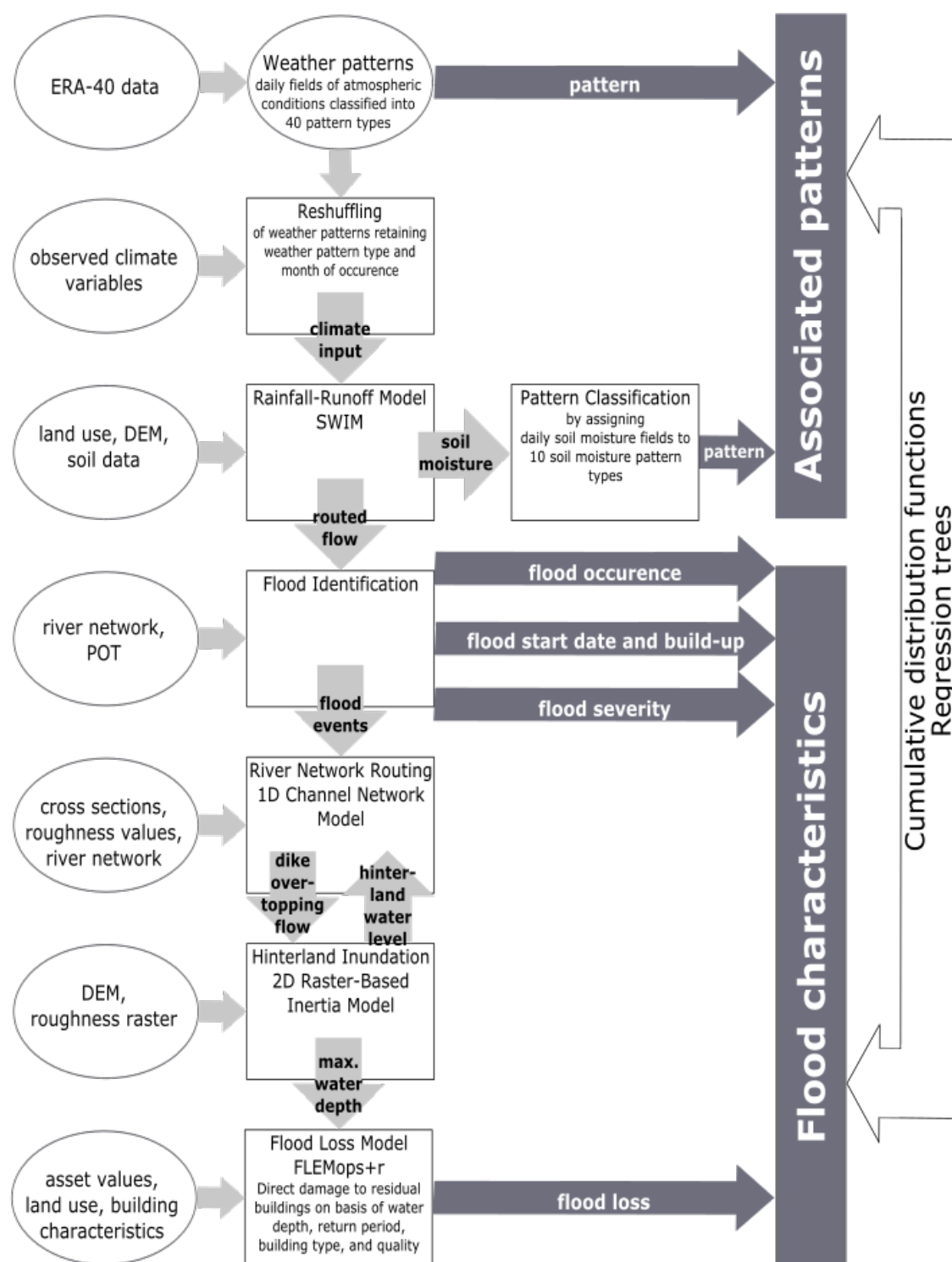


Figure 6.2: Flow chart of the analysis: modules (rectangles), their input data (ovals) and results (arrows). Weather patterns are reshuffled and used to drive the regional flood model (RFM) composed of a rainfall-runoff model to simulate soil moisture and discharge, a hydrodynamic model to simulate inundation, as well as a flood loss model. Flood events, their characteristics, as well as the involved soil moisture and weather patterns are identified. The relationship between the patterns and flood occurrence as well as flood characteristics are analyzed by cumulative distributions functions and regression trees.

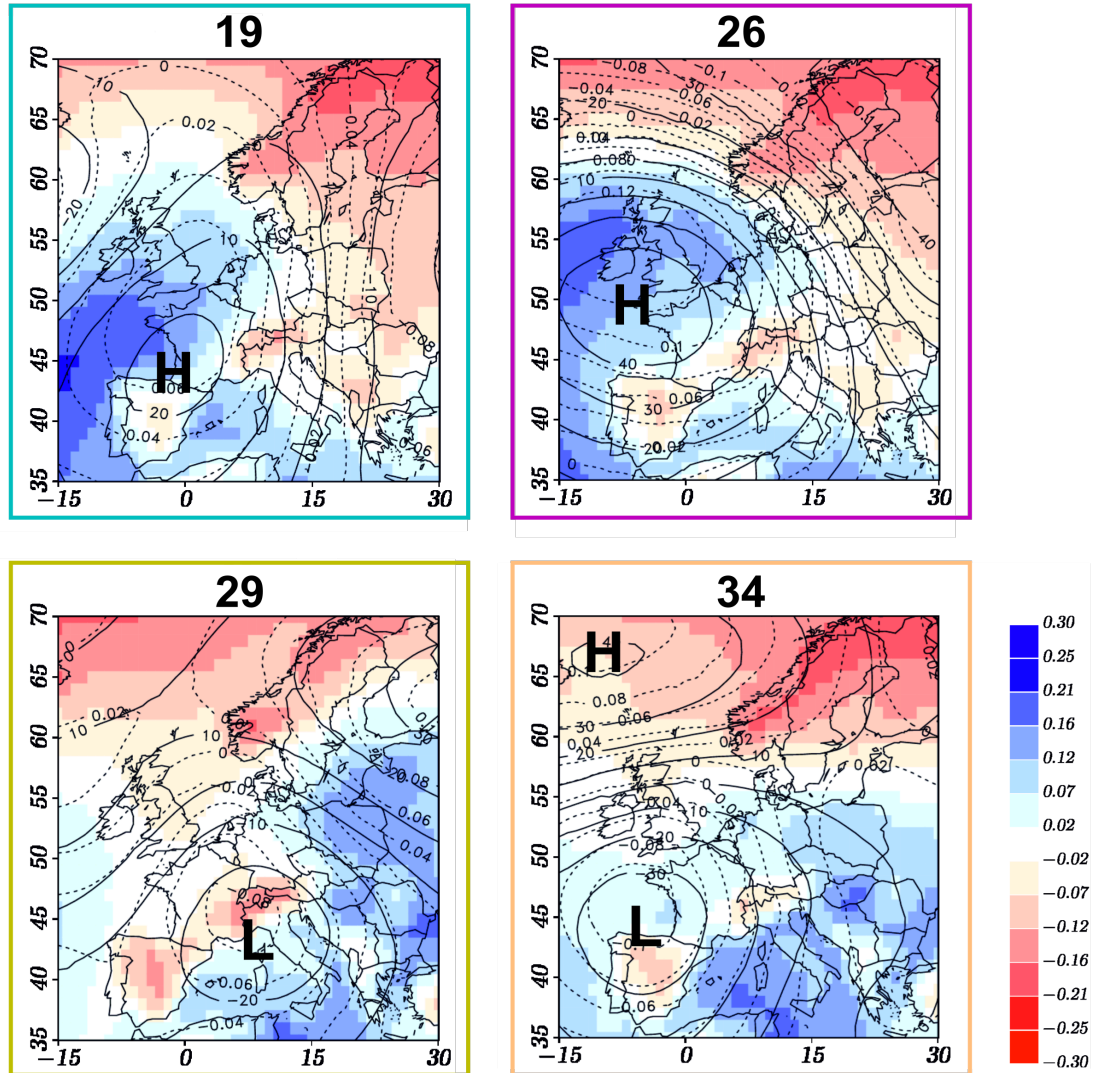


Figure 6.3: Meteorological cluster centroids of the selected weather patterns (19, 26, 29 and 34). Shaded contours show mean cluster anomalies in the vertically integrated moisture content [kg/m²], solid isolines show mean anomalies in the 500 hPa geopotential [m], and dashed isolines are mean anomalies in 500 hPa air temperature [°C]. Weather patterns are taken from Nied et al. (2014).

so, the reshuffling approach accounts for both, the synoptic-scale dependence between large-scale circulation and local meteorology, as well as the seasonal variability (Pathiraja et al., 2012). Furthermore, the spatial pattern as well as the interrelation of the meteorological variables is considered. In the median, a particular weather pattern - month combination occurs 31 times. The minimum value is 0, the maximum value 211 reflecting the different seasonality of the weather patterns. By reshuffling daily meteorological fields, the spatial coherence as well as the interdependence between the meteorological variables is preserved. However, the ‘meteorological genesis’ of weather phenomena lasting over several days may be disturbed. The method does neither produce new fields of meteorological variables, nor new sequences of weather patterns. Instead, it reshuffles the observed meteorological patterns, retaining the sequence of weather patterns and retaining the probability distributions of the local meteorological variables. The reshuffling is repeated 2000 times resulting in 90,000 yearly realizations (45 years of observations \times 2000).

Soil moisture patterns

The reshuffled meteorological time series are used to drive the subsequent flood risk model chain. From these simulations, the basin-wide distribution of soil moisture of each day is assigned to one of 10 soil moisture patterns. These patterns are taken from Nied et al. (2013). The patterns range from catchment wide soil saturation to dry conditions and vary seasonally. Figure 6.4 displays a selection of soil moisture patterns, which play a central role in this work. Pattern 9 is the wettest pattern characterized by catchment wide soil saturation. Pattern 3 is characterized by catchment wide soil saturation too. In previous studies (Nied et al., 2013; Nied et al., 2014), pattern 9 was primarily related to winter flood initiation whereas pattern 3 was relevant for flood initiation in summer as well as wintertime. Independent of the prevailing meteorological conditions, pattern 9 was identified to have the highest flood potential. In case of pattern 5, soil saturation is limited to the upstream Elbe. The pattern was found to be primarily relevant for flood initiation in summer (Nied et al., 2013; Nied et al., 2014).

For their pattern classification, Nied et al. (2013) simulated soil moisture for every Elbe subbasin with the SWIM model (details see section 6.3.2.1). A principal component analysis and a subsequent cluster analysis on the leading 4 principal components resulted in 10 soil moisture patterns. We use the classification of Nied et al. (2013) to assign the daily simulated soil moisture of the reshuffled model runs to these pre-defined patterns. The principal components (*PC*) of each reshuffled soil moisture simulation are obtained by projecting the simulated standardized (zero mean, unit variance) profile soil moisture (*SMI*) onto the eigenvectors u of the soil moisture classification of Nied et al. (2013).

$$PC = SMI \times u \quad (6.1)$$

Subsequently, the least squared deviation between the leading 4 *PCs* of the reshuffled simulation and the 10 cluster centroids of the soil moisture classification of Nied et al. (2013) is identified for each day. Each day of the reshuffled simulation is assigned to the soil moisture pattern with the least squared difference.

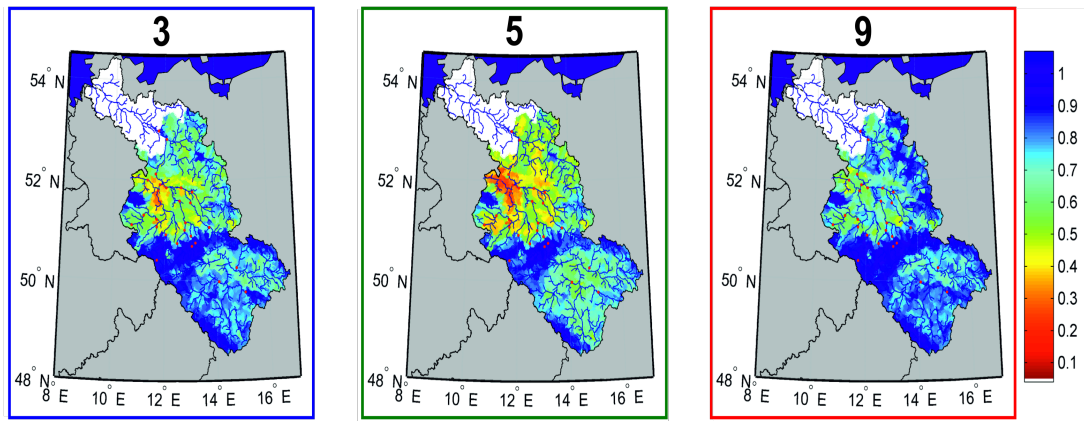


Figure 6.4: Selected soil moisture patterns (3, 5 and 9) as identified by Nied et al. (2013). Profile (layer-depth weighted average) soil moisture content is standardized by the field capacity of the respective soil type.

6.3.2 Regional flood model (RFM)

RFM comprises a rainfall-runoff model, a coupled 1D-2D hydrodynamic model as well as a flood loss model. The model chain assesses flood hazard and risk in a spatially consistent way and has been proven to derive plausible results in meso-scale (e.g. for the 6000 km² large Mulde catchment; (Falter et al., 2015)) as well as in macro-scale applications (e.g. for the Elbe catchment, (Falter et al., 2016)). The 1D-2D hydrodynamic model simulates the hydraulic processes in the river and adjacent flood floodplains, hence, its model domain is only a subarea of the model domain of the rainfall-runoff model (see Figure 6.1 for the different model domains).

Rainfall-runoff model

Runoff and soil moisture are simulated with the conceptual, semi-distributed rainfall-runoff model SWIM (Krysanova et al., 1998). The model calculates runoff based on hydrological response units which are delineated by soil type and land use class. Information on land use is taken from the CORINE 2000 land cover data set of the European Environment Agency (CORINE European Environment Agency, 2000). The soil map is created by merging the German soil map “BUECK 1000” provided by the Federal Institute for Geosciences and Natural Resources (BGR), and the FAO-UNESCO soil map for the Czech part.

Based on topography, the hydrological response units are aggregated into subbasins. In the model setup, the Elbe catchment is subdivided into 1945 subbasins upstream of gauge Wittenberge (see Figure 6.1 for the model domain). The reshuffled meteorological time series (section 6.1.1.1) serve as climate input to the model by interpolating the station data on the centroid of each subbasin.

On the next level of spatial disaggregation, the subbasins are aggregated into 27 regions, assuming homogeneous parameterization within each region. Nine parameters were calibrated progressively from upstream to downstream against observed discharge

at the outlet of each region (dots, Figure 6.1) by Nied et al. (2013). The calibration period extended from 1981 to 1989 and a weighted Nash-Sutcliffe efficiency coefficient (Hundecha and Bárdossy, 2004; Nash and Sutcliffe, 1970) was used as an objective function. 38 sets of parameter realizations have been identified as behavioral according to an a-priori set threshold of goodness of fit. All gauges had a median weighted Nash-Sutcliffe efficiency between 0.55 and 0.8. In the validation period which lasted from 1951 to 1980 as well as from 1990 to 2003, the gauges' median weighted Nash-Sutcliffe efficiency ranged between 0.53 and 0.81 (1951-1980) as well as 0.26 and 0.87 (1990-2003). In addition, it has been shown that the model is able to reproduce the temporal evolution of profile soil moisture by comparing simulated soil moisture against satellite derived soil moisture information (Nied et al., 2013). For more details on the model and the calibration as well as validation procedure see (Nied et al., 2013). For each gauge, the median simulated discharge is calculated from the 38 behavioral model runs and taken for further analysis.

Hydrodynamic model

As the rainfall-runoff model does not consider explicitly river channel geometry, slope and resistance, it is not able to simulate water levels and flood inundation. Therefore, a 1D river network routing model (see Figure 6.1 for the model domain) which considers hydraulic processes by taking into account the actual river cross-sections complements the regional flood model. The routed subbasin discharge derived from the rainfall-runoff model serves as its boundary condition.

The 1D routing model solves the simplified form of the Saint-Venant equations for flow in open channel with an adaptive explicit scheme (Falter et al., 2015). The model is able to simulate overbank flow. Whenever the routed water level exceeds the dike crest level, the overtopping flow triggers a 2D hinterland inundation model. This raster-based inertial model simulates inundation propagation and is based on the simplified shallow water equation, neglecting advective acceleration (Bates et al., 2010; Falter et al., 2015). The spatial resolution is 100 m. The 1D-2D coupled model was implemented in the CUDA Fortran environment to enable model simulation on highly parallelized NVIDIA Graphical Processor Units (GPU) and multicore processor Central Processing Unit (CPU). Dike breaching is not included in the current model version. Therefore, inundation extent may be underestimated (see (Falter et al., 2016)).

Profiles of overbank cross-sections including dike information are the most demanding model input and are very important for the quality of the model simulations (Falter et al., 2016). In total, 3717 cross-sections upstream of Tangermünde have been derived from a 10 m-DEM (Federal Agency for Cartography and Geodesy in Germany) using the HEC-GeoRas tool (US Army Corps of Engineers) in ArcGIS 10.1. The cross-section profiles have been extracted in 500 m distance, perpendicular to the flow direction. Inconsistencies, e.g. due to perpendicular cross-sections overlapping each other, have been corrected manually to generate a more realistic representation of channel geometry (see (Falter et al., 2015)).

The model has been validated by comparing the simulated inundation extent to a remotely sensed flood masks for the August 2002 flood in the Elbe basin (Falter et al., 2016).

Flood loss model

For each flood event (see section 6.3.3 for the definition of flood events), flood loss is calculated with the Flood Loss Estimation MOdel for the private sector (FLEMOps+r, (Elmer et al., 2010; Thielen et al., 2008a)). FLEMOps+r estimates direct damage to residential buildings using a rule based multi-variable approach differentiating between five classes of maximum inundation depth, three building types, two classes of building quality, three classes of contamination, three classes of private precaution and three classes of flood peak return periods. In summary, the loss estimation requires spatially detailed input data of asset values, building quality and building type, as well as the event dependent variables inundation depths and return period of peak flows.

All inputs are prepared as gridded data sets (spatial resolution of 100 m) to comply with the 2D hydrodynamic modelling output. Asset values of the regional stock of residential buildings are defined on the basis of standard construction costs (BMVBS, 2005) which reflect the market price of the construction works for restoring a damaged building with reference to the year 2010. The asset values are disaggregated to the digital basic landscape model (Basic DLM) of the German ATKIS (Authoritative Topographic Cartographic Information System; (GEODATENZENTRUM, 2009)) using the binary disaggregation scheme proposed by Wunsch et al. (2009). The characteristics of the municipal building stock are derived from the INFAS Geodaten data set (INFAS GEOdaten GmbH, 2009). Maximum inundation depth is the outcome of the 2D raster-based hinterland inundation model. Discharge return periods are estimated within each SWIM subbasin based on the annual maximum discharge series 1951 to 2003. As per (Elmer et al., 2010), precautionary measures and contamination are not taken into account in this study. For each flood event, absolute flood losses in Euros are calculated as the product of damage ratio and location-dependent asset value per raster cell.

The model has been validated both using observed loss data on the scale of individual buildings and on the meso-scale using official loss records for the 2002 flood in Saxony (Thielen et al., 2008a). Further, Falter et al. (2016) provide a comparison of loss model results with other damage estimates for the April 1994 and August 2002 floods in the Elbe basin in a proof of concept application of the RFM in the Elbe basin. Both validation exercises have shown a decent performance of the loss model.

6.3.3 Flood event identification and characteristics

Large-scale flood events are identified according to Uhlemann et al. (2010). Flood event detection is based on daily simulated discharge at all 27 gauges (see Figure 6.1, red dots). A systematic spatio-temporal peak-flow search is conducted around each simulated 10-year flood. In doing so, each flood event is characterized by its spatio-temporal extent. In general, a flood implies several discharge peaks of various magnitudes distributed in space and time which reflects the heterogeneity of floods at the river basin scale. The temporal flood progression is described by the event start date, the event end date and the event centroid. The event start date defines the date, up to three days in advance of a recorded 10-year flood, where the first gauge has a significant peak. The up to three days beforehand account for the catchment's concentration time which is determined by the catchment size, the catchment characteristics and its initial state. The event end date is the date where the last gauge shows a significant peak up to ten days after a

10-year flood. A peak is considered significant if it exceeds $P(t) + v$. Where $P(t)$ is the 13 days moving average of simulated discharge and v is the 90th percentile of the residuals between daily simulated discharge and $P(t)$. The event centroid C defines the day of the highest daily overall discharge increase at day t compared to the previous day ($t-1$) during a flood event of length d . Daily overall discharge is the discharge (Q) sum of all gauges n in the catchment standardized by their respective 2-year flood HQ_2 (Uhlemann et al., 2010).

$$C = \max \left(\sum_{i=1}^n \left(\frac{Q_{i,t}}{HQ_{2,i}} \right) - \sum_{i=1}^n \left(\frac{Q_{i,t-1}}{HQ_{2,i}} \right) \right) \quad t = \{2, 3, \dots, d\} \quad (6.2)$$

For each identified flood, the following characteristics, and their relationship to hydro-meteorological patterns are investigated:

- **Month event start date:** As different flood types dominate in different seasons (R. Merz and Blöschl, 2003; Nied et al., 2014), this characteristic is used to analyze the seasonal influence.
- **Length build-up period:** The period after the event start date including the event centroid date is named event build-up period. The length of the build-up period depends on flood type and spatial flood extent and accounts for the catchment reaction time as well as flood routing.
- **Total event length:** The event length marks the time between the event start date and the event end date.
- **Affected length:** The affected length describes the percentage of the regionalized river network affected by at least a 2-year flood. The regionalization scheme is based on the hierarchical ordering of river tributaries by Strahler (1964) accounting for river length and topology. The total length of the upstream river stretches is estimated in dependence of a gauge's Strahler-order. In case of nested catchments, regionalization stretches from the downstream gauge to the upstream gauge. Details on the regionalization scheme are provided by Uhlemann et al. (2010). The spatial flood extent depends on the flood type (R. Merz and Blöschl, 2003; Nied et al., 2014).
- **Affected gauges HQ_2 (affected gauges HQ_{10}):** The percentage of gauges, out of the 27 gauges in the analysis, which are affected by at least a 2-year flood (10-year flood). The measure characterizes the magnitude of a flood event.
- **Severity:** The severity S regionalizes gauges' discharge to represent the flood situation in a particular river stretch. It is a combined measure of flood magnitude and extent

$$S = \sum_{i=1}^n \left(\lambda_i \frac{HQ_i}{HQ_{2,i}} \right) HQ_i \geq HQ_{2,i}. (3) \quad (6.3)$$

HQ_i is the maximum discharge at gauge i for a respective flood event which is standardized by the gauge's 2-year flood HQ_2 . Only gauges exceeding

their $HQ2$ are included in the severity calculation as below $HQ2$ (assuming to represent bankfull river flow) no impact is expected. λ is a weighting factor. λ_i is the regionalized river network of gauge i in relation to the overall regionalized river network. i.e. $\sum \lambda_i$ equals unity.

- **Losses:** Flood losses are calculated according to section 6.3.2.3. In contrast to the severity, flood losses also take the spatial distribution of inundation areas and their superposition with assets into account.

For the comparability of results, the threshold values $HQ2$ and $HQ10$, applied in the flood identification as well as characterization, are estimated from the model simulation with undisturbed meteorological variables and kept constant for all reshuffled runs.

6.3.4 Linking patterns to flood events and their characteristics

The soil moisture patterns and weather patterns are assigned to the flood characteristics in two ways. Cumulative distributions functions analyze the separate impact of soil moisture patterns and weather patterns on the flood characteristics (section 6.3.4.1) whereas a regression tree analysis (section 6.3.4.2) estimates their combined impact. This allows for a quantitative investigation of the hydro-meteorological controls over the flood characteristics.

Since soil moisture patterns represent the pre-event catchment conditions, they are considered at the event start date. Weather patterns represent the meteorological influence of the event and are considered during the event build-up period. In the build-up period, each weather pattern is weighted in accordance with the number of days it occurs. The weighting coefficient is the ratio of number of days to the total length of the build-up period. Thus, each flood event receives the same weight (Nied et al., 2013; Nied et al., 2014). Minor flood events with a build-up period less than one day were removed from the analysis.

Cumulative distribution functions

A cumulative distribution function (CDF) describes the probability of a real random variable, i.e. in our case a flood characteristic. For each flood characteristic, a CDF is established to view the respective probability distribution. Second, the CDF of each flood characteristic is separated according to the prevailing soil moisture patterns as well as according to the prevailing weather patterns to view the patterns' influence on the flood characteristics.

Regression trees

Classification and regression trees (CART, Breiman et al. (1984) are binary trees to understand the structural relationship between a predictor, i.e. in our case soil moisture patterns/weather patterns and a response, i.e. the flood characteristic. Tree based models are chosen for this study as they do not make any implicit assumption on the relationship between the predictor and its response and can represent non-linear and non-monotonic dependencies. Therefore, they are well suited when there is little knowledge of the importance of the predictors as well as their interaction. However, tree based models can

only reflect those structures already present in the data and therefore can't draw any conclusions beyond the utilized data.

For regression trees, the response is predicted by subsequently separating the predictor values into homogeneous subgroups. The optimal split at each decision node is selected by calculating the within group variance of the response values of all possible splits. The partition that maximizes the decrease of the within group variance is chosen. This results in a tree that develops from the root node which unifies all predictor values, through the decision nodes that subsequently split the predictor values into two subgroups, to the terminal nodes (leaves) characterizing the response. Strongly ramified trees characterize the underlying data in the minutest detail. However, they can bear small leaf sample sizes where the predictive power for independent data is poor. Therefore, an optimal sized tree, complex enough to account for the relationship between predictors and response, and simple enough to avoid overfitting, has to be identified. One method is pruning. A ramified tree is sequentially pruned to a simplified subtree. Those branches are cut first that led to the smallest decrease in the predictive error. The predictive error R is defined over all leaves as the sum of the estimated probability of a leaf times its average squared error

$$R_T = \sum_{j=1}^{N_T} \left[\frac{T}{N} \frac{1}{N_T} \sum_{n=1}^T (y_n - \bar{y}_n)^2 \right] \quad (6.4)$$

where N_T is the number of leaves, N the total number of observations, T the number of observations of leaf j , y_n the observations in leaf j and n the simulation (median of observations in leaf j).

Ten-fold cross validation is applied to choose the tree size. The observations are randomly separated into 10 subsamples. Tree growing and pruning are repeatedly applied to the given data set excluding always one subsample. Taking the retained subsample, the predictive error of the grown tree is estimated. Afterwards, the predictive error is averaged over all subsamples and displayed as a function of the number of terminal nodes. The optimal tree is the smallest tree that is within one standard error of the subtree with the smallest predictive error.

The importance of a predictor variable (variable importance) with respect to the response is determined by estimating the predictive error at each decision node. The difference between the predictive error for the parent node and the total predictive error for the two children nodes, i.e. the decrease in the predictive error ΔI , is calculated. The importance of a variable m is defined as the sum over all ΔI where m is the splitting criteria. The higher the sum over all ΔI for a particular variable, the more important is the variable. The variable importance of the two predictor variables soil moisture patterns $\Sigma \Delta I_{m1}$ and weather patterns $\Sigma \Delta I_{m2}$ is estimated respectively for each response variable.

For the comparability of results, the delta of the variable importance is calculated for each response variable. The delta of the variable importance is defined as

$$D = \frac{\Sigma \Delta I_{m2}}{\max(\Sigma \Delta I_{m1}, \Sigma \Delta I_{m2})} - \frac{\Sigma \Delta I_{m1}}{\max(\Sigma \Delta I_{m1}, \Sigma \Delta I_{m2})} \quad (6.5)$$

Positive values illustrate the control of weather patterns, and negative values highlight the dominance of soil moisture patterns. The higher the absolute value, the stronger

the influence of weather or soil moisture patterns on the respective flood characteristic. The maximum value is one indicating that the flood characteristic is solely controlled by weather patterns in case of a positive value or by soil moisture patterns in case of a negative value. One has to be aware that the delta of the variable importance denotes only the importance of soil moisture patterns compared to weather patterns. Predictors not included in the regression tree analysis, like flood protection and management, may have an even larger control on the flood characteristics.

6.4 Results

6.4.1 Evaluation of the regional flood model and of the reshuffling approach

To prove the capability of the regional flood model to reproduce the flood characteristics (section 6.3.3), the simulated flood characteristics are compared against those retrieved from observed discharge. Therefore, the flood identification (section 6.3.3) is applied to observed discharge and simulated discharge generated by the undisturbed climate data, i.e. the observed meteorology. All flood events from September 1957 to August 2002 with a minimum build-up period of one day are evaluated. From the observed discharge time series, 15 flood events are identified (Figure 6.5, grey dashed line). The regional flood model simulates 7 events (Figure 6.5, grey solid line) when driven with the observed meteorology. Although the number of simulated events is half the number of observed events, the general agreement of the empirical cumulative distribution functions (CDFs), both in shape and magnitude, implies that the regional flood model is suitable to reproduce the observed event characteristics. According to the Kolmogorov Smirnov test, the hypothesis that the observed and simulated flood event characteristics are drawn from the same distribution cannot be rejected at the 5% significance level for all characteristics.

The underestimation of the number of flood events is due to the lower number of simulated significant peaks (43,507) than observed significant peaks (60,509). As a consequence, a higher number of flood events are detected in which a single 10-year flood is simulated and no additional significant peak three days beforehand the 10-year flood is found. The events' build-up period is less one day. Including these events, 32 events are observed whereas 37 events are simulated. In the current event set where minor flood events with a build-up period less one day are neglected, the number of significant peaks during the event is in the same order of magnitude for simulated and observed flood. On average, an observed flood event comprises 53 significant peaks whereas a simulated flood event comprises 49 significant peaks. Gauges underestimating the number of significant peaks are randomly distributed within the Elbe catchment. Therefore, the underestimation may be traced back to model deficits in simulating the runoff dynamics possibly due to deficits in the climate input data where small scale precipitation features like thunderstorms may not be present. The flood characteristic losses cannot be evaluated due to the scarcity and uncertainty of historical flood loss estimates (B. Merz et al., 2010b).

Within the reshuffling approach, 5970 flood events (Figure 6.5, black solid line) are identified from the reshuffled model runs. The comparison of the simulated characteristics (Figure 6.5, grey solid line vs. black solid line) shows that the reshuffling reproduces the event characteristics. According to the Kolmogorov Smirnov test, the hypothesis that

the characteristics are drawn from the same distribution cannot be rejected at the 5% significance level for all characteristics. However, flood severity (Figure 6.5, G), affected length (Figure 6.5, D) and the affected gauges HQ_2 (Figure 6.5, E) are in the median underestimated. Further, the reshuffling approach is able to generate events that are outside the range of previously (September 1957 to August 2002) observed events. For instance, the highest observed severity was 164 whereas the highest simulated severity obtained by the shuffling approach is 214. No events are generated where the entire catchment is affected by at least a 10-year flood (Figure 6.5, F). The maximum number of gauges affected by at least a 10-year flood during one specific flood event is 70.4%. This highlights that the commonly applied assumption of spatially uniform return periods within an entire river basin is invalid on the river basin scale and would result in overestimation of flood risk, as was shown for the Rhine river by (Thieken et al., 2014). Within the reshuffling approach, about 20% of the simulated flood events cause flood losses (Figure 6.5, H).

6.4.2 Separate control of hydrological pre-conditions and meteorological event conditions on flood characteristics

The separate impact of the hydrological pre-conditions and the meteorological event conditions on each flood characteristic is examined by deriving CDFs (Figure 6.6). The characteristics in dependence of weather patterns (soil moisture patterns) are shown on the left (right) hand side of each subplot. The color coded CDFs represent the patterns introduced in sect. 3.1. The remaining patterns are labeled in grey. The black colored CDF is in each case identical to the black solid line in Figure 6.5 representing the entire event set independent of the pattern. N is the sample size of the respective CDF.

The control of weather patterns/soil moisture patterns on a flood characteristic is expressed in the spread of the CDFs; the higher the spread the stronger the control. For instance, the CDFs of the length of the build-up period (Figure 6.6, B) and the total event length (Figure 6.6, C) are similar among the soil moisture patterns whereas they vary among the weather patterns. This indicates that the soil moisture conditions have little influence on these flood characteristics and that the impact of weather patterns is stronger. For other characteristics, the respective influence of soil moisture and event conditions is less clear and will be further investigated and discussed in section 6.4.3 and section 6.5.2.

Differences in the CDFs are not only visible between weather patterns and soil moisture patterns in general but also between the characteristics for specific weather patterns and soil moisture patterns. The patterns' different behavior in relation to the various characteristics can be explained by the patterns' associated flood types derived by Nied et al. (2014).

Weather pattern 19 is related to snowmelt as well as rain-on-snow events (Nied et al., 2014). In the Elbe catchment, snowmelt floods are limited to the winter season and characterized by a large spatial flood extent of minor magnitudes (Nied et al., 2014). The CDFs of weather pattern 19 reveal these characteristics. The pattern, related to flood generation in winter (Figure 6.6, A), shows high severities (Figure 6.6, G), a high affected length (Figure 6.6, D), a high affected gauges HQ_2 (Figure 6.6, E) as well as a low affected gauges HQ_{10} (Figure 6.6, F). Pattern 26 was linked to rain-on-snow events only (Nied et

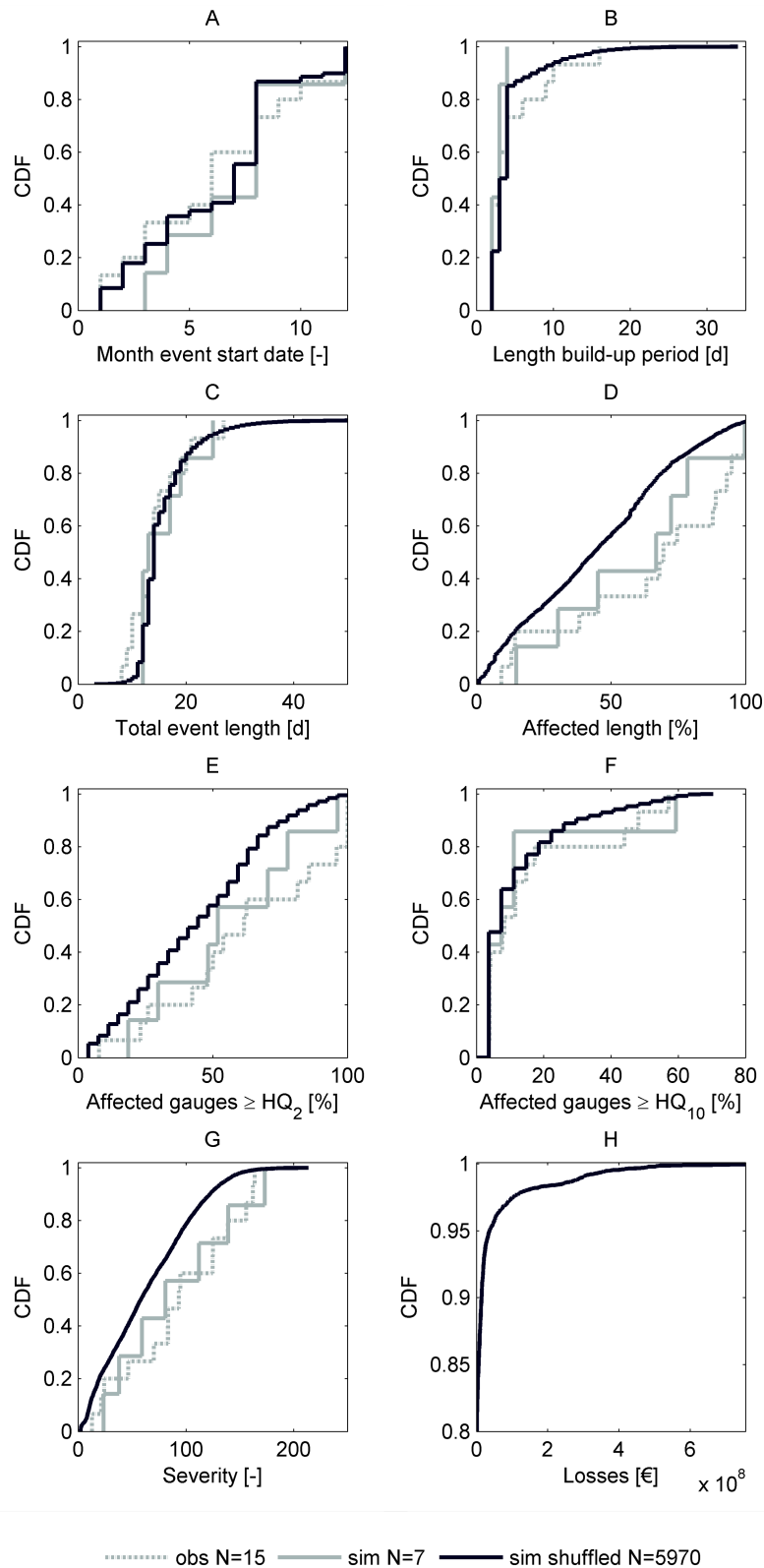


Figure 6.5: Cumulative distribution functions (CDF) of the different flood characteristics. The flood characteristics have been derived by the flood event identification applied to observed discharge (grey dashed line), simulated discharge generated by the undisturbed climate data, i.e. the observed meteorology (grey solid line), and simulated discharge generated by the shuffling approach (black solid line).

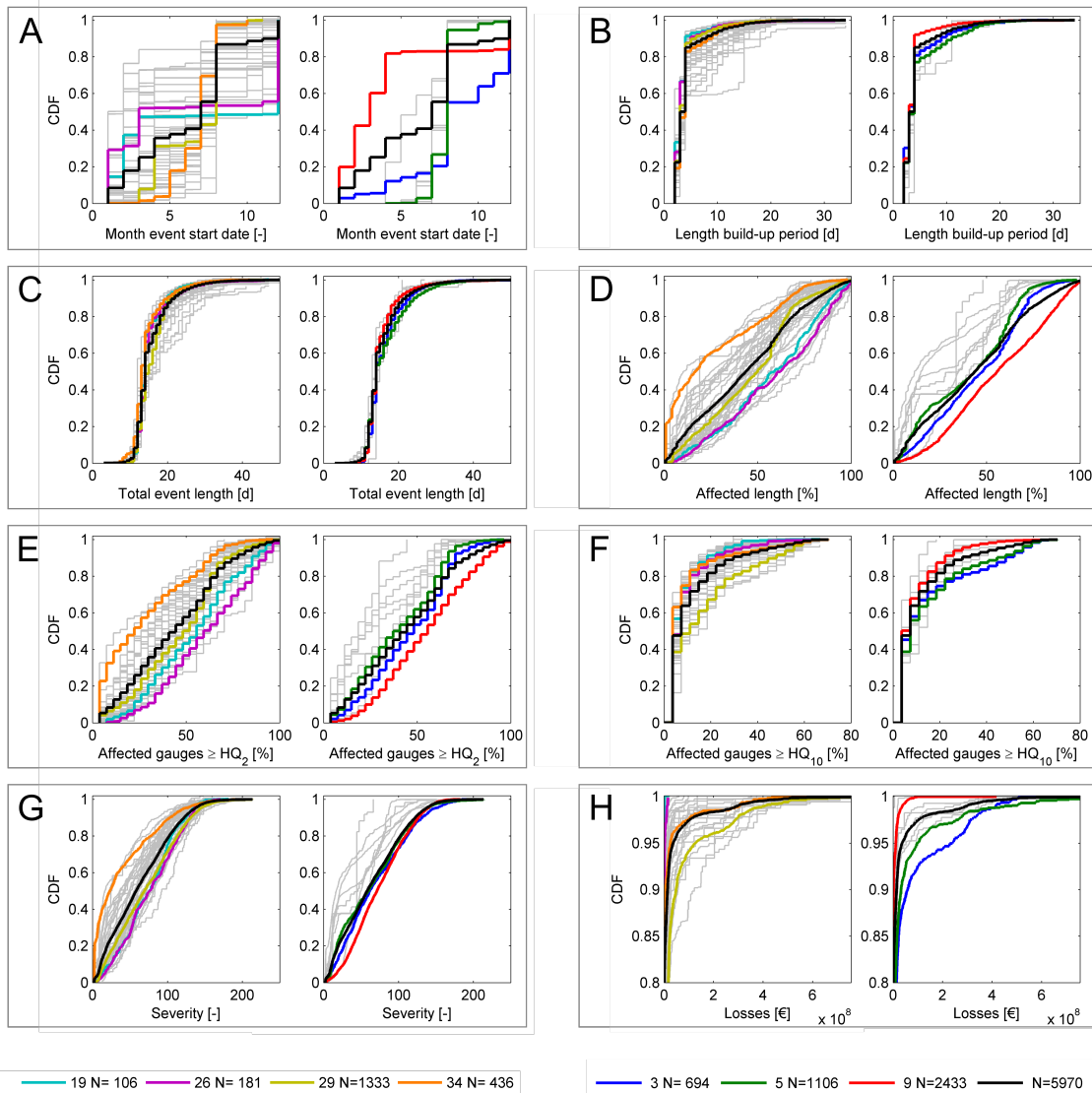


Figure 6.6: Cumulative distribution functions (CDFs) of the flood characteristics (subplots A-H) in dependence of weather patterns and soil moisture patterns. The grey and color coded CDFs represent the 40 weather patterns (left hand side of each subplot) and the 10 soil moisture patterns (right hand side of each subplot) respectively. The light blue CDF represents weather pattern 19, the purple weather pattern 26, the olive weather pattern 29 and the orange weather pattern 34. The blue CDF represents soil moisture pattern 3, the green soil moisture pattern 5 and the red soil moisture pattern 9. The respective patterns are displayed in sect. 3.1. The black CDFs represent the flood characteristics independent of patterns and are identical to the black CDFs in Figure 6.5. N refers to the sample size.

al., 2014). In these cases, rainfall can occur besides snowmelt (R. Merz and Blöschl, 2003). Therefore, CDFs of all characteristics under consideration are slightly more extreme for pattern 26 than for pattern 19.

The highest number of flood events (1333) is linked to weather pattern 29 which is associated with floods from March to October (maximum in August; Figure 6.6, A). The pattern is linked to short-rain floods, long-rain floods as well as flash floods (Nied et al., 2014). Flash floods are limited to the summer season. Long-rain floods predominantly occur in the winter season whereas short-rain floods have been observed all-year round (Nied et al., 2014). The CDFs of severity (Figure 6.6, G), affected length (Figure 6.6 D) and affected gauges HQ₂ (Figure 6.6, E) are around the non-stratified distribution (black solid line). However, the CDF of affected gauges HQ₁₀ (Figure 6.6, F) is much more extreme. Consequently, the pattern shows the most extreme loss behavior (Figure 6.6, H) among the patterns under consideration.

Weather pattern 34 is related to flash floods as well as short-rain floods (Nied et al., 2014). In case of flash floods and short-rain floods, discharge is expected to be high but spatially limited. The CDF of weather pattern 34 reveals the small spatial extent of these flood types (Figure 6.6, D). However, high discharge cannot be testified by the applied flood characteristics, i.e. affected gauges HQ₁₀ (Figure 6.6, F). The reason is that affected gauges HQ₁₀ is related to all gauges inside the catchment and not only to the fraction of flood affected gauges which is low in case of flash floods and short-rain floods. However, flood loss (Figure 6.6, H) gives a hint on the event impact of pattern 34 which is extreme but localized flood peaks with inundation and possibly loss. Flood loss related to pattern 34 is much higher than for the patterns associated with winter flooding (patterns 19 and 26).

Seasonal varying flood types also provide the explanation for the varying flood characteristics associated with the selected soil moisture patterns. Soil moisture pattern 9, the wettest pattern, is related to the winter flood types rain-on-snow and snowmelt, both characterized by a large spatial flood extent along with a high number of flood affected gauges (Nied et al., 2014). Accordingly, the pattern shows the most extreme CDF and even an almost linear behavior in affected length (Figure 6.6, D) and affected gauges HQ₂ (Figure 6.6, E). This observation does not hold true for affected gauges HQ₁₀ (Figure 6.6, F). Here, the CDF of pattern 9 is even below the non-stratified distribution. In line, losses associated with soil moisture pattern 9 are far below the non-stratified distribution (Figure 6.6, H).

Soil moisture pattern 5 related to summer flooding (Figure 6.6, A) comes along with long-rain floods, short-rain floods as well as flash floods. Flooding in summer is either characterized by a small spatial flood extent of miscellaneous magnitudes (short-rain floods), a local flood extent of high magnitude (flash flood), or a large spatial flood extent of high magnitudes (long-rain floods, (Nied et al., 2014). In the current analysis, it is not possible to assign the CDFs of pattern 5 to a particular summer flood type due to their partly contrasting characteristics, e.g. the wide range of the possible spatial flood extent. However, the CDF of affected gauges HQ₁₀ (Figure 6.6, F) and the CDF of losses (Figure 6.6, H) indicate that the overall impact of this pattern is high whereas the spatial extent (Figure 6.6, D) is less extreme which points towards the predominance of short-rain floods and flash floods in conjunction with pattern 5.

The all-year soil moisture pattern 3 (Figure 6.6, A) has no clear conjunction to a

specific flood type. The best linkage was detected to long-rain floods (Nied et al., 2014). Long-rain floods can occur all-year round but the majority of flood events related to this pattern occurs in the summer season. They are characterized by a large spatial flood extent of high magnitudes which is reflected in the CDFs of pattern 3. The CDF of losses (Figure 6.6, H) associated with pattern 3 depicts an extreme CDF. However, it can be observed, that for the most extreme losses (higher than the 98th percentile), the CDF of soil moisture pattern 5 overtakes the CDF of soil moisture pattern 3.

Although the non-color coded patterns are not discussed for the sake of brevity, similar conclusions could be drawn for them.

6.4.3 Combined control of soil moisture patterns and weather patterns on flood characteristics

The combined impact of soil moisture patterns and weather patterns on flood characteristics is studied with the help of regression trees. A regression tree is built for each flood characteristic. The root node, the overall tree complexity, the succession of decisions nodes separating soil moisture patterns or weather patterns as well as the number of terminal nodes change in dependence of the flood characteristic under consideration.

Figure 6.7 displays exemplarily the regression tree of the flood affected length. For reasons of simplification, only those patterns discussed in the previous section are labeled in the regression tree. Soil moisture patterns are indicated by a green number. Weather patterns are indicated by a blue number. For completeness, unlabeled patterns are indicated by their quantity. For instance '5+7P' means pattern 5 and additional 7 not further specified patterns. At each decision node visualized by a triangle, either soil moisture patterns (green triangles) or weather patterns (blue triangles) are split into two subgroups. The tree has 42 terminal nodes. The minimum number of flood events in a terminal node is 30. The median flood affected length of each subgroup is indicated at the respective terminal node. Terminal nodes with an affected length higher than the median value of the entire event set derived from the solid black line in Figure 6.5 are displayed in red. The numbers in brackets indicate the sample size of the specified pattern in the respective subgroup. The node position in the regression tree gives an indication on the importance of the respective soil moisture patterns or weather patterns. The closer a node is located to the root node the bigger is its importance for the flood characteristic under consideration.

The root node unites the entire flood event set, i.e. 5970 flood events. The first split separates the two wettest soil moisture patterns 3 and 9 to the right hand side of the tree, whereas the dryer patterns (8 in total) are pooled at the left hand side. On the right, soil moisture pattern 3 and 9 are further separated into two subgroups. All subsequent nodes separate weather patterns, as no further partition among the soil moisture patterns is possible. The first subgroup consists of 694 events all related to soil moisture pattern 3. The second subgroup consists of 2433 events all related to soil moisture pattern 9. Soil moisture pattern 9 is related to winter flooding. Therefore, the right-most branch can be considered a winter branch comprising mainly rain-on-snow and snowmelt events. Independent of the subsequent weather pattern, soil moisture pattern 9 is related to a high affected length which is characteristic for the winter flood types. The highest median affected length is observed in subgroups comprising weather pattern 19 (median

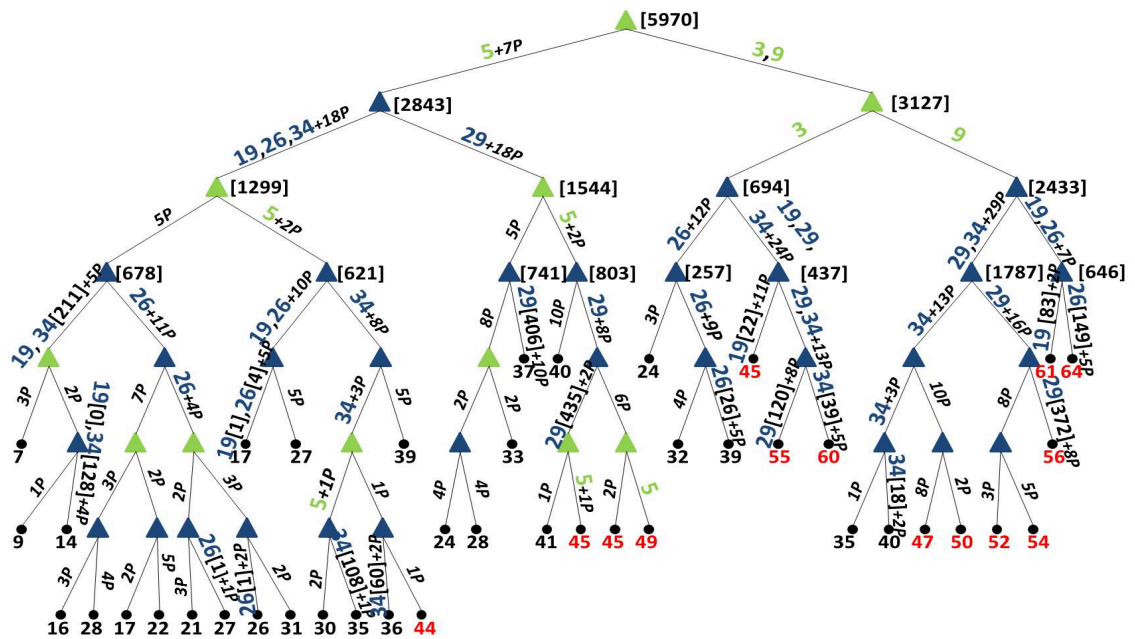


Figure 6.7: Regression tree of the flood affected length. Soil moisture patterns are indicated by a green number, weather patterns are indicated by a blue number. Unlabeled patterns are indicated by their quantity. Decision nodes are visualized by a green triangle (soil moisture pattern) or by a blue triangle (weather pattern). The median flood affected length of each subgroup is indicated at the respective terminal node. Terminal nodes with an affected length higher than the median value of the entire event set are displayed in red. In brackets, the sample size of the specified pattern in the subgroup is indicated.

of 61%) or weather pattern 26 (median of 64%). Among the weather patterns under consideration, these two patterns also showed the most extreme affected length in the separate view (see Figure 6.6, B) and are, like soil moisture pattern 9, related to winter flooding. 372 flood events are associated with soil moisture pattern 9 and weather pattern 29. In the separate view, weather pattern 29 was linked to all-year flooding. It is assumed that in this branch mainly the winter events associated with weather pattern 29 are present. In contrary, soil moisture pattern 3 is an all-year pattern. Hence, its branch can be considered an all-year branch.

The left hand side of the tree consists in general of soil moisture patterns related to flooding in summer. It can be considered a summer branch. Contrary to the right hand side of the tree, the node subsequent to the root node does not separate soil moisture patterns. Instead, weather patterns are separated. This indicates that the impact of weather patterns is higher in the summer branch (left hand side of the tree) whereas the impact of the soil moisture patterns is higher on the all-year/winter branch (right hand side of the tree).

In the summer branch, weather pattern 29 is grouped to the right and further separated according to the prevailing soil moisture conditions. The left hand side of the summer branch contains weather patterns 19, 26 and 34. It shows the smallest median affected length, revealing the spatial flood extent of the summer flood types flash flood and short-rain floods. As it is a summer branch, weather patterns related to winter flooding, i.e. 19 and 26, have a small sample size and are negligible. The sample size is highest for weather pattern 34 related to summer flooding.

In summary, the regression tree gives insight into which soil moisture – weather pattern combinations lead to most extreme flood impact and which ones result in small- or medium-sized impact. Second, based on the positions of the patterns in the regression tree, their importance in shaping the flood characteristic can be estimated. Finally, the regression tree delineates the seasonally varying flood processes.

To derive a quantitative estimate about the importance of catchment pre-conditions versus meteorological event characteristics, the variable importance is calculated. Figure 6.8 displays the delta of the variable importance derived for each flood characteristic. The graph shows, that the length of the build-up period, the total event length as well as the affected gauges HQ₁₀ are mostly controlled by weather patterns in the Elbe catchment. In contrary, the affected length and the affected gauges HQ₂ are mostly controlled by soil moisture patterns. In case of severity as well as losses, the control is less pronounced. Severity is slightly governed by soil moisture patterns whereas losses are slightly governed by weather patterns.

6.5 Discussion

6.5.1 Suitability of the developed approach

The reshuffling extends time series of various meteorological variables by taking into account their space-time pattern as well as their interrelation. The reshuffling is independent of the spatial scale and in particular suited for the river basin scale as it takes into account the catchment meteorology as well as large-scale atmospheric conditions. The former is required for hydrological modelling whereas the latter can be systematically as-

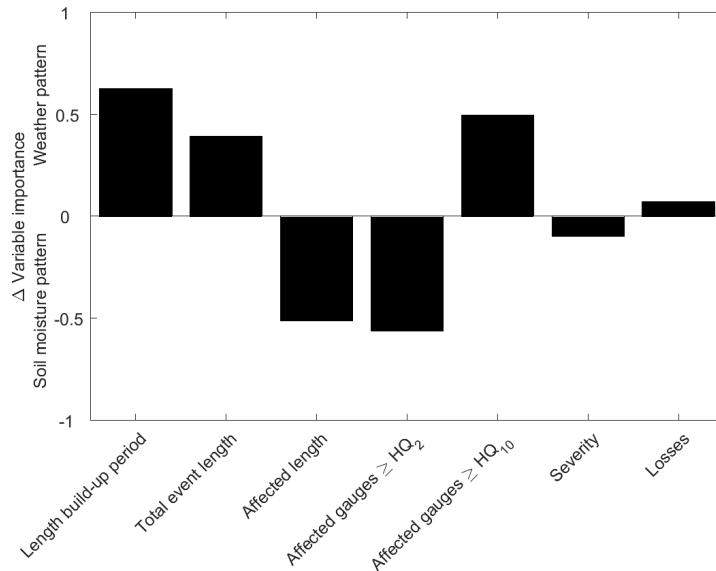


Figure 6.8: Delta of the variable importance for each flood characteristic. Positive values highlight the dominance of the weather patterns; negative values indicate the dominance of the soil moisture patterns. The higher the absolute value the stronger the influence on the respective flood characteristic. The maximum absolute value is one.

sociated with floods and guarantees a homogeneous subsample as each weather pattern can be attributed to specific flood generating processes (Nied et al., 2014). The reshuffling could be extended by altering the frequency and succession of the weather patterns to implement a change in climate. In the analysis, it is assumed that the length of the weather pattern time series is adequate to reproduce the present frequency, persistence and succession of weather patterns.

Studying the interacting control of soil moisture patterns, as a proxy for the hydrological pre-event conditions, and of weather patterns, as a proxy for the meteorological event conditions, over a variety of flood characteristics, the process-based approach proved its applicability (Figure 6.5). Although, each component of the model chain represents the system under study in a simplified manner and thus introduces uncertainties (Falter et al., 2016; Neal et al., 2013; Sampson et al., 2014), the validation against observations of soil moisture, discharge, inundation extent as well as losses (Falter et al., 2016; Nied et al., 2013; Thielen et al., 2008b) proved the feasibility to assess flood risk, including soil moisture conditions, rainfall-runoff processes, inundation as well as loss estimation, with the RFM. The benefits of the presented RFM are: First, no assumption on e.g. the catchment's saturation state prior to flooding has to be made as the regional flood model is a continuous simulation that explicitly accounts for the different controls. Second, such a distributed approach depicts spatially heterogeneous and consistent patterns of soil moisture, precipitation, discharge, inundation and losses. Compared to a lumped approach that assumes spatially uniform conditions and return periods in the entire river basin, e.g. (Alfieri et al., 2014; R. Merz et al., 2008), the distributed approach enables to understand flood generation and impact at the larger river basin scale in its chronological

order.

6.5.2 Hydro-meteorological controls on the flood characteristics

Flood generation in the Elbe catchment shows a high variation in terms of spatial patterns of flood peaks and return periods and in terms of process types (Nied et al., 2014). The reshuffling allows generating large samples of flood events reproducing the observed event characteristics. It enables to retrieve distributions of the flood characteristics in dependence of the hydro-meteorological (pre-)event conditions and to study their interaction by the use of regression tree analysis. Both analyses reveal the varying nature and origin of flood events as well as the hydro-meteorological controls on the flood characteristics. They give insight into the impact of specific soil moisture – weather pattern combinations and delineate the seasonal varying flood processes.

Otherwise, the governing hydro-meteorological controls of the flood characteristics are difficult to decipher. For instance, the spatial flood extent, i.e. the affected length, is influenced by the spatial rainfall extent. A larger portion of the river network may be flood affected in case of widespread heavy rainfall. However, if a large fraction of the catchment is saturated, modest rainfall may already generate large scale flooding. Hence, it is unclear whether the affected length is controlled by the extent and magnitude of rainfall, i.e. the weather patterns, or by the share of catchment saturation, i.e. the soil moisture patterns. In the following, the hydro-meteorological controls on the flood characteristics are discussed in light of the results provided in section 6.4.

Length build-up period

The control of weather patterns over the length of the build-up period is stronger than the control of soil moisture patterns. This is indicated by the higher spread of the CDFs in case of weather patterns compared to soil moisture patterns (Figure 6.6, B), as well as by the positive delta variable importance (Figure 6.8). The delta variable importance of the length of the build-up period has the highest absolute value and thereby highlights that the control is the strongest among all characteristics under consideration. The dominance can be traced back to the definition of the build-up period. As long as there is an increase in overall discharge the build-up period extends. The increase in overall discharge is either due to persistent rainfall or due to persistent positive air temperatures in case of a snow cover. Rainfall intensity has an influence on the length of the build-up period too. In case of intense rainfall, overland runoff can be generated if the soils' infiltration rate is exceeded. The control of the soil moisture conditions on the length of the build-up period is small compared to the weather patterns. A possible influence of the soil moisture conditions is given in case of preceding soil saturation where any rainfall is directly transformed into runoff resulting in a shorter build-up period.

Total event length

As for the build-up period, the control of the climate forcing, i.e. weather patterns, over the total event length is stronger than the control of the catchment state, i.e. soil moisture patterns. This is indicated by the higher spread of the CDFs in case of weather patterns compared to soil moisture patterns (Figure 6.6, C), as well as by the positive delta variable importance (Figure 6.8). For the total event length, the same consider-

ations apply as for the length of the build-up period. Besides the increase in overall discharge, the total event length also takes the recession time, i.e. the decrease of overall discharge, into account. For discharge recession, rainfall has either to stop or to decrease significantly. In case of snowmelt events, air temperature has either to decrease below zero degrees Celsius or the snow cover has to be depleted. This results in the meteorological event conditions as the controlling factor of the total event length. Similar findings were made by Gaál et al. (2012) who attribute flood duration to the type of climatic forcing (storm type as well as snowmelt or rain-on-snow events) in Austria. However, the authors also discovered regions where catchment processes, e.g. the antecedent soil moisture state, are the governing factor for flood duration. The travel time of the flood wave in the river network has a further influence on the total event length which is in our study accounted for by the flood event definition.

Affected length

Affected length is more strongly controlled by the soil moisture patterns. This is indicated by the delta of the variable importance (Figure 6.8). By the sole consideration of the CDFs (Figure 6.6, D), no unambiguous conclusion would have been possible. The regression tree (Figure 6.7) deciphered, exemplarily for all flood characteristics, the seasonal varying influence of the controls. In summer (left hand side of the regression tree in Figure 6.7), the influence of the weather patterns is stronger than during winter (right hand side of the regression tree in Figure 6.7). This is confirmed when estimating the variable importance separately for winter and summer. In both seasons, soil moisture patterns dominate over weather patterns. However, the absolute value of the delta variable importance is higher in winter than in summer. In addition, the regression tree showed which soil moisture – weather pattern combinations led to a high affected length and which ones resulted in small- or medium-sized affected length. As the soil moisture patterns and weather patterns can be linked to flood types (Nied et al., 2014), conclusions on the flood generation processes behind the pattern combinations can be drawn and their relative frequency can be estimated.

Affected gauges HQ_2

Like the affected length, affected gauges HQ_2 is controlled by the soil moisture conditions. Figure 6.5 D and E illustrates their similar behavior. Additionally, both characteristics have a similar regression tree (not shown). Therefore, the considerations made for the affected length hold true for the affected gauges HQ_2 too.

Affected gauges HQ_{10}

Affected gauges HQ_{10} is governed by the meteorological conditions. This can be partially explained by the upper limit of soil moisture. In case the catchment is saturated, any rainfall will be transferred into runoff. For these situations, discharge depends on precipitation only. Similarly, when the rainfall intensity exceeds the infiltration rate of the soil, discharge increases. The control of the meteorological conditions is in line with the studies which examined the relation between weather patterns and flood magnitude, e.g. (Bárdossy and Filiz, 2005; Petrow et al., 2007; Wilby and Quinn, 2013)). However, evidence exists that the spatial structure of soil moisture has an influence on discharge magnitude too, e.g. (Bronstert and Bárdossy, 1999; Castillo et al., 2003; B. Merz and E. J.

Plate, 1997; Minet et al., 2011; Paschalis et al., 2014). Accounting for the spatial variability of soil moisture was found to be most important for medium-sized rainfall events and led to an increase in discharge in small catchments ($< 7 \text{ km}^2$) and on the field scale ($< 0.25 \text{ km}^2$) (Castillo et al., 2003; B. Merz and E. J. Plate, 1997; Morbidelli et al., 2016). The authors relate this behavior to larger connected areas generating saturation excess overland flow. For extreme precipitation events, no significant influence was detected. (B. Merz and E. J. Plate, 1997) identified storms larger than the 10-year return period as the threshold above which soil moisture and its spatial structure is negligible in a catchment in Southern Germany. In the present analysis, the patterns related to high affected gauges HQ_{10} are not necessarily related to high values of affected gauges HQ_2 or affected length highlighting that flood magnitude and extent arise from different flood generation processes.

Severity

Severity is a combined measure of event magnitude and extent. Event magnitude is governed by the meteorological conditions whereas flood extent is dominated by the soil moisture conditions. As a result, the controls cancel each other in the severity measure which is reflected in the small absolute value of the delta variable importance.

Losses

Losses are slightly governed by the meteorological event conditions. It has to be noted that losses occur only for extreme streamflow values which overtax the flood defense structures and impact areas where assets are accumulated. Having the delta variable importance of affected gauges HQ_{10} and the control of weather patterns on this characteristic in mind, a stronger governance of weather patterns on losses could have been expected. However, the CDFs showed a similar spread when separating losses according to soil moisture patterns or according to weather patterns (Figure 6.6, H), indicating that neither the meteorological event conditions nor the catchment saturation state is the sole governing factor. Schröter et al. (2015) also have shown that large-scale flooding events can be generated either by extreme soil moisture conditions or by extreme event precipitation – or by a combination of both. In our study, soil moisture patterns 3 and 5 as well as weather pattern 29 associated with ‘Vb cyclones’ were identified as most costly with respect to flooding. The patterns are mainly related to summer flooding.

The methodology only allows quantifying the relative importance of soil moisture patterns and weather patterns with respect to the flood characteristics. The influence of factors (e.g. dike breaches, flood protection, flood management decisions) not taken into account may even be higher but cannot be quantified by the analysis at hand. However, the methodology allows including additional factors. For example, different flood protection scenarios could be realized in the model, and the simulation analysis could be repeated for the different scenarios. Then, in addition to soil moisture and weather pattern classes, flood protection classes (or scenarios) could be used in the regression tree analysis to understand the relative importance and the interplay of soil moisture, weather pattern and flood protection.

Since this research is based on the Elbe catchment, the conclusions might not hold true for other catchments. However, the methodology is applicable to other regions and allows studying floods at any scale. Besides the control of the hydrological pre-

conditions and the meteorological event conditions on the flood characteristics, the snow water equivalent, groundwater levels and frozen soils trigger may flood generation and have an impact on the flood characteristics. Furthermore, catchment attributes such as scale, river topology, vegetation, land use, geology, soils and climate (R. Merz and Blöschl, 2009b; R. Merz and Blöschl, 2009a) as well as anthropogenic factors like flood mitigation and management may also have an influence. In view of land use and climate change, the approach proposed is able to cope with instationarities. Climate and land use change might alter the relative frequency of weather patterns and soil moisture patterns. If the hydro-meteorological controls on the flood characteristics are known and assumed to persist, future changes in the flood characteristics could be assessed through changes in pattern frequency.

6.6 Conclusions

Understanding flood generation and the impacts of flooding on the large river basin scale is of special interest as this is the scale where national risk policy as well as disaster management and planning have to take place (EC, 2007b). At this scale, floods have to be seen in their spatio-temporal context rather than a single extreme value at one particular location (Falter et al., 2015; Uhlemann et al., 2010).

Whereas several studies have investigated the role of hydrological pre-conditions and of the meteorological event conditions on flood generation and flood peaks in small catchments, this question has hardly been addressed for large river basins. This study deciphers for the first time the large-scale control of the hydrological pre-event conditions and the meteorological event conditions on a set of flood characteristics, including flood losses. This is achieved by generating a large number of flood events. A reshuffling approach based on weather patterns and their month of occurrence is developed. The synthetic fields of catchment meteorology are used to drive a model chain. It is demonstrated that this approach reproduces the observed flood event characteristics. It also generates flood events beyond the existing range of observed variables. A further benefit of the approach is that the antecedent moisture state is continuously simulated by the rainfall-runoff model and takes into account pattern seasonality as well as realistic dry/wet sequences.

From the analysis by means of conditional cumulative distribution functions and regression trees, we conclude that the distinct flood characteristics do not have the same hydro-meteorological controls. Delineating the seasonal varying flood processes, regression trees give insight into which soil moisture – weather pattern combinations lead to most extreme flood characteristics and which ones result in small- or medium-sized flood characteristics. Variable importance quantifies the overall impact of soil moisture patterns and weather patterns on the flood characteristics that is not possible from hydrological reasoning only. In the Elbe catchment, the length of the build-up period, the total event length and affected gauges HQ_{10} are governed by weather patterns. The affected length and affected gauges HQ_2 are governed by soil moisture patterns. The controlling factor of flood severity, a combined measure of event magnitude and extent, is less pronounced. It is slightly governed by the pre-event catchment conditions. For the first time, flood loss has been linked to hydro-meteorological (pre-)event conditions. The

results indicate that flood loss is only slightly governed by weather patterns compared to soil moisture patterns.

The value of the current study lies in the probabilistic interconnection of soil moisture patterns/weather patterns and flood characteristics. The results outline that there is a potential to use soil moisture patterns as well as weather patterns not only to inform on possible flood occurrence but also on the involved flood processes and resulting flood characteristics.

The developed methodology is beneficial to the seasonal and sub-seasonal prediction of flooding and its associated flood characteristics without having to rely on the simulation of the complete flood chain. Therefore, special emphasis should be put on the (sub-)seasonal prediction of soil moisture and weather patterns. Furthermore, future changes in flood risk due to changes in pattern frequency evoked from climate and land use change can be embedded in the analysis. Flood risk management, agriculture, the shipping industry and the reinsurance business will greatly benefit from an improved (sub-)seasonal and long-term prediction of flooding. In dependence of the flood characteristic of interest, the soil moisture conditions or the meteorological conditions can be prioritized.

While the focus of this study is on patterns of antecedent soil moisture state and patterns of the meteorological conditions, the flood characteristics are summarized for each event in space and time. Whether a particular pattern of catchment/atmospheric state implies a particular pattern of e.g. inundation or flood losses is still an open question and of interest for flood risk management in particular in the preparation phase when an event is in its onset, as well as in the emergency response.

7 | Spatially coherent flood risk assessment based on long-term continuous simulation with a coupled model chain

Manuscript Info

Authors information:

Daniela Falter
Kai Schröter
Viet Dung Nguyen
Sergiy Vorogushyn
Heidi Kreibich
Yeshewastefa Hundecha
Heiko Apel
Bruno Merz

Published as:

Falter D., Schröter K.,
Nguyen V.D., Vorogushyn S.,
Kreibich H., Hundecha Y.,
Apel H., Merz B.
Spatially coherent
flood risk assessment
based on long-term
continuous simulation
with a coupled model chain
Journal of Hydrology
2015;524:182-193.
doi:10.1016/j.jhydrol.2015.02.021

Abstract

A novel approach for assessing flood risk in river catchments in a spatially consistent way is presented. The approach is based on a set of coupled models representing the complete flood risk chain, including a multisite, multivariate weather generator, a hydrological model, a coupled 1D–2D hydrodynamic model and a flood loss model. The approach is exemplarily developed for the meso-scale Mulde catchment in Germany. 10,000 years of meteorological fields at daily resolution are generated and used as input to the subsequent models, yielding 10,000 years of spatially consistent river discharge series, inundation patterns and damage values. This allows estimating flood risk directly from the simulated damage. The benefits of the presented approach are: (1) in contrast to traditional flood risk assessments, where homogenous return periods are assumed for the entire catchment, the approach delivers spatially heterogeneous patterns of precipitation, discharge, inundation and damage patterns which respect the spatial correlations of the different processes and their spatial interactions. (2) Catchment and floodplain processes are represented in a holistic way, since the complete chain of flood processes is represented by the coupled models. For instance, the effects of spatially varying antecedent catchment conditions on flood hydrographs are implicitly taken into account. (3) Flood risk is directly derived from damage yielding a more realistic representation of flood risk. Traditionally, the probability of discharge is used as proxy for the probability of damage. However, non-linearities and threshold behaviour along the flood risk chain contribute to substantial variability between damage probabilities and corresponding discharge probabilities.

7.1 Introduction

River flooding is increasingly seen from the risk perspective which considers not only the flood hazard, e.g. discharge and inundation extent, but also the vulnerability and adaptive capacity of the flood-prone regions (B. Merz et al., 2010a). This shift in perspective is visible, for instance, by the development of flood risk maps demanded by the European Flood Directive on the Assessment and Management of Flood Risks (EC, 2007b). These maps are now widely available throughout Europe and are important for risk communication and integrated flood risk management. Alfieri et al. (2014) argued, however, that these maps are generated with inconsistent methods on different spatial scales, using different data bases, and are therefore not comparable on the European scale. Even within European member states, methods might not be consistent, as it is the case for Germany where different federal states adopted different approaches for deriving and presenting flood maps (see e.g. (BfG, 2014b) for an overview). To enable comparisons, Alfieri et al. (2014) proposed the development of a pan-European flood hazard map with a spatial consistent methodology based on the assessment of uniform 100-year flood flows for all river stretches and piece-wise hydraulic modelling of corresponding flood areas.

This proposal alleviates the problem of method and data inconsistency, but it does not overcome the problem of assuming spatially uniform return periods for flood scenarios. This traditional approach in flood risk assessment derives scenarios with a constant T-year return period (e.g. $T = 100$) for flood peaks within the entire catchment. The assumption of spatially uniform return periods is valuable for local hazard and risk assessments, however, it is of limited use for large-scale assessments, for example, for national risk policy developments, for large-scale disaster management planning, and in the (re-)insurance industry. The assumption of a T-year flood peak for the entire river network gives an unrealistic large-scale picture. It is not realistic that a single flood reaches a 100-year return period in the entire large-scale river network. Flood risk would be overestimated, as the probability of a single flood reaching a 100-year return period throughout the catchment is much smaller than the probability of a 100-year flood at a single site. The overestimation of flood risk, derived with the traditional approach, was recently shown by Thieken et al. (2014) for the river Rhine in Germany.

There are different possibilities for generating flood events that respect the spatial variability of occurrence probability at the catchment scale. One approach that has recently gained attention is the application of multivariate distribution functions to represent the joint probability of flood peaks at multiple sites, e.g. (Lamb et al., 2010; Ghizzoni et al., 2012; Keef et al., 2013). A multivariate distribution function, considering the spatial dependence between gauging stations, is fitted to observed flood peaks at multiple gauges and can be used to generate spatial fields of flood peaks. A disadvantage of this method is that only flood peaks are provided. It is not obvious how such an event set could be used as input into unsteady inundation models, because hydraulic models require the entire hydrographs conserving flood volume in order to simulate the temporal evolution of flood waves within the river system. This problem can be bypassed when the event generation starts with the precipitation event. H.J.E. Rodda (2001) developed a stochastic model generating rainfall events for the UK. These events were used as input into a hydrological model to simulate the spatial distribution of the T-year discharge. A disadvantage of the event based simulation approach is the assumption that the return

period of flood discharge equals the return period of rainfall. This is usually not given, since storm characteristics, such as the rainfall time pattern, or the initial catchment state influence the relationship between rainfall probability and flood probability (Haberlandt and Radtke, 2014).

This simplifying assumption can be avoided by continuous hydrological simulation, e.g. (Boughton and Droop, 2003; Viviroli et al., 2009; Grimaldi et al., 2013; Haberlandt and Radtke, 2014). This increasingly popular concept consists of generating long synthetic meteorological time series and using them as input into a continuous hydrological model. Flood probabilities can then be derived from the simulated synthetic discharge time series. This ‘derived flood frequency approach based on continuous simulation’ has the advantage that the complete flood event, including antecedent processes, are modelled throughout the entire catchment in a consistent way. The importance of initial catchment conditions for the flood development was recently investigated by Nied et al. (2013) and also could be observed from the disastrous flood event in 2013 in Central Europe, where the interplay of event precipitation and very wet initial catchments played a dominant role for the exceptional event severity (Schröter et al., 2015). Grimaldi et al. (2013) demonstrated the effect of a continuous hydrologic-hydraulic simulation on floodplain inundation patterns compared to an event-based approach for a small-scale basin.

In this paper we extend the ‘derived flood frequency approach based on continuous simulation’ and propose a novel concept for assessing flood risks: the ‘derived flood risk approach based on continuous simulation’. Thereby we use the synthetic discharge time series as input into flood impact models and derive flood risk directly from the resulting synthetic damage time series. In this way, the processes, and their space–time interactions, underlying the flood risk in a catchment are represented in a consistent way. For instance, the hydrodynamic simulation of floodplain processes, such as storage effects or channel-floodplain interactions, allows considering the effects of floodplain processes on flood damage patterns.

A further advantage is that flood risk can be directly derived from the synthetic damage time series. The return period of damages is thus based on the empirical distribution constructed from long-term simulation. Ideally, risk is estimated as (probability \times damage), whereas probability is the probability of damage. Thielen et al. (2014) used this approach by generating a stochastic flood event set from discharge station data, combining it with a flood impact model and fitting an extreme value distribution directly to the synthetic damage data. This attempt to derive flood risk directly from the probability of damage is a rare exception in the flood risk literature. The usual way is to use the probability of discharge or the probability of precipitation as proxy for the probability of damage. However, the probability for the different phenomena (precipitation–discharge–inundation–damage) may change along the flood risk chain. For example, two events with the same flood peak discharge may lead to very different inundation and damage patterns.

In this paper, we explore the idea ‘derived flood risk approach based on continuous simulation’. The Mulde catchment, a meso-scale catchment in East Germany, is selected as example. A multisite, multivariate weather generator is linked to the Regional Flood Model (RFM). RFM is a coupled model chain, consisting of a continuous hydrological model, 1D/2D hydrodynamic models and a flood loss model. It has been recently

developed for risk assessments in large-scale river catchments and took part in a proof-of-concept study, driven by observed meteorological time series for a period of 14 years (Falter et al., 2016). For the first time, RFM is driven by synthetic meteorological data, generated by a multisite, multivariate weather generator, providing 100 realisations of 100 years of data. This virtual period of 10,000 years is simulated continuously, providing a sample of more than 2000 flood events with detailed information on inundation depth, extent and damage on a resolution of 100 m. On basis of this unique data set, we present a flood risk analysis directly on damage values. Additionally, this allows us to examine the assumption that probability of peak discharge is a suitable proxy for probability of damage. Derived damage probabilities are compared to corresponding flood peak probabilities to discuss problems that may arise from transformations of flood peak probabilities to damage probabilities.

7.2 Methods

7.2.1 Weather generator

The meteorological input data for the model chain is provided by a multisite, multivariate weather generator (Hundecha and B. Merz, 2012), further advanced from Hundecha et al. (2009). It provides spatially consistent realisations of meteorological fields for large-scale basins. The model generates synthetic daily meteorological forcing in two stages. In the first stage, precipitation series are generated at multiple sites by respecting the spatial and temporal correlations of the observed daily precipitation amounts on monthly basis. At each station, daily precipitation is sampled from a parametric distribution, which is estimated from the observed daily precipitation series as a mixture of Gamma and Generalized Pareto distributions. The mixing weight varies dynamically with respect to the precipitation intensity. The second stage of the model simulates daily maximum, minimum and average temperatures and solar radiation by keeping the correlations between the variables as well as their inter-site correlation and the autocorrelation of each variable. Temperature values are sampled from Gaussian distributions fitted to the corresponding observations, whilst for solar radiation a square root transformation was used prior to fitting a Gaussian distribution. Both temperature and solar radiation are conditioned on the state of precipitation. A multivariate autoregressive model is implemented to simulate the time series of all the daily forcing variables (precipitation, temperature and radiation). Details of the model are presented in Hundecha et al. (2009) and Hundecha and B. Merz (2012).

7.2.2 Regional Flood Model (RFM)

The Regional Flood Model (RFM) is a process-based model cascade developed for flood risk assessments of large-scale basins (Falter et al., 2016). It has been developed for basin areas in the order of several 10,000 km². RFM consists of four coupled models: the rainfall-runoff model SWIM, a 1D channel routing model, a 2D hinterland inundation model and the flood loss estimation model for residential buildings FLEMOps+r (Figure 7.1). We briefly describe the model chain and each model part here, for detailed information the reader is referred to Falter et al. (2016).

Rainfall-runoff model SWIM

The eco-hydrological model SWIM (Soil and Water Integrated Model, (Krysanova et al., 1998) is a conceptual, semi-distributed model that simulates the hydrological cycle on a daily basis. The model is spatially disaggregated on three levels: the primary unit is the river basin that is subdivided into subbasins and these are further disaggregated into hydrotopes. Water fluxes are computed for each hydrotope and aggregated on the subbasin scale. Computed daily runoff is routed from subbasin to subbasin using the Muskingum hydrological routing scheme. The routed discharges provide a boundary condition for the 1D hydrodynamic river network model.

Hydrodynamic models

The hydrological routing method integrated in SWIM routes the flow on a subbasin scale without considering explicitly the river channel geometry. However, for the prediction of flood defence overtopping and simulation of inundation processes in the hinterland, it is crucial to obtain water level information along the river network. Therefore, a 1D hydrodynamic channel routing model was developed to complement the SWIM routing. Additionally, a 2D hydrodynamic inundation model was implemented to simulate floodplain inundation processes. Both models are two-way coupled and exchange water level information during runtime.

The developed channel routing model solves a 1D representation of the diffusive wave equation with an explicit finite difference solution scheme. The diffusive wave equation is derived from the full dynamic shallow water equation by neglecting the local and advective acceleration terms. Due to the lack of precise information on the full cross-section geometry and in order to reduce the model run-times, the 1D hydrodynamic river network model only simulates flows exceeding bankfull discharge. The latter is assumed to be equivalent to a 2-year flood derived from the discharge series from the hydrological model at subbasin scale. Runoff time series at each SWIM subbasin outlet are used as boundary condition for the channel routing model. In case the bankfull flow threshold is exceeded within a subbasin, the excess flow is routed downstream subbasin-wise taking the new boundary condition from SWIM at each subbasin outlet into account. The cross-sections representing channel geometry are considered to cover the entire floodplain between flood protection dikes stretching from crest to crest. Whenever a dike crest height is exceeded, outflow into the hinterland is calculated with the broad-crested weir equation.

The dike overtopping discharge is treated as a point source boundary condition for the 2D floodplain model. The outflow of the 1D model is additionally controlled by the feedback of the 2D model. In case the water level in the hinterland is equal to the channel water level, the outflow into the hinterland is stopped. In that way, the uncontrolled water flux out of the 1D model domain is prevented in case the water level in the hinterland exceeds the channel water level.

The 2D inundation model uses a raster-based inertia formulation (Bates et al., 2010) implemented in the CUDA Fortran environment (PGI, Lake Oswego, Oregon, USA) which enables the application on the highly parallelised NVIDIA Graphical Processor Units (GPU; NVIDIA, Santa Clara, California, USA) with a strong performance gain compared to a CPU-based version. The model was benchmarked against a 2D fully dy-

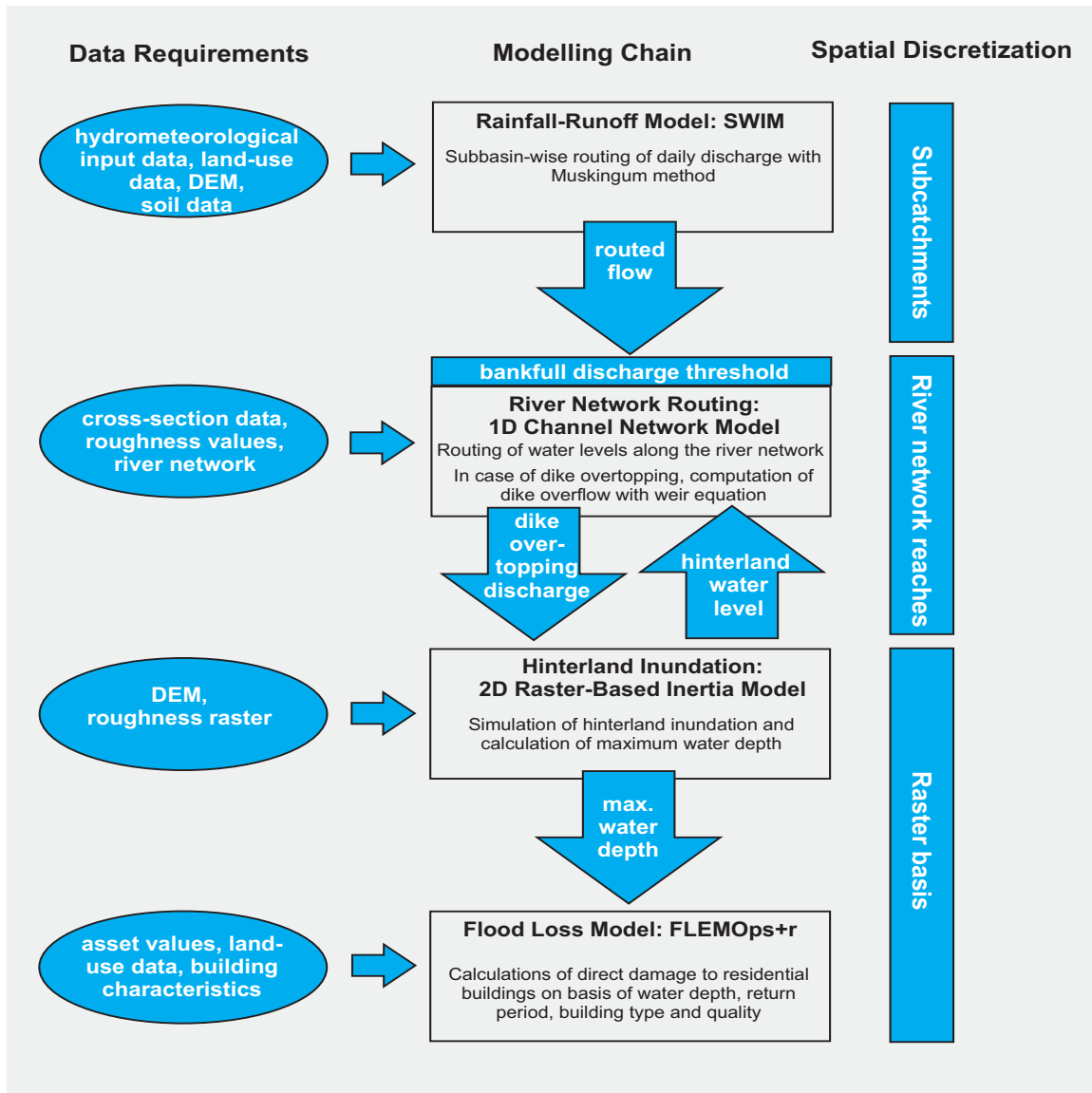


Figure 7.1: Components and data requirements of the Regional Flood Model (RFM). DEM, digital elevation model; FLEMOps+r, Flood Loss Estimation Model for the private sector; SWIM, Soil and Water Integrated Model.

dynamic shallow water model, regarding sensitivity of model performance and run-times to grid resolution (Falter et al., 2013).

For each flood event, where dike overtopping discharge and hinterland inundation occurred, grids of maximum water levels at each cell are extracted and used for calculation of flood loss with a multi-parametric damage model. A flood event starts as soon as bankfull discharge is exceeded anywhere along the river network and ends as soon as discharge drops below bankfull discharge along the whole river.

Flood loss model FLEMOps+r

From the maximum water level grids, damage to residential buildings is calculated for each flood event with the Flood Loss Estimation MOdel for the private sector (FLEMOps+r, (Elmer et al., 2010; Elmer et al., 2012), developed at the German Research Centre for Geosciences (GFZ), Potsdam. It uses a rule-based multifactorial approach to estimate direct economic damage to residential buildings. The base model version FLEMOps calculates the damage ratio for residential buildings using five different classes of inundation depth, three individual building types, two classes of building quality, three classes of contamination and three classes of private precaution (Thieken et al., 2008b). The advanced model version FLEMOps+r additionally considers the return period of the inundation at the affected residential building as an important damage influencing factor (Elmer et al., 2010). Within the RFM framework, FLEMOps+r is applied according to (Elmer et al., 2012) without taking into account the influence of precautionary measures and contamination.

7.3 Application to the Mulde catchment

7.3.1 Study area

The Mulde catchment comprises the Vereinigte Mulde – a sinistral tributary to the Elbe River, and its main frontal flows Zwickauer Mulde, Freiburger Mulde and Zschopau (Figure 7.2). The total catchment area is approximately 7400 km² (IKSE, 2005). About 70% of the catchment is dominated by mountain areas that drain a large part of the Ore Mountains, 30% of the catchment are lowland areas. The elevation ranges from 52 m to 1213 m a.s.l. The mean annual precipitation is about 770 mm, ranging from 1000 mm in the mountains to 550 mm in the lowlands.

The catchment was affected by several severe flood events during the last 100 years: 1954, 1958, 2002 (Petrow et al., 2007) and most recent in June 2013. The floods in July 1954, August 2002 and June 2013 were caused by intense and widespread precipitation. The flood in 2013 was additionally triggered by extraordinary initial wetness within the affected basins (Schröter et al., 2015). The August flood in 2002, mainly affecting the Elbe and Danube catchments, was the most expensive natural hazard that occurred in Germany so far and caused damage of around EUR 15 b in Germany alone (in values of 2013, (B. Merz et al., 2014b). The exceptional flood in June 2013 caused about EUR 8.8 b (Bundesregierung, 2013; GDV, 2013), , although it was more severe in hydrological sense, i.e. with the highest degree of affected river network (Schröter et al., 2015).

For this study, we selected river reaches of the Mulde catchment that have a drainage area larger than 600 km². The final study area comprises about 6000 km² catchment area and about 380 river kilometres (Figure 7.2).

7.3.2 Model set-up

The recent proof-of-concept study by Falter et al. (2016) applied the RFM model chain to the Elbe catchment (Germany) and demonstrated that flood risk assessment based on a continuous simulation approach, including rainfall-runoff, hydrodynamic and damage estimation models is feasible for large catchments. The study revealed however significant uncertainties especially associated with the 1D hydrodynamic model resulting from channel geometries. Therefore, an advanced set-up of the hydrodynamic models was implemented for the Mulde catchment based on high-resolution topography data.

Daily meteorological input data for 10,000 years were provided by the weather generator for the entire Elbe catchment. The long-term simulation of meteorological fields reflects the climatology from 1951 until 2003 and is assumed to provide a basis for estimating the current flood risk. Likewise, rainfall-runoff simulations with SWIM were performed for the entire Elbe catchment including parts belonging to the Czech Republic. Hydrodynamic models and the flood loss model FLEMOps+r were run only for the proposed study area of the Mulde catchment and were based on the most recent data on river system, dike geometry, topography, land use and building characteristics thus reflecting the present level of flood risk. Data used for flood damage estimation reflects the state as of 2010.

Rainfall-runoff model SWIM

For setting-up the semi-distributed model SWIM, the Elbe catchment was subdivided into 2268 subcatchments based on the SRTM digital elevation data. The historical hydrometeorological input data for SWIM calibration/validation and for parameterisation of the weather generator were provided by the German Weather Service (DWD) from all available stations within Germany and from the Czech Hydrometeorological Institute (CHMI) from stations within the Czech Republic. In addition to the hydrometeorological data, soil and land-use data were derived from the soil map for Germany (BÜK 1000 N2.3), obtained from Bundesanstalt für Geowissenschaften und Rohstoffe (BGR) and the European Soil Database map, obtained from the European Commission's Land Management and Natural Hazards unit and the CORINE (COoRdinated INformation on the Environment) land cover map. SWIM was run with historical daily input data and calibrated over the period from 1981 to 1989. A nested and automatic calibration technique was used in this work by employing the SCE-UA algorithm (Duan et al., 1992). A modified Nash–Sutcliffe efficiency (mNS) presented as normalised weighted sum of the squared differences between the observed and simulated discharges was employed as an objective function (Hundecha and Bárdossy, 2004) giving more emphasis to higher flows:

$$mNS = 1 - \frac{\sum_{i=1}^N w(\bullet) (Q_c(t_i) - Q_0(t_i))^2}{\sum_{i=1}^N w(\bullet) (Q_0(t_i) - \bar{Q}_0)^2} \quad (7.1)$$

where $Q_c(t_i)$ and $Q_0(t_i)$ are the simulated and observed discharges at time t_i , respec-

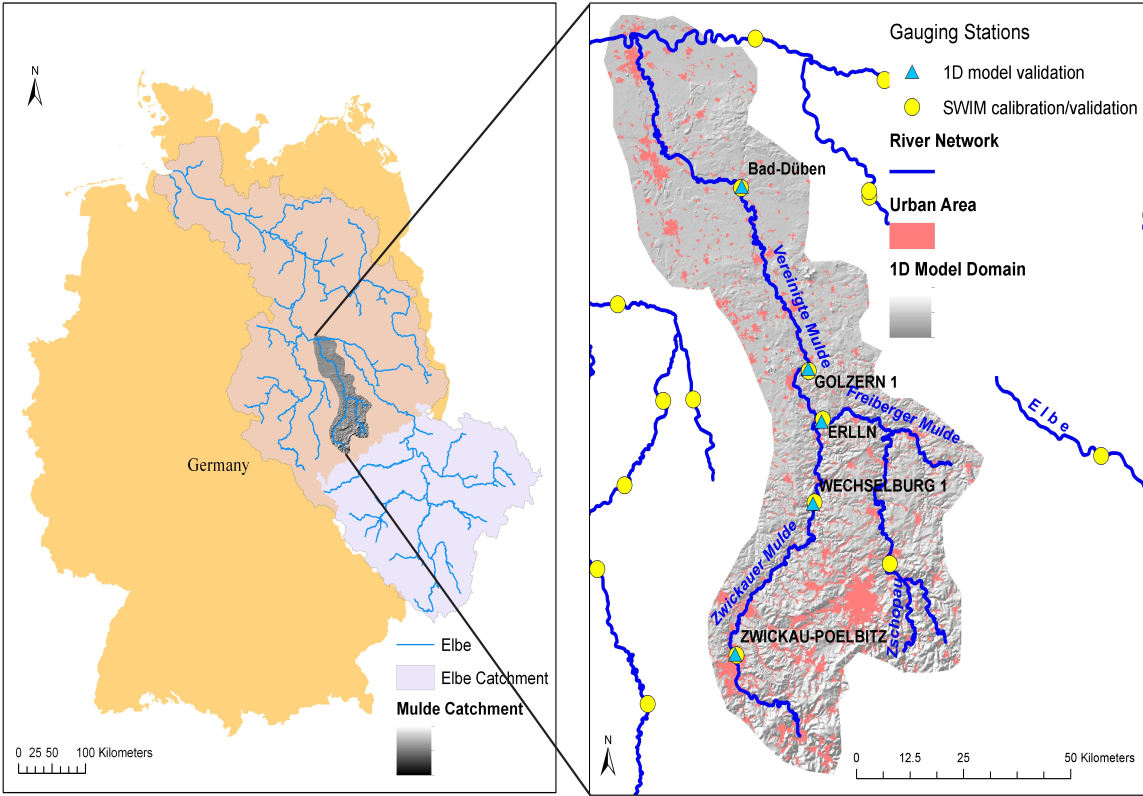


Figure 7.2: Study area, left panel: overview of the entire Elbe catchment including Czech areas; right panel: study area including the simulated river network, the 2D model domain and locations used for model calibration and validation

tively, and Q_0 is the mean observed discharge over the simulation period (N days), $w(\cdot)$ is a weight which is equal to the observed discharge $Q_0(t_i)$.

Hydrodynamic models

To simulate water levels along the selected river network with the 1D hydrodynamic river network model, the following input data is needed: river cross-section profiles, dike location and height information, Manning's roughness values and boundary conditions (Figure 7.1). The main data source for the acquisition of river cross-section profiles including dike location and elevation along the river network was a digital elevation model (DEM) with 10-m horizontal resolution, provided by the Federal Agency for Cartography and Geodesy in Germany (BKG), with a vertical accuracy of ± 0.5 –2 m. Additional information on dike location and channel width were taken from the digital basic landscape model (Base DLM) also provided by the BKG. Profiles were manually extracted in 500 m distance, perpendicular to the flow direction, with the GIS integrated tool Hec-GeoRas 10 for ArcGIS 10 (US Army Corps of Engineers, May 2012). Since only overbank flow above threshold was routed by the 1D model, cross-section profiles were corrected to represent only active floodplain without river channel. Cross-sections were further simplified to trapezoid-shape, by an algorithm that extracted the necessary parameters (channel location and width, dike location, bottom height of the dike, dike crest height and ground elevation, respectively bankfull depth) whilst conserving the original cross-section area. Dike heights are not well resolved by the DEM 10. Therefore a minimum dike height of 1.8 m was assumed at dike locations provided by the base DLM. The threshold for bankfull flow was assumed to be equivalent to a 2-year flood (Bradbrook et al., 2005; H. Rodda, 2005) and computed from simulated discharge series at each subbasin outlet. The runoff-boundary condition from SWIM assigned to the corresponding cross-section in the 1D hydrodynamic model is corrected by subtracting bankfull flow from the total runoff. The Manning's value ($n = 0.03$) was assumed to be homogenous for the whole river network. In case of dike overtopping, the width of overtopping flow was assumed to be 20 m. The 1D river network model is two-way coupled with the 2D hinterland inundation model and provides computed overtopping flow as boundary condition to the 2D model, whilst receiving hinterland water levels controlling the channel water level and overtopping flow.

The 2D raster-based inertia model was based on the computational grid of 100 m re-sampled from the DEM 10 to reduce model run-times. The 100 m resolution was selected based on the previous benchmark study by Falter et al. (2013) investigating the model sensitivity to grid resolution in terms of simulation of inundation depth and extent and computational time. The resolution of 100 m was found to offer a good compromise between model performance and computational time. The computationally intensive 2D modelling was performed only for the hinterland, and the channel and river banks embedded between dikes (1D model domain) were excluded from the 2D modelling domain. This simplification reduced run-time requirements considerably and seems justified for risk assessment studies along diked river stretches in Germany where assets in floodplains between dikes are minor compared to those on protected floodplains. Roughness grid was generated from CORINE land use maps by assigning roughness values from literature (Chow, 1959; Bollrich, 2000) to different land-use classes. The boundary condi-

tions derived from the 1D hydrodynamic channel network model in form of dike crest overtopping flow are assigned to the corresponding cell of the 2D calculation grid by location.

FLEMOps+r

The estimation of flood damage to residential buildings using FLEMOps+r requires spatially detailed information about asset values, building quality and building type. Inundation depths and return period of peak flows are used as impact variables to evaluate flood loss ratio. All input data in grid format were scaled to a spatial resolution of 100 m to comply with the 2D hydrodynamic modelling output.

Asset values of the regional stock of residential buildings are defined on the basis of standard construction costs (BMVBS, 2005), i.e. quantifying the market price of the construction works for restoring a damaged building (Kleist et al., 2006). The values used reflect the state of 2010. The asset values were disaggregated to the digital basic landscape model (Basic DLM) of the German ATKIS (Authoritative Topographic Cartographic Information System; (GEODATENZENTRUM, 2009) using the binary disaggregation scheme proposed by Wünsch et al. (2009). Within this procedure the ATKIS objects of the 'residential areas' (ATKIS code 2111) and 'areas of mixed use' (ATKIS code 2113) are used to determine residential areas.

The characteristics of the municipal building stock are derived from the INFAS Geodaten data set (INFAS GEOdaten GmbH, 2009). The composition of building types in each municipality is described using a cluster centre approach. In total, five clusters are defined differentiating the share of single-family houses, semi-detached/detached and multifamily houses (Thieken et al., 2008b). Average building quality is aggregated to two classes; high quality and medium/low quality (Thieken et al., 2008b).

The spatial distribution of inundation depths is provided by the 2D raster-based inertia model. Maximum inundation depths (h) for different flood events are classified according to the classes defined in the FLEMOps+r model ($0 \text{ m} < h < 0.2 \text{ m}$; $0.2 \text{ m} < h < 0.6 \text{ m}$; $0.6 \text{ m} < h < 1.0 \text{ m}$; $1.0 \text{ m} < h < 1.5 \text{ m}$; $1.5 \text{ m} < h$). Return periods of flood discharge peaks are estimated within each SWIM subbasin on the basis of extreme value statistics (GEV) derived from annual maximum discharge series generated through the long-term (10,000 years) continuous SWIM simulation of the Elbe catchment.

The estimation of flood losses comprises the determination of the damage ratio to residential buildings given the inundation depths and return periods, as well as the information about building quality and building type clusters in each location affected by flooding. Absolute flood losses in Euros are calculated as the product of damage ratio and location-dependent asset value per raster cell.

7.4 Results and discussion

7.4.1 RFM model performance evaluation

The performance of the coupled model chain was evaluated on the period of 1951–2003 where possible with observed data.

Table 7.1: Validation of SWIM at three gauging stations in the Mulde catchment

Gauging Station	NS	conventional NS
Bad Dueben	0.842	0.801
ErlIn	0.866	0.808
Wechselburg	0.818	0.692

Table 7.2: Water level evaluation in the Mulde catchment

Gauging station	Peak Error [m]	Bias [m]
Wechselburg 1	0.565	0.239
Zwickau-Poelbitz	0.304	0.212
Bad-Dueben	0.391	-0.255
Golzern 1	0.341	0.342
ErlIn	0.184	-0.014

Runoff validation

The hydrological model SWIM was calibrated and validated on 20 gauging stations in the entire Elbe catchment, whereas 3 gauging stations were located within the Mulde catchment (Figure 7.2). The validation was performed for the period 1951–2003 with observed discharge data, excluding the calibration period of 1981–1989. Results indicate a reasonable simulation, especially of high discharges, for the Mulde catchment with mNS larger than 0.8. Additionally, the conventional Nash–Sutcliffe (NS) values are displayed in Table 7.1 for reference. The results indicate that SWIM is particularly tuned to adequately simulate high flows relevant for flood risk assessment.

Water level evaluation

Water levels simulated by the 1D hydrodynamic model were validated at 5 gauging stations throughout the catchment (Figure 7.2) with observed water level data for the period of 1951–2003. Peak errors are in the range of 0.18–0.56 m (Table 7.2) and are in the range of uncertainty associated with dike crest heights controlling overtopping flow. As indicated by the bias, both an overall water level under- and overestimation occur likewise. Although dike overtopping is a threshold process sensitive to water level height, we consider the simulation acceptable for large-scale purposes aiming at providing the large-scale picture but not at representing local details.

Inundation extent evaluation

Evaluation of inundation extent simulations of past floods is difficult, as availability of inundation extents, e.g. from satellite data, is limited. Particularly, in non-natural

urbanised floodplains protected by dikes widespread inundations are exceptional and strongly controlled by performance of flood protection structures. In our case only for the flood in August 2002 inundation extents are documented by the National Aeronautics and Space Research Centre of the Federal Republic of Germany (DLR). A comparison of observed and simulated inundation extents is shown in Figure 7.3. For the Freiburger Mulde, inundated areas match quite well as partly constricted by topographic barriers. For the other parts of the catchment, over- and underestimation of inundated areas are present. Especially for the low-land part of the Vereinigte Mulde inundation patterns are widespread but were not exactly represented by the model resulting in a Flood Area Index (FAI) of 0.49. FAI is defined as follows:

$$FAI = \frac{M1D1}{M1D1 + M1D0 + M0D1} \quad (7.2)$$

where M1D1 is the number of cells correctly predicted as flooded, M1D0 is the number of cells flooded in the prediction and observed dry and M0D1 the number of cells dry in the prediction, however, observed wet. Only about 50% of the flood extent was correctly predicted by the simulation. Flood events at this scale are complex particularly when occurring dike breaches strongly shape inundation extent as was the case in the Mulde catchment in 2002. Within the current version of the hydrodynamic model dike breach processes are not implemented and no detailed information on the time and dynamics of breaching process was available. For large-scale applications, we consider the model to give a reasonable estimate on the dimension of the inundation extent and the severity of the event. Although, a general underestimation of inundation extents is to be expected by disregarding dike breach processes.

Damage estimation evaluation

Official damage estimates for the August 2002 flood are available for all 19 affected communities in the Federal State of Saxony in Germany which can be used to evaluate the results of the FLEMOps+r model. For these communities the sum of damage to residential buildings officially reported for the August 2002 flood (Staatskanzlei Freistaat Sachsen, 2003) and (SAB, personal communication 2004) amounts to EUR 240 M. The results obtained from the model chain in these communities amount to EUR 67 M, which are about 30% of the reported numbers.

Mainly two factors presumably contribute to this underestimation. First, the differences in inundated areas between the DLR flood footprint and hydraulic model results (FAI = 0.49) translates into differences in affected residential areas. According to the DLR flood footprint, 9.9 km² of residential areas have been affected in August 2002 in the study region. The hydraulic model estimated 7.9 km² affected residential areas which amounts about 80%. In addition, the simulated and observed inundation patterns are not exactly matching. The Flood Area Index computed only for residential areas (FAI_{res}), compare Eq. 7.2, for the hydraulic simulation is 0.29. Hence, the simulation correctly predicts about 30% of the affected residential areas. Accordingly, the areas where damage was actually caused by the 2002 flood differ considerably from the simulation. Therefore, the comparison of the damage values should be interpreted with caution. Second, former applications of FLEMOps+r on the meso-scale indicate a tendency to underestimate

damage, e.g. (Wünsch et al., 2009; Jongman et al., 2012). In this light, the systematic underestimation of reported damage may be also due to uncertainty in asset values and their spatial distribution and/or to the uncertainty of the damage model.

7.5 Long-term simulation results: flood risk in the Mulde catchment

For the continuous and long-term simulation, RFM was driven by meteorological input data, generated by the weather generator. The weather generator was set up to generate synthetic weather variables based on observed meteorological data for the years 1951–2003. Consequently, the weather generator reproduces the climate conditions of this time period. In total, 100 realisations of 100 years of daily weather variables were generated at 528 stations within Germany and neighbouring upstream countries. The virtual period of 10,000 years of meteorological data served as input for the rainfall-runoff model SWIM. The subsequent 1D/2D hydrodynamic simulations were run on a NVIDIA Tesla C1060 GPU server, containing four devices with each having 240 processor cores. The simulation of the virtual period of 10,000 years for the Mulde catchment took about 10 days run time. In total 2016 flood events, where hinterland inundation has occurred, were simulated. For each event, damage to residential buildings was calculated with the model FLEMOps+r. This resulted in a unique data set of about 2000 flood loss events including spatially detailed information on inundation depths and damage to residential buildings that served as basis for the subsequent flood risk analysis.

In Figure 7.4 we present the total count of flooding events for each computational cell of 100 m resolution. The frequency of flooding is unevenly distributed in space. There are areas that are flooded up to 1326 times in 10,000 years and others are never affected by inundation. Patterns like that are to be expected, as there are always areas that are more flood prone than others for several reasons. Remarkably, there are no areas inundated in all of the 2016 flood events.

This illustrates that the model chain provides different spatial patterns of flood generation and alternating inundation pathways within the Mulde catchment. As both tributaries Zwickauer and Freiburger Mulde seem to be affected nearly equally often, this suggests an alternating centre of flood impact between those tributaries.

Flood frequency estimation

The combined performance of the weather generator and SWIM was evaluated by comparing the flood frequency curve derived by simulation with the flood quantiles based directly on observed discharge. Figure 7.5 shows this comparison for gauge Bad Düben, the most downstream gauge of the Mulde catchment (see Figure 7.2). For this gauge daily flow was available for the 43-year period 1951–2003. The plotting positions were calculated according to Weibull. The derived flood frequency curve was estimated using the following resampling approach: annual maximum discharge values were extracted from the 10,000 years continuous simulation. 1000 random samples of length 43 were drawn with replacement from these 10,000 values, and the Generalised Extreme Value distribution was fitted to each sample. Parameters were estimated via L-moments (Hosk-

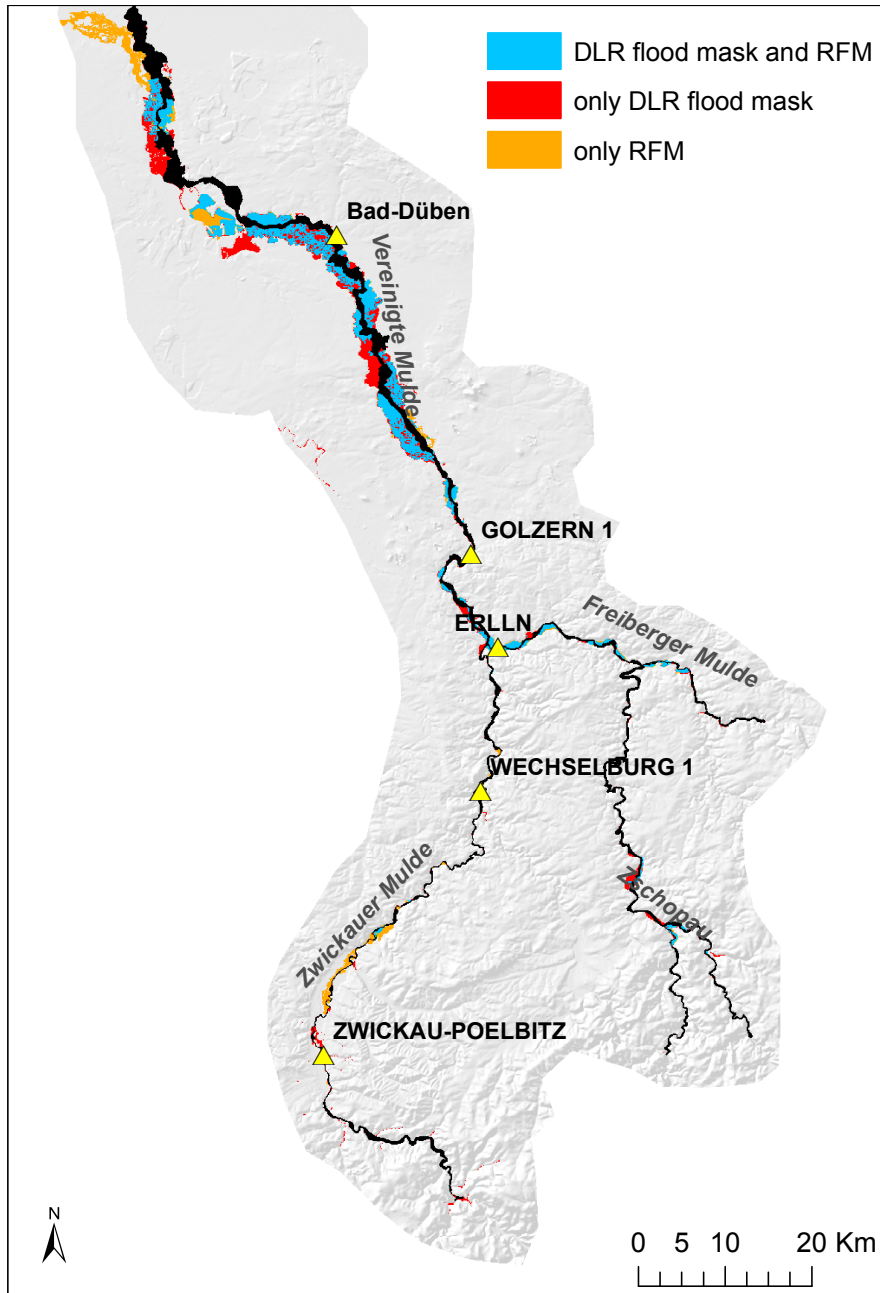


Figure 7.3: Comparison of simulated and observed inundation extents for the August 2002 flood.

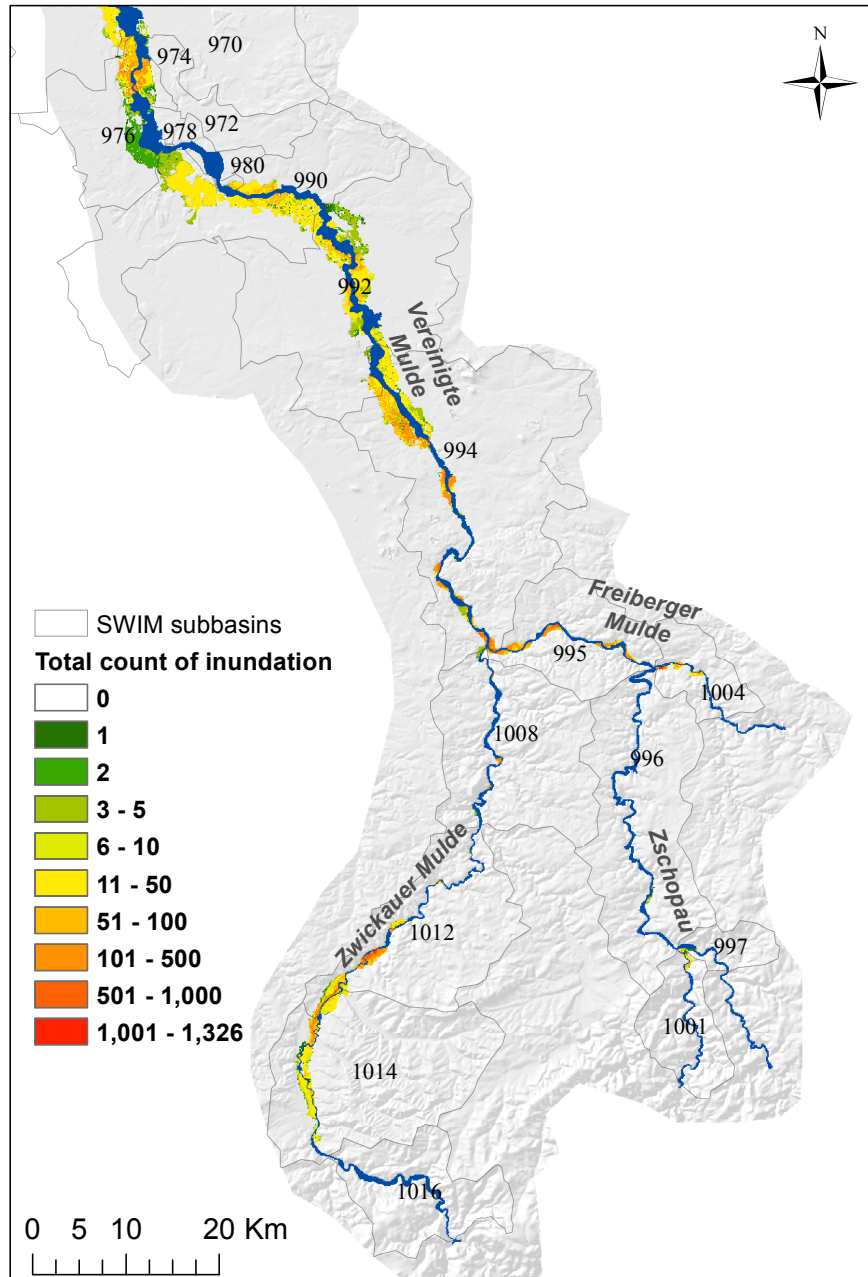


Figure 7.4: Inundation frequency in 10,000 years of simulation for each computational cell.

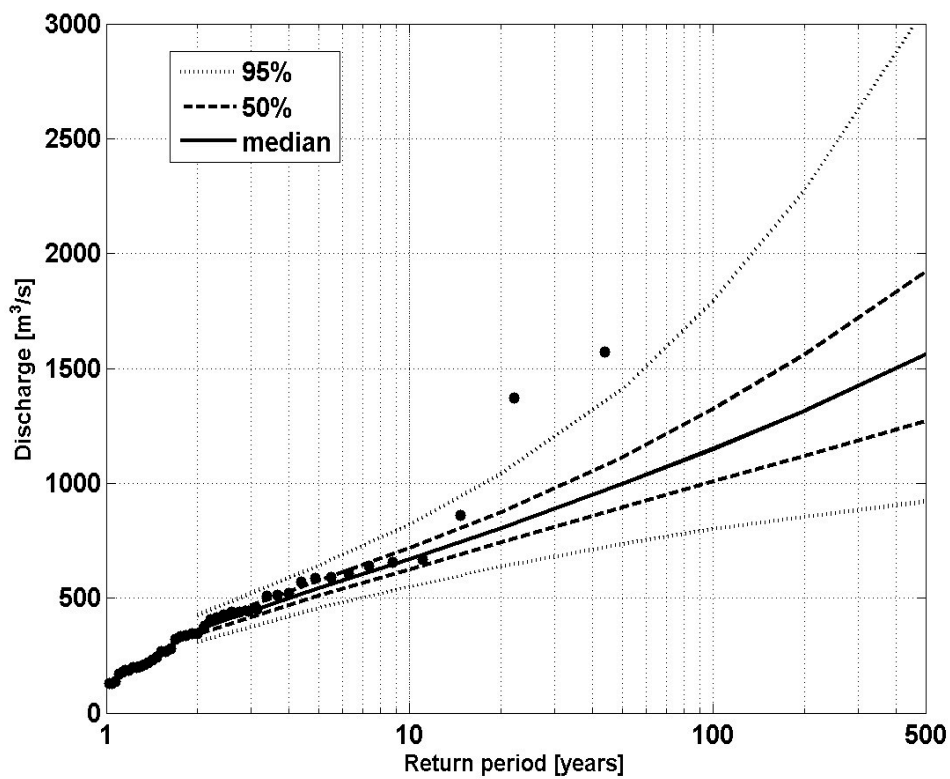


Figure 7.5: Comparison of derived flood frequency curve and plotting positions for gauge Bad Dübén. Dots are the observations; the solid line is the median of the derived frequency curves; the dashed and dotted lines show the 50% and 95% confidence interval, respectively.

ing and Wallis, 1997). The median and the 50% and 95% confidence intervals are derived from the 1000 flood frequency curves.

Figure 7.5 shows that the derived flood quantiles agree reasonably well with the observation based plotting positions. Two events are clearly outside the 95% sampling uncertainty, namely the floods in 1974 and 2002. These two largest events need to be put in perspective. They resulted from unusually high precipitation amounts in the Ore Mountains, the headwater areas of the Mulde catchment. A total of 312 mm within 24h was recorded on 12 and 13 August 2002 at Zinnwald. This is the highest amount of rainfall that has ever been measured in Germany (Ulbrich et al., 2003a). Given that the rainfall generator has been set up for the much larger Elbe catchment, thereby ignoring some of the local rainfall variability, and the extreme nature of these two events in the Mulde headwater catchments, Figure 7.5 shows a good agreement between observations and derived flood quantiles.

Flood risk curves

Usually, it is not possible to estimate flood loss probabilities directly from damage data, as information on flood loss is sparse or the number of synthetic event sets is not large enough to draw robust statistics. Here, the number of loss events derived from more than 2000 simulated floods within different subbasins ranges between 0 and 774. Apparently not every flood caused damage in each subbasin. This unique data set allowed for the first time to estimate the probabilities directly from damage data. Flood risk curves were derived for all 19 Mulde subbasins based on the aggregated damage values. However, the estimates for 7 subbasins were excluded from the analysis, as the number of damage events was too small (below 30).

In Figure 7.6, the histograms of damage values, aggregated to the subbasin level, and the risk curve are displayed for an example subbasin. The step in the risk curve visible for $p = 0.99$ (100-years return period) results from loss estimates of the FLEMOps+r model. FLEMOps+r uses the recurrence interval of the peak discharge as an explanatory variable on an ordinal scale which defines three different classes (below 10 years, above 10 years and below 100 years, above 100 years). As a consequence, loss estimates increase stepwise at 10 and 100 years causing also shifts in the loss estimate. This threshold behaviour implicitly reflects increasing damage propensity in areas which have been affected by low probability events only. This in turn is related to lower flood experiences, lower preparedness and lower resistance, and hence, higher damage (Elmer et al., 2010).

Figure 7.6a illustrates that the distribution of flood loss is strongly skewed. For the example subbasin, there were 646 loss events during the 10,000 years simulation period. Damage was smaller than 4 million in 85% (551 events) and smaller than 1 million in 48% (313 events), however, there were also a few very large loss events with more than 30 million damage.

To illustrate the advantage of our approach, we compared the risk curves based on our approach and on the traditional approach. In our approach, the probability of a loss event is directly derived from the sample of the damage data (empirical cumulative distribution function CDF in Figure 7.6b). In contrast, the traditional approach uses the probability of peak discharge as a proxy for damage probability, by fitting a Generalized Extreme Value (GEV) distribution to the simulated annual maximum flows of the 10,000

years period (GEV-based proxy in Figure 7.6b). Probabilities of peak flows scatter in varying degree around the loss probabilities (note the log scale of the y-axis). This highlights the strong variability in the relationship between probability of peak runoff and probability of damage.

Is probability of peak runoff a suitable proxy for probability of damage?

As discussed before, the probability of damage is commonly approximated by the probability of peak runoff as information on flood loss is rare. This approximation is based on the assumption that there is an unambiguous transformation between these probabilities. This assumption holds on average for individual subbasins, however, Figure 7.6b illustrates that there is significant variability around the mean behaviour, and that the return period of runoff peaks does not necessarily increase with increasing damage. For example, events in the range of 800 years return period may cause damage between EUR 1.5 and 2.5 M. Similarly, a loss event of EUR 1.2 M may be caused by events with return periods between 120 and 400 years.

To illustrate this observation, we selected two flood events with the same peak runoff but different damage. One simulation caused 122,058 damage within the subbasin 995, whereas another one almost the double loss of EUR 236,935. The return period of the corresponding peak flow was about $T = 50$ years. Although the peak runoff is the same, the shape of the hydrographs is different. The second flood featured a larger volume. When dikes are overtopped, this caused a larger volume of water flowing into the hinterland and, hence, higher inundation depth with differences up to 2.7 m (Figure 7.7) and higher damages. Of course, there are also examples where floods with different runoff peaks result in the same damage. For example, two simulations resulted in a damage of EUR 2,791,450 within subbasin 1012, whilst the peak runoffs corresponded to $T = 86$ years and $T = 51$ years, respectively.

A flood loss event is the outcome of complex interactions along the flood risk chain, from the flood-triggering rainfall event through the processes in the catchment and river system, the behaviour of flood defences, the spatial patterns of inundation processes, the superposition of inundation areas with exposure and flood damaging mechanisms. Hence, the common assumption that peak runoff corresponds proportionally to damage is not necessarily valid. The presented long-term, continuous simulation of the complete flood risk chain proved to be capable of partly representing these process interactions. Not represented by our current model setup, however, are dike breach processes and subsequent flood attenuation and storage effects. In case of a dike breach, the relationship between peak runoff and damage is all the more questionable. This is the case for the dike breach location, but also for the downstream part of the river. In case dike breach effects are represented it is to expect that differences in discharge probabilities and loss probabilities increase.

Our results show the discrepancy in traditional flood risk estimates, whereas risk is based on the probability of peak discharge, and the more comprehensive approach, where risk is based on the probability of damage. Relying on return periods of maximum flows may result in both under- and overestimation of risk values.

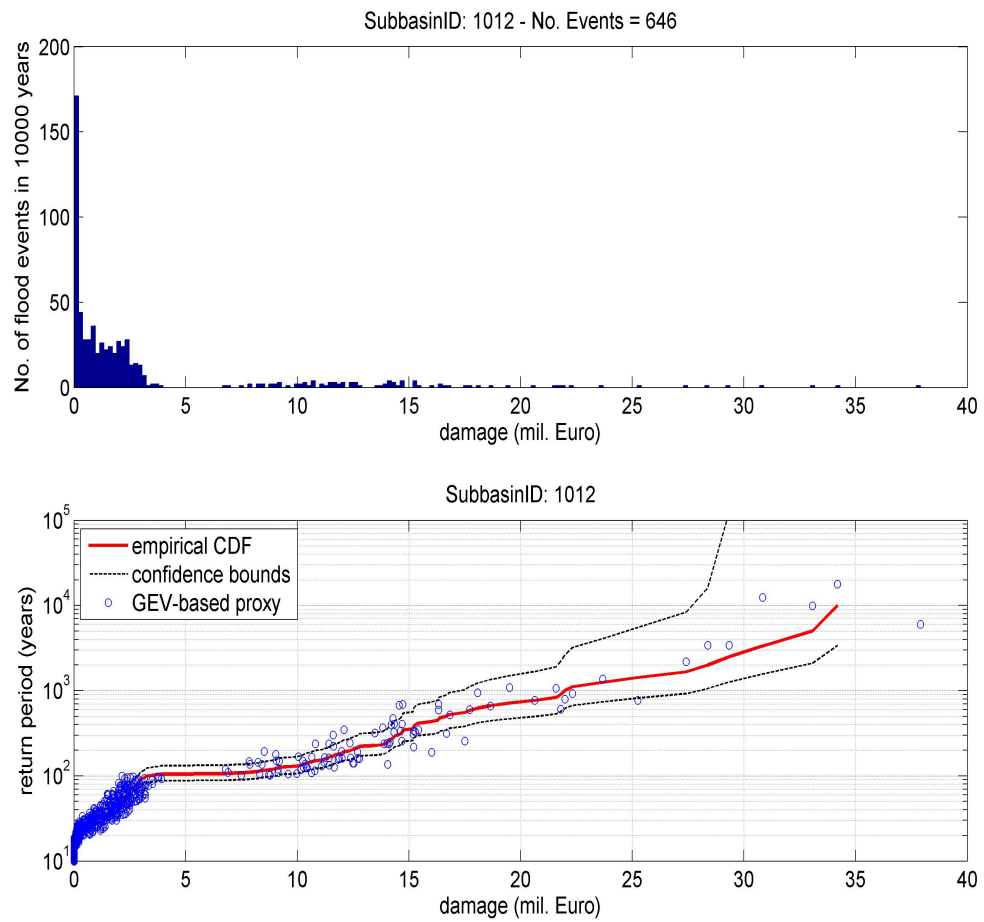


Figure 7.6: (a) Histogram of damage events and (b) comparison of traditional and simulation-based risk curves for an exemplarily subbasin.

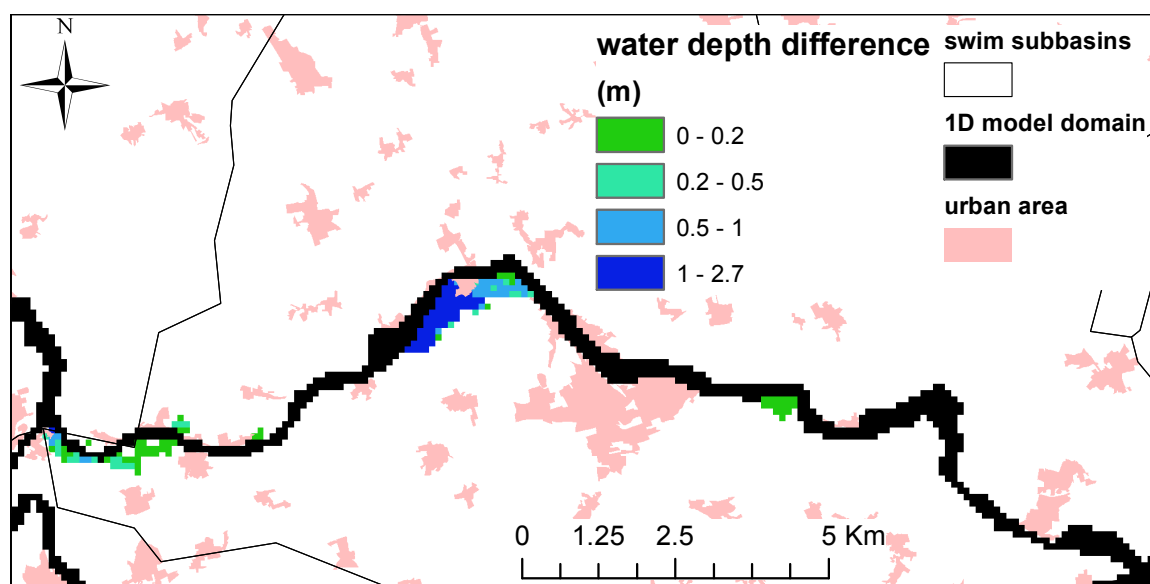


Figure 7.7: Differences in inundation depth for two flood events with the same flood peak in subbasin 995.

Spatial flood risk patterns and their variability

The presented coupled model chain allows deriving spatially consistent flood risk estimates at any scale – from the local scale to the catchment scale. Figure 7.8a shows, for example, the distribution of the expected annual damage (EAD) as risk indicator at the subbasin scale. The EAD values differ between subbasins, highlighting the spatial variability in both flood hazard (discharge, inundation extent and depth) and vulnerability (exposure, susceptibility).

Figure 7.8b–e compares the spatial distribution of discharge return periods and flood damage for two exemplary sets of flood events in the Mulde catchment with approximately 28 and 68 million Euro damage, respectively. Single flood events exhibit a strong variability of discharge return periods (more than two orders of magnitude) across different subbasins opposed to the steady values of damage return period of 114 years (standard deviation of damage return periods: $\sigma = 2.4$ years) and 238 years ($\sigma = 5.67$ years). This highlights the importance of explicitly considering the spatial variability of flood hazard contrary to the assumption of homogeneous return periods for large-scale basins.

The results further point out the presence of non-linear or threshold processes in the relationship between discharge return period and damage. For instance in subbasin 994 (Figure 7.8b–e), the damage value increases disproportionately above the return period of about 50 years. This can be a result of the dike overtopping process and/or jump in the affected assets. Furthermore, the order of flood events according to the discharge return period does not necessarily translates into the order of damage values as shown for subbasin 1012 (Figure 7.8b–e). This highlights the importance of different inundation pathways affecting spatially distributed assets in various manners with increasing flood hazard. These pathways can be shaped by both the flood generation processes, reflected in the flood wave form, and by river and floodplain processes such as dike overtopping

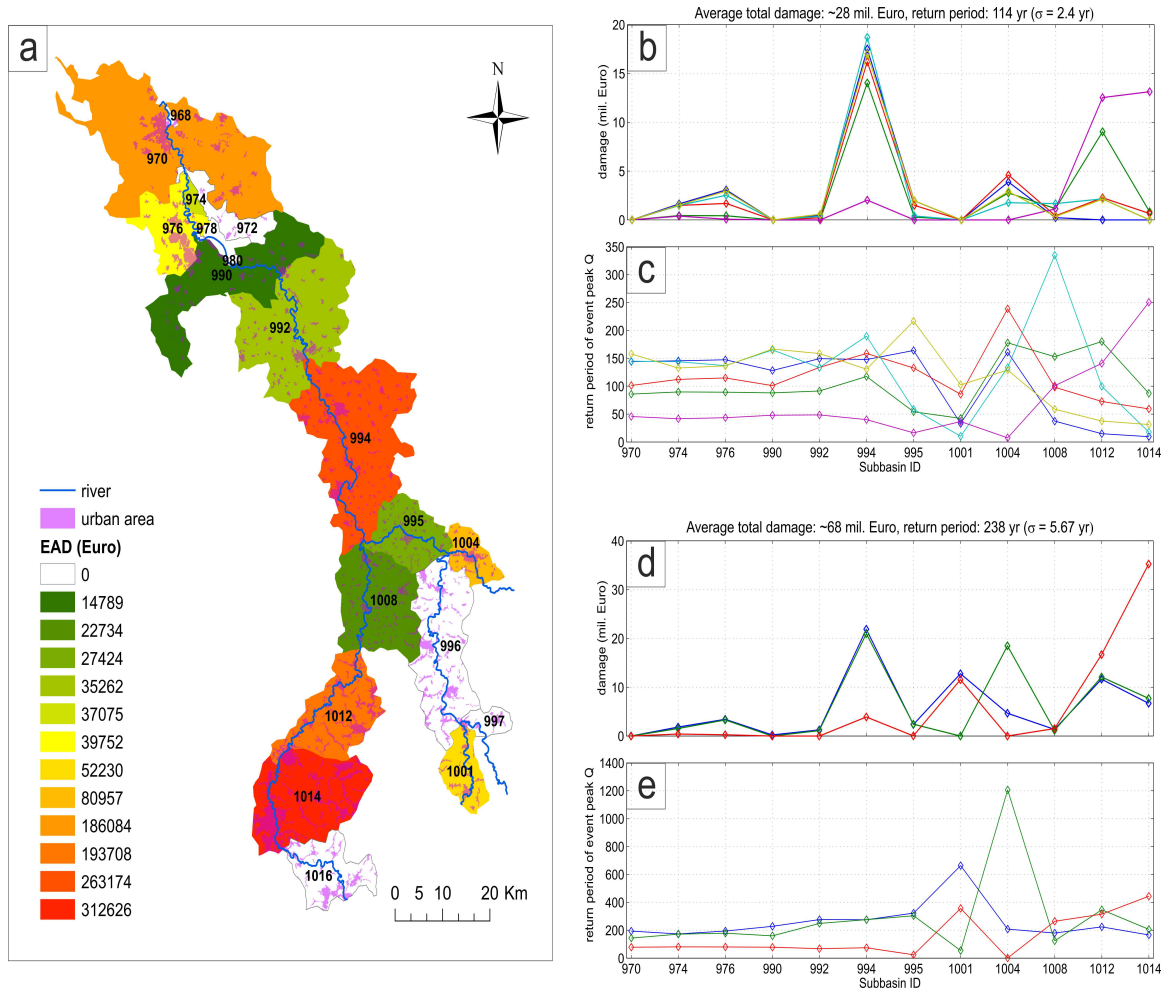


Figure 7.8: a) Distribution of expected annual damage to residential buildings in the Mulde catchment at the subbasin scale. (b)-(e) Comparison of total damage (b, d) and discharge return period (c, e) spatial distributions amongst subbasins (x-axis) and different flood events (coloured lines) for two different levels of total catchment damage. (For interpretation of the references to color in this figure legend, the reader is referred to the web version of this article.)

and inundation front propagation patterns. Once again, the return period of discharge attached to an entire subbasin is not capable of fully explaining the variability of damage and serving as a robust proxy for damage probability. This advocates our spatially distributed and continuous simulation approach to obtain spatially consistent distributed risk values. Assuming a homogeneous discharge return period across all subbasins as in the traditional risk assessment approach would also lead to a spatially distributed pattern of EAD values. Those would be, however, conditioned only by the spatial variability in vulnerability and neglect the spatial variability of hazard.

7.6 Conclusions

This paper presents a novel approach for assessing flood risk in river catchments in a spatially consistent way. The derived flood risk approach is based on a set of coupled models representing the complete flood risk chain, including a large-scale multisite, multivariate weather generator, a hydrological model, a coupled 1D–2D hydrodynamic model and a flood loss estimation model. Long time series of spatially consistent meteorological fields are generated and transformed, through the subsequent models, into long time series of flood damage. This allows deriving flood risk estimates directly from the simulated damage.

The approach is exemplarily developed for the meso-scale catchment Mulde, located in east of Germany. 10,000 years of spatially consistent meteorological time series are generated and used as input to the model chain, yielding 10,000 years of spatially consistent river discharge series, inundation patterns and damage values. This results in a unique data set of more than 2000 flood events, including detailed spatial information on inundation depth and damage at a resolution of 100 m. On this basis flood risk curves and risk indicators, such as expected annual damage, can be derived for any scale, from the grid cell scale to the catchment scale. The derived flood risk approach is per se transferable to other river basins without methodological limitations. The selection of models to simulate flood risk chain processes and case-specific hydro-meteorological and topographic data will certainly affect the accuracy of resulting risk estimates.

To the authors' knowledge, this is the first study which extends the derived flood frequency approach based on long-term continuous simulation and computes flood damage and associated risk. We foresee a number of advantages for this approach compared to the traditional flood risk assessments:

- (1) Spatially coherent patterns of catchment meteorology, hydrology and floodplain processes:

In contrast to traditional flood risk assessments, where homogeneous return periods are assumed for the entire catchment, the presented approach delivers spatially heterogeneous patterns which respect the spatial correlations of the different processes and their spatial interactions. For example, the spatial correlation structure of rainfall is modelled by the weather generator resulting in consistent event fields. Further, the superposition of flood waves at river confluences as function of rainfall characteristics and initial catchment state is implicitly considered. This advantage is particularly valuable for large-scale assessments, where it cannot be assumed that the catchment is uniformly affected by a single flood event.

(2) Holistic representation of flood processes:

Catchment and floodplain processes are represented in a holistic way, since the complete chain of flood processes is represented by the coupled model approach. For instance, the effects of spatially varying antecedent catchment conditions on the flood hydrographs are implicitly taken into account. Another example is the damage-reducing effect immediately downstream of a river reach where large water volumes overtop the dike. Running the coupled model in the continuous modes implicitly considers such effects. Contrary to the traditional event based approach, it is not necessary to define representative events based on flood frequency analysis and synthetic hydrographs.

(3) More realistic representation of damage probability, and hence, flood risk:

Traditional flood risk assessments use the probability of discharge as proxy for the probability of damage. Our approach of simulating the complete flood risk chain for long periods, e.g. 10,000 years, enables us to derive flood risk directly from damage data and their empirical frequency distribution. Problems associated with translating the probabilities of rainfall or peak runoff to probabilities of damage are bypassed. A comparison of damage probabilities and corresponding discharge probabilities shows a substantial variability in this relationship at the subbasin scale. Non-linearities and threshold behaviour along the flood risk chain contribute to this variability. For example, flood damage depends not only on the flood peak but on the hydrograph shape or floodplain hydraulics including dike overtopping and inundation pathways. Differences between traditional and derived flood risk approach in discharge and damage probabilities are expected to further increase, when dike breach processes are accounted for in the hydrodynamic modelling.

8 | Large-scale, seasonal flood risk analysis for agricultural crops in Germany

Manuscript Info

Authors information:

Stefan Klaus
Heidi Kreibich
Bernd Kuhlmann
Bruno Merz
Kai Schröter

Published as:

Stefan K., Kreibich H.,
Kuhlmann B., Merz B.
Schröter K.

Large-scale, seasonal
flood risk analysis
for agricultural crops
Env. Earth Sciences
2016;75;18:xxx-xxx.
doi:1007/s12665-016-6096-1

Abstract

In recent years, large-scale flood risk analysis and mapping has gained more attention. Regional to national risk assessments are needed, for example, for national risk policy developments, for large-scale disaster management planning and in the (re-)insurance industry. Despite increasing requests for comprehensive risk assessments some sectors have not received much scientific attention, one of these is the agricultural sector. In contrast to other sectors, agricultural crop losses depend strongly on the season. Also flood probability shows seasonal variation. Thus, the temporal superposition of high flood susceptibility of crops and high flood probability plays an important role for agricultural flood risk. To investigate this interrelation and provide a large-scale overview of agricultural flood risk in Germany, an agricultural crop loss model is used for crop susceptibility analyses and Germany wide seasonal flood-frequency analyses are undertaken to derive seasonal flood patterns. As a result, a Germany wide map of agricultural flood risk is shown as well as the crop type most at risk in a specific region. The risk maps may provide guidance for federal statewide coordinated designation of retention areas.

8.1 Introduction

Basin-wide flood risk analyses and mapping is demanded by the European Union Flood Risk Directive (EC, 2007b). Furthermore, large-scale risk assessments are needed for national risk policy developments, for regional flood risk management planning, and in the (re-)insurance industry (Moel et al., 2015). An example for a large-scale scientific study is the assessment of how the implementation of retention areas along the Elbe River impacts flood defence failure probabilities and risk for agricultural crops and residential buildings (Vorogushyn et al., 2012). Despite increasing requests for comprehensive risk assessments (BBK, 2010; Kreibich et al., 2014b) some sectors, including the agricultural sector, have not received much scientific attention (Tapia-Silva et al., 2011). This might be due to the fact, that for river flood disasters agricultural losses are small in comparison to losses in the built environment. For instance, the extreme flood in August 2002 caused losses of EUR 6.196 b in the federal state of Saxony of which only 1.3% (EUR 79 M) were losses in the agricultural sector (Staatskanzlei Freistaat Sachsen, 2003). However, the significance of agricultural flood losses is higher for small frequent floods, since arable land is commonly not as well protected as urban areas (Kuhlmann, 2010). This effect is even more important in view of the current strategy to give more room to rivers by restoring floodplains or creating retention areas, implying a higher protection for urban areas and a lower protection for agricultural land (Posthumus et al., 2009; Brémond and Grelot, 2013). Additionally, flood losses are important for the agricultural industry, since they are typically large at the individual farm scale (Posthumus et al., 2009). Agricultural flood loss comprises loss of crops, as well as loss of livestock, agricultural buildings, contents, and machinery, as well as loss due to soil erosion (Dutta et al., 2003; Pivot and P. Martin, 2002). Crop losses appear to be most important, e.g. for the 2007 summer floods in England on average 82% of the total loss per hectare flooded consisted of flood damage to crops, including grass (Posthumus et al., 2009).

In contrast to other sectors, agricultural crop losses depend strongly on the season. The time of flood occurrence with respect to crop phenology and critical field operations plays a crucial role for the magnitude of resulting loss (Penning-Rowsell et al., 2005). Brémond and Grelot (2013) report, that 88% of their reviewed studies considered the flood hazard parameter “season” for estimating losses to crops, for which temporal resolution varies and may be monthly, crop specific vegetative growth stages or four seasons per year. Other input variables for crop loss estimation may be crop type, water depth, inundation duration, flow velocity, deposited material and salinity. Overviews of available agricultural crop loss estimation models are presented by Förster et al. (2008), B. Merz et al. (2010b), and Brémond and Grelot (2013). For this study the MEDIS crop loss model is used which considers the following loss determining parameters: seasonality of the flood occurrence (on a monthly resolution), crop type, region and inundation duration (Kuhlmann, 2010).

Also flood probability shows seasonal variation due to different flood generating mechanisms that are often dominant during different seasons (Lecce, 2000; Cunderlik et al., 2004). Beurton and Thielen (2009) and Petrow and B. Merz (2009) and Uhlemann et al. (2010) have carried out comprehensive flood discharge analyses in Germany. They identified three regions showing pronounced differences concerning the seasonal occurrence of floods (Figure 8.1). The western region is dominated by winter flood events,

which are characterised by large spatial extent and rather long durations. The eastern region shows a considerable amount of winter floods, but in addition, a notable fraction of summer and spring floods. The southern region shows a multimodal distribution of floods throughout the year, with floods both during the period of snowmelt and in the summer months. These summer floods sometimes have particularly high discharges but their spatial extent is usually limited.

Sivapalan et al. (2005) propose a method to isolate the contributions of individual months or seasons to the annual flood frequency curve to account for the intra-annual variability in flood processes. Following this approach, Förster et al. (2008) performed frequency analysis by applying probability functions using annual maximum series (AMS) and monthly maximum series (MMS) for one gauge at the Elbe River. This approach is adapted in this study to derive seasonal patterns of flood probabilities for almost the entire area of Germany, only excluding coastal areas (Figure 8.1).

The objective of this study is a Germany wide flood risk analysis for agricultural crops with a strong focus on temporal superposition of high crop susceptibility and high flood probability. The monthly variation of flood occurrence is superimposed on the monthly variation of crop susceptibility. In this way, the effects of crop susceptibility being in phase with flood occurrence are quantified. The flood risk to crops as well as the crop type most at risk are estimated and mapped across Germany.

8.2 Methodology

For the analysis of large-scale seasonal flood risk of agricultural crops both, the seasonal variation of crop susceptibility and the seasonal flood probability are taken into consideration. The intra-annual variation of both influencing factors is characterized by twelve values covering each month of a year. The following subsections explain the derivation of intra-annual crop susceptibility and flood probability as well as the interaction of both risk drivers. Finally, the expected annual damage (EAD) is introduced as a risk parameter.

8.2.1 Seasonal crop susceptibility

One important aspect in risk analysis of agricultural areas is the seasonal varying susceptibility of agricultural crops. Considering the intra-annual growth cycle and harvesting seasons for most crops, the susceptibility to inundations can change substantially in short periods of time encompassing step changes between minimum potential damage to total loss and vice versa (Kuhlmann, 2007). Another important factor is the inundation duration. Many crops may overcome short periods of inundation during certain periods of their growth cycle, but will suffer severe damage if an inundation is long-lasting (Kuhlmann, 2007; Penning-Rowsell et al., 2005). This study focuses on seasonal crop susceptibility due to the intra-annual growth cycle of crop types, the effect of different inundation durations and spatial variations of loss due to regional differences in potential yield which results in different specific market values in Germany.

For the large-scale seasonal flood risk analysis the agricultural flood loss model MEDIS is applied. It considers the seasonality of a flood event on a monthly basis, inundation duration in four categories (1: 1-3 days, 2: 4-7 days, 3: 8-11 days and 4:

Table 8.1: Variation of specific loss ratios [%/ha] and specific losses [/ha] for potatoes depending on the month and inundation duration, based on (Kuhlmann, 2007). Market values exemplary for the administrative district Dresden.

Season	1-3 Days category 1		4-7 Days category 2		8-11 days category 3		>11 days category 4	
	[%/ha]	[EUR/ha]	[%/ha]	[EUR/ha]	[%/ha]	[EUR/ha]	[%/ha]	[EUR/ha]
January	0	0	0	0	0	0	0	0
February	0	0	0	0	0	0	0	0
March	0	0	0	0	0	0	0	0
April	30	1810.9	80	4829.1	100	6036.4	100	6036.4
May	40	2414.6	90	5432.8	100	6036.4	100	6036.4
June	50	3018.2	90	5432.8	100	6036.4	100	6036.4
July	50	3018.2	90	5432.8	100	6036.4	100	6036.4
August	50	3018.2	90	5432.8	100	6036.4	100	6036.4
September	50	3018.2	90	5432.8	100	6036.4	100	6036.4
October	0	0	0	0	0	0	0	0
November	0	0	0	0	0	0	0	0
December	0	0	0	0	0	0	0	0

>11 days), administrative districts (38 government districts in Germany) and crop type (canola, potatoes, corn, sugar beets, durum wheat and spelt, barley, rye). These crop types cover a major proportion of the agricultural crop cultivation in Germany. For instance, in 2014 they covered 84.33% of the cultivation area (Federal Statistical Office of Germany, 2015). Depending on these factors, the model estimates the specific loss ratio for the different crop types. The specific loss ratio is the percentile deduction of the perennial averaged yields, which are measured in EUR/ha, and represents the relative potential damage of the crops (Förster et al., 2008). In order to determine the actual monetary value at risk, the perennial averaged specific market value [EUR/ha] is considered. The specific market value for each crop varies between administrative districts due to regional differences in potential yield. As an example, Table 8.1 summarises seasonal variations of the specific loss ratio [%/ha] and the respective specific losses [EUR/ha] for sugar beets in the administrative district Dresden, considering the different inundation durations. In this study, averaged market values from 2008/2009 to 2012/2013 were used.

Table 8.1 illustrates abrupt changes of specific loss ratios and specific losses from one month to the next. A rapid decrease represents the time of harvest, where the crops susceptibility is at its highest level right before and at its lowest right after, e.g. from September to October. The seasonal pattern also depends on the inundation duration. Specific loss ratios and specific losses tend to increase with inundation duration, and seasonal variability of both decreases with longer inundation durations.

In this study the lowest and highest categories of inundation duration are considered. The first category illustrates the specific loss (ratios) inflicted by a flood with the shortest inundation duration of 1-3 days (category 1). The second category shows the effect of the longest inundation duration of more than eleven days (category 4).

8.2.2 Seasonal flood probability

Intra-annual flood probability is statistically analysed using daily time series (DTS) of discharges covering at least a period of 30 years. The discharge data used for this study were provided by the hydrometric services of the federal states of Germany and the water and shipment administration.

For the seasonal flood risk analysis, the monthly probability of floods with a specific annual return period is sought. In this work, extreme value statistics was carried out on the basis of AMS and MMS following the approach applied by Förster et al. (2008) and Weiler et al. (2000). AMS and MMS were derived from DTS for 269 gauging stations covering a time span of 53 years (1960-2013), Figure 8.1. Flood quantiles for return periods of 2 to 50 years were estimated, thus sampling uncertainties are considered marginal. An important issues in flood frequency analysis is the selection of the probability distribution function. We base our analysis on a composite distribution function approach (Apel et al., 2006; Wood and Rodríguez-Iturbe, 1975) in which the composite function results from the weighted average of individual distribution functions. The weights are based on the goodness of fit of the individual distribution functions. The Generalized Extreme Value (GEV), Weibull, Gumbel, 3-parameter Log-Normal and Pearson Type III distributions were fitted to the AMS and MMS of each gauge. The extremeStat - R package from Boessenkool (2015) was used for statistical analyses.

Figure 8.1 also illustrates the zones of different flood regimes in Germany based on the cluster analysis of discharge series from 481 gauging stations across Germany, carried out by Beurton and Thielen (2009). Detailed results will be presented for the gauges Cologne, Dresden and Munich. The procedure to derive seasonal flood probabilities will be exemplified for the gauge Dresden.

Figure 8.2 shows how the annual probability of having a certain flood peak in a certain month is related to the annual flood frequency. The probability of a peak of a given discharge value occurring in a certain month is smaller than its probability of occurrence at any time of the year. For instance, the peak discharge of a 5-years annual flood corresponds to a 100-years flood in the month of July.

8.2.3 Superposition of flood seasonality and seasonal crop susceptibility

Kuhlmann (2007) shows that the relative significance of agrarian flood losses increases if floods with smaller return periods are considered, which is reasonable because crop land is not necessarily protected by flood mitigation structures. Consequently, this analysis is limited to annual return periods of up to 50 years. For floods of larger return periods, which also affect urban areas, agricultural crop loss plays a minor role in total flood loss. Five flood scenarios are covered representing the annual return periods of two, five, ten, twenty and fifty years. For these scenarios, the seasonal flood probability [a^{-1}] is derived using the relation between the annual probabilities of a flood anytime in the year and of a flood in a certain month, resulting in a probability value for each month.

The example illustrated in Figure 8.3 shows for a flood with a 5-year return period the intra-annual changes of flood probability and crop susceptibility in relative and monetary terms for the inundation duration categories 1 and 4, cf. Table 8.1. The seasonal probability curve indicates a maximum during the first four months of the year. This is typical for the flood regime of the eastern part of Germany which is dominated by spring

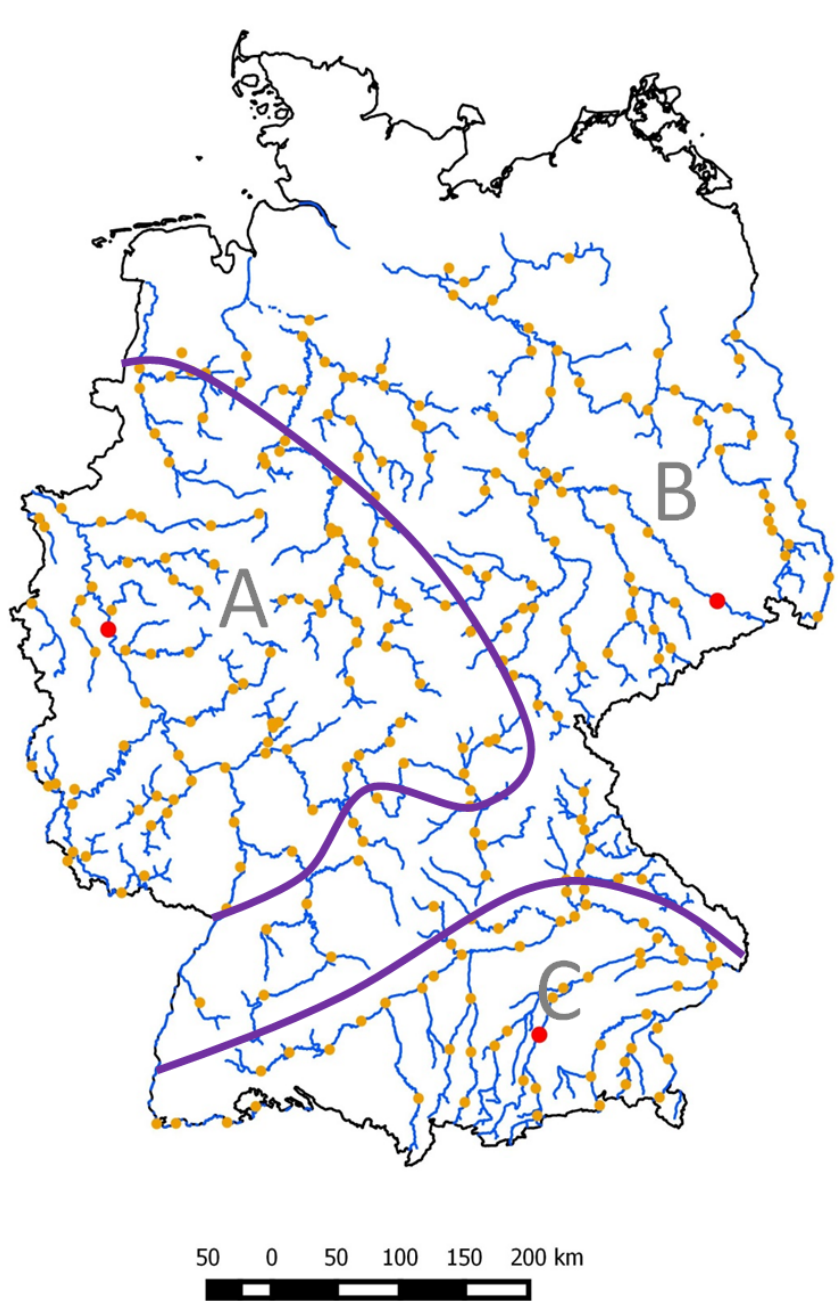


Figure 8.1: Locations of discharge gauging stations. Highlighted in red are the gauges Cologne, Dresden and Munich which represent the flood regime A, B and C identified by (Beurton and Thielen, 2009)

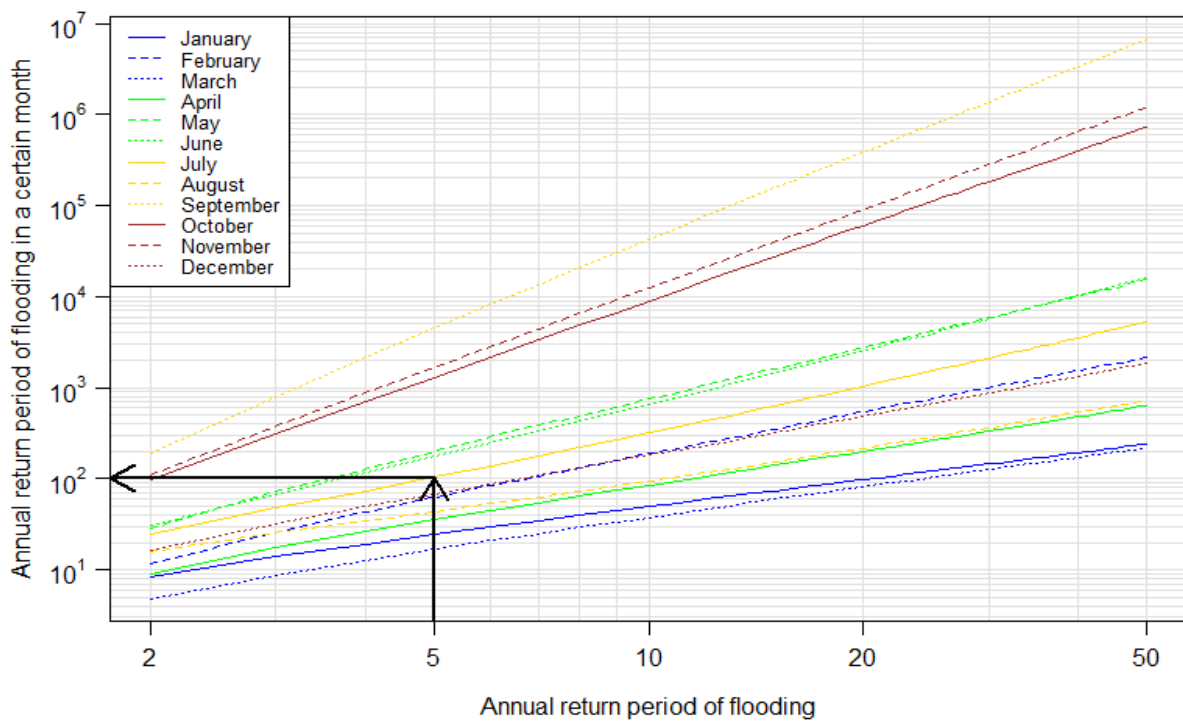


Figure 8.2: Relation between annual return period (flood occurrence anytime of the year) and annual return period of monthly floods (flood occurrence in the specified month). Example: Dresden gauge - Elbe River.

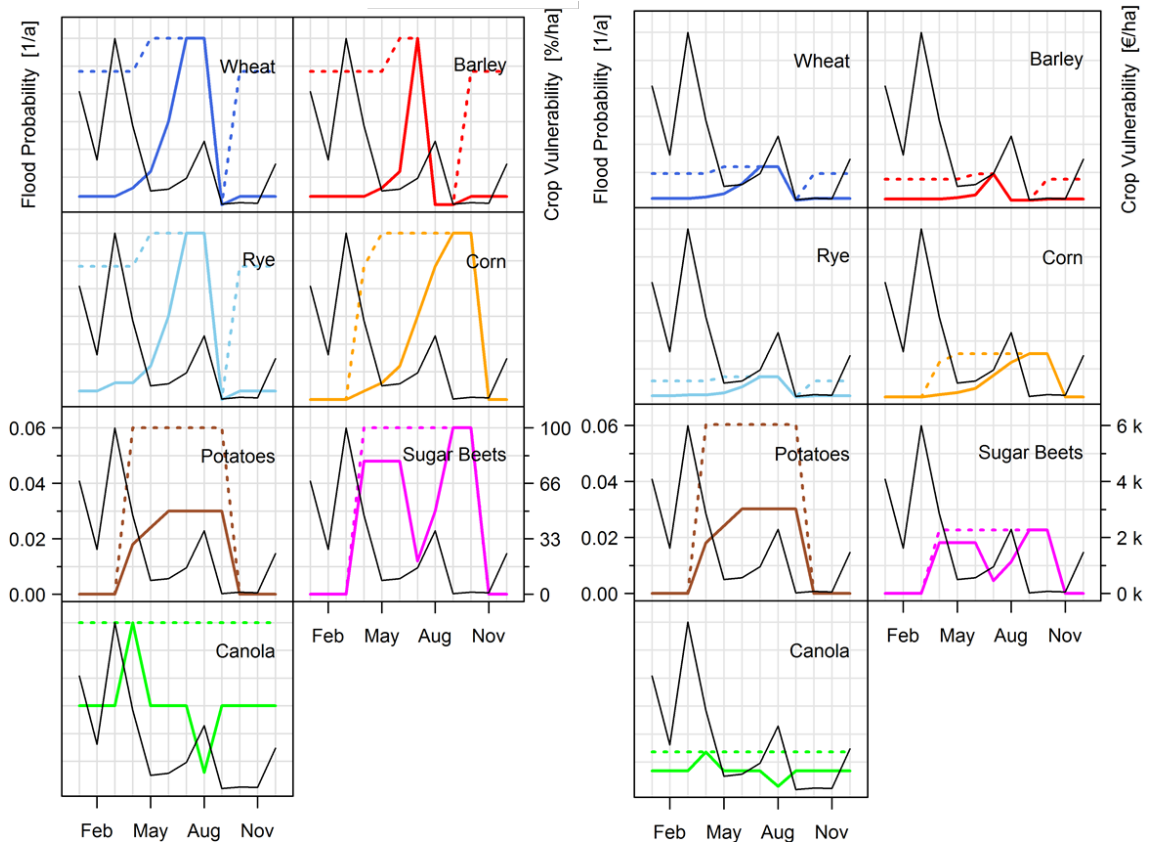


Figure 8.3: Seasonal flood probability [a^{-1}] and seasonal crop susceptibility. Susceptibility is given as specific loss ratio [%/ha] (left) and specific loss [EUR/ha] (right) and for inundation duration 1-3 days (solid line) and duration >11 days (dotted line) for HQ5 at the gauge Dresden (Elbe River).

floods (Beurton and Thielen, 2009). The left diagram in Figure 8.3 illustrates that cereal crops (wheat, rye and barley) take very small to no damage caused by an inundation of 1-3 days (solid lines) during most of the year except for the months June and July where a total loss would be the consequence. These sudden changes in specific loss ratios reflect the different stages of crop susceptibility depending on the growth cycles.

It can be observed that all crops except potatoes could potentially suffer a total yield loss in a certain period of the year. The rapid decrease after this maximum represents the harvest of the respective crop. Canola is the only crop with a distinct susceptibility pattern. Canola has a loss maximum in April and has a continuous specific loss ratio of 50%, except the month of August.

Canola also stands out, if inundation with duration of more than eleven days is inflicted upon an agricultural area (left diagram, dotted lines). In comparison to the shorter inundation duration scenario, the seasonal losses of all crops increase significantly. However, the canola yield will be lost entirely independent of the month of occurrence during the year if an inundation endures for more than eleven days.

The specific loss ratio, which represents the amount of crop yield [%/ha] lost due to flooding, can differ from the actual specific loss [EUR/ha]. Depending on location (i.e. administrative districts) and the mean market value, the specific loss can be considerable, even if only a small percentile of the crop yield is affected. This can be observed on the right panel of Figure 8.3. As a tuber crop, potatoes have a much higher market value than other crop types and are also more profitable than sugar beets (KTBL, 2015). For example, for the inundation duration of 1-3 days, the specific loss of potatoes are higher than for sugar beets, even though 80-100% of the sugar beet yield would be corrupted and only 50% of the potato yield would be lost at the most.

If the inundation duration category 4 (> 11 days) is considered, the specific loss ratio for potatoes increases strongly and reaches 100% in the period from April to September. Consequently, the maximum specific loss doubles and stands out even more among the crops considered.

8.2.4 Calculation of expected annual damage

Taking into account the seasonal flood probability [a^{-1}], specific loss ratio [%/ha] and specific loss [EUR/ha] for each crop in the administrative districts, the seasonal variation of agricultural risk across Germany is derived. Flood probabilities are derived for 269 gauge stations representing catchments, whereas crop loss ratios and specific losses are provided at the level of 45 administrative districts. To reconcile both spatial units, the catchments are intersected with the administrative districts.

The MEDIS model contains several administrative districts that are no longer in function. In this study those inactive districts will be considered and displayed.

Risk is quantified in terms of the expected annual damage (EAD), which is calculated for each month. We use discrete flood scenarios representing the 2, 5, 10, 20 and 50 years flood. In this case the continuous probability density function of the annual flood water level h , the expected annual damage can be approximated by:

$$EAD = \sum_{j=1}^m \Delta P_j D_j \quad (8.1)$$

where D_j is the crop damage inflicted by an inundation event with a specific annual return period for a respective month, and P_j represents the flood occurrence probability for the j -th interval of m probability increments (B. Merz and Thieken, 2009). Floods below a return period of 2 years are considered to cause no damage since the corresponding discharge will be within the bankfull capacity of the river channel.

The Damage D_j for the j -th interval is determined by:

$$D_j = \frac{1}{2}(D(h_j) + D(h_{j+1})) \quad (8.2)$$

and ΔP_j is defined as:

$$\Delta P_j = P(h_j) - P(h_{j+1}) \quad (8.3)$$

Based on the EAD for each month, two risk indicators are calculated. The first points out the crop most at risk in the region represented by a gauge station. The second indicates the average crop risk (EUR/ha/a and %/ha/a) for agricultural crop cultivation in a certain region. The average crop risk is a mean value derived from the monthly EAD of all crops, assuming that the probability of cultivation is the same for all crops in all regions. Further, we expect that a crop cultivation may be damaged only once per year. Hence, we calculate an annual mean value from the monthly average crop risk values.

Note that these risk indicators represent the damage inflicted in one year per hectare and as such are specific values which do not consider the spatial extent of inundation areas.

8.3 Results and Discussion

For the interpretation of the results, it is important to understand the spatial variation of flood seasonality and crop losses across Germany. (Beurton and Thieken, 2009) analysed the monthly occurrence of AMS values for 481 gauges across Germany. Based on a cluster analysis, they divided Germany in three regions with different seasonal flood patterns. The eastern part of Germany is dominated by late winter and spring floods. However, strong floods can also occur in summer. In the west and south-west, floods occur most likely in the winter months (November-January) and summer flood are very rare. In the pre-alpine region in South Germany, summer floods are predominant. Flood damage to crops depends on their susceptibility and their potential yield which determines their specific market values. The susceptibility is constant throughout Germany, and potential yield as well as market values differ regionally only to a small degree. Accordingly, the regional variations in seasonal flood probability will be mainly responsible for variations in seasonal flood risk for crops.

Figures 8.4 to 8.6 show the seasonal crop risk based on EAD for the gauges Cologne, Dresden and Munich that are representative for the three flood regimes in Germany, cf. Figure 8.1. These charts indicate that seasonal risk is particularly high when high loss ratios superimpose with high flood probability which is most prominently the case for the gauge Munich (Figure 8.6). The mean seasonal risk represented by the black curve shows an intra-annual risk pattern that is very similar across inundation duration categories as well as specific loss ratio and specific loss.

The comparison of Figures 8.4 and 8.6 illustrates that the intra-annual variation of

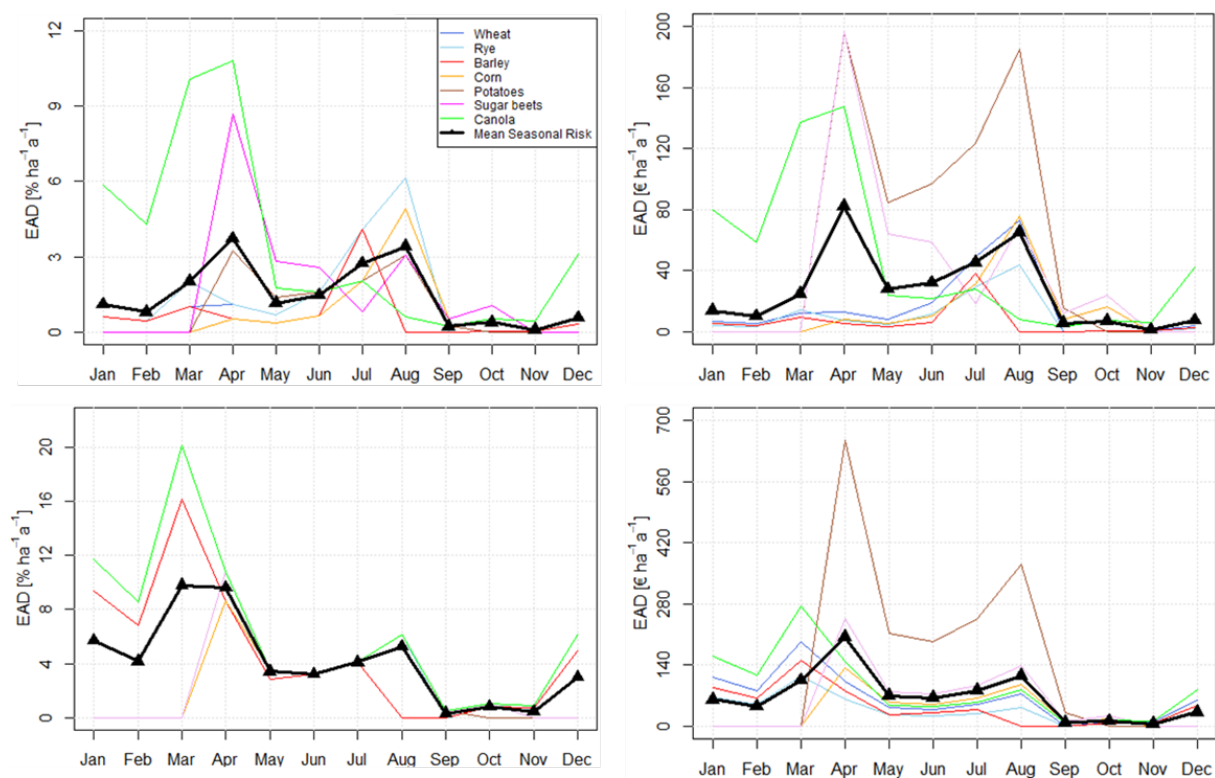


Figure 8.4: Seasonal crop risk (EAD) and mean risk averaged over all crop types (Left: loss ratio; Right: specific loss; Top: inundation duration 1-3 days; Bottom: inundation duration > 11 days). - Example: Dresden gauge – Elbe River, administrative district Dresden.

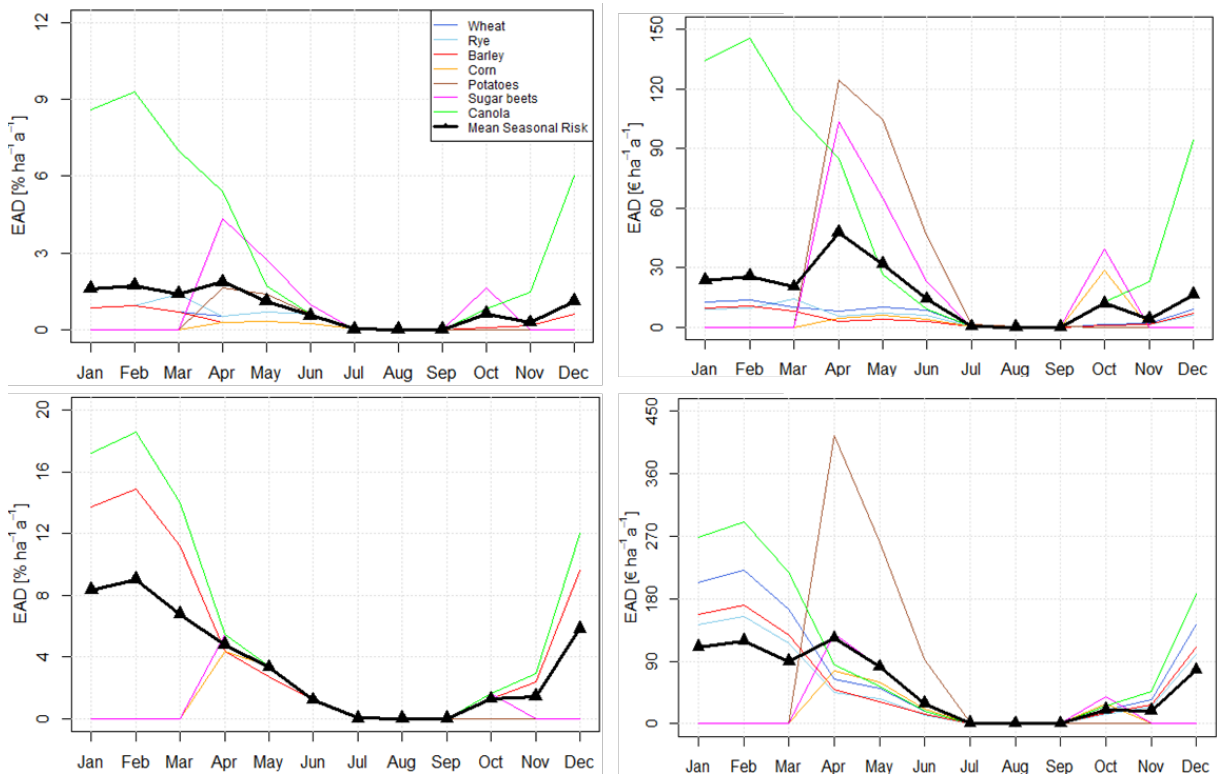


Figure 8.5: Seasonal crop risk (EAD) and mean risk averaged over all crop types (Left: loss ratio; Right: specific loss; Top: inundation duration 1-3 days; Bottom: inundation duration > 11 days). - Example: Cologne gauge – Rhine River, administrative district Cologne.

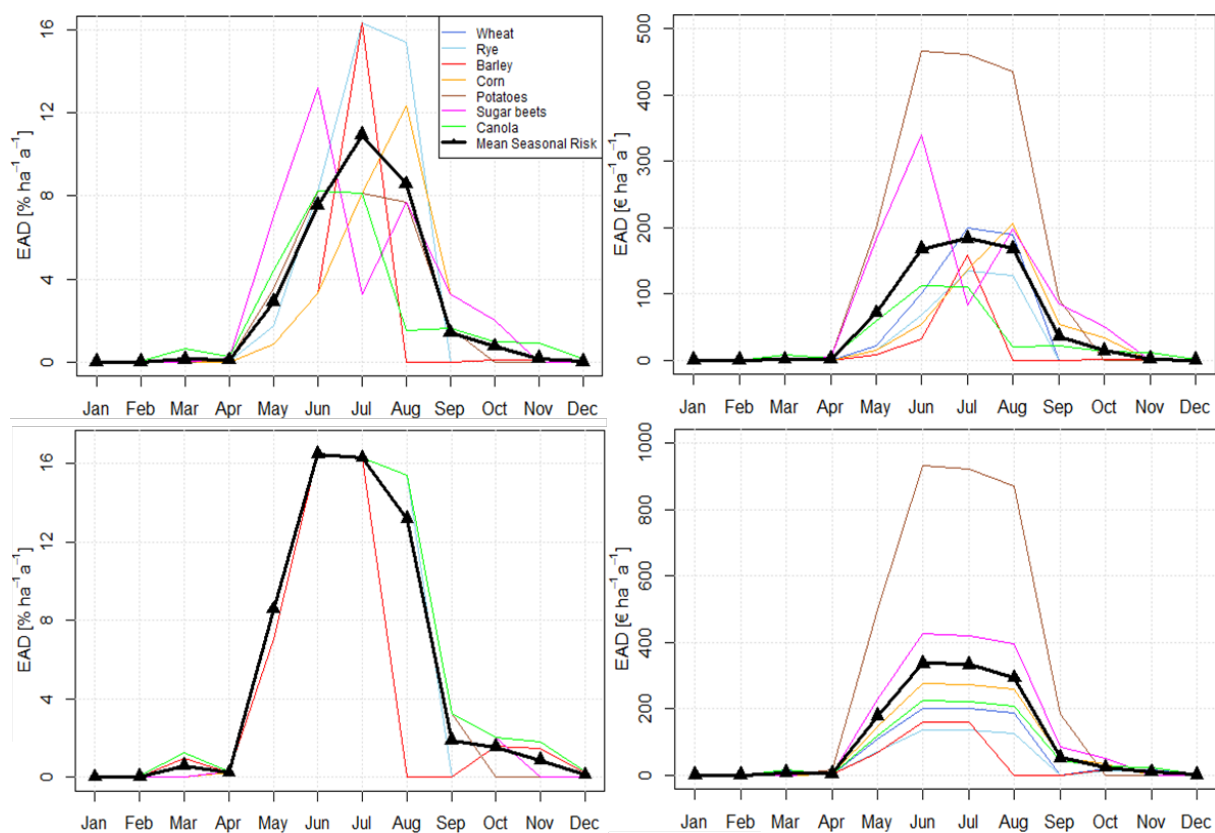


Figure 8.6: Seasonal crop risk (EAD) and mean risk averaged over all crop types (Left: loss ratio; Right: specific loss; Top: inundation duration 1-3 days; Bottom: inundation duration > 11 days). - Example: Munich gauge – Isar River, administrative district Upper Bavaria.

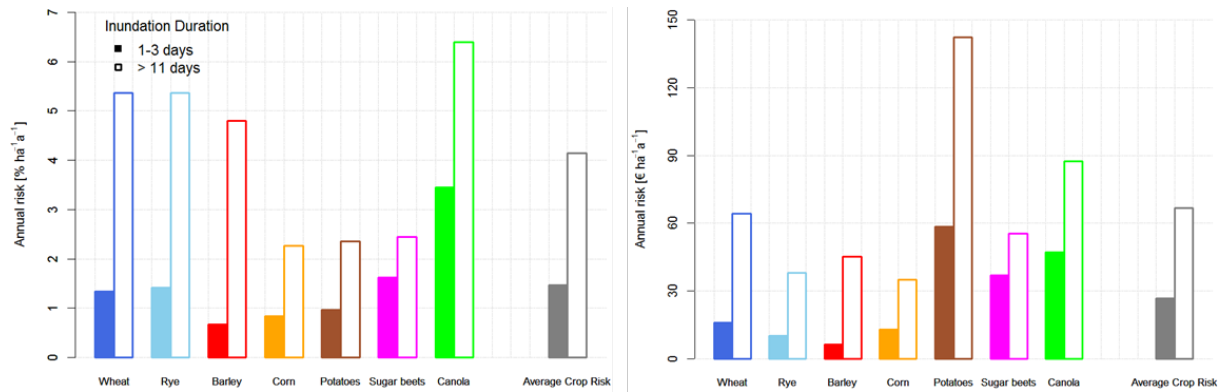


Figure 8.7: Annual risk as specific loss ratio (left) and specific loss (right) derived as the mean of the seasonal crop risk values. Example: Dresden gauge – Elbe River, administrative district Dresden.

flood probability dominates the seasonal crop risk when the loss is averaged across all crop types. In Figure 8.4, crop risk shows a bimodal behaviour with a peak in late winter and early spring and another peak in summer. This bimodality reflects that floods in the region represented by the gauge Dresden in East Germany typically occur both in late winter and during the summer months. In comparison, for the flood regime in West Germany represented by gauge Cologne (Figure 8.5) no peak of crop risk is present during the summer months which is a consequence of the very clear dominance of winter floods. Finally, Figure 8.6 shows seasonal crop risk in the region of the gauge Munich in South Germany which exhibits a marked summer flood regime. Consequently, crop risk is concentrated in the summer period.

Figures 8.7 to 8.9 display the annual crop risk for the gauges Cologne, Dresden and Munich and indicate which crop is most at risk. In most cases, canola or potatoes are the crops with the highest annual risk. Canola is at high risk due to its high susceptibility throughout the year, e.g. long inundations of more than 11 days always lead to total loss. Potatoes are at high risk due to their high market value. However, Figures 8.7 to 8.9 also illustrate the large variations in annual crop risk. This can be explained by the superposition of flood probability and crop susceptibility. Whether flood probability and crop susceptibility are in-phase or out-of-phase determines the crop most at risk as well as the average crop risk. The average crop risk (see Figure 8.7) serves as an indicator for the overall risk in a region.

The crop most at risk and the average crop risk are derived for every region in Germany (Figure 8.10). The average crop risk is particularly high in the South, where high susceptibility of most crops in summer and high summer flood probability superimpose. Additionally it is also high in the East, also due to relatively frequent summer floods in these regions. High average crop risk in some parts in the Middle of Germany, like in Central Hesse and in Thuringia, are the consequence of evenly distributed flood probabilities throughout the year, which are mostly due to anthropogenic structures like reservoirs, as for example the Edersee in Hesse, or lakes upstream of gauging stations. Figures 8.9 and d illustrate, that the annual crop risk is significantly increased due to longer inundation durations in comparison to the relatively short inundation of 1-3 days shown in Figures 8.7 and 8.8.

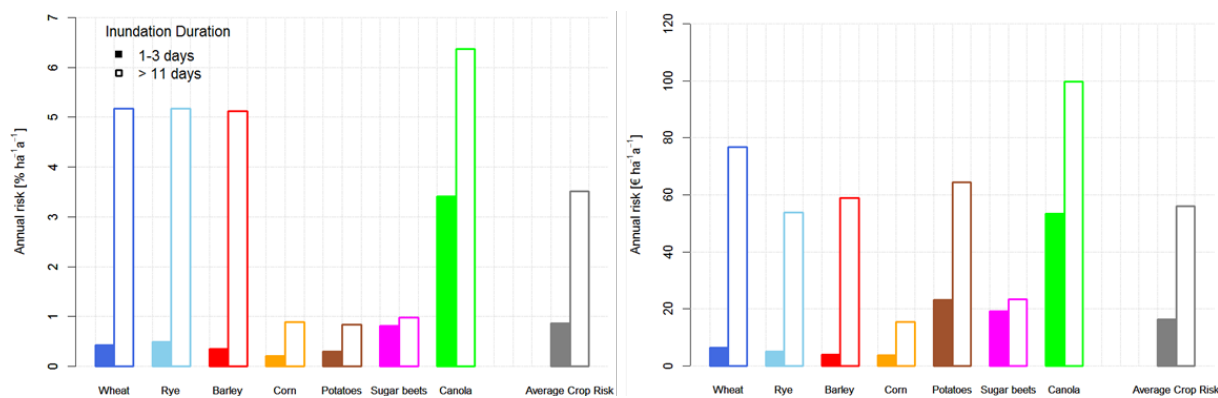


Figure 8.8: Annual risk as specific loss ratio (left) and specific loss (right) derived as the mean of the seasonal crop risk values. Example: Cologne gauge – Rhine River, administrative district Cologne.

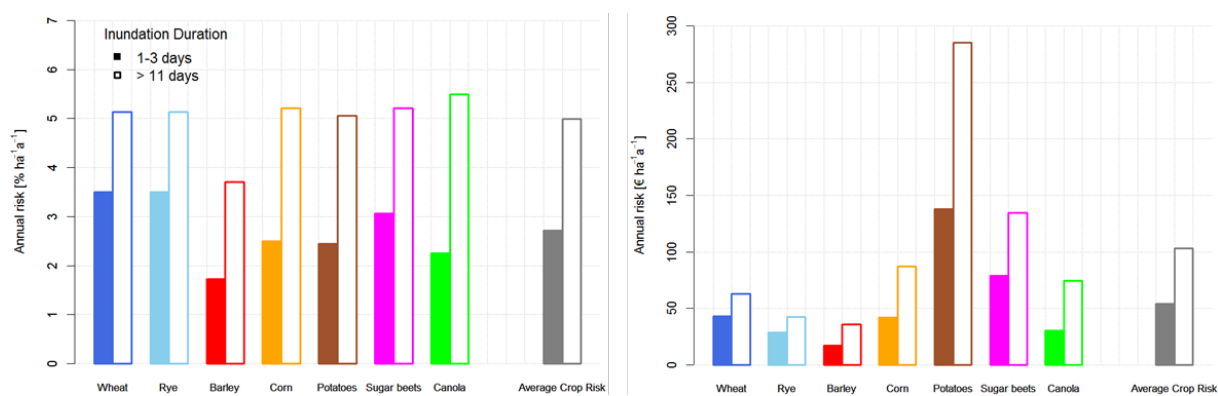


Figure 8.9: Annual risk as specific loss ratio (left) and specific loss (right) derived as the mean of the seasonal crop risk values. Example: Munich gauge – Isar River, administrative district Upper Bavaria.

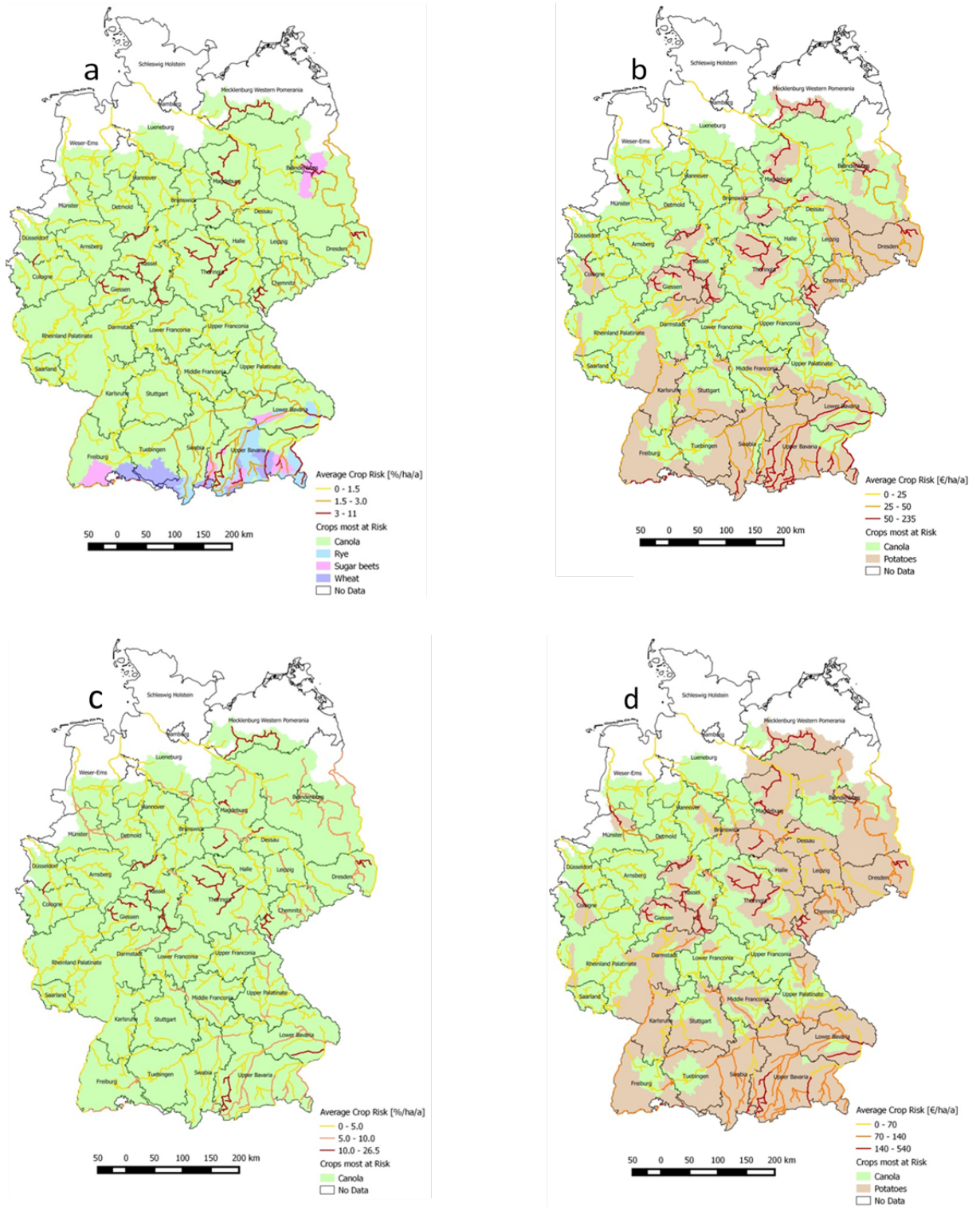


Figure 8.10: Flood risk for agricultural crops in Germany. Average crop risk is shown by the colored river sections, whereas the crop most at risk is shown by the colored regions. Left: specific loss ratio [%/ha/a]; Right: specific loss [EUR/ha/a]; Top: inundation duration 1-3 days; Bottom: inundation duration >11 days.

The maps highlight that canola and potatoes are most commonly the crops with the highest annual risk. Potatoes have by far the highest market value. Consequently, the monetary losses are comparatively high, even if the degree of superposition of high susceptibility and high flood probability is small. Farmers may probably not cultivate valuable crops like potatoes on areas endangered by flooding. Since potatoes are commonly cultivated for direct marketing or under cultivation contracts, farmers suffer not only from the high specific loss but also from disturbed customer relations when potato harvest is destroyed by flooding. Potato cultivation is particularly common in North-West Germany (Lower-Saxony), where fortunately flood risk is relatively low (Figure 8.10). Canola is at high risk because of its comparatively high susceptibility for almost the complete year, i.e. susceptibility does at no time go down to zero (see Figure 8.3). Hence, the degree of superposition is comparatively large, which translates in large relative risk values (Figures 8.10a) and 8.10c). Considering the monetary risk, canola is less important due to its small market value in comparison to potatoes. However, canola is very frequently cultivated, particularly in the eastern regions; it is the fourth most common crop in Germany (Federal Statistical Office of Germany, 2015)

Minor variations in seasonal flood probability can have large effects for the flood risk because they alter the superposition with susceptibility patterns. Therefore, the observed distribution of canola and potatoes as crops most at risk, especially within the monetary risk analysis, is the consequence of rather small regional variations in seasonal flood probability. The small differences in potential yield and market values between the administrative districts play a minor role.

Figure 8.10a indicates that other crops than canola and potatoes can be most at risk, if certain conditions apply. Wheat, rye and sugar beets are most at risk in the South of Germany, i.e. in an area with a marked summer flood regime (Beurton and Thieken, 2009). Figure 8.3 illustrates that maximum flood loss for cereal crops occurs in the summer months. Sugar beets also suffer high losses in June and September. The degree of superposition is therefore very high in the summer flood regime area, and particularly in the alpine tributaries to the Danube, and explains the predominance of these crops in South Germany on the risk map. The predominance of sugar beets in the Berlin-Brandenburg area is the consequence of unnatural seasonal flood probability patterns induced by considerable human interventions in the catchment of the gauge Berlin Mühlendamm which is located in the center of Berlin.

8.4 Conclusions

Flood risk to crops is driven by the temporal superposition of high crop susceptibility and high flood probability. Most crops are highly susceptible during summer, shortly before harvest. Thus, the average crop risk is particularly high in the South of Germany, due to the high probability of summer floods in the alpine tributaries of the Danube river. Average crop risk is additionally high in the East and at some river stretches in the middle of Germany since there summer and spring floods are also relatively frequent. Spatial differences in potential yield and market values play a minor role.

In contrast to other crops, canola is susceptible against floods throughout the whole year with a peak in spring and a singular low point in August. For long inundation

durations canola crops will be damaged completely throughout the whole year. For those reasons, canola is the crop most at risk. Canola is the fourth most cultivated crop in Germany (Federal Statistical Office of Germany, 2015) It is particularly common in the East of Germany. In respect to specific flood risk, potatoes are the crop most at risk in areas with summer floods, i.e. in the South and East, which is due firstly to their high susceptibility against floods during summer and secondly to their high market value. In Germany, the cultivation of potatoes has a relatively small share of the overall cultivation area. From a regional point of view potatoes are relatively frequently cultivated in the North-West of Germany, where their flood risk is relatively low.

Conscious crop selection can mitigate agricultural flood losses. Cultivation decisions are influenced by many farm-organisational, economic and horticultural factors. However, farmers, who cultivate crops in flood prone areas, particularly in flood polders or dike forelands should additionally take into account the flood regime and susceptibility of crops against floods when selecting crops for cultivation. Generally, in flood prone areas canola should be avoided as well as potatoes in the South and East. Agricultural consulting services provided by the chambers of agriculture of the German federal states should provide specific advice for cultivation on flood prone cropland. This Germany wide flood risk assessment for crops is helpful in this respect.

Part 2: Flood vulnerability modelling for loss estimation

9 | A review of flood loss models as basis for harmonization and benchmarking

Manuscript Info

Authors information:

Tina Gerl
Heidi Kreinich
Guillermo Franco
David Marechal
Kai Schröter

Published as:

Gerl T., Kreibich H.,
Franco G., Marechal D.,
Schröter K.

A review of flood loss
models as basis for
harmonization and
benchmarking

Plos One

2016;11,7:xxx-xxx.

doi:10.1371/journal.pone.0159791

Abstract

Risk-based approaches have been increasingly accepted and operationalized in flood risk management during recent decades. For instance, commercial flood risk models are used by the insurance industry to assess potential losses, establish the pricing of policies and determine reinsurance needs. Despite considerable progress in the development of loss estimation tools since the 1980s, loss estimates still reflect high uncertainties and disparities that often lead to questioning their quality. This requires an assessment of the validity and robustness of loss models as it affects prioritization and investment decision in flood risk management as well as regulatory requirements and business decisions in the insurance industry. Hence, more effort is needed to quantify uncertainties and undertake validations. Due to a lack of detailed and reliable flood loss data, first order validations are difficult to accomplish, so that model comparisons in terms of benchmarking are essential. It is checked if the models are informed by existing data and knowledge and if the assumptions made in the models are aligned with the existing knowledge. When this alignment is confirmed through validation or benchmarking exercises, the user gains confidence in the models. Before these benchmarking exercises are feasible, however, a cohesive survey of existing knowledge needs to be undertaken. With that aim, this work presents a review of flood loss –or flood vulnerability–relationships collected from the public domain and some professional sources. Our survey analyses 61 sources consisting of publications or software packages, of which 47 are reviewed in detail. This exercise results in probably the most complete review of flood loss models to date containing nearly a thousand vulnerability functions. These functions are highly heterogeneous and only about half of the loss models are found to be accompanied by explicit validation at the time of their proposal. This paper exemplarily presents an approach for a quantitative comparison of disparate models via the reduction to the joint input variables of all models. Harmonization of models for benchmarking and comparison requires profound insight into the model structures, mechanisms and underlying assumptions. Possibilities and challenges are discussed that exist in model harmonization and the application of the inventory in a benchmarking framework.

9.1 Introduction

The global increase of flood damage observed during recent decades (IPCC, 2012; Bouwer, 2010) is a prime mover to improve our understanding of flood impacts and consequences, for developing reliable loss models and efficiently reducing flood risk. Flood loss models –or flood vulnerability models– describe the relationship between hazard intensity metrics such as flood depth, velocity, etc. and a damage ratio that can be translated into a monetary quantity. These relationships constitute a critical component of flood risk analyses and consequently play an important role in the implementation of risk-oriented management approaches as described by legal frameworks such as the EU-flood risk management directive (EC, 2007b). Flood loss estimation is also important for insurance and reinsurance companies to design insurance products and set appropriate premiums (Michel-Kerjan and Kunreuther, 2011; Aerts and W. J. Botzen, 2011), as well as to estimate probable maximum losses to their portfolios, which in turn helps companies and regulators enforce the industry’s solvency requirements.

Using depth-damage curves for the estimation of flood loss dates back to the 1960s (White, 1945; Kates, 1965) and has been progressively accepted internationally as the standard approach for urban flood loss assessment (Grigg and Helweg, 1975; D. Smith, 1994). By now, a large variety of loss models have appeared differing in purpose, structure, and regional focus. Loss modelling in some instances is performed separately per sector, say residential, commercial, industrial, agricultural, etc. and on different spatial scales, where the units of analysis vary from individual elements at risk to aggregated land use units (B. Merz et al., 2010b). Furthermore, loss models differ in their damage metric, i.e. the model outcome may be the estimated absolute loss in monetary terms or it may be the relative loss, expressed as a fraction of the total value of the element at risk (Messner et al., 2007).

Besides the uni-variable depth damage curves, multi-variable loss functions have been developed that consider more variables in addition to water depth for loss estimation, for instance building type, or precautionary measures or impacts due to contamination (Zhai et al., 2005; Kreibich et al., 2010; Elmer et al., 2010). The extension of loss models into the probabilistic domain has introduced the possibility to provide quantitative information about model uncertainty (Schröter et al., 2014; B. Merz et al., 2004; K. Vogel et al., 2013; Kreibich et al., 2017a). This considerable progress (B. Merz et al., 2010b; Moel et al., 2015) has resulted in a highly heterogeneous landscape of functional forms of increasing complexity to describe flood damage. In the face of considerable uncertainty associated with loss estimates (Michel-Kerjan and Kunreuther, 2011; B. Merz et al., 2004; Apel et al., 2009; B. Merz and Thielen, 2009) probabilistic models show promise to increase the reliability of loss estimates impacting flood risk assessments (Schröter et al., 2014).

This growth in flood loss assessment methodologies has not always been accompanied by a sound and explicit model validation process that would document and demonstrate how well models perform the kind of task for which they were intended (Meyer et al., 2013). This lack of rigorous delineation of when and where a certain model should be applied might result in the adoption of models to geographical regions and flood events that differ from the settings for which they were originally designed. Since variations in local characteristics and systems such as the implementation of precautionary measures

have a strong impact on outcomes, models often require regional adjustments (Schröter et al., 2014; Cammerer et al., 2013).

Due to the uncertainties arising from these complexities, the reliability and robustness of flood loss models are often hard to assess. Frequent dispersion in the results leads to question their adequacy and validity in their application. Flood loss model benchmarking and validation are therefore becoming increasingly relevant for instance to public authorities in charge of flood risk assessment and management as well as to the insurance industry since regulatory standards in Europe and elsewhere expect companies to “own” their view of risk, i.e. to understand their risk assessment tools and to adopt a critical view to underpin their decisions on capital requirements, reinsurance, and enterprise risk management (Franco, 2013; Franco, 2014).

The robustness and validity of the flood loss models used in the risk assessment tools by the insurance companies should thus be tested by 1) comparing them with the models described in the scientific literature and 2) identifying whether such alignment is appropriate for the application in mind. As a consequence, the first step towards the benchmarking and validation of flood loss models should be a compilation of all available references from the scientific literature. Similar initiatives were recently made for other perils such as wind and earthquake (Lopeman et al., 2013; Spillatura et al., 2014). While this survey of scientific literature and the classification of flood loss models are instigated by the particular needs of the insurance industry, the authors believe that this taxonomic exercise is a useful contribution to the flood risk community in general.

This work thus presents an inventory of flood loss models, compiled from a review of scientific papers and research reports. The flood loss models are queried and catalogued according to various dimensions including model specification, geographical characteristics, sectors addressed, input variables used, completeness of model validation, transferability and mathematical formulations. The rationale of the review is to provide a basis for the development of model harmonization approaches and finally for model benchmarking. To build this catalogue of vulnerability functions we extract from the studies these functional relationships and analyze the accompanying descriptions regarding their usage, limitations, and scope. From this inventory we commence a discussion on the harmonization of models. Although this step is beyond the scope of this work, a benchmarking framework will eventually require that all or most models can be compared –at least approximately– within a common referential space.

9.2 Methods used to build the inventory

The compilation of the flood loss model inventory is carried out by collecting references that include original work on the development of loss models within a literature review. We focus on fluvial floods, while offering examples of other flood types such as coastal or lake floods. Only models for direct tangible flood losses are considered. Indirect tangible and all intangible damage are excluded. Direct losses occur as a result of the direct physical impact of a flood event while indirect losses occur outside the hazard area in temporal or spatial terms. Intangible losses refer to damage to people, objects and services that are not easily measurable in monetary terms because they are not directly traded in a market (Aerts and W. J. Botzen, 2011; B. Merz et al., 2010b; Hammond et al.,

2015).

The meta-data compiled in the inventory presented in this paper provides details about the general model philosophy in terms of underlying assumptions, regional embedding as well as units of analysis, flood type, input variables required and other model characteristics.

The functional forms themselves have not been included in the paper or in the supplemental material. However, all necessary references are given to lead the reader to the specific formulations, if that were of interest. In most cases, these references are publicly available and can be easily retrieved from the literature. In some limited instances, however, some models or model components might be subjected to intellectual property restrictions that may require the reader to ask for explicit permission from the relevant parties in order to access the information.

9.2.1 Literature review strategy

Our literature research uses the following mixed strategies: browsing, footnote chasing and consultation (P. Wilson, 1992).

Five experts with 60 collective years of experience in the field of flood loss modelling and with an approximate collective track record of 70 publications in the same field representing varied perspectives from the industry and academia, gave rise to the core recommendations and search strategy. Based on the recommendations of these experts, recent, comprehensive review papers and project reports were searched for flood loss model descriptions. This selection included five review papers (D. Smith, 1994; B. Merz et al., 2010b; Meyer et al., 2013; Hammond et al., 2015; Brémond and Grelot, 2013), six scientific papers (Kreibich et al., 2010; Elmer et al., 2010; Apel et al., 2009; Cammerer et al., 2013; Kelman and Spence, 2004; Jongman et al., 2012) and five project reports (IPCC, 2012; Helsten and Davidge, 2005; Sterr, 2005; Bubeck and Kreibich, 2011; Bank, 2014). Flood loss models were extracted from these documents and from their associated references, for which we searched in bibliographic databases using web-based research platforms.

As these papers mostly covered European studies, partly because other regions adopted standard models like in North America, additional references were searched in order to complement and update the inventory of flood loss models. Within this search, terms in English language were used since this is the international language of science. However, non-English references entered the inventory via cross-references in papers and reports of the core recommendations.

The search engines used were the web applications of Science, Scimedirect, Scopus, and Google or Google Scholar. The searches were carried out in the period from October 2014 to December 2014. The following keywords were searched in the different web search engines using the option 'search in all fields' without imposing any date or language restrictions: "flood catastrophe risk model", "flood damage function", "flood damage curve", "flood damage model", "flood vulnerability function", "flood vulnerability curve", "flood vulnerability model", "flood susceptibility", "flood damage assessment" and "cost of floods", "losses of floods", "cost of hazards", "losses of hazards". In this process the significance of the publication titles of the first 200 hits for each keyword search sorted by relevance were checked. Relevance of search results was determined by

the search engine according to the relative frequency that the search terms used appear in each publication. Next, publication titles were perused and potentially suitable publications were identified for subsequent eligibility assessment. The criterion for eligibility of a publication was if information about a flood loss model function is provided or not. The resulting inventory is the most complete public survey to date.

Review Limitations

The inventory does not represent an exhaustive compilation of all flood loss models, which exist worldwide. The recommendations of experienced experts may have biased the selection as a result of the experts' own backgrounds and experience. The additional search via web based engines may have introduced an bias towards scientific sources. The flood loss models included in the inventory mostly originate from publications in English although some were extracted from documents in Afrikaans, Japanese, German, Dutch or French which the authors translated with external support. Due to this language bias other existing references e.g. from South- and Central America, China and other countries have not been found. Other loss models, e.g. from commercial tools may not have been accessible.

9.2.2 Structure of the inventory

The structure of the flood loss model inventory is created on the basis of previous review papers (D. Smith, 1994; B. Merz et al., 2010b; Meyer et al., 2013; Hammond et al., 2015; Brémond and Grelot, 2013). It contains the following categories: (1) model specification, (2) geographical characteristics, (3) sectors addressed, (4) input variables used, (5) model validation, (6) transferability and (7) model functions. In addition, each category consists of several attributes which are described in Table 9.1. Category (1) gives general information about the model and its basic concept and application. Furthermore, the database used for model development is identified. Category (2) includes information on spatial scale and extent of the flood loss model, i.e. for which region/catchment the model was built. This category also contains information about the models' unit of analyses and land use classes as well as the flood type. Category (3) states the sector for which the model was developed. Category (4) specifies the input variables for the flood loss model, concerning flood impact, building characteristics, socio-economic factors and precautionary measures. Category (5) describes if and how the model results are validated. Category (6) describes the feasibility to transfer the model to different regions. Category (7) contains the actual model, i.e. the formula or matrix of flood loss separated for the various considered sectors.

9.3 Observations on the flood loss model inventory

Within the literature review we identified 66 publications from the search in web search engines. Another sixteen records were identified from the consultation of experts. Footnote chasing of the recommended review and original research papers as well as project reports contributed a number of nine additional project reports. After removal of duplicate publications, 89 records were retained for further analyses. All 89 records were

Table 9.1: Structure of the flood loss model inventory

Category	Attributes	Definition
Model specification	Model	refers to the model name and its abbreviation
	Reference	author name, year and publication title
	Domain (development background)	information about the publication type, e.g. scientific paper, proceedings, thesis, report, or software manual
	Approach	model approach type classified according to empirical (uses loss data collected after flood events), engineering/synthetic (uses loss data collected via what-if-questions), or a combination of both types
	Database	method of data acquisition for model development, e.g. interview data, building inspections, etc.; including number of cases
	Model type	distinguishes the model according to the number of damage-influencing factors considered possible types are univariate (assumption that flood damage is influenced only by one factor, mostly the inundation depth) and multivariate (flood damage is influenced by multiple factors)
	Model concept	differentiates deterministic (no stochastic elements are involved, so the input and output relation of the model is conclusively determined) and probabilistic models (multiple results with varying degree of uncertainty are possible due to the implementation of stochastic elements)
	Purpose of model	type of modelled damages, either insured damages or total economic loss
	Cost base	replacement costs (amount it would cost to replace an asset) or depreciated/repair costs (cost for the restoration of damaged property)
	Damage metric	model outcomes are relative (% of total value) or absolute (currency/unit, e.g. 2) damage
(2) Geographical characteristics	Geographical scope	regional context of the flood damage model, considering the categories continent (e.g. Europe), country (e.g. Great Britain), region/catchment (e.g. River Thames), city (e.g. London)
	Spatial resolution	differentiates deterministic (no stochastic elements are involved, so the input and output relation of the model is conclusively determined) and probabilistic models (multiple results with varying degree of uncertainty are possible due to the implementation of stochastic elements)
	Unit of analysis	major entity that is being analyzed, e.g. individual objects (single houses) or aggregated land use classes (combination of related objects)
	Land use classes	name of land use data set and data source (e.g. CORINE Land Cover provided by European Environment Agency) as well as land use classes (e.g. residential, industrial)
	Spatial category	rural (territory outside of a city, i.e. countryside) or urban (high-built up areas with high population density, i.e. a city)
	Flood type	flood source considered: fluvial flood (water overflows the river banks when surface water runoff exceeds the capacity of channels to accommodate the flow), flash flood (flood peak appears within a few hours originating from torrential rainfall), pluvial flood (caused by rainfall or snowmelt), groundwater rise (water table level rises to the surface level), coastal flood (arise from incursion by the ocean), or dam break (failing of dikes causes devastating floods)
(3) Sector	Sector	states the sector for which a flood damage function is available, e.g. residential (area in which housing is the predominant use, including building and its content, e.g. single-family house), commercial (buildings and its content that refer to the exchange of goods and services for money, e.g. bank, retail trade), industrial (includes buildings and its content that belong to processing of raw materials and manufacture of goods, e.g. heavy industry), public/municipal (institutional buildings used and run by the community, e.g. school, hospital, theatre), agriculture (refers to cultivated land for crop production and raising livestock, e.g. vegetables, stables), infrastructure (the installation of public transportation system, e.g. roads, railway), vehicles (includes cars and other transportation vehicles of private and business customers), mixed use (merged class of above mentioned sectors, e.g. industrial/commercial buildings), others (e.g. energy & water supply, forest)
(4) Input variables	flood impact	description of the flood event, considering parameters like water depth, inundation duration, flood velocity, contamination (e.g. oil), return period, time of flooding, recurrence interval, distance between object and water front, meteorological data and intercept
	Building characteristics	building type (e.g. single-family house, high-rise building, factory), number of floors, number of flats, floor space, construction material (e.g. masonry, concrete), age of building, heating system (e.g. district heating, oil), building quality, building value, building fragility, building content/inventory
	Socio-economic factors	household size (number of persons living in one house), ownership (e.g. rental, private), monthly net income, residing period, size of company (nr. employees), sector of company, equipment, goods/products/stock, crop type, gross value
	Precaution	precautionary measures (e.g. flood adapted building structure, mobile flood water barriers), flood experience, early warning
	Other	cost of replacement feed/additional costs incurred or saved, damage to building (no building damage or damage)
(5) Validation	Validation	type of model validation, either qualitative (cannot be measured with a numerical result) or quantitative (numeric estimation of uncertainty)
	Reference	author name, year and publication title should be given
(6) Transferability	Transferability	information if the transferability of the model is tested
	Reference	author name, year and publication title describing the transferability of the model
(7) Function	Type of function/matrix	univariate, multivariate
	Sector	see description of sectors in geographical characteristics
	Specific unit of analyses	specific object (e.g. single-family house) or land-use class (e.g. manufacturing)
	Damage function	damage function formula and legend
	Damage matrix	is expressed in water depth and damage value. The legend describes the units of input variables
	Damage matrix (for agriculture)	consists of time of flood event, damage value and flood duration

perused in order to check for eligibility to be included in the flood loss model inventory. Only those publications were retained which provide information about the flood loss model function. This step led to the exclusion of 28 records, so that 61 publications were included in the qualitative synthesis. Since, fourteen publications provided redundant information about flood loss models functions finally 47 references are included in the flood loss model inventory.

In this section, we summarize our main observations with regards to the main traits used in the flood loss model taxonomy organized accordingly.

Model specification (category 1)

An important distinguishing feature for the specification of flood loss models is the model approach or philosophy. There are two approaches that are typically used in developing flood loss functions (A. Kron, 2007), empirical or engineering/synthetic, as specified in Table 9.1. A model may also be derived from a combination of both approaches. While the empirical approach uses observed flood damage data collected after flood events, the generation of synthetic damage models is based on hypothetical damage estimates by experts through what-if-analysis (i.e. what is the potential loss if a specific building type is flooded with an inundation depth of 1 meter?). This second approach is often used when detailed empirical damage data are not available or if they are of dubious quality. 49% of the catalogued flood loss models are empirical models while synthetic models account for about 19%. 32% result from a combination of these two approaches (Figure 9.8).

Model concept, i.e. whether a model is deterministic or probabilistic, is a key attribute. The first type is frequently used to describe the damage processes in terms of a functional relation between flood loss and the variables involved (R. M. Vogel, 1999). Models in this category provide point estimates of flood loss. In contrast, probabilistic models provide a distribution of flood loss estimates due to the inclusion of stochastic elements such as the probability of a building being affected by a flood event (Zhai et al., 2005) or the random behavior of certain model parameters or variables (Zhai et al., 2005; Schröter et al., 2014). By far the largest share of 96% corresponds to deterministic models versus only 4% of probabilistic approaches. The scarcity of probabilistic models in the literature betrays the rampant epistemic uncertainty and is a strong argument to investigate these models in greater depth in order to leverage their potential to increase the reliability of loss estimates.

We distinguish models depending on whether they use one or many parameters to estimate damages. Uni-variable models are based on the assumption that the response variable, flood loss, is influenced by only one factor, usually the inundation depth, in contrast to multi-variable models which use more than one predictor. Although it is internationally accepted that flood damage is mainly influenced by the inundation depth, this parameter cannot fully explain the damage data variance (B. Merz et al., 2010b; Thielen et al., 2005). Commonly one distinguishes between impact parameters, reflecting specific characteristics of a flood event (e.g. inundation depth, flow velocity, contamination), and resistance parameters that describe the capability of a flood prone object to resist the flood impact, e.g. building type or construction material. The analysis of the flood loss model inventory shows that the most frequently used impact parameters are water depth, inundation duration and flow velocity. Furthermore, some models use contamina-

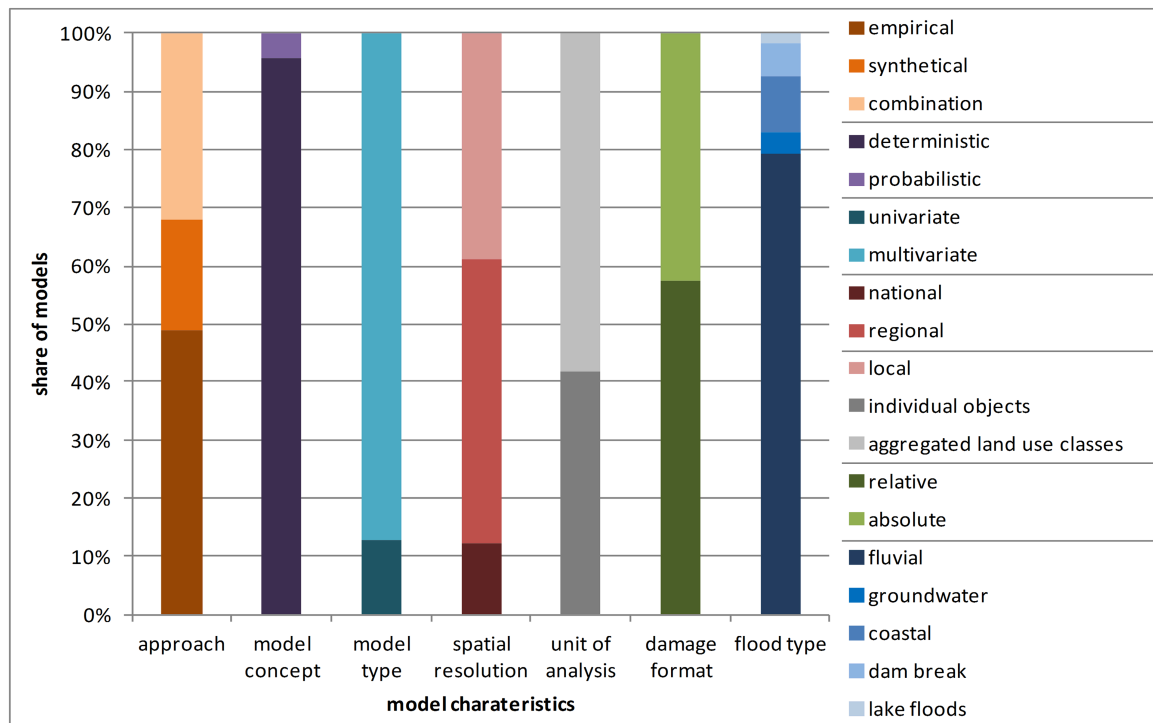


Figure 9.1: Characteristics of flood loss models contained in the inventory.

tion, return period and time of flood event as factors influencing damage (Schröter et al., 2014; Förster et al., 2008; Chau et al., 2015). In the agricultural sector, the inundation duration and timing of the flood event are particularly important for flood loss assessment (Brémond and Grelot, 2013). Building characteristics like building type, number of floors, floor space, construction material, building value and building content/inventory are important resistance parameters in flood damage assessment for urban areas (B. Merz et al., 2013; FEMA, 2009; Dutta et al., 2003). Additionally, the implementation of precautionary measures in order to reduce flood losses is an important factor (Thieken et al., 2008b; Torterotot, 1993). Several models consist of a set of uni-variable loss functions which differentiate for example for building or crop type and other impacts of resistance characteristics. Hence, these models eventually do consider multiple variables to estimate flood loss.

Another criterion for distinguishing flood loss models is the damage metric used. Absolute damage functions estimate the loss in monetary units, while relative damage functions express the expected loss as a proportion of the total asset value of an element at risk. 57% of the flood loss models are relative and 43% are absolute models. The advantage of relative loss models is the better transferability in space and time due to the independence from the local economic setting. On the other hand, information on object assets is required for the estimation of monetary damage. While this is not necessary for absolute damage functions, these models require a regular recalibration. Furthermore, since absolute loss models are developed for a particular study area, it is difficult to transfer them to other regions (B. Merz et al., 2010b; Poussin et al., 2012).

Geographical characteristics (category 2)

The inventory contains 47 flood loss models that are distributed across 23 countries (Figure 9.2). Most of them arise from Europe (60%), followed by Asia (21%), North America (6%), Australia (6%), Africa (4%), and Central and South America (2%). 40 models or about 85% were published as scientific papers and reports. The remaining seven models originate from proceedings, theses, and software manuals.

The large variety of flood loss models around the world can be explained mainly by variations in the objective of country or regional studies as well as national or regional differences in data availability and level of data precision (spatial and temporal resolution), which may depend on budget or time restrictions (Kreibich et al., 2017a). The amount of loss models developed in a country is most likely also influenced by the availability of a standard method like the HIS-SSM model in the Netherlands (Kind, 2011; Kok et al., 2005) or the HAZUS model in the US (FEMA, 2009; Scawthorn et al., 2006).

Flood loss estimation is performed on different scales (spatial resolution/unit of analysis), which is mainly determined by data availability. For national or regional studies aggregated land use classes (e.g. residential buildings, commerce) are the norm. In smaller investigation areas (local or object-based scale) the integration of spatial high-resolution land use data with information about individual buildings is more common (Messner et al., 2006). On this scale building types are often differentiated by building age, construction material or floor space, for instance. Often separate damage functions are available regarding building structure and building content. The majority of flood loss models are generated to work on regional (49%) and local (39%) scales, i.e. flood damage assessment is performed for entire catchments or urban sprawls. About 12% of the loss models are applicable on a national scale. All in all, 58% consider aggregated land use classes and 42% use individual objects as the unit of analysis.

Due to our search focus on riverine floods, most of the flood loss models contained in the inventory refer to fluvial floods with low flow velocities (79%). Some specialised models focus on estimating losses that occur through dam breaks (6%), groundwater rising (4%) or coastal floods (9%). One model in the inventory tackles lake-flood induced losses (Grahm and Nyberg, 2014). Most studies focus on urban areas, because the largest damages are expected in cities. In contrast, flood losses in agricultural regions are usually much lower (Brémond and Grelot, 2013).

Sector (category 3)

The flood loss model inventory contains 936 flood loss functions although not all loss functions that belong to a model are included in the inventory. For example, the Multi-Coloured Manual (MCM) (Penning-Rowsell et al., 2005) and HAZUS-MH (FEMA, 2009) contain several hundred functions due to the numerous sub-categories of individual sectors. For these models the average loss functions for individual sectors were selected. Dominant land use categories in the inventory are residential buildings (36%) and their contents (13%), commercial/service sector (8%) and accompanying equipment (10%), public and municipal buildings (7%), and industrial buildings (4%) and their contents (3%). The share of damage functions for the agricultural sector is almost 10%. Infrastructure (1%) and vehicles (<1%) have a significantly lower proportion. About 6% belong to mixed and other uses, see Figure 9.2.

Input variables (category 4)

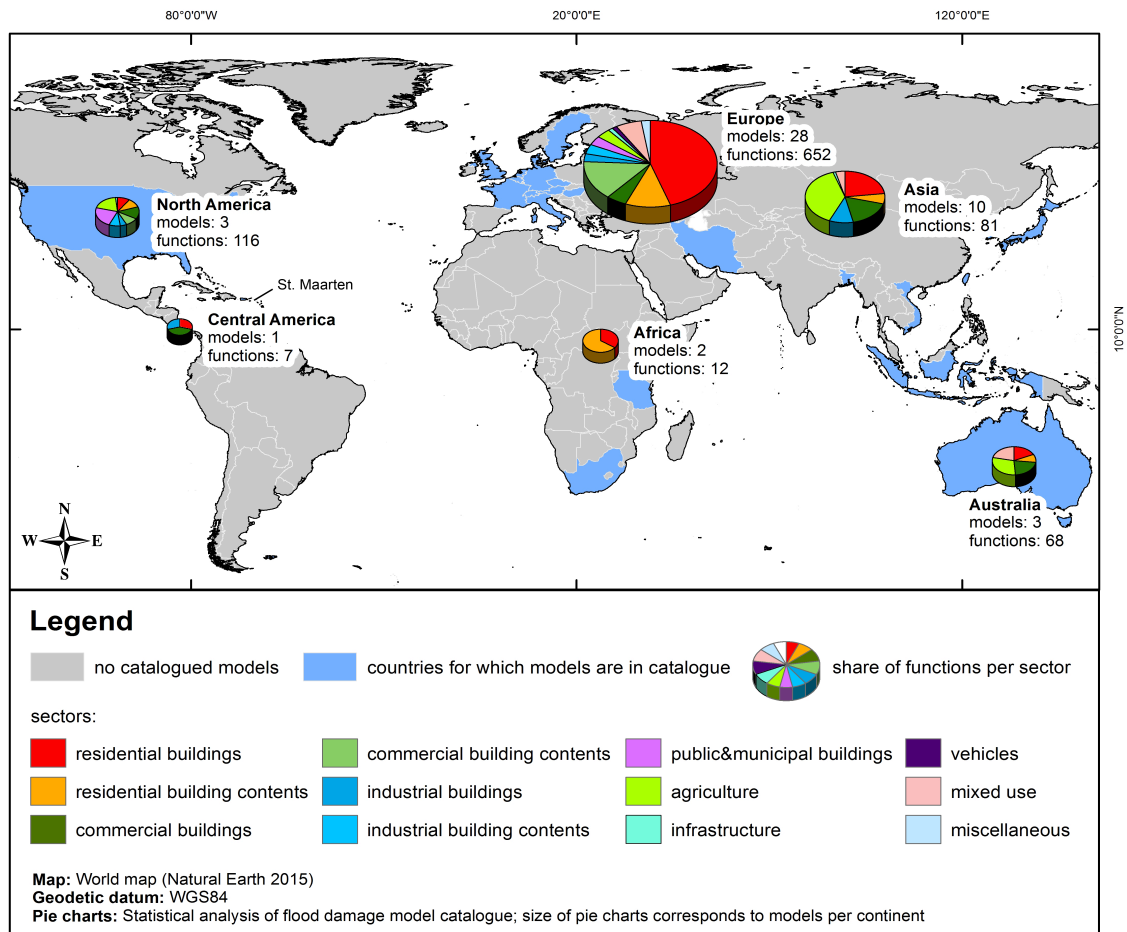


Figure 9.2: Global distribution of flood loss models and functions for different sectors contained in the inventory.

The inventory contains 47 loss models covering different sectors in which different damaging processes are important. Accordingly, the loss models include differing types and number of input variables. 94% of the models use, among others, water depth as an explanatory variable for flood loss. The remaining models (6%) utilize inundation duration and time of flood event as impact parameters (Förster et al., 2008; NRC, 2000; Y.-O. Kim et al., 2012). The second most utilized input variable is the floor space of a building (51%) followed by number of flats and socio-economic factors (23%). Flow velocity, goods, products, stock, vehicles, crop type and total area of crop cultivation and contamination are used by 17% of the models. Other input variables used by at least 10% of the models are: construction material, building fragility, flood experience, recurrence interval and age of building, Variables describing information about return period, time of flood event, building value, heating system, flood warning etc. currently seem to play a minor role in loss modeling even though their usefulness to explain flood loss has been demonstrated in various studies. For instance flood warning, and the quality of external response in a flood situation has been shown to have a strong impact on loss, e.g. (D. Smith, 1994; Wind et al., 1999; Kreibich et al., 2009; Penning-Rowsell and Green, 2000; Kreibich et al., 2005) and return period has been shown to play a role as well (Elmer et al., 2010).

Validation and transferability (categories 5 and 6)

An important prerequisite for flood loss assessment is the quality and extent of loss model validation. For 45% of the models, estimated flood losses were validated by comparison with observed loss data, often including an analysis of the relevant factors that affect loss. For the rest of the models the evaluation status is rather unknown and the validation process is not explicitly described in the paper or report that contains the model development description. However, validation of these models may have been undertaken and described in other posterior follow-on literature not included in our review. This holds also true for transferability of the models to other regions. While one cannot bluntly assume that validation and transferability assumptions do not exist for roughly half of the loss models found in our review, it is worrisome that this information is not put forward at the time of the development of the model. One cannot help but wonder whether such validation and transferability exercises were tackled at all when the loss model was proposed. This is not a contributor to increasing our confidence in the models that we use for risk assessments.

Functional form (category 7)

The functional form of the flood loss models varies considerably depending on the concept, the approach, the sector, and the input variables used. The functions extracted from the literature range from constant loss values for different land uses or sectors, respectively, to complex analytical functions and conditional probability functions. The spectrum of analytical functions covers linear, exponential, logarithmic, polynomial, and square root functions as well as non-linear regression equations to describe the relation between the input variables and flood loss. These analytical functions are usually used within deterministic empirical loss models, where the functions are selected and parameters are derived by curve fitting to observations. In contrast, synthetic models are usually provided as value pair matrices, e.g. in MCM (Penning-Rowsell et al., 2005) and HAZUS-

Table 9.2: Characteristics of the selected example models

Model characteristic		Example models (Reference)				
		HAZUS-MH for residential buildings (FEMA, 2009)	(Zhai et al., 2005)	BN-FLEMOps (Schröter et al., 2014)	(Yazdi and Salehi Neyshabouri, 2012)	(Hess and Morris, 1988)
Sector	Residential	x	x	x		
	Agricultural				x	x
Damage metric	Absolute		x			x
	Relative	x		x	x	
Type of function	Uni-variable	x			x	
	Multi-variable		x	x		x
Model concept	Deterministic	x	x		x	x
	Probabilistic			x		

MH (FEMA, 2009).

9.4 An illustration of model diversity

As stated above, the heterogeneity found in existing flood loss models is daunting. To illustrate the challenges that arise when one aims to compare these loss models with one another or with other models external to the inventory, we choose five arbitrary models and depict their characteristics in this section. These models represent different damage metrics, types of function and model concepts (Table 9.2). The analysis focuses on two particular sectors only, residential and agricultural.

The North American deterministic model HAZUS-MH (FEMA, 2009) is selected as an example for the residential sector. It contains numerous uni-variable functions that calculate relative flood losses dependent on the inundations depth. The functions are derived based on a combination of empirical and synthetic databases. Individual loss functions are available for residential buildings according to building type, number of floors, and building contents (Figure 9.3). Loss estimates can be obtained for individual objects; however these values represent average values for a group of similar buildings and hence are usually aggregated for census blocks.

Zhai et al. (Zhai et al., 2005) derived an empirical deterministic loss function for residential buildings of the megacity of Nagoya in Japan. Considering the loss influencing factors of house ownership, residing period, income and inundation depth this multi-variable model calculates absolute flood losses based on individual buildings. Income is classified into (1) less than YEN 3 M, (2) YEN 3-4 M, (3) YEN 4-5 M, (4) YEN 5-6 M, (5) YEN 6-7 M, (6) YEN 7-8 M, (7) YEN 8-10 M and (8) >YEN 10 M. Residing period is classified as (1) 1-10 years, (2) 10-20 years, (3) 20-30 years, (4) 30-40 years, (5) 40-50 years, or (6) >50 years. Figure 9.4 shows three two-dimensional views on the variation of flood loss in YEN M within this multi-variable model space. These sections map water depth and income class, water depth and residing period as well as income and residing period class. For each section the remaining variable is set to its mean value. Loss increases with inundation depth, residing period class and income class. The steepest gradient is observed for increasing water depth in combination with increasing income class and to a lesser extent with increasing residing period class.

Figure 9.5 presents the structure of the multi-variable probabilistic model BN-FLEMOps (Schröter et al., 2014) which uses Bayesian Networks to describe the joint probability distribution of the explanatory variables involved. The model was derived from empirical

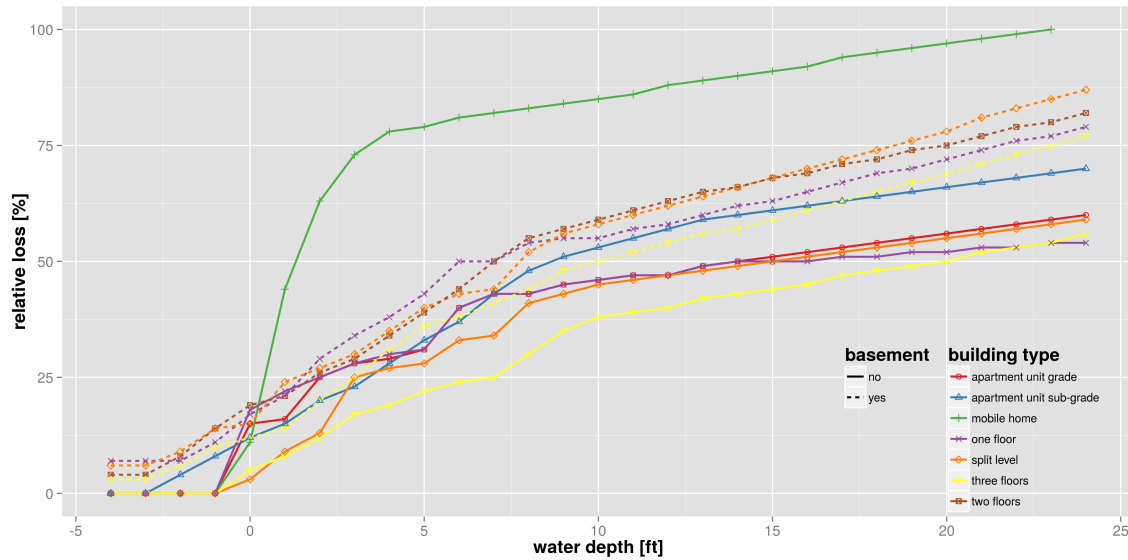


Figure 9.3: Loss functions of residential buildings in HAZUS-MH (FEMA, 2009); example of a relative, deterministic model using uni-variable loss functions (negative inundation depth refers to inundation in the basement of a building).

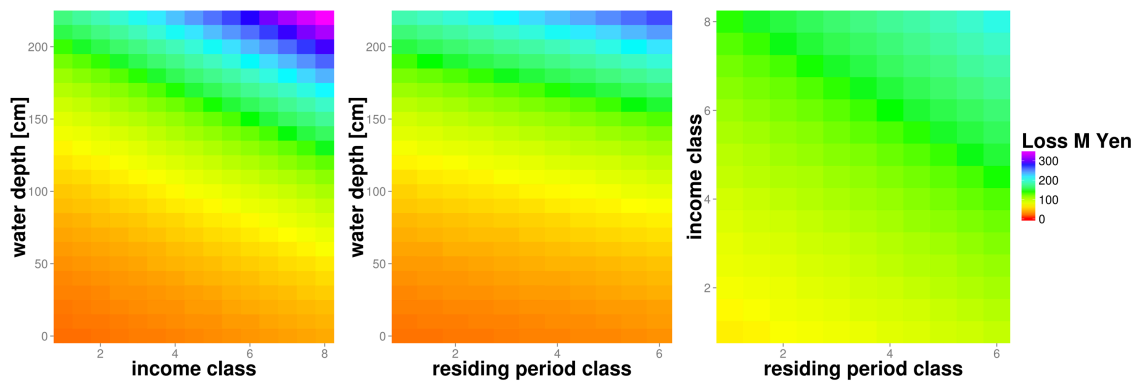


Figure 9.4: Damage model of Zhai et al. (2005) with the damage-influencing factors residing period, income and inundation depth; example for an absolute, deterministic model using multi-variable loss functions.

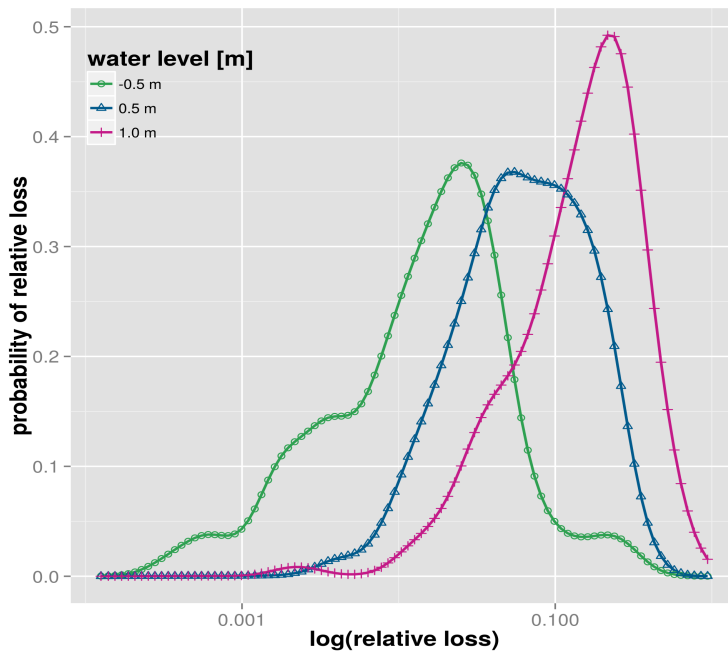


Figure 9.5: Structure and example distributions of loss estimates for selected water levels of BN-FLEMOps; example for a multi-variable, relative, probabilistic model.

flood damage data for the Elbe and Danube catchments in Germany and can be used to estimate relative loss to residential buildings on the object level. The model considers ten explanatory variables including water depth, contamination, inundation duration, flow velocity, return period, building quality, building value, building type, emergency measures and precaution. On the left in Figure 9.5 the directed acyclic graph (DAG) of the model is shown which describes the probabilistic independences of the variables. The DAG, discretization and conditional probability distributions were learned from observed data (K. Vogel et al., 2013). The marginal probability distributions of relative loss for varying water levels (-0.5, 0.5, and 1.0) but constant observations for precaution and contamination are plotted on the right hand-side of Figure 9.5. This plot illustrates the shift in probability of relative loss towards higher relative damage with increasing water levels. In contrast to deterministic models the probability distribution of relative loss provides a quantitative estimate of the uncertainty associated with the predicted relative damage.

For the agricultural sector the deterministic models of Yazdi and Salehi Neyshabouri (2012) and Hess and Morris (1988) are selected. The first one is developed based on empirical data from the Kan basin in Iran and contains several uni-variable functions for calculating relative flood losses to different crop types (Figure 9.6). The second model includes a multi-variable loss function for grassland that is based on an empirical-synthetic approach (Figure 9.7). This function uses information about the energy from grass lost due to flooding (GMJ), cost of replacement feed (RF) and additional costs (C) incurred or saved in order to estimate absolute flood losses in England based on aggregated land use classes.

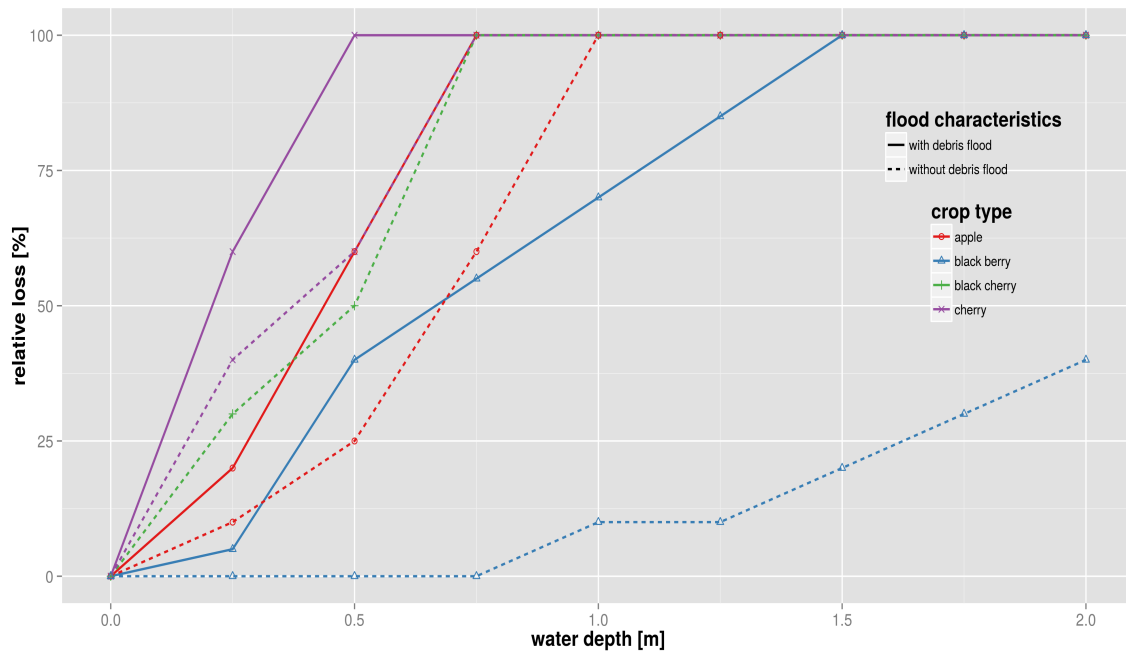


Figure 9.6: Loss functions of crop types (Yazdi and Salehi Neyshabouri, 2012); example for a relative, deterministic model using uni-variable loss functions.

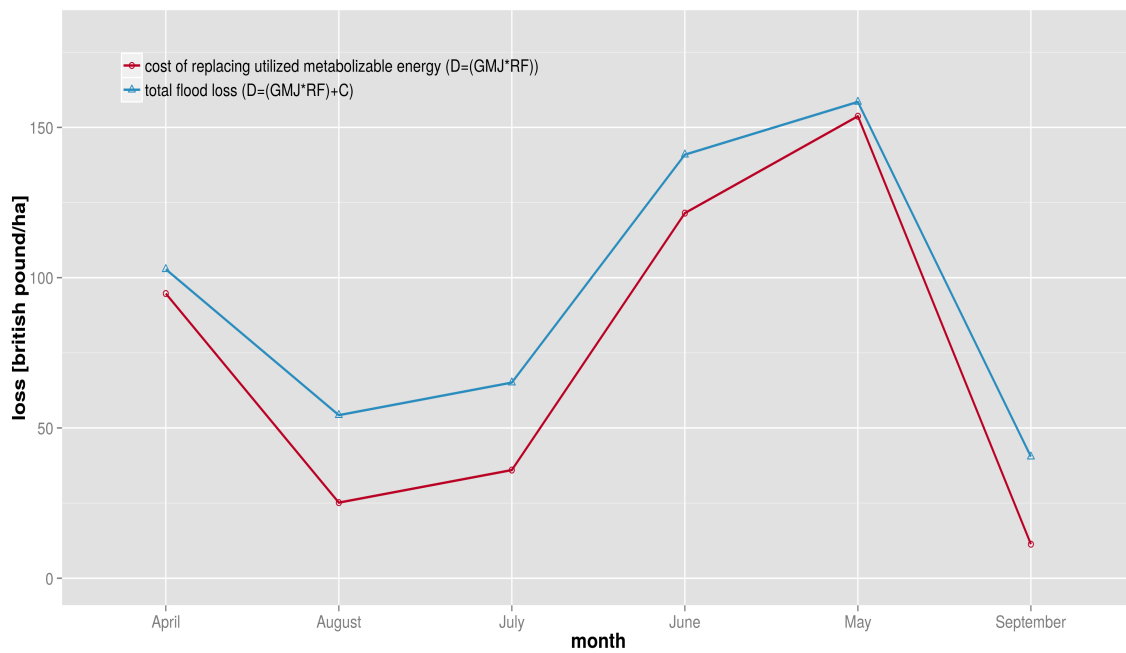


Figure 9.7: Loss functions for one-cut silage (Hess and Morris, 1988); example for an absolute, deterministic model using multi-variable loss functions. D =total damage [GBP/ha], GMJ =energy from grass lost due to flooding [MJ/ha], RF =cost of replacement feed [GBP/ha], C =additional costs incurred (+) or saved (-) [GBP/ha].

These examples illustrate typical differences between loss models contained in the inventory which, for the purpose of comparison and benchmarking, need to be harmonized somehow. For instance, models may require different input information in terms of number and type of variables to estimate flood loss. Further, the model outcome might be either in relative or absolute format and might represent loss to varying spatial entities e.g. individual objects or aggregated land use classes.

A strategy to project heterogeneous models onto a common reference space needs to be devised. Otherwise, these models exist in isolation and their performance cannot be easily evaluated against each other's.

9.4.1 Challenges in model harmonization

Recall that the ultimate aim that instigated this research is to use the inventory of flood loss models as a broad compendium of reference information against which to judge whether commercial flood risk models are reasonably aligned in their assumptions with the existing corpus of science and knowledge. Therefore, the mechanics required to establish comparisons across models are of critical importance.

It is evident, however, in light of the existing heterogeneity of models and approaches that using a common reference frame to carry out sensible comparisons across models is extremely difficult. Devising a strategy that would make this possible in general is well beyond the scope of this paper. Nevertheless, in order to illustrate approaches to tackle this challenge that seem reasonable to the authors at this stage, an exercise is presented in this section to attempt the harmonization of three of the models contained in the inventory.

In this pursuit we ask ourselves whether there exists guidance in the literature as to how to maneuver through this challenge but despite the relevance of this problem, there is no generic procedure available. Therefore, we consider two starting strategies. First, we consider the possibility that all the flood loss models that we wish to compare are transported to a common set of reference variables. In practice this means that for example inundation duration as a flood-impact factor would have to be translated to inundation depth – the most commonly used flood impact variable – in order to compare two models across this dimension. This transformation would ideally provide a set of unique functions using the same common variables. However, due to the heterogeneous nature of the input variables and their ambiguous interrelations and conversion uncertainties, this approach seems tortuous.

As a second option, one could restrict the comparison across flood loss functions to their common intrinsic variables, i.e. the models are driven using only the input variables which are used by all the other models as well. The non-common variables must be set to assume reasonable estimates or a distribution of likely values. In this approach the differences in terms of the number of input variables are maintained and may lead to the comparison of single uni-variable loss functions across models, for instance, differentiating flood loss functions by building types, building material or topographical circumstances. If the number of common variables is relatively low, the dispersion in loss estimates can be expected to be large.

Both approaches aim at harmonizing the dimensionality of uni-variable and multi-variable models and to reconcile differences between the models as regards the model

concept (deterministic, probabilistic), their damage format (relative, absolute) and the unit of analysis (individual objects, aggregated land use classes) which may require additional considerations.

To tackle an actual example, we illustrate the harmonization of flood loss models for the residential sector used in the previous section. Within this exercise we aim to compare these three models based on their common variables, following the second approach described above. The target space for harmonization is given by the relative building loss in percent in dependence on water depth in meters which is the only variable common to all three models. For the deterministic relative flood loss model HAZUS-MH (FEMA, 2009) the harmonization is straightforward. As this model already provides relative building loss as a function of water depth, the only adjustment needed is to convert water depth from feet into meters. This model then provides a set of relative flood loss functions which differentiate residential buildings according to number of floors, presence of basement, and location within special flood hazard areas (Figure 9.8). The deterministic multi-variable damage model of Zhai et al. (2005) provides absolute loss values as a function of water depth, ownership, residing period and income, and thus requires a two-tiered approach for harmonization. First, a set of uni-variable loss functions are obtained from the multi-variable model functions by determining the marginal functions which only depend on water depth. For this purpose, fixed values for house ownership (rental=0 and owner=1), residing period (short=1 and long=0) and income (low=1 and high=8) are used in combination with variable water depth values. The outcome is a set of damage functions depending on water depth which differentiate for house ownership, residing period and income level. Second, the absolute loss values are converted to relative values by dividing absolute values by the average single-family house price. Actually, different house prices or a price distribution should be taken into account e.g. for low and high income. For the sake of this exercise, however, we simply assume the average value of YEN 72.11M suggested by Shimizu (2014) for the year 2000 (Figure 9.8).

The harmonization of the multi-variable probabilistic model BN-FLEMOps (Schröter et al., 2014) also requires two steps. First, a best estimate for relative loss needs to be inferred from the probability distribution. Second, the multi-variable joint probability distribution function has to be marginalized to obtain a uni-variable relation between relative damage and water depth. Within this illustrative example we use the median of the probability distribution as the best estimate for relative damage. The dimension of the multi-variable distribution is reduced by extracting separate functions for different combinations of values, the variables contamination 'con' and precaution 'pre' might take. This results in a set of damage functions each of them representing the expectation of relative flood damage for varying water levels given the specific combination of observations for the variables 'con' and 'pre'. Figure 9.8 exemplifies the outcome of this procedure for the combination of 'high contamination and high precaution', 'high contamination and low precaution', 'low contamination and high precaution', and 'low contamination and low precaution'. Each case is represented by a curve which depicts the expected relative damage, i.e. the median of the probability distribution, for three discrete water depth classes. The error bars show the inter-quartile range (IQR) of the probability distribution for the different combinations and water depth values and provide insight into uncertainty associated with the loss estimate.

Figure 9.9 shows all three models in the joint target space defined by relative building

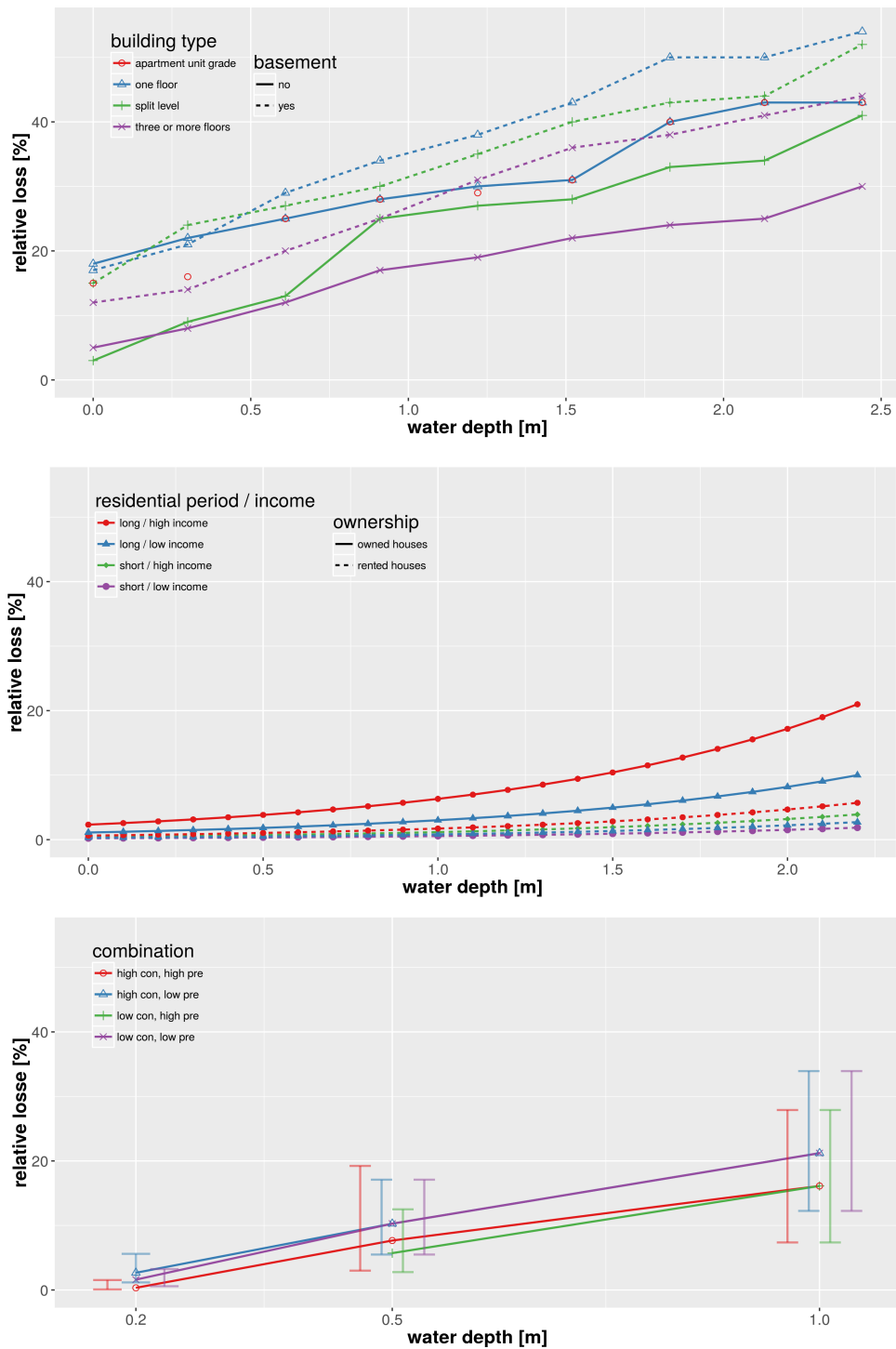


Figure 9.8: Harmonized flood loss models for residential buildings in dependence of water depth; top: HAZUS (FEMA, 2009), middle: Zhai et al. (Zhai et al., 2005), bottom: BN-FLEMOps (Schröter et al., 2014).

loss in percent and water depth in meters. The variability within HAZUS loss curves is due to building types and the presence of a basement, in the model of Zhai et al. (2005) it is due to income class and residing period, and for BN-FLEMO (Schröter et al., 2014) due to precaution and contamination. The information on different building types in different geographic regions is lost within the process of harmonization. Most striking is the large variability of relative loss estimates provided by the different models. This is consistent with previous findings of Schröter et al. (2014), Jongman et al. (2012), and Moel and Aerts (2011) who showed the high sensitivity of model structure and loss function shape with regard to loss estimation. Further, our results show that model structural differences persist in spite of the adjustments made within harmonization. For example, the HAZUS functions show almost uniform loss gradients across the whole scale of water depths, whereas the functions of Zhai et al. (2005) are based on a loss gradient which increases non-linearly with water depth. Note that the transformation of absolute loss estimates of Zhai et al. (2005) to the harmonized relative loss estimates is clearly sensitive to the building value applied. For example, the variation of the average building value by $\pm 50\%$ gives a reduction of relative loss estimates by $\frac{1}{2}$ and an increase by a factor of 2 respectively (not shown). Still, inter-model variability seems to be more important than intra-model variations due to differentiation of building type, number of floors, ownership structure, income and other characteristics. In this regard, the set of HAZUS loss functions shows the largest variability across the whole range of water depths. Zhai et al. (2005) functions we observe that the spread of loss estimates increases with water depth. The BN-FLEMOs functions show the smallest amount of intra-model variability. The uncertainty range indicated by IQR is within the range of the alternative models HAZUS and Zhai et al. (2005).

These findings emphasize the difficulties involved in assessing the suitability of a specific single model in comparison to other models within a harmonization framework. Our example illustrates the harmonization of only three alternative flood loss models for direct damage to residential buildings but the inventory contains various other models which could be included in a model suitability analysis framework with the aim of assessing the reasonability of model assumptions for application in risk assessments. The meta-data compiled in the inventory support the selection of suitable candidate models for benchmarking and comparison and thus may substantially reduce the effort required for model harmonization.

9.5 Conclusions

The survey of 47 flood loss models, including nearly a thousand flood vulnerability relationships comprised in the inventory reveals model types of vastly heterogeneous characteristics. The large majority of models are based on a deterministic model concept. While they are still scarce, probabilistic models seem to be emerging in the literature. Most models are based, at least partly, on empirical data. Multi-variable models are widespread. They typically consist of a selection of uni-variable loss functions differentiated by building use, type, etc. From the inventory we see an almost equal share of relative and absolute loss estimation formats. Most models in the inventory refer to the residential sector; and clearly fewer models are available for other sectors like industry

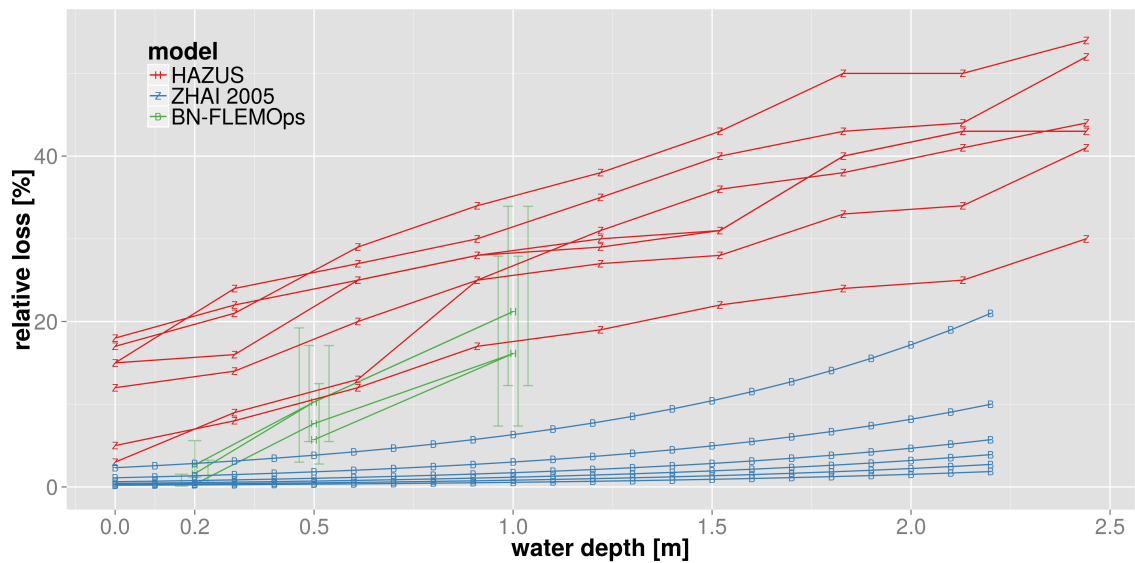


Figure 9.9: Compilation of harmonized flood loss models for residential buildings based on common variables.

and infrastructure. Research efforts should be focused on these sectors if the objective were to perform risk assessments of public services. Validation seems not to be a standard step in model development, which is concerning. Quite a large share of papers that describe or propose flood loss models do not include any validation process or exhibits. Sometimes validation has been done later on in application studies or separately, in specific validation campaigns.

This flood loss model inventory constitutes a critical first step in the development of benchmarking and suitability analyses to support the evaluation and selection of models depending on the desired usage or regional focus in the insurance industry as well as in the flood risk community in general.

The harmonization of models for benchmarking and comparison is a tedious and difficult task that requires profound insight into the model structures, mechanisms and underlying assumptions. The most promising approach to achieve a quantitative comparison of disparate models probably relies on using variables that are common to the models. However, if the number of common variables is low the explanatory power of sophisticated multi-variable or probabilistic models is reduced, and thus the dispersion of loss estimates may become larger. This will make a relative quality assessment more challenging. This work has established the foundation to commence this harmonization exercise, critical for the validation of flood loss models in a common framework.

10 | How useful are complex flood damage models?

Manuscript Info

Authors information:

Kai Schröter
Heidi Kreibich
Kristin Vogel
Carsten Riggelsen
Frank Scherbaum
Bruno Merz

Published as:

Schröter K., Kreibich H.,
Vogel K., Riggelsen C.,
Scherbaum F., Merz B.

How useful are complex
flood damage models?

Water Resour. Res.

2014;50,4:3378-3395.

doi:10.1002/2013WR014396

Abstract

We investigate the usefulness of complex flood damage models for predicting relative damage to residential buildings in a spatial and temporal transfer context. We apply eight different flood damage models to predict relative building damage for five historic flood events in two different regions of Germany. Model complexity is measured in terms of the number of explanatory variables which varies from one variable up to ten variables which are singled out from 28 candidate variables. Model validation is based on empirical damage data, whereas observation uncertainty is taken into consideration. The comparison of model predictive performance shows that additional explanatory variables besides the water depth improve the predictive capability in a spatial and temporal transfer context, i.e. when the models are transferred to different regions and different flood events. Concerning the trade-off between predictive capability and reliability the model structure seem more important than the number of explanatory variables. Among the models considered, the reliability of Bayesian Network based predictions in space-time transfer is larger than for the remaining models and the uncertainties associated with damage predictions are reflected more completely.

10.1 Introduction

Flood losses have increased worldwide during the last decades (Barredo, 2009; W. Kron et al., 2012; UNISDR, 2011). At the same time, the perception that floods are recurrent natural phenomena and the recognition that both the hazard and the vulnerability ultimately control flood losses have pushed the implementation of risk oriented approaches to flood design and flood risk management (B. Merz et al., 2004; EC, 2007b).

Hence, flood damage assessments are of growing importance since damage has to be estimated in any deliberation of cost-effectiveness of flood mitigation measures, analyses of vulnerability and resilience, land use planning, flood risk mapping, comparative risk analyses and financial appraisal (B. Merz et al., 2010b). For these tasks reliable models to estimate flood damage are an essential component (Dutta et al., 2003; Kang et al., 2005; Thielen et al., 2005).

Flood damaging processes are complex: they are influenced by the interplay of various hydrological, hydraulic and socioeconomic factors, e.g. (Kelman and Spence, 2004; Thielen et al., 2005; Schwarz and Maiwald, 2007; Kreibich and Thielen, 2009). In contrast to this complexity, common damage estimation methods are simple (B. Merz et al., 2010b). Traditional damage models are based on the type and/or use of the element at risk and the water depth as the exclusive determining factors for the estimation of damage (NRC, 2000; Green, 2003). Essentially, this is due to limited data and knowledge about the single and joint effects of other damage influencing factors. Important challenges remain to advance the understanding of the damaging process (Bubeck and Kreibich, 2011), to deepen its theoretical foundations (Wind et al., 1999) and to develop reliable damage models (B. Merz et al., 2013). Flood damage modeling is subject to considerable uncertainty (B. Merz and Thielen, 2005; Moel and Aerts, 2011). This uncertainty stems from various sources including an incomplete knowledge about the damaging process, which crystallizes for instance in generalizations concerning the damage influencing factors and aggregated input data. Further, numerous quantities involved in the damage process are inherently variable as for example the flow velocity or inundation duration.

There are several examples of model developments aimed at a more comprehensive consideration of damage influencing variables. Wind et al. (1999) account for flood warning time and flood experience in flood damage estimation. Zhai et al. (2005) include house type, length of residence and household income in a probabilistic damage model. Thielen et al. (2008b) set up the rule based model FLEMOps+ using inundation depth, building type and quality, contamination and precaution as explanatory variables for flood damage. Elmer et al. (2010) includes flood frequency as an additional variable to FLEMOps+r. B. Merz et al. (2013) derive a multivariate model using tree-based methods considering 28 potential explanatory variables describing the flooding situation, early warning and emergency measures, precaution, building characteristics and the socioeconomic characteristics. Using the same set of candidate variables, K. Vogel et al. (2012) take a data driven Bayesian Network perspective for the development of a probabilistic damage model.

One important step in model development is model validation. The purpose of validation is to evaluate model-generated and real system data, and thus to prove the suitability of the model to describe real system behavior. The level of model validation has

to reflect the intended purpose of the model application (Power, 1993). The validation of a model to predict flood damage has to evaluate the performance of the model not only in replicative applications but more importantly in predictive applications. In this context, replicative applications refer to a comparison of model results to observed damages which have been used to develop and/or fit the model. Predictive applications correspond to estimating damage and comparing model outcomes to damage data which have not been included in the model development.

In general, model validation is scarcely performed in loss modeling. This might be due to limited or missing data: damage data are rarely gathered, repair cost estimates are uncertain and data are not updated systematically (M. Downton and Pielke, 2005). Some damage model validation studies are available: Penning-Rowsell and Green (2000) compared synthetic damage functions of Penning-Rowsell and Chatterton (1977) against post-flood surveys derived by damage adjusters. This validation resulted in a general agreement between surveys and synthetic results. Ding et al. (2008) report a good agreement between damage estimates using the HAZUS -MH "level 2" flood damage model (Scawthorn et al., 2006) and the outcomes of an alternative detailed approach to flood damage estimation, hence the validation is not based on observations in this case. Elmer et al. (2010) successfully tested the model FLEMOps+r against other models using a leave-one-out cross validation method. Similar to Kreibich and Thielen (2008) who used a split sampling technique to analyze the performance of twelve different versions of stage-damage functions and two different versions of rule-based damage models predicting groundwater flood damage, Thielen et al. (2008b) compared damage estimates of FLEMOps+ with observed repair costs for the August 2002 flood for several municipalities in Saxony (Germany) and showed that the model delivers very good damage estimates. However, the model has been developed using damage data for the same flood in the same region. Testing the model predictive capability by applying it to the 1993 flood in a different region in Germany (Baden-Wuerttemberg) showed much larger deviations. Jongman et al. (2012) compared seven damage models on a predictive validation level. They reported considerable differences in model predictive capability across regions. Recently, Cammerer et al. (2013) investigated the transferability of flood damage models to other geographical regions by comparing model results to official damage data. The study confirms that flood damage models which have been derived on data from geographical regions with comparable building and flood event characteristics perform better than those based on more heterogeneous data sets encompassing different regions and floods.

These findings suggest that the predictive capability of flood damage models is rather weak, especially when a temporal and spatial transfer is involved, i.e. the damage models are applied to different flood events and/or in different regions than those which have been used to derive the model. Against this background we investigate, whether and to which extent complex flood damage models are useful to improve the predictive performance in terms of variation, precision and reliability. In this context, model complexity is basically related to the ability of the model to capture and to reproduce complex processes, and thus depends on various factors such as the number and type of explanatory variables included, the interactions between those variables described by the model, and the functional form of those interactions. The functional form is ultimately defined by the model structure and varies from predefined functional relations, e.g. traditional stage-

Table 10.1: Characteristics of flood damage models

Damage model	Knowledge basis for model derivation	Number of expl. variables	Explanatory variables ¹⁾	Input requirements	Outcome	Reference
1	square root function	1	wst	requires complete observations	point estimate for rloss	(Buck and Merkel, 1999)
2	FLEMOps+r	6	wst, bv, bq, con, pre, rp	requires complete observations	point estimate for rloss	(Elmer et al., 2010)
3	RT12	5	wst, bv, age, con, rp	approximate prediction for incomplete observations	point estimate for rloss	(B. Merz et al., 2013)
4	RT4	2	wst, bv	approximate prediction for incomplete observations	point estimate for rloss	(B. Merz et al., 2013)
5	BNd29	6 ²⁾	wst, d, con, v, pre, epre	able to predict with incomplete observations	distribution of rloss	(K. Vogel et al., 2012)
6	BNd11	3 ²⁾	wst, con, pre	able to predict with incomplete observations	distribution of rloss	(K. Vogel et al., 2012)
7	BNe28	10 ²⁾	wst, con, d, v, rp, bq, bv, bt, em, pre	able to predict with incomplete observations	distribution of rloss	-
8	BNe10	8 ²⁾	wst, con, d, rp, bv, bt, bq, pre	able to predict with incomplete observations	distribution of rloss	-

¹⁾ cf. 10.4 for detailed explanations ²⁾ considering the variables on the markov blanket only

damage functions, to probabilistic dependencies derived from observations without any prior assumption concerning the functional form, e.g. Bayesian networks. In view of these conceptual differences a general and consistent measure of model complexity can hardly be defined. Measures such as the Akaike or Bayesian information criterion (AIC or BIC) are of little value in this regard, since they are not consistent across the different model approaches. Therefore, we use the number of explanatory variables (predictors) included in the model as an indicator for model complexity.

To test the hypothesis that increasing complexity of flood damage models improves the predictive capability in a spatial and temporal transfer context, we apply eight flood damage models for three flood events in two different regions in Germany. This enables us to distinguish between different model usages, namely local, cross regional and/or temporal transfer applications. We focus on the estimation of direct damage to residential buildings. Flood damage estimation is carried out on the scale of the individual buildings in terms of relative damage (*rloss*), whereas relative building damage is defined as the ratio of the actual building loss and its total replacement value (Elmer et al., 2010). The predictive performance of the models is assessed by comparing modelled to observed relative building damage.

10.2 Set up of validation exercise

The damage models compared are a stage-damage function, using only water depth as explanatory variable, FLEMOps+r, a rule based model using six variables, and data mining approaches, namely regression trees and Bayesian networks, using up to 28 explanatory variables. Table 10.1 summarizes key qualities of these damage models. A detailed description will be given in section 10.3.

The comparison of model performance is based on empirical damage data. Flood damage records are available from computer aided telephone interviews that were com-

Table 10.2: Usage of data sub-samples from different flood events and river basins

sub-sample	year	location	interviews completed	rloss given	usage
Elbe 2002 id	2002	Elbe	850	426	model derivation
Elbe 2002 pr	2002	Elbe	398	235	local validation
Danube 2002	2002	Danube	449	286	cross regional validation
Danube 2005	2005	Danube	275	116	cross regional and temporal validation
Elbe 2006	2006	Elbe	126	46	temporal validation

piled after the floods in 2002, 2005 and 2006, respectively, in the Elbe and Danube catchments in Germany (Thieken et al., 2007; Kreibich and Thieken, 2009; Kreibich et al., 2011a). The considered flood events and data sets are portrayed in sections 10.2.1 and 10.2.2. The location of the communities in which interviews have been undertaken is shown in Figure 10.1. For the most part, varying localities were affected by the different flood events except for some communities mainly in the region of Dresden (Elbe catchment).

This data base is split up according to different floods (2002, 2005 and 2006) and to different regions (Elbe and Danube catchments), see Table 10.2. Furthermore, the sub-sample for the 2002 flood in the Elbe catchment is partitioned randomly into two parts: two third of the data set is used to derive the damage models (Elbe 2002 id), the remaining third (Elbe 2002 pr) is used for local validation.

The derivation of the models includes all steps to set up the model for the estimation of *rloss*. Depending on the model approach this involves the selection of the model structure (i.e. functional forms and functional relations), the estimation of model parameters, scaling factors, parameter distributions and their discretization.

Next, the models are applied to predict *rloss* for the flood events (Elbe 2002 pr, Danube 2002, Danube 2005 and Elbe 2006). For each event, the models are validated by comparing model results to observed damage data using the criteria detailed in section 10.4. The sub-division of damage data according to different events and regions allows for the evaluation of model predictive capability in spatial and temporal transfer applications.

In view of the uncertainty present in flood damage modeling, we are particularly addressing the uncertainty associated with the observations of the explanatory variables, which have been acquired via surveys with flood affected private households, e.g. uncertainties due to imprecise observations, bad memory, reluctant answers and misunderstandings. To ensure the robustness of the results against disturbances induced by observation uncertainty, we explicitly consider this uncertainty. In this way, we substantiate that the differences in the predictive performance of the various damage models are actually a consequence of different model complexity and not the outcome of uncertainties in the underlying database. The procedure to consider observation uncertainty is outlined in section 10.3.

10.2.1 Flood events

The extreme flood in central Europe in August 2002 was caused by intense long-lasting precipitation covering large areas in Austria, Slovakia, the Czech-Republic and Germany. As a result, flash floods were observed in the headwaters of the Elbe tributaries in the

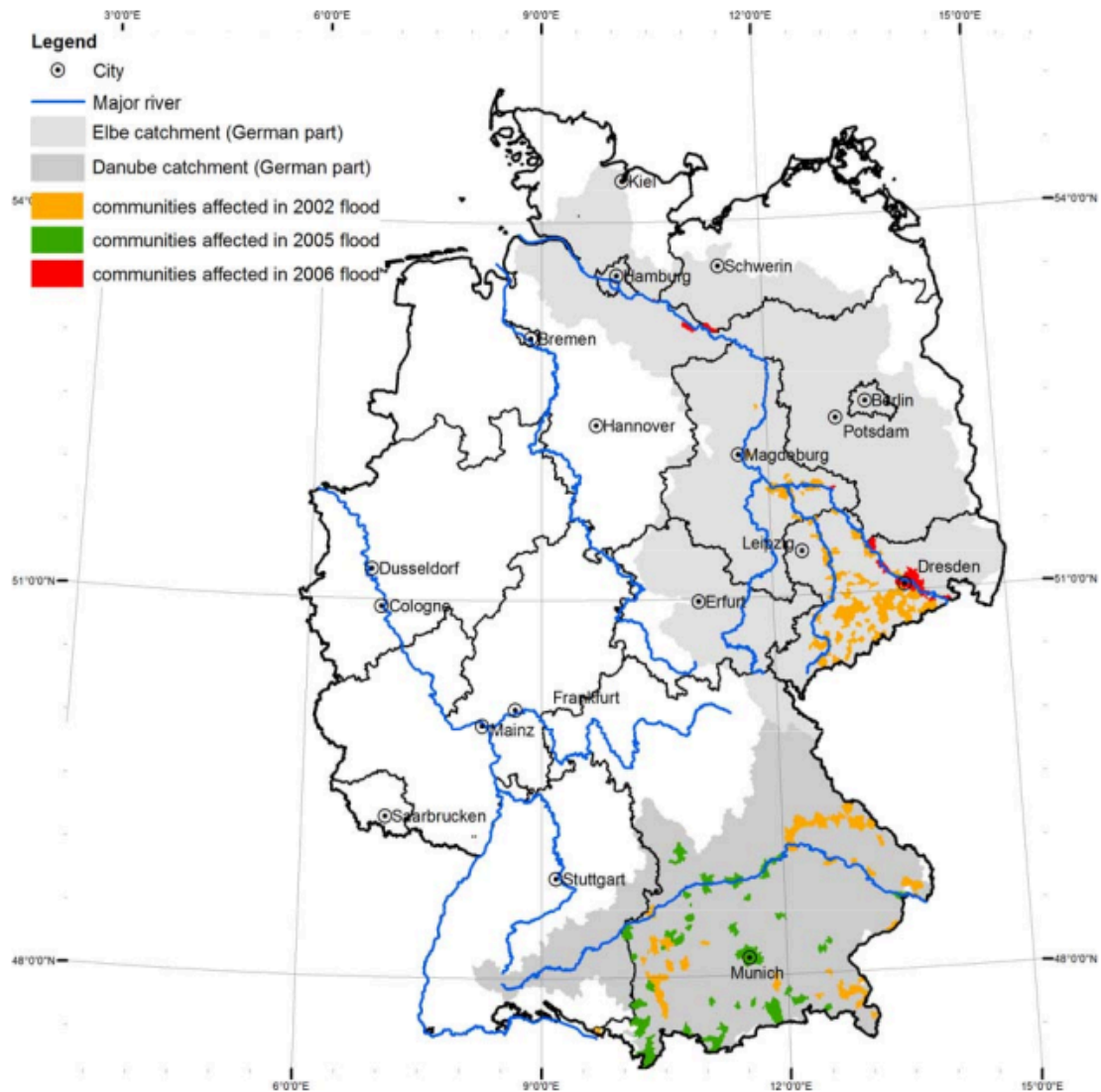


Figure 10.1: Location of communities in which interviews had been undertaken after the 2002, 2005 and 2006 flood events in the Elbe and Danube catchments (Germany), data sources: rivers and administrative borders: DLM1000 of (GEODATENZENTRUM, 2009); cities: Esri, DeLorme Publishing Company, inc.; catchment areas: CCM2 data of JRC (Vogt, 2007)

Ore Mountains as well as in some alpine tributaries of the Danube and in the Bohemian Forest. Further downstream, floods came along with unprecedented water levels, flooding of polders and vast inundated areas as a result of levee overtopping and numerous levee breaches, in particular in the Elbe catchment. Twenty two people were killed in Germany during this flood. Infrastructures and buildings suffered substantial damage. As shown in Figure 10.1, mainly the tributaries in the Ore Mountains (Saxony, Elbe catchment), the river Regen in Bavaria and several southern tributaries of the Danube were affected. Total damage amounted to EUR 9.9 b in the German part of the Elbe catchment and EUR 0.2 b in the German part of the Danube catchment (IKSE, 2004).

In August 2005 another considerable flood affected the Alpine region, particularly Switzerland but also the German part of the Danube catchment. The alpine foothills were affected by flash floods characterized by a rapid increase of discharges and water levels. Inundations occurred along the Danube and its southern tributaries being the main areas reporting damage in Germany (see Figure 10.1). Flood protection measures and effective operation of dams reduced the flood impact. The total economic damage is estimated at about EUR 190 M (LfU, 2006).

In the Elbe catchment another flood event followed in April 2006 which was caused by the combination of widespread heavy rainfall and snowmelt in the upper catchment. In Dresden the maximum water level was clearly below the 2002 flood peak. In contrast, the flood situation downstream of the Havel confluence was comparable or even worse than during the 2002 flood. Several towns in the Saxon Elbe valley and in the lower reaches of the Elbe were inundated (Figure 10.1). Several hundreds of people were evacuated. The resulting damage in Germany was estimated to be EUR 75 M (Munich Re, 2009).

10.2.2 Empirical damage data collection

After the floods of 2002, 2005 and 2006 in the Elbe and Danube catchments in Germany damage data have been collected from affected households via computer aided telephone interviews. In total, data from 2098 interviews are available, see Table 10.2. The survey for the 2002 flood resulted in 1248 completed interviews in the Elbe catchment and 449 completed interviews in the Danube catchment. The survey for the 2005 flood in the Danube basin provided 275 interviews. For the 2006 flood in the Elbe catchment 126 interviews were completed. However, the loss ratio for the damaged buildings (*rloss*) could not be provided for all interviews. As *rloss* is the variable to be predicted by the model, the data set is limited to 1109 damage cases.

The households interviewed were randomly sampled from lists which have been compiled of all streets affected by flooding with the help of information from local authorities, flood reports or press releases as well as with the help of flood footprints derived from satellite radar data (DLR, Centre for Satellite Based Crisis information, ¹). The raw data were supplemented by estimates of return period, building values, loss ratio, i.e. the relation between the actual building damage and replacement costs, and indicators for flow velocity, contamination, flood warning, emergency measures, precautionary measures, flood experience and socio-economic variables (Thieken et al., 2005; Elmer et al., 2010)

From this extensive data set 28 candidate variables were preselected to be used in a modeling context for predicting the loss ratio of residential buildings (*rloss*), see 10.3.

¹<http://www.zki.dlr.de/>

These candidate variables were selected according to experiences from previous analyses (Thieken et al., 2005; B. Merz et al., 2013) : five variables are related to the hydrological and hydraulic aspects of the flooding situation at the affected building, ten variables are related to damage reduction, particularly to early warning and emergency measures undertaken, as well as to the state of precaution of the household, and 13 variables are related to the residential building characteristics and the socioeconomic status of the household.

10.2.3 Consideration of observation uncertainty

The collection of empirical damage data via computer aided telephone interviews applied cross checks of answers during the interviews to avoid contradictions and to improve data quality. The information retrieved from the interviews is considered to be of comparatively high quality and to be free of a strategic response bias (Kreibich et al., 2010; Thieken et al., 2007). This was confirmed via a comparison of the damage data collected after the 2002 flood with official damage data in the federal state of Saxony (Thieken et al., 2005). Nonetheless, to ensure the robustness of the findings against disturbances resulting from observation uncertainty, we assume that the observations, i.e. the interview responses, are uncertain. Uncertainty is understood as the deviation of the interview responses to the real situation. For the consideration of the observation uncertainty within the evaluation of the predictive performance we need to discern the fundamentally different modelling approaches considered in this study. Bayesian Networks are probabilistic models which as a basic principle treat all quantities involved as random variables, and do not distinguish between explanatory and response variables. This enables to capture the joint probability distribution of all variables. Consequently, the Bayesian Network models the probabilistic dependency among the variables. Thereby, it is assumed that observations are uncertain. On that note, the Bayesian Network inherently captures the uncertainty that is related to the observations of the individual variables and thus implicitly includes this uncertainty in the joint probability distribution modelled. Accordingly, the joint probability distribution reflects both the probabilistic dependence of the variables and the observation uncertainty associated with the variables. An explicit consideration of observation uncertainty is not indicated since it would be double accounted. However, Bayesian Networks do not allow to distinguish between observation uncertainty and other uncertainty sources uncertainty, i.e. it cannot be determined to which extent the uncertainty in the probabilistic dependence is actually due to uncertain observations.

In contrast, stage-damage functions, FLEMOPs+r, and regression trees assume a deterministic relation between explanatory and predicted variables, providing point estimates for specific observations of explanatory variables. For the derivation of these models methods of regression analysis are applied. Usually in regression analysis, the observations are assumed to be error free. In this framework, a feasible approach to account for the observation uncertainty is to explicitly describe this uncertainty and to feed it into the analysis (Saltelli et al., 2000). This includes the following steps: (i) define uncertainty models which quantify the uncertainty associated with the observations of each explanatory variable, (ii) generate a large number of variations of the observed data set Elbe 2002 id by random sampling from the different uncertainty models using Monte

Table 10.3: Description of candidate variables for flood damage modeling

abbr.	Variable	Scale and range	Uncertainty model	
flooding situation				
1	wst	Water depth*	c: 248 cm below ground to 670 cm above ground	~N(m,sd)
2	d	Inundation duration	c: 1 to 1,440 h	~N(m,sd)
3	v	Flow velocity indicator	o: 0=still to 3=high velocity	C(Px)
4	con	Contamination indicator	o: 0=no contamination to 6=heavy contamination	C(Px)
5	rp	Return period	c: 1 to 848 yrs	C(Px)
early warning and emergency measures				
6	wt	Early warning lead time	c: 0 to 336 h	~N(m,sd)
7	wq	Quality of warning	o: 1=receiver of warning knew exactly what to do to 6=receiver of warning had no idea what to do	C(Px)
8	ws	Indicator of flood warning source	o: 0=no warning to 4=official warning through authorities	C(Px)
9	wi	Indicator of flood warning information	o: 0=no helpful information to 11=many helpful information	C(Px)
10	wte	Lead time period elapsed without using it for emergency measures	c: 0 to 335 h	~N(m,sd)
11	em	Emergency measures indicator	o: 1=no measures undertaken to 17=many measures undertaken	C(Px)
precaution				
12	pre	Precautionary measures indicator	o: 0=no measures undertaken to 38=many, efficient measures undertaken	C(Px)
13	epre	Perception of efficiency of private precaution	o: 1=very efficient to 6=not efficient at all	C(Px)
14	fe	Flood experience indicator	o: 0=no experience to 9=recent flood experience	C(Px)
15	kh	Knowledge of flood hazard	n (yes / no)	C(Px)
building characteristics				
16	bt	Building type	n (1=multifamily house, 2= semi-detached house, 3=one-family house)	C(Px)
17	nfb	Number of flats in building	c: 1 to 45 flats	~N(m,sd)
18	fsb	Floor space of building	c: 45 to 18,000 m ²	~N(m,sd)
19	bq	Building quality	o: 1=very good to 6=very bad	C(Px)
20	bv	Building value	c: EUR 92,244 to EUR 3,718,677	~N(m,sd)
socioeconomic status				
21	age	Age of the interviewed person	c: 16 to 95 yrs	-
22	hs	Household size, i.e. number of persons	c: 1 to 20 people	-
23	chi	Number of children (<14 years) in household	c: 0 to 6	-
24	eld	Number of elderly people (>65 years) in household	c: 0 to 4	-
25	own	Ownership structure	n (1=tenant; 2=owner of flat; 3=owner of building)	-
26	inc	Monthly net income in classes	o: 11=below EUR 500 to 16= EUR 3,000 and more	C(Px)
27	socp	Socioeconomic status according to Plapp (2003)	o: 3=very low socioeconomic status to 13=very high socioeconomic status	C(Px)
28	socs	Socioeconomic status according to Schnell et al (1999)	o: 9=very low socioeconomic status to 60=very high socioeconomic status	C(Px)
flood damage				
29	rloss	loss ratio of residential building	c: 0 = no damage to 1 = total damage	~N(m,sd)

c: continuous, o: ordinal, n: nominal * the depth of the basement of a building is assumed to be 250 cm below ground level

Carlo techniques, (iii) derive a sample of models using each realization of the data set variations generated in step ii, (iv) predict flood damage for the other data sub-samples (Elbe 2002 pr, Danube 2002, Danube 2005 and Elbe 2006) using each sample member of the models derived in step iii. As a result, for each damage model and data sub-sample we obtain a distribution of model predictions which represents the predictive uncertainty of the models given the assumed uncertainty in data observations.

The definition of uncertainty models for the 28 explanatory variables is difficult, since knowledge about the degree and characteristics of observation uncertainty is hardly available. As an exception, the water depths (*wst*) obtained from the telephone interviews after the Elbe 2002 flood have been compared with a sample of water marks at 409 buildings in the community of Eilenburg (Saxony) (Poser and Dransch, 2010). A bias of 0.37 m and a root mean square error of 0.76 m are reported indicating the order of magnitude of the deviation (in this case ca. 30%), and thus the degree of uncertainty concerning *wst* based on telephone interviews. However, the results from this localized comparison can hardly be generalized.

In this light, we need to resort to several assumptions concerning the degree and the characteristics of observation uncertainty. Firstly, the explanatory variables are distinguished concerning their underlying scale: continuous, ordinal or nominal scale. For the continuous variables (e.g. *wst*, *d*) we describe the uncertainty in the measurement process using an uncertainty model which adds Gaussian Noise to the observed values. In this model the mean (*m*) defines the systematic deviation from the unobservable true value and the standard deviation (*sd*) controls the magnitude of the deviations. We parameterize the uncertainty model in such a way that $m=0$ and *sd* corresponds to a constant percentage of the individual observations.

The variables based on ordinal or nominal scales describe differences in the observations using a spectrum of values (e.g. *con*: 0 no contamination, 6 = heavy contamination) or qualitative classifications (e.g. *kh*: yes, no). Hence, for these variables observation uncertainty refers to the attribution to a specific category (*C*). We describe this uncertainty by setting a probability level (*Px*) for an erroneous categorization of an observation. When an observation is wrongly classified, the observation is allocated to a wrong category assuming uniform probability for all possible categories. For the variables *age*, *hs*, *chi*, *eld*, and *own* we assume that the uncertainty of the measurement process is negligible. The uncertainty models for Gaussian Noise ($\sim N(m, sd)$) and categorical uncertainty ($C(Px)$) applied to the explanatory variables are listed in Table 10.3.

As there is hardly any evidence to quantitatively frame the observation uncertainty and the cross correlation structure of the explanatory variables, we investigate the potential implications for the predictive performance of the deterministic damage models in terms of different uncertainty scenarios comprising (i) no uncertainty, (ii) small uncertainty and (iii) large uncertainty. Within these scenarios we assume that the observations of the different variables are independent from each other. Further we control the degree of uncertainty by varying both the magnitude of the standard deviation for continuous variables and the probability level for erroneous observations for ordinal and nominal variables. The first scenario (no uncertainty) corresponds to a deterministic regression approach, i.e. error free input data which yields point estimates for *rloss*. Within the small uncertainty scenario we set the standard deviation to 5% of the observed value and the probability level for an observation to be erroneous to 5%. Large uncertainty

corresponds to a standard deviation of 20% of the observed value and a probability level for erroneous observations of 20%. For the latter two uncertainty scenarios we generate a sample size of 5,000 realizations for each observation of explanatory variables. This sample size has been checked for stable convergence using the median and the quantile range at the 90% level as diagnostics. Note we have also conducted the analyses for an additional scenario of ‘very large uncertainty’ defined by a standard deviation of 50% and a probability level for erroneous observations of 50%. The outcomes for this scenario are very similar to the ‘large uncertainty’ scenario and, therefore, are not discussed in detail.

10.2.4 Evaluation criteria

The predictive capability of the various damage models is evaluated with regard to precision, variation and reliability. For the scenarios of small and large uncertainty we use the median (Q_{50}) as a summary statistic of the distribution of model predictions. The Bayesian networks naturally provide the conditional probabilities of the predicted variable $rloss$ and thus also capture the prediction uncertainty. For the model comparison also use the median of $rloss$ distribution.

The model precision is evaluated in terms of the mean bias (mbe) and the mean absolute error (mae) as listed in Table 10.4. Both criteria evaluate the model residuals, i.e. the differences between predictions (Q_{50}) and observations (O) of $rloss$. The mean bias error (mbe) provides information about a systematic deviation, i.e. an average over- or under-prediction. The mean absolute error (mae) describes the average magnitude of the residuals and allows for a dimensioned comparison of average model precision (Willmott and Matsuura, 2005).

The variation of the model predictions is quantified using the quantile-range at the 90 percent level (QR_{90}), see Table 10.4. A smaller value for QR_{90} corresponds to a smaller spread in the predictions, i.e. the model predictions are less uncertain.

Concerning the model reliability we evaluate whether the predictive distribution actually covers the observed values of $rloss$. For this purpose we compute the hit-rate (HR) which represents the proportion of the number of observations that fall within the 95-quantile and 5-quantile predictive interval and the total number of observations available, see Table 10.4. The 95-quantile to 5-quantile range corresponds to a nominal coverage of 0.9, and thus a $HR = 0.9$ indicates that the coverage of model predictions is equal to the nominal coverage representing a perfect reliability of model prediction on this level (Thordarson et al., 2012).

We derive the models and calculate the model predictions for the log-transformed variable $rloss$ ($\log-rloss$). This transformation reduces the influence of the few very high loss ratios present in the data sample.

10.3 Damage models

We compare eight flood damage models of different complexity, see Table 10.1. In particular, we examine a ‘traditional’ depth-damage function based on a root function (Buck and Merkel, 1999), the rule based model FLEMOPs+r (Elmer et al., 2010), two variants

Table 10.4: Model evaluation criteria

Criterion	LB	UB	OPT
$MBE = \frac{1}{n} \sum_{i=1}^n (Q_{50_i} - O_i)$	-inf	inf	0
$MAE = \frac{1}{n} \sum_{i=1}^n Q_{50_i} - O_i $	0	inf	0
$QR_{90} = \frac{1}{n} \sum_{i=1}^n (Q_{95_i} - Q_{05_i})$	0	inf	0
$HR = \frac{1}{n} \sum_{i=1}^n h_i ; h_i = \{ 1, \text{ if } O_i \in [Q_{95_i}, Q_{5_i}]; 0, \text{ otherwise} \}$	0	1	0.9*

LB: lower bound, UB: upper bound, OPT: perfect prediction

* depending on the nominal coverage rate applied, e.g. 0.9 for the 95-to 5-quantile range

of the regression tree model approach using different numbers of explanatory variables proposed by B. Merz et al. (2013), and two variants of Bayesian network approaches: first, completely data based (K. Vogel et al., 2012) and, second, using both expert knowledge and data to derive the network structure. Further, the Bayesian network approach is applied taking into consideration two different numbers of explanatory variables.

10.3.1 Depth-damage function

Damage functions are a central concept of damage estimation. They relate the damage for the respective element at risk to characteristics of the inundation (B. Merz et al., 2010b). Most often, damage is estimated for the type or use of the element at risk and the inundation depth (Wind et al., 1999; NRC, 2000). Such depth-damage curves were for the first time proposed in the USA (White, 1945) and, since then have been applied in numerous models and case studies. Depth-damage functions remain the standard approach to assessing urban flood damage (D. Smith, 1994; B. Merz et al., 2010b). For Germany, stage-damage curves as separate square-root functions for water depths in the basement and above ground floor were suggested by (Buck and Merkel, 1999).

In this study we apply a combination of root functions to predict $rloss$ in the basement and in the building above ground level separately. The model structure is defined as given in Eq. 10.1 for the basement and Eq. 10.2 above the ground-level:

$$rloss = a_b + b_b \sqrt{w_b} ; w_b = w + 250 \{w|w < 0\} \quad (10.1)$$

$$rloss = a + b \sqrt{w} \{w|w \geq 0\} \quad (10.2)$$

With w (water depth in relation to the ground level), w_b (water depth above basement level) and a, b, a_b, b_b parameters of the respective root functions. A general basement height of 250 cm is assumed.

The derivation of the model consists in estimating the parameters a, b and a_b, b_b . This is done in a regression approach by minimizing the sum of squared residuals, i.e. the differences between modeled and observed damage ($rloss$) in the sub-sample Elbe 2002 id. These best estimates of model parameters are used to predict flood damage ($rloss$) for observed water levels during the other events.

10.3.2 FLEMOps+r

The Flood Loss Estimation MOdel for the private sector (FLEMOps) uses a rule based multi-factorial approach to estimate direct tangible damage to residential buildings. It has been developed at the German Research Centre for Geosciences, primarily for scientific flood risk analyses from the local to national scale, e.g. (Apel et al., 2009; Vorogushyn et al., 2012).

Since the initial version proposed by (Thieken et al., 2008b), the model has undergone several enhancements including an increasing number of explanatory variables. We apply the most recent version FLEMOps+r (Elmer et al., 2010). This version incorporates six explanatory variables. Flood damage is calculated using five different classes of water depth, three classes of contamination, and three classes of flood frequency, three individual building types, two classes of building quality and three classes of private precaution. The class limits for inundation depth, building types and building quality have been defined in a way to appropriately reflect the range and variability included in available observations and other basic data as defined in Büchele et al. (2006) and Thieken et al. (2008b).

The derivation of the model within this study comprises two steps. Firstly, for each class combination of inundation depth, building types and building quality mean damage values are determined from observed damage records (Elbe 2002 id). Secondly, a set of scaling factors are derived for each class combination to reflect the impact of contamination, precaution and flood frequency. Again, these scaling factors are derived from observed damage records (Elbe 2002 id).

10.3.3 Regression Trees

Following the approach by B. Merz et al. (2013), a regression tree has been grown based on 28 candidate explanatory variables (Tabel 10.3) within the sub-sample Elbe 2002 id. For the scenario of 'no uncertainty' this results in a tree with 12 terminal nodes (Figure 10.2) considering five variables. The most important variable is water depth, followed by building value, age, contamination and return period.

Using regression trees, overfitting needs careful attention. Hence, the large tree RT is cut back to obtain a simpler tree, which however, should have a predictive error comparable to the most accurate large tree. For this purpose, branches which give less improvement in error cost have been pruned from RT. RT_p is the tree which results in the lowest cost. For the 'no uncertainty' scenario it consists of four leaves and considers only water depth and building value to predict r_{loss} . The trees derived from uncertain observations within the frame of the 'small uncertainty' and 'large uncertainty' scenarios differ from this solution, since the sub-division of the explanatory variable space strives for the minimization of the error for each realization of the data set variations.

Tree-based models are a simple means to multi-variate damage modeling, since they permit inclusion of both continuous and categorical variables and they allow for nonlinearities and predictor interactions (B. Merz et al., 2013). Regression trees can handle incomplete data. In this case predictions are made by considering only the leaves that can be reached given the available data.

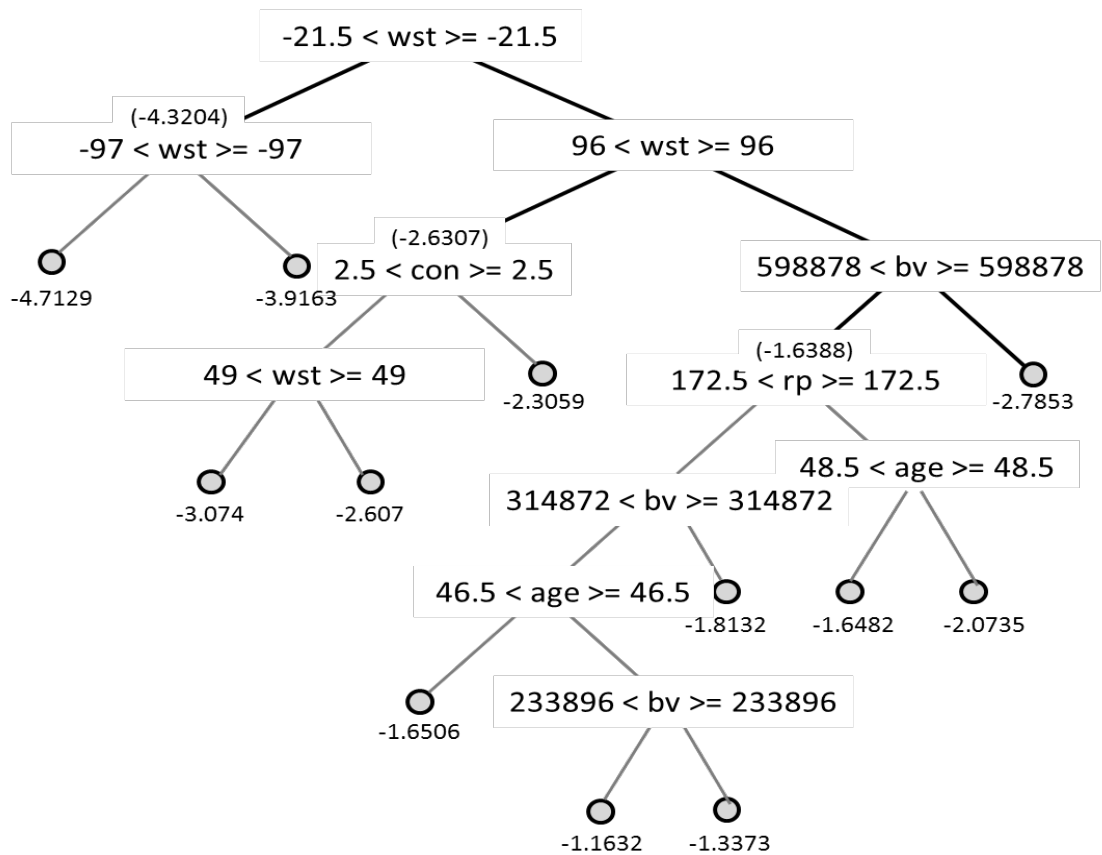


Figure 10.2: Regression tree RT with 12 leaves considering five variables for estimating $\log(\text{rloss})$ and pruned regression tree (RT_p, indicated by bold joins) with 4 leaves considering two variables for estimating $\log(\text{rloss})$ grown within the 'no uncertainty' scenario

10.3.4 Data based Bayesian networks

The Bayesian network approach relies on a probabilistic formalism which aims to describe the joint distribution of all variables involved in the system. The number of parameters that is needed to describe the distribution is reduced by decomposing the joint probability into a product of conditional probabilities according to a directed acyclic graph (DAG) capturing probabilistic independencies between the variables. The joint probability of a Bayesian network is given in Eq. 10.3.

$$P(A_1, \dots, A_n) = \prod_{i=1}^n P(A_i | \text{parents}(A_i)) \quad (10.3)$$

Where A_i are the variables and $\text{parents}(A_i)$ denotes the set of parent nodes of the node A_i as defined by the DAG.

Using a completely data-driven approach the graph structure as well as the parameters of the conditional distributions can be learned from data, such that the learning algorithm respects various model complexity issues relating to sample size, overfitting, etc. For a detailed description of the learning procedure we refer to K. Vogel et al. (2012) and K. Vogel et al. (2013).

In contrast to other models the Bayesian network allows use of all 850 records of the Elbe 2002 id sub-sample for the model derivation, thus exploiting information present in partially observed records. This also includes those cases where $rloss$ is unobserved. A Bayesian Network treats all quantities involved as random variables, and does not distinguish between explanatory and response variables. This enables to capture the joint probability distribution of all variables and to infer in any direction as new evidence, i.e. observations, become available. The network learned for 29 variables (including $rloss$) is shown in Figure 10.3 (left). Its graph structure gives insight into the (in-)dependency structure of the involved variables (note that this is different from causality).

The gray shaded variables in Figure 10.3 form the so called Markov Blanket of $rloss$, which is the minimal set of variables having influence on $rloss$. This means that in this specific case of Bayesian network learning the estimation of $rloss$ depends only on six variables: water depth (wst), contamination indicator (con), inundation duration (d), flow velocity indicator (v), precautionary measure indicator (pre) and perception of efficiency of private precaution ($epre$), and that all other variables can be ignored provided that the Markov Blanket is fully observed. However, if observations of some of these variables are unknown or missing, observations on variables from outside the Markov Blanket provide indirect knowledge “flowing” towards $rloss$, thus helping to improve the prediction thereof.

In Bayesian network learning, in general, we strive to approximate the joint distribution of all variables. Hence, we consider all variables equally important. However, in this study we are particularly interested in the variable $rloss$. Therefore, in another attempt of learning a Bayesian network we restrict attention to those variable assumed to be highly relevant for the prediction of this target. The selection of these variables is based on available knowledge and experience from previous studies, e.g. (Thieken et al., 2005; B. Merz et al., 2010b). For $rloss$ this amounts to a subset of ten variables from the original set of 28 explanatory variables. The resulting network is shown in Figure 10.3 (right) where the Markov Blanket of $rloss$ shows that only contamination (con), water depth (wst) and

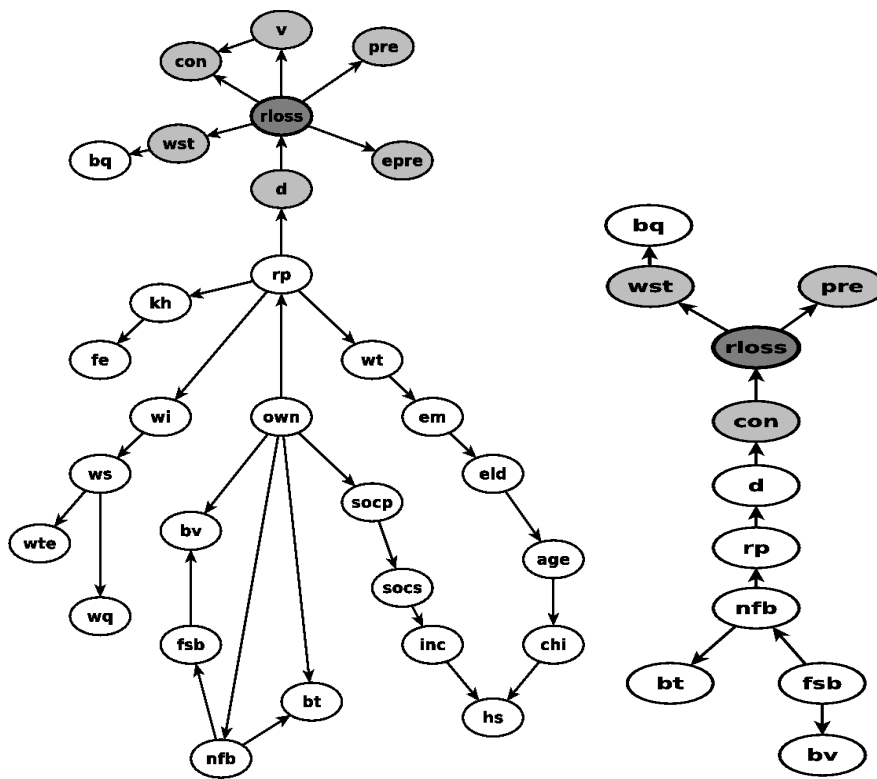


Figure 10.3: DAG of data based Bayesian network for 29 explanatory variables including rloss (left), data based Bayesian network for 11 explanatory variables including rloss (right)

precaution (*pre*) have direct predictive relevance.

Predictions of any of the variables represented in the Bayesian networks are achieved by inferring the respective conditional probabilities given the observations of other variables. For instance, the prediction of *rloss* given observations of water depth, return period and precautionary measures corresponds to the operation of forward inference and is accomplished by marginalization of the conditional probability for *rloss*. In this context, we stress the fundamental property of Bayesian networks providing conditional probabilities of the target variable and thus inherently capturing the uncertainty of the prediction. This is in contrast to the other models examined, which, without the additional efforts for uncertainty analysis, offer only a single deterministic point estimate.

10.3.5 Expert Bayesian networks

The construction of a Bayesian network can also incorporate domain or expert knowledge. This knowledge may be included in the definition of the network structure, the direction of the arcs and the distribution of the parameters. This is of interest because a totally data-driven approach for Bayesian network learning can result in models that capture unwanted artefacts of the data. Especially, when the data set used for model derivation is sparse, those artefacts may overrule physical/causal relationships. The inclusion of expert knowledge into Bayesian network construction might reduce the effect of data anomalies.

For the construction of expert Bayesian networks we define the graph skeleton based on domain knowledge and learn only the arc directions, the discretization of the ordinal variables and the parameters of the conditional probabilities from the data.

For the definition of the network skeleton we adopt a causal mapping approach as proposed by Nadkarni and Shenoy (2001). This procedure involves in a first step the derivation of a causal map for the variables of interest. The causal map depicts the cause-effect relations among these variables according to expert knowledge in terms of a directed graph (Nadkarni and Shenoy, 2001). Next, the causal map is modified using the idiomatic introduced by Fenton and Neil (2012) in order to construct a Bayesian causal map which satisfies the requirement of conditional independence among variables and acyclic structure of the graph in order to represent a proper Bayesian network.

The causal map has been derived by using an adjacency matrix which is defined by the 29 candidate variables (including *rloss*) listed in . This matrix was independently completed by three flood damage experts. In this matrix the experts indicated whether there is a causal relation between any two variables and defined the direction of these relations. On this basis a causal map was derived as a directed graph by superimposing the relations identified from the different experts.

Next, within a discussion among the experts any inconsistency in this draft directed graph was reviewed and modified to be compatible with a Bayesian network. This is to ensure that the presence of a link between variables represents dependence and that the lack of a link represents independence between these variables. Further, the presence of direct and indirect relations between subsets of variables was scrutinized and any circular relations were eliminated.

Two alternative versions of expert Bayesian networks are derived: first, accounting for the complete set of candidate explanatory variables and second, for a sub-set of eleven

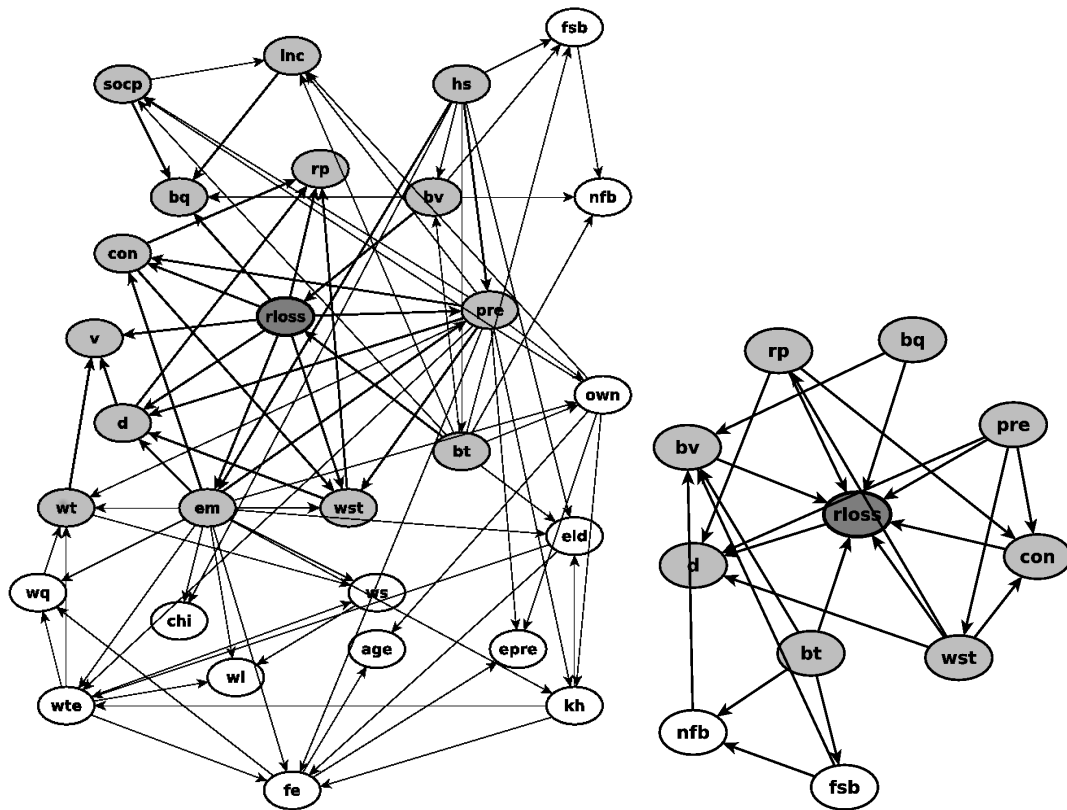


Figure 10.4: DAG of expert Bayesian network for 28 explanatory variables (left), expert Bayesian network for 10 explanatory variables (right) constructed with the specific goal to predict rloss

of these variables which have been identified to be most informative to predict *rloss* on the basis of existing knowledge and damage modeling experience (Thieken et al., 2005; Kreibich and Thieken, 2009; B. Merz et al., 2010b; Elmer et al., 2010). The resulting networks are shown in Figure 10.4.

The definition of the network skeleton based on expert knowledge is a non-trivial task. Wrong independence assumptions cannot be corrected by the data and should be avoided. A dense network structure leads to a large number of combinations in the node probability tables. The automatic regularization of network complexity which is ensured in a data driven approach by means of a structure fitness score (Riggelsen, 2008; K. Vogel et al., 2013) is thereby impaired by the network structure imposed. Therefore, the Markov Blanket of *rloss* in an expert Bayesian network will be much larger than in a fully data-driven well-regularized learned Bayesian network. This can be realized from the comparison of the data based DAGs shown in Figure 10.3 and the expert DAGs shown in Figure 10.4.

Predictions within the expert Bayesian network follow the same procedure as within the data based networks.

10.4 Results and discussion

We test the hypothesis that increasing complexity improves the predictive capability of flood damage models by comparing the performance of the different models for the data sub-samples defined in Table 10.2 with regard to precision, variation and reliability.

In the first instance, we examine the scores for the evaluation criteria *mbe* and *mae* within the 'no uncertainty' scenario. The scores which are achieved by the models for each sub-sample are compiled in Table 10.5 with the best score for each criterion marked bold. Obviously, different models perform best with regard to *mbe* or *mae* within the different sub-samples. Noticeably, the magnitude of *mbe* and *mae* increases from the Elbe 2002 id sub-sample to the Elbe 2002 pr, Danube 2002, Elbe 2006 and Danube 2005 sub-samples reflecting the increasing difficulty to predict *rloss* in spatial and temporal transfer applications. At the same time the differences between the *mae* and *mbe* scores achieved by the different model approaches become more pronounced. Whereas the variations of model performance scores are small for the Elbe 2002 id sub-sample, they are clearly larger for cross regional and temporal validation exercises based on the sub-samples Danube 2002, Elbe 2006 and Danube 2005. This suggests that the model approach makes a difference in terms of the predictive precision, in particular in a spatial and temporal transfer context; but is there a relation between model predictive capability and model complexity?

To investigate this question we use the Euclidean Distance (*ED*) of *mbe* and *mae* to the point of optimum model performance as a multi-criteria measure of model predictive precision. *ED* values for the different models and data sub-samples are listed in Table 10.5. We relate *ED* to the number of explanatory variables included by the different models (cf. Table 10.1). For each model we calculate the average *ED* out of the results obtained for the sub-samples Danube 2002, Danube 2005 and Elbe 2006 which involve a temporal or spatial transfer. The results are plotted in Figure 10.5 against the number of explanatory variables. This graph illustrates a trade-off between model complexity and predictive performance. However, this relationship is not monotonic, but interfered by differences in the performance of different model approaches. In this regard, for instance the data based Bayesian Networks utilize fewer explanatory variables to predict *rloss* than the expert Bayesian Networks but still, on average, provide predictions with higher precision. Comparing alternatives of different complexity within similar modeling approaches, e.g. the pruned regression tree and the complete regression tree, the data based or expert Bayesian Networks based on a reduced number of explanatory variables and the complete set of variables, we recognize that the more complex variant performs better in any case.

However, the results obtained for the deterministic models are based on the assumption that the explanatory variables are observed without uncertainty. The implications of potential observations uncertainty on the predictive performance are shown in Figure 10.6. Essentially, two effects are apparent. First, the noise added to the observations used for model derivation propagates to the model predictions and impairs the precision of the models. Unsurprisingly, the more variables are used to predict *rloss*, the larger the decline of predictive precision, since with additional variables additional sources of uncertainty take effect. Accordingly, RTp and the sdf model achieve best predictive

Table 10.5: Precision of damage model predictions for no uncertainty scenario

sub-sample	criterion	model							
		sdf	Flemops+r	RT	RT	BNe10	BNe28	BNd11	BNd29
model derivation									
Elbe 2002id	mbe	0.00	0.02	0.00	0.00	0.04	0.07	0.08	0.07
	mae	0.76	0.77	0.72	0.67	0.60	0.69	0.73	0.71
	ED	0.76	0.77	0.72	0.67	0.60	0.69	0.73	0.71
local validation									
Elbe 2002pr	mbe	0.18	0.05	0.15	0.08	0.03	0.05	0.18	0.03
	mae	0.96	0.90	0.94	0.95	1.05	1.00	0.91	0.93
	ED	0.98	0.90	0.95	0.95	1.05	1.00	0.93	0.93
cross regional and temporal validation									
Danube 2002	mbe	0.48	0.72	0.77	0.65	0.75	0.77	0.76	0.51
	mae	1.29	1.29	1.26	1.21	1.47	1.36	1.23	1.19
	ED	1.38	1.48	1.48	1.37	1.65	1.56	1.45	1.29
Danube 2005	mbe	0.96	1.03	1.08	0.99	0.75	0.77	0.91	0.42
	mae	1.71	1.69	1.51	1.51	1.70	1.60	1.55	1.54
	ED	1.96	1.98	1.86	1.81	1.86	1.78	1.80	1.60
Elbe 2006	mbe	1.13	0.92	1.26	1.20	0.10	0.57	0.79	0.55
	mae	1.75	1.55	1.55	1.49	1.54	1.35	1.31	1.35
	ED	2.08	1.80	2.00	1.91	1.54	1.47	1.53	1.46

ED: Euclidian distance to the perfect prediction in the two-dimensional space defined by mbe and mae.
Best scores for each criterion and data sub-sample are marked with bold numbers

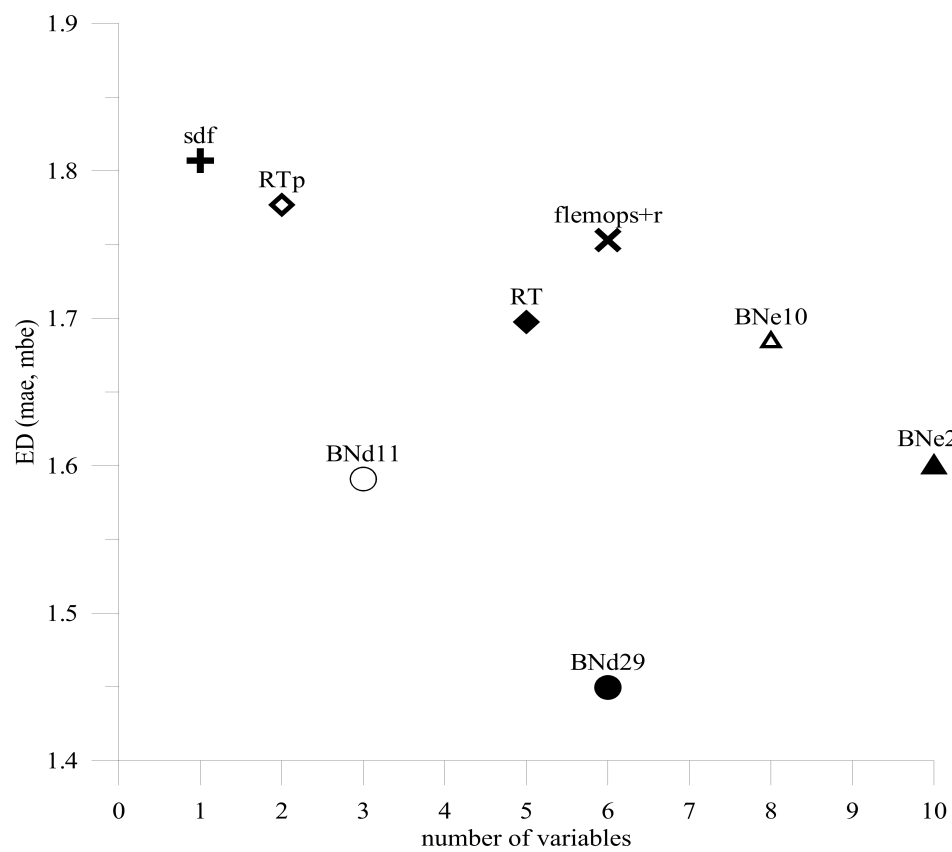


Figure 10.5: Average model predictive precision ED (mbe and mae) in cross regional and temporal validations against model complexity (number of explanatory variables used to predict rloss) for 'no uncertainty' scenario

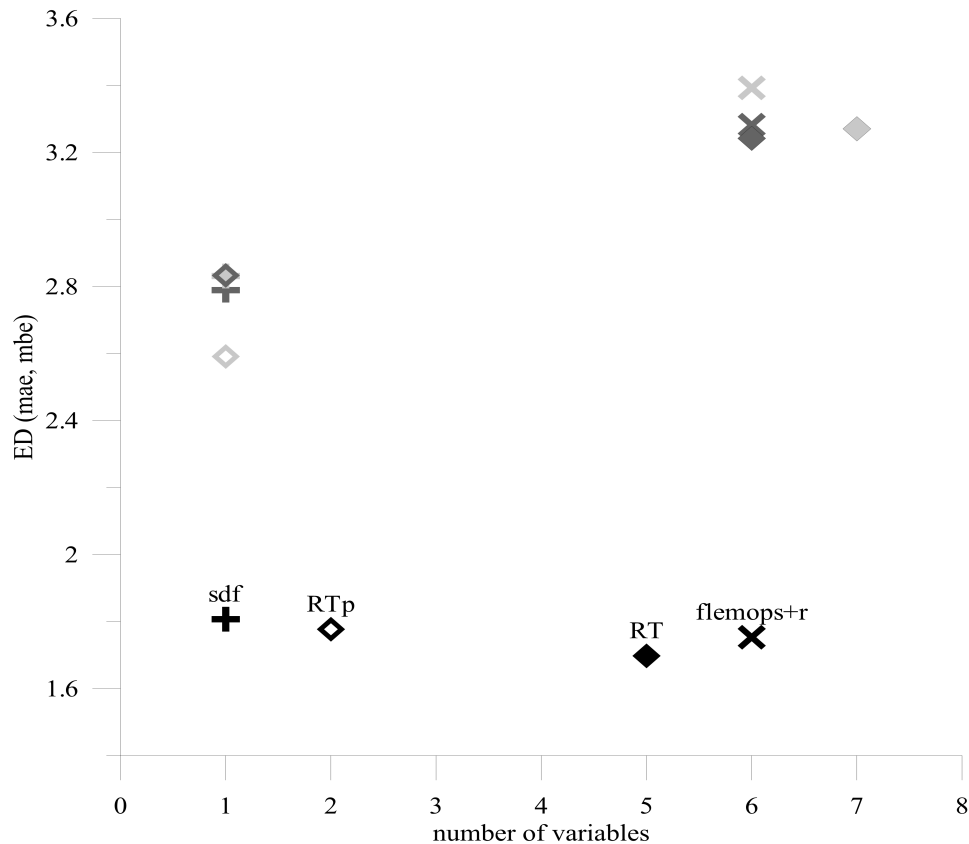


Figure 10.6: Average model predictive precision ED (mbe and mae) of deterministic models in cross regional and temporal validations against model complexity (number of explanatory variables used to predict $rloss$) within the uncertainty scenarios, model approaches are described by different symbols, uncertainty scenarios are represented by different colors: black (no uncertainty), grey (small uncertainty), light grey (large uncertainty)

precision given uncertain observations. Second, observation uncertainty influences the structure of the regression trees derived from the data and hence the complexity of the resulting model. Mostly, RTp models trained with uncertain observations include only one variable defining a single branch. In contrast, RT models tend to include more variables in the tree structure than without considering observation uncertainty (within the sample of models on average six variables (± 4 based on IQR) are assuming 'small uncertainty', seven variables (± 5 based on IQR) are used assuming 'large uncertainty'). In this context, the regression trees derived within 'no uncertainty' scenario have to be thought of as a single realization of the sample of models considered within the uncertainty scenarios.

To compare the variation and reliability of the model predictions (using the criteria QR_{90} and HR), we evaluate the predictive distributions of $rloss$ for the different damage models, whereat we discern on the one hand the predictive distributions obtained for the deterministic models for the small and large uncertainty scenarios and on the other hand the joint probability distributions of $rloss$ from the Bayesian Networks. Table 10.6 documents QR_{90} and HR scores for the different sub-samples and models. For the de-

Table 10.6: Variation and reliability of predictive distributions of deterministic models (sdf, flemops+r, RTp, RT) within small and large uncertainty scenarios (su, lu) and joint probability distributions of Bayesian Network (BN) variants

sub-sample	criterion	model											
		sdf		FLEMOps+r		RTp		RT		BNe10	BNe28	BNd11	BNd29
		su	lu	su	lu	su	lu	su	lu				
<i>model derivation</i>													
Elbe 2002id	QR90	0.04	0.16	0.28	0.13	0.30	0.00	0.72	0.41	1.41	1.48	1.47	1.41
	HR	0.05	0.13	0.16	0.57	0.25	0.00	0.50	0.41	0.96	0.94	0.92	0.92
<i>local validation</i>													
Elbe 2002pr	QR90	0.01	0.03	0.37	0.65	0.32	0.00	0.66	0.63	1.39	1.41	1.38	1.30
	HR	0.00	0.02	0.13	0.44	0.26	0.00	0.46	0.42	0.86	0.87	0.86	0.85
<i>cross regional and temporal validation</i>													
Danube 2002	QR90	0.01	0.03	0.35	0.44	0.42	0.00	0.70	0.64	1.20	1.41	1.20	1.10
	HR	0.00	0.01	0.09	0.15	0.16	0.00	0.37	0.33	0.73	0.83	0.83	0.83
Danube 2005	QR90	0.01	0.03	0.33	0.52	0.40	0.00	0.68	0.60	1.25	1.36	1.27	1.10
	HR	0.00	0.01	0.09	0.15	0.16	0.00	0.31	0.28	0.62	0.64	0.69	0.66
Elbe 2006	QR90	0.01	0.03	0.36	0.36	0.33	0.00	0.68	0.56	1.16	1.39	1.28	1.16
	HR	0.00	0.00	0.08	0.08	0.12	0.00	0.28	0.23	0.63	0.67	0.67	0.65

terministic models sdf and FLEMOps+r, QR_{90} increases with the degree of uncertainty added to the observations. This relation is reverse for the RTp and RT models. For RTp this is due to the difficulty to derive meaningful tree structures from increasingly uncertain observations which results in very simple model structures, and in turn zero variability of model predictions with $QR_{90} = 0$ and $HR = 0$. For the BN model variants QR_{90} is clearly larger (by a factor of 2). In this regard, we recall that the joint probability distribution inferred by BN reflects both the probabilistic dependence of the variables and the observation uncertainty associated with the variables. Overall, the variability of model predictions increases with model complexity since with additional variables additional sources of uncertainty take effect. Hence, more complex models tend to provide more variable predictions.

For the prediction interval to be of use it should be reliable. The HR criterion quantifies the proportion of the observations that fall within the prediction interval. The HR scores are listed in Table 10.6. Obviously, HR increases with QR_{90} . Among the deterministic models RT provides the most reliable predictions. Further, the HR scores provide evidence to which extent the uncertainty associated with the damage estimation is represented by the model. According to this interpretation the closer HR is to the nominal coverage (0.9 for the 95-quantile to 5-quantile range) the better the representation of the uncertainty. In this regard, the Bayesian Networks apparently embrace the prediction uncertainty more completely than the deterministic models. This is comprehensible since for the derivation of the deterministic models the uncertainty in the observations has been considered but the uncertainty concerning the probabilistic dependence of variables is not accounted for.

Figure 10.7 relates the average HR achieved by the different models in cross-regional and temporal validations to the number of explanatory variables. This graph illustrates that the reliability of model predictions seems to depend more on the model approach and the underlying concept to handle predictive uncertainty than on model complexity. In this regard, the largest values for HR are achieved by BNd11 using three explanatory

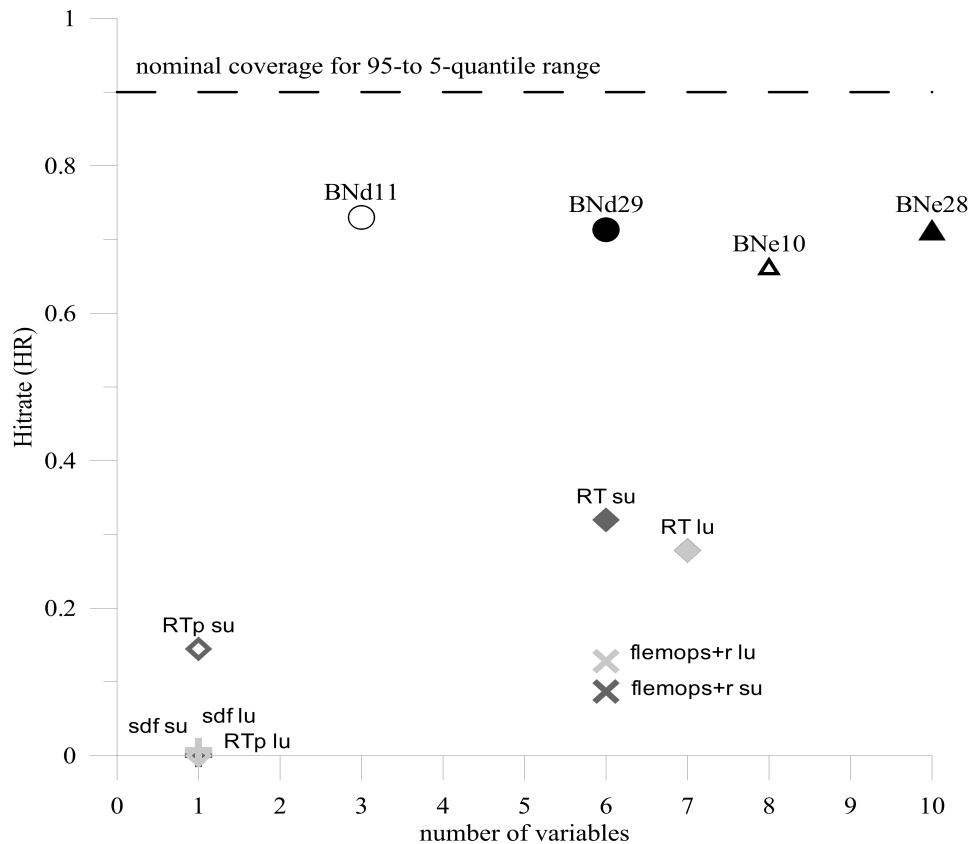


Figure 10.7: Average predictive reliability HR in cross regional and temporal validations against model complexity (number of explanatory variables used to predict *rloss*) for the predictive distributions of deterministic models within uncertainty scenarios (su, lu) and joint probability distribution of Bayesian Networks, model approaches are described by different symbols, uncertainty scenarios applied to deterministic models are represented by different colors: grey (small uncertainty), light grey (large uncertainty).

variables to predict *rloss*. Overall, the reliability of BN based predictions in space-time transfer is larger than for the remaining models and the uncertainties associated with damage predictions are reflected more completely. For these models the average HR is quite close to the nominal coverage of 0.9 for the 95-quantile to 5-quantile range and, hence, the joint probability distribution of *rloss* describes the predictive uncertainty relatively well.

10.5 Conclusions

In this paper we investigated the usefulness of complex flood damage models for the improvement of predicting relative damage to residential buildings. The results confirm the hypothesis that increasing complexity of flood damage models improves the capability to predict flood damage. In particular, this applies to model transfer applications to different regions and different flood events. Using additional explanatory variables

besides water depth improves the precision of predictions assuming that there is 'no uncertainty' in the observed explanatory variables. However, the relation between predictive capability and model complexity is not monotonic but is interfered by differences in the performance of different model approaches. In this regard, using the number of explanatory variables as a proxy for model complexity obviously falls short in capturing the various facets of model complexity, as for instance the representation of interactions between explanatory variables and their functional form implemented within the different model approaches. Still, it is shown that the more complex variants of similar model approaches outperform the simpler alternatives.

Uncertainty is of high relevance in flood damage modeling as all models show difficulties in completely explaining the real damage processes given the damage data available. The analysis of different uncertainty scenarios has shown that observation uncertainty can considerably impair the predictive performance of the deterministic models and may impede the derivation of appropriate model structures. In relation to model complexity, on the one hand the use of additional explanatory variables incorporates additional knowledge, but, on the other hand, as these observations are uncertain it also introduces additional uncertainty. In the light of the magnitude of model prediction errors it is mandatory to quantify the uncertainty of model predictions. For a realistic estimation of model predictive uncertainty not only observation uncertainty but also other uncertainty sources, e.g. model structure uncertainty, have to be taken into account. In this regard, probabilistic model approaches, as for instance Bayesian Networks, provide a consistent framework to comprehensively consider uncertainty. The results obtained for the hit rate in relation to the nominal coverage show that the joint probability distribution of damage estimates provided by Bayesian Networks represents the prediction uncertainty very well given the damage data available.

Overall, for the improvement of flood damage predictions more complex models including more details about the damaging process are useful. However, the application of these models requires a sufficient amount of data and a detailed and structured acquisition of explanatory variables preferably gathered within the study region and hence representing local characteristics. Despite this, the variability of damage records and related explanatory variables will remain considerable, thus the uncertainty of flood damage predictions must be analyzed, quantified and communicated.

11 | Tracing the value of data for flood loss modelling

Manuscript Info

Authors information:

Kai Schröter
Stefan Lüdtke
Kristin Vogel
Heidi Kreibich
Bruno Merz

Published as:

Schröter K., Lüdtke S.,
Vogel K., Kreibich H.,
Merz B.
Tracing the value
of data for flood
loss modelling
E3S Web of Conferences.
2016;7:xxx-xxx.
doi:10.1051/e3sconf/20160705005

Abstract

Flood loss modelling is associated with considerable uncertainty. If prediction uncertainty of flood loss models is large, the reliability of model outcomes is questionable, and thus challenges the practical usefulness. A key problem in flood loss estimation is the transfer of models to geographical regions and to flood events that may differ from the ones used for model development. Variations in local characteristics and continuous system changes require regional adjustments and continuous updating with current evidence. However, acquiring data on damage influencing factors is usually very costly. Therefore, it is of relevance to assess the value of additional data in terms of model performance improvement. We use empirical flood loss data on direct damage to residential buildings available from computer aided telephone interviews that were compiled after major floods in Germany. This unique data base allows us to trace the changes in predictive model performance by incrementally extending the data base used to derive flood loss models. Two models are considered: a uni-variable stage damage function and RF-FLEMO, a multi-variable probabilistic model approach using Random Forests. Additional data are useful to improve model predictive performance and increase model reliability, however the gains also seem to depend on the model approach.

11.1 Introduction

Flood loss modelling is associated with considerable uncertainty which is due to an incomplete knowledge about the damaging process and to the inherent variability of quantities involved (B. Merz et al., 2004). In view of large uncertainty in flood loss model predictions, the reliability of model outcomes is questionable and challenges the practical usefulness of model results; particularly when this affects the quality of decision as for instance on the investment in flood defences (Wagenaar et al., 2016). Therefore, it is of high importance to complement model outcomes with quantitative information about prediction uncertainty (Schröter et al., 2014). In comparison to traditional stage-damage functions which simply relate flood loss to inundation depth, multi-variable flood loss models, which take additional factors as for instance building characteristics, precaution, contamination etc. into account are an improvement to explain the variability of observed flood loss data (Thieken et al., 2008b; Elmer et al., 2010). In spite of this, uncertainty ranges of flood loss predictions are still large, and thus probabilistic modelling approaches which take uncertainty into account and provide quantitative information about model prediction uncertainty are required (Schröter et al., 2014).

A key problem in flood loss estimation is the transfer of models to geographical regions and to flood events that may differ from the ones used for model development (Cammerer et al., 2013). Variations in local characteristics and continuous system changes require regional adjustments by updating the model with local evidence (Schröter et al., 2014).

In this light, the demand for more and systematically collected data is an obvious conclusion. However, the acquisition of information on flood loss and influencing factors is elaborate and costly. Therefore, it is of relevance to assess the value of additional data in terms of model reliability improvement.

We use empirical flood loss data on direct damage to residential buildings available from computer aided telephone interviews (CATI) that were compiled after major floods in Germany (Thieken et al., 2005). This unique data base allows us to trace the changes in predictive model performance and reliability within a split-sample validation test by incrementally extending the data base used to derive flood loss models. Further, it offers the possibility to gain insight into the benefit of incorporating local evidence to a flood loss model. To study the implications of additional data on model prediction uncertainty, the analysis is conducted for probabilistic flood loss modelling approaches.

11.2 Data and Models

11.2.1 Empirical flood loss data

Empirical data of direct flood damage to residential buildings and related damage influencing variables are available from CATI that were carried out after the floods in 2002, 2005, 2006, 2010, 2011 and 2013 in Germany. A compilation of loss cases broken down for events and river basins is provided in Table 11.1. In total 2,254 empirical loss cases are available. Regional focuses of loss cases are in the Elbe and Danube river basins.

Within the CATI campaigns a broad range of information were gathered covering damage influencing aspects related to flood impacts, building characteristics, socio eco-

Table 11.1: Loss cases for different flood events and regions in Germany

Set	River basin/ region	Event year	Number of loss cases
E02	Elbe	2002	661
D02	Danube	2002	286
D05	Danube	2005	116
E06	Elbe	2006	43
De10	Germany	2010	242
De11	Germany	2011	103
E13	Elbe	2013	649
D13	Danube	2013	130
De13	Germany outside Elbe of Danube	2013	24
		Total	2254

conomic status, precaution and early warning. From this extensive data set, 28 candidate variables were preselected to be used in a modelling context for predicting the relative loss ratio of residential buildings (*rloss*). These candidate variables were selected according to experiences from previous analyses (Thieken et al., 2005; B. Merz et al., 2013). This selection of variables for flood loss modelling is narrowed further in this study based on the analysis of the out-of-bag feature importance as an indicator for the relevance of individual variables (B. Merz et al., 2013). Accordingly, the variables water depth (*wst*), building value (*bv*), floor space of building (*fsb*), contamination indicator (*con*), return period of flood peak discharge (*rp*), inundation duration (*d*), precautionary measures indicator (*pre*), emergency measures indicator (*em*), age of interviewed person (*age*) and indicator of flood warning information (*wi*) are used to predict *rloss*. Further details about the variables are documented in Merz et al. 2013 (B. Merz et al., 2013).

11.2.2 Loss models

Two flood loss models are considered: (i) uni-variable stage-damage function and (ii) multi-variable RF-FLEMO which is based on the machine learning technique of random forests (Breiman, 2001).

The model structure of the stage-damage function (*sdf*) for the estimation of *rloss* is defined as a two parameter (*a*, *b*) square root function of water depth (*wst*) as given in Eq. 11.1:

$$rloss = a + b(wst)^{1/2} \quad (11.1)$$

To evaluate predictive uncertainty, the *sdf* model is cast in a Bayesian modelling framework using a Monte Carlo Markov Chain approach for Gaussian linear regression using Gibbs sampling. Within this framework, the posterior distributions of model parameters *a* and *b* are used to sample the predictive distribution of *rloss* which describes model predictive uncertainty. Calculations are carried out using the R-package MCMCpack (A. Martin et al., 2011).

The multi-variable model RF-FELMO is built using the machine learning technique of random forests (RF). RF is an ensemble of Regression Trees (RT) derived by generating

many bootstrap replicas of the data set and by growing a RT on each replica. RTs are tree-building algorithms for predicting continuous dependent variables (Breiman et al., 1984). They recursively sub-divide the predictor data space into smaller regions in order to approximate a nonlinear regression structure. At each split the data set is partitioned into two sub-spaces in such a way that the improvement in predictive accuracy is maximised. Bootstrapping captures the effects of data variability as one source of uncertainty in flood loss modelling (Breiman, 1996). The ensemble of candidate RT composing the RF represents a variety of model structures reflecting model structure uncertainty. The sample of *rloss* predictions provided by RF-FLEMO represents the prediction uncertainty of the multi-variable modelling framework. RF-FLEMO model derivation and *rloss* predictions are carried out using the R-package randomForest (Liaw and Wiener, 2002).

11.3 Analysis framework

The implications of additional data on model performance are investigated in a split-sample validation test framework. Basically this involves a splitting of available data into two sub-sets which are either used for model derivation or for an independent evaluation of model predictive performance also referred to as model validation (Klemes, 1986). Evaluation of model predictive performance and predictive uncertainty is implemented by means of a set of performance criteria for accuracy, reliability, and sharpness and prediction skill.

11.3.1 Split-sample validation experiments

Two validation experiments are designed. The first investigates the value of data within a gradual learning setting. In this case, the amount of data available for model derivation is incrementally increased and model performance and predictive uncertainty are evaluated using an independent split-sample of the data. This validation sample is randomly drawn from the complete sample and is not used to derive the models.

The second experiment examines the effect of using local evidence, i.e. regional specific observations to update a basic model. In this context basic flood loss sdf and RF-FLEMO models are derived using randomly selected loss cases from the complete data sample and then gradually including regional data available from specific local data sets of different CATI campaigns in the derivation of the models. Accordingly, the regional updating of the basic models for instance in the Danube catchment includes a model derivation sequence using the data sub-set D02, next the data sub-sets D02 and D05 and finally the sub-sets D02, D05 and D13. Model predictive performance is evaluated using the observations of the sub-set D13. All experiments conducted are compiled in Table 11.2.

11.3.2 Performance criteria and scores

Model predictive performance and model predictive uncertainty are evaluated in terms of mean bias error (equation 2), mean absolute error (equation 3), quantile range of pre-

Table 11.2: Split-sample validation experiments for incremental model derivation

Experiment	Derivation set	Validation set
Incremental split-sample	100 increments of ca. 20 loss cases	200 loss cases randomly selected from complete sample
Regional updating Danube	200 random loss cases from complete sample D02 D02 + D05 D02 + D05 + D13	D13
Regional updating Elbe	200 random loss cases from complete sample E02 E02 + E06 E02 + E06 + E13	E13

dictions (equation 4), hit rate (equation 5) and the interval score (equation 6); where Q_{50} refers to the median (50-quantile), Q_{95} to the 95-quantile and Q_{05} to the 5-quantile of the predictive distribution and O represents observed values of the predicted variable $rloss$.

$$MBE = \frac{1}{n} \sum_{i=1}^n (Q_{50_i} - O_i) \quad (11.2)$$

$$MAE = \frac{1}{n} \sum_{i=1}^n |Q_{50_i} - O_i| \quad (11.3)$$

$$QR_{90} = \frac{1}{n} \sum_{i=1}^n (Q_{95_i} - Q_{05_i}) \quad (11.4)$$

$$HR = \frac{1}{n} \sum_{i=1}^n h_i ; h_i = \{ 1 \text{ if } O_i \in [Q_{95_i}, Q_{05_i}], 0 \text{ otherwise} \} \quad (11.5)$$

$$IS = QR_{90} + \frac{1}{n} \sum_{i=1}^n \frac{2}{\beta} (Q_{05_i} - O_i) | \{O_i < Q_{05_i}\} + \frac{2}{\beta} (O_i - Q_{95_i}) | \{O_i > Q_{95_i}\} \quad (11.6)$$

Mean bias (MBE) and mean absolute error (MAE) give information about the accuracy and the exactness of model predictions. MBE and MAE are calculated using the 50-quantile (Q_{50}) of the predictive distributions for each loss case. The quantile range (QR_{90}), Hit rate (HR) and interval score (IS) enable to evaluate the sharpness, reliability and overall performance of the interval predictions generated by the probabilistic models and are outlined in detail in (Gneiting and Raftery, 2007) and (Thordarson et al., 2012). QR_{90} is defined as the mean quantile range of model predictions between the 95-quantile and 5-quantile. It is an accuracy measure of the prediction interval with smaller values representing smaller ranges of the model prediction interval. HR is an indicator for model reliability by quantifying the ratio of observations within the prediction interval. IS combines sharpness and reliability scores in a single overall performance measure.

The second term in Equation 6 penalises observations outside the prediction interval by the distance to either the upper or lower boundary of the interval. This penalty depends on the quantile range considered in terms of the coefficient which is defined as $= 1 - 0.9$ for the 95 to 5-quantile range as upper and lower boundaries of the prediction interval. Smaller *IS* values indicate a narrow quantile range and higher coverage of observations within the prediction interval.

11.4 Results and Discussion

The results of the incremental split-sample validation test are shown in Figure 11.1 for the sdf-model and in Figure 11.2 for RF-FLEMO in terms of performance traces for the different criteria and scores depending on the sample size used for model derivation.

For the sdf-model larger datasets tend to reduce the bias of predictions. In contrast, a slight improvement but no substantial change is seen concerning *MAE*. The *QR₉₀* decreases clearly with larger datasets reflecting a higher sharpness of predictions. However, this smaller prediction interval hardly covers any of the observations used for model validation which can be recognized from the decreasing *HR*. Both developments are also reflected in a continuous deterioration of the interval score *IS* for the predictive distribution. *QR₉₀*, *HR* and *IS* seem to be stabilizing above a sample size of ca. 1500 loss cases. Beyond that additional data do not contribute substantially to a further improvement.

For the RF-FLEMO model larger datasets reduce the bias and minimize the *MAE*. The *QR₉₀* of the RF-FLEMO prediction interval increases as additional data are taken into account for model derivation and indicates a larger uncertainty in the model predictions. However, this development is paralleled by a clear improvement of the reliability of model predictions which can be recognized from the *HR* score. *HR* approximates a value of 0.85 which is very close to the nominal coverage rate of 0.9 for the 95 to 5-quantile range and expresses an almost complete representation of uncertainty in the framework. The development of *QR₉₀* and *HR* results in a continuous improvement of the interval score *IS* for the prediction interval. As for the sdf-model the performance scores appear to be stabilizing with increasing sample size above 1500 loss cases, yet a clear improvement of model performance is achieved already with ca. 500 loss cases indicating a more rapid learning curve for the multi-variable RF-FLEMO model in comparison to the uni-variable sdf model.

The results of the regional updating experiments in the Danube and Elbe catchments are summarized in Figure 11.3. Performance measures are shown for each updating step, i.e. starting from the basic model and gradually extending the data basis for deriving the models, cf. Table 11.2.

The improvement of model performance by including gradually local specific observations in the model derivation can be recognized for both models in terms of reduced bias (*MBE*) and smaller *MAE*. For RF-FLEMO the *HR* is continuously improved while *QR₉₀* is reduced which is also reflected in smaller *IS* values, indicating an improved reliability and sharpness of the predictive distribution. In contrast, similar to the incremental split-sample learning experiment for the sdf model additional regional data are not effective to increase model prediction reliability. The benefit of additional data is more obvious in the Elbe updating sequence. In the Danube catchment additional data

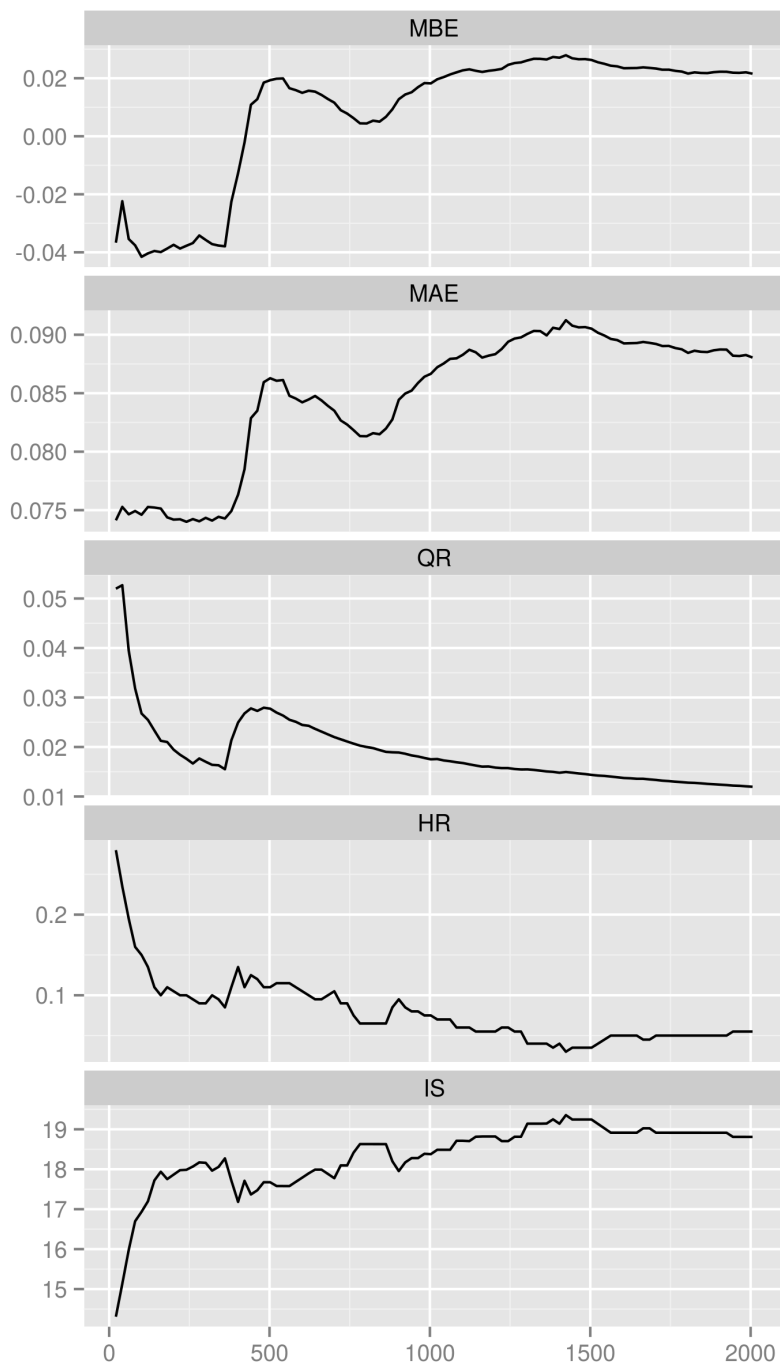


Figure 11.1: Performance traces for incremental split-sample evaluation of sdf model, x-axis: sample size, y-axes performance values.

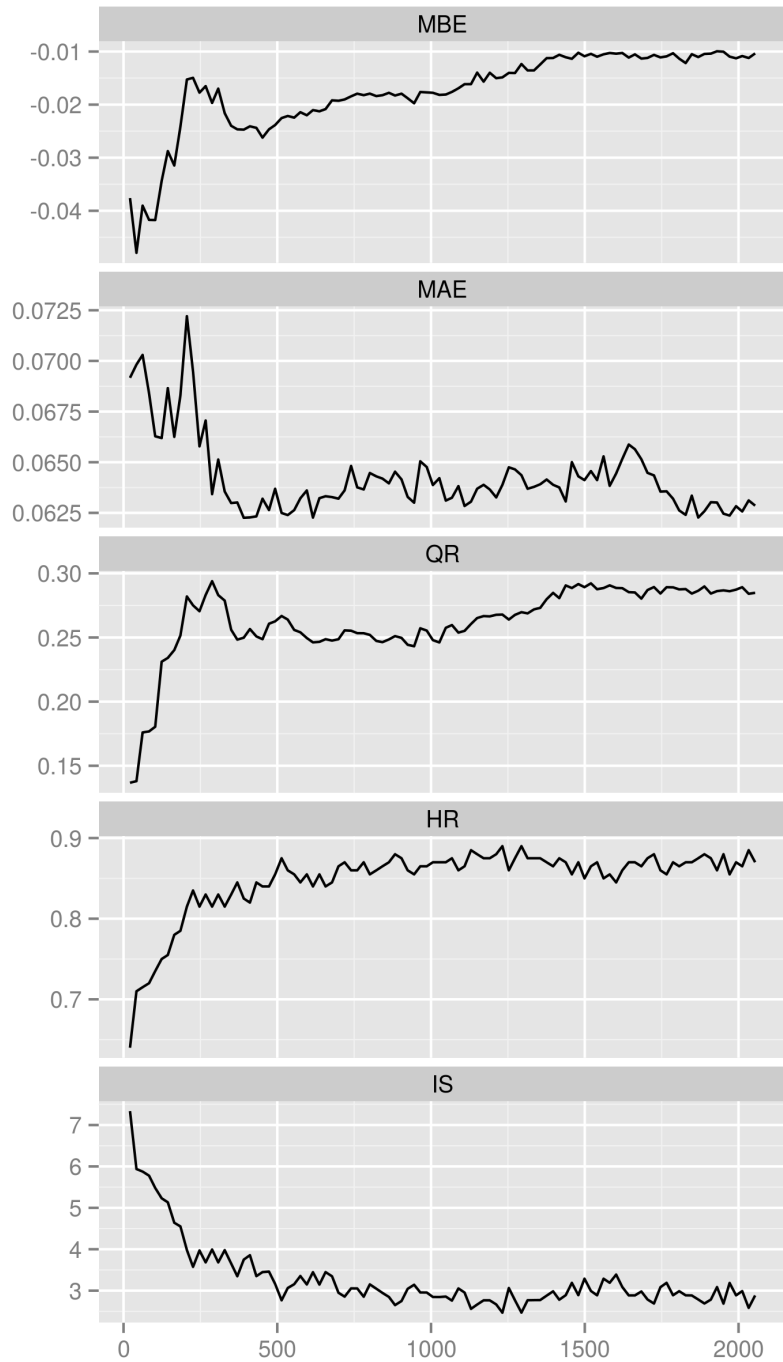


Figure 11.2: Performance traces for incremental split-sample evaluation of RF-FLEMO, x-axis: sample size, y-axes performance values.

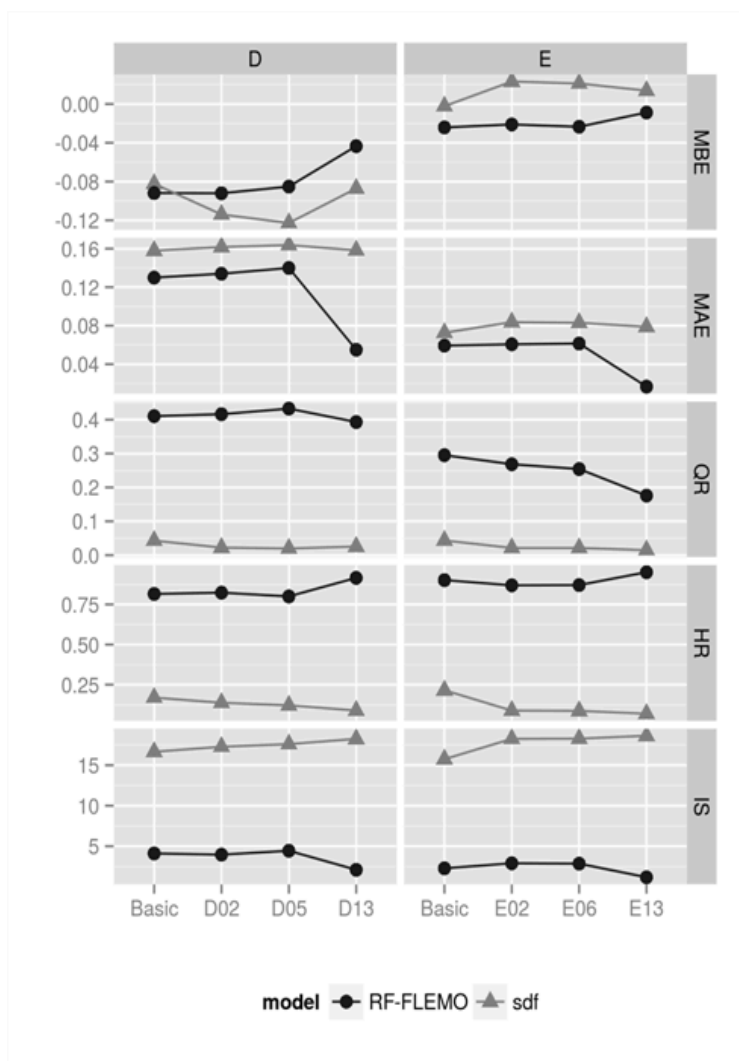


Figure 11.3: Model performance of sdf and RF-FLEMO models in regional updating in the Danube (D) and Elbe (E) catchments.

appear to be of less value to achieve better predictions for the D13 validation set. A clear improvement is only achieved if the D13 sub-set is included in model derivation. A possible explanation for this is that in this specific sub-set many loss cases are related to inundation as a result of major dike breaches. This resulted in large inundation depths and high relative losses (not shown), which are not represented well in the sub sets of the earlier campaigns D05 and D05.

Overall, even though the prediction uncertainty remains considerable, the performance measures achieved by sdf and RF-FLEMO model updated with local specific information are superior to the performance values achieved within the incremental split-sample validation. This supports the hypothesis that local information is useful to improve the reliability of flood loss estimation.

11.5 Conclusions

The value of data for the performance and reliability of flood loss predictions has been analysed within incremental split-sample and regional updating validation tests conducted for two probabilistic flood loss models. Both experiments demonstrate that additional data are useful to improve model predictive performance and reliability. The importance of local specific information to adjust loss models to regional characteristics is stressed. Comparing both model approaches the performance gain is higher for the multi-variable model. Even though predictive uncertainty ranges for RF-FLEMO are larger, which is due to the fact that with additional variables additional uncertainty sources are revealed, the modelling framework seems to more realistically represent the uncertainty. In contrast, the predictions provided by the sdf model are clearly less reliable. Apparently the uni-variable model approach is not capable to adequately describe the variability in loss observations. Therefore, one recommendation is to develop methods and to establish procedures which enable decision makers to take uncertain model predictions explicitly into account.

The effort to collect additional loss data seems to be justified as it is useful to improve model predictive performance and reliability. However, the gain also depends on the model approach applied. In this context, it is rewarding to not only focus on inundation depth but to comprehensively gather information for other loss influencing factors which enable the application of multi-variable flood loss models. As an extension of the analysis framework the connection of costs for data acquisition and monetary gains of more informed decisions should be investigated.

12 | Flood loss estimation using 3D city models and remote sensing data

Manuscript Info

Authors information:

Kai Schröter
Stefan Lüdtke
Richard Redweik
Jessica Meier
Mathias Bochow
Lutz Ross
Claus Nagel
Heidi Kreibich

Published as:

Schröter K., Lüdtke S.,
Redweik R., Meier J.,
Bochow M., Ross L.,
Nagel C., Kreibich H.
Flood loss estimation
using 3D city models
and remote sensing
data
Environmental Modelling &
Software.
2018;105:118-111.
doi:10.1016/j.envsoft.2018.03.032

Abstract

Flood loss modeling provides the basis to optimize investments for flood risk management. However, detailed object-related data are not readily available to generate spatially explicit risk information. Virtual 3D city models and numerical spatial measures derived from remote sensing data provide standardized data and hold promise to fill this gap. The suitability of these data sources to characterize the vulnerability of residential buildings to flooding is investigated using the city of Dresden as a case study, where also empirical data on relative flood loss and inundation depths are available. Random forests are used for predictive analysis of these heterogeneous data sets. Results show that variables depicting building geometric properties are suitable to explain flood vulnerability. Model validation confirms that predictive accuracy and reliability are comparable to alternative models based on detailed empirical data. Furthermore, virtual 3D city models allow embedding vulnerability information into flood risk sensitive urban planning.

12.1 Introduction

With the transition to flood risk management, for which flood risk analyses are an essential basis, loss estimation is becoming increasingly important (B. Merz et al., 2010a; Bubeck et al., 2017). This is also recognised by the European Flood Directive (2007/60/EC) which requires the assessment and mapping of flood risk, and to draft flood risk management plans. Risk assessments aim to quantify the probability of expected losses resulting from interactions between hazard, exposure and vulnerability, e.g. (Moel et al., 2015).

Risk analyses are undertaken on different spatial scales (Meyer and Messner, 2005; Moel et al., 2015). Our study focuses on the local or micro-scale, i.e. on the level of individual objects. These assessments are primarily undertaken to optimise investments for risk management concepts, including protection measures, urban planning, etc. Additionally, micro-scale, spatially explicit risk information enables communities, companies, and people to prepare for disasters, e.g. (Takeuchi, 2001; B. Merz and Thieken, 2004). At the micro-scale the assessment is based on single elements at risk. For instance, in order to estimate the loss to a community in case of a certain flood scenario, losses are calculated for each affected object, e.g. buildings. These analyses require detailed object-related data. Accurate flood modelling at high spatial and temporal resolutions remains a significant challenge (B. Merz et al., 2010b). Likewise, this concerns the spatial resolution and geo-location of the exposed objects as well as object characteristics, which determine their vulnerability towards inundation. This is challenging, since such detailed data are hardly available (Apel et al., 2009).

A standard approach to determine the expected direct monetary loss to buildings are depth-damage functions based on the type or use of the building and the inundation depth (Grigg and Helweg, 1975; D. Smith, 1994; Penning-Rowsell et al., 2005). Accordingly, inundation depth is the variable which is most commonly included in flood loss models (B. Merz et al., 2010b; Gerl et al., 2016). However, making use of additional variables to explain vulnerability and to develop predictive models for loss estimation has been shown to offer substantial advancements to explain flood loss (Thieken et al., 2008b; Schröter et al., 2014). The domain of flood loss modelling is experiencing a boom of tree based data analysis since (B. Merz et al., 2013) have demonstrated the suitability and superior performance of regression trees and bagging decision trees for flood loss estimation. Also graphical models (Bayesian Networks) have been successfully applied to the domain of flood loss estimation, e.g. (K. Vogel et al., 2012; Schröter et al., 2014). Decision trees have been used by (Spekkers et al., 2014) to gain new insights into damage influencing factors for pluvial floods. Chinh et al. (2015) and Nafari et al. (2016), and Wagenaar et al. (2017) have derived multi-variable flood loss models based on decision-tree approaches for the Mekong delta (Vietnam), Australia, and the Maas River (The Netherlands), respectively. The model validation experiment of Schröter et al. (2014) has shown that regression trees do also outperform traditional models in cross-regional and temporal transfer applications. Kreibich et al. (2017a) have proposed a novel flood loss model for meso-scale applications based on bagging decision trees which provides uncertainty information of loss estimates. In the broader context of flood hazard and flood risk assessment tree based model approaches have also been successfully applied, e.g. (Z. Wang et al., 2015; Chapi et al., 2017).

The application of multi-variable models poses high requirements on the availabil-

ity of input data (B. Merz et al., 2013), which is particularly challenging for the spatial transfer of these models. Kreibich et al. (2017a) used empirical flood vulnerability data gathered via surveys to estimate the model input variables on municipality level. However, such data is costly and time consuming to collect and is therefore unavailable in many regions (Thieken et al., 2017; Kreibich et al., 2017c). By necessity, flood loss models are often taken from the literature and transferred in space and applied to different built environments and other settings, e.g. (Balica et al., 2013). Model transfer and application is eased when data from standard databases or sources can be used because then the specification and definition of variables is similar across regions. For instance, Kreibich et al. (2010) used macro-economic data from the Federal Statistical Office Germany and the Federal Employment Agency together with geo-marketing data for the application of the multi-variable model FLEMOcs- Flood loss estimation model for the commercial sector on the meso-scale. As such, the Germany wide application of FLEMOcs was enabled. However, due to the spatially coarse data base, uncertainties in loss estimates are high. Gerl et al. (2014) examined the use of urban structure type information which is automatically derived from remote sensing data for flood loss estimation. Their analyses show that different urban structure types comprising the categories “closed block development”, “semi-open block development”, “mid-rise dwellings”, and “single-family/semi-detached houses” and the information about their specific location are valuable for flood loss modelling. However, they suggest that additional data about building characteristics which cannot be derived from remote sensing would be useful to make further advancements.

Detailed building location and characteristics can be stored in (virtual) 3D city models, which are based on CityGML. CityGML is an open standard application schema of the Geography Markup Language (GML), which represents the 3D geometry, 3D topology, semantics, and appearance of objects on different levels of detail (LOD). Hence, 3D city models provide a framework for detailed spatial information in terms of geo-located building footprints (based on cadastral data) which is useful to describe the exposure as well as detailed information about buildings characteristics and geometries which are useful to describe the vulnerability of residential buildings at risk. CityGML is the reference model for the building model in the Infrastructure for spatial information in Europe (INSPIRE; Directive 2007/2/EC). They have been widely adopted for diverse applications in environmental simulations (Biljecki et al., 2015) including also examples from flooding and flood damage assessment, e.g. (Amirebrahimi et al., 2016). However, currently building information contained in 3D city models is available for low levels of detail (LOD), i.e. LOD1 or LOD2, whereas relevant data about building openings and/or interior structures of a building are available only for high levels of detail, i.e. LOD3 or LOD4. The concept of LODs is described in detail in section 12.2.2.2. Therefore, a combination with remote-sensing data might be advantageous. For instance, numerical spatial measures from remote-sensing data have been used to characterize the physical properties of landscapes (Uuemaa et al., 2009) and urban areas, e.g. (Bochow et al., 2010; Graesser et al., 2012) and have been used as proxies for information like “socio-economic characteristics” or “energy demand” (J. R. Jensen and Cowen, 1999; Taubenböck et al., 2009).

The objective of this study is to develop multi-variable flood loss models which are based on standardized data sources to characterize the vulnerability of buildings towards

flooding. We investigate the potential of virtual 3D city models and numerical spatial measures derived from remote sensing data to support the estimation of flood losses to residential buildings. Section 12.2 and section 12.3 introduce the data sources and the methods applied. The results of these analyses are presented in section 12.4. Further, the potential of 3D city database systems to store data, embed flood loss modelling as a functional extension for risk assessment, and visualize results is explored. In this regard the prototype implementation and a case study application in the city of Dresden (Germany) are described in section 12.5. In section 12.6 the results are discussed and concluded in section 12.7.

12.2 Data

12.2.1 Study area

The city of Dresden (Saxony, Germany) is used as a case study for this research. Figure 12.1 shows the location of Dresden along the Elbe river banks and its tributaries. In the past, floods have caused severe impacts as for instance in June 2011, April 2006 and in August 2002. The flood in August 2002 caused more than EUR 1 Bn economic damage in the city of Dresden with losses to residential buildings of EUR 305 Mn (Kreibich and Thielen, 2009)

Dresden is characterised by a heterogeneous architectural structure including historical as well as modern multi-storey buildings in the densely built-up city center, and multi-storey residential buildings as well as one-to-three-storey developments in the neighboring city districts (Gerl et al., 2014) which is the outcome of a series of eventful historic developments with drastic impacts on the building stock development such as World War II, communist planned economy and the reunion of Germany. Given this diversity of building characteristics, differences in terms of building vulnerability towards flooding are expected.

Driven by the recent floods, flood risk assessment and management is a highly relevant topic on the urban planning agenda in the city of Dresden and comprehensive flood management concepts have been put into practice (Dresden, 2011). As part of this planning hydro-numeric simulations have been conducted to determine inundation depth maps for historic floods and for design flood scenarios. For this study, inundation depth maps for three different water levels at the gauge Dresden are available for several focus areas in Dresden. In (Dresden, 2011) flood impacts have been estimated using simple flood damage curves relating inundation depth to specific loss [EUR/m²] for different land use classes. This damage model had been derived for the river Rhine (ICPR, 2001) and from this model the damage curve for residential buildings will be also compared to the outcomes of the flood loss models developed in this study.

Other data sources (cf. Figure 12.1) are a dataset of computer aided telephone interviews (CATI) carried out after the floods August 2002 and April 2006 in Dresden (Thielen et al., 2007), building data from the 3D city model of Dresden in LOD1 and LOD2 (citydb) saved in the 3D City Database, spatial measures (SM) for the residential building stock derived from IKONOS hyper-spectral images mapped on the German Official Topographic Cartographic Information System (ATKIS) building blocks (Bochow et al., 2010). These data sets provide input variables for the derivation of predictive flood

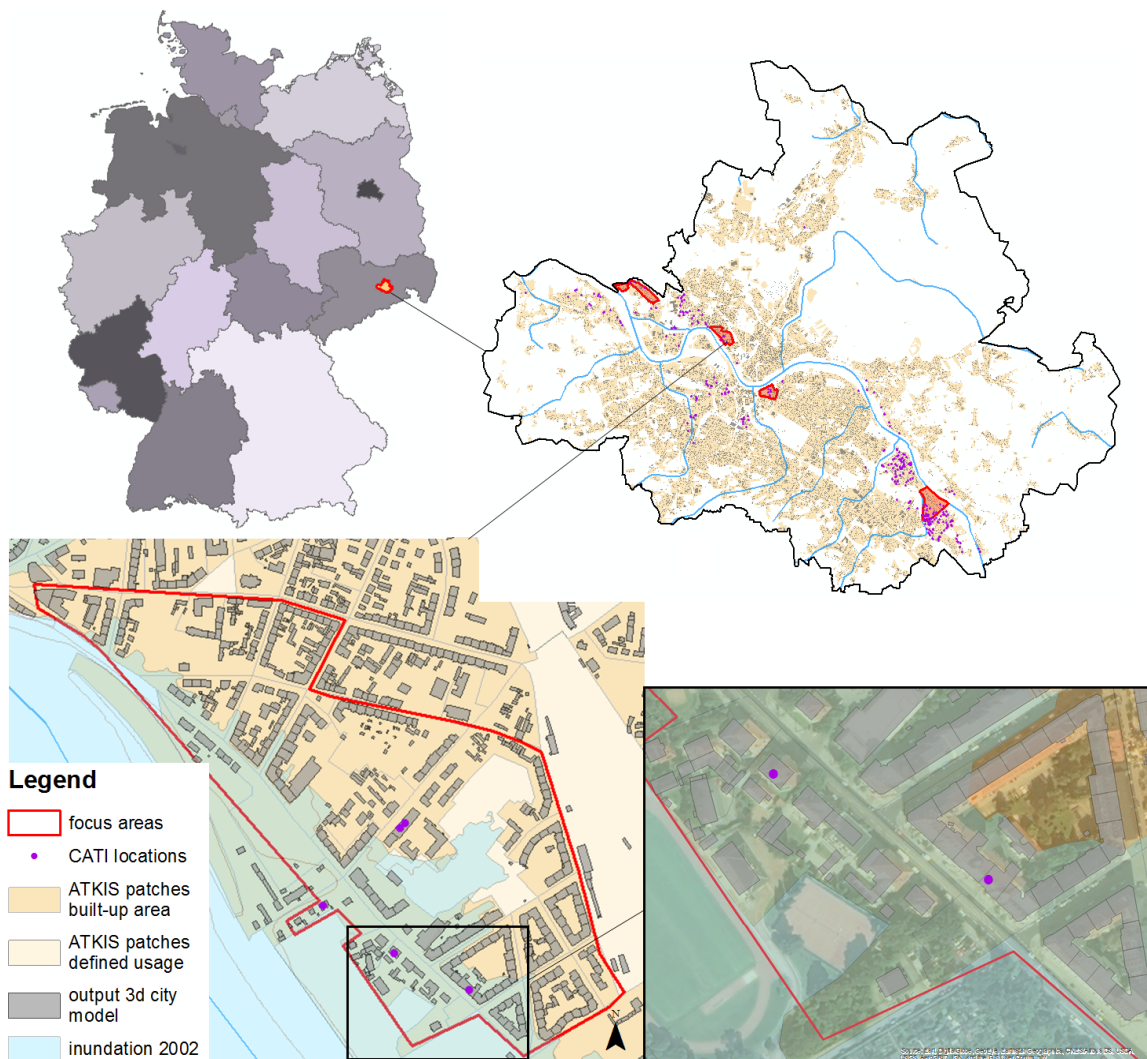


Figure 12.1: Map of Dresden in Germany with focus areas, interview locations, building outlines and ATKIS land use classes, the detail cutout shows the focus area Pieschen

loss models and are described in detail in the following sections. Beyond that, estimates of the regional stock of residential buildings (Kleist et al., 2006) are used to quantify the asset values of residential buildings exposed to flooding in the application case in the city of Dresden in section 3.4. A digital elevation model (DEM10; Federal Agency for Cartography and Geodesy in Germany (BKG)) with a spatial resolution of 10 m is used to estimate the elevation of residential buildings and to derive inundation depths maps for the flood scenarios used in the application case.

12.2.2 Data sources

Computer aided telephone interview data

Empirical loss data have been collected from flood affected households via computer aided telephone interviews (CATI) after the major floods in August 2002 and April

2006. These questionnaires cover aspects about the flooding situation, early warning and emergency measures, precaution, building characteristics and the socio-economic status (Thieken et al., 2007). From these campaigns 292 geo-located interviews are available in the city of Dresden. Further, the interview data were supplemented by estimates of the return period of the flood peak discharge as well as aggregated indicators for flow velocity, contamination, flood warning, emergency measures, precautionary measures, flood experience, and socioeconomic variables. Building values were estimated according to the VdS guideline 772 1988-10 (Dietz, 1999), and the loss ratio of the buildings has been calculated as the quotient of replacement costs and building value. However, the building value could be determined for only 80 buildings due a lack of information in the other interviews. As we are interested in investigating data sources to describe residential building resistance in flood loss models, from the broad range of information about flood influencing factors, those variables of the CATI dataset are of central interest which provide specific information about the building characteristics. Beyond that, the interview datasets provide information about the flooding situation in terms of water depth and the flood impact in terms of relative loss to the individual buildings. These building related information used from the CATI data set are listed in Table 12.1. For a detailed description of the complete set of variables derived from CATI refer to B. Merz et al. (2013).

3D-city model data

For this study the City of Dresden provided a virtual 3D city model which is based on the international standard CityGML. CityGML is the Open Geospatial Consortium (OGC) standard for the representation, storage, and exchange of virtual 3D city models. CityGML is a XML based application schema of the Geography Markup Language 3 (GML3) (version 3.1.1). Hence, its usage is suitable for Spatial Data Infrastructures (SDI) in the context of OGC web services. Unlike purely graphical or geometrical models, CityGML represents semantic and topological aspects of features which are relevant for city models as well (Gröger and Plümer, 2012). Hence, CityGML based 3D city models can be used for visualization purposes and for thematic analysis. For that, CityGML provides a semantic “geospatial information model (ontology) for urban landscapes based on the ISO 191xx family” (Gröger and Plümer, 2012). In general, CityGML defines classes and relations with respect to geometrical, topological, semantical, and appearance properties (Gröger and Plümer, 2012). CityGML makes use of a level of detail concept discerning five levels (LOD0 to LOD4), where the same object can be represented in different LODs at the same time. For instance, in LOD0 a building is only represented by the horizontal 3D surface representing the footprint or the roof edge. In LOD1 buildings are represented as simple block models specified either by multi surfaces or a solid body. LOD2 introduces *BoundarySurfaces* as thematic features, e.g. *WallSurface*, *RoofSurfaces*, *GroundSurfaces*, and other surface information. LOD3 allows to model openings of *BoundarySurfaces* such as *doors* and *windows*. LOD4 adds interior structures of buildings as for instance *Rooms* or *BuildingFurniture*. The LODs describe geometrical and semantical aspects. That means the objects become more accurate and detailed with an increasing LOD level. An additional important design principle of CityGML is the coherent semantical-geometrical modeling, which means real-world entities are represented

Table 12.1: Variables available from computer aided telephone interviews, 3d city model and remote sensing

Abbreviation	Variable	Scale and range
flooding situation and impact from cati data set		
wd	Water depth	c: 212 cm below ground to 476 cm above ground
rloss	loss ratio of residential building	c: 0 = no damage to 1 = total damage
building characteristics from cati data set		
bt	Building type	n (1=multifamily house, 2= semi-detached house, 3=one-family house)
nfb	Number of flats in building	c: 1 to 12 flats
fsb	Floor space of building	c: 60 to 2,000 m ²
bq	Building quality	o: 1=very good to 6=very bad
bv	Building value	c: 130,088 to 3,718,677 EUR
year	Construction year	c: 1800 to 2001
heat	Heating system	N (gas, coal, heating oil, night storage, wood pellet, long distance heating)
building characteristics from citydb data set		
ba	Building area	c: 37.6 to 362.5 m ²
rt	Roof type	n: 3100, 3200, 3300, 3400, 3500, 5000
mh	Measured height	c: 4.42 to 19.01 m
sag	Storeys above ground	c: 1 to 5
year	Year of construction	c: 2000 to 2012
Variables of spatial measures data set		
BT_AREA	Area of a city block calculated as the sum of the pixel areas of the rasterized city block	c: 2302 - 43726
BT_LSI	Linear-Segment-Indicator calculated as the ratio between the first and second principal component of the pixel positions of a rasterized city block in the 2D space	c: 1.04 6.75
BT_DIST	Distance of a city block to the city center	c: 467 - 738
CL_POFA	Percentage of area of a Land use/Land Cover (LULC) class (or LULC class group) within a UST patch	c: 0.0726, 0.339
CL_GRAV	Degree of compactness of a LULC class (or LULC class group) according to Newtons Universal Law of Gravitation	c: 0.00186, 0.0286
CL_CEPPE, CL_CEPPE_HEIGHT	Mean distance of class pixels from a central region (3% innermost pixels) of a building block normalized by the mean distance of the block boundary from the central region. A second variant of this basic type ignores pixels below a minimum height value in the DSM to exclude small buildings like garages.	c: 0.01, 1
CL_NUMSEG	Number of segments of a LULC class (or LULC class group)	d: 2, 37
CL_NUMSEG_PER_ AREA	Number of segments of a LULC class (or LULC class group) divided by the area of the building block	c: 0.0322, 0.319
CL_SEGORI	Mean value of the angles between the first Eigenvectors (indicating the orientation of the segments in the 2D space) of each pair of two segments of a LULC class (or LULC class group)	c: 0.318, 40.2
CL_HEIGHT	Height of a LULC class (or LULC class group)*	c: 33.8, 141
SEG2CL_AREA	Area (m ²) of the segments of a LULC class (or LULC class group)*	c: 68.1, 830
SEG2CL_LSI	Linear-Segment-Indicator calculated as the ratio between the first and second principal component of a segments pixel positions in the 2D space*	c: 1.27, 4.79
SEG2CL_SEGDIST	The shortest distance between the centroid of a segment of a LULC class (or LULC class group) and the centroid of the closest segment of the same class (group)*	c: 8.45, 62.6
SEG2CL_VOL	3D volume of the segments of a LULC class (or LULC class group)*	c: 409, 9764
SEG2CL_HEIGHT	Height of the segments of a LULC class (or LULC class group)**	c: 38.8, 115
ust_type	The urban structure type of the building block	n: 2,3,4,5,7,8,B,E,I

c: continuous, d: discrete, o: ordinal, n: nominal, *: 4 variants: min, max, mean, sdev, **: 20 variants: min, max, mean, followed by min, max, mean, sdev over all resulting values of the buildings within a building block

as features at semantic level and as geometry objects (that are assigned to the semantic features) at geometry level. It follows that "geometrical objects 'know' what they are" and "semantic entities 'know' where they are and what are their spatial extents" (Stadler and Kolbe, 2007). For example, 3D city models can be queried for all wall surfaces with their material in an inundated area.

CityGML organizes the features into different thematic modules which cover different thematic fields of virtual cities (e.g. Building, Bridge, Vegetation, Water Body, etc.) with each of them containing specific feature types. Still, the data model is flexible to combine any of these modules as needed by the application or application domain (Gröger and Plümer, 2012). In this research, the focus is on the data contained in the building module

For the Dresden case study a 3D city model in LOD1 and LOD2 was available and thus providing geometrical information about the location and the extent of the buildings (*building area*). Additional available thematic attributes on the building level are: *function*, e.g. residential, industry, etc., *roof_type*, *measured_height*, *storeys_above_ground*, and *year of construction*, see Table 12.1. The attributes *function* and *roof_type* are specified separately from the CityGML schema using code lists which specify the values given admissible ranges. To give an example, a *roof_type* encoded by the value 3100 is a gabled roof, a *roof_type* encoded by the value 3200 is a hipped roof. Roof types are useful to distinguish building types which is a relevant detail to characterize building vulnerability. The usefulness of these variables for flood loss estimation will be explored within the model development step.

Numerical spatial measures derived from remote sensing data

Numerical spatial measures as implemented by Bochow et al. (2010) are based on standardized calculation procedures. They describe the amount, proportions, size, shape, spatial arrangement and distribution of land cover classes and classified image objects (e.g. houses, trees, lawns) within the building blocks. For some of these measures (e.g. the footprint size of a building) it is obvious or has been already shown that they directly affect the vulnerability to floods. For others hidden relations might exist which we aim to explore in this work.

Multispectral IKONOS Geo Ortho Kit satellite images (GeoEye, 2006) acquired between 2004 and 2008 have been geometrically and atmospherically corrected, pan-sharpened to a spatial resolution of 1 m using principal component pan-sharpening, and mosaicked to a single image covering the complete city area of Dresden. A land use/land cover (LULC) classification has been produced using a maximum likelihood classifier. The initial classification result has been enhanced by incorporating object height information derived from LiDAR data using a decision tree built with the ERDAS Imagine Knowledge Engineer. Misclassified pixels (e.g. pixels of roofs and ground surface pixel with similar spectral properties) are reclassified according to their object height into a roof class or a ground surface class, respectively. In a further processing step the LULC classes are combined into thematic groups, as for instance the class group "vegetation" integrates the classes "meadow" and "trees", which are stored as additional layers to the original LULC classes. The resulting layer stack contains the original 15 LULC classes, as well as 12 thematic class groups, namely vegetation, trees, soils, roofs, roofs_metal, roofs_tiles, roofs_flat, traffic, sports, roofs_industry, water, and shadow. In the next processing step

sequentially numbered image segments consisting of adjacent pixels of the same class are created and stored for each LULC class and class group.

The resulting layers enable the computation of class specific and image object based numerical spatial measures as implemented by Bochow et al. (2010) which can be used as the basis for urban structure type mapping. The numerous spatial measures are organized into five categories assessing the size and shape, orientation, and distribution, percentage of area, neighborhood, or spatial position of classified pixels or image segments. They are calculated either based on the entire building blocks (taken from the ATKIS-DLM), based on individual classes or class groups within the building blocks, or based on the segments of a class within the city blocks. Furthermore, if present, the interior (backyard) of a building block or its border area can be considered separately for the calculation. For all basic features distinctive statistical parameters like minimum, maximum, mean, and standard deviation can be calculated. In this work we focus on the mean values for the basic spatial measures which are related to buildings, i.e. the class group "roofs", see Table 12.1.

The Building blocks from the ATKIS-DLM data also serve as spatial mapping units for urban structure types. The urban structure types are distinguished in terms of their composition of different objects like buildings, trees, and surface material as for instance roof materials or vegetation types as well as about their distribution and arrangement within space. Within this study the following urban structure types are considered: semi open block development (2), terraced houses, (3), single/semi detaches houses (4), mixed types of buildings (5), sport facilities/playgrounds (7), garden plots (8), green spaces (B), water surfaces (F), traffic areas (I).

12.3 Methods

12.3.1 Model development

For the development of multi-variable flood loss models based on 3D city models and numerical spatial measures derived from remote sensing images two central tasks are addressed: a) selecting variables from the variety of candidate variables of standardized data sources according to their usefulness to explain flood loss, and b) deriving a good predictive model for flood loss to residential buildings.

Model development is carried out using a variety of sub-sets with different number of variables from the different data-sets described above, see Table 12.1. In this way, models of different complexity are derived and compared in terms of predictive performance also from the angle of model parsimony. This comprises the development of flood loss models using i) the complete set of variables available from the surveys using computer aided telephone interviews (CATI_complete), ii) a reduced set of variables from computer aided telephone interviews which are related to building characteristics (CATI_reduced), iii) water depth at the building as the only explanatory variable referring to established stage damage functions (sdf), iv) geometrical information and thematic attributes provided by the 3D city model (citydb), v) building roof related numerical spatial measures derived from remote sensing images representing the mean values per building block (sm), and vi) the concatenation of 3D city model data and spatial measures (citydb_sm). All datasets are amended with the observations of wa-

ter depth and relative building loss available from the empirical surveys (CATI) for the selection of variables and the derivation of predictive models.

The underlying question of variable selection is: which variables are most useful to explain flood damage? This step in data analytics aims to improve the predictive performance of a model in terms of faster and more cost-effective predictors in the sense that the trade-off between the number of explanatory variables used in the predictive model and the performance of the prediction is reflected according to the principle of parsimony. Accordingly, the task is to choose those variables from the data that will give as good or better predictive performance while requiring less data (Guyon and Elisseeff, 2003). The general strategy involves a ranking of the candidate explanatory variables and an assessment of model predictive performance. While the 'ad-hoc' selection of variables requires deep knowledge of the problem domain, data-mining algorithms entail a variety of methods for the automated analysis of large data sets and also provide metrics for comparing the relevance of each candidate variable. Guyon and Elisseeff (2003) distinguish filter methods which rank the variables independent on the model approach like correlation coefficients, wrapper methods which assess subsets of variables according to the predictive performance within the chosen model approach like recursive feature elimination algorithms, and embedded methods which incorporate variable ranking and selection as part of the model derivation process as for instance classification and regression trees (Breiman et al., 1984). Embedded methods include the interaction with the model learning and are computationally more efficient than wrapper methods (Saeys et al., 2007).

Previous research, e.g. (B. Merz et al., 2013; Schröter et al., 2014; Spekkers et al., 2014; Kreibich et al., 2017a) has emphasized a number of advantages of tree based algorithms for problems faced in flood loss modeling. First, the approach is non-parametric, thus assumptions concerning the covariance between explanatory variables and response variable are not needed. Second, non-linear and non-monotonic dependencies can be represented by a tree. Third, these algorithms can deal with heterogeneous data, i.e. a mixture of continuous and categorical variables, as well as incomplete data. Fourth, no assumptions about the independence of data are needed. However, tree based models require large data sets to detect and represent complex inter-relationships. Random Forests (RF, (Breiman, 2001) are one member of Tree-Based algorithms which make use of bagging predictors (Breiman, 1996) and have become popular across a broad range of disciplines due to its versatile applicability and efficient solution to multi-variable prediction problems facing complex interactions among variables with different scales (Huang and Boutros, 2016).

For the problem addressed in this study the method of RF is a suitable approach because it first provides a concept to estimate the importance of candidate explanatory variables and thus enables a well-founded selection of variables and second is an efficient algorithm to learn models with superior predictive performance even for data with more variables (p) than samples (n) (Genuer et al., 2010; Huang and Boutros, 2016). In this study we have applied the R package implementation `randomForest` by (Liaw and Wiener, 2002).

RF belongs to the family of ensemble methods: it uses many regression trees and strives to reduce the uncertainty associated with the selection of a single model, by aggregating an ensemble of alternative models. RFs are derived by generating many bootstrap

replicas of the data set and by growing a regression tree on each replica. At each node of a regression tree a subset of explanatory variables (m_{try}) is randomly chosen and the best split is determined within this subset. This distinguishes RF from the bagging tree method where all variables are considered at each split. Sub-setting the variables considered for each split enables a more diverse set of variables to contribute to the ensemble prediction. This also brings the advantage that the individual trees of the forest are less correlated than in the bagging approach, and thus are less biased. A bootstrap replica is generated by randomly drawing with replacement observations of the sample n . On average, 37% of observations are excluded for building an individual tree. These observations are called out-of-bag observations (OOB) and are used to evaluate the predictive performance of the tree in terms of the out-of-bag error. While OOB error evaluation supersedes the need for cross-validation, bootstrapping and a minimum number of five data points in a node makes RF robust against changes in data and avoids overfitting. The response of RF is an aggregation of the responses of all individual regression trees in the ensemble while the distribution of responses provides an estimate of model structure and input data related uncertainty.

Further, RFs include an efficient way for ranking candidate explanatory variables based on variable importance, and thus supports the selection of the most suitable variables for the development of predictive models. In the permutation based approach the RF algorithm estimates the importance of a variable by evaluating the increase of the prediction mean squared error when data for that variable is permuted in the OOB sample: the higher the increase, the more important the variable. This approach is popular due to its unconditional properties and as the algorithm is sensitive to informative variables and to relations among variables it supports the identification of relevant variables (Hapfelmeier and Ulm, 2013).

The underlying question for deriving a good predictive model is: how well does the model predict the target variable? To evaluate and compare the performance of the predictive models MSE is computed as the average squared deviation of the ensemble mean prediction and the out-of-bag observations as given in Eq. 12.1

$$MSE = \frac{1}{n} \sum_{i=1}^n (\bar{P}_i - O_i)^2 \quad (12.1)$$

With \bar{P}_i the ensemble mean prediction of observation i , O the observation i and n the number of observations.

Additionally, the mean bias error (MBE, Eq. 12.2) and the mean absolute error (MAE, Eq. 12.3) which give information about the accuracy and the precision of the model predictions are used as model performance criteria.

$$MBE = \frac{1}{n} \sum_{i=1}^n (P_{50_i} - O_i) \quad (12.2)$$

$$MAE = \frac{1}{n} \sum_{i=1}^n |P_{50_i} - O_i| \quad (12.3)$$

MBE and MAE are calculated using the median (P_{50}) of the predictive distributions of the Random Forest models. The distribution of responses available from the Random

Forest model offers additional information about the prediction uncertainty. We analyze this property using the 95-5-quantile range (QR_{90} , Eq. 12.4) and the hit rate (HR , Eq. 12.5) as indicators for sharpness and reliability of model performance, respectively (Gneiting and Raftery, 2007).

$$QR_{90} = \frac{1}{n} \sum_{i=1}^n (P_{95_i} - P_{5_i}) / P_{50_i} \quad (12.4)$$

$$HR = \frac{1}{n} \sum_{i=1}^n h_i ; h_i = \{ 1, \text{ if } O_i \in [P_{95_i}, P_{5_i}] 0, \text{ otherwise} \} \quad (12.5)$$

QR_{90} is a measure of sharpness of the prediction interval with smaller values representing smaller ranges of the model prediction interval. HR is an indicator for model reliability by quantifying the ratio of observations within the prediction interval defined by the 95 and 5 quantile range. The 95–5 quantile range corresponds to a nominal coverage of 0.9, and thus a HR=0.9 indicates that the coverage of model predictions is equal to the nominal coverage representing a perfect reliability of model prediction on this level.

12.3.2 Software and data availability

The model development of the 3dcfd module was implemented in R 3.4.1 (2017-06-30), using the attached packages scales 0.4.1, (Wickham, 2016), doParallel 1.0.10 (Analytics and Weston, 2015a), foreach 1.4.3 (Analytics and Weston, 2015b), hydroGOF 0.3.8 (Zambrano-Bigiarini, 2014), tidyr 0.6.1 (Wickham and Henry, 2017), stringr 1.2.0 (Wickham, 2017), dplyr 0.5.0 (Wickham et al., 2017a), reshape2 1.4.2 (Wickham, 2007), readr 1.1.1 (Wickham et al., 2017b), randomForest (Liaw and Wiener, 2002), ggplot2 4.6.12 (Wickham, 2009; Schloerke et al., 2017), _RODBC 1.3.15 (Ripley and Lapsley, 2017), RODBCext 0.3.0 (Zoltak et al., 2017). A prototype implementation for the case study Dresden is available online (Schröter et al., 2017); [doi:10.5880/GFZ.5.4.2017.001]). Further information can be obtained from the corresponding author of this paper.

12.4 Results

12.4.1 Variable selection

The RF implementation randomForest uses two parameters: *mtry*, the number of explanatory variables which are randomly chosen at each node, and *ntree* which defines the number of trees in the forest (Liaw and Wiener, 2002). As the variable importance derived by RF is sensitive to these parameters (Genuer et al., 2010), we pursue an averaging approach to derive stable results for variable importance as a basis to select the variables from the different data sub-sets for the predictive models. The averaging is carried out for the variable importance obtained from a set of random forests with different numbers of trees (*ntree* \in [500, 1000, 2000, 3000]) whereby each realisation of *ntree* has in turn been derived using three values for *mtry*: the default $p/3$ and the recommended lower and upper limits $p/6$ and $2p/3$ where p is the number of predictors in the dataset (Breiman, 2001). The motivation for this variation and averaging of variable importance is to identify the variables which are consistently important across a reasonable range of settings for the RF algorithm. The results for the normalized mean importance of the variables

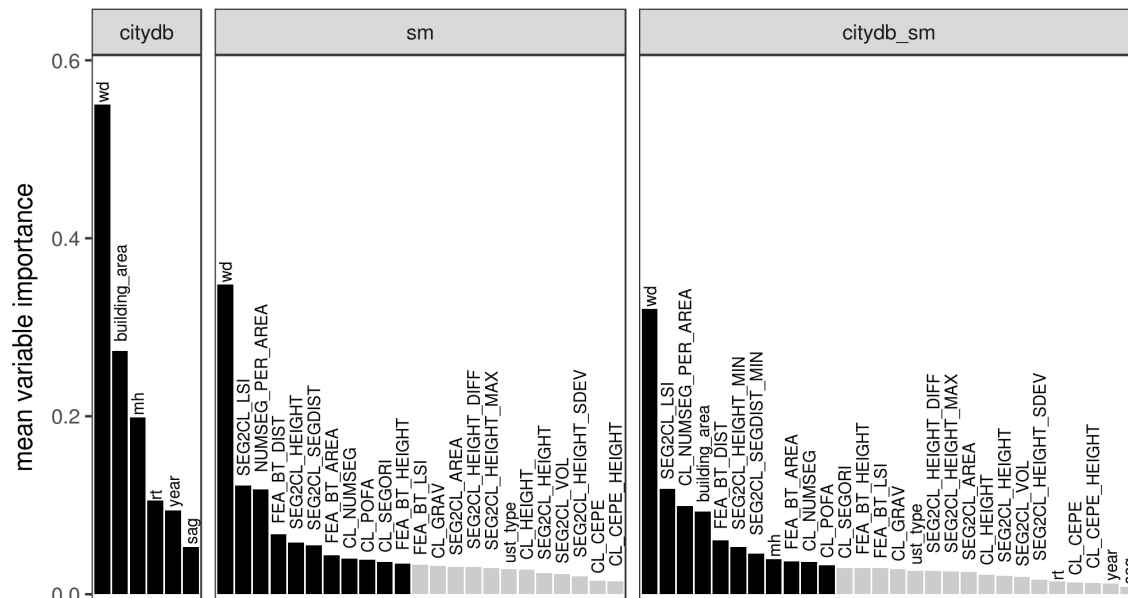


Figure 12.2: Ordered importance for building related variables for 3D City database and spatial measures data sub sets based on $n = 80$ observations including water depth from the cati data base. Top 10 important variables used for predictive modeling are colored black.

related to building characteristics from the different data sub-sets are summarized in Figure 12.2.

Water depth (emphwd) is the most important variable to explain flood loss in comparison to the other variables available from the different data sub-sets. The analysis of the citydb data sub-set results in a large importance of *building area* and *measured height (mh)*, followed by *roof type (rt)*. These variables are related to building characteristics as for instance the floor space which is a function of building footprint area and height or typical roof types for different building types. B. Merz et al. (2013) have shown that both building type and floor space are strongly correlated and that their relationship to relative building loss can be explained by the finding that single-family houses (with smaller floor spaces) have a higher loss ratio in comparison to multi-family houses (with larger floor spaces). From the spatial measures data sub-set the linear segment indicator (LSI) and the numbers of segments per area (NUMSEG_PER_AREA) achieve the highest importance for the estimation of relative flood loss. LSI is an indicator for the elongated shape of an area. Hence, the LSI for the roof areas of the building block provides information about the geometry of the building footprint which in turn provides proxy information for different building types, and/or building values. NUMSEG_PER_AREA describes the density of buildings in the area with higher numbers being an indicator for the presence of single family houses and lower number an indicator for multi-family houses. Again, this information may serve as a proxy for building types and related properties. This complements the findings of (Thieken et al., 2005; Gerl et al., 2014; Schröter et al., 2014) that the differentiation of building types is useful to explain flood

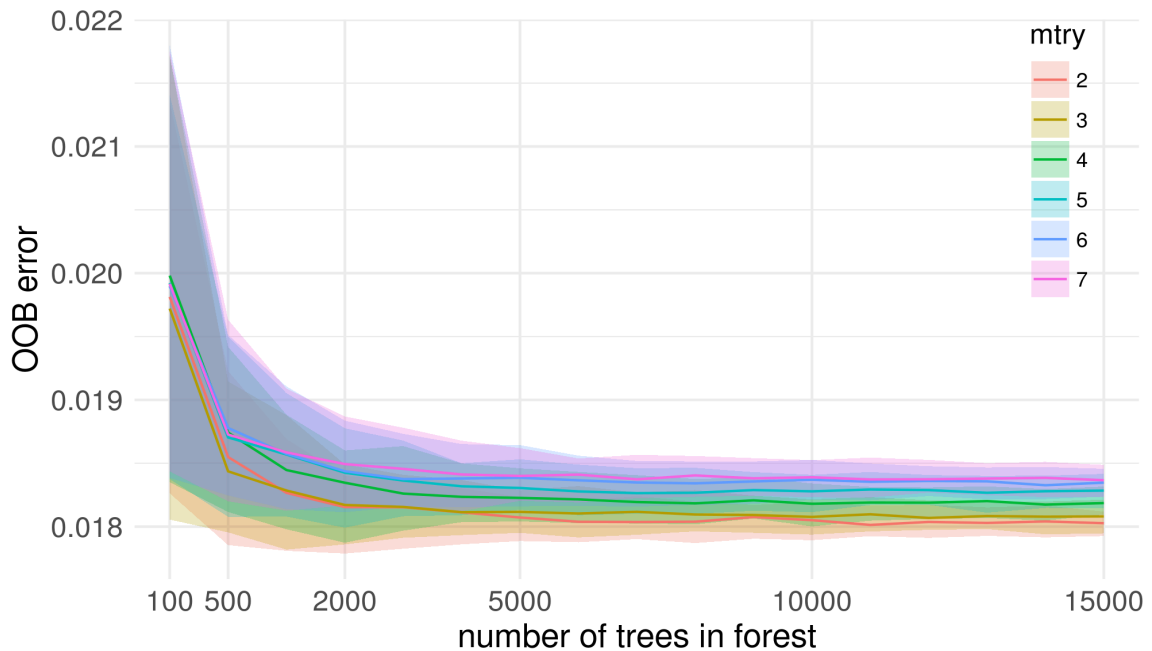


Figure 12.3: OOB error distributions of the citydb_sm data set for repeated simulations using different mtry values and increasing tree sizes

loss. The analysis of the combined data sets citydb_sm confirms the importance of LSI, NUMSEG_PER_AREA, and building area information.

12.4.2 Model derivation and evaluation

The analysis of variable importance indicates that the data sources citydb and sm contain variables which are informative for the estimation of flood loss. On that basis, the performance of predictive models for flood loss to residential buildings using these variables is examined. The derivation predictive flood loss models uses the top 10 important variables from the outcomes documented in Figure 12.2.

First the two parameters of the RF algorithm need to be optimized with the aim to find stable models. To this end we repeatedly ($i = 100$ repetitions) build random forests with different n_{tree} values ($n_{tree} \in [100, 500, 1000, \dots, 15.000]$) and varying values for $mtry$ ($mtry = \in [p/6, \dots, 2p/3]$), record the mean OOB error of i repetitions and see the number of trees where the OOB error asymptotically reaches a stable minimum. Figure 12.3 shows the 90-quantile range and the median of OOB distributions grouped for $mtry$ parameter values. For smaller forests ($n_{tree} < 500$) the variability of OOB is large but decreases with growing numbers of trees in the RFs. RF models with 6000 trees seem to achieve stable predictions. For RF models above this size, the parameter $mtry$ dominates the OOB error with optimum performance for $mtry = 2$ to 3 which is close to the recommended default value $p/3$ (for the data sub-set with $p = 11$ variables) (Liaw and Wiener, 2002).

On this basis we work with RF models with $n_{tree} = 6000$ and $mtry = p/3$ with p depending on the data sub-set used for learning predictive models for relative flood loss to residential buildings. Model performance is evaluated in terms of MSE, MAE, MBE,

Table 12.2: RF model performance using different data sub-sets with city DB and sm models also including water depth from the empirical data and icpr standard model performance, best performance values are marked bold

Model approach	mtry	MAE	MBE	MSE	QR	HR
cati complete	9	0.015	-0.009	0.0016	0.25	0.95
cati reduced	3	0.016	-0.008	0.0013	0.23	0.95
cityDB model	2	0.021	-0.011	0.0018	0.24	0.93
sm model	3	0.019	-0.009	0.0028	0.25	0.95
cityDB_sm model	3	0.014	-0.01	0.0017	0.26	0.97
sdf model	1	0.03	-0.003	0.0018	0.19	0.69
icpr model	-	0.135	-0.002	0.0481	NA	NA

QR₉₀, and HR for all observed relative loss values in the data sample (n=80). The performance of RF models to reproduce the learning data is reported in Table 12.2. As mentioned earlier bootstrapping and the minimum number of data points in a node avoids overfitting of RF models. Model performance for independent data within a leave-one-out cross validation procedure is reported subsequently.

The empirical survey data can be assumed to be the most comprehensive and most detailed set of information available for flood loss estimation to individual residential buildings (Thieken et al., 2007; B. Merz et al., 2013). Therefore, the models based on these data sub-sets (cati complete and cati reduced) represent upper benchmarks for the models based on standardized data sources. In contrast, the sdf model which uses only water depth as predictor for relative building loss is a lower benchmark for the models based on standardized data sources, because it is expected that using additional variables improves predictive model performance (Schröter et al. 2014). Further, we also include the icpr model in the comparison which is the standard model for flood risk management and planning of mitigation measures in the city of Dresden (Dresden, 2011). The icpr stage damage function ($relative_loss = (2_wd^2 + 2wd) / 100$) has been originally derived for regional risk assessment in the River Rhine (ICPR, 2001) and has been transferred without any further local adjustments to the city of Dresden in the Elbe catchment.

The RF models based on standardized data sources achieve comparable performance values as the models based on the cati complete and cati reduced data sets. In particular the citydb_sm model which uses both data from the 3D city database and the spatial measures outperforms the alternatives in terms of MAE and MSE. However, the citydb model achieves best scores in terms of QR and HR and thus provides smallest predictive uncertainty intervals in combination with most reliable predictions; recall that HR is evaluated using the 95–5 quantile range, and thus should ideally yield a nominal coverage of 0.9.

The sdf model shows inferior performance particularly in terms of MAE and MSE which indicates less accurate predictions. In contrast, for the sdf model the QR is underestimated in comparison to the other models as it is combined with a clearly smaller HR, which indicates that only 69% of the observations are within the QR₉₀ interval. This

is a signal for the predictions of the sdf model being less reliable than from the other models, which cover more than 90% of the observations. One explanation for this is the number of variables used in the sdf model and the other models: while the sdf model uses only water depth to predict relative loss to residential buildings, the other models use up to 10 additional variables which in turn reveal additional sources of uncertainty. Hence, the sharpness of the predictions is reduced resulting in larger quantile ranges, but as the results show, these predictions are more accurate and more reliable with HR close to the nominal coverage of 0.9. This insight supports similar findings by B. Merz et al. (2013), Schröter et al. (2014), and Wagenaar et al. (2017) that using additional variables improves the predictive performance of flood loss models and reliability. Both, the sdf model and icpr use only water depth as a predictor. In comparison, the sdf model yields clearly smaller MAE and MSE values which emphasizes the usefulness of local data to derive a flood loss model as also pointed out by Cammerer et al. (2013), and the increased flexibility of the RF approach to reflect underlying complexities in comparison to an analytical function (Wagenaar et al., 2017).

As a next step we investigate the performance of the models to predict independent data, i.e. data which is unused to derive the models. As the data sample with only 80 observations is rather small it is not sensible to conduct a split sample testing procedure. Instead, we follow a leave-one-out cross validation procedure to test the transferability of the models.

In this regard, the models are derived 80 times while excluding each time one of the records from the learning sample. For this independent data point we predict the relative building loss and evaluate the predictive performance in terms of MBE, MSE, and MAE. In this way, samples of performance values for the 80 model tests are obtained which are illustrated as box plots in Figure 12.4.

Again, the performance of the model based on standardized data sources is comparable the results of the cati based models. Both the citydb and citydb_sm models yield comparable results for MAE, MBE and MSE as well as in terms of median, inter quartile range, hinges, and outliers. The sdf model performs worse than the other models based on local data. Also the variability of sdf model performance is higher indicating less reliable model predictions in transfer applications. Similar to the performance values reported in, the icpr model performs clearly worse than the other models in particular regarding MAE and MSE. Obviously, models based on local data perform better than a model transferred from a different region which confirms the conclusions of Cammerer et al. (2013) and Schröter et al. (2014). In terms of MBE, the difference in performance of the icpr model is not that pronounced. This is due to the fact that for the given data sample, over and underestimation errors favorably cancel out.

Overall, the differences in model performance within the standardized data based approaches (citydb, sm, and citydb_sm) are rather small and it is impossible to conclude if one model is always better than all the others for all evaluation criteria. However, the results provide support for the hypothesis that standardized data sources provide useful information to describe the vulnerability characteristics of buildings for the estimation of flood losses to residential buildings with a comparable performance to models based on detailed empirical survey data. Hazard related information including inundation depth is still needed as an additional input variable.

For all models, the model performance boxplots show outliers, which indicate that

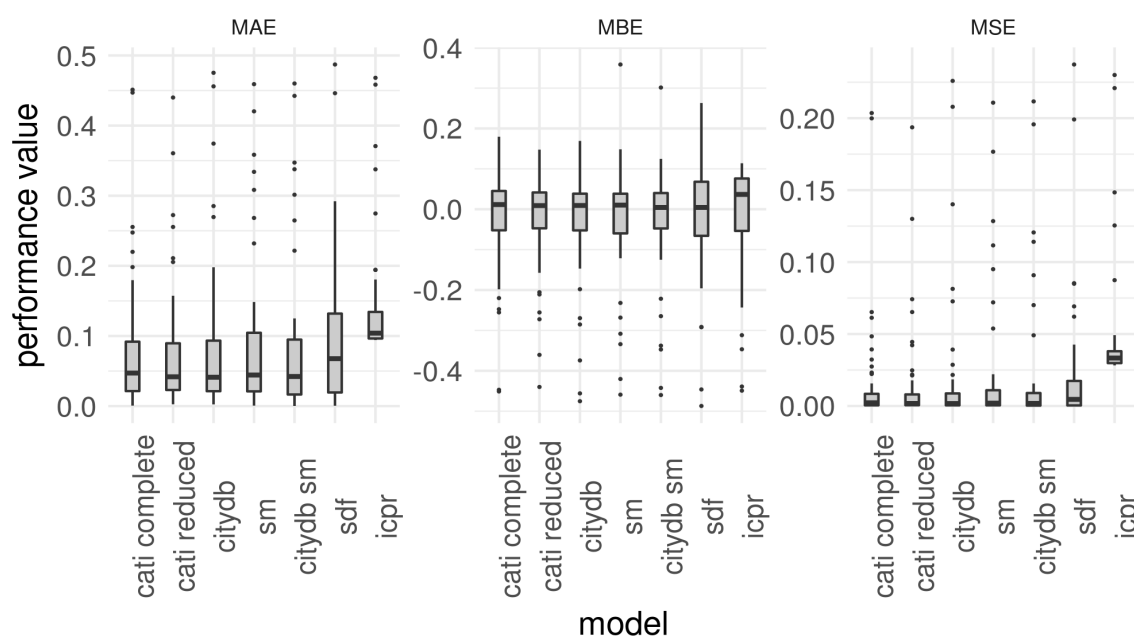


Figure 12.4: Model predictive performance in leave-one-out cross validation, median values for performance metrics are given as labels.

a number of observations cannot be reproduced by the models well. These cases apparently deviate from the overall relationships derived from the data which offer too little support for capturing these particularities and adequately representing them in the models. Recall that flood loss estimation on the micro-scale, i.e. on the level of individual buildings, is particularly challenging (Dottori et al., 2016), and as shown by B. Merz et al. (2013), given the large variability of individual objects is usually associated with large uncertainty. Neither the empirical survey data nor the standardized data used in this study do currently provide these details. In the future 3D city models could offer additional information, when data become available on higher levels of detail, i.e. LOD3 or LOD4. However, for current practical purposes the use of standardized data sources seems to enable flood loss estimation on a comparable level of performance as the empirical survey data. Further, 3D city models are readily available for urban areas and using the underlying standardized data for flood loss modeling will ease the spatial transfer of models. In addition, 3D city models also open for opportunities to embed risk oriented urban planning in these tools.

12.5 Prototype

12.5.1 Implementation

Beyond the usefulness of data about residential building characteristics for flood loss modeling, 3D city models offer additional possibilities to embed building vulnerability information into flood risk sensitive urban planning. This includes storing building related and other data in a standardized way, simulating urban and environmental processes and visualizing information (Gröger and Plümer, 2012). To demonstrate the

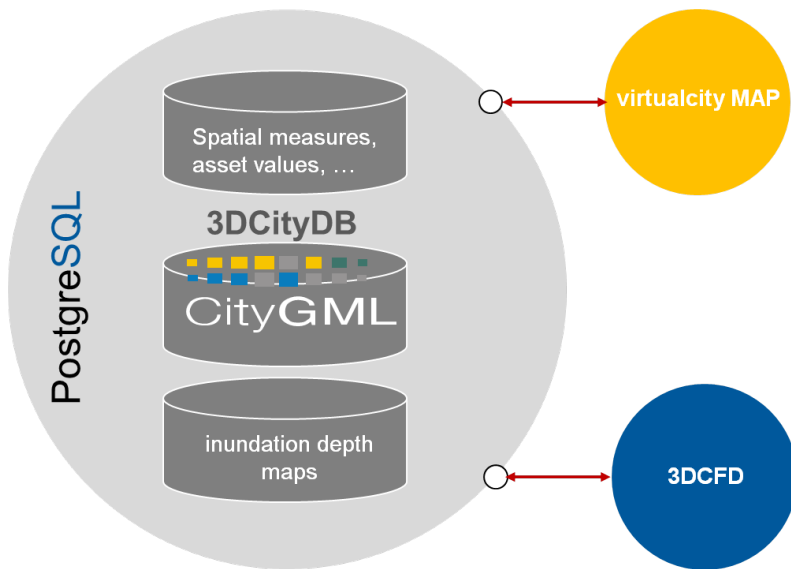


Figure 12.5: Prototype component diagram

functioning and utilization of 3D city models for flood risk assessment and management, the flood loss model 'citydb' derived in section 3.2 has been implemented as the 3D city flood damage module (3DCFD) to the 3D City Database (3DCityDB). The 3DCFD module is applied to the city of Dresden (Germany) as an example. The 3DCityDB is a free 3D geo database to store and manage 3D city models, which is implemented as a schema compliant to CityGML 2.0 for the relational database management systems PostgreSQL/PostGIS and Oracle (Kunde et al., 2013). Hence, the 3DCityDB enables the efficient management and processing of large city models. The components and links of the 3DCFD prototype implementation are shown in Figure 12.5.

The core of the PostgreSQL implementation form a number of database schema including the 3DCityDB which holds the geometrical, thematic, and generic attribute information of the 3D city model according to the CityGML standard. An additional schema contains further information about buildings like spatial measures or building asset values which are required for the calculation of economic loss. Further, spatial information about inundation extent and inundation depths are stored in a separate schema. The 3DCFD module is linked to the database using SQL queries. This module queries the attributes of the buildings affected by flooding and the inundation depths at the residential buildings for an inundation depth map of interest from the database. The result of this query provides the input to the flood loss model 'citydb', i.e. the RF flood loss model derived in section 12.3.2. The 3DCFD module calculates the relative loss for each affected building and returns them to the database where they are added to the features of the specific buildings using generic attributes. The concept of generic attributes allows extending CityGML applications during runtime by providing a name, a data type and a value. Thus, it is possible to add attributes that are not explicitly modeled in CityGML without changing the schema (Gröger and Plümer, 2012). Loss modeling in combination with high resolution visualization allows identifying those buildings which should be protected with precautionary measures which is an important component of flood prevention and risk management concepts.

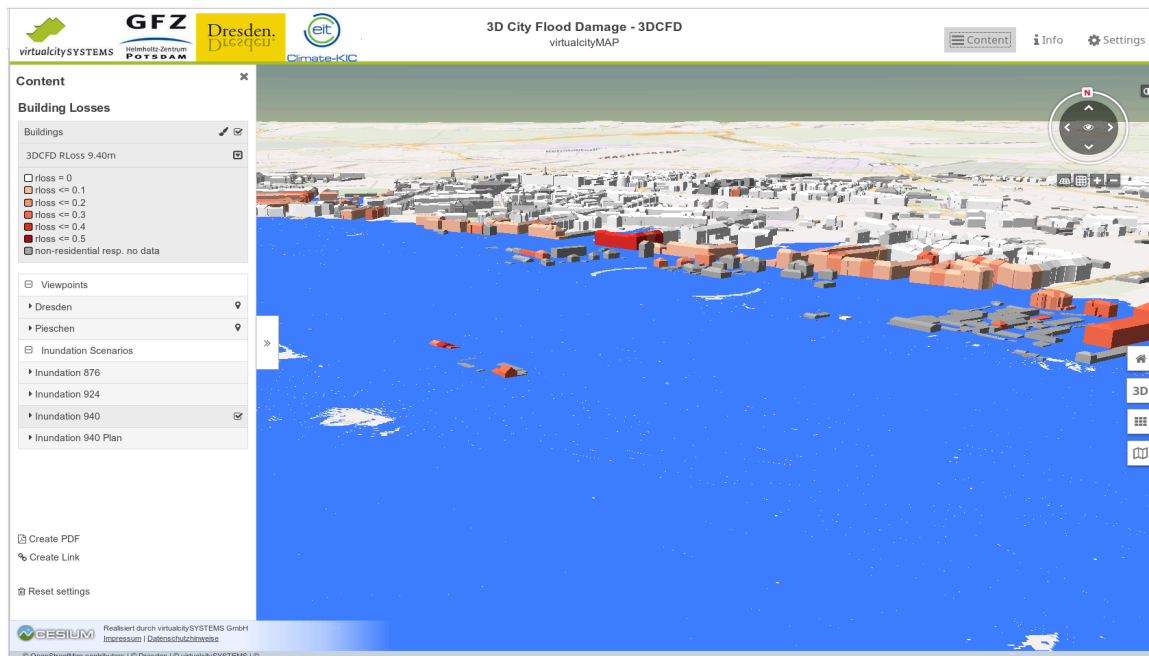


Figure 12.6: 3DCFD online prototype implementation showing the inundation area for the flood scenario 9.4 m in Dresden with color coded residential buildings according to relative building loss.

The prototype implementation demonstrates the functioning using the 3DCFD module as an example. Driven by the idea to provide a flexible framework, alternative simulation modules can be linked to the database. Hence, similar to the 3DCFD module any other flood loss model which uses input data provided by the database can be linked to the framework using appropriate SQL queries. Further processing of the data to calculate economic losses to residential buildings as the product of relative loss and building asset values is straightforward and can be easily conducted using spatial SQL queries or GIS software tools.

In addition, the prototype offers functionalities to visualize the loss estimation results and the underlying data in an interactive web framework (virtualcityMAP). The user may browse through the 3D city model, colorize the residential buildings regarding their relative damage values caused by different flooding scenarios, and get detailed information for individual buildings, see Figure 12.6. This prototype application is based on the virtualcityMAP technology. It contains an integrated viewer for oblique images, 2D and 3D maps. The virtualcityMAP can be used from any computer or workstation with a modern browser which enables the execution of JavaScript and WebGL. WebGL is an API for rendering 3D computer graphics within a browser without the use of plugins; see Schröter et al. (2017) for an online version of the prototype.

12.5.2 Application example Dresden

The 3DCFD module is used to estimate flood loss to residential buildings for three flood scenarios within the focus area of Pieschen in Dresden (see Figure 12.1). The flood scenarios are defined in terms of water levels above the Dresden gauge datum (112.3 m):

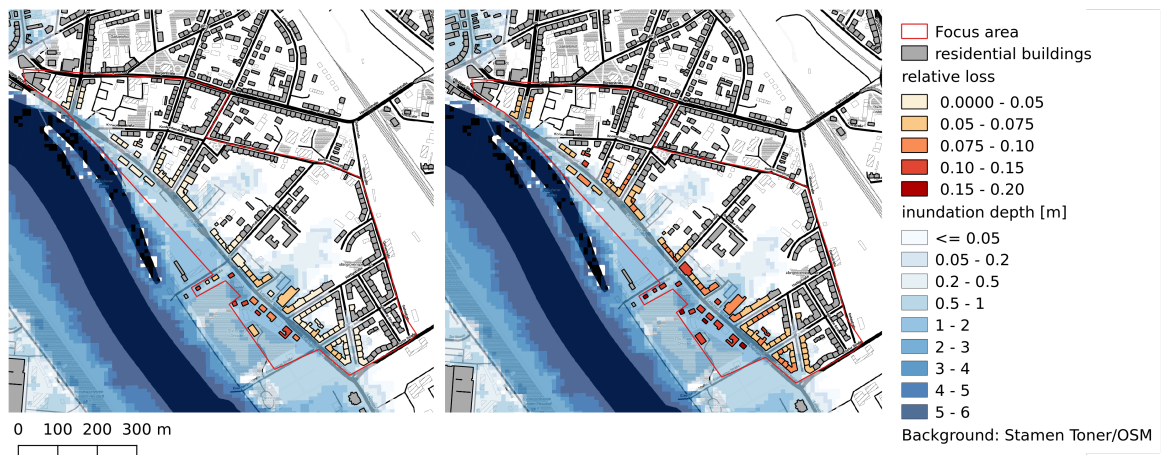


Figure 12.7: Relative loss estimates for residential buildings in the focus area Pieschen for 9.4 m flood scenario: left panel icpr model, right panel citydb model

8.76 m which correspond to the June 2011 flood (50 years return period), 9.24 m, which is the statistically expected 1% (1 in 100) years flood, and 9.40 m which has been registered during the August 2002 flood (approx. 200 years return period). The 3DCFD loss estimation results are compared with the outcomes of the icpr model on the level of individual buildings (in total 272 residential buildings) as well as on the aggregated level of the entire focus area (33.6 ha). Figure 12.7 illustrates the inundation depth and the resulting relative losses to the buildings affected in the Pieschen area for the 9.4 m flood scenario which affects 95 residential buildings with maximum inundation depths of 1.5 m.

As can be seen by the color codes of the affected buildings, the icpr model tends to predict lower relative damages than the citydb model. To illustrate this point, Figure 12.8 compares the relative loss estimates of both models as a function of inundation depth. The citydb model consistently estimates higher loss ratios than the icpr model with a more pronounced difference (ca. 0.05) for inundation depths values below 0.5 m. The plot also shows the relative loss values and inundation depths from the cati data set for the whole Dresden area but limited to the range of inundation depths present in the Pieschen focus area for the flood scenarios.

The citydb model nicely reproduces the mean of the empirical relative loss values along the range of inundation depths which is approximated by a spline interpolation (grey line in Figure 12.8) without taking the outliers into account. As the citydb model uses additional variables like building area and measured height, it reproduces parts of the variability of relative loss for comparable inundation depths which is also visible for the cati data.

The implications of these differences in relative loss estimates on the estimation of risk in terms of the expected annual damage (EAD) are investigated for the Pieschen focus area. For the calculation of economic loss the regional values for residential building stock derived by Kleist et al. (2006) are disaggregated to the level of individual buildings. The product of relative loss and building value yields an estimate for the economic loss in terms of the reinstatement costs for the affected buildings in the different flood scenar-

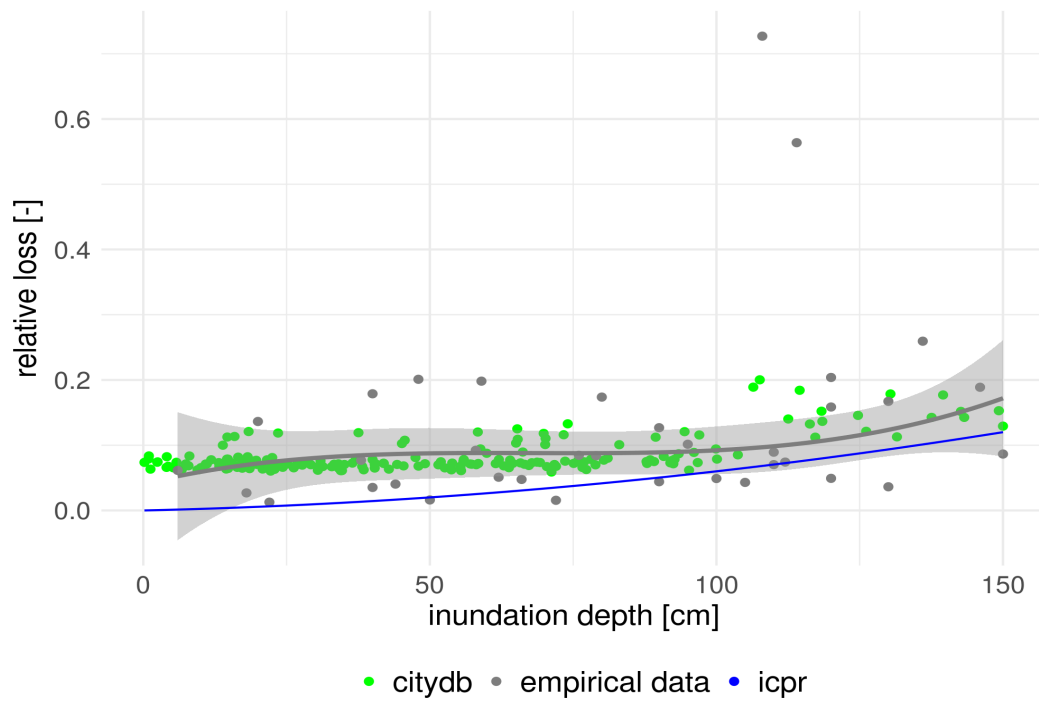


Figure 12.8: Relative loss to residential buildings as a function of inundation depth in the Pieschen focus area for different inundation scenarios using icpr and citydb flood loss models, empirical data are from the cati surveys for the whole Dresden area. The grey line is a spline approximation with standard errors to the cati data (neglecting the outliers).

Table 12.3: Flood loss to residential buildings in the focus area Pieschen for different flood scenarios using icpr and citydb flood loss model

Flood scenario	approx. Flood probability	Loss icpr model [EUR]	Loss citydb model [EUR]
9.4	0.005	3,611,000	7,928,000
9.24	0.01	2,245,000	6,848,000
8.76	0.02	629,000	3,940,000
EAD		33,200	118,000

ios, Table 12.3. EAD is calculated as the probability weighted sum of losses for different flood scenarios. Probability weights are defined as the differences of flood probabilities (inverse of return period) between different flood scenarios.

The differences in economic losses for both models are considerable. Notably, larger differences occur for higher probable flood scenarios which are associated with smaller inundation depths where the differences in the loss models are most distinct. This directly translates into considerable deviations in the calculation of the EAD as the probability weighted mean of loss incurred for discrete flood scenarios (Kaplan and Garrick, 1981). Using the citydb model instead of the icpr model yields a difference of a factor 3.5 in EAD which results in a substantially different assessment of investments in flood mitigation measures. These findings are in line with the results published by (Wagenaar et al., 2016) and underline the high relevance of flood loss model uncertainty in risk assessments. In this respect, the 3DCFD prototype makes a contribution to overcome the reluctance to use more sophisticated and complex modeling approaches instead of overly simplified models either due to convenience and/or lower efforts.

12.6 Discussion

Flood loss modeling on the micro scale, i.e. on the level of individual buildings, is important to optimize investments for the implementation of flood risk management concepts in urban areas. The application and even more the spatial transfer of multi-variable flood loss models are challenging, because input data need to be available with high spatial detail. Standard data sources may ease the set-up of flood loss models and spatial transfer.

3D city models can store detailed information of building locations and building characteristics. However, presently 3D city models mostly include information only on LOD1 or LOD2 which corresponds to geometric building information. Therefore, numerical spatial measures derived from remote sensing data are another promising standardized data source to feed flood loss models. This paper investigates the potential of 3D city models and numerical spatial measures to support the estimation of flood losses to residential buildings. The study is carried out in the city of Dresden where data on relative flood losses and inundation depths are available from empirical surveys which can be used to derive and to validate new flood loss models. For this purpose Random Forests are used to first analyze the usefulness of variables available from 3D city models and re-

remote sensing based spatial measures and to identify the most important ones to explain flood loss.

The sample size of 80 available data points for the study may influence the outcomes of variable importance and predictive model performance analyses. On the one hand it is possible that the Random Forest does not find any reasonable splits in the data space, and thus does not provide any meaningful predictions. On the other hand it may overfit the data and achieve overly optimistic performance results. The study includes several steps to reduce these potential influences. First bootstrapping i.e. using only a subset of data to learn an individual tree of the forest, a minimum number of five data points per node, and a limited number of candidate variables for each split effectively reduce overfitting. Second, within the leave-one-out cross-validation procedure model predictive performance is tested against independent data. Third, the models derived are assessed using more complex data sets for model learning and a simple standard flood loss model as benchmarks. The performance of the models using standardized input data ranges between both benchmarks.

The acid test for the derived flood loss models will be the application and performance testing in another city. In this context, the ability to assimilate local data will be an interesting question to answer.

For practical applications the trade-off between number of input variables, model performance and effort to collect input data needs further investigation. In our study we assumed that all input data are readily available with the 3D city model. Also, the various spatial measures are derived from remote sensing using automated classification algorithms. Therefore, we assume that all variables will be generated within the same data processing operation. However, the collection of individual variables may require substantial efforts. Therefore, the knowledge about their relevance/importance for loss modeling is valuable to set priorities.

The exemplary calculation of the expected annual damage within the application case in the city of Dresden shows the potential effects of model biases on the outcomes of economic assessments and decisions about efficient measure. This emphasizes the importance of model validation and selection. In this regard, the information about predictive uncertainty provided by the predictive distribution of Random Forests offers additional possibilities for quantifying the reliability of model predictions. How this additional information can be used to support decision making and how it can be visualized to illustrate and communicate uncertainty are interesting questions for following research. Overall the 3D city model based technology shows good opportunities to use more sophisticated and complex modeling approaches by exploiting available data sources.

Beyond that, 3D city models also open for opportunities to embed building vulnerability information into flood risk sensitive urban planning including the storage of a variety of ancillary information, simulation of urban and environmental processes and visualization. Concerning simulations, the use of building geometries as boundary conditions for hydro-numerical simulation of flood dynamic processes is obvious. Concerning visualization, this tool provides large potential to increase transparency in risk assessment, to support the identification of damage hotspots as well as to improve risk communication and raising awareness.

12.7 Conclusions

The assessment of variable importance reveals that those variables of standardized data sources which provide information about building geometric properties such as building area, height, roof type, shape, and density of buildings are most suitable to explain flood loss. All these variables are directly or indirectly linked to different building types and associated characteristics.

Predictive flood loss models are derived using a set of important variables. Model validation confirms that using multiple variables for flood loss modeling improves the predictive performance and reliability. The results also show that standardized data sources provide useful information for the estimation of flood losses to residential buildings. For current practical purposes the use of standardized data sources enables predictive flood loss modeling with a comparable performance as modeling based on detailed empirical survey data.

Further, 3D city models are readily available for urban areas and using the underlying standardized data for flood loss modeling will ease the spatial transfer of models. In the future, even more can be expected from 3D city models, when data become available on higher levels of detail, i.e. LOD3 or LOD4, which provides details about building openings, sill level heights and building internal facilities.

13 | Multi-model ensembles for assessment of flood losses and associated uncertainty

Manuscript Info

Authors information:

Rui Figueiredo
Kai Schröter
Alexander Weiss-Motz
Mario L.V. Martina
Heidi Kreibich

Published as:

Figueiredo R., Schröter K.,
Weiss-Motz A.,
Martina M.L.V., Kreibich H.
Multi-model ensembles
for assessment of
flood losses and
associated uncertainty
Nat. Hazards Earth Syst. Sci.
2018;18,5:1297-1314.
doi:10.5194/nhess-18-1297-
2018

Abstract

Flood loss modelling is a crucial part of risk assessments. However, it is subject to large uncertainty that is often neglected. Most models available in the literature are deterministic, providing only single point estimates of flood loss, and large disparities tend to exist among them. Adopting any one such model in a risk assessment context is likely to lead to inaccurate loss estimates and sub-optimal decision-making. In this paper, we propose the use of multi-model ensembles to address these issues. This approach, which has been applied successfully in other scientific fields, is based on the combination of different model outputs with the aim of improving the skill and usefulness of predictions. We first propose a model rating framework to support ensemble construction, based on a probability tree of model properties, which establishes relative degrees of belief between candidate models. Using twenty flood loss models in two test cases, we then construct numerous multi-model ensembles, based both on the rating framework and on a stochastic method, differing in terms of participating members, ensemble size and model weights. We evaluate the performance of ensemble means, as well as their probabilistic skill and reliability. Our results demonstrate that well-designed multi-model ensembles represent a pragmatic approach to consistently obtain more accurate flood loss estimates and reliable probability distributions of model uncertainty.

13.1 Introduction

Effective management of flood risk requires comprehensive risk assessment studies that consider not only the hazard component, but also the impacts that the phenomena may have on the built environment, economy and society (Messner et al., 2006). This integrated approach has gained importance over recent decades, and with it so has the scientific attention given to flood vulnerability models describing the relationships between flood intensity metrics and damage to physical assets, also known as flood loss models. A large number of models have become available in the scientific literature. However, despite progress in this field, many challenges persist in their development, and flood loss models tend to be quite heterogeneous. This often results in practical difficulties when they are to be applied in risk assessment studies (Gerl et al., 2016; Jongman et al., 2012), as described below.

Flood damage mechanisms are complex, being dependent on different properties of flood events, such as water depth, flow velocity and flood duration, as well as on the physical characteristics of the exposed assets (Kelman and Spence, 2004). Precautionary and socio-economic factors can also influence their degree of vulnerability (Thieken et al., 2005). Building accurate and reliable flood loss models that account for all these factors is a challenging task. Model development is hampered by limited knowledge about damage-influencing factors, as well as limited data availability (B. Merz et al., 2010b). It is therefore unsurprising that traditional flood loss models tend to be rather simple, often using water depth as the only explanatory variable to describe damage and loss to coarsely defined groups of assets (Green et al., 2011; D. Smith, 1994). However, the limited predictive ability and high degree of uncertainty associated with such models has been acknowledged (Krzysztofowicz and Davis, 1983; B. Merz et al., 2004), and more complex models that consider additional explanatory variables have been developed (Dottori et al., 2016; Elmer et al., 2010; B. Merz et al., 2013). Regardless, uncertainty in flood loss modelling is to some extent inevitable (Schröter et al., 2014).

Furthermore, flood loss models are usually developed for specific regions, ranging from country to catchment or municipality level, with smaller scales making up the majority of models (Gerl et al., 2016). Lack of available flood loss models in many regions often leads to the transfer of models in space, resulting in their application to contexts with different built environments and/or socio-economic settings than originally intended. However, this is generally done with insufficient justification, and flood loss models have been shown to offer lower predictive ability under such circumstances (Cammerer et al., 2013; Jongman et al., 2012; Schröter et al., 2014).

In addition, flood loss models are most often constructed for specific flood types (e.g. fluvial flood, flash flood, coastal flood), and will usually be poorly suited to estimate loss due to flood events with other dominant damaging processes (Kreibich and Dimitrova, 2010; Kreibich and Thieken, 2008). Models also vary in the way loss is expressed, which can be either in monetary terms or as a fraction of the value of the element at risk (Messner et al., 2007). These are referred to respectively as absolute and relative flood loss models, the latter being better suited than the former for application across different study cases (Krzysztofowicz and Davis, 1983). Further differences may exist in terms of other model attributes.

Due to this large heterogeneity, it is difficult to identify flood loss models that, given

their attributes, are potentially the most appropriate for application in specific risk assessment studies. Ideally, for any given application setting, a perfectly suited model (e.g. similar type of asset, no spatial transferability required, validated with local evidence) would be available and unambiguously identifiable, but unfortunately, this is far from the case. The lack of an established procedure to select suitable flood loss models from the many available in the literature means that model selection is often done rather arbitrarily (Scorzini and Frank, 2017), which can negatively impact the quality of flood loss estimations and lead to suboptimal investment decisions based on model outcomes (Wagenaar et al., 2016).

A critical issue in flood loss modelling is uncertainty (B. Merz et al., 2004), which is usually high and can significantly contribute to overall uncertainty in flood risk analyses (Moel and Aerts, 2011). Model uncertainty is mainly related with parameter representation, whereby fewer parameter than those theoretically needed to describe physical damage processes are used, and with insufficient data and/or knowledge about damage processes (Wagenaar et al., 2016). Quantifying uncertainty is imperative, as this information is required to make informed decisions in the context of flood risk management (M. W. Downton et al., 2005; Peterman and Anderson, 1999; USACE, 1992). However, the vast majority of flood loss models currently available in the literature are deterministic (Gerl et al., 2016), providing single point estimates of loss. Such estimates are unable to meet the decision needs of different stakeholders, who may have differing risk attitudes or cost-benefit ratios for risk mitigation measures (B. Merz and Thielen, 2009). Moreover, the uncertain nature of flood loss estimations means that the performance of any given deterministic model that appears appropriate for a certain application can be limited, as large disparities may exist even among seemingly comparable models (Jongman et al., 2012; B. Merz and Thielen, 2009). This makes flood risk estimates highly sensitive to loss model selection (Apel et al., 2009; Wagenaar et al., 2016). It is thus clear that adopting a single deterministic model for the estimation of flood losses is not recommended, as the information it provides is insufficient for optimal decision-making, and the results will potentially, and very likely, be inaccurate. Even though research on flood loss modelling has recently started to move into the probabilistic domain (Custer and Nishijima, 2015; Dottori et al., 2016; Schröter et al., 2014; K. Vogel et al., 2012; Kreibich et al., 2017a), probabilistic models are still scarce.

Multi-model ensembles have been successfully applied in scientific fields such as hydrology or weather forecasting to tackle similar issues to those discussed above. Ensemble means have been shown to almost always outperform individual models (Georgakakos et al., 2004; Gleckler et al., 2008; Reichler and J. Kim, 2008), and the combination of the output of different models can be a pragmatic approach to estimate model uncertainty (Palmer et al., 2004; Weigel et al., 2008). However, in the context of vulnerability modelling, the concept of combining multiple models is relatively new. Rossetto et al. (2014) and Spillatura et al. (2014) have proposed the use of mean model estimates as part of their studies on respectively fragility and vulnerability curves for seismic risk assessment, but model performance is not evaluated and uncertainty quantification is not discussed. The potential use of multi-model ensembles in flood vulnerability assessment has not been addressed before.

This study therefore aims to answer the following research questions:

1. Can multi-model ensembles be used to improve the accuracy of flood loss estimations?
2. Are multi-model ensembles able to represent model uncertainty and provide reliable probabilistic estimates of flood loss?
3. How should such ensembles be constructed?

We first propose a framework to rate flood loss models according to their potential skill and suitability as participating members in such ensembles. We then construct various multi-model ensembles, based both on the rating framework and on a state of simulated non-informativeness, differing in terms of participating members, ensemble size, and weighting criteria, and evaluate their performance. Twenty flood loss models available in the literature are adopted, and losses are modelled for residential buildings in two application cases, corresponding to flood events that took place in Germany in 2002 and in Italy in 2010. Based on the results, which are shown and discussed in Section 13.3, conclusions are drawn regarding the application of multi-model ensembles in flood loss estimations.

13.2 Setup of validation exercise

13.2.1 Flood loss models

The flood loss model catalogue developed by Gerl et al. (2016) was used as the basis for model selection in this study. We first identified all deterministic models describing loss to residential buildings, and then excluded models based on following criteria:

- The documentation is insufficient for model implementation;
- The model uses explanatory variables that are not available in most practical applications;
- The model has a functional form that is considered inappropriate (e.g. too simplistic or discretised);
- The model is based on the same dataset as another model deemed more appropriate for the application settings (this is to ensure model independence and avoid potential biases in the resulting ensembles).

Based on this procedure, twenty deterministic flood loss models for residential buildings were adopted. The catalogue developed by Gerl et al. (2016) provides information on the properties of each model, which is necessary to assess model suitability according to the framework proposed in Section 13.3.1. Table 13.1 shows the model properties relevant for this study, as well as the corresponding references, where model formulations can be consulted.

Each model is implemented to compute flood losses for the two application cases described in Section 13.2.3, for which the available hazard and exposure data are shown in

Table 13.1: Models included in this study, including some of their properties

Name	Hazard variables *	Exposure variables**	Country	Region/Catchment	Flood type	Damage metric	Reference
ANUFlood	wd	fa	Australia	-	fluvial	absolute	(DNRM, 2002)
Budiyono	wd	bt	Indonesia	Ciliwung River	fluvial	relative	(Budiyono et al., 2014)
DSM	wd	bt	The Netherlands	-	fluvial, coastal	relative	(Klijn et al., 2007)
Dutta	wd	str	Japan	Ichinomiya river basin, Chiba prefecture	fluvial	relative	(Dutta et al., 2003)
FLEMO	wd, con, rp	bt, bq, pre	Germany	Elbe, Danube	fluvial	relative	(Elmer et al., 2010)
HAZUS-MH	wd	bt, nf, bas	USA	-	fluvial, coastal	relative	(Scawthorn et al., 2006)
HOWAS	wd	bt, bas	Germany	-	fluvial	absolute	(Buck and Merkel, 1999)
HWS-GIS	wd	-	Germany Switzerland,	Lippe	fluvial	relative	(Hydrotec, 2002)
ICPR	wd	-	Germany, France, Netherlands	Rhine	fluvial	relative	(ICPR, 2001)
IKSE	wd	-	Germany	Elbe	fluvial	relative	(IKSE, 2003)
Luino	wd	-	Italy	Boesio basin, in the Lombardy Region	fluvial	relative	(Luino et al., 2009)
MCM	wd, id	bt	England, Wales	-	fluvial, coastal	absolute	(Penning-Rowse et al., 2005)
MERK	wd	nf, bas	Germany	Coast of Schleswig-Holstein	coastal	relative	(Reese et al., 2003)
Pistrika and Jonkman	wd, fv	-	USA	Mississippi River	fluvial, levee breach	relative	(Pistrika and Jonkman, 2010)
Riha and Marcikova	wd, id	bt, oth	Czech Republic	-	fluvial	relative	(Riha and Marcikova, 2009)
Toth	wd	bt, str, nf	Hungary	Körös corner flood area	fluvial	relative	(Tóth et al., 2008)
TYROL	wd	-	Austria	Tyrol	fluvial	absolute	(Huttenlau et al., 2010)
Vanneuville	wd	bt	Belgium	-	fluvial	relative	(Vanneuville et al., 2006)
Vojinovic	wd	fa	St Maarten	-	fluvial	absolute	(Vojinovic et al., 2008)
Yazdi and Neyshabouri	wd	-	Iran	Kan basin	fluvial	relative	(Yazdi and Salehi Neyshabouri, 2012))

* Hazard variables: wd: water depth; fv: flow velocity; id: inundation duration; con: contamination; rp: return period. ** Exposure variables: bt: building type; str: building structure; bq: building quality; nf: number of floors; bas: presence of basement; fa: floor area; pre: precautionary measures.

Table 13.2. This consists in the largest to date application of different flood loss models within the scope of a scientific study on flood risk. In the estimation of losses for each asset, the best-matching function from each model is selected. In cases where this cannot be done unambiguously (e.g. due to mismatch in asset description between the exposure dataset and the model documentation), the selection is based on expert judgement. When models do not use some of the available hazard or exposure data, the unused variables are not considered. Losses given in absolute terms are adjusted for inflation. The modelled losses are provided as supplementary material.

13.2.2 Evaluation methods

Deterministic predictions

The predictive performance of single loss models and ensemble means is evaluated in terms of accuracy and systematic bias, using respectively the root mean squared error (RMSE) and the mean bias error (MBE). These are given by

$$RMSE = \sqrt{\frac{1}{n} \sum_{i=1}^n (\hat{X}_i - X_i)^2} \quad (13.1)$$

and

$$MBE = \frac{1}{n} \sum_{i=1}^n (\hat{X}_i - X_i), \tag{13.2}$$

where \hat{X} is a vector of n predictions and X is the vector of observed values of flood loss.

Ensemble predictions

The probabilistic skill of ensembles is evaluated using the continuous ranked probability score (CRPS), which is defined as the integrated squared difference between the cumulative distributions of predictions and observations (Weigel, 2011). We adopt the expression for the CRPS derived by Hersbach (2000), which is described as follows. Consider a set of n elements affected by a flood with corresponding observed losses x_1, \dots, x_n . Let there be m ensemble members, and let $\hat{x}_{t,i}$ be the prediction of loss given by i^{th} ensemble member for the t^{th} element, sorted in ascending order. Define $\hat{x}_{t,0} = -\infty$ and $\hat{x}_{t,m+1} = +\infty$. The CRPS is given by

$$CRPS = \frac{1}{n} \sum_{t=1}^n \left[\sum_{i=1}^m \alpha_{t,i} \left(\frac{i}{m} \right)^2 + \sum_{i=0}^{m-1} \beta_{t,i} \left(1 - \frac{i}{m} \right)^2 \right] \tag{13.3}$$

where

$$\alpha_{t,i} = \{ 0 \text{ if } x_t \leq \hat{x}_{t,i} \text{ or } x_t - \hat{x}_{t,i} < \hat{x}_{t,i} - \hat{x}_{t,i-1} \text{ or } x_t - \hat{x}_{t,i} < \hat{x}_{t,i+1} - \hat{x}_{t,i} \}$$

and

$$\beta_{t,i} = \{ \hat{x}_{t,i+1} - \hat{x}_{t,i} \text{ if } x_t \leq \hat{x}_{t,i} \text{ or } x_t - \hat{x}_{t,i} < \hat{x}_{t,i+1} - \hat{x}_{t,i} \text{ or } x_t - \hat{x}_{t,i} < \hat{x}_{t,i+1} - \hat{x}_{t,i} \}$$

The CRPS can be interpreted as an error measure, with lower values corresponding to higher probabilistic skill.

To assess ensemble reliability (i.e. whether ensemble predictions and observations are statistically indistinguishable), the rank histogram is adopted, which is constructed as follows. Consider an m -member ensemble prediction $\hat{x} = (\hat{x}_1, \dots, \hat{x}_m)$ and a corresponding observation x . The rank of x in relation to the ensemble members of \hat{x} is given by $r = M + 1$, where M is the number of ensemble members that x exceeds ($M \leq mi$). For example, if x is smaller than all ensemble members, the observation has rank $r = 1$, while if x exceeds all ensemble members, then $r = m + 1$. If an ensemble is reliable, for a set of n prediction-observation pairs there should be $n/(m + 1)$ observations with each $m + 1$ possible rank values, i.e. the histogram should be flat. Systematic deviations from flatness can indicate deficiencies in terms of ensemble dispersion and bias. Note that no ensemble is perfectly reliable, and random deviations from flatness are expected due to sampling uncertainty (Talagrand et al., 1997; Weigel, 2011).

13.2.3 Application cases

2002 flood along the Mulde River, Germany

Floods are a recurring natural hazard in the Mulde catchment (7,400 km²) located in Saxony, Germany. In recent years, this area has been severely affected by the June 2013 and August 2002 floods (Engel, 2004; B. Merz et al., 2014a). The latter was triggered by record-breaking precipitation amounts in the Ore Mountains, which form the headwaters of the Mulde River. At the Zinnwald-Georgenfeld station, operated by the German Weather Service, 312 mm of rainfall were recorded within 24h (Ulbrich et al., 2003a). The flood caused many dike breaches and resulted in considerable loss in 19 Saxonian municipalities along the Mulde (Figure 13.1).

The data used for this application case are listed in Table 13.2, and the results of individual model applications in terms of error statistics are shown in Table 13.3. The flood extension and water depths were estimated through hydro-numeric simulations (Apel et al., 2009) and hydraulic transformation (Grabbert, 2006). Return periods of flood peak discharges were derived from annual maximum series of mean daily discharges by (Elmer et al., 2010). For the estimation of contamination indicators, inundation durations, flow velocity indicators and precautionary measures indicators, computer aided telephone interviews with affected households have been used (Thieken et al., 2005). The average floor areas of residential buildings and average building values are based on official statistical data about total living area for different types of residential buildings per district, and standard construction costs per square meter gross floor area (Kleist et al., 2006). Asset values with a spatial resolution corresponding to the inundation map (i.e. 10x10 m²) have been derived by applying a binary disaggregation method and using the digital basic landscape model ATKIS as ancillary information (Wünsch et al., 2009). Residential building type composition and mean residential building quality per municipality were derived by (Thieken et al., 2008b) using geo-marketing data from INFAS GEOdaten GmbH from 2001. Flood losses to residential buildings have been documented by the Saxon Relief Bank on the municipality level (SAB, 2005) and amount to a total of EUR 240.6 million. For more details, see Kreibich et al. (2017a).

2010 flood in Caldogno, Italy

From 31 October to 2 November 2010, the Veneto Region was affected by persistent rain, particularly in the pre-Alpine and foothill areas, with accumulated rainfall exceeding 500 mm in some locations (Veneto, 2011a). This caused multiple rivers to overflow, resulting in floods that inundated an area of 140 km² and had a considerable human and economic impact. Three people lost their lives and 3500 had to evacuate their homes. Flood losses to residential, commercial and public assets were estimated to be 426 million Euro. Caldogno, a municipality with a population of about 11 000 located in the province of Vicenza, was among the most affected, with reported losses to those sectors reaching EUR 25.7 M (Veneto, 2011b). In this study, we adopt it as the second application case (Figure 13.2).

The data used for this application case are listed in Table 13.2, and the results of

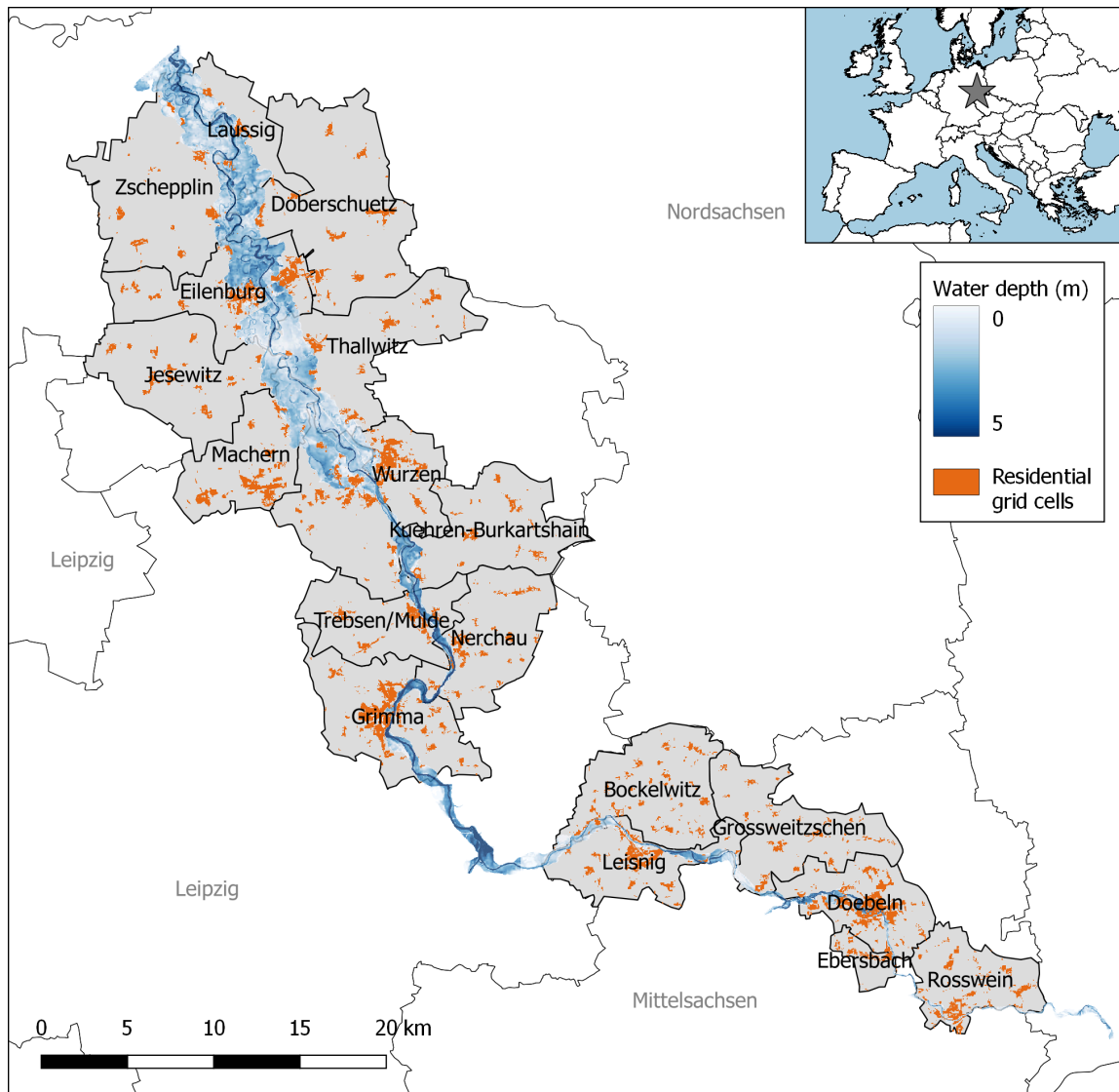


Figure 13.1: 2002 flood along the Mulde River, in Germany. The figure shows the municipalities considered in the case study (grey), the estimated flood extension and water depths (blue), and the location of the residential grid cells (orange).

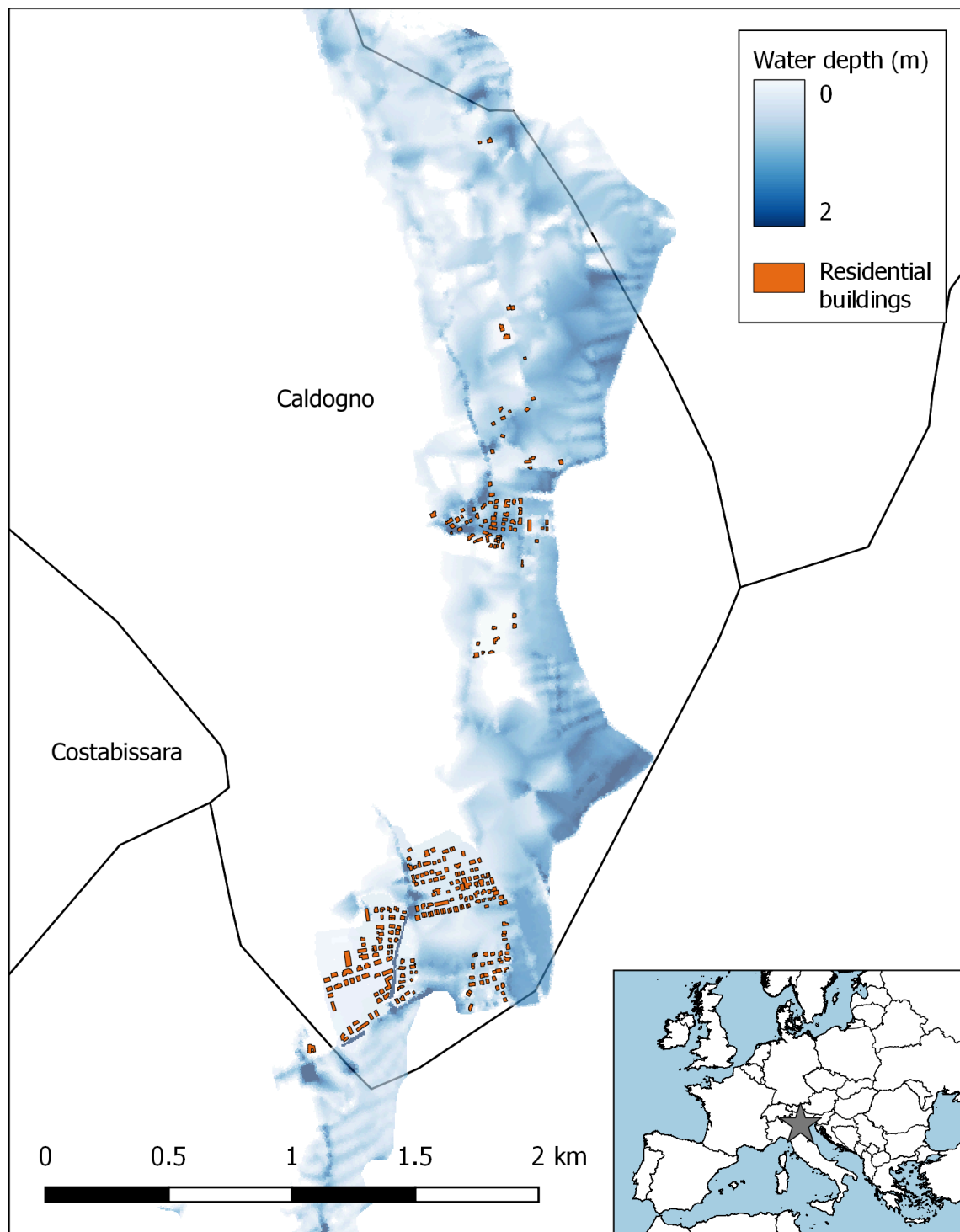


Figure 13.2: 2010 Bacchiglione river flood in Caldogno, Italy. The figure shows the estimated flood extension and water depths (blue), and the location of the residential buildings considered in the study (orange).

Table 13.2: Input variables for the Mulde and Caldogno application cases

Component	Variable	Resolution	
		Mulde	Caldogno
Hazard	Water depth (m)	10x10 m ² grid cell	5x5 m ² grid cell
	Flow velocity*	Municipality	5x5 m ² grid cell
	Inundation duration (h)	Municipality	-
	Return period (yr)	Catchment	-
	Contamination indicator	Municipality	-
Exposure	Building floor area (m ²)	Municipality**	Building
	Value (EUR)	10x10 m ² grid cell	Building
	Building type	Municipality	Building
	Building quality	Municipality	Building
Building structure	Building structure	-	Building
Number of floors	Number of floors	-	Building
Presence of basement	Presence of basement	-	Building
Year of construction	Year of construction	-	Building
	Precautionary measures indicator	Municipality	-
Loss	Reported loss (EUR)	Municipality	Building

* indicator for Mulde; m/s for Caldogno. ** Mean value

individual model applications in terms of error statistics are shown in Table 13.4. The inundation characteristics were estimated using a coupled 1D/2D model of the study area between the municipalities of Caldogno and Vicenza, and validated using data from sources such as aerial surveys and interviews with the local population. Building areas were derived from the cadastral map issued by the Veneto region. Building properties (i.e. building type, structural type, quality, number of floors and year of construction) were assessed through direct surveys to each damaged building. Building values were estimated based on data from the Chamber of Commerce of Vicenza. Losses to residential buildings were provided by the municipality of Caldogno and amount to a total of EUR 7.55 M. These correspond to actual restoration costs that were collected and verified within the scope of the loss compensation process by the State. Further details can be found in (Scorzini and Frank, 2017).

13.3 Ensemble construction and evaluation

Ensembles are finite sets of deterministic realisations of a random variable, whereby the prediction given by each ensemble member is assumed to represent an independent sample from an underlying true probability distribution (Hamill and Colucci, 1997). Ensembles can be used to account for various sources of uncertainty in physical processes, namely initial conditions, parameter and model uncertainty. The latter can be achieved by combining the output of different models to create a so-called multi-model ensemble (Weigel, 2011). In this section, we investigate how best to translate this concept to the field of flood loss modelling, and to which extent multi-model ensembles can improve

the skill and usefulness of flood loss estimations.

13.3.1 Model rating

Method

The first challenge in constructing a multi-model ensemble to estimate flood loss for a certain future application is identifying models that are better suited to be participating members. One of the requirements for the construction of successful multi-model ensembles is that participating models are skilful; if a model is consistently worse than the others in terms of prediction quality, it should not be included (Hagedorn et al., 2005). Unfortunately, testing the level of skill of a model in predicting loss, for a certain type of asset and application setting, is often not possible. Such exercise would involve applying each candidate model to estimate loss for a past flood event with similar characteristics, and quantifying its performance based on past loss observations for the same assets. However, data required to perform such assessments are usually not available, as scarcity of data is still a major problem in the field of flood risk (B. Merz et al., 2010b). Moreover, exposure and vulnerability tend to change over time, which is likely to affect loss estimates (Tanoue et al., 2016). Another issue of a more practical nature is that collecting, implementing and comparing flood loss models is laborious and time consuming. Because of the economic constraints that inevitably exist in any practical application, most users will likely have limited time to invest in that task. This becomes more problematic as the already large number of models available in the literature continues to increase.

A more practicable approach is to evaluate the suitability and potential performance of each model in estimating loss, for a given application setting, based on its properties. This is advantageous, as it does not require that each model be tested explicitly, and can instead be achieved by making use the information contained in a model metadata catalogue such as the ones developed by Gerl et al. (2016) or Pregnolato et al. (2015). However, models differ at various levels, and a model that is potentially superior regarding some of its properties may be inferior in terms of others (see Section 13.1). Consequently, directly evaluating the potential performance of flood loss models is arduous, and currently no established procedure exists to this end. In this subsection, we address this gap by proposing a framework to rate a set of flood loss models based on their properties. The framework is described as follows:

1. A probability tree of model properties is set up through expert elicitation. A set of N independent properties that characterize flood loss models and that are likely to be informative for model performance are identified (e.g. damage metric). For each property (i.e. tree node) n , a set of mutually exclusive and collectively exhaustive categories are defined (e.g. relative and absolute). A subjective probability is then assigned to each category, corresponding to the degree of belief that a model that falls into that category will offer higher predictive performance than if it did in others. It follows that for each property n , the probabilities of the different categories sum to 1. Each path of the tree will have an associated probability that is obtained through the product of each node's probabilities p_n along the path, therefore reflecting the degree of belief that that combination of model properties is the one that should be used;

2. Once the probability tree is set up, it can be used to assign scores to and rank flood loss models. Because the tree covers the entire space of possible categories within each property, all flood loss models will necessarily have a set of properties that matches one of the tree paths. Any model can thus be assigned a score that is equal to the probability of its respective path. When assigned to a certain number of *models* rather than to all the possible combinations of *model properties*, such scores no longer have a specific probabilistic meaning, nor are they intended to. Instead, the scores of different candidate models in a pool can be used to establish a relative degree of belief among them. This effectively provides users with information on their potential performance, in relation to the other models in the pool, through a structured and simple to use procedure.

Application

We apply this framework to the models and test cases presented in Section 13.2. We first propose a probability tree referring to flood loss models for buildings. It condenses expert knowledge and current state of the art in flood vulnerability of buildings, as well as experience from previous model transfer studies. The selection of properties and categories aims to balance comprehensiveness, objectivity and simplicity. Figure 13.5 presents the different properties, a succinct justification of their potential relevance in assessing model performance, and the respective categories and assigned subjective probabilities. Note that the maximum partial score that can be assigned to a model for properties 1 and 2 (shown in Figure 13.5) depends not only on the model but also on the hazard and exposure data sets. For example, if in a certain application case only water depth data is available, loss models that use additional explanatory variables (e.g. velocity) should not be rated higher. We then use this setup to rate the flood loss models. The results are shown in Tables 13.5 and 13.6.

While model properties are expected to be informative for performance, they are not presumed to explain it fully. However, if model properties do have usefulness in assessing the performance of models in relation to one other, some degree of correlation between model scores and different performance metrics should exist. We evaluate this using the Spearman's rank correlation coefficient r_s respectively between the scores shown in Tables 13.5 and 13.6 and the error metrics shown in Tables 13.3 and 13.4. Results show a significant strong negative correlation between the variables ($-0.79 < r_s < -0.51$, $p < 0.01$), which suggests that model rating based on expert judgement is indeed informative for model performance. Note that no attempt was made to maximize correlations by fine-tuning the subjective probabilities, as not only would those not correspond to the experts' degrees of belief, but more importantly, because that would be no more than an exercise in overfitting to these two case studies. This topic is revisited in Section 13.3.2.2.

13.3.2 Ensemble-mean performance

The objective of the analyses presented in this section is twofold: to assess to which extent ensemble-means are able to improve skill in the estimation of flood losses, and

Table 13.3: Results of individual model applications in the Mulde case: root mean square error (RMSE) and mean bias error (MBE), sorted by RMSE

Model name	Error metrics (million EUR)	
	RMSE	MBE
Luino	8.143	-1.23
IKSE	9.16	-2.433
Dutta	9.177	1.87
DSM	9.469	1.359
FLEMO	10.918	-3.85
HAZUS-MH	10.964	3.998
Riha&Marcikova	11.449	2.986
Vanneuville	13.608	-5.302
Toth	13.906	-6.05
MCM	14.405	-4.266
HWS-GIS	15.796	-7.237
ICPR	15.888	-7.201
MERK	16.497	-7.656
Pistrika and Jonkman	16.883	8.235
Yazdi and Neyshabouri	17.174	7.398
Budiyono	18.258	8.19
Vojinovic	19.095	-8.667
HOWAS	20.982	-9.863
TYROL	21.16	-9.979
ANUFlood	21.559	-10.273

Table 13.4: Results of individual model applications in the Caldogno case: root mean square error (RMSE) and mean bias error (MBE), sorted by RMSE

Model name	Error metrics (EUR)	
	RMSE	MBE
IKSE	28,324.2	3742
Toth	28,381.9	-6154
HWS-GIS	28,901.2	-7974.5
FLEMO	29,147.5	2899.9
DSM	29,950.1	8437
Riha and Marcikova	30,248.8	-12,084.7
MCM	30,798.3	-11,106.9
HAZUS-MH	30,829.7	13,131.2
Luino	31,050.4	12,688.3
Dutta	31,242.9	11,470
MERK	32,078.9	-16,228.1
Vojinovic	32,605.8	-15,581.1
TYROL	33,798.5	-17,867.9
ANUFlood	34,010.5	-18,510.8
Vanneuville	34,925.9	-20,809
HOWAS	34,954.3	-19,213.4
ICPR	35,356.4	-21,224.3
Yazdi and Neyshabouri	40,614.3	25,441.6
Budiyono	43,112.8	6602.7
Pistrika and Jonkman	109,444.7	101,296.1

Table 13.5: Model scores for the Mulde application case

Model name	Node probabilities					Score (10 ⁻²)	Score rank
	p1	p2	p3	p4	p5		
FLEMO	0.65	0.35	0.3	0.7	0.7	3.34	1
IKSE	0.35	0.2	0.4	0.7	0.7	1.37	2
Riha and Marcikova	0.65	0.2	0.2	0.7	0.7	1.27	3
HAZUS-MH	0.35	0.35	0.2	0.7	0.7	1.2	4
HWS-GIS	0.35	0.2	0.3	0.7	0.7	1.03	5
MCM	0.65	0.35	0.2	0.7	0.3	0.96	6
DSM	0.35	0.2	0.2	0.7	0.7	0.69	7
Dutta	0.35	0.2	0.2	0.7	0.7	0.69	7
ICPR	0.35	0.2	0.2	0.7	0.7	0.69	7
Luino	0.35	0.2	0.2	0.7	0.7	0.69	7
Toth	0.35	0.2	0.2	0.7	0.7	0.69	7
Vanneuville	0.35	0.2	0.2	0.7	0.7	0.69	7
Pistrika and Jonkman	0.65	0.2	0.2	0.3	0.7	0.55	13
HOWAS	0.35	0.2	0.3	0.7	0.3	0.44	14
MERK	0.35	0.2	0.3	0.3	0.7	0.44	14
Budiyono	0.35	0.2	0.1	0.7	0.7	0.34	16
Yazdi and Neyshabouri	0.35	0.2	0.1	0.7	0.7	0.34	16
ANUFlood	0.35	0.2	0.2	0.7	0.3	0.29	18
TYROL	0.35	0.2	0.2	0.7	0.3	0.29	18
Vojinovic	0.35	0.2	0.1	0.7	0.3	0.15	20

Table 13.6: Model scores for the Caldogno application case

Model name	Node probabilities					Score (10 ⁻²)	Score rank
	p1	p2	p3	p4	p5		
FLEMO	0.65	0.35	0.2	0.7	0.7	2.23	1
Riha and Marcikova	0.65	0.2	0.2	0.7	0.7	1.27	2
HAZUS-MH	0.35	0.35	0.2	0.7	0.7	1.2	3
Toth	0.35	0.35	0.2	0.7	0.7	1.2	3
Luino	0.35	0.2	0.3	0.7	0.7	1.03	5
MCM	0.65	0.35	0.2	0.7	0.3	0.96	6
DSM	0.35	0.2	0.2	0.7	0.7	0.69	7
Dutta	0.35	0.2	0.2	0.7	0.7	0.69	7
HWS-GIS	0.35	0.2	0.2	0.7	0.7	0.69	7
ICPR	0.35	0.2	0.2	0.7	0.7	0.69	7
IKSE	0.35	0.2	0.2	0.7	0.7	0.69	7
Vanneuville	0.35	0.2	0.2	0.7	0.7	0.69	7
Pistrika and Jonkman	0.65	0.2	0.2	0.3	0.7	0.55	13
MERK	0.35	0.35	0.2	0.3	0.7	0.51	14
Budiyono	0.35	0.2	0.1	0.7	0.7	0.34	15
Yazdi and Neyshabouri	0.35	0.2	0.1	0.7	0.7	0.34	15
ANUFlood	0.35	0.2	0.2	0.7	0.3	0.29	17
HOWAS	0.35	0.2	0.2	0.7	0.3	0.29	17
TYROL	0.35	0.2	0.2	0.7	0.3	0.29	17
Vojinovic	0.35	0.2	0.1	0.7	0.3	0.15	20

to investigate how such ensembles should be constructed. Regarding the latter, two questions require particular attention: firstly, which and how many models to include as participating members, and secondly, how to weight those members. Both the ensemble size and the model weighting scheme are likely to have an effect on skill.

Based on model rating

In this exercise, the models and application cases described in Section 13.2 are used. For the construction of the various multi-model ensembles, we mimic the most common practical situation whereby it is necessary to estimate losses for a certain scenario for which past observational data is not available. Because in such situation, the skill of the individual models is not known, the potential suitability of each model for inclusion in a multi-model ensemble is evaluated through their properties, following the framework proposed in Section 13.3.1. Accordingly, different ensembles with increasing number of members are built, by including models sequentially from highest to lowest scores, according to Tables 13.5 and 13.6. Models with the same score are added to the ensemble simultaneously. The ensembles of different sizes constructed for each case study are shown in the x-axes of Figure 13.3, where 1 refers to the highest-ranked single model.

Losses given by ensemble means are estimated using two approaches: firstly, by assigning equal weights to all models, and secondly, by weighting them differently. Concerning this point, we now present some considerations. In the construction of an equal-weighted multi-model ensemble, the underlying hypothesis is that each model is independent and equally skilful, whereas this condition is most often not satisfied. For this reason, adopting different weights may increase the quality of multi-model predictions. However, finding optimal weights is not straightforward, and previous studies show that weighting models differently may result in different outcomes ranging from slight increases to degradation in performance (Doblas-Reyes et al., 2005; Hagedorn et al., 2005; Knutti et al., 2010). Here, we aim to assess how weights affect ensemble-mean performances in estimating flood loss, again by reproducing a practical situation where the skill of models in a certain future application is not known. Therefore, assigned weights instead reflect the user's confidence in each model (Marzocchi et al., 2015). Because the framework proposed in Section 13.3.1 provides scores that are proportional to relative degrees of belief among models, in principle they may be used as weights. This is achieved by normalizing the weights of the participating models in each ensemble so that they sum to 1 (Spillatura et al., 2014). As mentioned in Section 13.2.1, in this study we aimed to ensure model independence by selecting a set of models developed independently, by different authors, using non-overlapping datasets (Cotton et al., 2006; Palmer et al., 2004). We therefore assume that possible model dependences are not relevant and have no bearing on the weighting scheme. Section 13.3.2.2 further discusses the effect of model weighting on ensemble-based loss estimation.

Ensemble-mean performances are calculated in terms of RMSE and MBE, which are shown in Figure 13.3 for the ensembles of different sizes – starting with a single model, the highest ranked for each case – and using the two weighting schemes described above. A number of observations can be made from this figure. Firstly, multi-model ensembles of any size, built by adding models with the highest degrees of belief first, considerably outperform the highest ranked single model in terms of both RMSE and MBE. This is

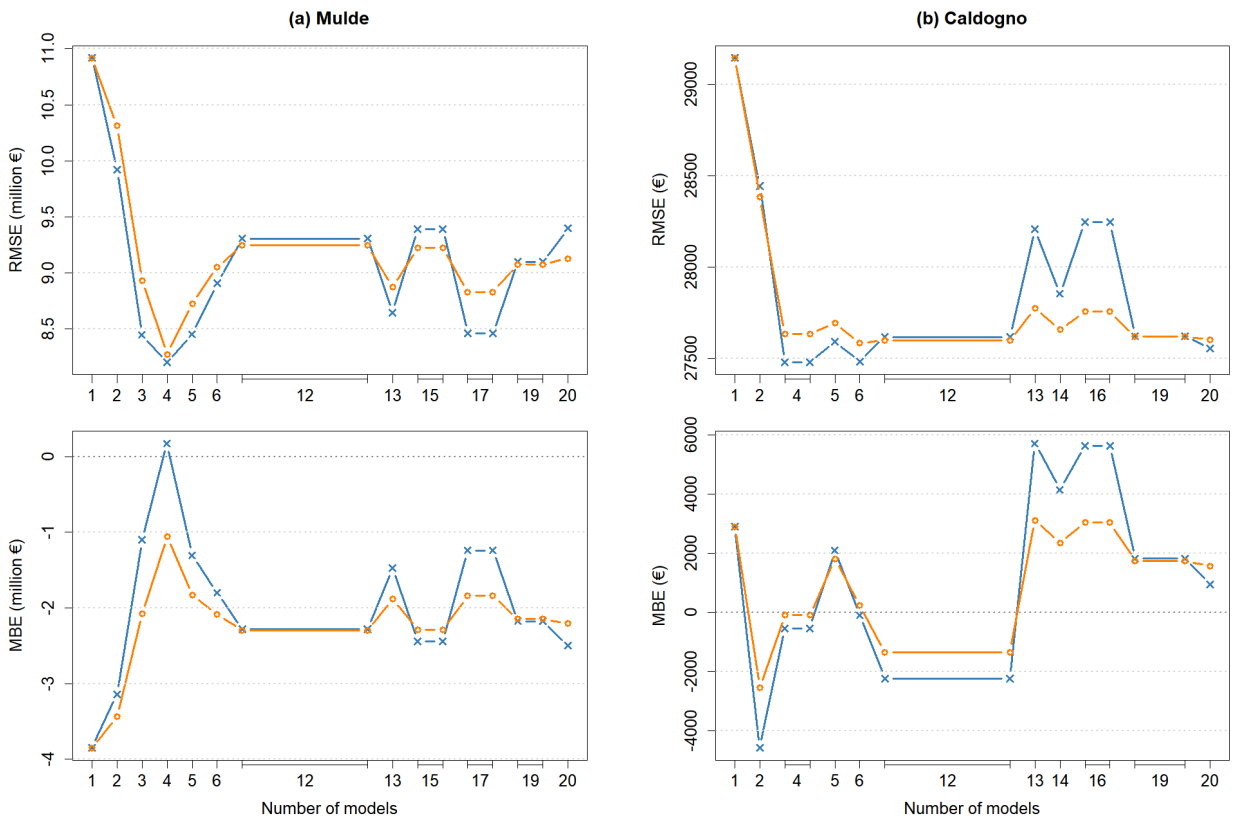


Figure 13.3: Root mean square error (RMSE) and mean bias error (MBE) of the means of ensembles of increasing size, with models included sequentially from highest to lowest score, starting with the highest ranked single model. Blue crosses and orange circles refer to ensembles weighted equally and differently, respectively.

observed for both application cases, the only exception being the MBE of some ensembles in the Caldugno case. Secondly, the performances obtained using the two different weighting approaches is mixed; while in some cases there is improvement by weighting ensemble members differently, in others the opposite is observed. The weighting approach generally does not have a significant impact on error metrics, especially when compared to the model selection. Thirdly, in both cases, the largest improvements in ensemble-mean performances are obtained after the first few highest ranked models are added. In relative terms, the impact of including additional models after that is lower. For example, in the Mulde and Caldugno case studies, the best performances are obtained with ensembles using respectively the highest-scoring four and six models. From a practical point of view, this is a particularly interesting finding because, as mentioned previously, it may not be feasible to implement a large number of models, and users may therefore be interested in parsimonious ensembles with the least number of models that lead to high predictive skill. However, in terms of probabilistic estimates of loss, smaller ensembles are less useful, which also needs to be taken into account when deciding on which ensemble size to use, as further discussed in Section 13.3.3.

Note that from here on, the equal-weighted expert-based multi-model ensembles shown in Figure 13.3 will be used as a basis for other analyses and further discussion, and for the sake of brevity will be referred to as EEM-ensembles.

Some of the above observations draw comparisons between multi-model ensembles and individual models, for which the highest ranked single model is used as reference. Even though that model may not necessarily correspond to the highest performing model (which it does not in either of the application cases used here; see Tables 13.3, 13.4 and 13.5, 13.6, in a practical application case, users have no way of knowing which model is the 'best'. The above results very clearly demonstrate that in such situation, using a multi-model ensemble is preferable. However, it is also insightful to assess how the constructed multi-model ensembles perform in relation to the other single models. Therefore, in Figure 13.4, the error metrics of the predictions given by EEM-ensemble-means and single models are presented, showing that the former consistently outperform the latter. Note that ensembles are not expected to outperform every single model in every possible situation, and it is possible that in some application cases, certain models have such high accuracy that combining them with other models results in lower performances. The problem is that it is usually not possible to identify such models beforehand. For example, in the Mulde case, the Luino model slightly outperforms the constructed ensembles in terms of RMSE. This model consists in a simple stage-damage function that refers to a single building type, and was derived from data relative to a flood in Italy. Therefore, it is not expectable that it would consistently perform as well if applied to other analogous case studies. Overall, better performances should be obtained by using multi-model ensembles (Hagedorn et al., 2005).

Based on simulated non-informativeness

The framework proposed in Section 13.3.1 and the subjective probabilities proposed in Figure 13.5 provide a basis for model selection and weighting in the development of multi-model ensembles. In Section 13.3.2.1, we constructed various ensembles using this approach and evaluated their performance in estimating loss. However, in principle, it

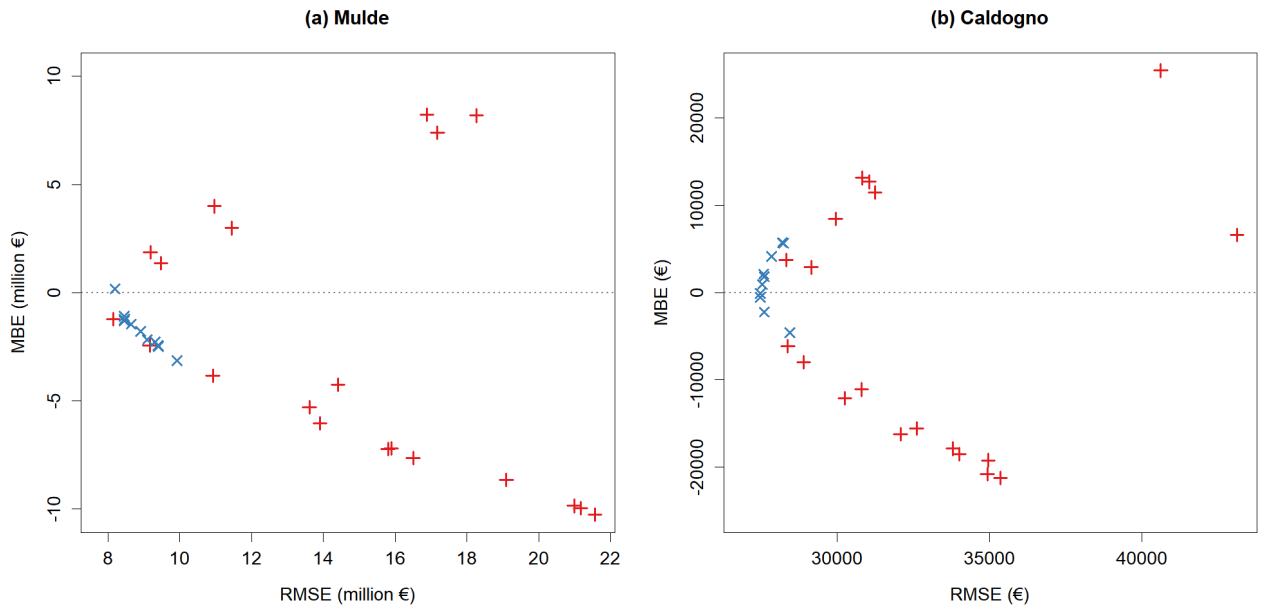


Figure 13.4: RMSE and MBE of the EEM-ensemble means, represented by blue crosses, and single model predictions, by red plus signs.

is possible that multi-model ensembles developed differently, i.e. by selecting different models and/or assigning different weights, would have higher skill. To investigate this issue, we simulate a so-called state of non-informativeness in terms of model suitability. This consists in assuming we have no knowledge about how particular model characteristics might affect model predictive performance (Scherbaum and Kuehn, 2011), and therefore have no way of rating models. Accordingly, we implement a probabilistic sampling procedure that, for a large number of realisations, randomly generates weights for individual models regardless of their properties. On this basis, model ensembles are built and their predictive performance is calculated for the Mulde and the Caldugno case studies. The weight generation follows the stick-breaking method, whereby models are first randomly ordered and then assigned weights sequentially. For each model, the weight is drawn from a continuous uniform distribution with a minimum value of 0 and a maximum value of 1 minus the sum of weights that have already been assigned. This approach, based on a large number of realisations, aims to cover all possible ensembles that can be constructed using the twenty flood loss models from Table 13.1, using not only different weighting approaches (i.e. ensemble members weighted both equally and differently) but also different combinations of models. The latter is because according to the stick-breaking method, once the model weights sum to 1, all other models receive a weight of 0 and are thus not included in the ensemble.

Scatter plots of the RMSE and MBE that result from the above procedure are presented in Figure 13.6 for both case studies. The same error metrics regarding the EEM-ensembles and the single models are also included. The plots show that a wide range of possible

1. Flood intensity measures
Flood damage processes are influenced by multiple factors. Although water depth is considered the most important intensity measure, additional variables tend to improve model predictive skill.

Water depth and additional variables	0.65
Water depth only	0.35

2. Characterization of exposed assets
The degree of characterization of assets in flood loss model is directly related with potential performance, as insufficient distinction may result in their inappropriate application to assets for which they are not suited.

Building type and physical properties (e.g. material, no. of floors)	0.45
Building type only (e.g. single family house)	0.35
Occupancy type only (e.g. residential)	0.20

3. Similarity of local context with application setting
Models generally perform better in regions with a socio-economic context comparable to the one for which they were developed, as they tend to have more similarities in terms of construction quality and practices.

Same region	0.40
Same country	0.30
Same WESP classification ¹	0.20
Different WESP classification ¹	0.10

¹ According to UN World Economic Situation and Prospects 2016. A: developed economies; B: economies in transition; C: developing countries; D: least developed countries.

4. Flood type in relation to application setting
Flood loss models are usually constructed for specific types of inundation (e.g., fluvial flood), and will usually perform worse when applied to flood events with different dominant damaging processes.

Identical	0.70
Different	0.30

5. Damage metric
Relative loss models, which express loss as a fraction of the total asset value, offer better transferability, whereas absolute loss models have little applicability outside the specific case for which they were developed.

Relative	0.70
Absolute	0.30

Figure 13.5: Proposed set of properties (probability tree nodes) that are considered relevant to assess the performance of flood loss models for buildings, and respective categories and subjective probabilities.

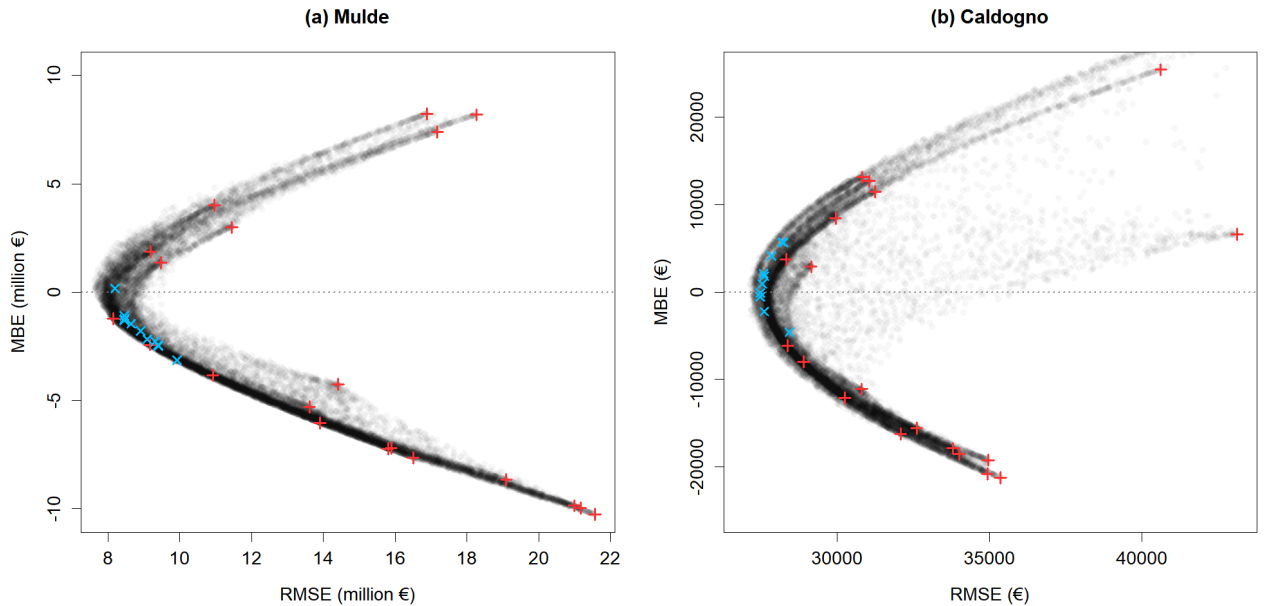


Figure 13.6: RMSE and MBE of 20 000 multi-model ensemble means, generated by simulating a state of non-informativeness, whereby each participating member is assigned a random weight. Blue crosses and red plus signs refer respectively to the EEM-ensemble means and the single model predictions.

outcomes in terms of RMSE and MBE exist when random weights are assigned to models within the framework of a state of non-informativeness. While the lower bounds of the resulting convex hull are defined by the error metrics of the lowest-performing models, the upper bounds (i.e. highest performances) are given not by any single model, but instead by multi-model ensembles, as expected. In this regard, it is clear that the model rating framework based on expert judgement and subjective probabilities proposed in Section 13.3.1 add value to the ensemble development process. Indeed, ensembles that are constructed by adding models prioritized in terms of potential suitability (shown in Figure 13.3) are among the highest performing ensembles, considering all the existing possibilities. It is interesting to highlight that the simple unweighted mean of all models also performs relatively well, which suggests that if no knowledge is available on model properties and/or on how they influence performance, it is better to include all models than to wrongly select them.

The plots also show that it is possible to create certain ensembles that lead to better skill in relation to the ones developed based on expert judgement. However, the potential relative degree of improvement is very low in both test cases, more markedly so in the Caldogno case, which reinforces the idea that the approach proposed in Section 13.3.1 provides a good basis for ensemble construction. We do not attempt to maximize the performance of the constructed multi-model ensembles based on the results obtained in this exercise, as this would be of little relevance. Analogously to the ‘best’ model discussion in Section 13.3.2.1, in a practical application the ensembles cannot be tested beforehand. Finding specific weights that maximize performance for the Mulde and the Caldogno

case studies would consist in pointless overfitting, as such weights necessarily vary from case to case. In addition, it is likely that such weights would not make sense from the perspective of an expert. Instead, the objective here is that ensembles are constructed in a manner that leads to good performances in all situations, which the results support. Finally, Figure 13.6 corroborates that correctly selecting models for an ensemble is more important than weighting them. The EEM-ensembles, which result from model selection only, display error metrics close to the minimum obtainable from a wide range of possible outcomes. In comparison, further improvements that could possibly be achieved by assigning different weights to ensemble members are very small.

13.3.3 Probabilistic application

In Section 13.3.2, multi-model ensemble-means have been shown to provide more skilful estimates of flood losses than single models. Another motivation for the use of such ensembles is that they may be used to quantify model uncertainty and obtain probabilistic distributions of possible outcomes rather than single point estimates, which is, as discussed previously, required for optimal decision-making. In this section, we offer some discussion on this topic.

It is first necessary to make clear what the probabilistic meaning of a multi-model ensemble is. Multi-model ensembles do not directly provide probability distributions of a certain variable; instead, ensemble predictions are *a priori* only finite sets of deterministic realisations of that variable. The question then arises how a probability distribution can be obtained from such ensembles. The simplest approach is to adopt a frequentist interpretation of the ensembles, whereby the probability of a certain event to happen is estimated by the fraction of ensemble members predicting it. However, such approach can only produce reasonable probabilistic estimates if many ensemble members are available. Better probabilistic estimates may in principle be obtained by dressing the ensemble members with kernel functions or by fitting a suitable parametric distribution to them, provided that this is done in an appropriate manner (Weigel, 2011).

Skill and reliability

Regardless of the method that is used to obtain probabilistic estimates from multi-model ensembles, it is first important to evaluate the ‘raw’ ensembles, with minimum interference from the ensemble interpretation model that is used. This can be achieved using the continuous ranked probability score (CRPS) (Bröcker, 2012; Hersbach, 2000). We calculate the CRPS for the EEM-ensembles, and present the results in Figure 13.7. This is done for the Caldugno case study, as the low number of data points in the Mulde case (19) are insufficient for such analysis.

The probabilistic skill of the ensembles is observed to have an increasing trend (i.e. decreasing CRPS) with the number of participating members. This is to some extent expected, as ensemble size is known to have an effect on probabilistic skill scores, which is explained by the fact that probabilistic estimates derived from ensembles become more unreliable as the size of the ensemble gets smaller (Weigel, 2011). This highlights the need of using a considerable number of models when the objective is to obtain reliable (i.e. statistically consistent) probabilistic estimates of flood loss. Another requirement to

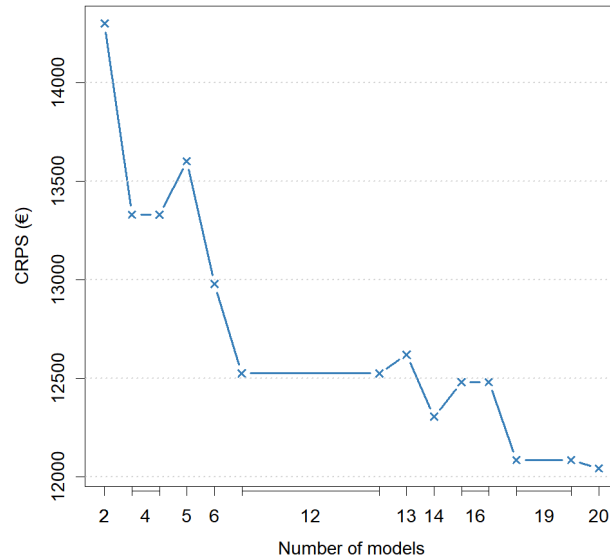


Figure 13.7: Continuous ranked probability score (CRPS) of the EEM-ensembles for the Caldogno application case.

achieve this is that the ensemble itself is reliable, in the sense that ensemble members and observations are sampled from the same underlying probability distributions or, in other words, that they are statistically indistinguishable from each other (Leutbecher and Palmer, 2008). Even an ensemble of infinite size is unable to yield reliable probabilistic estimates if its member are not reliable (e.g. if they are heavily biased). For illustration, we assess reliability considering an ensemble comprising all twenty models implemented in this study using the rank histogram, which is shown in Figure 13.8. As expected, the ensemble is not perfectly reliable; however, the counts do tend to oscillate around $\frac{n}{m+1} = \frac{296}{21}$, which suggests a reasonable degree of reliability. In addition, the ensemble appears to be slightly overdispersive, due to an overpopulation of central ranks of the histogram.

Loss estimation

Finally, we illustrate the simplest approach to obtain a probabilistic distribution of flood losses using a multi-model ensemble. For each building, a value of loss is randomly generated using the reverse transform sampling method, whereby a number $u[0, 1]$ is sampled from the standard uniform distribution, and the corresponding quantile is sampled from the empirical cumulative distribution function (ECDF) of losses given by ensemble members through linear interpolation. The losses for each building are then summed, and a total loss is obtained. This process is repeated a large number of times, yielding a loss distribution for the flood event. The results for the Caldogno application, based on 10,000 realisations, are shown in Figure 13.9 in the form of a histogram and ECDF of total loss.

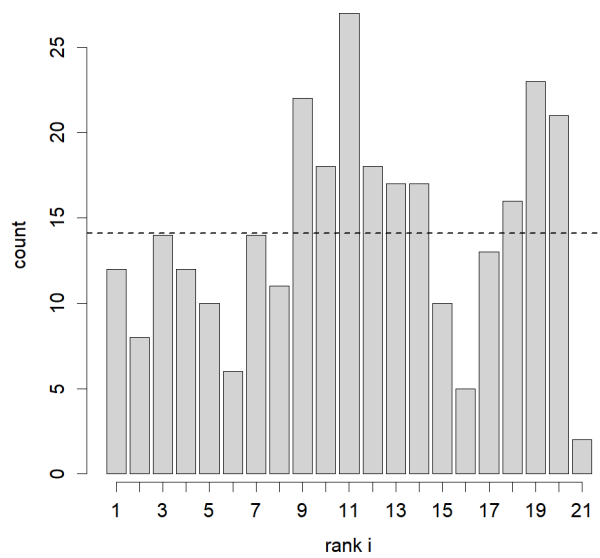


Figure 13.8: Rank histogram relative to the 20-model ensemble for the Caldogno application case.

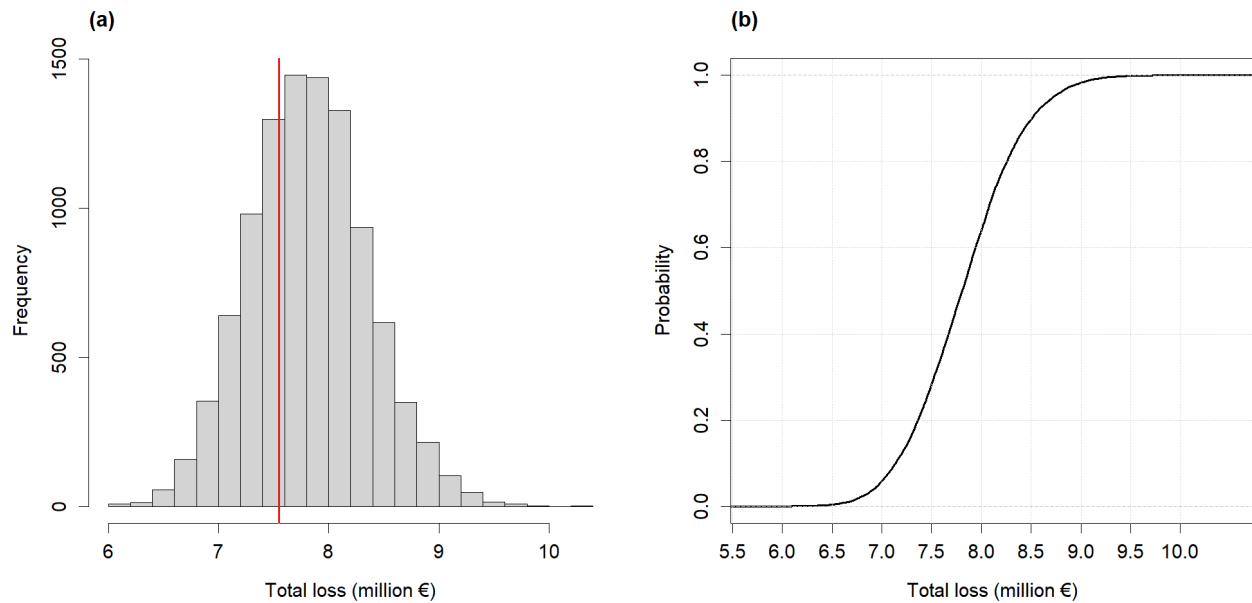


Figure 13.9: Probabilistic estimates of total loss, relative to model uncertainty, for the Caldogno application case, based on 10,000 realisations of loss to each building. (a) Histogram, with observed loss shown by the vertical red line. (b) Empirical cumulative distribution function (ECDF).

Statistical post-processing techniques may be used to improve the reliability of probabilistic predictions. This is common practice in the field of numerical weather prediction, for example. However, in that case, relatively long time series of past observational data for a certain variable (e.g. temperature) at a certain location are usually available, and such data continue to be collected, which allows the predictive system to be calibrated and the forecasts verified. This is in contrast with the case of flood loss estimations, where loss models necessarily need to be transferred due to the rarity of the events and the difficulty in obtaining data. In the particular case of probabilistic loss estimates based on ensembles, it is therefore necessary to investigate how best to improve their reliability for future applications by considering data from previous flood events often occurring in different contexts. In addition, as mentioned previously, the reliability of probabilistic estimates may also be improved by using a more sophisticated ensemble interpretation method (i.e., kernel dressing or parametric distribution fitting). However, the most appropriate approach to do this in the case of flood loss modelling also needs to be investigated. These topics are beyond the scope of this article.

13.4 Conclusions

Flood loss modelling is associated with considerable uncertainty that is often neglected. In fact, most currently available flood loss models are deterministic, providing only single point estimates of loss. Users interested in performing a risk assessment will typically select one such model from the large number available in the literature, based on their perception of which one is the most suitable for the application case at hand. However, this is generally done rather arbitrarily. Moreover, the uncertain nature of flood loss estimations means that the performance of any single deterministic model may vary considerably from case to case, as large disparities in model outcomes exist even among apparently comparable models. This approach is therefore flawed at two main levels: first, flood risk estimates are highly sensitive to the selection of the flood loss model, and second, deterministic estimates of loss do not lead to optimal decision-making. In this study, we have proposed a novel approach to tackle these issues and advance the state of the art in flood loss modelling, based on the application of the concept of multi-model ensembles. This technique, which is widely used in fields such as weather forecasting, consists in combining the outcomes of different models in order to improve prediction skill and sample model uncertainty.

In order to support ensemble construction, we have first proposed a framework to assess the suitability of flood loss models to specific application cases, based on some of their main properties, through expert knowledge. This approach is advantageous as it does not require that all candidate models are implemented beforehand, which is often not achievable in practice. Based on such framework, we have proposed a scoring scheme for flood loss models for residential buildings, and applied it to the twenty models and two applications cases used in this study. The obtained model scores show significant strong negative rank correlation with error metrics, suggesting that the proposed approach is useful, and that expert judgement is informative for model performance and selection.

The constructed ensembles have been shown to considerably outperform the high-

est ranked single models in the estimation of flood losses. This demonstrates that in a practical application, where model performances cannot be tested beforehand, using multi-model ensembles will result in more skilful loss estimates. Ensemble-means were also tested against all single models, consistently showing higher accuracy. Equal-weighted ensembles generally displayed performances comparable to the score-weighted ones. The largest improvements in ensemble-mean performances were observed after the first few highest ranked models were added to the ensembles, which is a useful finding for practical applications, where it is not always feasible to implement a large number of models. We have also simulated a state of non-informativeness and randomly generated a large set of multi-model ensembles, representative of all possible ensembles that can be constructed using the twenty flood loss models adopted in this study. The ensembles based on expert-based scoring approach were among the most skilful, highlighting its value in the construction of multi-model ensembles. Results also suggest that model selection is more important than weighting. Further insight may be gained by testing the approach in other application cases and using a different set of flood loss models.

Larger ensembles showed higher probabilistic skill than smaller ones, which results from the increased intrinsic unreliability of ensembles as the number of participating members decreases. Therefore, if on the one hand only a limited number of models is necessary to obtain accurate mean estimates of loss, on the other additional effort in model implementation is recommended when the objective is to derive a probabilistic distribution of loss that captures model uncertainty. For the Caldogno case study, we have illustrated how such a distribution can be constructed, adopting a simple equal-weighted ensemble comprising all twenty models. The results demonstrate that the use of multi-model ensembles represents a simple and pragmatic way of obtaining reliable flood loss distributions, which are more useful for decision-making than single point estimates of loss. Reliability may be further improved by calibrating the ensembles and/or adopting more sophisticated ensemble interpretation models, which warrants further research.

14 | Probabilistic, multi-variable flood loss modelling on the meso-scale with BT-FLEMO

Manuscript Info

Authors information:

Heidi Kreibich
Anna Botto
Bruno Merz
Kai Schröter

Published as:

Kreibich H., Botto A.,
Merz B., Schröter K.
Probabilistic,
multi-variable
flood loss modelling
on the meso-scale
with BT-FLEMO
Risk Analysis.
2017;37,4:774-784.
doi:10.1111/risa.12650

Abstract

Flood loss modelling is an important component for risk analyses and decision support in flood risk management. Commonly, flood loss models describe complex damaging processes by simple, deterministic approaches like depth-damage functions and are associated with large uncertainty. To improve flood loss estimation and to provide quantitative information about the uncertainty associated with loss modelling, a probabilistic, multi-variable **B**agging decision **T**ree based **F**lood **L**oss **E**stimation **M**odel (BT-FLEMO) for residential buildings was developed. The application of BT-FLEMO provides a probability distribution of estimated losses to residential buildings per municipality. BT-FLEMO was applied and validated at the meso-scale in 19 municipalities which have been affected during the 2002 flood by the River Mulde in Saxony, Germany. Validation was undertaken on the one hand via a comparison with six deterministic loss models, including both depth-damage functions and multi-variable models. On the other hand the results were compared with official loss data. BT-FLEMO outperforms deterministic, uni-variable and multi-variable models with regard to model accuracy, though the prediction uncertainty remains high. An important advantage of BT-FLEMO is the quantification of prediction uncertainty. The probability distribution of loss estimates by BT-FLEMO represents well the variation range of loss estimates of the other models in the case study.

14.1 Introduction

Risk-based approaches have been increasingly accepted and operationalised in flood risk management during recent decades (B. Merz et al., 2010a). They support optimum investments and enable decisions on cost-efficient measures (Al-Futaisi and Stedinger, 1999; Apel et al., 2009; Kreibich et al., 2011a). The European Flood Risk Management Directive (EC, 2007b) requests the EU member states to provide risk management plans for areas with potentially significant flood risk. Flood risk analyses combine analyses of hazard and resulting consequences. Flood loss models provide quantitative estimates of flood damage in monetary terms. In this respect, they are a key tool to fulfil the requirements of the EU Flood Directive. However, the development of models for reliable flood loss assessment is still a challenge.

Damage processes during floods are complex because they are influenced by physical and socio-economic processes and their interaction. Thielen et al. (2005) and B. Merz et al. (2013) investigate single and joint effects of impact factors (i.e. flood characteristics) and resistance factors, e.g. characteristics of the building at risk) on flood loss ratios of private households. These studies highlight that flood impact variables, particularly water depth, return period, inundation duration and contamination are important determinants for building and contents loss. Similarly, the resistance variables floor space of building, the building value and indicators representing precautionary measures proved to be of relevance. Kreibich et al. (2005) and Kreibich et al. (2011a) quantify the loss-reducing effects of different precautionary measures for residential buildings.

In contrast to this diversity of important loss influencing factors, common loss models are simple, often only based on the relationship between water-depth and loss (depth-damage functions). For instance, various depth-damage functions are developed for Germany based on different mathematical functions, e.g. linear (NRW, 2000), cubic (ICPR, 2001) and square-root functions (Buck and Merkel, 1999; Emschergerossenschaft and Hydrotec, 2004).

Some loss models take into account further impact and resistance factors: For instance, Wind et al. (1999) account for flood warning time and flood experience in flood loss estimation. Nicholas et al. (2001) suggest a model which defines important variables to be considered in flood loss estimation but without quantifying their effect on the loss. Zhai et al. (2005) consider the following resistance variables in their loss model: building type, length of residence and household income. Multi-variable flood loss estimation models for private households and companies (FLEMOps, FLEMOcs) have been developed, applied and validated at the micro- and meso-scale in Germany (Bücheler et al., 2006; Thielen et al., 2008b; Kreibich and Thielen, 2008; Kreibich et al., 2010; Seifert et al., 2010; Elmer et al., 2010). K. Vogel et al. (2012) and Schröter et al. (2014) first apply Bayesian Networks to develop probabilistic multi-variable loss models. Schröter et al. (2014) compare different loss models and demonstrate that additional explanatory variables besides water depth improve the predictive capability. This applies particularly to model transfer applications to different regions, i.e. the loss model is developed based on empirical data from a certain region and is applied in another region, and to different flood events, i.e. the model is developed based on data from a certain flood and is applied to another flood.

An important aspect in loss modelling is the spatial scale, which can be micro-, meso-

or macro-scale, depending on the spatial resolution of the analysis (Messner et al., 2006; Messner et al., 2007). Micro-scale models calculate loss for single objects, e.g. buildings. Meso-scale models consider aggregated land use units, e.g. residential areas or industrial areas. Macro-scale models typically consider much larger spatial units and are used for risk assessments at the national or continental scale. The choice of the scale depends on the objective of the risk analysis and on the available data. According to Moel et al. (2015) meso-scale flood risk assessments are used for regional flood risk management and mapping and in the re-insurance industry (Olsen et al., 1998; Ganoulis, 2003). An example is the assessment of how the implementation of retention areas along rivers impact flood defence failure probabilities and risk (Vorogushyn et al., 2012). Micro-scale approaches are used for object-targeted project appraisals and detailed information for policy makers (Messner et al., 2007). Another crucial point is data availability: micro-scale approaches require detailed object-related data, whereas for meso-scale analysis data with lower spatial resolution are used which are commonly available in national statistical datasets (Apel et al., 2009).

B. Merz et al. (2013) derive multi-variable flood loss models at the micro-scale using tree-based methods. The present study builds upon this study by transferring their BT flood loss model from the micro-scale to the meso-scale. It is possible to transfer flood loss models from one scale to another by means of aggregation/disaggregation techniques. Usually object-specific, i.e. micro-scale, models are developed on the basis of object-related empirical or synthetic loss data (B. Merz et al., 2010b). Hence, for meso-scale analyses, micro-scale models have to be scaled to suitable spatial units, e.g. land use classes (Lekuthai and Vongvisessomjai, 2001; Kreibich et al., 2010). Likewise, exposed asset values have to be allocated to these spatial entities. Asset values are required to derive monetary values from relative loss estimates provided by the models. As asset values are usually available at spatially aggregated units, e.g. municipalities, disaggregation techniques, e.g. dasymetric mapping, have to be used to obtain data with higher resolution (Chen et al., 2004; Wünsch et al., 2009). For multi-variable loss models, scaling is a crucial issue since suitable data to describe the various influencing factors on different scales is not readily available.

It is essential to quantify the uncertainty involved in flood risk assessments in order to enable informed decisions (M. Downton and Pielke, 2005; B. Merz and Thielen, 2009). Whereas uncertainty considerations are widespread when assessing flood hazard, uncertainty of loss modelling is rarely considered. However, Apel et al. (2009) and Notaro et al. (2014) stress the important contribution of flood loss modelling to the overall uncertainty in flood risk analysis. Uncertainty in loss modelling arises both from a lack of knowledge concerning the relevant processes and data, and the natural variability of the underlying processes and variables (Ferson and Ginzburg, 1996; B. Merz and Thielen, 2009). Uncertainty sources are the hazard characteristics (e.g. inundation depth, duration, contamination), the resistance characteristics of the elements at risk (e.g. building type, building quality, precautionary measures), the value of the elements at risk, and their susceptibility which is described by the loss model (Apel et al., 2004; Moel and Aerts, 2011). Additional uncertainty stems from spatial aggregation of heterogeneous data, e.g. within scale transfers.

In this paper we propose a novel probabilistic flood loss model for meso-scale applications which quantifies the model uncertainty. The **Bagging decision Tree Flood Loss**

Estimation Model BT-FLEMO is a multi-variable model which is derived using the ensemble modelling approach of bagging decision trees (BT) (Breiman, 1996). BTs are an ensemble of many regression trees (RT). BT-FLEMO provides quantitative estimates of model prediction uncertainty which reflects the uncertainty inherent to the flood loss model due to model structure, the variability of input data and data errors. We present, for the first time, the application and validation of a probabilistic, multi-variable flood loss model on the meso-scale which enables for instance the consideration of flood loss model uncertainty in regional flood risk analysis.

14.2 Data and methods

14.2.1 Case study area

Model application and validation are conducted in 19 municipalities located at the river Mulde in Saxony, Germany (Figure 14.1). During the extreme flood of August 2002, flood peak return periods of up to 500 years have been estimated at the river Mulde (IKSE, 2004; Engel, 2004) which caused major losses also due to a large number of dike breaches. Altogether losses of about EUR 11.6 b (values of 2002) in Germany has been reported, of which EUR 8.7 b occurred in Saxony (Thieken et al., 2005).

Flood losses have been well documented by the Saxon Relief Bank (SAB, 2005), which has been in charge of the loss adjustment and management in Saxony after the flood in 2002. According to the loss compensation guidelines (SMI, 2002) the eligible repair costs represent the total residential building loss in terms of financial costs, i.e. costs due to repairing damage to the building structure (Wünsch et al., 2009). Costs for repairing or replacing damaged household contents or damaged outside facilities (e.g. fences, plants) were excluded from the compensation. Since the official loss data from Saxon Relief Bank and the estimated flood losses both represent financial costs, they can be compared on the municipality level for model validation purposes.

14.2.2 Bagging Decision Tree (BT) based loss model for the micro-scale

Tree-based modelling has been introduced by Breiman et al. (1984). BTs are an ensemble of regression trees. They are derived by generating many bootstrap replicas of the data set and by growing a regression tree (RT) on each replica. The data set consists of predictors, i.e. variables possibly influencing the loss (Table 14.1), and the response variable, i.e. the building loss ratio. In this study, the building loss includes all costs associated with repairing the damage to the building structure, such as plastering, replacing broken windows and repairing the heating system. Contents loss is not included. The building loss ratio is the relation between the building loss and the building value, i.e. the relative building loss. The building values were estimated according to the VdS guideline 772 1988-10 (Dietz, 1999) which is commonly used in the insurance sector.

In contrast to regression approaches where a global relation between predictors and response variable is sought which holds across the complete data space, RTs are a form of local regression. The data space is recursively split into sub-spaces. At each split the data set is partitioned into two sub-spaces in such a way that the homogeneity of the response variable in the resulting sub-spaces is maximized. The succession of binary



Figure 14.1: Location of the municipalities in the case study area at the Mulde River in Germany

splits leads to a set of tree branches subdividing the data space into disjoint partitions of the response variable (leaves). The prediction for a given input of predictors is simply the average of the response variable of all the samples of the training data set that belong to this leaf. RTs can easily handle incomplete data, since when data is missing, the predictions are based only on the leaves that can be reached given the available data. RTs do not require any assumption on the relationship between predictors and the response variable, and non-linear and non-monotonic dependencies can be represented by a tree. They are able to consider interactions between predictor variables. They are particularly well suited when there is little knowledge of which potential predictor variables are of importance and how the important predictors and the response variable relate to each other. Disadvantages of RTs are, that a large database is needed for model development and that RTs only reflect the relationships that are contained within the data (B. Merz et al., 2013). Additionally, it is important to avoid overfitting. Large trees may agree well with the training data, but their prediction ability may be poor. Tree pruning where large trees are cut back to obtain simpler trees are a helpful approach in this respect.

Bagging of plausible candidate RT can give substantial gain in prediction accuracy and is useful to reduce the predictive limitations associated with the selection of a single model (B. Merz et al., 2013; Breiman, 1996). Bootstrapping captures the effects of data variability as one source of uncertainty in flood loss modelling. The ensemble of candidate RT composing the BT represents a variety of model structures reflecting model structure uncertainty. The prediction of a BT is available as the distribution of the individual predictions from all tree ensemble members or can be aggregated in terms of a summary statistic, e.g. the average over the predictions.

B. Merz et al. (2013) derived a BT flood loss model for the micro-scale, which is further developed in this study to be applicable at the meso-scale. The micro-scale database contained 1103 data sets of damaged residential buildings which have been collected via computer aided telephone interviews after the floods in 2002, 2005 and 2006 in the Elbe and Danube catchments in Germany. 28 candidate predictors were tested for their importance in respect to estimating the loss ratio of residential buildings. The BT loss model is an ensemble of 200 RTs, of which one example RT is shown in Figure 14.2. It uses the following predictors: water depth (wst), return period (rp), contamination indicator (con), inundation duration (d), flow velocity indicator (v), floor space of building (fsb), building value (bv) and precautionary measures indicator (pre). The same model structure which was developed on the micro-scale is used for the meso-scale, but the input variables are estimated for meso-scale units, e.g. municipalities (Table 14.1).

14.2.3 Spatial scale transfer

The micro-scale BT loss model is the starting point for the development of BT-FLEMO for the meso-scale. The up-scaling approach of Kreibich et al. (2010) is followed, i.e. the model structure is not changed, but the predictors of the micro-scale BT loss model are estimated area-wide for spatially aggregated meso-scale units. For this purpose suitable data representations or proxies need to be identified. These meso-scale proxies should reflect the differences in the micro-scale, i.e. building specific data. This bottom-up approach assumes no changes in the processes and their importance due to spatial aggregation. However, only an analysis on how meso-scale variables interact and influence the

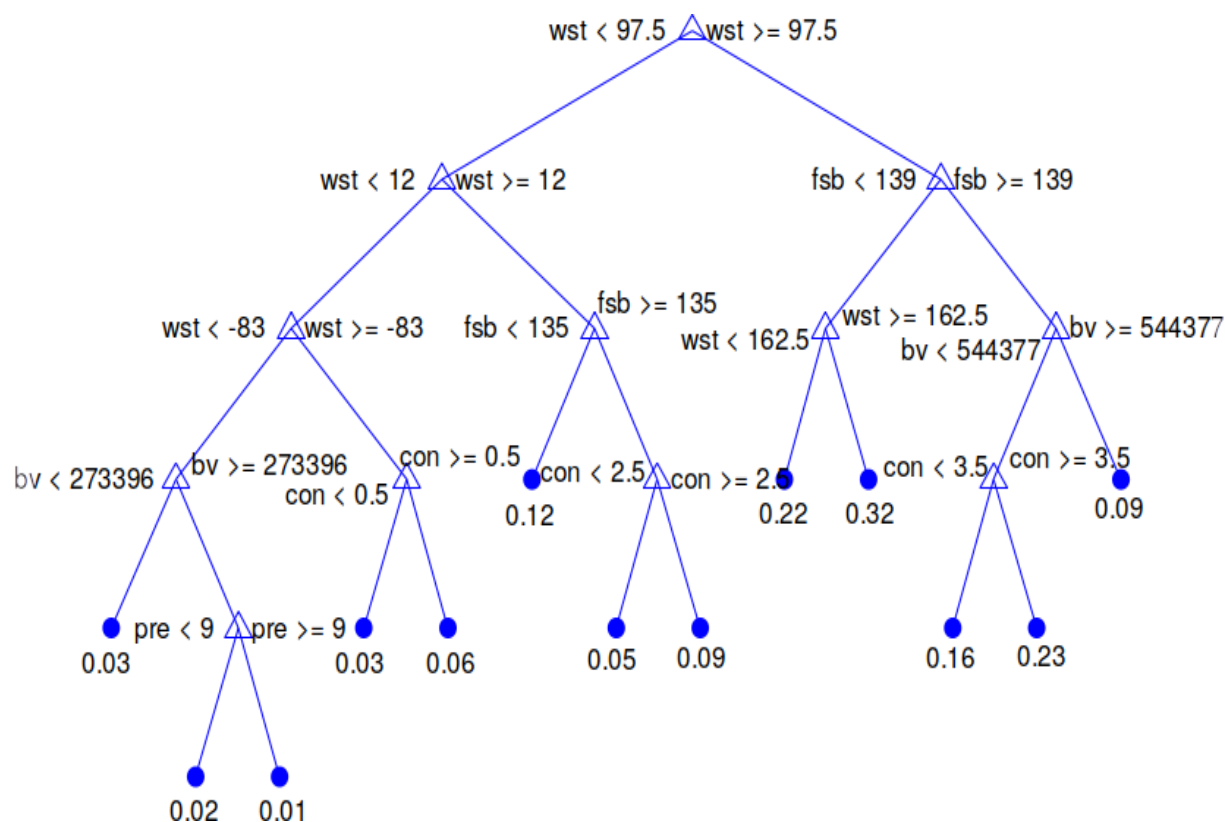


Figure 14.2: Example of RT representation of BT-FLEMO (water depth (*wst*), return period (*rp*), contamination indicator (*con*), inundation duration (*d*), flow velocity indicator (*v*), floor space of building (*fsb*), building value (*bv*) and precautionary measures indicator (*pre*); for further description of predictors see Table 14.1).

Table 14.1: Compilation of variable characteristics and spatial scale transfer methods

Variables	Type and range on micro-scale	Spatial scale transfer method	Meso-scale units
<i>flood impact variables</i>			
Water depth	wst C*: 248 cm below ground to 670 cm above ground	Hydraulic transformation (Kleist et al., 2006), (M. Downton and Pielke, 2005)	Area-wide on 10 m grid level
Return period	rp C: 1 to 848 years	Extreme value statistics (Elmer et al., 2010)	Sub-catchments
Contamination indicator	con O: 0 = no contamination to 6=heavy contamination	Regionalised median values from empirical flood damage data (Thieken et al., 2005)	Municipality
Inundation duration	d C: 1 to 1,440 h	Regionalised median values from empirical flood damage data (Thieken et al., 2005)	Municipality
Flow velocity indicator	v O: 0 = still to 3 = high velocity	Regionalised median values from empirical flood damage data (Thieken et al., 2005)	Municipality
<i>resistance variables</i>			
Floor space of building	fsb C: 45 to 18,000 m ²	Exposure estimation on basis of official statistical data (Kleist et al., 2006)	Municipality
Building value	bv C: EUR 92,244 to EUR 3,718,677	Exposure estimation on basis of official statistical data (Kleist et al., 2006)	Municipality
Precautionary measures indicator	pre O: 0=no measures undertaken to 38=many, efficient measures undertaken	Regionalised median values from empirical flood damage data (Thieken et al., 2005)	Municipality
Building type	bt N: 1=multifamily house, 2= semi-detached house, 3=one-family house	Cluster analyses with INFAS geomarketing data (Thieken et al., 2008b)	Municipality
Building quality	bq O: 1=high, 2-6=medium to low quality	Average from INFAS geomarketing data (Thieken et al., 2008b)	Municipality
Monthly net income in classes	inc O: 11=below EUR 500 to 16= EUR 3,000 and more	Regionalised median values from empirical flood damage data (Thieken et al., 2005)	Municipality

* C: continuous, O: ordinal, N: nominal

loss at the meso-scale could verify if all important meso-scale variables are considered for the meso-scale loss estimation. Such an analysis appears hardly possible due to a lack of data. This up-scaling procedure showed good results in a validation study (Kreibich et al., 2010; Seifert et al., 2010). In addition to the variables used by BT-FLEMO, also the variables building type (bt), building quality (bq), and income (inc) need to be estimated for meso-scale units, since they are required for the application of the loss models used for model comparison. The type and range of the variables on the micro-scale, the spatial scale transfer method (i.e. estimation method for meso-scale units) and the meso-scale units are compiled in Table 14.1.

The inundation patterns including water depths (wst) distribution of the 2002 flood in the 19 case study municipalities were taken from Grabbert (2006) and Apel et al. (Apel et al., 2007). In the municipalities Döbeln and Eilenburg, water depths were calculated with Lisflood-FP (Bates et al., 2010) and were provided by Apel et al. (2007). In the other

17 municipalities, water depths of 10-m resolution were derived by hydraulic transformation undertaken by Grabbert (2006), following the approach of H. Rodda (2005).

Return periods (rp) were taken from Elmer et al. (2010), who applied the following procedure: Per gauge the annual maximum series were derived from discharge data with at least 30 years of observations. The Generalised Extreme Value distribution function was fitted to the annual maximum series using the L-Moment method. The resulting return period for the maximum annual discharge in 2002 was assigned to the respective catchment of each gauge (Elmer et al., 2010). The return period of the 2002 flood event has been estimated to be equal to 500 years for the entire study area.

Contamination indicator (con), inundation duration (d), flow velocity indicator (v), precautionary measures indicator (pre) and monthly net income (inc) were estimated on basis of empirical flood damage data collected via computer aided telephone interviews with households affected by the 2002 flood in the case study area (Thieken et al., 2005). Development of the indicators (con, v, pre) is described in Thieken et al. (2005). Interview data was available in seven out of the 19 municipalities. For these municipalities the median value of the variables (con, d, v, pre, inc) per municipality is used as estimate. Via a regionalisation approach, i.e. in case of identical estimates in neighbouring municipalities along the river stretch, these estimates were also used as the estimate for the municipalities without interview data. Via this approach, meso-scale variables con, v, pre, inc are estimated for all municipalities. For inundation duration the spatial heterogeneity was large, so that no regionalisation is undertaken and estimates are only available in the seven municipalities with interview data.

The average floor space of residential buildings (fsb) as well as the average building value (bv) per municipality were taken from the Germany-wide exposure dataset of Kleist et al. (2006) who based their estimates on official statistical data like the information on total living area for three classes of residential buildings per district provided by the Federal Statistical Office of Germany and the standard construction costs per square meter gross floor space.

The residential building type (bt) composition and the mean residential building quality (bq) per municipality were derived following the approach of Thieken et al. (2008b). This approach is based on the geo-marketing data from INFAS Geodaten (INFAS Geodaten GmbH, 2001) which contain information about the numbers of different building types and their quality per municipality in Germany. On the basis of the share of each building type the municipalities were classified by means of a cluster analysis (Thieken et al., 2008b). The mean building quality per municipality was calculated from the information about the building quality in INFAS Geodaten which is distinguished in six classes from 1 "exclusive building quality" to 6 "very poor quality" (Thieken et al., 2008b).

The meso-scale loss calculation uses tools in ArcGIS and Matlab. All input variables were processed to be available as raster data sets with a cell size of 10 m x 10 m to fit to the water depth information. For each grid cell, the loss ratio is estimated by applying BT-FLEMO (and the other loss models, see section 14.2.4) on basis of the meso-scale input variables (Table 14.1). These loss ratios are then multiplied by the specific building value assigned to the corresponding grid cell. Finally, the loss estimates are summed up per municipality. The specific building values [EUR/m²] were extracted from the disaggregated asset value dataset from Wünsch et al. (2009). Their most detailed and reliable disaggregation result named A1+ was chosen. Asset estimation for residential buildings

was based on total replacement costs, with reference to the year 2000 (Kleist et al., 2006) which were transferred to the year 2002 by the construction price index (INFAS GEOdaten GmbH, 2001). The binary disaggregation procedure A1+ of Wünsch et al. (2009) was conducted with the use of ancillary information, namely the digital basic landscape model ATKIS Basic DLM (GEODATENZENTRUM, 2009) and data of residential building type and number at the subordinate constituency level of INFAS Geodaten (INFAS GEOdaten GmbH, 2001; INFAS GEOdaten GmbH, 2005). For the 12 small municipalities under study (i.e. Zschepplin, Bennewitz, Kuehren-Burkartshain, Jesewitz, Thallwitz, Bockelwitz, Nerchau, Trebsen/Mulde, Ebersbach, Grossweitzschen, Doberschuetz and Laussig), municipality and constituency are the same, so that no differentiation of building densities within one municipality was possible (see disaggregation A1 in Wünsch et al. (2009)).

14.2.4 Model validation

BT-FLEMO is validated by comparing estimated flood loss to official loss data and to alternative estimates of a variety of established loss models. The loss models are used to estimate direct economic losses of residential buildings caused by the 2002 flood at the meso-scale for the 19 municipalities of the case study area. The modelled absolute loss to residential buildings per municipality is compared to the official loss information which had been reported by the Saxon Relief Bank (SAB, 2005). Thus, model evaluation is based on 19 records.

In total, six deterministic, meso-scale loss models are applied for comparison purposes: two multi-variable models (FLEMOps+r and RT2), and four traditional uni-variable depth-damage functions. The rule based FLEMOps+r model (Elmer et al., 2010) calculates flood loss using five different classes of water depth (*wst*), three individual building types (*bt*), two classes of building quality (*bq*) and three classes of flood frequency (i.e. return period (*rp*)). The regression tree loss model (RT2) developed by B. Merz et al. (2013) has eight leaves using the predictors water depth (*wst*), floor space of building (*fsb*), return period (*rp*), and monthly net income (*inc*). Three depth-damage functions commonly used in Germany are applied (NRW, 2000; ICPR, 2001; Hydrotec, 2001; Hydrotec, 2002). MURL (NRW, 2000) calculates the loss ratio of residential buildings by the equation $r_{loss} = 0.02 wst$, where *wst* is the water depth [*m*] and *rloss* is the loss ratio [-]. For water levels of more than 5 m the loss ratio is set to 0.1 (i.e. 10%). ICPR (ICPR, 2001) estimates the loss ratios of residential buildings by the relation $r_{loss} = (2 wst^2 + 2 wst) / 100$. HYDROTEC (Hydrotec, 2001; Hydrotec, 2002) uses the root function $r_{loss} = (27\sqrt{wst}) / 100$. In the latter two models, estimated loss ratios >1 are set to 1 (i.e. total loss). The fourth depth-damage function (*sd-f*) is taken from Merz et al. (B. Merz et al., 2013) and uses the equation $r_{loss} = 0.0142 + 0.0127 * \sqrt{wst * 100}$. It was derived at the micro-scale using the same empirical flood loss database as the models FLEMOps+r, RT2 and BT-FLEMO, i.e. data sets of damaged residential buildings which have been collected via computer aided telephone interviews after the floods in 2002, 2005 and 2006. The other three depth-damage functions (MURL, ICPR, HYDROTEC) were developed differently, i.e. on basis of expert judgement and data from the old German flood loss database HOWAS which contained loss data from floods between 1978 and 1994 in Germany. This difference needs to be taken into consideration for the model

comparison.

As performance measures for the loss models in comparison with the official loss values the mean bias error (MBE), the mean absolute error (MAE) and the root mean square error (RMSE) were used. The MBE provides the average deviation of the estimated flood loss values from the officially reported values and indicates the systematic error of the model, i.e. its accuracy. A positive MBE indicates an average over-estimation of the model, while a negative MBE corresponds to an average under-estimation. The MAE provides the average absolute deviation of the estimated loss from the reported values and indicates the precision of the model results. The RMSE provides information on the variation of the estimated loss values from the officially reported values. As the square root of a variance, RMSE can be interpreted as the standard deviation of the unexplained variance.

In contrast to the deterministic loss models, the probabilistic model BT-FLEMO provides not only a single prediction but supplies a distribution of model predictions. For the evaluation of BT-FLEMO results in terms of the above criteria we use the average of all individual predictions. The distribution of model predictions represents the prediction uncertainty due to uncertainties in the model structure, data variability and data errors. For BT-FLEMO to provide reliable predictions, the 90% confidence interval should contain 90% of the officially reported loss values, in case there are no other significant sources of uncertainty along the flood loss estimation chain.

14.3 Results and discussions

14.3.1 Meso-scale BT-FLEMO

For the meso-scale BT-FLEMO the same model structure is used as for the micro-scale. The meso-scale input variables of BT-FLEMO were estimated on the municipal level as shown in Table 14.2, except for water depth and return period which are given in a more spatially differentiated way as described in Table 14.1. In some cases no estimation of the inundation duration (d) was possible due to the high heterogeneity of the empirical flood damage data. However, BT-FLEMO is robust in respect to missing data. In these cases, loss estimates are based on the RT-leaves that can be reached given the available data. The relatively coarse spatial differentiation on the municipality level has a smoothing effect on spatial data variability and does not reflect the real heterogeneity of inundation patterns as well as building and household characteristics. Heterogeneity also differs from area to area, for instance, the precautionary measures indicator in Döbeln is estimated to be one and shows a standard deviation of 1.4 and in Eilenburg it is also estimated to be one but shows a standard deviation of 5 (data not shown). Further research should develop more spatially differentiated estimation methods for key input variables used in flood loss estimation. The use of remote sensing data is a way forward in respect to resistance variables (Gerl et al., 2014). For an improved spatial differentiation of impact variables like inundation duration (d) or flow velocity indicator (v) a 2-D hydraulic modelling of the inundation scenario should be undertaken. Regional 2-D hydraulic modelling is feasible due to improved computer performance and numerical solvers (Vorogushyn et al., 2010; Falter et al., 2015).

Table 14.2: *Input variable values which have been estimated on the municipality level for BT-FLEMO (contamination indicator (con), inundation duration (d), flow velocity indicator (v), floor space of building (fsb), precautionary measures indicator (pre), building value (bv)) as well as for the models FLEMOps+r and RT2 (building type (bt), building quality (bq), and income (inc))*

Municipality	con	d	v	fsb	pre	bv	bt*	bq	inc
	[-]	[h]	[-]	[mš]	[-]	[EUR]	[-]	[-]	[-]
Bennewitz	3	120	1	102	1	118,394	5	4	15
Bockelwitz	3	-	2	95	1	111,709	5	4	15
Doberschuetz	3	-	2	89	1	104,715	5	4	15
Döbeln	1	48	2	215	1	260,860	2	4	15
Ebersbach	1	-	2	89	1	106,172	5	3	15
Eilenburg	3	144	2	183	1	219,840	2	4	15
Grimma	3	36	2	159	1	194,877	3	4	15
Grossweitzschen	1	-	2	111	1	129,749	5	4	15
Jesewitz	3	-	2	97	1	114,059	5	4	15
Kuehren-Burkartshain	3	-	2	95	1	117,802	5	3	15
Laussig	3	-	2	165	1	193,962	5	4	15
Leisnig	1	24	2	139	1	163,731	4	4	15
Machern	3	-	2	103	1	117,043	5	4	15
Nerchau	3	-	2	92	1	106,143	4	4	15
Rosswein	3	39	2	139	1	166,444	4	4	15
Thallwitz	3	-	2	106	1	128,326	5	3	15
Trebsen/Mulde	3	24	1	106	2	124,929	4	4	15
Wurzen	3	-	2	199	1	243,413	2	4	15
Zschepplin	3	-	2	90	1	101,936	5	4	15

* Building type clusters: 1 Dominated by multifamily houses; 2 Mixed (high share of multifamily houses); 3 Mixed (high share of semi-detached houses); 4 Mixed (high share of one-family houses); 5 Dominated by one-family houses

14.4 Loss estimates and model validation

BT-FLEMO provides a probability distribution of aggregated loss to residential buildings for each municipality under study. Figure 14.3 shows the histograms, i.e. probability distributions resulting from the 200 regression trees of BT-FLEMO. The vertical red line represents the official loss reported for the municipality by the Saxon Relief Bank (SAB, 2005).

The comparison between the probability distribution of the loss estimates and the official reported loss shows, that only in three of the 19 municipalities, i.e. in 16% of the cases (Eilenburg, Döbeln, Rosswein), the official loss information is located within the 90% confidence interval of the BT-FLEMO loss estimates (Figure 14.3). This suggests that other significant uncertainty sources exist, besides uncertainty due to the loss modelling component which is captured by the probabilistic BT-FLEMO.

The comparison of BT-FLEMO with the other loss models shows that the 90% confidence interval of BT-FLEMO represents relatively well the variation range of loss estimates of the other models, except for the MURL (NRW, 2000) model (Figure 14.4). However, it was shown by Thieken et al. (Thieken et al., 2008b) that the MURL model tends to strongly underestimate losses in comparison with official loss data from the Elbe 2002 flood. This is in accordance with MURL's strong bias towards underestimation in our case study (Table 14.4). Thus, BT-FLEMO captures well the uncertainty due to the loss modelling component.

The different loss models provide coherent results in terms of underestimation in some municipalities and overestimation in others. The within model variation of loss predictions seems to be smaller than within municipalities (Table 14.3 and Figure 14.4). In some of the municipalities, the estimated losses are one order of magnitude off the reported values. The strongest underestimation is given in Bennewitz (mean estimate of all models: EUR 1.5 M; reported: EUR 20.8 M), whereas the models most strongly overestimate the loss in Grossweitzschen (mean estimate of all models: EUR 37.7 M; reported: EUR 0.9 M). In municipalities where all loss models significantly over- or underestimate the official loss report it is likely that errors and uncertainty result from other sources along the loss estimation chain, e.g. from inundation modelling or exposure estimation. A further source is the uncertainty of the official loss data. These additional, other sources of uncertainty are not addressed in this study, but have been investigated in previous case studies, e.g. by B. Merz and Thieken (2009), Apel et al. (2009) and Notaro et al. (2014). Seifert et al. (2010) reported similar patterns for loss estimation for the commercial sector. They relate large errors in loss estimation to high uncertainties in the exposure estimation, i.e. disaggregated asset values, particularly in municipalities with a small fraction of affected companies. This is in accordance with our results, where we see smaller errors in loss estimation in municipalities with larger total loss in comparison with municipalities with total loss below about EUR 3 M officially reported loss (with the exception of Bennewitz; Table 14.3 and Figure 14.4).

The compilation of error statistics for all loss models averaged over all 19 municipalities is shown in Table 14.4. For BT-FLEMO the average loss estimate is used for calculating the errors. In contrast to the other models, BT-FLEMO provides a virtually unbiased prediction of flood loss. In terms of MAE it performs comparably well as the

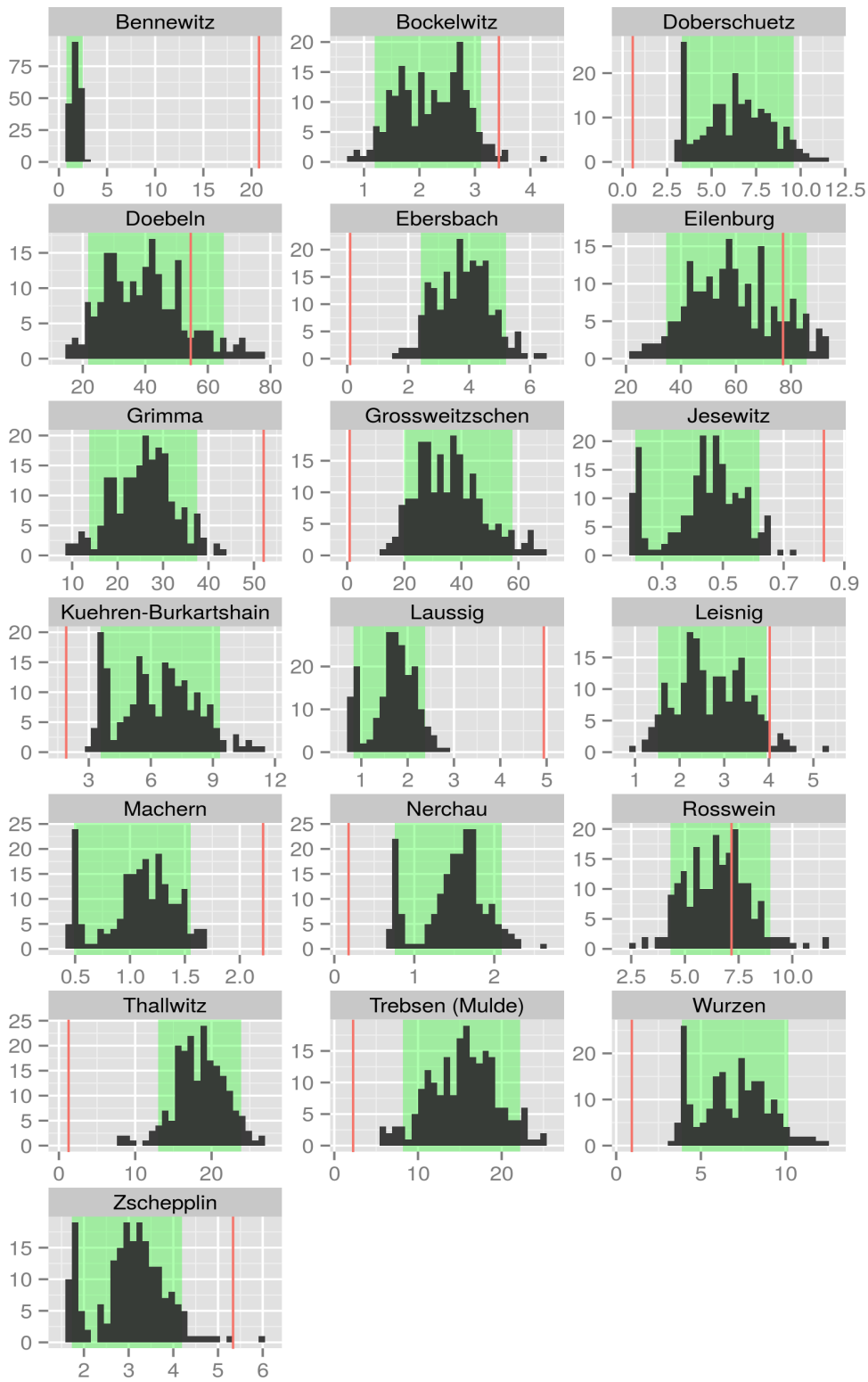


Figure 14.3: Results of BT-FLEMO (black histograms, x-axes represent losses in million euros, y-axes represent frequency, 90% confidence interval is marked in green) as well as official loss information (red lines) in the 19 municipalities under study.

Table 14.3: Overview of official loss data and loss estimates in the 19 municipalities in the case study area

Municipalities with official loss [mill. EUR]	Loss estimates by different models [mill. EUR]							
	MURL	ICPR	HYDROTEC	sd-f	FLEMOps+r	RT2	mean BT-FLEMO	
Bennewitz	20.8	0.3	0.8	2.6	1.3	1.5	2	1.7
Bockelwitz	3.4	0.3	1.1	3.6	1.8	2.1	2.4	2.2
Doberschuetz	0.6	1.2	4.2	11.2	5.7	6.2	5.1	6.3
Döbeln	54.5	9.9	42.7	80.4	40.5	50.3	32.9	39.9
Ebersbach	0.1	0.6	1.7	5.6	2.9	3.4	2.7	3.8
Eilenburg	77.1	9	28.3	88.2	45.1	62.3	42.3	59
Grimma	52.1	3.9	12.5	38.6	19.8	25.3	18.3	25.8
Grossweitzschen	0.9	8.7	36.8	71.6	36.1	45.1	29.6	35.9
Jesewitz	0.8	0.1	0.2	0.6	0.3	0.4	0.5	0.4
Kuehren-Burkartshain	1.9	1.3	4.5	12.1	6.1	8.3	5.6	6.3
Laussig	4.9	0.3	0.9	2.6	1.3	1.4	1.8	1.7
Leisnig	4	0.5	1.6	4.9	2.5	2.9	3.3	2.7
Machern	2.2	0.2	0.5	1.6	0.8	1	1.2	1.1
Nerchau	0.2	0.2	0.5	2.1	1.1	1.2	1.5	1.5
Rosswein	7.2	0.9	2.6	9.5	4.9	5.8	4.6	6.5
Thallwitz	1.3	2.4	7.6	23.9	12.3	13.9	17	18.4
Trebsen/Mulde	2.2	2.4	8	23.3	11.9	15.1	10.9	15.4
Wurzen	0.9	1.4	4.5	13	6.6	9.1	6.2	6.9
Zschepplin	5.3	0.4	0.9	4.4	2.3	2.5	2.7	3.1

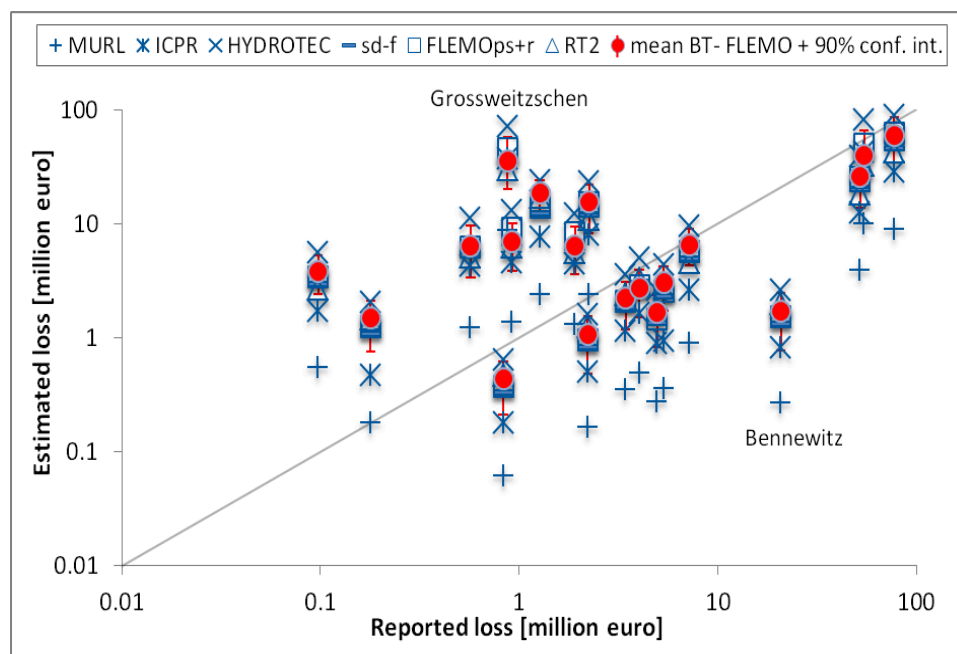


Figure 14.4: Loss model comparison and validation with official loss data for the 19 municipalities in the case study area at the Mulde River.

Table 14.4: Comparison of model performance (MBE: mean bias error, MAE: mean absolute error, RMSE: root mean square error)

	MURL	ICPR	HYDROTEC	sd-f	FLEMO _{ps+r}	RT2	BT-FLEMO
No. of input variables	1	1	1	1	4	4	8
MBE [Mill. EUR]	-10.4	-4.2	8.4	-2	0.9	-2.6	-0.1
MAE [mill. EUR]	11.5	10.5	12.1	9.8	9	10.1	9.2
RMSE [mill. EUR]	22.4	17.7	20.1	14.9	14.1	15.3	13.4

FLEMO_{ps+r} model which ranks first place. BT-FLEMO shows the smallest RMSE of all models. The error statistic is strongly influenced by five municipalities which appear particularly problematic for loss estimation (Table 14.3). These are Bennewitz, Eilenburg, Grimma and Döbeln where most models underestimate the absolute loss as well as Grossweitzschen where all models strongly overestimate the absolute loss. Additionally, apparent are the strong biases of under- and overestimation by the Models MURL and HYDROTEC, respectively (Figure 14.4). The models which have been developed on basis of empirical loss data from recent flood events in 2002, 2005 and 2006, namely sd-f, FLEMO_{ps+r}, RT2 and BT-FLEMO, perform better than the other models MURL, ICPR, and HYDROTEC which have been developed on basis of expert judgement and loss data from floods between 1978 and 1994.

In summary, multi-variable models outperform depth-damage functions and seem to be as such an improvement in flood loss modelling. This is in accordance with previous findings of B. Merz et al. (2013) and Schröter (2015). However, more input parameters also introduce additional uncertainty, even more in upscaling procedures for meso-scale applications, where the parameters need to be estimated on a regional area-wide basis. Thus, when looking for the “best” loss model, one actually looks for a loss model with best performance and the smallest number of variables (principle of parsimony). The models sd-f with one input variable and FLEMO_{ps+r} with four input variables show in comparison still relatively good error statistics (Table 14.4). Thus, these models are also suitable for meso-scale loss estimation. However, bagging of RTs significantly improves prediction accuracy and reduces the predictive limitations associated with a single model. The basically unbiased loss estimation and the additional advantage of inherent uncertainty estimation by BT-FLEMO justifies the use of this model despite its high number of input variables. The MBE shows that the majority of the loss models tend to underestimate flood losses, exceptions are the models HYDROTEC and FLEMO_{ps+r}. These results are consistent with previous validation studies using the 2002 flood as a case study (Thieken et al., 2008b; Elmer et al., 2010; Wunsch et al., 2009). Generally, uncertainties of loss estimation remain high, which underlines the importance of uncertainty quantification. The probabilistic loss model BT-FLEMO is as such a significant advancement.

14.5 Conclusions

Reliable loss modelling is essential for risk analysis. Loss models are supposed to account for the complexity of the damaging processes, though remaining as simple as possible. Recent studies demonstrated that multi-variable flood loss models using several impact and resistance variables outperform depth-damage functions. The proposed loss model BT-FLEMO is a probabilistic, multi-variable, meso-scale model based on eight input variables: water depth, return period, contamination indicator, inundation duration, flow velocity indicator, floor space of building, building value and precautionary measures indicator. BT-FLEMO is robust in respect to missing values, i.e. loss estimates are still possible for cases where certain variables are not available. Additionally, it provides quantitative information on uncertainty associated both with the random heterogeneity of input data (i.e. data variability and errors) and model structure. BT-FLEMO was transferred from the micro-scale to the meso-scale. Validation at the meso-scale shows the suitability of the up-scaling approach. In the case study based model comparison and validation, BT-FLEMO showed the smallest systematic error (MBE) and smallest RMSE of all applied models, whereas the multi-variable model FLEMOps+r showed the smallest MAE. In accordance with previous studies these results show that multi-variable models provide an improvement in flood loss modelling. Additionally, the probabilistic BT-FLEMO model inherently provides an estimate of the uncertainty in the flood loss modelling component, which is an important innovation. It is crucial to capture and quantify uncertainties in flood loss estimates for risk communication and informed decision making.

15 | Discussion, conclusions and outlook

15.1 Summary of achievements

Floods impact individuals and communities globally and may have significant social, economic and environmental consequences. With USD 100 b economic loss on average every year, floods are among the most harmful natural hazards worldwide. Confronting an increasing trend in flood risk, the sustainable reduction of flood impacts needs a rigorous implementation of integrated risk management. While risk-oriented approaches are increasingly pursued and operationalized on administrative level as well as in the re-insurance industry, important questions remain regarding the interactions, feedbacks and dynamics in flood risk. Research is needed to obtain an improved understanding of flood risk systems regarding the interplay of underlying hazard, exposure and vulnerability processes. Rapidly increasing amounts and diversity of data require further efforts to enhance the capability to process large data sets, as well as to develop and test methods and models for less uncertain and more reliable flood risk assessments. The thirteen papers of this habilitation thesis contribute new insights and findings to this field of research, and thus improve the foundations of flood risk management and in particular the assessment of flood risk. The first part of the thesis investigated questions regarding flood risk systems and the second part looked into aspects of vulnerability modelling for loss estimation. The research on these topics was organized in three overarching themes addressing the *analysis of flood events*, *data sources* and *flood risk modelling*. The contributions and main findings with regard to the according research questions are as follows:

Flood event analysis: What can be learnt from flood events about controls and impacts and how do flood events need to be monitored and documented?

Schröter et al. (2015) and Thielen et al. (2016) demonstrated that flood event analyses are a suitable approach for gaining insights into the generation and evolution of floods as well as into the response of flood risk systems and impacts. Further, it has been shown that closely monitoring floods provides unique opportunities for collecting data during extreme situations and for learning about data gaps to improve monitoring and documentation systems.

The hydro-meteorological analysis of the June flood 2013 in Germany and the statistical analyses of precipitation and discharge data for large-scale floods in Germany conducted by Schröter et al. (2015) showed that hydrological extremes are more due to the unusual combination of different hydro-meteorological factors than to unusual magnitudes of the individual factors alone. This emphasises the need to take interactions of various flood drivers into account in flood hazard assessment. The newly created dataset of past large-scale floods in Germany provides consistent information about initial catchment wetness,

initial river discharge levels, event precipitation and resulting flood magnitudes. This knowledge constitutes a basis for the development of plausible worst-case flood scenarios and for additional investigations of flood controls including the spatial and temporal variability of these factors, and their superposition. In future works, factors related to additional hydrological processes, as for instance snow-melt or seasonal variation in water storage should be included.

Regarding flood impacts, the analyses of the June flood 2013 in Germany (Thielen et al., 2016) showed that many information about consequences of flooding are available but considerably differ in detailedness, completeness and accuracy. In view of this large heterogeneity in data sources, formats and accessibility, an agreement on reporting standards is an important step towards a consistent documentation of flood impacts. These standards should define the scope and level of detail of data as for instance the sectors, types and number of affected entities. Such a framework would be the foundation to implement a systematic data collection and information system for flood impacts and expenditures related to flood management.

The structured compilation of event related data and the targeted retrieval of data during and after flood events makes it possible to capture and document flood and impact processes more comprehensively and in higher detail. In this regard, post disaster event survey data of affected people and entities have been shown to give new insights into the relevance of factors and interrelationships. Knowledge about actual occurrence of damage and concerns of affected people is useful to inform the process of weighing social, economic and other impacts in flood risk assessments.

Data sources: How can new data sources be utilized in flood risk modelling and assessment?

Capturing data during flood events supports the situation assessment and secures evidence on extreme states of the flood risk system for post event analyses. Tapping new data sources open up new opportunities to expand and complement established sensors and monitoring systems, and to enrich our view to flood processes and impacts. The utilization of new data sources for flood risk assessment has been approached by example of volunteered geographic information (VGI), by example of post event surveys on flood losses and influencing factors, and by example of open data sources based on data standards.

Fohringer et al. (2015) have demonstrated that VGI from social media are a useful source to extract quantitative information from geo-located images for inundation mapping. The inundation depth maps derived from the image content complement observations from water level gauges or are even exclusive in situ data. However, the joint usage of VGI with other data sources requires further investigation concerning the pre-selection of photos by automatic image analyses, the integration of more detailed information about the reference environment, and the use of ancillary data such as flood footprints or hydrodynamic model based flood hazard maps to reasonably constrain inundated areas. In addition, it has to be recognized that VGI are associated with uncertainty concerning the timing, the geo-location and the derived water depths. Also the spatial coverage of information support from social media within the target area cannot be controlled but depends on the arbitrary activity of social media users. In this regard, ways need to be

explored for the targeted acquisition of VGI in areas where information is missing or not clear. One approach would be mapping quests, which are directly addressing people in the affected region, voluntary helpers or emergency responders in the field.

For the example of post event surveys on flood losses and influencing factors Schröter et al. (2014), and Schröter et al. (2016) have investigated the implications of the number of variables and the amount of data used for flood loss modelling for predictive model performance. Post event survey data provide local, context related data which link hazard, exposure and vulnerability characteristics. The incorporation of such additional knowledge into vulnerability models intends to achieve a better representation of flood damaging processes. In Schröter et al. (2014) it has been questioned whether increasing complexity of flood damage models - by adding predictive variables to flood vulnerability models - improves the capability to reliably predict flood damage. It has been shown that the improvement depends not only on the number of variables used to predict flood loss, but also on the model approach, and thus on the complexity inherent to the model structure, i.e. the representation of damage processes. One important finding was that newly introduced multi-variable probabilistic models more reliably predict flood loss. As these models require a larger number of input variables, this implies increased efforts for the detailed and structured acquisition of explanatory variables. To get a better understanding of the required amount of data, Schröter et al. (2016) tested different models within split sample validation experiments using incremental amounts of data from different regions and event contexts. The outcomes of these tests revealed that model predictive performance and reliability improves with increasing amounts of data, and exhibiting larger performance gains for the more complex models.

However, the acquisition of post event survey data is laborious and costly, and not always possible. Therefore, the suitability of alternative data sources for vulnerability modelling is of interest. The suitability of open data sources for flood loss estimation has been investigated by Schröter et al. (2018a) for the example of 3D city models using a predictive data analytics approach. The outcomes suggest that variables representing building geometric properties such as building area, height, roof type, shape, and density of buildings are useful to explain flood loss of residential buildings with slightly reduced model performance in comparison to detailed post event data. Nevertheless, the variability of flood loss on individual building level is huge, and thus uncertainty associated with flood loss estimates models must be analyzed, quantified, and communicated. Probabilistic model approaches are an important advancement in this direction and need to be further developed for the broad application. This has to address the implementation of these models as deployable software, as well as provision of procedures for the use of uncertainty information in risk assessment.

Risk Modelling: How can interactions and dynamics in flood risk systems be incorporated in flood risk modelling and assessment?

Comprehensive and consistent data on floods and impacts give new insights into flood risk systems, their feedbacks and interactions, and thus provide a basis to improve, evaluate and test risk models. Regarding vulnerability modelling, multi-model ensembles and machine learning ensemble approaches have been examined with a view to model performance and model predictive uncertainty. In the broader context of flood risk systems, the controls on flood characteristics and impacts have been investigated, an approach for assessing flood risk in a spatially consistent way has been developed, and the interplay of flood seasonality with susceptibility of agricultural crops has been examined.

Based on the inventory of flood vulnerability models presented in Gerl et al. (2016) and using the included meta data about model specification, geographical characteristics, transferability and mathematical formulations the concept of multi-model ensembles has been implemented for flood vulnerability models in Figueiredo et al. (2018). On a similar line, Kreibich et al. (2017a) have applied a machine learning approach for multi-variable vulnerability modelling on the meso-scale. The used algorithm of Bagging Decision Trees is an ensemble method and provides quantitative information on the predictive uncertainty which enables the consideration of flood loss model uncertainty in regional flood risk analysis.

Interactions, feedbacks and dynamics in flood risk systems shape the implications and importance of controls on flood characteristics and impacts. As revealed by the analyses of the June flood 2013 (Schröter et al., 2015), flood magnitude and extent arise from the combination of different factors including catchment wetness and precipitation. Accordingly, initial wetness, weather patterns and event precipitation inform on flood occurrence, involved processes and flood characteristics. The simulations of the complete flood risk chain conducted by Nied et al. (2017) showed that distinct flood characteristics have different hydro-meteorological controls. Importantly, for flood losses no single governing control has been identified and it is still an open question whether a particular catchment and atmospheric state implies particular patterns of inundation and flood losses.

Accordingly, in flood risk assessment continuous long term simulations of the flood risk chain are needed for a holistic representation of flood processes considering their spatial correlations and interactions. Using a coupled model chain as proposed by Falter et al. (2015) allows deriving flood risk estimates directly from the simulated damage. The comparison of damage probabilities derived from simulated loss samples and corresponding peak discharge probabilities showed substantial differences in risk estimates which arises from non-linearities and threshold behaviour along the flood risk chain. Flood damage depends not only on the maximum flood intensity, i.e. the flood peak but also on other flood characteristics as for instance hydrograph shape and/or floodplain hydraulics including dike overtopping.

While these findings corroborate the importance to take interactions in flood risk systems into account, additional complexities arise with hazard and vulnerability characteristics changing with time. Temporal dynamics of flood risk systems have been inves-

tigated by Klaus et al. (2016) for the case of seasonal changes in flood risk of agricultural crops. In this research the variation of flood occurrence is superimposed on the monthly variation of crop susceptibility to quantify the implications of these effects in terms of flood risk. With spatially varying flood regimes, agricultural flood risk differs across regions and results in different crop types most at risk. Equipped with this knowledge, conscious crop selection can mitigate agricultural flood losses.

15.2 Discussion

In view of quickly changing flood risk, with expanding floodplains, land use change transforming watersheds, and population migration shifting demographics and accumulation of assets, increasingly different parts of the society face the need to plan and adapt to risks. The public sector, the insurance and financial industries realize an increasing need for advanced methods and tools for risk assessments to reduce flood disaster risk, assess and manage solvency of insured portfolios, and evaluate investments. The research papers of this thesis relate to various challenges these sectors are facing. This concerns aspects of understanding flood risk systems, analysing flood events, exploring and applying data sources, and modelling flood risk which deserve a discussion in the context of emerging trends and progresses in reducing risk.

Understanding risk is the first priority of actions to achieve the targets of the Sendai framework for disaster risk reduction (UNISDR, 2015). Likewise, the insurance and financial industries need to keep up with evolving risk (UNEP FI, 2018; Geneva Association, 2018). In a shrinking world, with an increasing interconnectedness at many levels, flood risk assessment and management has to deal with a growing complexity of tasks: risk is becoming systemic (UNDRR, 2019). The need to overcome organisational, sectoral and disciplinary silos is obvious and requires a rethinking of self-images, competencies and commitments by the parties involved, e.g. (Surminski and Thielen, 2017). Further, developments in open data, shared and interoperable software, computing power and other technologies are increasingly recognized to enable improved data analytics, risk assessment and management, as well as reporting and informed policies.

The achievements of this thesis contribute to our knowledge about flood risk systems, our capabilities to analyse and make use of data as well as to improve risk modelling approaches. Hence, it offers advancements which are relevant for risk assessment and risk management in the public, insurance and financial sectors. The possible avenues and links to these domains are illustrated in Figure 15.1 and comprise insights into flood risk systems, data usage and analytic capabilities, as well as advanced risk modelling approaches.

Insights into flood risk systems

Flood risk is complex. The challenge for a sound system framing is to identify the important processes to be considered in which detail or to neglect. Therefore, an understanding is needed how to balance practical risk assessment approaches and (over)

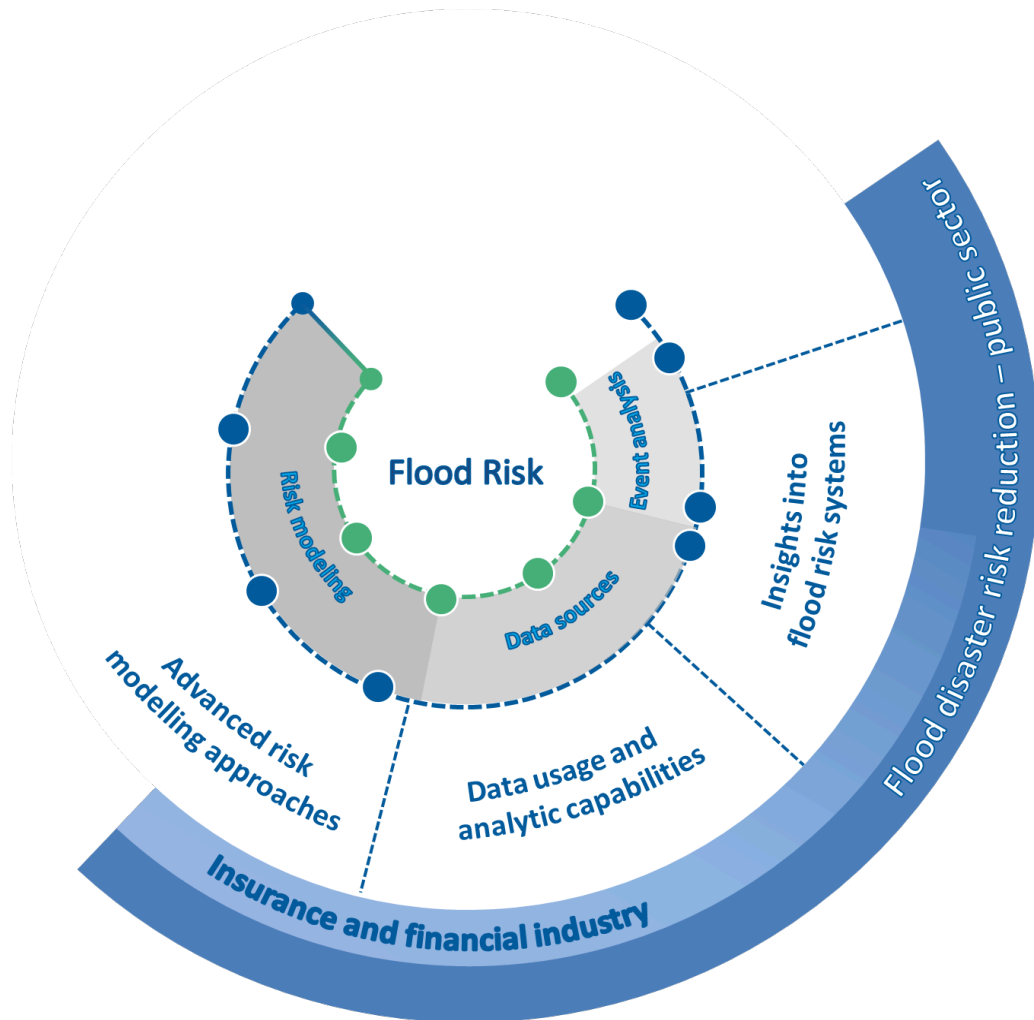


Figure 15.1: Thesis outcomes: avenues and links to flood disaster risk reduction

simplifying assumptions that ignore the essential features of the flood risk system. The analysis, monitoring and documentation of extreme events covering both hazard and impacts give useful insights into system behaviour (IRDR, 2015b; Schröter et al., 2018b). The idea of learning from disasters is adopted and operationalized in the post event review capability (PERC), (Venkateswaran et al., 2013). With the aim to capture the hazard, institutional and socio-economic landscape which shape the impact of the event, this framework is geared towards unveiling the interactions of hazard and vulnerability as well as the mechanisms within the implemented disaster risk management practice. PERC may be seen as a catalyst to strengthen and improve local institutional frameworks and planning processes for disaster risk reduction. Though, the further deepening of extreme flood event analyses needs also technical frameworks for the documentation, quantitative analysis and evaluation. Event catalogues as proposed by Paprotny et al. (2018a) for European floods are suitable to structure and compile available knowledge. In addition, linking flood severity indices and impact indicators give deepened insights into how flood risk systems respond to extreme events (Schröter et al., 2015; Thielen et al., 2016). Such extended data sets support the comparisons of events, e.g. Kreibich et al. (2017b), and are an important addition for the evaluation of flood risk reduction strategies and identification of options for action.

Data usage and analytical capabilities

The lack of reliable, consistent and comparable data is seen as a major obstacle for effective and long-term loss prevention. In the most recent global assessment report, UNDRR (2019) stresses that reliable risk assessments underpinning flood risk reduction strategies and plans need *good data*. Basically, good data is useful and usable. This implies accurate and consistent data in appropriate spatial and temporal detail with thorough quality control. Beyond that, good data should also involve, verbose description of datasets including the generation processes, date specification, as well as accessibility and reliable availability. Currently, fragmented and heterogeneous data from dispersed sources involve disproportionate efforts to compile useful data sets, particularly for flood impacts (Thielen et al., 2016). The UNDRR Desinventar open source initiative¹ is one example for a global disaster information management system which collects hazard and impact data time-stamped, geo-referenced and disaggregated to sub-national administrative units. Still, quality checks, completeness and consistency with other datasets, e.g. EM-DAT, MunichRe NATCATservice, SwissRe Sigma, PERILS etc. are unsolved issues.

Evolving technologies have the potential to enrich and innovate flood risk assessment by delivering locally up to date information as for instance citizen-science, internet of things, remote sensing with new satellites or drones. Machine Learning offers useful algorithms to leverage new and increasing amounts of heterogeneous data, explore and effectively analyse data, and build novel data-driven risk models. In combination with growing computational capacities these approaches become feasible. At the same time, the expanding use of new technologies is closely linked to and depending on developments in open data.

Interoperable data are a prerequisite to enable the exchange of knowledge and in-

¹www.desinventar.net

formation and are the technical groundwork to make progress in implementing systems approaches. In this context, the agreement and adherence to data standards is an indispensable step. The infrastructure for spatial information in Europe (INSPIRE), EC (2007a) and CityGML ² are examples for geospatial data standards which should be used more widely. For the domain of vulnerability and exposure data examples are the open exposure database ³, and open building map ⁴. Such approaches embody the idea that environmental and economic data are pooled in a common or compatible database which is open, visible and available for cross-sectoral planning, e.g. in urban planning (Schröter et al., 2018a).

Concerning the data generation process, citizen-generated data or VGI offer appealing innovations in all phases of flood risk management (Irwin, 2018; Paul et al., 2018). Exposure mapping and vulnerability characterisation are important aspects for preparedness and ex-ante risk assessment. During disasters VGI contribute to situation assessments supporting emergency response and rapid assessments of consequences (Fohringer et al., 2015). The Humanitarian OpenStreetmapTeam for disaster response ⁵ is a striking example for the capacity of this approach. Multi-directional exchange of information as well as targeted acquisition of missing data are further possibilities to improve the effectiveness of disaster relief (Paul et al., 2018). Finally, loss reporting by affected citizens after the event is useful for simplified loss and claim reporting. It also offers a good opportunity to collect first hand information about damaging processes and consequences including intangible effects and how affected people experience risk and loss. The implementation of a common data base for property level flood impact information could improve the empirical data basis for model development and testing and promote the exchange of experiences about mitigation measures. The technological development and implementation of such systems is presumably a matter of time. However, the utilisation of these information may be subject to data protection regulations which often means a loss of information detail, e.g. about geo-locations. Actively engaging people in the data generation and collection process also affects the ownership of data. Citizens as the originators of data are likely to find additional usages of these data for other purposes. While this assumption will need to be corroborated, it is plausible that these data can find application in site-specific multi-risk assessments which will enable the identification and utilisation of synergies to mitigate consequences of different hazards and risks.

Advanced risk modelling approaches

With growing demands to provide dynamic risk profiling and management of risk, not only comprehensive high quality data are requested, but also realistic simulations of extreme events in terms of hazard intensity and impacts. Continuous simulations of the flood risk chain and derived flood risk (Falter et al., 2015; Falter et al., 2016) enable the sensitivity analysis of flood risk to changes in various factors in the flood risk system as for instance conducted by Metin et al. (2018). Risk models also offer possibilities to study effects of system behaviour on the performance of flood risk reduction strategies

²<https://www.opengeospatial.org/standards/citygml>

³<https://github.com/simplitium/oed>

⁴<http://www.openbuildingmap.org>

⁵<https://hotosm.org>

(Ciullo et al., 2019). As with data, interoperability of risk models is key to account for the interconnectedness in flood risk systems.

Open modelling and model interface standards are the basis for modular concepts which facilitate the development of combined and tailored risk models for the problem under study. Modular approaches will simplify the procedure to extend boundaries of risk models regarding represented processes, interactions and dynamics. Further, interoperable models enable the exchange of models, model outputs and underlying assumptions. Talking the same language regarding data and models opens communication capabilities across administrative, economic and academic sectors. As risk assessments are associated with large uncertainty, rigorous testing and validation of flood risk models is essential and has to be a standard step in risk model development. Decision making needs to be aware of the underlying assumptions and sensitivity to the outcomes of risk assessments. In this regard, open data and modelling standards increase transparency and reproducibility of model simulations which are crucial for the credibility and trust in risk assessments. Reliability and transparency of risk assessments are key requirements to support the public discussion about how to manage risks.

15.3 Concluding remarks and outlook

The work and findings presented in this thesis mark progresses in several aspects of flood risk assessment and management. Concluding, a number of points are stressed with emerging importance for future advancements of the field.

Consolidate the analysis of extreme flood events: Establish institutional and technical frameworks for the structured documentation of events which support comprehensive assessments and testing of current risk management strategies.

Expand the use of new technologies and open data: Take advantage of evolving technologies regarding observations, monitoring, data exploration and predictive analytics. The domain of machine learning offers useful algorithms to leverage new and increasing amounts of heterogeneous data and build novel data-driven risk models. Open data and modelling standards are a vehicle to broaden the perspective of risk assessments to more comprehensively capture flood risk systems.

Consider the broader risk context: Take system behaviour into consideration for flood risk assessment and management. Beyond that, risk analyses are usually carried out separately for the pertinent hazards in a region without considering interaction, triggering of cascading hazards etc. Comprehensive, harmonised and site-specific multi-risk assessments are needed, enabling the identification and utilisation of synergies to mitigate consequences of different hazards.

Keep up with changing risk: Maintain the data basis and refresh risk assessments. This underlines the necessity to implement increasingly efficient, adaptable and robust approaches for dynamic risk profiling and flood risk management.

Understand and quantify the uncertainties and limitations of risk information: Risk assessments are associated with large uncertainty. Rigorous testing and validation of flood risk models is essential and has to be a standard step in risk model development. Decision making needs to be aware of underlying assumptions and sensitivity to the outcomes of risk assessments.

Ensure credibility and transparency of risk information: Reliability and transparency of risk assessments are key requirements to support the public discussion about how to manage risks. At the same time increasingly different parts of the society face the need to plan and adapt to future risks. Understanding these risks is critical and requires broad accessibility of these information. Such knowledge also comes along with individual responsibility, and thus requires not only improved risk communication but also needs suitable legal frameworks.

In conclusion, we must acknowledge that complex systems and processes determine our reality. However, we do not deal with these systems directly, but we plan, decide and make predictions on the basis of our perception of reality. Though, our view of the world is not only distorted but always incomplete⁶. Hence, the real behaviour of complex and dynamic systems will always lead to unpredictable surprises, and thus nourish research.

⁶based loosely on Dietrich Dörner: <https://www.uni-bamberg.de/trac/emeriti-of-excellence/doerner/>

Annex 1

Contribution to papers included in the thesis:

Paper	Citation	Design of study	Performed research	Analysed data	Wrote Manuscript
1	Kreibich, H., Bubeck, P., Kunz, M., Mahlke, H., Parolai, S., Khazai, B., Daniell, J., Lakes, T., Schröter, K., 2014. A review of multiple natural hazards and risks in Germany. Nat Hazards 126. https://doi.org/10.1007/s11069-014-1265-6	20%	20%	20%	20%
2	Schröter, K., Kunz, M., Elmer, F., Mühr, B., Merz, B., 2015. What made the June 2013 flood in Germany an exceptional event? A hydro-meteorological evaluation. Hydrol. Earth Syst. Sci. 19, 309327. https://doi.org/10.5194/hess-19-309-2015	40%	40%	40%	50%
3	Thieken, A.H., Bessel, T., Kienzler, S., Kreibich, H., Müller, M., Pisi, S., Schröter, K., 2016. The flood of June 2013 in Germany: how much do we know about its impacts? Nat. Hazards Earth Syst. Sci. 16, 15191540. https://doi.org/10.5194/nhess-16-1519-2016	20%	20%	20%	20%
4	Fohringer, J., Dransch, D., Kreibich, H., Schröter, K., 2015. Social media as an information source for rapid flood inundation mapping. Nat. Hazards Earth Syst. Sci. 15, 27252738. https://doi.org/10.5194/nhess-15-2725-2015	30%	30%	20%	40%
5	Nied, M., Schröter, K., Lüdtke, S., Nguyen, V.D., Merz, B., 2017. What are the hydro-meteorological controls on flood characteristics? Journal of Hydrology 545, 310326. https://doi.org/10.1016/j.jhydrol.2016.12.003	15%	20%	20%	25%
6	Falter, D., Schröter, K., Dung, N.V., Vorogushyn, S., Kreibich, H., Hundedea, Y., Apel, H., Merz, B., 2015. Spatially coherent flood risk assessment based on long-term continuous simulation with a coupled model chain. Journal of Hydrology 524, 182193. https://doi.org/10.1016/j.jhydrol.2015.02.021	25%	20%	20%	20%
7	Klaus, S., Kreibich, H., Merz, B., Kuhlmann, B., Schröter, K., 2016. Large-scale, seasonal flood risk analysis for agricultural crops in Germany. Environmental Earth Sciences 75. https://doi.org/10.1007/s12665-016-6096-1	30%	20%	25%	30%
8	Gerl, T., Kreibich, H., Franco, G., Marechal, D., Schröter, K., 2016. A Review of Flood Loss Models as Basis for Harmonization and Benchmarking. PLOS ONE 11, e0159791. https://doi.org/10.1371/journal.pone.0159791	30%	10%	20%	40%
9	Schröter, K., Kreibich, H., Vogel, K., Riggelsen, C., Scherbaum, F., Merz, B., 2014. How useful are complex flood damage models? Water Resour. Res. 50, 33783395. https://doi.org/10.1002/2013WR014396	40%	40%	40%	50%
10	Schröter, K., Lüdtke, S., Vogel, K., Kreibich, H., Merz, B., 2016. Tracing the value of data for flood loss modelling. E3S Web of Conferences 7, 05005. https://doi.org/10.1051/e3sconf/20160705005	40%	30%	50%	40%
11	Schröter, K., Lüdtke, S., Redweik, R., Meier, J., Bochow, M., Ross, L., Nagel, C., Kreibich, H., 2018. Flood loss estimation using 3D city models and remote sensing data. Environmental Modelling & Software 105, 118131. https://doi.org/10.1016/j.envsoft.2018.03.032	40%	40%	50%	40%
12	Figueiredo, R., Schröter, K., Weiss-Motz, A., Martina, M.L.V., Kreibich, H., 2018. Multi-model ensembles for assessment of flood losses and associated uncertainty. Nat. Hazards Earth Syst. Sci. 18, 12971314. https://doi.org/10.5194/nhess-18-1297-2018	30%	20%	20%	25%
13	Kreibich, H., Botto, A., Merz, B., Schröter, K., 2017. Probabilistic, Multivariable Flood Loss Modeling on the Mesoscale with BT-FLEMO. Risk Analysis 37, 774787. https://doi.org/10.1111/risa.12650	30%	20%	30%	20%

List of Figures

1.1	Thematic framework, overarching themes and composition of the thesis. Arrows indicate links between papers regarding methods, methodological approaches and interrelated research design	23
2.1	The risk management cycle (adapted from (DKKV, 2003b; PLANAT, 2004))	28
2.2	Distribution of the different natural hazards that caused fatalities and economic damage between 1950 and 2013 in Germany. Damage given in USD in EM-DAT are converted into EUR using the exchange rate of 1.37 as at December 2013 (DAT, 2006)	29
2.3	a: Maximum gust wind speeds in Germany on a 1 x 1 km ² grid for a 10-year return period according to model simulations and observations (1971-2000) obtained during the CEDIM www.cedim.de project “Risk Map Germany” (Hofherr and Kunz, 2010); b: lightning density in Germany obtained from the Siemens Network BLIDS 2000-2009 (Damian, 2011). . . .	36
2.4	Groundwater flood damage to residential buildings in Dresden estimated on basis of different groundwater flood scenarios (adapted from (Kreibich et al., 2011b)	42
2.5	Estimated seismic risk [millions of Euro] in communities of Germany for an exceedance probability of 10% in 50 years (adapted from (Tyagunov et al., 2006))	43
3.1	500 hPa geopotential height, 16-day mean for 16 – 31 May 2013 (left) and anomaly in respect to the climatology based on 1979-1995 (right). Credit: Data/image provided by the NOAA/OAR/ESRL PSD, Boulder, Colorado, USA, from their Web site at http://www.esrl.noaa.gov/psd/ (accessed 4 April 2014)	58
3.2	Weather charts for 30 May (a) and 01 June 2013(b) 00 UTC with analysis of 500 hPa geopotential height (black lines), surface pressure (white lines) and 1000/500 hPa relative topography (colors) from the Global Forecast System (GFS). Image credit: wetter3.de (Accessed 7 May 2014).	59
3.3	Time series of cumulated areal mean precipitation for the upper Elbe catchment in Germany up to the inflow of the Saale River (area: 63,171 km ² ; a) and for the upper Danube catchment in Germany (area: 51,379 km ² ; b). The x-axis marks the days prior to the 3-day maximum precipitation totals. Event precipitation is highlighted in grey.	60
3.4	The 3-day maximum precipitation according to REGNIE data sets for June 2013 (left), August 2002 (middle) and July 1954 (right).	60
3.5	Day of the year at each REGNIE grid point where the event related maximum R3d total according to Figure 3.4 occurred (end of the 3-day total) for June 2013 (left), August 2002 (middle), and July 1954 (right). The day 152 corresponds to 1 June, 220 to 8 August, and 190 to 9 July. The indicated days refer to the end of R3d.	61

3.6	Return periods of 3-day maximum precipitation for each REGNIE grid point derived from data of the period from 1960 to 2009 for the corresponding rain totals displayed in Figure 3.4: June 2013 (left), August 2002 (middle), and July 1954 (right).	63
3.7	Antecedent Precipitation Index API over 30 days for the floods in June 2013 (left), August 2002 (middle), and July 1954 (right). See text for further details.	64
3.8	Return periods of the API displayed in Figure 3.7 derived from 30-day API of large-scale floods in the period from 1960 to 2009: June 2013 (left), August 2002 (middle), and July 1954 (right).	64
3.9	Initial flow ratio at meteorological event start Q_i normalized for MHQ (calculated from AMS 1950-2009) for June 2013 (left), August 2002 (middle), and July 1954 (right).	65
3.10	Return periods of initial flow ratio at meteorological event start (Q_i normalized for MHQ) derived from Q_i /MHQ ratios of large-scale floods in the period from 1969 to 2009: June 2013 (left), August 2002 (middle), and July 1954 (right)	66
3.11	Regionalized return periods (T_n) of flood peak discharges for June 2013 (left), August 2002 (middle), and July 1954 (right). Gauge data were made available by the Water and Shipping Management of the Fed. Rep. (WSV) prepared by the Federal Institute for Hydrology (BfG) and environmental state offices of the federal states.	67
3.12	Locally-weighted scatter plot smooth (LOWESS) for the relationship between precipitation and wetness indices as predictors for the flood severity index (grey color code) of past large scale flood events in Germany. Top left: Reference (5-years return period as reference level for severity indices, R3d, API 30 days, $k = 0.9$), top right: 10-years return period as reference level for severity indices, bottom left: R7d, bottom right: API k0.98. Note that all severity indices have been normalized to the respective maximum values and that the upper right corners do not contain observed data. . . .	69
3.13	Spearman's rank correlation coefficients between the reference scenario and the variations examined within the sensitivity analysis; for the scenario definition see Table 3.3	72
3.14	Outline map of referred geographic locations.	74
3.15	Same as Figures 3.4 and 3.6, but for 7-day maximum precipitation (top line: 7-day maximum precipitation; bottom line: Return periods June 2013, left; August 2002, middle; July 1954, right).	75
4.1	River reaches with flood discharges (Q_p) exceeding a 10-year-discharge (HQ10) or a 100-year discharge (HQ100), exceedance of highest navigable water level (NavWL) in days at selected gauges (data source: (BfG, 2014a), p. 152), as well as hot spots of inundation in June 2013 including major dike breach locations; details for a) Fischbeck, b) confluence of the rivers Saale and Elbe, c) Fischerdorf at the confluence of the rivers Isar and Danube as well as d) the city of Passau (Source: (Schröter et al., 2015), based on satellite images of TerraSAR-X and MODIS).	79

4.2	Geographic overview of affected federal states and districts that declared a state of emergency (a) as well as the number of surveyed households and companies (b).	85
4.3	Average perception of the severity flood impacts witnessed by flood-affected residents and assessed on a scale of 1 (= impact was not very serious) to 6 (= impact was very serious).	90
4.4	Frequency of the flood memories of affected private households in the six months preceding the survey (information is given in percentages of respondents; the first two categories of answers – (several times) daily – were not provided to the respondents in autumn 2012).	92
4.5	Distribution of the overall direct losses of the flood event in June 2013 according to loss-incurring sectors in the federal states of Bavaria (EUR 1.3 b) and Saxony (EUR 1.9 b) according to the Federal Ministry of Finance (BMF, 2013).	96
4.6	Chronological sequence of the number of traffic obstructions on German roads related to the flood event in the period from 19 th May to 1 st July 2013, subdivided into causes and as a total number.	99
4.7	Overall duration of the obstructions in road traffic induced by the flood event shown in terms of administrative districts.	100
4.8	Number of train routes with disruptions or interferences caused by extreme weather conditions (low-speed routes, platform or route closures; Information source: German Railways Corporation’s internal survey maps detailing interferences caused by extreme weather, in part updated several times a day).	101
4.9	Share of surveyed companies that reported on the different flood impacts.	102
5.1	PostDistiller system architecture.	118
5.2	PostExplorer: media view and map view (map tiles by Stamen Design), under a Creative Commons Attribution (CC BY 3.0) license. Data by OpenStreetMap, under Open Data Commons Open Database license (ODbL).	120
5.3	Study region and data sources for flood inundation depth mapping.	125
5.4	Process chain, timeframe and number of tweets for the Dresden flood in June 2013 handled within <i>PostCrawler</i> , <i>PostStorage</i> , <i>PostExplorer</i> and GIS environment for automatic and manual filtering of tweets.	127
5.5	Location of useful photos retrieved with PostDistiller and inundation depths estimates (Photos by Denny Tumlirsch (@Flitzpatrick), @ubahnverleih, Sven Wernicke (@SvenWernicke), Leo Käßner (@leokaesner)).	128
5.6	Inundation maps and inundation depths derived from online water level observations (panel a), social media content (panel b), inundated area from reference remote sensing flood footprint (panel c) and differences between inundation depths for overlapping areas in maps (a) and (b) (panel d).	130
6.1	Topographic map of the Elbe River catchment, hydrologic model domain, 1D model river network and 2D model domain. Red dots show the gauges which are used to calibrate and validate the rainfall-runoff model, and to identify large-scale flood events. Map of the regional setting of the Elbe catchment (upper right). The map delineates the spatial extent the weather pattern classification is based on.	138

- 6.2 Flow chart of the analysis: modules (rectangles), their input data (ovals) and results (arrows). Weather patterns are reshuffled and used to drive the regional flood model (RFM) composed of a rainfall-runoff model to simulate soil moisture and discharge, a hydrodynamic model to simulate inundation, as well as a flood loss model. Flood events, their characteristics, as well as the involved soil moisture and weather patterns are identified. The relationship between the patterns and flood occurrence as well as flood characteristics are analyzed by cumulative distributions functions and regression trees. 141
- 6.3 Meteorological cluster centroids of the selected weather patterns (19, 26, 29 and 34). Shaded contours show mean cluster anomalies in the vertically integrated moisture content [kg/m^2], solid isolines show mean anomalies in the 500 hPa geopotential [m], and dashed isolines are mean anomalies in 500 hPa air temperature [$^{\circ}\text{C}$]. Weather patterns are taken from Nied et al. (2014). 142
- 6.4 Selected soil moisture patterns (3, 5 and 9) as identified by Nied et al. (2013). Profile (layer-depth weighted average) soil moisture content is standardized by the field capacity of the respective soil type. 144
- 6.5 Cumulative distribution functions (CDF) of the different flood characteristics. The flood characteristics have been derived by the flood event identification applied to observed discharge (grey dashed line), simulated discharge generated by the undisturbed climate data, i.e. the observed meteorology (grey solid line), and simulated discharge generated by the shuffling approach (black solid line). 152
- 6.6 Cumulative distribution functions (CDFs) of the flood characteristics (subplots A-H) in dependence of weather patterns and soil moisture patterns. The grey and color coded CDFs represent the 40 weather patterns (left hand side of each subplot) and the 10 soil moisture patterns (right hand side of each subplot) respectively. The light blue CDF represents weather pattern 19, the purple weather pattern 26, the olive weather pattern 29 and the orange weather pattern 34. The blue CDF represents soil moisture pattern 3, the green soil moisture pattern 5 and the red soil moisture pattern 9. The respective patterns are displayed in sect. 3.1. The black CDFs represent the flood characteristics independent of patterns and are identical to the black CDFs in Figure 6.5. N refers to the sample size. 153
- 6.7 Regression tree of the flood affected length. Soil moisture patterns are indicated by a green number, weather patterns are indicated by a blue number. Unlabeled patterns are indicated by their quantity. Decision nodes are visualized by a green triangle (soil moisture pattern) or by a blue triangle (weather pattern). The median flood affected length of each subgroup is indicated at the respective terminal node. Terminal nodes with an affected length higher than the median value of the entire event set are displayed in red. In brackets, the sample size of the specified pattern in the subgroup is indicated. 156

6.8	Delta of the variable importance for each flood characteristic. Positive values highlight the dominance of the weather patterns; negative values indicate the dominance of the soil moisture patterns. The higher the absolute value the stronger the influence on the respective flood characteristic. The maximum absolute value is one.	158
7.1	Components and data requirements of the Regional Flood Model (RFM). DEM, digital elevation model; FLEMOps+r, Flood Loss Estimation MOdel for the private sector; SWIM, Soil and Water Integrated Model.	170
7.2	Study area, left panel: overview of the entire Elbe catchment including Czech areas; right panel: study area including the simulated river network, the 2D model domain and locations used for model calibration and validation	173
7.3	Comparison of simulated and observed inundation extents for the August 2002 flood.	179
7.4	Inundation frequency in 10,000 years of simulation for each computational cell.	180
7.5	Comparison of derived flood frequency curve and plotting positions for gauge Bad Döben. Dots are the observations; the solid line is the median of the derived frequency curves; the dashed and dotted lines show the 50% and 95% confidence interval, respectively.	181
7.6	(a) Histogram of damage events and (b) comparison of traditional and simulation-based risk curves for an exemplarily subbasin.	184
7.7	Differences in inundation depth for two flood events with the same flood peak in subbasin 995.	185
7.8	a) Distribution of expected annual damage to residential buildings in the Mulde catchment at the subbasin scale. (b)-(e) Comparison of total damage (b, d) and discharge return period (c, e) spatial distributions amongst subbasins (x-axis) and different flood events (coloured lines) for two different levels of total catchment damage. (For interpretation of the references to color in this figure legend, the reader is referred to the web version of this article.	186
8.1	Locations of discharge gauging stations. Highlighted in red are the gauges Cologne, Dresden and Munich which represent the flood regime A, B and C identified by (Beurton and Thielen, 2009)	194
8.2	Relation between annual return period (flood occurrence anytime of the year) and annual return period of monthly floods (flood occurrence in the specified month). Example: Dresden gauge - Elbe River.	195
8.3	Seasonal flood probability [a^{-1}] and seasonal crop susceptibility. Susceptibility is given as specific loss ratio [%/ha] (left) and specific loss [EUR/ha] (right) and for inundation duration 1-3 days (solid line) and duration >11 days (dotted line) for HQ5 at the gauge Dresden (Elbe River).	196
8.4	Seasonal crop risk (EAD) and mean risk averaged over all crop types (Left: loss ratio; Right: specific loss; Top: inundation duration 1-3 days; Bottom: inundation duration > 11 days). - Example: Dresden gauge – Elbe River, administrative district Dresden.	199

8.5	Seasonal crop risk (EAD) and mean risk averaged over all crop types (Left: loss ratio; Right: specific loss; Top: inundation duration 1-3 days; Bottom: inundation duration > 11 days). - Example: Cologne gauge – Rhine River, administrative district Cologne.	200
8.6	Seasonal crop risk (EAD) and mean risk averaged over all crop types (Left: loss ratio; Right: specific loss; Top: inundation duration 1-3 days; Bottom: inundation duration > 11 days). - Example: Munich gauge – Isar River, administrative district Upper Bavaria.	201
8.7	Annual risk as specific loss ratio (left) and specific loss (right) derived as the mean of the seasonal crop risk values. Example: Dresden gauge – Elbe River, administrative district Dresden.	202
8.8	Annual risk as specific loss ratio (left) and specific loss (right) derived as the mean of the seasonal crop risk values. Example: Cologne gauge – Rhine River, administrative district Cologne.	203
8.9	Annual risk as specific loss ratio (left) and specific loss (right) derived as the mean of the seasonal crop risk values. Example: Munich gauge – Isar River, administrative district Upper Bavaria.	203
8.10	Flood risk for agricultural crops in Germany. Average crop risk is shown by the colored river sections, whereas the crop most at risk is shown by the colored regions. Left: specific loss ratio [%/ha/a]; Right: specific loss [EUR/ha/a]; Top: inundation duration 1-3 days; Bottom: inundation duration >11 days.	204
9.1	Characteristics of flood loss models contained in the inventory.	214
9.2	Global distribution of flood loss models and functions for different sectors contained in the inventory.	216
9.3	Loss functions of residential buildings in HAZUS-MH (FEMA, 2009); example of a relative, deterministic model using uni-variable loss functions (negative inundation depth refers to inundation in the basement of a building).	219
9.4	Damage model of Zhai et al. (2005) with the damage-influencing factors residing period, income and inundation depth; example for an absolute, deterministic model using multi-variable loss functions.	219
9.5	Structure and example distributions of loss estimates for selected water levels of BN-FLEMOps; example for a multi-variable, relative, probabilistic model.	220
9.6	Loss functions of crop types (Yazdi and Salehi Neyshabouri, 2012); example for a relative, deterministic model using uni-variable loss functions.	221
9.7	Loss functions for one-cut silage (Hess and Morris, 1988); example for an absolute, deterministic model using multi-variable loss functions. D=total damage [GBP/ha], GMJ=energy from grass lost due to flooding [MJ/ha], RF=cost of replacement feed [GBP/ha], C=additional costs incurred (+) or saved (-) [GBP/ha].	221
9.8	Harmonized flood loss models for residential buildings in dependence of water depth; top: HAZUS (FEMA, 2009), middle: Zhai et al. (Zhai et al., 2005), bottom: BN-FLEMOps (Schröter et al., 2014).	224

9.9	Compilation of harmonized flood loss models for residential buildings based on common variables.	226
10.1	Location of communities in which interviews had been undertaken after the 2002, 2005 and 2006 flood events in the Elbe and Danube catchments (Germany), data sources: rivers and administrative borders: DLM1000 of (GEODATENZENTRUM, 2009); cities: Esri, DeLorme Publishing Company, inc.; catchment areas: CCM2 data of JRC (Vogt, 2007)	232
10.2	Regression tree RT with 12 leaves considering five variables for estimating $\log(rloss)$ and pruned regression tree (RTp, indicated by bold joins) with 4 leaves considering two variables for estimating $\log(rloss)$ grown within the 'no uncertainty' scenario	240
10.3	DAG of data based Bayesian network for 29 explanatory variables including $rloss$ (left), data based Bayesian network for 11 explanatory variables including $rloss$ (right)	242
10.4	DAG of expert Bayesian network for 28 explanatory variables (left), expert Bayesian network for 10 explanatory variables (right) constructed with the specific goal to predict $rloss$	244
10.5	Average model predictive precision ED (mbe and mae) in cross regional and temporal validations against model complexity (number of explanatory variables used to predict $rloss$) for 'no uncertainty' scenario	247
10.6	Average model predictive precision ED (mbe and mae) of deterministic models in cross regional and temporal validations against model complexity (number of explanatory variables used to predict $rloss$) within the uncertainty scenarios, model approaches are described by different symbols, uncertainty scenarios are represented by different colors: black (no uncertainty), grey (small uncertainty), light grey (large uncertainty)	248
10.7	Average predictive reliability HR in cross regional and temporal validations against model complexity (number of explanatory variables used to predict $rloss$) for the predictive distributions of deterministic models within uncertainty scenarios (su, lu) and joint probability distribution of Bayesian Networks, model approaches are described by different symbols, uncertainty scenarios applied to deterministic models are represented by different colors: grey (small uncertainty), light grey (large uncertainty).	250
11.1	Performance traces for incremental split-sample evaluation of sdf model, x-axis: sample size, y-axes performance values.	259
11.2	Performance traces for incremental split-sample evaluation of RF-FLEMO, x-axis: sample size, y-axes performance values.	260
11.3	Model performance of sdf and RF-FLEMO models in regional updating in the Danube (D) and Elbe (E) catchments.	261
12.1	Map of Dresden in Germany with focus areas, interview locations, building outlines and ATKIS land use classes, the detail cutout shows the focus area Pieschen	267
12.2	Ordered importance for building related variables for 3D City database and spatial measures data sub sets based on $n = 80$ observations including water depth from the cati data base. Top 10 important variables used for predictive modeling are colored black.	275

12.3	OOB error distributions of the citydb_sm data set for repeated simulations using different <i>mtry</i> values and increasing tree sizes	276
12.4	Model predictive performance in leave-one-out cross validation, median values for performance metrics are given as labels.	279
12.5	Prototype component diagram	280
12.6	3DCFD online prototype implementation showing the inundation area for the flood scenario 9.4 m in Dresden with color coded residential buildings according to relative building loss.	281
12.7	Relative loss estimates for residential buildings in the focus area Pieschen for 9.4 m flood scenario: left panel icpr model, right panel citydb model . .	282
12.8	Relative loss to residential buildings as a function of inundation depth in the Pieschen focus area for different inundation scenarios using icpr and citydb flood loss models, empirical data are from the cati surveys for the whole Dresden area. The grey line is a spline approximation with standard errors to the cati data (neglecting the outliers).	283
13.1	2002 flood along the Mulde River, in Germany. The figure shows the municipalities considered in the case study (grey), the estimated flood extension and water depths (blue), and the location of the residential grid cells (orange).	294
13.2	2010 Bacchiglione river flood in Caldogno, Italy. The figure shows the estimated flood extension and water depths (blue), and the location of the residential buildings considered in the study (orange).	295
13.3	Root mean square error (RMSE) and mean bias error (MBE) of the means of ensembles of increasing size, with models included sequentially from highest to lowest score, starting with the highest ranked single model. Blue crosses and orange circles refer to ensembles weighted equally and differently, respectively.	304
13.4	RMSE and MBE of the EEM-ensemble means, represented by blue crosses, and single model predictions, by red plus signs.	306
13.5	Proposed set of properties (probability tree nodes) that are considered relevant to assess the performance of flood loss models for buildings, and respective categories and subjective probabilities.	307
13.6	RMSE and MBE of 20 000 multi-model ensemble means, generated by simulating a state of non-informativeness, whereby each participating member is assigned a random weight. Blue crosses and red plus signs refer respectively to the EEM-ensemble means and the single model predictions.	308
13.7	Continuous ranked probability score (CRPS) of the EEM-ensembles for the Caldogno application case.	310
13.8	Rank histogram relative to the 20-model ensemble for the Caldogno application case.	311
13.9	Probabilistic estimates of total loss, relative to model uncertainty, for the Caldogno application case, based on 10,000 realisations of loss to each building. (a) Histogram, with observed loss shown by the vertical red line. (b) Empirical cumulative distribution function (ECDF).	311
14.1	Location of the municipalities in the case study area at the Mulde River in Germany	319

14.2	Example of RT representation of BT-FLEMO (water depth (wst), return period (rp), contamination indicator (con), inundation duration (d), flow velocity indicator (v), floor space of building (fsb), building value (bv) and precautionary measures indicator (pre); for further description of predictors see Table 14.1).	321
14.3	Results of BT-FLEMO (black histograms, x-axes represent losses in million euros, y-axes represent frequency, 90% confidence interval is marked in green) as well as official loss information (red lines) in the 19 municipalities under study.	328
14.4	Loss model comparison and validation with official loss data for the 19 municipalities in the case study area at the Mulde River.	329
15.1	Thesis outcomes: avenues and links to flood disaster risk reduction	338

List of Tables

1.1	List of Papers included in habilitation thesis	22
2.1	Most severe events with respect to fatalities and economic loss in Germany between 1950 and 2013 according to (DAT, 2006)	30
2.2	Spatial-temporal characteristics of important natural hazards in Germany (adapted from (B. Merz and Emmermann, 2006; Bittner et al., 2009)	32
2.3	Indication of relevant risk management measures for storms, floods, extreme temperatures and earthquakes in Germany (++ = very relevant; + = relevant; (+) = partly relevant; - = not relevant/not applicable)	45
3.1	Data sources, resolution and analysis methods for hydro-meteorological parameters	53
3.2	Severity indices for June 2013, August 2002 and July 1954 floods	68
3.3	Variation scenarios examined within sensitivity analysis	70
4.1	Overview of human loss indicators as recommended by (Corbane et al., 2015) or (IRDR, 2015a) accessible for the flood in June 2013 per federal state (data sources: BMF, 2013 including annexes; GMLZ, 2014 without annexes; ND: no data reported)	89
4.2	Damage and loss indicators as recommended by Corbane et al. (2015) and IRDR (2015) available for the flood of June 2013 in Germany per federal state (Data sources: BMF, 2013; Saxon State Chancellery, 2013; Brandenburg pers. communication in May 2014; Federal Parliament, 2015; ND: no data reported)	94
4.3	Financial losses of companies affected by the flood in June 2013	103
4.4	Overview of minimum information requested by recently published loss documentation guidelines (Corbane et al. 2015; IRDR 2015) and information reported for the 2013-flood	107
7.1	Validation of SWIM at three gauging stations in the Mulde catchment	176
7.2	Water level evaluation in the Mulde catchment	176
8.1	Variation of specific loss ratios [%/ha] and specific losses [/ha] for potatoes depending on the month and inundation duration, based on (Kuhlmann, 2007). Market values exemplary for the administrative district Dresden.	192
9.1	Structure of the flood loss model inventory	212
9.2	Characteristics of the selected example models	218
10.1	Characteristics of flood damage models	230
10.2	Usage of data sub-samples from different flood events and river basins	231
10.3	Description of candidate variables for flood damage modeling	235
10.4	Model evaluation criteria	238
10.5	Precision of damage model predictions for no uncertainty scenario	246
10.6	Variation and reliability of predictive distributions of deterministic models (sdf, flemops+r, RTp, RT) within small and large uncertainty scenarios (su, lu) and joint probability distributions of Bayesian Network (BN) variants	249

11.1	Loss cases for different flood events and regions in Germany	255
11.2	Split-sample validation experiments for incremental model derivation . . .	257
12.1	Variables available from computer aided telephone interviews, 3d city model and remote sensing	269
12.2	RF model performance using different data sub-sets with city DB and sm models also including water depth from the empirical data and icpr stan- dard model perfor- mance, best performance values are marked bold . . .	277
12.3	Flood loss to residential buildings in the focus area Pieschen for different flood scenarios using icpr and citydb flood loss model	284
13.1	Models included in this study, including some of their properties	291
13.2	Input variables for the Mulde and Caldogno application cases	296
13.3	Results of individual model applications in the Mulde case: root mean square error (RMSE) and mean bias error (MBE), sorted by RMSE	299
13.4	Results of individual model applications in the Caldogno case: root mean square error (RMSE) and mean bias error (MBE), sorted by RMSE	300
13.5	Model scores for the Mulde application case	301
13.6	Model scores for the Caldogno application case	302
14.1	Compilation of variable characteristics and spatial scale transfer methods .	322
14.2	Input variable values which have been estimated on the municipality level for BT-FLEMO (contamination indicator (con), inundation duration (d), flow velocity indicator (v), floor space of building (fsb), precautionary mea- sures indicator (pre), building value (bv)) as well as for the models FLE- MOps+r and RT2 (building type (bt), building quality (bq), and income (inc)	326
14.3	Overview of official loss data and loss estimates in the 19 municipalities in the case study area	329
14.4	Comparison of model performance (MBE: mean bias error, MAE: mean absolute error, RMSE: root mean square error)	330

Bibliography

- [1] F. Abel, C. Hauff, G. - . Hoube, K. Tao, and R. Stronkman. "Semantics + Filtering + Search = Twitcident exploring information in social web streams". In: *HT'12 - Proceedings of 23rd ACM Conference on Hypertext and Social Media*. 2012, pp. 285–294.
- [2] J. Aerts and W. J. Botzen. "Climate change impacts on pricing long-term flood insurance: A comprehensive study for the Netherlands". In: *Global Environmental Change* 21.3 (2011), pp. 1045–1060.
- [3] J. Aerts, W. J. Botzen, K. C. Clarke, et al. "Integrating human behaviour dynamics into flood disaster risk assessment". In: *Nature Climate Change* 8.3 (Mar. 2018), pp. 193–199. ISSN: 1758-6798. DOI: 10.1038/s41558-018-0085-1.
- [4] N. U. Ahmed. "Estimating soil moisture from 6.6 GHz dual polarization, and/or satellite derived vegetation index". In: *International Journal of Remote Sensing* 16.4 (1995), pp. 687–708.
- [5] L. Alfieri, P. Salamon, A. Bianchi, J. Neal, P. Bates, and L. Feyen. "Advances in pan-European flood hazard mapping". In: *Hydrological Processes* 28.13 (2014), pp. 4067–4077.
- [6] A. Allmann, E. Rauch, and A. Smolka. "New paleoseismological findings on major earthquakes in Central Europe. Possible consequences for the earthquake loss potential in Germany". In: *Proceedings 11th ECEE Paris/France* (1998).
- [7] S. Amirebrahimi, A. Rajabifard, P. Mendis, and T. Ngo. "A framework for a microscale flood damage assessment and visualization for a building using BIMGIS integration". In: *International Journal of Digital Earth* 9.4 (2016), pp. 363–386. DOI: 10.1080/17538947.2015.1034201.
- [8] AMS. *AMS Glossary*. 2013. URL: http://glossary.ametsoc.org/wiki/Main_Page.
- [9] R. Analytics and S. Weston. "doParallel: foreach parallel adaptor for the parallel package. [online] available from". In: (2015).
- [10] R. Analytics and S. Weston. "Foreach: provides foreach looping construct for R. [online] available from". In: (2015).
- [11] H. Apel, G. T. Aronica, H. Kreibich, and A. Thielen. "Evaluation of different modelling strategies for flood risk assessment in urban areas". In: *Proceedings of the 32nd Congress of IAHR July 16 2007, Venice, Italy*. 2007.
- [12] H. Apel, G. T. Aronica, H. Kreibich, and A. Thielen. "Flood risk analyses how detailed do we need to be?" In: *Nat Hazards* 49.1 (Apr. 1, 2009), pp. 79–98. ISSN: 0921-030X, 1573-0840. DOI: 10.1007/s11069-008-9277-8.
- [13] H. Apel, A. Thielen, B. Merz, and G. Blöschl. "A Probabilistic Modelling System for Assessing Flood Risks". In: *Nat Hazards* 38.1 (May 1, 2006), pp. 79–100. ISSN: 0921-030X, 1573-0840. DOI: 10.1007/s11069-005-8603-7.

- [14] H. Apel, A. Thieken, B. Merz, and G. Blöschl. "Flood risk assessment and associated uncertainty". In: *Nat. Hazards Earth Syst. Sci.* 4.2 (Apr. 16, 2004), pp. 295–308. ISSN: 1684-9981. DOI: 10.5194/nhess-4-295-2004.
- [15] T.H. Assumpção, I. Popescu, A. Jonoski, and D.P. Solomatine. "Citizen observations contributing to flood modelling: opportunities and challenges". In: *Hydrology and Earth System Sciences* 22.2 (Feb. 28, 2018), pp. 1473–1489. ISSN: 1027-5606. DOI: <https://doi.org/10.5194/hess-22-1473-2018>.
- [16] Deutsche Bahn. *Wieder freie Fahrt zwischen Hannover und Berlin*. Press Release. Nov. 4, 2013.
- [17] S. F. Balica, I. Popescu, L. Beevers, and N. G. Wright. "Parametric and physically based modelling techniques for flood risk and vulnerability assessment: A comparison". In: *Environmental Modelling & Software* 41 (Mar. 1, 2013), pp. 84–92. ISSN: 1364-8152. DOI: 10.1016/j.envsoft.2012.11.002.
- [18] World Bank. *Review of open source and open access software packages available to quantify risk from natural hazards*. World Bank, 2014.
- [19] J. C. Banks, J. V. Camp, and M. D. Abkowitz. "Adaptation planning for floods: A review of available tools". In: *Natural Hazards* 70.2 (2014), pp. 1327–1337.
- [20] A. Bárdossy and F. Filiz. "Identification of flood producing atmospheric circulation patterns". In: *Journal of Hydrology*. Palaeofloods, hystorical data & climate variability: Applications in flood risk assessment 313.1 (Nov. 5, 2005), pp. 48–57. ISSN: 0022-1694. DOI: 10.1016/j.jhydro1.2005.02.006.
- [21] M.H. Barendrecht, A. Viglione, and G. Blöschl. "A dynamic framework for flood risk". In: *Water Security* 1 (July 2017), pp. 3–11. ISSN: 24683124. DOI: 10.1016/j.wasec.2017.02.001.
- [22] A. G. Barnett, S. Hajat, A. Gasparrini, and J. Rocklöv. "Cold and heat waves in the United States". In: *Environmental research* 112 (2012), pp. 218–224.
- [23] J. I. Barredo. "Major flood disasters in Europe: 1950-2005". In: *Natural Hazards* 42.1 (2007), pp. 125–148.
- [24] J. I. Barredo. "No upward trend in normalised windstorm losses in Europe: 1970-2008". In: *Natural Hazards and Earth System Sciences* 10.1 (2010), pp. 97–104.
- [25] J. I. Barredo. "Normalised flood losses in Europe: 1970-2006". In: *Natural Hazards and Earth System Science* 9.1 (2009), pp. 97–104.
- [26] P. Bates. "Integrating remote sensing data with flood inundation models: how far have we got?" In: *Hydrological Processes* 26.16 (2012), pp. 2515–2521. ISSN: 1099-1085. DOI: 10.1002/hyp.9374.
- [27] P. Bates, M.S. Horritt, and T.J. Fewtrell. "A simple inertial formulation of the shallow water equations for efficient two-dimensional flood inundation modelling". In: *Journal of Hydrology* 387.1 (June 2010), pp. 33–45. ISSN: 00221694. DOI: 10.1016/j.jhydro1.2010.03.027.

- [28] Bavarian Parliament. *Written enquiry by the representative R. Steinberger BÜNDNIS 90/DIE GRÜNEN, answer by the Bavarian State Ministry of Environment and Consumer Protection*. Drucksache 17/889. Munich: Deutscher Bundestag, Mar. 21, 2014.
- [29] BBK. *Neue Strategie zum Schutz der Bevölkerung in Deutschland*. Bundesamt für Bevölkerungsschutz und Katastrophenhilfe, 2010.
- [30] K. M. Bedka. "Overshooting cloud top detections using MSG SEVIRI Infrared brightness temperatures and their relationship to severe weather over Europe". In: *Atmospheric Research* 99.2 (2011), pp. 175–189.
- [31] G. Benito, R. Brázdil, J. Herget, and M. J. Machado. "Quantitative historical hydrology in Europe". In: *Hydrology and Earth System Sciences* 19.8 (Aug. 10, 2015), pp. 3517–3539. ISSN: 1027-5606. DOI: <https://doi.org/10.5194/hess-19-3517-2015>.
- [32] S. Beurton and A. Thielen. "Seasonality of floods in Germany". In: *Hydrological Sciences Journal* 54.1 (2009), pp. 62–76. ISSN: 0262-6667. DOI: 10.1623/hysj.54.1.62.
- [33] BfG. "Das Hochwasserextrem des Jahres 2013 in Deutschland: Dokumentation und Analyse". In: *Report, BfG-Mitteilung* 31 (2014).
- [34] BfG. "Das Juni-Hochwasser des Jahres 2013 in Deutschland". In: *Report, BfG-1793* (2013).
- [35] BfG. *Geoportal der BfG*. 2014.
- [36] F. Biljecki, J. Stoter, H. Ledoux, S. Zlatanova, and A. Çöltekin. "Applications of 3D City Models: State of the Art Review". In: *ISPRS International Journal of Geo-Information* 4.4 (Dec. 18, 2015), pp. 2842–2889. DOI: 10.3390/ijgi4042842.
- [37] R. Bittner, K. Günther, and B. Merz. "Naturkatastrophen in deutschland". In: *Hochwasserschutz Und Katastrophenmanagement* 6 (2009), pp. 7–10.
- [38] B. J. Blanchard, M. J. McFarland, T. J. Schmutge, and E. Rhoades. "ESTIMATION OF SOIL MOISTURE WITH API ALGORITHMS AND MICROWAVE EMISSION". In: *JAWRA Journal of the American Water Resources Association* 17.5 (1981), pp. 767–774.
- [39] R. Blong. "Residential building damage and natural perils: Australian examples and issues". In: *Building Research and Information* 32.5 (2004), pp. 379–390.
- [40] G. Blöschl, T. Nester, J. Komma, J. Parajka, and R. A. P. Perdigão. "The June 2013 flood in the Upper Danube Basin, and comparisons with the 2002, 1954 and 1899 floods". In: *Hydrol. Earth Syst. Sci.* 17.12 (2013), pp. 5197–5212. ISSN: 1607-7938. DOI: 10.5194/hess-17-5197-2013.
- [41] BMF. *Antrag der Bundesrepublik Deutschland Vom 24 Juli 2013 Auf Finanzielle Unterstützung Aus Dem Solidaritätsfonds der Europäischen Union Zur Bewältigung der Durch das Hochwasser in Mehreren Bundesländern im Zeitraum Vom 18 Mai 2013 Bis 26 Juni*(TRUNCATED). Bundesministerium für Finanzen, 2013.
- [42] BMI. *Bericht Zur Flutkatastrophe 2013: Katastrophenhilfe, Entschädigung, Wiederaufbau*. Bundesinnenministerium, 2013.

- [43] BMU. *Dem Klimawandel begegnen – Die Deutsche Anpassungsstrategie*. Berlin: Bundesministerium für Umwelt, Naturschutz und Reaktorsicherheit, 2009.
- [44] BMVBS. *Normalherstellungskosten 2005 (NHK 2005)*. Berlin: Bundesministerium für Verkehr, Bau und Stadtentwicklung, 2005.
- [45] M. Bochow, H. Taubenböck, K. Segl, and H. Kaufmann. "An automated and adaptable approach for characterizing and partitioning cities into urban structure types". In: *International Geoscience and Remote Sensing Symposium (IGARSS)*. 2010, pp. 1796–1799.
- [46] Berry Boessenkool. *Fit, plot and compare several (extreme value) distributions by means of a plot with return periods on a linear scale: brry/extremeStat*. original-date: 2014-09-30T09:39:36Z. Feb. 2, 2015.
- [47] O. Bogenrieder. "Vortrag Auf Dem Dresdner Forum Zur Versicherungsmathematik". 2004.
- [48] M. Böhme, F. Krüger, K. Ockenfeld, and W. Geller. *Schadstoffbelastung nach dem Elbe-Hochwasser 2002*. Leipzig: UFZ, 2005, p. 101.
- [49] G. Bollrich. *Technische Hydromechanik 1*. 5. Auflage. 2. Spezielle Probleme. Berlin [u.a.]: Verl. für Bauwesen, 2000. 456 pp. ISBN: 3-345-00744-4.
- [50] W. J. W. Botzen, J. Aerts, and J. C. J. M. van den Bergh. "Individual preferences for reducing flood risk to near zero through elevation". In: *Mitig Adapt Strateg Glob Change* 18.2 (Feb. 1, 2013), pp. 229–244. ISSN: 1573-1596. DOI: 10.1007/s11027-012-9359-5.
- [51] W. Boughton and O. Droop. "Continuous simulation for design flood estimation - A review". In: *Environmental Modelling and Software* 18.4 (2003), pp. 309–318.
- [52] L.M. Bouwer. "Have Disaster Losses Increased Due to Anthropogenic Climate Change?" In: *Bull. Amer. Meteor. Soc.* 92.1 (Aug. 20, 2010), pp. 39–46. ISSN: 0003-0007. DOI: 10.1175/2010BAMS3092.1.
- [53] L.M. Bouwer, J. E. Vermaat, and J. Aerts. "Winter atmospheric circulation and river discharge in northwest Europe". In: *Geophysical Research Letters* 33.6 (2006).
- [54] I.C. Bovolo, S. J. Abele, J. C. Bathurst, D. Caballero, M. Ciglan, G. Eftichidis, and B. Simo. "A distributed framework for multi-risk assessment of natural hazards used to model the effects of forest fire on hydrology and sediment yield". In: *Computers and Geosciences* 35.5 (2009), pp. 924–945.
- [55] K. Bradbrook, S. Waller, and D. Morris. "National floodplain mapping: Datasets and methods - 160,000 km in 12 months". In: *Natural Hazards* 36.1 (2005), pp. 103–123.
- [56] O. Brasseur. "Development and application of a physical approach to estimating wind gusts". In: *Monthly Weather Review* 129.1 (2001), pp. 5–25.
- [57] L. Breiman. "Bagging predictors". In: *Machine Learning* 24.2 (Aug. 1996), pp. 123–140. ISSN: 0885-6125, 1573-0565. DOI: 10.1007/BF00058655.
- [58] L. Breiman. "Random Forests". In: *Machine Learning* 45.1 (Oct. 2001), pp. 5–32. ISSN: 0885-6125, 1573-0565. DOI: 10.1023/A:1010933404324.

- [59] L. Breiman, J. H. Friedman, R. A. Olshen, and C. J. Stone. *Classification and Regression Trees*. 1984.
- [60] P. Brémond and F. Grelot. "Review Article: Economic evaluation of flood damage to agriculture - Review and analysis of existing methods". In: *Natural Hazards and Earth System Sciences* 13.10 (2013), pp. 2493–2512.
- [61] J. Bröcker. "Evaluating raw ensembles with the continuous ranked probability score". In: *Quarterly Journal of the Royal Meteorological Society* 138.667 (2012), pp. 1611–1617.
- [62] J. Brombach. "Modifikation der Strömung über Mittelgebirgen und die Auswirkungen auf das Auftreten hochreichender Konvektion". PhD thesis. Karlsruhe: Karlsruhe Institute of Technology (KIT), 2012.
- [63] A. Bronstert and A. Bárdossy. "The role of spatial variability of soil moisture for modelling surface runoff generation at the small catchment scale". In: *Hydrology and Earth System Sciences* 3.4 (1999), pp. 505–516.
- [64] K. de Bruijn, J. Buurman, M. Mens, R. Dahm, and F. Klijn. "Resilience in practice: Five principles to enable societies to cope with extreme weather events". In: *Environmental Science & Policy* 70 (Apr. 1, 2017), pp. 21–30. ISSN: 1462-9011. DOI: 10.1016/j.envsci.2017.02.001.
- [65] P. Bubeck, W. Botzen, and J. Aerts. "A Review of Risk Perceptions and Other Factors that Influence Flood Mitigation Behavior". In: *Risk Anal.* 32.9 (Sept. 2012). WOS:000307930900005, pp. 1481–1495. ISSN: 0272-4332. DOI: 10.1111/j.1539-6924.2011.01783.x.
- [66] P. Bubeck, L. Dillenardt, L. Alfieri, L. Feyen, A. Thieken, and P. Kellermann. "Global warming to increase flood risk on European railways". In: *Climatic Change* (Apr. 26, 2019). ISSN: 1573-1480. DOI: 10.1007/s10584-019-02434-5.
- [67] P. Bubeck and H. Kreibich. "Natural Hazards: Direct costs and losses due to the disruption of production processes". In: *CONHAZ Costs of Natural Hazards 2011* (2011).
- [68] P. Bubeck, H. Kreibich, E.C. Penning-Rowsell, W.J.W. Botzen, H. de Moel, and F. Klijn. "Explaining differences in flood management approaches in Europe and in the USA - a comparative analysis: Differences in flood management approaches". In: *Journal of Flood Risk Management* 10.4 (Dec. 2017), pp. 436–445. ISSN: 1753318X. DOI: 10.1111/jfr3.12151.
- [69] B. Büchele, H. Kreibich, A. Kron, A. Thieken, J. Ihringer, P. Oberle, B. Merz, and F. Nestmann. "Flood-risk mapping: contributions towards an enhanced assessment of extreme events and associated risks". In: *Nat. Hazards Earth Syst. Sci.* 6.4 (June 12, 2006), pp. 485–503. ISSN: 1684-9981. DOI: 10.5194/nhess-6-485-2006.
- [70] W. Buck and U. Merkel. *Auswertung der HOWAS-Schadendatenbank*. HY98/15. Institut für Wasserwirtschaft und Kulturtechnik: Universität Karlsruhe, 1999.
- [71] Y. Budiyo, J. Aerts, J. Brinkman, M. A. Marfai, and P. Ward. "Flood risk assessment for delta mega-cities: a case study of Jakarta". In: *Nat Hazards* 75.1 (July 20, 2014), pp. 389–413. ISSN: 0921-030X, 1573-0840. DOI: 10.1007/s11069-014-1327-9.

- [72] Bundesregierung. *Bericht zur Flutkatastrophe 2013-Katastrophenhilfe, Entschädigung*. Drucksache 17/14743. Berlin: Deutscher Bundestag, Sept. 19, 2013.
- [73] T. Camelbeeck, H. Martin, K. Vanneste, M. Meghraoui, K. Verbeeck, and M. Brondeel. "Geomorphic evidence of active faulting in slow deformation area: The example of the Lower Rhine Embayment". In: *Workshop Evaluation of the Potential for Large Earthquakes in Region of Present-day Low Seismic Activity* (2000), pp. 31–34.
- [74] T. Camelbeeck and M. Meghraoui. "Geological and geophysical evidence for large palaeo-earthquakes with surface faulting in the Roer Graben (northwest Europe)". In: *Geophysical Journal International* 132.2 (1998), pp. 347–362.
- [75] T. Camelbeeck, K. Vanneste, K. Verbeeck, M. Meghraoui, R. Pelzing, K. Hinzen, B. Dost, and M. van der Berg. "Long term seismic activity in the Lower Rhine Embayment". In: *European Centre for Geodynamics and seismology workshop. Evaluation of the Potential for large Earthquakes in regions of present day low seismic activity in Europe*. Han-sur-Lesse, Belgium, 2000, pp. 35–38.
- [76] H. Cammerer, A. Thielen, and J. Lammel. "Adaptability and transferability of flood loss functions in residential areas". In: *Nat. Hazards Earth Syst. Sci.* 13.11 (Nov. 29, 2013), pp. 3063–3081. ISSN: 1684-9981. DOI: 10.5194/nhess-13-3063-2013.
- [77] O.D. Cardona, M.K. van Aalst, J. Birkmann, et al. "Determinants of Risk: Exposure and Vulnerability". In: *Managing the Risks of Extreme Events and Disasters to Advance Climate Change Adaptation. A Special Report of Working Groups I and II of the Intergovernmental Panel on Climate Change (IPCC)*. Ed. by C. B. Field, V. R. Barros, T.F. Stocker, et al. Cambridge, United Kingdom and New York, NY, USA: Cambridge University Press, 2012, pp. 65–108.
- [78] V. M. Castillo, A. Gómez-Plaza, and M. Martínez-Mena. "The role of antecedent soil water content in the runoff response of semiarid catchments: A simulation approach". In: *Journal of Hydrology* 284.1 (2003), pp. 114–130.
- [79] CEDIM. *June 2013 Flood in Central Europe - Focus Germany Report 1 - Update 2: Preconditions, Meteorology, Hydrology*. Potsdam: Center for Disaster Management and Risk Reduction Technology, June 20, 2013, p. 13.
- [80] CEDIM. *June 2013 Flood in Central Europe - Focus Germany Report 2 - Update 1: Impact and Management*. Potsdam: Center for Disaster Management and Risk Reduction Technology, June 27, 2013, p. 22.
- [81] S. A. Changnon. "Hailstreaks". In: *Journal of the Atmospheric Sciences* 27.1 (1970), pp. 109–125.
- [82] S. A. Changnon. "Shifting economic impacts from weather extremes in the United States: A result of societal changes, not global warming". In: *Natural Hazards* 29.2 (2003), pp. 273–290.
- [83] K. Chapi, V.P. Singh, A. Shirzadi, H. Shahabi, D.T. Bui, B.T. Pham, and K. Khosravi. "A novel hybrid artificial intelligence approach for flood susceptibility assessment". In: *Environmental Modelling & Software* 95 (Sept. 1, 2017), pp. 229–245. ISSN: 1364-8152. DOI: 10.1016/j.envsoft.2017.06.012.

- [84] V. N. Chau, S. Cassells, and J. Holland. "Economic impact upon agricultural production from extreme flood events in Quang Nam, central Vietnam". In: *Natural Hazards* 75.2 (2015), pp. 1747–1765.
- [85] K. Chen, J. McAneney, R. Blong, R. Leigh, L. Hunter, and C. Magill. "Defining area at risk and its effect in catastrophe loss estimation: A dasymetric mapping approach". In: *Applied Geography* 24.2 (2004), pp. 97–117.
- [86] D. T. Chinh, A.K. Gain, N.V. Dung, D. Haase, and H. Kreibich. "Multi-Variate Analyses of Flood Loss in Can Tho City, Mekong Delta". In: *Water* 8.1 (Dec. 25, 2015), p. 6. DOI: 10.3390/w8010006.
- [87] V.T. Chow. *Open-channel hydraulics*. McGraw-Hill, 1959. 710 pp.
- [88] Alessio Ciullo, Karin M. de Bruijn, Jan H. Kwakkel, and Frans Klijn. "Accounting for the uncertain effects of hydraulic interactions in optimising embankments heights: Proof of principle for the IJssel River". In: *Journal of Flood Risk Management* 0.0 (Apr. 29, 2019), e12532. ISSN: 1753-318X. DOI: 10.1111/jfr3.12532.
- [89] W.S. Cleveland. "Robust Locally Weighted Regression and Smoothing Scatterplots". In: *Journal of the American Statistical Association* 74.368 (Dec. 1979), pp. 829–836. ISSN: 01621459. DOI: 10.2307/2286407.
- [90] T. Conradt, M. Roers, K. Schröter, F. Elmer, P. Hoffmann, H. Koch, F.F. Hattermann, and F. Wechsung. "Comparison of the extreme floods of 2002 and 2013 in the German part of the Elbe River basin and their runoff simulation by SWIM-live". In: *Hydrologie und Wasserbewirtschaftung* 57.5 (2013), pp. 241–245. ISSN: 1439-1783. DOI: 10.5675/HyWa-2013,5-4.
- [91] C. Corbane, T. De Groeve, and D. Ehrlich. "Guidance for Recording and Sharing Disaster Damage and Loss Data-Towards the development of operational indicators to translate the Sendai Framework into action". In: *Report, JRC95505, EUR 27192 en* (2015).
- [92] F. Cotton, F. Scherbaum, J. J. Bommer, and H. Bungum. "Criteria for selecting and adjusting ground-motion models for specific target regions: Application to central Europe and rock sites". In: *Journal of Seismology* 10.2 (2006), pp. 137–156.
- [93] CRED. *EM-DAT | The international disasters database*. 2019. URL: <https://www.emdat.be/> (visited on 01/31/2019).
- [94] CRED. *The human cost of natural disasters: a global perspective*. Centre for Research on the Epidemiology of Disasters, 2015, p. 58.
- [95] R. Cremades, S. Surminski, M. Mánuez Costa, P. Hudson, P. Shrivastava, and J. Gascoigne. "Using the adaptive cycle in climate-risk insurance to design resilient futures". In: *Nature Climate Change* 8.1 (Jan. 2018), p. 4. ISSN: 1758-6798. DOI: 10.1038/s41558-017-0044-2.
- [96] J. M. Cunderlik, T. B. M. J. Ouarda, and B. Bobee. "Determination of flood seasonality from hydrological records". In: *Hydrological Sciences Journal* 49.3 (2004), pp. 511–526.
- [97] R. Custer and K. Nishijima. "Flood vulnerability assessment of residential buildings by explicit damage process modelling". In: *Natural Hazards* 78.1 (2015), pp. 461–496.

- [98] A. D'Addabbo, A. Refice, G. Pasquariello, F. P. Lovergine, D. Capolongo, and S. Manfreda. "A Bayesian Network for Flood Detection Combining SAR Imagery and Ancillary Data". In: *IEEE Transactions on Geoscience and Remote Sensing* 54.6 (June 2016), pp. 3612–3625. ISSN: 0196-2892. DOI: 10.1109/TGRS.2016.2520487.
- [99] T. Damian. "Blitzdichte im Zusammenhang mit Hagelereignissen in Deutschland und Baden-Württemberg". In: *Seminar thesis at the Institute for Meteorology and Climate Research (IMK)* (2011).
- [100] M. Danard, A. Munro, and T. Murty. "Storm surge hazard in Canada". In: *Natural Hazards* 28.2 (2003), pp. 407–431.
- [101] J. E. Daniell. *Deterministic Earthquake Scenarios for the Northern Rhine Region (Deterministische Erdbeben Szenarien für die nördliche Rhein-Region)*. Research Report 10-02. Karlsruhe, Germany: CEDIM, 2010.
- [102] EM DAT. *EM-DAT: The OFDA/CRED International Disaster Database*. EM-DAT: The OFDA/CRED International Disaster Database. 2006. URL: www.emdat.be (visited on 05/16/2014).
- [103] T. De Groeve, K. Poljansek, and D. Ehrlich. *Recording Disaster Losses*. JRC83743, EUR 26111. Ispra: JRC, 2013.
- [104] T. De Groeve, K. Poljansek, D. Ehrlich, and C. Corbane. *Current Status and Best Practices for Disaster Loss Data Recording in EU Member States*. JRC92290, EUR 26879 en. Ispra: JRC, 2014.
- [105] H. De Moel, J. Van Alphen, and J. Aerts. "Flood maps in Europe - Methods, availability and use". In: *Natural Hazards and Earth System Science* 9.2 (2009), pp. 289–301.
- [106] J. M. Delgado, B. Merz, and H. Apel. "A climate-flood link for the lower Mekong River". In: *Hydrology and Earth System Sciences* 16.5 (2012), pp. 1533–1541.
- [107] P. M. Della-Marta, H. Mathis, C. Frei, M. A. Lininger, J. Kleinn, and C. Appenzeller. "The return period of wind storms over Europe". In: *International Journal of Climatology* 29.3 (2009), pp. 437–459.
- [108] Deutsche Deutsche Bahn. *Wettbewerbsbericht 2014*. German Railways, 2014.
- [109] Deutscher Bundestag. *Gesetz zur Ordnung des Wasserhaushalts (Wasserhaushaltsgesetz - WHG)*. Jan. 3, 2010.
- [110] G. Di Baldassarre, H. Kreibich, S. Vorogushyn, et al. "Hess Opinions: An interdisciplinary research agenda to explore the unintended consequences of structural flood protection". In: *Hydrology and Earth System Sciences* 22.11 (Oct. 30, 2018), pp. 5629–5637. ISSN: 1607-7938. DOI: 10.5194/hess-22-5629-2018.
- [111] G. Di Baldassarre, G. Schumann, and P. Bates. "Near real time satellite imagery to support and verify timely flood modelling". In: *Hydrol. Process.* 23.5 (Feb. 28, 2009), pp. 799–803. ISSN: 1099-1085. DOI: 10.1002/hyp.7229.

- [112] G. Di Baldassarre, A. Viglione, G. Carr, L. Kuil, K. Yan, L. Brandimarte, and G. Blöschl. "Debates-Perspectives on socio-hydrology: Capturing feedbacks between physical and social processes: A socio-hydrological approach to explore flood risk changes". In: *Water Resources Research* 51.6 (June 2015), pp. 4770–4781. ISSN: 00431397. DOI: 10.1002/2014WR016416.
- [113] H Dietz. *Wohngebäudeversicherung Kommentar*. 2nd ed. Karlsruhe: VVW Verlag Versicherungswirtschaft GmbH, 1999.
- [114] DieWelt. "Wasserfluten Richtung Norden". In: *Die Welt* (June 5, 2013).
- [115] DIN. *DIN1055-4: Einwirkungen auf Tragwerke - Teil 4: Windlasten*. 2005.
- [116] DIN. *DIN4149 Bauten in deutschen Erdbebengebieten. Lastannahmen, Bemessung Ausführung üblicher Hochbauten*. 1981.
- [117] A. Ding, J.F. White, P.W. Ullman, and A.O. Fashokun. "Evaluation of HAZUS-MH flood model with local data and other program". In: *Natural Hazards Review* 9.1 (2008), pp. 20–28. ISSN: 15276988. DOI: 10.1061/(ASCE)1527-6988(2008)9:1(20).
- [118] DKKV. *Das Hochwasser im Juni 2013-Bewährungsprobe für das Hochwasserrisikomanagement in Deutschland*. 53. Bonn: Deutsches Komitee Katastrophenvorsorge e.V. (DKKV), 2015.
- [119] DKKV. *Detecting Root Causes of Disasters*. 48. Bonn: Deutsches Komitee Katastrophenvorsorge e.V. (DKKV), 2012.
- [120] DKKV. *Deutsches Komitee für r Katastrophenvorsorge (2003) Hochwasservorsorge in Deutschland- Lernen aus der Katastrophe 2002 im Elbegebiet*. 29. Bonn: Deutsches Komitee für Katastrophenvorsorge, 2003.
- [121] DKKV. *Lessons Learned-Hochwasservorsorge in Deutschland-Lernen Aus der Katastrophe 2002 im Elbegebiet*. 29. Bonn: Deutsches Komitee Katastrophenvorsorge e.V. (DKKV), 2003.
- [122] DNRM. *Guidance on the Assessment of Tangible Flood Damage*. Australia: Department of Natural Resources and Mines, Queensland Government, 2002.
- [123] F. J. Doblas-Reyes, R. Hagedorn, and T. N. Palmer. "The rationale behind the success of multi-model ensembles in seasonal forecasting - II. Calibration and combination". In: *Tellus, Series A: Dynamic Meteorology and Oceanography* 57.3 (2005), pp. 234–252.
- [124] F. Dottori, R. Figueiredo, M. L. V. Martina, D. Molinari, and A. R. Scorzini. "INSYDE: a synthetic, probabilistic flood damage model based on explicit cost analysis". In: *Nat. Hazards Earth Syst. Sci.* 16.12 (Dec. 2, 2016), pp. 2577–2591. ISSN: 1684-9981. DOI: 10.5194/nhess-16-2577-2016.
- [125] N. Dotzek. "Tornadoes in Germany". In: *Atmospheric Research* 56.1 (2000), pp. 233–251.
- [126] M. W. Downton, R. E. Morss, O. V. Wilhelmi, E. Gruntfest, and M. L. Higgins. "Interactions between scientific uncertainty and flood management decisions: Two case studies in Colorado". In: *Environmental Hazards* 6.3 (2005), pp. 134–146.

- [127] M.W. Downton and R.A. Pielke. "How Accurate are Disaster Loss Data? The Case of U.S. Flood Damage". In: *Nat Hazards* 35.2 (June 1, 2005), pp. 211–228. ISSN: 0921-030X, 1573-0840. DOI: 10.1007/s11069-004-4808-4.
- [128] D. Dransch, J. Fohringer, K. Poser, and C. Lucas. "Volunteered geographic information for disaster management". In: *Citizen E-Participation in Urban Governance: Crowdsourcing and Collaborative Creativity*. 2013, pp. 98–118.
- [129] Landeshauptstadt Dresden. "Plan Hochwasservorsorge Dresden. Dresden: Landeshauptstadt Dresden". In: (2011).
- [130] Q. Duan, S. Sorooshian, and V. Gupta. "Effective and efficient global optimization for conceptual rainfallrunoff models". In: *Water Resources Research* 28.4 (1992), pp. 1015–1031.
- [131] L. Duckstein, A. Bárdossy, and I. Bogárdi. "Linkage between the occurrence of daily atmospheric circulation patterns and floods: an Arizona case study". In: *Journal of Hydrology* 143.3 (1993), pp. 413–428. ISSN: 0022-1694. DOI: 10.1016/0022-1694(93)90202-K.
- [132] D. Dutta, S. Herath, and K. Musiakcec. "A mathematical model for flood loss estimation". In: *J. Hydrol.* 277.1 (June 1, 2003), pp. 24–49. ISSN: 0022-1694. DOI: 10.1016/S0022-1694(03)00084-2.
- [133] DWD-Deutscher Wetterdienst. *Das Hochwasser An Elbe und Donau im Juni 2013*. 242. Offenbach: Deutscher Wetterdienst, 2013.
- [134] G. Dyke, S. Gill, R. Davies, et al. "Dream project: Applications of earth observations to disaster risk management". In: *Acta Astronautica* 68.1 (2011), pp. 301–315.
- [135] EC. *Directive 2000/60/EC of the European Parliament and of the Council establishing a framework for the Community action in the field of water policy*. 2000.
- [136] EC. *Directive 2001/42/EC of the European Parliament and of the Council on the Assessment of the Effects of Certain Plans and Programmes on the Environment*. 2001.
- [137] EC. *Directive 2007/2/EC of the European Parliament and of the Council of 14 March 2007 establishing an Infrastructure for Spatial Information in the European Community (INSPIRE) | INSPIRE*. 2007. URL: <https://inspire.ec.europa.eu/documents/directive-20072ec-european-parliament-and-council-14-march-2007-establishing> (visited on 07/24/2017).
- [138] EC. *Directive 2007/60/EC of the European Parliament and of the Council on the assessment and management of flood risks*. 2007.
- [139] EC. *Directive 2011/92/EC of the European Parliament and of the Council of 13 December 2011 on the Assessment of the Effects of Certain Public and Private Projects on the Environment*. 2011.
- [140] EC. *Proposal for a Directive of the European Parliament and of the Council amending Directive 2011/92/EU on the assessment of the effects of certain public and private projects on the environment*. Commission staff working paper. 2014.
- [141] EC. *Risk assessment and mapping guidelines for disaster management*. Commission staff working paper. 2011.

- [142] F. Elmer, J. Hoymann, D. DÜthmann, S. Vorogushyn, and H. Kreibich. "Drivers of flood risk change in residential areas". In: *Nat. Hazards Earth Syst. Sci.* 12.5 (2012), pp. 1641–1657. ISSN: 1684-9981. DOI: 10.5194/nhess-12-1641-2012.
- [143] F. Elmer, A. Thielen, I. Pech, and H. Kreibich. "Influence of flood frequency on residential building losses". In: *Nat. Hazards Earth Syst. Sci.* 10.10 (2010), pp. 2145–2159. ISSN: 1684-9981. DOI: 10.5194/nhess-10-2145-2010.
- [144] P. Embrechts, C. Klüppelberg, and T. Mikosch. *Modelling Extremal Events - for Insurance and Finance*. Vol. Vol. 33. Berlin, Heidelberg: Springer, 1997. 648 pp. ISBN: ISBN 978-3-642-33483-2.
- [145] Emschergenossenschaft and Hydrotec. *Hochwasser-Aktionsplan Emscher, Kapitel 1: Methodik der Schadensermittlung*, Essen: Emschergenossenschaft, 2004.
- [146] H. Engel. "The flood event 2002 in the Elbe river basin causes of the flood, its course, statistical assessment and flood damages". In: *Houille Blanche* 6 (2004), pp. 33–36. ISSN: 00186368.
- [147] T. M. Ettrick, J. A. Mawdlsey, and A. V. Metcalfe. "The influence of antecedent catchment conditions on seasonal flood risk". In: *Water Resour. Res.* 23.3 (1987), pp. 481–488. ISSN: 1944-7973. DOI: 10.1029/WR023i003p00481.
- [148] D. Falter, N. V. Dung, S. Vorogushyn, et al. "Continuous, large-scale simulation model for flood risk assessments: Proof-of-concept". In: *Journal of Flood Risk Management* 9.1 (2016), pp. 3–21.
- [149] D. Falter, K. Schröter, N.V. Dung, S. Vorogushyn, H. Kreibich, Y. Hundecha, H. Apel, and B. Merz. "Spatially coherent flood risk assessment based on long-term continuous simulation with a coupled model chain". In: *Journal of Hydrology* (2015). ISSN: 0022-1694. DOI: 10.1016/j.jhydro.2015.02.021.
- [150] D. Falter, S. Vorogushyn, J. Lhomme, H. Apel, B. Gouldby, and B. Merz. "Hydraulic model evaluation for large-scale flood risk assessments". In: *Hydrol. Process.* 27.9 (Apr. 30, 2013), pp. 1331–1340. ISSN: 1099-1085. DOI: 10.1002/hyp.9553.
- [151] Federal Statistical Office of Germany. *Anbauflächen, Hektarerträge und Erntemengen ausgewählter Anbaukulturen im Zeitvergleich*. Statistisches Bundesamt. 2015. URL: <https://www.destatis.de/DE/Themen/Branchen-Unternehmen/Landwirtschaft-Forstwirtschaft-Fischerei/Feldfruechte-Gruenland/Tabellen/liste-feldfruechte-zeitreihe.html> (visited on 11/26/2015).
- [152] G. Felder, J.J. Gómez-Navarro, A.P. Zischg, C.C. Raible, V. Röthlisberger, D. Bozhinova, O. Martius, and R. Weingartner. "From global circulation to local flood loss: Coupling models across the scales". In: *Science of The Total Environment* 635 (Sept. 1, 2018), pp. 1225–1239. ISSN: 0048-9697. DOI: 10.1016/j.scitotenv.2018.04.170.
- [153] FEMA. *Multi-Hazard Loss Estimation Methodology Flood Model HAZUS1MH MR4 Technical Manual*. 43. Federal Emergency Management Agency (US), 2009.
- [154] N. Fenton and M. Neil. *Risk Assessment and Decision Analysis With Bayesian Networks*. Boca Raton, FL, USA: Taylor & Francis, Nov. 5, 2012. 552 pp. ISBN: 978-1-4398-0910-5.

- [155] S. Ferson and L.R. Ginzburg. "Different methods are needed to propagate ignorance and variability". In: *Reliability Engineering & System Safety* 54.2 (Nov. 1996), pp. 133–144. ISSN: 09518320. DOI: 10.1016/S0951-8320(96)00071-3.
- [156] R. Figueiredo, K. Schröter, A. Weiss-Motz, M. L. V. Martina, and H. Kreibich. "Multi-model ensembles for assessment of flood losses and associated uncertainty". In: *Nat. Hazards Earth Syst. Sci.* 18.5 (May 3, 2018), pp. 1297–1314. ISSN: 1684-9981. DOI: 10.5194/nhess-18-1297-2018.
- [157] E. M. Fischer and C. Schär. "Future changes in daily summer temperature variability: Driving processes and role for temperature extremes". In: *Climate Dynamics* 33.7 (2009), pp. 917–935.
- [158] J. Fohringer, D. Dransch, H. Kreibich, and K. Schröter. "Social media as an information source for rapid flood inundation mapping". In: *Nat. Hazards Earth Syst. Sci.* 15.12 (2015), pp. 2725–2738. ISSN: 1684-9981. DOI: 10.5194/nhess-15-2725-2015.
- [159] J.D. Ford, S.E. Tilleard, L. Berrang-Ford, et al. "Opinion: Big data has big potential for applications to climate change adaptation". In: *PNAS* 113.39 (Sept. 27, 2016), pp. 10729–10732. ISSN: 0027-8424, 1091-6490. DOI: 10.1073/pnas.1614023113.
- [160] S. Förster, B. Kuhlmann, K.-E. Lindenschmidt, and A. Bronstert. "Assessing flood risk for a rural detention area". In: *Nat. Hazards Earth Syst. Sci.* 8.2 (Apr. 10, 2008), pp. 311–322. ISSN: 1684-9981.
- [161] G. Franco. "Uncertainty in Catastrophe Models: How Much of it is Reasonable?" In: *Guy Carpenter's Capital Ideas Blog* (2013).
- [162] G. Franco. "Validation and Adjustment of Assumptions in Catastrophe Models". In: *Insurance ERM* (2014).
- [163] F. Fundel and M. Zappa. "Hydrological ensemble forecasting in mesoscale catchments: Sensitivity to initial conditions and value of reforecasts". In: *Water Resources Research* 47.9 (2011).
- [164] A. Al-Futaisi and J. R. Stedinger. "Hydrologic and economic uncertainties and flood-risk project design". In: *Journal of Water Resources Planning and Management* 125.6 (1999), pp. 314–324.
- [165] L. Gaál, J. Szolgay, S. Kohnová, J. Parajka, R. Merz, A. Viglione, and G. Blöschl. "Flood timescales: Understanding the interplay of climate and catchment processes through comparative hydrology". In: *Water Resources Research* 48.4 (2012).
- [166] K. M. A. Gabriel and W. R. Endlicher. "Urban and rural mortality rates during heat waves in Berlin and Brandenburg, Germany". In: *Environmental Pollution* 159.8 (2011), pp. 2044–2050.
- [167] M. Gall, K.A. Borden, and S.L. Cutter. "When do losses count?" In: *Bulletin of the American Meteorological Society* 90.6 (2009), pp. 799–809. ISSN: 00030007. DOI: 10.1175/2008BAMS2721.1.
- [168] J. Ganoulis. "Risk-based floodplain management: A case study from Greece". In: *International Journal of River Basin Management* 1.1 (2003), pp. 41–47.

- [169] F. Garavaglia, M. Lang, E. Paquet, J. Gailhard, R. Garçon, and B. Renard. "Reliability and robustness of rainfall compound distribution model based on weather pattern sub-sampling". In: *Hydrology and Earth System Sciences* 15.2 (2011), pp. 519–532.
- [170] E. Gaume, V. Bain, P. Bernardara, et al. "A compilation of data on European flash floods". In: *Journal of Hydrology* 367.1 (2009). <http://www.Hydrate.tesaf.unipd.it>, pp. 70–78. ISSN: 0022-1694. DOI: 10.1016/j.jhydro1.2008.12.028.
- [171] GDV. *2003 Yearbook: The German Insurance Industry*. Berlin: German Insurance Association, 2003.
- [172] GDV. *Erste Schadenbilanz: Hochwasser 2013 verursacht 180.000 versicherte Schäden in Höhe von fast 2 Milliarden Euro*. 2013.
- [173] GDV. *Geo-Informationssystem Zü RS Geo: Zonierungssystem für ü berschwemmungsrisiko und Einschätzung von Umweltrisiken*. Geo-Informationssystem Zü RS Geo: Zonierungssystem für ü berschwemmungsrisiko und Einschätzung von Umweltrisiken. 2008. URL: <http://www.gdv.de/2008/08/geo-informationssystem-zuers-geo-zonierungssystem-fuer-ueberschwemmungsrisiko-und-einschaetzung-von-umweltrisiken/> (visited on 10/24/2012).
- [174] GDV. *Naturgefahrenreport 2014 - Die Schadenchronik der deutschen Versicherer in Zahlen, Stimmen und Ereignissen*. Berlin: Gesamtverband der Deutschen Versicherungswirtschaft e.V., 2014.
- [175] GDV. *Naturgefahrenreport 2015 - Die Schadenchronik der deutschen Versicherer in Zahlen, Stimmen und Ereignissen*. Berlin: Gesamtverband der Deutschen Versicherungswirtschaft e.V., 2015.
- [176] Geneva Association. *Managing Physical Climate Risk Leveraging Innovations in Catastrophe Risk Modelling*. Zurich: The Geneva Association International Association for the Study of Insurance Economics, Nov. 18, 2018, p. 48.
- [177] R. Genuer, J. -. Poggi, and C. Tuleau-Malot. "Variable selection using random forests". In: *Pattern Recognition Letters* 31.14 (2010), pp. 2225–2236.
- [178] BKG GEODATENZENTRUM. *ATKIS-Basis-DLM*. 2009.
- [179] E. GeoEye. *Ikonos-imagery products guide (Ver.1.5)*. 2006, p. 19.
- [180] K. P Georgakakos, D. J Seo, H. Gupta, J. Schaake, and M. B Butts. "Towards the characterization of streamflow simulation uncertainty through multimodel ensembles". In: *Journal of Hydrology* 298.1 (2004). Cited References: *WMO, 2001, EXPT TEAM ENS PRED S BEVEN K, 2001, J HYDROL, V249, P11 CARPENTER TM, 2001, J HYDROL, V249, P148 CARPENTER TM, 2004, J HYDROL, V298, P202 FRITSCH JM, 2000, WEATHER FORECAST, V15, P571 GEORGAKAKOS KP, 2001, J HYDROL, V249, P1 GEORGAKAKOS KP, 2002, MATH MODELS SMALL WA, P593 KHARIN VV, 2002, J CLIMATE, V15, P793 KRISHNAMURTI TN, 1999, SCIENCE, V285, P1548 KRISHNAMURTI TN, 2000, J CLIMATE, V13, P4196 KRZYSZTOFOWICZ R, 1999, WATER RESOUR RES, V35, P2739 MASON SJ, 2002, Q J ROY METEOR SOC B, V128, P2145 RAISANEN J, 2001, J CLIMATE, V14, P3212 REED S, 2004, J HYDROL, V298, P27 SCHWEPPE FC, 1973, UNCERTAIN DYNAMIC SY SMITH MB, 2004, J HYDROL, V298, P4 SRINATH MD, 1979,

- INTRO STAT SIGNAL PR TOTTH Z, 2002, P ECMWF SEM PRED WEA, P1 VIS-LOCKY RL, 1995, B AM METEOROL SOC, V76, P1157 WANDISHIN MS, 2001, MON WEATHER REV, V129, P729 WILKS DS, 1995, STAT METHODS ATMO-SPH ZHU YJ, 2002, B AM METEOROL SOC, V83, P73, pp. 222–241.
- [181] T. Gerl, M. Bochow, and H. Kreibich. “Flood Damage Modeling on the Basis of Urban Structure Mapping Using High-Resolution Remote Sensing Data”. In: *Water* 6.8 (Aug. 11, 2014), pp. 2367–2393. DOI: 10.3390/w6082367.
- [182] T. Gerl, H. Kreibich, G. Franco, D. Marechal, and K. Schröter. “A Review of Flood Loss Models as Basis for Harmonization and Benchmarking”. In: *PLOS ONE* 11.7 (July 25, 2016), e0159791. ISSN: 1932-6203. DOI: 10.1371/journal.pone.0159791.
- [183] T. Ghizzoni, G. Roth, and R. Rudari. “Multisite flooding hazard assessment in the Upper Mississippi River”. In: *Journal of Hydrology* 412-413 (2012), pp. 101–113.
- [184] D. Giordan, D. Notti, A. Villa, et al. “Low cost, multiscale and multi-sensor application for flooded area mapping”. In: *Nat. Hazards Earth Syst. Sci.* 18.5 (May 30, 2018), pp. 1493–1516. ISSN: 1684-9981. DOI: 10.5194/nhess-18-1493-2018.
- [185] R. Glaser and H. Stangl. “Climate and floods in Central Europe since AD 1000: Data, Methods, Results and Consequences”. In: *Surveys in Geophysics* 25.5 (2004), pp. 485–510. ISSN: 0169-3298. DOI: 10.1007/s10712-004-6201-y.
- [186] P. J. Gleckler, K. E. Taylor, and C. Doutriaux. “Performance metrics for climate models”. In: *Journal of Geophysical Research Atmospheres* 113.6 (2008).
- [187] GMLZ. *Abschlussbericht zur Hochwasserlage Juni 2013*. internal report. Bonn: GMLZ-Gemeinsames Melde-und Lagezentrum, 2014.
- [188] T. Gneiting and A.E. Raftery. “Strictly Proper Scoring Rules, Prediction, and Estimation”. In: *Journal of the American Statistical Association* 102.477 (Mar. 2007), pp. 359–378. ISSN: 0162-1459, 1537-274X. DOI: 10.1198/016214506000001437.
- [189] M. F. Goodchild and J. A. Glennon. “Crowdsourcing geographic information for disaster response: A research frontier”. In: *International Journal of Digital Earth* 3.3 (2010), pp. 231–241.
- [190] P. Goovaerts. “Geostatistics for natural resources evaluation”. In: *Geostatistics for natural resources evaluation*. 1997.
- [191] S. N. Gosling, J. A. Lowe, G. R. McGregor, M. Pelling, and B. D. Malamud. “Associations between elevated atmospheric temperature and human mortality: A critical review of the literature”. In: *Climatic Change* 92.3 (2009), pp. 299–341.
- [192] J.H. Grabbert. “Analyse der schadensbeeinflussenden Faktoren des Hochwassers 2002 und Ableitung eines mesoskaligen Abschätzungsmodells für Wohngebäudeschäden [Analysis of parameters influencing loss during the flood event 2002 and development of a meso-scale estimation model for residential building damages].” Unpublished Thesis. Potsdam: University of Potsdam, 2006. 109 pp.
- [193] J. Graesser, A. Cheriyyadat, R. R. Vatsavai, V. Chandola, J. Long, and E. Bright. “Image based characterization of formal and informal neighborhoods in an urban landscape”. In: *IEEE Journal of Selected Topics in Applied Earth Observations and Remote Sensing* 5.4 (2012), pp. 1164–1176.

- [194] U. Graewe and H. Burchard. "Storm surges in the Western Baltic Sea: the present and a possible future". In: *Clim. Dyn.* 39.1 (July 2012). WOS:000305745100010, pp. 165–183. ISSN: 0930-7575. DOI: 10.1007/s00382-011-1185-z.
- [195] T. Grahn and R. Nyberg. "Damage assessment of lake floods: Insured damage to private property during two lake floods in Sweden 2000/2001". In: *International Journal of Disaster Risk Reduction* 10, Part A (2014), pp. 305–314. ISSN: 2212-4209. DOI: 10.1016/j.ijdr.2014.10.003.
- [196] C. M. Grams, H. Binder, S. Pfahl, N. Piaget, and H. Wernli. "Atmospheric processes triggering the central European floods in June 2013". In: *Nat. Hazards Earth Syst. Sci.* 14.7 (July 4, 2014), pp. 1691–1702. ISSN: 1684-9981. DOI: 10.5194/nhess-14-1691-2014.
- [197] C. Green. *The handbook of water economics: principles and practice*. Chichester, England: Wiley, May 15, 2003. 470 pp. ISBN: 978-0-471-98571-6.
- [198] C. Green, C. Viavattene, and P. Thompson. "Guidance for Assessing Flood Losses. CONHAZ Report". In: *Guidance for Assessing Flood Losses* (2011).
- [199] M. R. Greenberg, M. Lahr, and N. Mantell. "Understanding the economic costs and benefits of catastrophes and their aftermath: A review and suggestions for the U.S. federal government". In: *Risk Analysis* 27.1 (2007), pp. 83–96.
- [200] S. Greiving and M. Fleischhauer. *Spatial planning response to natural and technological hazards*. Special Paper of the Geological Survey of Finland 42. 2006. 109-123.
- [201] N. S. Grigg and O. J. Helweg. "STATEOFTHEART OF ESTIMATING FLOOD DAMAGE IN URBAN AREAS". In: *JAWRA Journal of the American Water Resources Association* 11.2 (1975), pp. 379–390.
- [202] S. Grimaldi, A. Petroselli, E. Arcangeletti, and F. Nardi. "Flood mapping in ungauged basins using fully continuous hydrologic-hydraulic modeling". In: *Journal of Hydrology* 487 (2013), pp. 39–47.
- [203] G. Gröger and L. Plümer. "CityGML - Interoperable semantic 3D city models". In: *ISPRS Journal of Photogrammetry and Remote Sensing* 71 (2012), pp. 12–33.
- [204] G. Grünthal, D. Mayer-Rosa, and W. A. Lenhardt. "Seismic hazard assessment for the D-A-CH countries - Germany, Austria, and Switzerland". In: *Bautechnik* 75.10 (1998), pp. 753–767.
- [205] G. Grünthal, A. Thieken, J. Schwarz, K. S. Radtke, A. Smolka, and B. Merz. "Comparative Risk Assessments for the City of Cologne Storms, Floods, Earthquakes". In: *Natural Hazards* 38.1 (May 2006), pp. 21–44. ISSN: 0921-030X, 1573-0840. DOI: 10.1007/s11069-005-8598-0.
- [206] G. Grünthal and R. Wahlström. "The European-Mediterranean earthquake catalogue (EMEC) for the last millennium". In: *Journal of Seismology* 16.3 (2012), pp. 535–570.
- [207] D. Guha-Sapir and R. Below. "The quality and accuracy of disaster data - A comparative analyses of three global data sets". In: *Working Paper for the Disaster Management Facility* (2002).

- [208] E. J Gumbel. *Statistics of extremes*. OCLC: 923876437. Place of publication not identified: Echo Point Books & Media, 2013. ISBN: 978-1-62654-987-6.
- [209] I. Guyon and A. Elisseeff. "An Introduction to Variable and Feature Selection". In: *Journal of Machine Learning Research* 3 (Mar 2003), pp. 1157–1182. ISSN: ISSN 1533-7928.
- [210] U. Haberlandt and I. Radtke. "Hydrological model calibration for derived flood frequency analysis using stochastic rainfall and probability distributions of peak flows". In: *Hydrol. Earth Syst. Sci.* 18.1 (Jan. 30, 2014), pp. 353–365. ISSN: 1607-7938. DOI: 10.5194/hess-18-353-2014.
- [211] R. Hagedorn, F. J. Doblas-Reyes, and T. N. Palmer. "The rationale behind the success of multi-model ensembles in seasonal forecasting - I. Basic concept". In: *Tellus, Series A: Dynamic Meteorology and Oceanography* 57.3 (2005), pp. 219–233.
- [212] Y. H Haimes. *Risk Modelling, Assessment and Management*. Wiley Series in System Engineering. Bibliothek Siegel: MAT HAI chapter 1 uncertainty, chapter 6 to copy. Wiley & Sons, 1998.
- [213] S. Hallegatte. "Strategies to adapt to an uncertain climate change". In: *Global Environmental Change. Traditional Peoples and Climate Change* 19.2 (2009), pp. 240–247. ISSN: 0959-3780. DOI: 10.1016/j.gloenvcha.2008.12.003.
- [214] S. Hallegatte, C. Green, R.J. Nicholls, and J. Corfee-Morlot. "Future flood losses in major coastal cities". In: *Nature Clim. Change* 3.9 (Sept. 2013), pp. 802–806. ISSN: 1758-678X. DOI: 10.1038/nclimate1979.
- [215] T. M. Hamill and S. J. Colucci. "Verification of Eta-RSM short-range ensemble forecasts". In: *Monthly Weather Review* 125.6 (1997), pp. 1312–1327.
- [216] M. J. Hammond, A. S. Chen, S. Djordjevi, D. Butler, and O. Mark. "Urban flood impact assessment: A state-of-the-art review". In: *Urban Water Journal* 12.1 (2015), pp. 14–29.
- [217] J. Handmer, J. Abrahams, R. Betts, and M. Dawson. "Towards a consistent approach to disaster loss assessment across Australia". In: *Australian Journal of Emergency Management* 20 (2005), pp. 10–18. ISSN: 1324-1540.
- [218] A. Hapfelmeier and K. Ulm. "A new variable selection approach using Random Forests". In: *Computational Statistics and Data Analysis* 60.1 (2013), pp. 50–69.
- [219] S. L. Harlan and D. M. Ruddell. "Climate change and health in cities: Impacts of heat and air pollution and potential co-benefits from mitigation and adaptation". In: *Current Opinion in Environmental Sustainability* 3.3 (2011), pp. 126–134.
- [220] F.F. Hattermann, S. Huang, O. Burghoff, W. Willems, H. Österle, M. Büchner, and Z. Kundzewicz. "Modelling flood damages under climate change conditions a case study for Germany". In: *Nat. Hazards Earth Syst. Sci.* 14.12 (Dec. 2, 2014), pp. 3151–3168. ISSN: 1684-9981. DOI: 10.5194/nhess-14-3151-2014.
- [221] F.F. Hattermann, M. Wattenbach, V. Krysanova, and F. Wechsung. "Runoff simulations on the macroscale with the ecohydrological model SWIM in the Elbe catchment - Validation and uncertainty analysis". In: *Hydrological Processes* 19.3 (2005), pp. 693–714.

- [222] F.F. Hattermann, M. Wortmann, S. Liersch, et al. "Simulation of flood hazard and risk in the Danube basin with the Future Danube Model". In: *Climate Services* (Nov. 7, 2018). ISSN: 2405-8807. DOI: 10.1016/j.cliser.2018.07.001.
- [223] M. Helsten and D. Davidge. *Flood Damage Estimation in the Upper Thames River Watershed CFCAS Project: Assessment of Water Resources Risk and Vulnerability to Changing Climatic Conditions*. Project Report 7. 2005.
- [224] P. Heneka and T. Hofherr. "Probabilistic winter storm risk assessment for residential buildings in Germany". In: *Nat Hazards* 56.3 (Mar. 1, 2011), pp. 815–831. ISSN: 0921-030X, 1573-0840. DOI: 10.1007/s11069-010-9593-7.
- [225] P. Heneka, T. Hofherr, B. Ruck, and C. Kottmeier. "Winter storm risk of residential structures - Model development and application to the German state of Baden-Württemberg". In: *Natural Hazards and Earth System Science* 6.5 (2006), pp. 721–733.
- [226] B. Herfort, J. P. de Albuquerque, S. -. Schelhorn, and A. Zipf. "Exploring the geographical relations between social media and flood phenomena to improve situational awareness: A study about the river Elbe flood in June 2013". In: *Lecture Notes in Geoinformation and Cartography*. 2014, pp. 55–71.
- [227] J. Herget, A. Kapala, M. Krell, E. Rustemeier, C. Simmer, and A. Wyss. "The millennium flood of July 1342 revisited". In: *CATENA. Past Hydrological Extreme Events in a Changing Climate* 130 (July 1, 2015), pp. 82–94. ISSN: 0341-8162. DOI: 10.1016/j.catena.2014.12.010.
- [228] H. Hersbach. "Decomposition of the continuous ranked probability score for ensemble prediction systems". In: *Weather and Forecasting* 15.5 (2000), pp. 559–570.
- [229] T. M. Hess and J. Morris. "Estimating the value of flood alleviation on agricultural grassland". In: *Agricultural Water Management* 15.2 (1988), pp. 141–153.
- [230] Y. Hirabayashi, R. Mahendran, S. Koirala, L. Konoshima, Dai Yamazaki, S. Watanabe, H. Kim, and S. Kanae. "Global flood risk under climate change". In: *Nature Clim. Change* 3.9 (Sept. 2013), pp. 816–821. ISSN: 1758-678X. DOI: 10.1038/nclimate1911.
- [231] E. Hirata, M. A. Giannotti, A. P. C. Larocca, and J. A. Quintanilha. "Flooding and inundation collaborative mapping use of the Crowdmap/Ushahidi platform in the city of Sao Paulo, Brazil". In: *Journal of Flood Risk Management* 11 (2018), S98–S109.
- [232] P. Hoeppe. "Trends in weather related disasters Consequences for insurers and society". In: *Weather and Climate Extremes. Observed and Projected (Longer-term) Changes in Weather and Climate Extremes* 11 (Mar. 1, 2016), pp. 70–79. ISSN: 2212-0947. DOI: 10.1016/j.wace.2015.10.002.
- [233] T Hofherr and M Kunz. "Extreme wind climatology of winter storms in Germany". In: *Climate Research* 41 (Mar. 17, 2010), pp. 105–123. ISSN: 0936-577X, 1616-1572. DOI: 10.3354/cr00844.
- [234] M. S. Horritt and P. Bates. "Evaluation of 1D and 2D numerical models for predicting river flood inundation". In: *Journal of Hydrology* 268.1 (Nov. 1, 2002), pp. 87–99. ISSN: 0022-1694. DOI: 10.1016/S0022-1694(02)00121-X.

- [235] J. R. M. Hosking and J. R. Wallis. *Regional Frequency Analysis: An Approach Based on L-Moments*. Cambridge, UK: Cambridge University Press, 1997. 224 pp.
- [236] J. Howe. "The Rise of Crowdsourcing". In: *Wired* (June 1, 2006). ISSN: 1059-1028.
- [237] B.F.F. Huang and P.C. Boutros. "The parameter sensitivity of random forests". In: *BMC Bioinformatics* 17.1 (Dec. 2016). ISSN: 1471-2105. DOI: 10.1186/s12859-016-1228-x.
- [238] P. Hudson, M. Pham, and P. Bubeck. "An evaluation and monetary assessment of the impact of flooding on subjective well-being across genders in Vietnam". In: *Climate and Development* (Feb. 20, 2019), pp. 1–15. ISSN: 1756-5529, 1756-5537. DOI: 10.1080/17565529.2019.1579698.
- [239] Y. Hundecha and A. Bárdossy. "Modeling of the effect of land use changes on the runoff generation of a river basin through parameter regionalization of a watershed model". In: *Journal of Hydrology* 292.1 (June 15, 2004), pp. 281–295. ISSN: 0022-1694. DOI: 10.1016/j.jhydrol.2004.01.002.
- [240] Y. Hundecha and B. Merz. "Exploring the relationship between changes in climate and floods using a model-based analysis". In: *Water Resour. Res.* 48.4 (Apr. 1, 2012), W04512. ISSN: 1944-7973. DOI: 10.1029/2011WR010527.
- [241] Y. Hundecha, M. Pahlow, and A. Schumann. "Modeling of daily precipitation at multiple locations using a mixture of distributions to characterize the extremes". In: *Water Resources Research* 45.12 (2009), n/a–n/a. ISSN: 1944-7973. DOI: 10.1029/2008WR007453.
- [242] M. Huttenlau, J. Stötter, and H. Stiefelmeyer. "Risk-based damage potential and loss estimation of extreme flooding scenarios in the Austrian Federal Province of Tyrol". In: *Natural Hazards and Earth System Science* 10.12 (2010), pp. 2451–2473.
- [243] J. Huza, A. J. Teuling, I. Braud, J. Grazioli, L. A. Melsen, G. Nord, T. H. Raupach, and R. Uijlenhoet. "Precipitation, soil moisture and runoff variability in a small river catchment (Arde'che, France) during HyMeX Special Observation Period 1". In: *Journal of Hydrology* 516 (2014), pp. 330–342.
- [244] Hydrotec. *Hochwasser-Aktionsplan Lippe - Grundlagen, Überflutungsgebiete, Schadenspotenzial, Defizite und MaSSnahmen*. Aachen, 2002.
- [245] Hydrotec. *Hochwasseraktionsplan Angerbach [Flood action plan for the river Angerbach]*. Aachen: Hydrotec, 2001.
- [246] ICPR. *Atlas of Flood Danger and Potential Damage Due to Extreme Floods of the Rhine, Rhine-Atlas*. Koblenz: International Commission for the Protection of the Rhine, 2001.
- [247] IKSE. *Aktionsplan Hochwasserschutz Elbe*. Internationale Kommission zum Schutz der Elbe, 2003.
- [248] IKSE. *Die Elbe und ihre Einzugsgebiete*. Magdeburg: International Commission for the Protection of the Elbe, 2005.
- [249] IKSE. *Dokumentation des Hochwassers vom August 2002 im Einzugsgebiet der Elbe*. Magdeburg: International Commission for the Protection of the Elbe, 2004.

- [250] M. Imran, C. Castillo, J. Lucas, P. Meier, and S. Vieweg. "AIDR: Artificial intelligence for disaster response". In: *WWW 2014 Companion - Proceedings of the 23rd International Conference on World Wide Web*. 2014, pp. 159–162.
- [251] M. Imran, S. Elbassuoni, C. Castillo, F. Diaz, and P. Meier. "Practical extraction of disaster-relevant information from social media". In: *WWW 2013 Companion - Proceedings of the 22nd International Conference on World Wide Web*. 2013, pp. 1021–1024.
- [252] INFAS GEOdaten GmbH. *Das DataWherehouse*. Bonn: INFAS GEOdaten GmbH, 2001.
- [253] INFAS GEOdaten GmbH. *Das DataWherehouse*. Bonn: INFAS GEOdaten GmbH, 2005.
- [254] INFAS GEOdaten GmbH. *Das DataWherehouse*. Bonn: INFAS GEOdaten GmbH, 2009.
- [255] IPCC. *Managing the risks of extreme events and disasters to advance climate change adaptation*. New York, 2012, p. 582.
- [256] IRDR. *Forensic investigations of Disasters: The FORIN project*. Beijing: Integrated Research on Disaster Risk, 2011.
- [257] IRDR. *Guidelines on Measuring Losses from Disasters: Human and economic Impact Indicators*. 2. Beijing, China: Integrated Research on Disaster Risk, 2015, p. 28.
- [258] IRDR. *The FORIN Project: Understanding the Causes of Disasters*. Beijing: Integrated Research on Disaster Risk, 2015, p. 16.
- [259] A. Irwin. "No PhDs needed: how citizen science is transforming research". In: *Nature* 562 (Oct. 23, 2018), p. 480. DOI: 10.1038/d41586-018-07106-5.
- [260] J. Jacobeit, A. Philipp, and M. Nonnenmacher. "Atmospheric circulation dynamics linked with prominent discharge events in Central Europe". In: *Hydrological Sciences Journal* 51.5 (2006), pp. 946–965.
- [261] J. R. Jensen and D. C. Cowen. "Remote sensing of urban/suburban infrastructure and socio-economic attributes". In: *Photogrammetric Engineering and Remote Sensing* 65.5 (1999), pp. 611–622.
- [262] B. Jongman, H. Kreibich, H. Apel, et al. "Comparative flood damage model assessment: towards a European approach". In: *Nat. Hazards Earth Syst. Sci.* 12.12 (2012), pp. 3733–3752. ISSN: 1684-9981. DOI: 10.5194/nhess-12-3733-2012.
- [263] B. Jongman, H.C. Winsemius, J.C.J.H. Aerts, E.C. Perez, M.K. van Aalst, W. Kron, and P. Ward. "Declining vulnerability to river floods and the global benefits of adaptation". In: *PNAS* 112.18 (May 5, 2015), E2271–E2280. ISSN: 0027-8424, 1091-6490. DOI: 10.1073/pnas.1414439112.
- [264] K. Joseph, P. M. Landwehr, and K. M. Carley. "An approach to selecting keywords to track on twitter during a disaster". In: *ISCRAM 2014 Conference Proceedings - 11th International Conference on Information Systems for Crisis Response and Management*. 2014, pp. 672–676.

- [265] J.-L. Kang, M.-D. Su, and L.-F. Chang. "Loss functions and framework for regional flood damage estimation in residential area". In: *Journal of Marine Science and Technology* 13.3 (2005), pp. 193–199. ISSN: 1023-2796.
- [266] S. Kaplan and B.J. Garrick. "On The Quantitative Definition of Risk". In: *Risk Analysis* 1.1 (1981), pp. 11–27. ISSN: 1539-6924. DOI: 10.1111/j.1539-6924.1981.tb01350.x.
- [267] M. S. Kappes, M. Keiler, K. von Elverfeldt, and T. Glade. "Challenges of analyzing multi-hazard risk: A review". In: *Natural Hazards* 64.2 (2012), pp. 1925–1958.
- [268] M. Kasperski. "A new wind zone map of Germany". In: *Journal of Wind Engineering and Industrial Aerodynamics* 90.11 (2002), pp. 1271–1287.
- [269] R. W. Kates. "Industrial Flood Losses: Damage Estimation in the Lehigh Valley. Research Paper No. 98". In: *Industrial Flood Losses: Damage Estimation in the Lehigh Valley* (1965).
- [270] C. Keef, J.A. Tawn, and R Lamb. "Estimating the probability of widespread flood events". In: *Environmetrics* 24.1 (Feb. 1, 2013), pp. 13–21. ISSN: 1099-095X. DOI: 10.1002/env.2190.
- [271] S. Keller and A. Atzl. "Mapping Natural Hazard Impacts on Road Infrastructure The Extreme Precipitation in Baden-Württemberg, Germany, June 2013". In: *International Journal of Disaster Risk Science* 5.3 (2014), pp. 227–241.
- [272] I. Kelman. "Physical flood vulnerability of residential properties in coastal, eastern England". In: *Physical Flood Vulnerability of Residential Properties in Coastal, Eastern England* (2002).
- [273] I. Kelman and R. Spence. "An overview of flood actions on buildings". In: *Engineering Geology* 73.3 (June 2004), pp. 297–309. ISSN: 0013-7952. DOI: 10.1016/j.enggeo.2004.01.010.
- [274] S. Kienzler, I. Pech, H. Kreibich, M. Müller, and A. Thielen. "After the extreme flood in 2002: changes in preparedness, response and recovery of flood-affected residents in Germany between 2005 and 2011". In: *Nat. Hazards Earth Syst. Sci.* 15.3 (2015), pp. 505–526. ISSN: 1684-9981. DOI: 10.5194/nhess-15-505-2015.
- [275] Y.-O. Kim, S.B. Seo, and O.-J. Jang. "Flood risk assessment using regional regression analysis". In: *Nat Hazards* 63.2 (June 4, 2012), pp. 1203–1217. ISSN: 0921-030X, 1573-0840. DOI: 10.1007/s11069-012-0221-6.
- [276] J. Kind. *Maatschappelijke kosten-batenanalyse Waterveiligheid 21e eeuw*. 1204144-006-ZWS-0012. Delft, Netherlands: Deltares, 2011.
- [277] J. Kind, W.J.W. Botzen, and J. Aerts. "Accounting for risk aversion, income distribution and social welfare in cost-benefit analysis for flood risk management". In: *Wiley Interdisciplinary Reviews: Climate Change* 8.2 (2017), e446. ISSN: 1757-7799. DOI: 10.1002/wcc.446.
- [278] S. Klaus, H. Kreibich, B. Merz, B. Kuhlmann, and K. Schröter. "Large-scale, seasonal flood risk analysis for agricultural crops in Germany". In: *Environmental Earth Sciences* 75.18 (Sept. 2016). ISSN: 1866-6280, 1866-6299. DOI: 10.1007/s12665-016-6096-1.

- [279] M. Klawa and U. Ulbrich. "A model for the estimation of storm losses and the identification of severe winter storms in Germany". In: *Natural Hazards and Earth System Science* 3.6 (2003), pp. 725–732.
- [280] L. Kleist, A. Thieken, P. Köhler, M. Müller, I. Seifert, D. Borst, and U. Werner. "Estimation of the regional stock of residential buildings as a basis for a comparative risk assessment in Germany". In: *Nat. Hazards Earth Syst. Sci.* 6.4 (June 15, 2006), pp. 541–552. ISSN: 1684-9981. DOI: 10.5194/nhess-6-541-2006.
- [281] V. Klemes. "Operational testing of hydrological simulation models". In: *Hydrological Sciences Journal -Journal des Sciences Hydroliques* 31.1 (1986). Article A3015 English Times Cited:92 Cited References Count:10, pp. 13–24.
- [282] V. Klemes. "Probability of extreme hydrometeorological events - a different approach". In: *Extreme Hydrological Events: Precipitation, Floods and Droughts*. Yokohama Symposium. Vol. 213. Yokohama: IAHS, 1993, pp. 167–176.
- [283] V. Klemes. "Risk Analysis: The unbearable cleverness of bluffing". In: *Common Sense and other heresis - Selected Papers on Hydrology and Water resources engineering*. Ed. by E. D Sellars. Cambridge, Ontario, Canada: Canadian Water Resources Association, 2000, pp. 197–209.
- [284] F. Klijn, P. J. A. Baan, K. M. De Bruijn, and J. Kwadijk. "Overstromingsrisico's in Nederland in een veranderend klimaat-Verwachtingen, schattingen en berekeningen voor het project Nederland Later". In: *Overstromingsrisico's in Nederland in Een Veranderend Klimaat* (2007).
- [285] F. Klijn, H. Kreibich, H. de Moel, and E. Penning-Rowsell. "Adaptive flood risk management planning based on a comprehensive flood risk conceptualisation". In: *Mitig Adapt Strateg Glob Change* 20.6 (Aug. 1, 2015), pp. 845–864. ISSN: 1573-1596. DOI: 10.1007/s11027-015-9638-z.
- [286] R. Knutti, R. Furrer, C. Tebaldi, J. Cermak, and G. A. Meehl. "Challenges in combining projections from multiple climate models". In: *Journal of Climate* 23.10 (2010), pp. 2739–2758.
- [287] M. A. Kohler and R. K. Linsley. *Predicting the runoff from storm rainfall*. U.S. Weather Bureau, 1951.
- [288] M. Kok, H. J. Huizinga, A. C. W. M. Vrouwenvelder, and A. Barendregt. "Standaardmethode 2004Schade en Slachtoffers als gevolg van overstromingen". In: *Standaardmethode2004-Schade en Slachtoffers Als Gevolg Van Overstromingen* (2005).
- [289] E. Koks. "Moving flood risk modelling forwards". In: *Nature Climate Change* 8.7 (July 2018), pp. 561–562. ISSN: 1758-6798. DOI: 10.1038/s41558-018-0185-y.
- [290] H. Kreibich, J. C. J. M. van den Bergh, L.M. Bouwer, et al. "Costing natural hazards". In: *Nature Clim. Change* 4.5 (2014), pp. 303–306. ISSN: 1758-678X. DOI: 10.1038/nclimate2182.
- [291] H. Kreibich, A. Botto, B. Merz, and K. Schröter. "Probabilistic, Multivariable Flood Loss Modeling on the Mesoscale with BT-FLEMO". In: *Risk Analysis* 37.4 (2017), pp. 774–787. ISSN: 1539-6924. DOI: 10.1111/risa.12650.

- [292] H. Kreibich, P. Bubeck, M. Kunz, et al. "A review of multiple natural hazards and risks in Germany". In: *Nat Hazards* (June 6, 2014), pp. 1–26. ISSN: 0921-030X, 1573-0840. DOI: 10.1007/s11069-014-1265-6.
- [293] H. Kreibich, P. Bubeck, M. Van Vliet, and H. De Moel. "A review of damage-reducing measures to manage fluvial flood risks in a changing climate". In: *Mitigation and Adaptation Strategies for Global Change* 20.6 (Aug. 2015), pp. 967–989. ISSN: 1381-2386, 1573-1596. DOI: 10.1007/s11027-014-9629-5.
- [294] H. Kreibich, S. Christenberger, and R. Schwarze. "Economic motivation of households to undertake private precautionary measures against floods". In: *Nat. Hazards Earth Syst. Sci.* 11.2 (Feb. 3, 2011), pp. 309–321. ISSN: 1684-9981. DOI: 10.5194/nhess-11-309-2011.
- [295] H. Kreibich, G. Di Baldassarre, S. Vorogushyn, et al. "Adaptation to flood risk - results of international paired flood event studies: Adaptation to flood risk". In: *Earth's Future* (July 26, 2017). ISSN: 23284277. DOI: 10.1002/2017EF000606.
- [296] H. Kreibich and B. Dimitrova. "Assessment of damages caused by different flood types". In: *WIT Transactions on Ecology and the Environment* 133 (2010), pp. 3–11.
- [297] H. Kreibich, S. Meyer, and B. Diekkrüger. "Further development of FLEMOps for the modelling of damage to residential buildings due to high groundwater levels". In: *Hydrologie und Wasserbewirtschaftung* 55.6 (2011), pp. 300–309.
- [298] H. Kreibich, M. Müller, A. Thielen, and B. Merz. "Flood precaution of companies and their ability to cope with the flood in August 2002 in Saxony, Germany". In: *Water Resources Research* 43.3 (2007). ISSN: 00431397. DOI: 10.1029/2005WR004691.
- [299] H. Kreibich, K. Piroth, I. Seifert, H. Maiwald, U. Kunert, J. Schwarz, B. Merz, and A. Thielen. "Is flow velocity a significant parameter in flood damage modelling?" In: *Nat. Hazards Earth Syst. Sci.* 9.5 (2009), pp. 1679–1692. ISSN: 1684-9981. DOI: 10.5194/nhess-9-1679-2009.
- [300] H. Kreibich, I. Seifert, B. Merz, and A. Thielen. "Development of FLEMOcs - a new model for the estimation of flood losses in the commercial sector". In: *Hydrological Sciences Journal* 55.8 (2010), pp. 1302–1314.
- [301] H. Kreibich and A. Thielen. "Assessment of damage caused by high groundwater inundation". In: *Water Resources Research* 44.9 (2008), n/a–n/a. ISSN: 1944-7973. DOI: 10.1029/2007WR006621.
- [302] H. Kreibich and A. Thielen. "Coping with floods in the city of Dresden, Germany". In: *Nat Hazards* 51.3 (Dec. 1, 2009), pp. 423–436. ISSN: 0921-030X, 1573-0840. DOI: 10.1007/s11069-007-9200-8.
- [303] H. Kreibich, A. Thielen, S. Haubrock, and K. Schröter. "HOWAS21 the German flood damage database. in: flood damage survey and assessment: new insights from research and practice". In: *AGU, Geophysical Monograph* 228 5 (2017), pp. 65–78.
- [304] H. Kreibich, A. Thielen, Th Petrow, M. Müller, and B. Merz. "Flood loss reduction of private households due to building precautionary measures - Lessons learned from the Elbe flood in August 2002". In: *Natural Hazards and Earth System Science* 5.1 (2005), pp. 117–126.

- [305] A. Kron. "Flood damage estimation and flood risk mapping". In: *Advances in Urban Flood Management* (2007), pp. 213–235.
- [306] W. Kron. "Flood Risk = Hazard Values Vulnerability". In: *Water International* 30.1 (2005), pp. 58–68. ISSN: 0250-8060. DOI: 10.1080/02508060508691837.
- [307] W. Kron. "Zunehmende Überschwemmungsschäden: Eine Gefahr für die Versicherungswirtschaft?" In: ATV-DVWK Bundestagung. Würzburg: DCM, Meckenheim, 2004, pp. 47–63.
- [308] W. Kron, M. Steuer, P. Löw, and A. Wirtz. "How to deal properly with a natural catastrophe database - Analysis of flood losses". In: *Natural Hazards and Earth System Science* 12.3 (2012), pp. 535–550.
- [309] J. p. Kropp, A. Block, F. Reusswig, K. Zickfeld, and H. J. Schellnhuber. "Semiquantitative Assessment of Regional Climate Vulnerability: The North-Rhine Westphalia Study". In: *Climatic Change* 76.3 (June 2006), pp. 265–290. ISSN: 0165-0009, 1573-1480. DOI: 10.1007/s10584-005-9037-7.
- [310] V. Krysanova, D. -. Müller-Wohlfeil, and A. Becker. "Development and test of a spatially distributed hydrological/water quality model for mesoscale watersheds". In: *Ecological Modelling* 106.2 (1998), pp. 261–289.
- [311] R. Krzysztofowicz and D. R. Davis. "Category unit loss functions for flood forecast-response system evaluation". In: *Water Resources Research* 19.6 (1983), pp. 1476–1480.
- [312] KTBL. *Standdeckungsbeiträge für Feldfrüchte in Deutschland*. KTBL-SDB-Application. 2015. URL: <https://daten.ktbl.de/sdb/source.do> (visited on 02/02/2015).
- [313] C. Kuhlicke, C. Begg, M. Beyer, I. Callsen, A. Kunath, and N. Löster. *Hochwasservorsorge und Schutzgerechtigkeit: Erste Ergebnisse Einer Haushaltsbefragung Zur Hochwassersituation in Sachsen*. 15/2014. Leipzig: UFZ, 2014, p. 39.
- [314] B. Kuhlmann. "Methods for the evaluation of direct and indirect flood losses (MEDIS): Methods for the evaluation of direct and indirect flood losses in agriculture and forestry". PhD thesis. Giessen, Germany: Justus Liebig University, 2007.
- [315] B. Kuhlmann. "Schäden in der Landwirtschaft (Damages in Agriculture): In: Thielen AH, Seifert". In: *Hochwasserschäden Erfassung, Abschätzung und Vermeidung*. Ed. by I. Thielen A. and Seifert and B. Merz. 2010, p. I.
- [316] F. Kunde, C. Nagel, J. Herrerruela, L. Ross, and T. H. Kolbe. "3D-Stadtmodelle in PostGIS mit der 3D City Database". In: *Tagungsband der FOSSGIS-Konferenz* (2013).
- [317] M. Kunz. "Characteristics of Large-Scale Orographic Precipitation in a Linear Perspective". In: *J. Hydrometeor* 12.1 (2011), pp. 27–44. ISSN: 1525-755X. DOI: 10.1175/2010JHM1231.1.
- [318] M. Kunz, B. Mühr, T. Kunz-Plapp, et al. "Investigation of superstorm Sandy 2012 in a multi-disciplinary approach". In: *Nat. Hazards Earth Syst. Sci.* 13.10 (2013), pp. 2579–2598. ISSN: 1684-9981. DOI: 10.5194/nhess-13-2579-2013.
- [319] M. Kunz and M. Puskeiler. "High-resolution assessment of the hail hazard over complex terrain from radar and insurance data". In: *Meteorologische Zeitschrift* 19.5 (Oct. 1, 2010), pp. 427–439. ISSN: 0941-2948. DOI: 10.1127/0941-2948/2010/0452.

- [320] W. Kuttler. "Climate change in urban areas. Part 2, Measures". In: *Environmental Sciences Europe* 23.1 (2011), p. 21. ISSN: 2190-4715. DOI: 10.1186/2190-4715-23-21.
- [321] P. Lagadec. "Understanding the French 2003 Heat Wave Experience: Beyond the heat, a Multi-Layered Challenge". In: *Journal of Contingencies and Crisis Management* 12.4 (Dec. 2004), pp. 160–169. ISSN: 0966-0879, 1468-5973. DOI: 10.1111/j.0966-0879.2004.00446.x.
- [322] R. Lamb, C. Keef, J. Tawn, S. Laeger, I. Meadowcroft, S. Surendran, P. Dunning, and C. Batstone. "A new method to assess the risk of local and widespread flooding on rivers and coasts". In: *Journal of Flood Risk Management* 3.4 (2010), pp. 323–336.
- [323] Landtag Rheinland-Pfalz. *Antwort des Ministeriums der Finanzen auf die Große Anfrage der Fraktion der CDU Hilfe bei Hochwasser- und Elementarschäden*. Drucksache 14/4195. Mainz: Landtag Rheinland-Pfalz, 2005.
- [324] D. Lang, S. Molina-Palacios, C. Lindholm, and S. Balan. "Deterministic earthquake damage and loss assessment for the city of Bucharest, Romania". In: *Journal of Seismology* 16.1 (Jan. 2012), pp. 67–88. ISSN: 1383-4649, 1573-157X. DOI: 10.1007/s10950-011-9250-y.
- [325] S. A. Lecce. "Seasonality of flooding in North Carolina". In: *Southeastern Geographer* 40.2 (2000), pp. 168–175.
- [326] R. Leichenko. "Climate change and urban resilience". In: *Current Opinion in Environmental Sustainability* 3.3 (May 1, 2011), pp. 164–168. ISSN: 1877-3435. DOI: 10.1016/j.cosust.2010.12.014.
- [327] A. Lekuthai and S. Vongvisessomjai. "Intangible flood damage quantification". In: *Water Resources Management* 15.5 (2001), pp. 343–362.
- [328] M. Leutbecher and T. N. Palmer. "Ensemble forecasting". In: *Journal of Computational Physics* 227.7 (2008), pp. 3515–3539.
- [329] LfU. *August-Hochwasser 2005 in Südbayern*. Augsburg: Bayerisches Landesamt für Umwelt, 2006, p. 49.
- [330] LfU. *Junihochwasser 2013 Wasserwirtschaftlicher Bericht*. Augsburg: Bayerisches Landesamt für Umwelt, Aug. 2013, p. 97.
- [331] LFULG. *Gewässerkundlicher Monatsbericht mit vorläufiger Auswertung des Hochwassers Juni 2013*. Dresden: Sächsisches Landesamt für Umwelt und Geologie, June 2013.
- [332] J. Li and A.D. Heap. "Spatial interpolation methods applied in the environmental sciences: A review". In: *Environmental Modelling & Software* 53 (2014), pp. 173–189. ISSN: 1364-8152. DOI: 10.1016/j.envsoft.2013.12.008.
- [333] L. Li, J. Wang, H. Leung, and C. Jiang. "Assessment of Catastrophic Risk Using Bayesian Network Constructed from Domain Knowledge and Spatial Data". In: *Risk Anal.* 30.7 (July 2010). WOS:000279939700016, pp. 1157–1175. ISSN: 0272-4332. DOI: 10.1111/j.1539-6924.2010.01429.x.
- [334] A. Liaw and M. Wiener. "Classification and Regression by randomForest". In: *R News* 2.3 (2002), pp. 18–22.

- [335] A.H. te Linde, P. Bubeck, J. E. C. Dekkers, H. de Moel, and J. Aerts. "Future flood risk estimates along the river Rhine". In: *Natural Hazards and Earth System Science* 11.2 (Feb. 15, 2011), pp. 459–473. ISSN: 1684-9981. DOI: 10.5194/nhess-11-459-2011.
- [336] M. Lopeman, G. Deodatis, and G. Franco. "A critical comparison of windstorm vulnerability models with application to extra-tropical cyclones in Northern Europe". In: *Safety, Reliability, Risk and Life-Cycle Performance of Structures and Infrastructures - Proceedings of the 11th International Conference on Structural Safety and Reliability, ICOSSAR 2013*. 2013, pp. 1311–1318.
- [337] N. Luger, Z. Kundzewicz, E. Genovese, S. Hochrainer, and M. Radziejewski. "River flood risk and adaptation in Europe assessment of the present status". In: *Mitigation and Adaptation Strategies for Global Change* 15.7 (2010), pp. 621–639. ISSN: 1381-2386. DOI: 10.1007/s11027-009-9211-8.
- [338] F. Luino, C. Cirio, M. Biddoccu, A. Agangi, W. Giulietto, F. Godone, and G. Nigrelli. "Application of a model to the evaluation of flood damage". In: *GeoInformatica* 13.3 (2009), pp. 339–353. ISSN: 1384-6175. DOI: 10.1007/s10707-008-0070-3.
- [339] A. M. MacEachren, A. Jaiswal, A. C. Robinson, S. Pezanowski, A. Savelyev, P. Mitra, X. Zhang, and J. Blanford. "SensePlace2: GeoTwitter analytics support for situational awareness". In: *VAST 2011 - IEEE Conference on Visual Analytics Science and Technology 2011, Proceedings*. 2011, pp. 181–190.
- [340] A. Malcharek. *Gezeiten und Wellen - Die Hydromechanik der Küstengewässer*. Wiesbaden, Germany: Vieweg-Teubner, 2010.
- [341] G. Mandlbürger, C. Hauer, B. Höfle, H. Habersack, and N. Pfeifer. "Optimisation of LiDAR derived terrain models for river flow modelling". In: *Hydrol. Earth Syst. Sci.* 13.8 (Aug. 14, 2009), pp. 1453–1466. ISSN: 1607-7938. DOI: 10.5194/hess-13-1453-2009.
- [342] A.D. Martin, K.M. Quinn, and J.H. Park. "MCMCpack: Markov Chain Monte Carlo in R". In: *Journal of Statistical Software* 42.9 (2011), p. 22.
- [343] W. Marzocchi, A. Garcia-Aristizabal, P. Gasparini, M.L. Mastellone, and A. Di Ruocco. "Basic principles of multi-risk assessment: a case study in Italy". In: *Natural Hazards* 62.2 (June 2012), pp. 551–573. ISSN: 0921-030X, 1573-0840. DOI: 10.1007/s11069-012-0092-x.
- [344] W. Marzocchi, M. Taroni, and J. Selva. "Accounting for epistemic uncertainty in PSHA: Logic tree and ensemble modeling". In: *Bulletin of the Seismological Society of America* 105.4 (2015), pp. 2151–2159.
- [345] D. C. Mason, G. J. -P. Schumann, J. C. Neal, J. Garcia-Pintado, and P. Bates. "Automatic near real-time selection of flood water levels from high resolution Synthetic Aperture Radar images for assimilation into hydraulic models: A case study". In: *Remote Sensing of Environment* 124 (Sept. 2012), pp. 705–716. ISSN: 0034-4257. DOI: 10.1016/j.rse.2012.06.017.

- [346] P. Matgen, G. Schumann, J.-B. Henry, L. Hoffmann, and L. Pfister. "Integration of SAR-derived river inundation areas, high-precision topographic data and a river flow model toward near real-time flood management". In: *International Journal of Applied Earth Observation and Geoinformation* 9.3 (Aug. 2007), pp. 247–263. ISSN: 0303-2434. DOI: 10.1016/j.jag.2006.03.003.
- [347] R. Mechler and L.M. Bouwer. "Understanding trends and projections of disaster losses and climate change: is vulnerability the missing link?" In: *Climatic Change* 133.1 (Nov. 1, 2015), pp. 23–35. ISSN: 0165-0009, 1573-1480. DOI: 10.1007/s10584-014-1141-0.
- [348] G. A. Meehl and C. Tebaldi. "More Intense, More Frequent, and Longer Lasting Heat Waves in the 21st Century". In: *Science* 305.5686 (Aug. 13, 2004), pp. 994–997. ISSN: 0036-8075, 1095-9203. DOI: 10.1126/science.1098704.
- [349] B. Menne and V. Murray. *Floods in the WHO European Region: Health Effects and Their Prevention*. Copenhagen, Denmark: WHO, 2013, p. 116.
- [350] M. J. P. Mens and F. Klijn. "The added value of system robustness analysis for flood risk management illustrated by a case on the IJssel River". In: *Nat. Hazards Earth Syst. Sci.* 15.2 (Feb. 4, 2015), pp. 213–223. ISSN: 1684-9981. DOI: 10.5194/nhess-15-213-2015.
- [351] M. J. P. Mens, F. Klijn, K.M. de Bruijn, and E. van Beek. "The meaning of system robustness for flood risk management". In: *Environmental Science & Policy* 14.8 (Dec. 1, 2011), pp. 1121–1131. ISSN: 1462-9011. DOI: 10.1016/j.envsci.2011.08.003.
- [352] B. Merz. *Hochwasserrisiken - Grenzen und Risiken der Risikoabschätzung*. Stuttgart: Schweizerbart, 2006. 334 pp. ISBN: 3-510-65220-7.
- [353] B. Merz, J. Aerts, K. Arnbjerg-Nielsen, et al. "Floods and climate: emerging perspectives for flood risk assessment and management". In: *Nat. Hazards Earth Syst. Sci.* 14.7 (July 30, 2014), pp. 1921–1942. ISSN: 1684-9981. DOI: 10.5194/nhess-14-1921-2014.
- [354] B. Merz, F. Elmer, M. Kunz, B. Mühr, K. Schröter, and S. Uhlemann-Elmer. "The extreme flood in June 2013 in Germany". In: *La Houille Blanche* 1 (Feb. 2014), pp. 5–10. ISSN: 0018-6368. DOI: 10.1051/lhb/2014001.
- [355] B. Merz, F. Elmer, and A. Thielen. "Significance of "high probability/low damage" versus "low probability/high damage" flood events". In: *Nat. Hazards Earth Syst. Sci.* 9.3 (June 30, 2009), pp. 1033–1046. ISSN: 1684-9981. DOI: 10.5194/nhess-9-1033-2009.
- [356] B. Merz and R. Emmermann. *Zum Umgang mit Naturgefahren in Deutschland: Vom Reagieren zum Risikomanagement*. Dec. 2006. DOI: info:doi/10.14512/gaia.15.4.9. URL: <https://www.ingentaconnect.com/contentone/oekom/gaia/2006/00000015/00000004/art00009> (visited on 12/02/2018).
- [357] B. Merz, J. Friedrich, M. Disse, J. Schwarz, J.G. Goldammer, and J. Wächter. "Possibilities and Limitations of Interdisciplinary, User-oriented Research: Experiences from the German Research Network Natural Disasters". In: *Nat Hazards* 38.1 (May 1, 2006), pp. 3–20. ISSN: 1573-0840. DOI: 10.1007/s11069-005-8597-1.

- [358] B. Merz, J. Hall, M. Disse, and A. Schumann. "Fluvial flood risk management in a changing world". In: *Nat. Hazards Earth Syst. Sci.* 10.3 (2010), pp. 509–527. ISSN: 1561-8633.
- [359] B. Merz, H. Kreibich, and U. Lall. "Multi-variate flood damage assessment: a tree-based data-mining approach". In: *Nat. Hazards Earth Syst. Sci.* 13.1 (Jan. 11, 2013), pp. 53–64. ISSN: 1684-9981. DOI: 10.5194/nhess-13-53-2013.
- [360] B. Merz, H. Kreibich, R. Schwarze, and A. Thielen. "Review article "Assessment of economic flood damage"". In: *Nat. Hazards Earth Syst. Sci.* 10.8 (2010), pp. 1697–1724. ISSN: 1684-9981. DOI: 10.5194/nhess-10-1697-2010.
- [361] B. Merz, H. Kreibich, A. Thielen, and R. Schmidtke. "Estimation uncertainty of direct monetary flood damage to buildings". In: *Nat. Hazards Earth Syst. Sci.* 4.1 (2004), pp. 153–163. ISSN: 1684-9981. DOI: 10.5194/nhess-4-153-2004.
- [362] B. Merz, Z. W. Kundzewicz, J.M. Delgado, Y. Huntecha, and H. Kreibich. "Detection and Attribution of Changes in Flood Hazard and Risk". In: *Changes in Flood Risk in Europe*. Ed. by Z. W. Kundzewicz. Vol. 10. Special Publication. Wallingford, UK: IAHS Press, 2012.
- [363] B. Merz and E. J. Plate. "An analysis of the effects of spatial variability of soil and soil moisture on runoff". In: *Water Resources Research* 33.12 (1997), pp. 2909–2922.
- [364] B. Merz and A. Thielen. "Flood risk analysis: Concepts and challenges". In: *Osterreichische Wasser- und Abfallwirtschaft* 56.3 (2004), pp. 27–34.
- [365] B. Merz and A. Thielen. "Flood risk curves and uncertainty bounds". In: *Natural Hazards* 51.3 (2009), pp. 437–458. ISSN: 0921-030X. DOI: 10.1007/s11069-009-9452-6.
- [366] B. Merz and A. Thielen. "separating natural and epistemic uncertainty in flood frequency analysis". In: *Journal Of Hydrology* 309 (2005), pp. 114–132.
- [367] B. Merz, S. Vorogushyn, U. Lall, A. Viglione, and G. Blöschl. "Charting unknown waters On the role of surprise in flood risk assessment and management". In: *Water Resour. Res.* (Aug. 1, 2015), n/a–n/a. ISSN: 1944-7973. DOI: 10.1002/2015WR017464.
- [368] R. Merz and G. Blöschl. "A process typology of regional floods". In: *Water Resour. Res.* 39.12 (Dec. 5, 2003), p. 1340. ISSN: 0043-1397. DOI: 10.1029/2002WR001952.
- [369] R. Merz and G. Blöschl. "A regional analysis of event runoff coefficients with respect to climate and catchment characteristics in Austria". In: *Water Resources Research* 45.1 (2009).
- [370] R. Merz and G. Blöschl. "Flood frequency hydrology: 2. Combining data evidence". In: *Water Resources Research* 44.8 (2008), n/a–n/a. ISSN: 1944-7973. DOI: 10.1029/2007WR006745.
- [371] R. Merz and G. Blöschl. "Process controls on the statistical flood moments - A data based analysis". In: *Hydrological Processes* 23.5 (2009), pp. 675–696.
- [372] R. Merz, G. Blöschl, and G. Humer. "National flood discharge mapping in Austria". In: *Natural Hazards* 46.1 (2008), pp. 53–72.

- [373] F. Messner, V. Meyer, J. Schanze, E. Zeman, and J. Marsalek. "Flood damage, vulnerability and risk perception-challenges for flood damage research". In: *Flood Risk Management: Hazards, Vulnerability and Mitigation Measures*. Dodrecht: Springer, 2006, pp. 149–167.
- [374] F. Messner, E. Penning-Rowsell, C. Green, V. Meyer, S. Tunstall, and A. van der Veen. *Evaluating Flood Damages: guidance and recommendations on principles and methods*. D9.1. UFZ, 2007.
- [375] A.D. Metin, N.V. Dung, K. Schröter, B. Guse, H. Apel, H. Kreibich, S. Vorogushyn, and B. Merz. "How do changes along the risk chain affect flood risk?". In: *Natural Hazards and Earth System Sciences* 18.11 (Nov. 19, 2018), pp. 3089–3108. ISSN: 1561-8633. DOI: <https://doi.org/10.5194/nhess-18-3089-2018>.
- [376] V. Meyer, N. Becker, V. Markantonis, et al. "Review article: Assessing the costs of natural hazards-state of the art and knowledge gaps". In: *Natural Hazards and Earth System Science* 13.5 (2013), pp. 1351–1373.
- [377] V. Meyer and F. Messner. "National flood damage evaluation methods, a review of applied methods in England, the Netherlands, the Czech Republic and Germany UFZ Discussion Papers 21/2005 Department of Economics, Leipzig". In: *National Flood Damage Evaluation Methods - A Review of Applied Methods in England, the Netherlands, the Czech Republic and Germany* (2005).
- [378] E. Michel-Kerjan and H. Kunreuther. "Redesigning Flood Insurance". In: *Science* 333.6041 (July 22, 2011), pp. 408–409. ISSN: 0036-8075, 1095-9203. DOI: 10.1126/science.1202616.
- [379] J. Minet, E. Laloy, S. Lambot, and M. Vanclooster. "Effect of high-resolution spatial soil moisture variability on simulated runoff response using a distributed hydrologic model". In: *Hydrology and Earth System Sciences* 15.4 (2011), pp. 1323–1328.
- [380] H. de Moel and J. Aerts. "Effect of uncertainty in land use, damage models and inundation depth on flood damage estimates". In: *Nat Hazards* 58.1 (July 1, 2011), pp. 407–425. ISSN: 0921-030X, 1573-0840. DOI: 10.1007/s11069-010-9675-6.
- [381] H. de Moel, B. Jongman, H. Kreibich, B. Merz, E. Penning-Rowsell, and P. Ward. "Flood risk assessments at different spatial scales". In: *Mitig Adapt Strateg Glob Change* (May 22, 2015), pp. 1–26. ISSN: 1381-2386, 1573-1596. DOI: 10.1007/s11027-015-9654-z.
- [382] R. Morbidelli, C. Saltalippi, A. Flammini, C. Corradini, L. Brocca, and R. S. Govindaraju. "An investigation of the effects of spatial heterogeneity of initial soil moisture content on surface runoff simulation at a small watershed scale". In: *Journal of Hydrology* 539 (2016), pp. 589–598.
- [383] F. Morstatter, S. Kumar, H. Liu, and R. Maciejewski. "Understanding twitter data with tweetexplorer". In: *Proceedings of the ACM SIGKDD International Conference on Knowledge Discovery and Data Mining*. Vol. Part F128815. 2013, pp. 1482–1485.
- [384] C. Mudersbach and J. Jensen. "Küstenschutz an der Deutschen Ostseeküste. Zur Ermittlung von Eintrittswahrscheinlichkeiten extremer Sturmflutwasserstände". In: *Korrespondenz Wasserwirtschaft* 3.3 (2010), pp. 136–144.
- [385] Munich Re. *NatCatSERVICE*. 2009. URL: www.munichre.com (visited on 11/20/2009).

- [386] Munich Re. *NatCatSERVICE*. Münchener Rückversicherungs-Gesellschaft, GeoRisiko-Forschung. 2012. URL: <http://www.ergo.com/de/Presse/Overview/Pressemappen/Wetterereignisse/~ /media/ERG0com/PDF/Praesentationen/2012/201207-Naturkatastrophen-Deutschland-1970-2011.ashx> (visited on 09/15/2012).
- [387] Munich Re. *Natural Catastrophes 2013 Analyses, assessments, positions*. Issue 2014. Munich: Munich Re, Sept. 7, 2013, p. 65.
- [388] Munich Re. *Naturkatastrophen in Deutschland. Publication of Munich Re*. 2798-E-d. Munich: Munich Re Insurance, 1999.
- [389] Munich Re. *Winterstürme in Europa*. 2041-E-d. Munich: Munich Re Insurance, 1993.
- [390] H.P. Nachtnebel. "Cost-Benefits Evaluation of Risk Reduction Options". In: *Flood Risk Management Research - from extreme events to citizen involvement*. European Symposium on Flood Risk Management Research (EFRM 2007). Ed. by J. Schanze. Dresden, Germany: Leibniz Institute of Ecological and Regional Development (IOER), 2007, p. 278. ISBN: 978-3-933053-5.
- [391] N. C. Nadal, R. E. Zapata, I. Pagán, R. López, and J. Agudelo. "Building Damage due to Riverine and Coastal Floods". In: *Journal of Water Resources Planning and Management* 136.3 (May 1, 2010), pp. 327–336. DOI: 10.1061/(ASCE)WR.1943-5452.0000036.
- [392] S. Nadkarni and P. P. Shenoy. "Bayesian network approach to making inferences in causal maps". In: *European Journal of Operational Research* 128.3 (2001), pp. 479–498.
- [393] R. H. Nafari, T. Ngo, and P. Mendis. "An assessment of the effectiveness of tree-based models for multi-variate flood damage assessment in Australia". In: *Water (Switzerland)* 8.7 (2016).
- [394] J. E. Nash and J. V. Sutcliffe. "River flow forecasting through conceptual models part I - A discussion of principles". In: *Journal of Hydrology* 10.3 (1970), pp. 282–290.
- [395] J. Neal, C. Keef, P. Bates, K. Beven, and D. Leedal. "Probabilistic flood risk mapping including spatial dependence". In: *Hydrological Processes* 27.9 (2013), pp. 1349–1363. ISSN: 1099-1085. DOI: 10.1002/hyp.9572.
- [396] J. Nicholas, G. D. Holt, and D. G. Proverbs. "Towards standardising the assessment of flood damaged properties in the UK". In: *Structural Survey* 19.4 (Oct. 1, 2001), pp. 163–172. ISSN: 0263-080X. DOI: 10.1108/02630800110406667.
- [397] M. Nied, Y. Hundecha, and B. Merz. "Flood-initiating catchment conditions: a spatio-temporal analysis of large-scale soil moisture patterns in the Elbe River basin". In: *Hydrol. Earth Syst. Sci.* 17.4 (Apr. 12, 2013), pp. 1401–1414. ISSN: 1607-7938. DOI: 10.5194/hess-17-1401-2013.
- [398] M. Nied, T. Pardowitz, K. Nissen, U. Ulbrich, Y. Hundecha, and B. Merz. "On the relationship between hydro-meteorological patterns and flood types". In: *Journal of Hydrology* 519 (PD 2014), pp. 3249–3262. ISSN: 0022-1694. DOI: 10.1016/j.jhydrol.2014.09.089.

- [399] M. Nied, K. Schröter, S. Lüdtke, V.D. Nguyen, and B. Merz. "What are the hydro-meteorological controls on flood characteristics?" In: *Journal of Hydrology* 545 (Feb. 2017), pp. 310–326. ISSN: 0022-1694. DOI: 10.1016/j.jhydrol.2016.12.003.
- [400] NLWKN. *Jahresbericht 2013*. Norden: Niedersächsisches Landesamt für Wasserwirtschaft, Küsten- und Naturschutz, 2014, p. 52.
- [401] V. Notaro, M. De Marchis, C. M. Fontanazza, G. La Loggia, V. Puleo, and G. Freni. "The effect of damage functions on urban flood damage appraisal". In: *Procedia Engineering*. Vol. 70. 2014, pp. 1251–1260.
- [402] NRC. *Risk Analysis and Uncertainty in Flood Damage Reduction Studies*. Washington, D.C.: The National Academies Press, 2000. 216 pp. ISBN: 0-309-07136-4.
- [403] MURL NRW. *Potentielle Hochwasserschäden am Rhein in NRW*. Düsseldorf: Ministerium für Umwelt, Raumordnung und Landwirtschaft des Landes Nordrhein-Westfalen, 2000, p. 87.
- [404] H. Oesterle. "Reconstruction of daily global radiation for past years for use in agricultural models". In: *Physics and Chemistry of the Earth, Part B: Hydrology, Oceans and Atmosphere* 26.3 (2001), pp. 253–256. ISSN: 1464-1909. DOI: 10.1016/S1464-1909(00)00248-3.
- [405] H. Oesterle, F. W. Gerstengarbe, and P. C. Werner. "Ein neuer meteorologischer Datensatz für Deutschland, 1951-2003. Klimatrends: Vergangenheit und Zukunft". In: *Proceedings der 7* (2006), p. 3.
- [406] J. R. Olsen, P. A. Beling, J. H. Lambert, and Y. Y. Haimes. "Input-output economic evaluation of system of levees". In: *Journal of Water Resources Planning and Management* 124.5 (1998), pp. 237–245.
- [407] T. N. Palmer, A. Alessandri, U. Andersen, et al. "Development of a European multimodel ensemble system for seasonal-to-interannual prediction (DEMETER)". In: *Bulletin of the American Meteorological Society* 85.6 (2004), pp. 853–872.
- [408] D. Paprotny, O. Morales-Nápoles, and S.N. Jonkman. "HANZE: a pan-European database of exposure to natural hazards and damaging historical floods since 1870". In: *Earth System Science Data* 10.1 (Mar. 16, 2018), pp. 565–581. ISSN: 1866-3508. DOI: <https://doi.org/10.5194/essd-10-565-2018>.
- [409] D. Paprotny, A. Sebastian, O. Morales-Napoles, and S.N. Jonkman. "Trends in flood losses in Europe over the past 150 years". In: *Nat. Commun.* 9 (May 29, 2018). WOS:000433297300001, p. 1985. ISSN: 2041-1723. DOI: 10.1038/s41467-018-04253-1.
- [410] E. Paquet, F. Garavaglia, R. Garçon, and J. Gailhard. "The SCHADEX method: A semi-continuous rainfall-runoff simulation for extreme flood estimation". In: *Journal of Hydrology* 495 (2013), pp. 23–37.
- [411] Federal Parliament. *Answer of the Federal Government to the Minor Enquiry of the Representatives B.Höhn, S.-Ch.Kindler, P.Meiwald, Further Representatives and the Parliamentary Party BÜNDNIS 90/DIE GRÜNEN, 18th Legislative Period*. 18/5641. 2015.

- [412] S. Parolai, G. Grünthal, and R. Wahlström. "Site-specific response spectra from the combination of microzonation with probabilistic seismic hazard assessment—An example for the Cologne (Germany) area". In: *Soil Dynamics and Earthquake Engineering* 27.1 (Jan. 1, 2007), pp. 49–59. ISSN: 0267-7261. DOI: 10.1016/j.soildyn.2006.03.007.
- [413] A. Paschalis, S. Fatichi, P. Molnar, S. Rimkus, and P. Burlando. "On the effects of small scale space-time variability of rainfall on basin flood response". In: *Journal of Hydrology* 514 (2014), pp. 313–327.
- [414] S. Pathiraja, S. Westra, and A. Sharma. "Why continuous simulation? the role of antecedent moisture in design flood estimation". In: *Water Resources Research* 48.6 (2012).
- [415] Jonathan D. Paul, Wouter Buytaert, Simon Allen, et al. "Citizen science for hydrological risk reduction and resilience building". In: *Wiley Interdisciplinary Reviews: Water* 5.1 (2018), e1262. ISSN: 2049-1948. DOI: 10.1002/wat2.1262.
- [416] E. Penning-Rowsell and J. B. Chatterton. "The benefits of flood alleviation. A manual of assessment techniques." In: (1977).
- [417] E. Penning-Rowsell and C. Green. "New Insights into the Appraisal of Flood-Alleviation Benefits: (1) Flood Damage and Flood Loss Information". In: *Water and Environment Journal* 14.5 (2000), pp. 347–353. ISSN: 1747-6593. DOI: 10.1111/j.1747-6593.2000.tb00272.x.
- [418] E. Penning-Rowsell, C. Johnson, S. Tunstall, S. Tapsell, J. Morris, J. Chatterton, and C. Green. *The Benefits of Flood and Coastal Risk Management: A Manual of Assessment Techniques*. London: Flood Hazard Research Centre, Middlesex University, 2005.
- [419] E. Penning-Rowsell and T. Wilson. "Gauging the impact of natural hazards: The pattern and cost of emergency response during flood events". In: *Transactions of the Institute of British Geographers* 31.2 (2006), pp. 99–115.
- [420] M.A. Perry and J.D. Niemann. "Analysis and estimation of soil moisture at the catchment scale using EOFs". In: *Journal of Hydrology* 334.3 (Feb. 28, 2007), pp. 388–404. ISSN: 0022-1694. DOI: 10.1016/j.jhydro1.2006.10.014.
- [421] R. M. Peterman and J. L. Anderson. "Decision analysis: A method for taking uncertainties into account in risk-based decision making". In: *Human and Ecological Risk Assessment (HERA)* 5.2 (1999), pp. 231–244.
- [422] M Petersen and H Rohde. *Sturmflut - Die groSSen Fluten an den Küsten Schleswig-Holsteins und in der Elbe*. Wachholtz, Neumünster, 1991.
- [423] T. Petrow and B. Merz. "Trends in flood magnitude, frequency and seasonality in Germany in the period 1951-2002". In: *Journal of Hydrology* 371.1 (2009), pp. 129–141.
- [424] T. Petrow, B. Merz, K.-E. Lindenschmidt, and A. Thielen. "Aspects of seasonality and flood generating circulation patterns in a mountainous catchment in south-eastern Germany". In: *Hydrol. Earth Syst. Sci.* 11.4 (July 26, 2007), pp. 1455–1468. ISSN: 1607-7938. DOI: 10.5194/hess-11-1455-2007.

- [425] T. Petrow, J. Zimmer, and B. Merz. "Changes in the flood hazard in Germany through changing frequency and persistence of circulation patterns". In: *Nat. Hazards Earth Syst. Sci.* 9.4 (Aug. 12, 2009), pp. 1409–1423. ISSN: 1684-9981. DOI: 10.5194/nhess-9-1409-2009.
- [426] C. Pfuertscheller and A. Thielen. "The price of safety: costs for mitigating and coping with Alpine hazards". In: *Nat. Hazards Earth Syst. Sci.* 13.10 (Oct. 22, 2013), pp. 2619–2637. ISSN: 1684-9981. DOI: 10.5194/nhess-13-2619-2013.
- [427] A. Philipp, P. M. Della-Marta, J. Jacobeit, D. R. Fereday, P. D. Jones, A. Moberg, and H. Wanner. "Long-term variability of daily North Atlantic-European pressure patterns since 1850 classified by simulated annealing clustering". In: *Journal of Climate* 20.16 (2007), pp. 4065–4095.
- [428] R. A. Pielke Jr. and C. W. Landsea. "Normalized hurricane damages in the United States: 1925-95". In: *Weather and Forecasting* 13.3 (1998), pp. 621–631.
- [429] N. Pinter. "One Step Forward, Two Steps Back on U.S. Floodplains". In: *Science* 308.5719 (Apr. 8, 2005), pp. 207–208. ISSN: 0036-8075, 1095-9203. DOI: 10.1126/science.1108411.
- [430] J.G. Pinto. *personal communication*. 2012.
- [431] J.G. Pinto, E. L. Fröhlich, G. C. Leckebusch, and U. Ulbrich. "Changing European storm loss potentials under modified climate conditions according to ensemble simulations of the ECHAM5/MPI-OM1 GCM". In: *Natural Hazards and Earth System Sciences* 7.1 (Feb. 8, 2007), pp. 165–175. ISSN: 1684-9981. DOI: 10.5194/nhess-7-165-2007.
- [432] A. K. Pistrika and S. N. Jonkman. "Damage to residential buildings due to flooding of New Orleans after hurricane Katrina". In: *Natural Hazards* 54.2 (2010), pp. 413–434.
- [433] J. -. Pivot and P. Martin. "Farms adaptation to changes in flood risk: A management approach". In: *Journal of Hydrology* 267.1 (2002), pp. 12–25.
- [434] PLANAT. *The cycle of integrated risk management*. (National Platform for Natural Hazards), 2004.
- [435] E.J. Plate. "Flood risk and flood management". In: *Journal of Hydrology* 267.1 (2002), pp. 2–11. ISSN: 0022-1694. DOI: 10.1016/S0022-1694(02)00135-X.
- [436] S. K. Ploeger, G. M. Atkinson, and C. Samson. "Applying the HAZUS-MH software tool to assess seismic risk in downtown Ottawa, Canada". In: *Natural Hazards* 53.1 (Apr. 2010), pp. 1–20. ISSN: 0921-030X, 1573-0840. DOI: 10.1007/s11069-009-9408-x.
- [437] Saxon Police. *Latest Traffic Information of the Saxon Police*. Traffic Information. 2013.
- [438] J. Pollner. "Financial and Fiscal Instruments for Catastrophe Risk Management: Addressing the Losses from Flood Hazards in Central Europe". In: *Financial and Fiscal Instruments for Catastrophe Risk Management: Addressing the Losses from Flood Hazards in Central Europe* (2012).

- [439] K. Poser and D. Dransch. "Volunteered geographic information for disaster management with application to rapid flood damage estimation". In: *Geomatica* 64.1 (2010), pp. 89–98.
- [440] H. Posthumus, J. Morris, T. M. Hess, D. Neville, E. Phillips, and A. Baylis. "Impacts of the summer 2007 floods on agriculture in England". In: *Journal of Flood Risk Management* 2.3 (2009), pp. 182–189.
- [441] J. Poussin, P. Ward, P. Bubeck, L. Gaslikova, A. Schwerzmann, and C. C. Raible. "Flood Risk Modeling". In: *Climate Adaptation and Flood Risk in Coastal Cities*. Ed. by J. Aerts, W. Botzen, M. J. Bowman, P. Ward, and P. Dircke. London, New York: earthscan, 2012.
- [442] M. Power. "The predictive validation of ecological and environmental models". In: *Ecological Modelling* 68.1 (1993), pp. 33–50. ISSN: 03043800.
- [443] M. Pregolato, C. Galasso, and F. Parisi. "A compendium of existing vulnerability and fragility relationships for flood: Preliminary results". In: *12th International Conference on Applications of Statistics and Probability in Civil Engineering, ICASP 2015*. 2015.
- [444] C. Prudhomme and M. Geneviev. "Can atmospheric circulation be linked to flooding in Europe?" In: *Hydrological Processes* 25.7 (2011), pp. 1180–1190. ISSN: 1099-1085. DOI: 10.1002/hyp.7879.
- [445] C. Prudhomme, S. Parry, M. Geneviev, J. Hannaford, and Z. W. Kundzewicz. "Large Scale Flooding in Europe 1961 - 2005". In: *Changes in Flood Risk in Europe*. Vol. 10. IAHS Special Publications. Balkema: IAHS/ CRC Press, 2012, pp. 55–82. ISBN: 978-1-907 161-28-5.
- [446] H. J. Punge, K. M. Bedka, M. Kunz, and A. Werner. *A new physically based stochastic event catalog for hail in Europe*. Natural Hazards. Sept. 2014. URL: <http://link.springer.com/10.1007/s11069-014-1161-0> (visited on 01/15/2019).
- [447] M Puskeiler. *Radarbasierte Analyse der Hagelgefährdung in Deutschland*. Wiss. Reports Institute for Meteorology and Climate Researc 59. Karlsruhe, Germany, 2013.
- [448] J Ramirez, WL Adamowicz, KW Easter, and T Graham-Tomasi. "Ex post analysis of flood control: benefit-cost analysis and the value of information". In: *Water Resources Research* 24 (1988), pp. 1397–140. DOI: 10.1029/WR024i008p01397.
- [449] Fitch Ratings. *German Flood Claims May Hit EUR3bn*. Nov. 6, 2013.
- [450] M. Rauthe, H. Steiner, U. Riediger, A. Mazurkiewicz, and A. Gratzki. "A Central European precipitation climatology - Part I: Generation and validation of a high-resolution gridded daily data set (HYRAS)". In: *Meteorol. Z.* 22.3 (Oct. 2013). WOS:000326063600001, pp. 235–256. ISSN: 0941-2948. DOI: 10.1127/0941-2948/2013/0436.
- [451] J. T. Reager, B. F. Thomas, and J. S. Famiglietti. "River basin flood potential inferred using GRACE gravity observations at several months lead time". In: *Nature Geosci* advance online publication (July 6, 2014). ISSN: 1752-0894. DOI: 10.1038/ngeo2203.

- [452] S. Reese, H. -. Markau, and H. Sterr. *MERK-Mikroskalige Evaluation der Risiken in überflutungsgefährdeten Küstenniederungen*. Kiel, 2003.
- [453] T. Reichler and J. Kim. "How well do coupled models simulate today's climate?" In: *Bulletin of the American Meteorological Society* 89.3 (2008), pp. 303–311.
- [454] J.W.F Remo and N. Pinter. "Hazu-MH earthquake modeling in the central USA". In: *Natural Hazards* 63.2 (Sept. 2012), pp. 1055–1081. ISSN: 0921-030X, 1573-0840. DOI: 10.1007/s11069-012-0206-5.
- [455] O. Renn. "Concepts of Risk: An Interdisciplinary Review Part 1: Disciplinary Risk Concepts". In: *GAIA - Ecological Perspectives for Science and Society* 17.1 (2008), pp. 50–66.
- [456] C. Riggelsen. "Learning Bayesian Networks: A MAP Criterion for Joint Selection of Model Structure and Parameter". In: *Eighth IEEE International Conference on Data Mining, 2008. ICDM '08*. Eighth IEEE International Conference on Data Mining, 2008. ICDM '08. 2008, pp. 522–529. DOI: 10.1109/ICDM.2008.14.
- [457] J. Riha and M. Marcikova. "Classification and estimation of flood losses". In: *International Symposium on Water Management and Hydraulic Engineering* (2009), pp. 863–872.
- [458] B. Ripley and M. Lapsley. "RODBC: ODBC database access. [online] available from". In: (2017).
- [459] H. Rodda. "The Development and Application of a Flood Risk Model for the Czech Republic". In: *Natural Hazards* 36.1 (2005), pp. 207–220. ISSN: 0921-030X. DOI: 10.1007/s11069-004-4549-4.
- [460] H.J.E. Rodda. "The development of a stochastic rainfall model for UK flood modelling". In: *Generation of Hydrometeorological Reference Conditions for the Assessment of Flood Hazard in Large River Basins* (2001).
- [461] J. Rogstadius, V. Kostakos, J. Laredo, and M. Vukovic. "Towards real-time emergency response using crowd supported analysis of social media". In: *Proceedings of CHI Workshop on Crowdsourcing and Human Computation, Systems, Studies and Platforms* (2011).
- [462] J. Rogstadius, M. Vukovic, C. A. Teixeira, V. Kostakos, E. Karapanos, and J. A. Laredo. "CrisisTracker: Crowdsourced social media curation for disaster awareness". In: *IBM Journal of Research and Development* 57.5 (2013).
- [463] A. Rosner, R.M. Vogel, and P.H. Kirshen. "A risk-based approach to flood management decisions in a nonstationary world". In: *Water Resour. Res.* 50.3 (2014), pp. 1928–1942. ISSN: 1944-7973. DOI: 10.1002/2013WR014561.
- [464] T. Rossetto, D. D'Ayala, I. Ioannou, and A. Meslem. *Evaluation of Existing Fragility Curves*. Vol. 27. Geotechnical, Geological and Earthquake Engineering. 2014. 47-93.
- [465] SAB. *Schäden durch das Hochwasser 2002. Angaben aus der Fördermitteldatenbank [Damages of the Flood 2002]*. Sächsische Aufbau Bank - Saxon Relief Bank, 2005.
- [466] Y. Saeys, I. Inza, and P. Larrañaga. "A review of feature selection techniques in bioinformatics". In: *Bioinformatics* 23.19 (Oct. 1, 2007), pp. 2507–2517. ISSN: 1367-4803. DOI: 10.1093/bioinformatics/btm344.

- [467] Safecoast. *Coastal flood risk and trends for the future in the North Sea region: Synthesis report*. The Hague, Netherlands: The safecoast project team, 2008.
- [468] T. Sakaki, M. Okazaki, and Y. Matsuo. "Earthquake shakes Twitter users: Real-time event detection by social sensors". In: *Proceedings of the 19th International Conference on World Wide Web, WWW '10*. 2010, pp. 851–860.
- [469] A. Saltelli, K. Chan, and E. M Scott. *Sensitivity Analysis*. Wiles Series in Probability and Statistics. Chichester: John Wiley & Sons, LTD, 2000. 475 pp.
- [470] C. C. Sampson, T. J. Fewtrell, F. O'Loughlin, F. Pappenberger, P. Bates, J. E. Freer, and H. L. Cloke. "The impact of uncertain precipitation data on insurance loss estimates using a Flood Catastrophe Model". In: *Hydrology and Earth System Sciences Discussions* 11.1 (Jan. 3, 2014), pp. 31–81. ISSN: 1812-2116. DOI: 10.5194/hessd-11-31-2014.
- [471] Saxon State Chancellery. *Der Wiederaufbau im Freistaat Sachsen Nach Dem Hochwasser im Juni 2013*. Freestate of Saxony, Wiederaufbaustab 2013, 2013, p. 85.
- [472] Saxony-Anhalt Ministry of the Interior. *Katastrophenschutzreport Zum Hochwasser 2013 in Sachsen-Anhalt*. 2013, p. 61.
- [473] P. B. Sayers, J. W. Hall, and I. C. Meadowcroft. "Towards risk-based flood hazard management in the UK". In: *Proc. Inst. Civil Eng.-Civil Eng.* 150 (May 2002). WOS:000175759000008, pp. 36–42. ISSN: 0965-089X. DOI: 10.1680/cien.2002.150.5.36.
- [474] C. Scawthorn, N. Blais, H. Seligson, E. Tate, E. Mifflin, W. Thomas, J. Murphy, and C. Jones. "HAZUS-MH flood loss estimation methodology. I: Overview and flood hazard characterization". In: *Natural Hazards Review* 7.2 (2006), pp. 60–71. ISSN: 15276988. DOI: 10.1061/(ASCE)1527-6988(2006)7:2(60).
- [475] J. Schanze. "FLOOD RISK MANAGEMENT A BASIC FRAMEWORK". In: *Flood Risk Management: Hazards, Vulnerability and Mitigation Measures*. Ed. by J. Schanze, E. Zeman, and J. Marsalek. NATO Science Series. Springer Netherlands, 2006, pp. 1–20. ISBN: 978-1-4020-4598-1.
- [476] F. Scherbaum and N.M. Kuehn. "Logic Tree Branch Weights and Probabilities: Summing Up to One Is Not Enough". In: *Earthquake Spectra* 27.4 (Nov. 2011), pp. 1237–1251. ISSN: 8755-2930. DOI: 10.1193/1.3652744.
- [477] B. Schloerke, J. Crowley, D. Cook, F. Briatte, M. Marbach, E. Thoen, A. Elberg, and J. Larmarange. "GGally: extension to ggplot2. [online] Available from". In: (2017).
- [478] J. Schmidt, I. Matcham, S. Reese, et al. "Quantitative multi-risk analysis for natural hazards: a framework for multi-risk modelling". In: *Natural Hazards* 58.3 (Sept. 2011), pp. 1169–1192. ISSN: 0921-030X, 1573-0840. DOI: 10.1007/s11069-011-9721-z.
- [479] P. Schmidt-Thomé, S. Greiving, H. Kallio, M. Fleischhauer, and J. Jarva. "Economic risk maps of floods and earthquakes for European regions". In: *Quaternary International*. Impact of rapid environmental changes on humans and ecosystems 150.1 (June 1, 2006), pp. 103–112. ISSN: 1040-6182. DOI: 10.1016/j.quaint.2006.01.024.

- [480] E. Schnebele and G. Cervone. "Improving remote sensing flood assessment using volunteered geographical data". In: *Nat. Hazards Earth Syst. Sci.* 13.3 (2013), pp. 669–677. ISSN: 1684-9981. DOI: 10.5194/nhess-13-669-2013.
- [481] K. Schröter. "Hydrologie und hydro-meteorologische Einordnung in überregionale Hochwasser in Deutschland". In: *Das Hochwasser im Juni 2013: Bewährungsprobe Für das Hochwasserrisikomanagement in Deutschland* 53 (2015), pp. 23–31.
- [482] K. Schröter, H Kreibich, K Vogel, C Riggelsen, F Scherbaum, and B Merz. "How useful are complex flood damage models?" In: *Water Resour. Res.* 50.4 (Apr. 1, 2014), pp. 3378–3395. ISSN: 1944-7973. DOI: 10.1002/2013WR014396.
- [483] K. Schröter, M. Kunz, F. Elmer, B. Mühr, and B. Merz. "What made the June 2013 flood in Germany an exceptional event? A hydro-meteorological evaluation". In: *Hydrol. Earth Syst. Sci.* 19.1 (Jan. 16, 2015), pp. 309–327. ISSN: 1607-7938. DOI: 10.5194/hess-19-309-2015.
- [484] K. Schröter, S. Lüdtkke, R. Redweik, J. Meier, M. Bochow, L. Ross, C. Nagel, and H. Kreibich. "Flood loss estimation using 3D city models and remote sensing data". In: *Environmental Modelling & Software* 105 (July 2018), pp. 118–131. ISSN: 1364-8152. DOI: 10.1016/j.envsoft.2018.03.032.
- [485] K. Schröter, S. Lüdtkke, K. Vogel, H. Kreibich, and B. Merz. "Tracing the value of data for flood loss modelling". In: *E3S Web of Conferences* 7 (2016). Ed. by M. Lang, F. Klijn, and P. Samuels, p. 05005. ISSN: 2267-1242. DOI: 10.1051/e3sconf/20160705005.
- [486] K. Schröter, D. Molinari, M. Kunz, and H. Kreibich. "Preface: Natural hazard event analysis for risk reduction and adaptation". In: *Nat. Hazards Earth Syst. Sci.* 18.3 (Mar. 26, 2018), pp. 963–968. ISSN: 1684-9981. DOI: 10.5194/nhess-18-963-2018.
- [487] K. Schröter, R. Redweik, S. Lüdtkke, J. Meier, M. Bochow, H. Kreibich, L. Ross, and C. Nagel. "3d-City Flood Damage Module Prototype Implementation". In: (2017).
- [488] G. Schumann, G. Di Baldassarre, and P. Bates. "The Utility of Spaceborne Radar to Render Flood Inundation Maps Based on Multialgorithm Ensembles". In: *IEEE Transactions on Geoscience and Remote Sensing* 47.8 (Aug. 2009), pp. 2801–2807. ISSN: 0196-2892. DOI: 10.1109/TGRS.2009.2017937.
- [489] S.S. Schuster, R.J. Blong, and K.J. McAneney. "Relationship between radar-derived hail kinetic energy and damage to insured buildings for severe hailstorms in Eastern Australia". In: *Atmospheric Research* 81.3 (Sept. 2006), pp. 215–235. ISSN: 01698095. DOI: 10.1016/j.atmosres.2005.12.003.
- [490] J. Schwarz and H. Maiwald. "Prognosis of building damage due to flood impact". In: *Bautechnik* 84.7 (2007), pp. 450–464.
- [491] R. Schwarze and G.G. Wagner. "The political economy of natural disaster insurance: lessons from the failure of a proposed compulsory insurance scheme in Germany". In: *European Environment* 17.6 (Nov. 2007), pp. 403–415. ISSN: 09610405, 10990976. DOI: 10.1002/eet.456.

- [492] A. R. Scorzini and E. Frank. "Flood damage curves: new insights from the 2010 flood in Veneto, Italy". In: *Journal of Flood Risk Management* 10.3 (2017), pp. 381–392.
- [493] I. Seifert, H. Kreibich, B. Merz, and A. Thieken. "Application and validation of flemocs - a flood-loss estimation model for the commercial sector". In: *Hydrological Sciences Journal* 55.8 (2010), pp. 1315–1324.
- [494] C. Shimizu. "Estimation of hedonic single-family house price function considering neighborhood effect variables". In: *Sustainability (Switzerland)* 6.5 (2014), pp. 2946–2960.
- [495] T. Sieg, K. Vogel, B. Merz, and H. Kreibich. "Tree-based flood damage modeling of companies: Damage processes and model performance". In: *Water Resources Research* 53.7 (2017), pp. 6050–6068. ISSN: 1944-7973. DOI: 10.1002/2017WR020784.
- [496] ML Silver. "International best practices in disaster mitigation and management recommended for Mongolia". In: National Conference Strengthening the Disaster Mitigation and Management System in Mongolia. Ulaanbaatar: Gov. of Mongolia, 2001.
- [497] F. Silvestro and N. Rebori. "Impact of precipitation forecast uncertainties and initial soil moisture conditions on a probabilistic flood forecasting chain". In: *Journal of Hydrology* 519 (PA 2014), pp. 1052–1067.
- [498] F. Sirocko, S. Dietrich, D. Veres, et al. "Multi-proxy dating of Holocene maar lakes and Pleistocene dry maar sediments in the Eifel, Germany". In: *Quaternary Science Reviews* 62 (Feb. 2013), pp. 56–76. ISSN: 02773791. DOI: 10.1016/j.quascirev.2012.09.011.
- [499] M. Sivapalan, G. Blöschl, R. Merz, and D. Gutknecht. "Linking flood frequency to long-term water balance: Incorporating effects of seasonality". In: *Water Resources Research* 41.6 (2005), pp. 1–17.
- [500] SMI. *Verwaltungsvorschrift des Sächsischen Staatsministeriums des Innern zur Behebung von Hochwasserschäden an Wohngebäuden [Administrative regulation on the compensation of flood damages of residential buildings]*. 2002.
- [501] D.I. Smith. "Flood damage estimation - a review of urban stage-damage curves and loss functions". In: *Water SA* 20.3 (1994), pp. 231–238. ISSN: 03784738.
- [502] K. Smith and R. C. Ward. *Floods: physical processes and human impacts*. Wiley, 1998. 412 pp. ISBN: 978-0-471-95248-0.
- [503] R.B. Smith and I. Barstad. "A Linear Theory of Orographic Precipitation". In: *J. Atmos. Sci.* 61.12 (June 1, 2004), pp. 1377–1391. ISSN: 0022-4928. DOI: 10.1175/1520-0469(2004)061<1377:ALTOOP>2.0.CO;2.
- [504] M. H. Spekkers, M. Kok, F. H. L. R. Clemens, and J. A. E. ten Veldhuis. "Decision-tree analysis of factors influencing rainfall-related building structure and content damage". In: *Nat. Hazards Earth Syst. Sci.* 14.9 (Sept. 24, 2014), pp. 2531–2547. ISSN: 1684-9981. DOI: 10.5194/nhess-14-2531-2014.
- [505] A. Spillatura, E. Fiorini, P. Bazzurro, and D. Pennucci. "Harmonization of Vulnerability Curves for Masonry and RC Buildings". In: *2nd European Conference on Earthquake Engineering and Seismology* (2014).

- [506] Bayerische Staatskanzlei. *Bayerisches Wassergesetz*. Feb. 25, 2010.
- [507] Staatskanzlei Freistaat Sachsen. *Schadensausgleich und Wiederaufbau im Freistaat Sachsen*. Dresden: Leitstelle Wiederaufbau, 2003, p. 126.
- [508] A. Stadler and T. H. Kolbe. "Spatio-semantic coherence in the integration of 3D city models". In: *Proceedings of the 5th International Symposium on Spatial Data Quality* (2007).
- [509] K. Starbird and J. Stamberger. "Tweak the tweet: Leveraging microblogging proliferation with a prescriptive syntax to support citizen reporting". In: *ISCRAM 2010 - 7th International Conference on Information Systems for Crisis Response and Management: Defining Crisis Management 3.0, Proceedings*. 2010.
- [510] P.C. Stern and V. Fineberg, eds. *Understanding Risk: Informing Decisions in a Democratic Society*. Washington: National Academies Press, July 5, 1996. 264 pp. ISBN: 978-0-309-08956-2.
- [511] H. Sterr. "Status Report. Analyses of previous vulnerability studies in the pilot site German bight coast". In: *FLOODsite Report T27-05-01* (2005).
- [512] H. von Storch and K. Woth. "Storm surges, perspectives and options". In: *Sustainability Science* 3.1 (2008).
- [513] A.N. Strahler. "Quantitative analysis of watershed geomorphology". In: *Transactions, American Geophysical Union* 38 (1957), pp. 913–920. DOI: 10.1029/TR038i006p00913.
- [514] A.N. Strahler. "Quantitative geomorphology of drainage basins and channel networks". In: *Quantitative geomorphology of drainage basins and channel networks* (1964).
- [515] S. Surminski and A. Thielen. "Promoting flood risk reduction: The role of insurance in Germany and England". In: *Earth's Future* 5.10 (2017), pp. 979–1001. ISSN: 2328-4277. DOI: 10.1002/2017EF000587.
- [516] J. Sutton, L. Palen, and I. Shklovski. "Backchannels on the front lines: Emergent uses of social media in the 2007 Southern California Wildfires". In: *Proceedings of ISCRAM 2008 - 5th International Conference on Information Systems for Crisis Response and Management*. 2008, pp. 624–631.
- [517] T. Swierczynski, S. Lauterbach, P. Dulski, J. Delgado, B. Merz, and A. Brauer. "Mid- to late Holocene flood frequency changes in the northeastern Alps as recorded in varved sediments of Lake Mondsee (Upper Austria)". In: *Quaternary Science Reviews* 80 (Nov. 15, 2013), pp. 78–90. ISSN: 0277-3791. DOI: 10.1016/j.quascirev.2013.08.018.
- [518] Swiss Re. *Sigma preliminary estimates: natural catastrophes and man-made disasters in 2013 cost insurers worldwide USD 44 billion*. Preliminary catastrophe estimates for 2013 | Swiss Re - Leading Global Reinsurer. Dec. 18, 2013. URL: http://www.swissre.com/media/news_releases/nr_20131218_sigma_natcat_2013.html (visited on 12/18/2013).
- [519] K. Takeuchi. "Increasing vulnerability to extreme floods and societal needs of hydrological forecasting". In: *Hydrological Sciences Journal* 46.6 (2001), pp. 869–881.
- [520] O. Talagrand, R. Vautard, and B. Strauss. "Evaluation of probabilistic prediction systems". In: *Proc.ECMWF Workshop on Predictability* (1997), pp. 1–25.

- [521] M. Tanoue, Y. Hirabayashi, and H. Ikeuchi. "Global-scale river flood vulnerability in the last 50 years". In: *Scientific Reports* 6 (2016).
- [522] F.-O. Tapia-Silva, S. Itzerott, S. Foerster, B. Kuhlmann, and H. Kreibich. "Estimation of flood losses to agricultural crops using remote sensing". In: *Phys. Chem. Earth* 36.7 (2011). WOS:000291375300005, pp. 253–265. ISSN: 1474-7065. DOI: 10.1016/j.pce.2011.03.005.
- [523] H. Taubenböck, M. Wurm, N. Setiadi, N. Gebert, A. Roth, G. Strunz, J. Birkmann, and S. Dech. "Integrating remote sensing and social science: The correlation of urban morphology with socioeconomic parameters". In: *2009 Joint Urban Remote Sensing Event*. 2009.
- [524] W. L. Teng, J. R. Wang, and P. C. Doraiswamy. "Relationship between satellite microwave radiometric data, antecedent precipitation index, and regional soil moisture". In: *International Journal of Remote Sensing* 14.13 (Sept. 1993), pp. 2483–2500. ISSN: 0143-1161, 1366-5901. DOI: 10.1080/01431169308904287.
- [525] A. Thielen. "Schadstoffmuster in der Regionalen Grundwasserkontamination der Mitteldeutschen Industrie- und Bergbauregion Bitterfeld-Wolfen". PhD thesis. Halle (Saale): Martin-Luther University Halle-Wittenberg, 2001. 154 pp.
- [526] A. Thielen, H. Apel, and B. Merz. "Assessing the probability of large-scale flood loss events: a case study for the river Rhine, Germany: Assessing the probability of large-scale flood loss events". In: *Journal of Flood Risk Management* (Feb. 2014), n/a–n/a. ISSN: 1753318X. DOI: 10.1111/jfr3.12091.
- [527] A. Thielen, T. Bessel, S. Kienzler, H. Kreibich, M. Müller, S. Pisi, and K. Schröter. "The flood of June 2013 in Germany: how much do we know about its impacts?" In: *Nat. Hazards Earth Syst. Sci.* 16.6 (July 1, 2016), pp. 1519–1540. ISSN: 1684-9981. DOI: 10.5194/nhess-16-1519-2016.
- [528] A. Thielen, H. Kreibich, M. Müller, and J. Lamond. "Data collection for a better understanding of what causes flood damage: experiences with telephone surveys: in Flood damage survey and assessment: new insights from research and practice". In: *Geophysical monograph* 228 7 (2017), pp. 95–106.
- [529] A. Thielen, H. Kreibich, M. Müller, and B. Merz. "Coping with floods: preparedness, response and recovery of flood-affected residents in Germany in 2002". In: *Hydrological Sciences Journal* 52.5 (2007), pp. 1016–1037. ISSN: 0262-6667. DOI: 10.1623/hysj.52.5.1016.
- [530] A. Thielen, M. Müller, L. Kleist, I. Seifert, D. Borst, and U. Werner. "Regionalisation of asset values for risk analyses". In: *Nat. Hazards Earth Syst. Sci.* 6.2 (2006), pp. 167–178. ISSN: 1684-9981. DOI: 10.5194/nhess-6-167-2006.
- [531] A. Thielen, M. Müller, H. Kreibich, and B. Merz. "Flood damage and influencing factors: New insights from the August 2002 flood in Germany". In: *Water Resources Research* 41.12 (2005), pp. 1–16. ISSN: 0043-1397. DOI: 10.1029/2005WR004177.
- [532] A. Thielen, A. Olschewski, H. Kreibich, S. Kobsch, and B. Merz. "Development And Evaluation Of FLEMops - A New Flood Loss Estimation Model For The Private Sector". In: *Development and Evaluation of FLEMops-A New Flood Loss Estimation Model for the Private Sector* (2008).

- [533] A. Thielen, A. Olschewski, H. Kreibich, S. Kobsch, and B. Merz. "Development and evaluation of FLEMOps - a new Flood Loss Estimation MOdel for the private sector". In: International Conference on Flood Recovery, Innovation and Response. London, 2008.
- [534] A. Thielen, T. Petrow, H. Kreibich, and B. Merz. "Insurability and Mitigation of Flood Losses in Private Households in Germany". In: *Risk Analysis* 26.2 (Apr. 1, 2006), pp. 383–395. ISSN: 1539-6924. DOI: 10.1111/j.1539-6924.2006.00741.x.
- [535] A. Thielen, I. Seifert, and B. Merz. *Hochwasserschäden - Erfassung, Abschätzung und Vermeidung*. München: oekom, 2010. 304 pp.
- [536] Fannar Örn Thordarson, A. Breinholt, J.K. Møller, P.S. Mikkelsen, M. Grum, and H. Madsen. "Evaluation of probabilistic flow predictions in sewer systems using grey box models and a skill score criterion". In: *Stoch Environ Res Risk Assess* 26.8 (Dec. 1, 2012), pp. 1151–1162. ISSN: 1436-3240, 1436-3259. DOI: 10.1007/s00477-012-0563-3.
- [537] G.A. Tobin. "The Levee Love Affair: A Stormy Relationship?1". In: *JAWRA Journal of the American Water Resources Association* 31.3 (June 1, 1995), pp. 359–367. ISSN: 1752-1688. DOI: 10.1111/j.1752-1688.1995.tb04025.x.
- [538] J. P. Torterotot. "Estimation et analyse des incertitudes". In: *Ecole Nationale des Ponts et Chaussées* 1993 (1993).
- [539] S. Tóth, S. Kovács, and L. Kummer. "Vulnerability Analysis in the Koros-Corner Flood Area Along the Middle-Tisza river Pilot Study Application of General Vulnerability Analysis Techniques". In: *Vulnerability Analysis in the Körös-Corner Flood Area Along the Middle-Tisza River - Pilot Study Application of General Vulnerability Analysis Techniques* (2008).
- [540] P.A. Troch, J.A. Smith, E.F. Wood, and F.P. de Troch. "Hydrologic controls of large floods in a small basin: central Appalachian case study". In: *Journal of Hydrology* 156.1 (Apr. 1994), pp. 285–309. ISSN: 0022-1694. DOI: 10.1016/0022-1694(94)90082-5.
- [541] S. Tyagunov, G. Grünthal, R. Wahlström, L. Stempniewski, and J. Zschau. "Seismic risk mapping for Germany". In: *Natural Hazards and Earth System Sciences* 6.4 (June 29, 2006), pp. 573–586. ISSN: 1561-8633. DOI: <https://doi.org/10.5194/nhess-6-573-2006>.
- [542] K. Tzavella, A. Fekete, and F. Fiedrich. "Opportunities provided by geographic information systems and volunteered geographic information for a timely emergency response during flood events in Cologne, Germany". In: *Nat Hazards* 91.1 (Apr. 1, 2018), pp. 29–57. ISSN: 1573-0840. DOI: 10.1007/s11069-017-3102-1.
- [543] S. Uhlemann, A. Thielen, and B. Merz. "A consistent set of trans-basin floods in Germany between 1952-2002". In: *Hydrology and Earth System Sciences* 14.7 (2010), pp. 1277–1295.
- [544] U. Ulbrich, T. Brücher, A.H. Fink, G.C. Leckebusch, A. Krüger, and J.G. Pinto. "The central European floods of August 2002: Part 1 Rainfall periods and flood development". In: *Weather* 58.10 (2003), pp. 371–377. ISSN: 1477-8696. DOI: 10.1256/wea.61.03A.

- [545] U. Ulbrich, T. Brücher, A.H. Fink, G.C. Leckebusch, A. Krüger, and J.G. Pinto. "The central European floods of August 2002: Part 2 Synoptic causes and considerations with respect to climatic change". In: *Weather* 58.11 (Nov. 1, 2003), pp. 434–442. ISSN: 1477-8696. DOI: 10.1256/wea.61.03B.
- [546] UNDRR. *Mitigating natural disasters: phenomena, effects and options, A Manual for Policy Makers and Planners*. New York: United Nations, 1991.
- [547] UNDRR. *Global assessment report on disaster risk reduction 2019*. United Nations Office for Disaster Risk Reduction, 2019, p. 425.
- [548] UNEP FI. *Navigating a new climate: Assessing credit risk and opportunity in a changing climate*. PART 2: Physical risks and opportunities. UN Environment Finance Initiative (UNEP FI), 2018, p. 78.
- [549] UNISDR. *Global Assessment Report on Disaster Risk Reduction - Revealing Risk, re-defining development*. Geneva: United Nations, 2011, p. 178.
- [550] UNISDR. *Sendai Framework for Disaster Risk Reduction 2015-2030*. United Nations International Strategy for Disaster Reduction, 2015.
- [551] S. M. Uppala, P. W. Kållberg, A. J. Simmons, et al. "The ERA-40 re-analysis". In: *Quarterly Journal of the Royal Meteorological Society* 131.612 (2005), pp. 2961–3012.
- [552] USACE. *Guidelines for Risk and Uncertainty Analysis In Water Resources Planning*. Fort Belvoir, VA. USA, 1992.
- [553] E. Uuema, M. Antrop, J. Roosaare, R. Marja, and Ü. Mander. "Landscape metrics and indices: An overview of their use in landscape research". In: *Living Reviews in Landscape Research* 3 (2009).
- [554] A. Van Der Veen, A. E. Steenge, M. Bockarjova, and C. Logtmeijer. "Structural economic effects of large scale inundation: A simulation of the Krimpen dike breakage". In: *The Role of Flood Impact Assessment in Flood Defence Policies* (2003), pp. 1–50.
- [555] W. H. J. M. Van Eck, J. P. M. Lenssen, H. M. Van De Steeg, C. W. P. M. Blom, and H. De Kroon. "Seasonal dependent effects of flooding on plant species survival and zonation: A comparative study of 10 terrestrial grassland species". In: *Hydrobiologia* 565.1 (2006), pp. 59–69.
- [556] N. Van Steenbergen and P. Willems. "Increasing river flood preparedness by real-time warning based on wetness state conditions". In: *Journal of Hydrology* 489 (2013), pp. 227–237. ISSN: 0022-1694. DOI: 10.1016/j.jhydro1.2013.03.015.
- [557] K. Vanneste, K. Verbeeck, T. Camelbeeck, E. Paulissen, M. Meghraoui, F. Renardy, D. Jongmans, and M. Frechen. "Surface-rupturing history of the Bree fault scarp, Roer Valley graben: Evidence for six events since the late Pleistocene". In: *Journal of Seismology* 5.3 (July 1, 2001), pp. 329–359. ISSN: 1573-157X. DOI: 10.1023/A:1011419408419.
- [558] W. Vanneuville, R. Maddens, C. Collard, P. Bogaert, P. de Maeyer, and M. Antrop. *Impact op mens en economie t.g.v. overstromingen bekeken in het licht van wijzigende hydraulische condities, omgevingsfactoren en klimatologische omstandigheden*. 2006, pp. 3–121.

- [559] Regione del Veneto. *31 ottobre-2 novembre 2010: L'alluvione dei Santi*. Rapporto Statistico. 2011, pp. 410–425.
- [560] Regione del Veneto. *Veneto, la Grande Alluvione*. 2011.
- [561] K. Venkateswaran, K. MacClune, A. Keating, and M. Szoenyi. *The PERC manual*. Zurich Insurance Group Ltd, 2013.
- [562] S. Verma, S. Vieweg, W. J. Corvey, L. Palen, J. H. Martin, M. Palmer, A. Schram, and K. M. Anderson. "Natural language processing to the rescue? Extracting situational awareness tweets during mass emergency". In: *ICWSM (2011)*, pp. 385–392.
- [563] W. Viessman and G. L. Lewis. *Introduction to Hydrology*. 5th edition. New York, USA: Prentice Hall, 2002. 612 pp.
- [564] S. Vieweg, A. L. Hughes, K. Starbird, and L. Palen. "Microblogging during two natural hazards events: What twitter may contribute to situational awareness". In: *Conference on Human Factors in Computing Systems - Proceedings*. Vol. 2. 2010, pp. 1079–1088.
- [565] R Vitolo, DB Stephenson, IM Cook, and K Mitchell-Wallace. "Serial clustering of intense European storms". In: *Meteorologische Zeitschrift* 18 (2009), pp. 411–424. doi: 10.1127/0941-2948/2009/0393.
- [566] D. Viviroli, M. Zappa, J. Schwanbeck, J. Gurtz, and R. Weingartner. "Continuous simulation for flood estimation in ungauged mesoscale catchments of Switzerland - Part I: Modelling framework and calibration results". In: *Journal of Hydrology* 377.1 (2009), pp. 191–207.
- [567] K. Vogel, C. Rigg, H. Kreibich, B. Merz, and F. Scherbaum. "Flood Damage and Influencing Factors: A Bayesian Network Perspective". In: *Proceedings of the 6th European Workshop on Probabilistic Graphical Models (PGM 2012)*. 6th European Workshop on Probabilisit Graphical Models. Granada, Spain, 2012, pp. 347–354.
- [568] K. Vogel, C. Riggelsen, F. Scherbaum, K. Schröter, H. Kreibich, and B. Merz. "Challenges for Bayesian Network Learning in a Flood Damage Assessment Application". In: *ICOSSAR 2013*. 11th international Conference on Structural Safety & Reliability. New York, 2013.
- [569] K. Vogel, L. Weise, K. Schröter, and A. Thielen. "Identifying Driving Factors in Flood-Damaging Processes Using Graphical Models". In: *Water Resources Research* 54.11 (Nov. 2018), pp. 8864–8889. ISSN: 00431397. DOI: 10.1029/2018WR022858.
- [570] R. M. Vogel. "Stochastic and Deterministic World Views". In: *Journal of Water Resources Planning and Management* 125.6 (1999), pp. 311–313.
- [571] J. Vogt. "A Pan-European River and Catchment Database". In: *Eur.Comm.Luxembourg* (2007).
- [572] Z. Vojinovic, J. C. W. Ediriweera, and A. A. Fikri. "An approach to the model-based spatial assessment of damages caused by flash floods". In: *11th Int.Conf.on Urban Drainage*. 31 (2008).

- [573] S. Vorogushyn, P. Bates, K. Bruijn, et al. "Evolutionary leap in large-scale flood risk assessment needed". In: *Wiley Interdisciplinary Reviews: Water* 5.2 (2018), e1266. ISSN: 2049-1948. DOI: 10.1002/wat2.1266.
- [574] S. Vorogushyn, K.-E. Lindenschmidt, H. Kreibich, H. Apel, and B. Merz. "Analysis of a detention basin impact on dike failure probabilities and flood risk for a channel-dike-floodplain system along the river Elbe, Germany". In: *Journal of Hydrology* 436437 (2012), pp. 120–131. ISSN: 0022-1694. DOI: 10.1016/j.jhydrol.2012.03.006.
- [575] S. Vorogushyn, B. Merz, K.-E. Lindenschmidt, and H. Apel. "A new methodology for flood hazard assessment considering dike breaches". In: *Water Resour. Res.* 46.8 (Aug. 1, 2010), W08541. ISSN: 1944-7973. DOI: 10.1029/2009WR008475.
- [576] D. Wagenaar, K. M. de Bruijn, L.M. Bouwer, and H. de Moel. "Uncertainty in flood damage estimates and its potential effect on investment decisions". In: *Natural Hazards and Earth System Sciences* 16.1 (Jan. 15, 2016), pp. 1–14. ISSN: 1561-8633. DOI: 10.5194/nhess-16-1-2016.
- [577] D. Wagenaar, J. de Jong, and L.M. Bouwer. "Multi-variable flood damage modelling with limited data using supervised learning approaches". In: *Nat. Hazards Earth Syst. Sci.* 17.9 (Sept. 29, 2017), pp. 1683–1696. ISSN: 1684-9981. DOI: 10.5194/nhess-17-1683-2017.
- [578] Y. Wang. "Mapping extent of floods: What we have learned and how we can do better". In: *Natural Hazards Review* 3.2 (2002), pp. 68–73. ISSN: 1527-6988. DOI: 10.1061/(ASCE)1527-6988(2002)3:2(68).
- [579] Z. Wang, C. Lai, X. Chen, B. Yang, S. Zhao, and X. Bai. "Flood hazard risk assessment model based on random forest". In: *Journal of Hydrology* 527 (Aug. 2015), pp. 1130–1141. ISSN: 00221694. DOI: 10.1016/j.jhydrol.2015.06.008.
- [580] P. Ward, W. Beets, L.M. Bouwer, J. Aerts, and H. Renssen. "Sensitivity of river discharge to ENSO". In: *Geophysical Research Letters* 37.12 (2010).
- [581] P. Ward, S. Eisner, M. Flo Rke, M. D. Dettinger, and M. Kummu. "Annual flood sensitivities to el nintild;O-Southern Oscillation at the global scale". In: *Hydrology and Earth System Sciences* 18.1 (2014), pp. 47–66.
- [582] P. Ward, B. Jongman, J. Aerts, et al. "A global framework for future costs and benefits of river-flood protection in urban areas". In: *Nature Climate Change* 7.9 (Sept. 2017), p. 642. ISSN: 1758-6798. DOI: 10.1038/nclimate3350.
- [583] P. Ward, B. Jongman, P. Salamon, et al. "Usefulness and limitations of global flood risk models". In: *Nature Clim. Change* 5.8 (Aug. 2015), pp. 712–715. ISSN: 1758-678X. DOI: 10.1038/nclimate2742.
- [584] P. Ward, H. de Moel, and J. Aerts. "How are flood risk estimates affected by the choice of return-periods?" In: *Nat. Hazards Earth Syst. Sci.* 11.12 (2011), pp. 3181–3195. ISSN: 1684-9981.
- [585] P. Watkiss, T. Downing, C. Handley, and R. Butterfield. *The Impacts and Costs of Climate Change*. Final Report Commissioned by European Commission DG Environment. 2005.

- [586] P. R. Waylen and C. N. Caviedes. "El Niño and annual floods on the north Peruvian littoral". In: *Journal of Hydrology* 89.1 (1986), pp. 141–156.
- [587] A. P. Weigel. "Ensemble forecasts". In: *Forecast Verification: A Practitioner's Guide in Atmospheric Science* (2011), pp. 141–166.
- [588] A. P. Weigel, M. A. Liniger, and C. Appenzeller. "Can multi-model combination really enhance the prediction skill of probabilistic ensemble forecasts?" In: *Quarterly Journal of the Royal Meteorological Society* 134.630 (2008), pp. 241–260.
- [589] K. Weiler, T. Walter, M. F. Walter, E. S. Brooks, and C. A. Scott. "Seasonal risk analysis for floodplains in the Delaware River Basin". In: *Journal of Water Resources Planning and Management* 126.5 (2000), pp. 320–329.
- [590] A. Werritty. "Sustainable flood management: oxymoron or new paradigm?" In: *Area* 38.1 (Mar. 1, 2006), pp. 16–23. ISSN: 0004-0894. DOI: 10.1111/j.1475-4762.2006.00658.x.
- [591] G.F. White. *Human adjustments to floods*. 29. Chicago: Department of Geography, University of Chicago, 1945, p. 119.
- [592] G.F. White. "The Limit of Economic Justification for Flood Protection". In: *The Journal of Land & Public Utility Economics* 12.2 (1936), pp. 133–148. ISSN: 1548-9000. DOI: 10.2307/3158294.
- [593] H. Wickham. "Ggplot2: Elegant Graphics for Data Analysis". In: *Ggplot2: Elegant Graphics for Data Analysis* (2009).
- [594] H. Wickham. "Reshaping Data with the reshape Package". In: *Journal of Statistical Software* 21.12 (2007), pp. 1–20.
- [595] H. Wickham. "Scales: scale functions for visualization. [online] available from". In: (2016).
- [596] H. Wickham. "Stringr: simple, consistent wrappers for common string operations. [online] available from". In: (2017).
- [597] H. Wickham, R. Francois, L. Henry, and K. Müller. "Dplyr: a grammar of data manipulation. [online] available from". In: (2017).
- [598] H. Wickham and L. Henry. "tidyr: Easily Tidy Data with spread and gather Functions. [online] available from". In: (2017).
- [599] H. Wickham, J. Hester, and R. Francois. "Readr: read rectangular text data. [online] available from". In: (2017).
- [600] J. Wieringa. "Roughness-dependent geographical interpolation of surface wind speed averages". In: *Quarterly Journal of the Royal Meteorological Society* 112.473 (July 1986), pp. 867–889. ISSN: 00359009, 1477870X. DOI: 10.1002/qj.49711247316.
- [601] R. L. Wilby and N. W. Quinn. "Reconstructing multi-decadal variations in fluvial flood risk using atmospheric circulation patterns". In: *Journal of Hydrology* 487 (2013), pp. 109–121.
- [602] O.V. Wilhelmi and M.H. Hayden. "Connecting people and place: a new framework for reducing urban vulnerability to extreme heat". In: *Environmental Research Letters* 5.1 (Jan. 2010), p. 014021. ISSN: 1748-9326. DOI: 10.1088/1748-9326/5/1/014021.

- [603] C.J. Willmott and K. Matsuura. "Advantages of the mean absolute error (MAE) over the root mean square error (RMSE) in assessing average model performance". In: *Clim Res* 30.1 (Dec. 19, 2005), pp. 79–82. DOI: 10.3354/cr030079.
- [604] S.N. Willner, C. Otto, and A. Levermann. "Global economic response to river floods". In: *Nature Climate Change* 8.7 (July 2018), pp. 594–598. ISSN: 1758-6798. DOI: 10.1038/s41558-018-0173-2.
- [605] P. Wilson. "Searching: Strategies and evaluation". In: *For Information Specialists: Interpretations of Reference and Bibliographic Work* (1992), pp. 153–181.
- [606] H. G. Wind, T. M. Nierop, C. J. de Blois, and J. L. de Kok. "Analysis of flood damages from the 1993 and 1995 Meuse Floods". In: *Water Resources Research* 35.11 (1999), pp. 3459–3465. ISSN: 1944-7973. DOI: 10.1029/1999WR900192.
- [607] H.C. Winsemius, J. Aerts, L. P. H. van Beek, et al. "Global drivers of future river flood risk". In: *Nature Clim. Change* 6.4 (Apr. 2016), pp. 381–385. ISSN: 1758-678X. DOI: 10.1038/nclimate2893.
- [608] H.C. Winsemius, L. P. H. Van Beek, B. Jongman, P. Ward, and A. Bouwman. "A framework for global river flood risk assessments". In: *Hydrol. Earth Syst. Sci.* 17.5 (2013), pp. 1871–1892. ISSN: 1607-7938. DOI: 10.5194/hess-17-1871-2013.
- [609] WMO. *Comprehensive Risk Assessment for Natural Hazards*. 955. Geneva, Switzerland: World Meteorological Organisation, 1999, p. 100.
- [610] E.F. Wood and I. Rodríguez-Iturbe. "A Bayesian approach to analyzing uncertainty among flood frequency models". In: *Water Resources Research* 11.6 (1975), pp. 839–843. ISSN: 0043-1397. DOI: 10.1029/WR011i006p00839.
- [611] K. Woth, R. Weisse, and H. von Storch. "Climate change and North Sea storm surge extremes: an ensemble study of storm surge extremes expected in a changed climate projected by four different regional climate models". In: *Ocean Dynamics* 56.1 (May 2006), pp. 3–15. ISSN: 1616-7341, 1616-7228. DOI: 10.1007/s10236-005-0024-3.
- [612] A. Wunsch, U. Herrmann, H. Kreibich, and A. Thielen. "The Role of Disaggregation of Asset Values in Flood Loss Estimation: A Comparison of Different Modeling Approaches at the Mulde River, Germany". In: *Environmental Management* 44.3 (2009), pp. 524–541. ISSN: 0364-152X. DOI: 10.1007/s00267-009-9335-3.
- [613] J. Yazdi and S. A. A. Salehi Neyshabouri. "Optimal design of flood-control multi-reservoir system on a watershed scale". In: *Natural Hazards* 63.2 (2012), pp. 629–646.
- [614] S.W. Yeo. "Flooding in Australia: A review of events in 1998". In: *Nat Hazards* 25 (2002), p. 177.191. DOI: 10.1023/A:1013765303567.
- [615] J. Yin, A. Lampert, M. Cameron, B. Robinson, and R. Power. "Using social media to enhance emergency situation awareness". In: *IEEE Intelligent Systems* 27.6 (2012), pp. 52–59.
- [616] M. Zambrano-Bigiarini. "HydroGof: Goodness-of-fit Functions for Comparison of Simulated and Observed Hydrological Time Series". In: *hydroGOF: Goodness-of-fit functions for comparison of simulated and observed hydrological time series* (2014).

- [617] G. Zhai, T. Fukuzono, and S. Ikeda. "Modeling flood damage: Case of Tokai flood 2000". In: *Journal of the American Water Resources Association* 41.1 (2005), pp. 77–92. ISSN: 1093474X.
- [618] P Zimmerli. *Hagelstürme in Europa*. Zurich, Switzerland: Swiss Re, 2005.
- [619] A.P. Zischg, P. Hofer, M. Mosimann, V. Röthlisberger, J.A. Ramirez, M. Keiler, and R. Weingartner. "Flood risk (d)evolution: Disentangling key drivers of flood risk change with a retro-model experiment". In: *Science of The Total Environment* 639 (Oct. 15, 2018), pp. 195–207. ISSN: 0048-9697. DOI: 10.1016/j.scitotenv.2018.05.056.
- [620] M. Zoltak, B. Ripley, and M. Lapsley. "RODBCext: parameterized queries extension for RODBC. [online] available from". In: (2017).
- [621] H. Zwenzner and S. Voigt. "Improved estimation of flood parameters by combining space based SAR data with very high resolution digital elevation data". In: *Hydrolog. Earth Syst. Sci.* 13.5 (2009), pp. 567–576. ISSN: 1607-7938. DOI: 10.5194/hess-13-567-2009.